



University  
of Glasgow

King, Vicky (2010) *Assessment of the therapeutic potential of the atypical chemokine receptor, D6*. PhD thesis.

<http://theses.gla.ac.uk/2165/>

Copyright and moral rights for this thesis are retained by the author

A copy can be downloaded for personal non-commercial research or study, without prior permission or charge

This thesis cannot be reproduced or quoted extensively from without first obtaining permission in writing from the Author

The content must not be changed in any way or sold commercially in any format or medium without the formal permission of the Author

When referring to this work, full bibliographic details including the author, title, awarding institution and date of the thesis must be given

# **Assessment of the Therapeutic Potential of the Atypical Chemokine Receptor, D6.**

**Vicky King**

**B.Sc (Hons)**

**Submitted in fulfilment of the requirements for  
the Degree of Doctor of Philosophy**

**Department of Immunology, Infection and Inflammation  
Faculty of Medicine  
University of Glasgow**

**February 2010**

## Abstract

Infiltration of inflammatory cells into the tissue during the inflammatory response is beneficial to the host. Chemokines and their receptors are instrumental in this process by influencing the migration and behaviour of leukocytes in the tissue. However, prolonged inflammation is associated with many diseases.

In recent years, a family of atypical receptors have emerged which do not seem to signal. One of these receptors, D6, is able to internalise and degrade 12 pro-inflammatory CC chemokines and has a role in the resolution of the inflammatory response. Here, using a murine transgenic approach, the potential therapeutic role of D6 in suppressing cutaneous inflammation *in vivo* has been investigated, using a well-characterised model of skin inflammation. In addition, expression of D6 in a range of inflammatory disorders has also been characterised.

Transgenic mice were generated (K14D6), using an epidermis-specific transgene, in which expression of the D6 transgene was driven by the human keratin 14 promoter in epidermal keratinocytes. K14D6 mice were validated and we have shown that D6 is expressed in K14D6 but not in wild-type epidermal keratinocytes. The K14D6 transgene was shown to be functional as only K14D6 keratinocytes were able to bind CCL2 and progressively deplete extracellular CCL3. K14D6 mice can dampen down cutaneous inflammation in response to a topical application of TPA. In addition, K14D6 mice displayed reduced infiltration of epidermal T cells and mast cells compared to wild-type mice.

Using a microarray approach, we examined the transcriptional consequences of non-ligated D6 and after ligand binding in primary murine keratinocytes from K14D6 and wild-type mice. Although limited conclusions could be made from the microarray data, our results suggest the possibility that non-ligated D6 in murine keratinocytes may have a negative impact on the transcription of some genes, such as chemokines.

In a previous study, D6 null mice displayed a human psoriasis-like pathology after chemical induced skin inflammation, suggesting a possible involvement of D6-

dysfunction as a contributing factor in the pathogenesis of psoriasis. We have investigated the possible correlation between D6 expression levels and cutaneous disease development. Analysis of skin biopsies revealed that D6 mRNA levels were 8-fold higher in uninvolved psoriatic skin compared to matching psoriatic lesional skin, atopic dermatitis and control skin. In PBMCs, there was no significant difference in D6 mRNA expression in psoriasis patients compared to control. A preliminary study examining surface D6 expression on leukocytes from control and rheumatoid arthritis patients revealed enhanced D6 expression on B cells and myeloid DCs.

In this study, we have shown for the first time that increased expression of D6 *in vivo* can limit cutaneous inflammation, therefore providing a rationale for exploring the therapeutic potential of D6 in human inflammatory diseases. In addition, we provide evidence that D6 expression is dysregulated in inflammatory disorders further suggesting an involvement of this receptor in the pathogenesis of these diseases.

# Table of contents

Abstract .....	2
Table of contents .....	4
List of Tables .....	9
List of Figures .....	11
List of publications arising from this work .....	14
Acknowledgements.....	15
Author's Declaration .....	17
Abbreviations.....	18
Chapter 1 Introduction .....	21
1.1 Haemopoiesis.....	22
1.2 The immune system .....	24
1.2.1 <i>The immune response</i> .....	24
1.2.1.1 Recognition of pathogens in innate immunity .....	25
1.2.1.2 Immune response to endogenous danger signals .....	27
1.2.1.3 Cells of the innate immune system .....	27
1.2.1.4 Cells of adaptive immunity .....	32
1.3 Cutaneous immune system .....	36
1.3.1 <i>Structure of the skin</i> .....	36
1.3.2 <i>Immune response within the skin</i> .....	38
1.4 Acute inflammation .....	41
1.4.1 <i>Cytokines in inflammation</i> .....	41
1.4.2 <i>Resolution of inflammation</i> .....	44
1.4.3 <i>Chronic inflammation</i> .....	46
1.4.3.1 Psoriasis .....	46
1.4.3.2 Psoriatic arthritis .....	51
1.4.3.3 Rheumatoid arthritis .....	51
1.4.4 <i>Treatment of inflammatory diseases</i> .....	52
1.5 Chemokines.....	52
1.5.1 <i>Nomenclature</i> .....	53
1.5.2 <i>Chemokine receptors</i> .....	55
1.5.2.1 Chemokine receptor signalling.....	63
1.5.2.2 Chemokine receptor internalisation .....	63
1.5.3 <i>Functions of chemokines and their receptors</i> .....	65
1.5.3.1 Leukocyte migration.....	65

1.5.3.2	Cell trafficking and surveillance.....	69
1.5.3.3	Haemopoiesis .....	71
1.5.3.4	Angiogenesis .....	72
1.5.4	<i>Role of chemokines and their receptors in disease</i> .....	74
1.5.4.1	Human immunodeficiency virus .....	75
1.5.4.2	Cancer .....	77
1.5.4.3	Psoriasis .....	79
1.5.4.4	Rheumatoid arthritis .....	80
1.6	Atypical chemokine receptors .....	82
1.6.1	<i>DARC</i> .....	82
1.6.2	<i>CCX-CKR</i> .....	84
1.6.3	<i>CXCR7</i> .....	86
1.6.4	<i>D6</i> .....	87
1.7	Aims .....	92
<b>Chapter 2 Materials and Methods.....</b>		<b>93</b>
2.1	Materials .....	94
2.1.1	<i>Antibodies</i> .....	94
2.1.2	<i>Chemicals, reagents and solutions</i> .....	95
2.1.3	<i>Chemokines</i> .....	96
2.1.4	<i>Enzymes, kits and PCR master mix</i> .....	97
2.1.5	<i>Primers</i> .....	98
2.1.6	<i>Tissue culture media and reagents</i> .....	100
2.2	Methods .....	101
2.2.1	<i>Molecular Biology</i> .....	101
2.2.1.1	Preparation of genomic DNA from tail tips .....	101
2.2.1.2	RNA extraction using Trizol .....	101
2.2.1.3	RNA extraction using RNeasy Mini Kit.....	102
2.2.1.4	RNA clean up .....	103
2.2.1.5	RNA quality test.....	103
2.2.1.6	cDNA synthesis from RNA .....	103
2.2.1.7	Polymerase chain reaction .....	104
2.2.1.8	Agarose gel electrophoresis .....	105
2.2.1.9	Quantitative polymerase chain reaction .....	105
2.2.2	<i>In vivo analysis</i> .....	112
2.2.2.1	Maintenance of mice .....	112
2.2.2.2	Genotyping of mice.....	112

2.2.2.3	Epidermal sheet preparation.....	112
2.2.2.4	Harvesting of primary keratinocytes.....	113
2.2.2.5	Staining of primary keratinocytes .....	113
2.2.2.6	Assessment of keratinocyte purity .....	113
2.2.2.7	Incubation of keratinocytes with biotinylated CCL3.....	114
2.2.2.8	Detection of biotinylated CCL3 by western blotting.....	114
2.2.2.9	Assessment of CCL2 binding by keratinocytes using flow cytometry .....	115
2.2.2.10	Testing an anti-mouse D6 antibody .....	115
2.2.2.11	Cutaneous skin inflammation model .....	116
2.2.2.12	Haematoxylin staining.....	116
2.2.2.13	Measuring skin thickness.....	116
2.2.3	<i>Keratinocyte microarray</i> .....	117
2.2.3.1	Keratinocyte incubation and RNA extraction .....	117
2.2.3.2	Microarray analysis .....	117
2.2.4	<i>Human analysis</i> .....	118
2.2.4.1	Collection of human psoriasis skin biopsies.....	118
2.2.4.2	Collection of peripheral blood samples.....	120
2.2.5	<i>Statistical Analysis</i> .....	122
<b>Chapter 3</b>	<b>Characterisation of K14D6 Mice</b> .....	<b>123</b>
3.1	Introduction .....	124
3.2	Generation of K14D6 transgenic mice .....	125
3.3	The D6 transgene is expressed in the epidermis in K14D6 mice .....	126
3.4	The D6 transgene is expressed by K14D6 epidermal keratinocytes ....	130
3.5	Detection of mouse D6 protein .....	135
3.6	Characterisation of chemokine receptor transcripts in primary keratinocytes.....	137
3.7	The function of D6 in K14D6 epidermal keratinocytes .....	140
3.7.1	<i>K14D6 keratinocytes can bind CCL2, a D6 ligand</i> .....	140
3.7.2	<i>K14D6 keratinocytes can remove extracellular CCL3 from the media.</i> .....	143
3.8	Transgenic expression of D6 dampens cutaneous inflammation.....	145
3.9	Summary of Chapter 3 .....	148
<b>Chapter 4</b>	<b>Characterisation of the transcriptional consequences of D6 ligand binding</b> .....	<b>149</b>
4.1	Introduction .....	150

4.2	Experimental details .....	151
4.3	Generation and validation of RNA for microarray application .....	152
4.4	Analysis of microarray Data .....	153
4.4.1	<i>Rank product differential expression analysis reports</i> .....	153
4.4.1.1	WT keratinocytes versus K14D6 keratinocytes .....	154
4.4.1.2	WT keratinocytes versus WT keratinocytes + CCL3 .....	157
4.4.1.3	K14D6 keratinocytes versus K14D6 + CCL3 .....	161
4.4.1.4	WT + CCL3 versus K14D6 + CCL3 .....	165
4.4.1.5	Summary of rank product differential analysis reports .....	169
4.4.2	<i>Iterative group analysis</i> .....	173
4.4.2.1	WT control v K14D6 control keratinocytes .....	174
4.4.2.2	WT control v WT control + CCL3 .....	177
4.4.2.3	K14D6 control v K14D6 + CCL3 .....	180
4.4.2.4	WT + CCL3 v K14D6 + CCL3 .....	184
4.4.2.5	Summary of iGA analysis .....	188
4.5	Validation of microarray data by QPCR .....	192
4.5.1	<i>Identifying potentially upregulated genes to validate by QPCR</i> ..	192
4.5.2	<i>Identifying potentially downregulated genes to validate</i> .....	197
4.5.3	<i>Design and validation of primers</i> .....	198
4.5.4	<i>Validation of outer primers</i> .....	199
4.5.4.1	Calculation of gene transcripts numbers within standards ...	200
4.5.5	<i>Optimisation of 'nested' primers</i> .....	201
4.5.6	<i>QPCR results</i> .....	202
4.5.6.1	Validation of genes potentially induced by CCL3 in both wild-type and K14D6 transgenic keratinocytes. ....	202
4.5.6.2	Validation of genes potentially induced by CCL3 only in K14D6 keratinocytes .....	206
4.5.6.3	Validation of genes potentially upregulated between wild-type and K14D6 keratinocytes at rest .....	208
4.5.7	<i>Summary of quantitative PCR results</i> .....	210
4.6	Discussion of Chapter 4 .....	211
4.7	Conclusion of Chapter 4 .....	213
<b>Chapter 5</b>	<b>D6 in human psoriasis</b> .....	<b>214</b>
5.1	Introduction .....	215
5.2	Collection of human skin samples .....	216
5.3	D6 transcripts in human skin .....	217

5.4	D6 protein in human skin .....	219
5.5	D6 transcripts in peripheral blood .....	236
5.6	D6 surface expression on peripheral blood cells .....	238
5.7	Summary of Chapter 5 .....	251
<b>Chapter 6</b>	<b>General Discussion .....</b>	<b>252</b>
<b>References</b>	<b>.....</b>	<b>265</b>
<b>Appendix One</b>	<b>.....</b>	<b>317</b>
<b>Appendix Two</b>	<b>.....</b>	<b>322</b>
<b>Appendix Three</b>	<b>.....</b>	<b>366</b>

## List of Tables

Table 1-1. Clinical spectrum of psoriasis .....	47
Table 1-2. Classification of chemokines and their receptors .....	62
Table 2-1. Example of normalisation of QPCR data using a housekeeping gene to determine levels of ‘gene of interest’. .....	111
Table 3-1. Summary of D6 ligands, which CCR1, CCR2, CCR3, CCR4 and CCR5 can bind.....	138
Table 4-1. Concentration and total yield of RNA extracted from keratinocytes analysed by a Nanodrop ND-1000. ....	152
Table 4-2. The top 6 genes listed by RP score as potentially upregulated genes in K14D6 keratinocytes compared to wild-type keratinocytes.....	155
Table 4-3. Twenty-five top genes potentially downregulated in K14D6 keratinocytes compared to wild-type keratinocytes. ....	156
Table 4-4. The first 25 genes listed as potentially upregulated by CCL3 in wild-type keratinocytes. ....	158
Table 4-5. Top 15 genes potentially downregulated gene by CCL3 in wild-type keratinocytes.....	160
Table 4-6. Top 25 genes potentially upregulated by CCL3 in K14D6 keratinocytes. ....	162
Table 4-7. Top 4 genes listed as potentially downregulated after CCL3 treatment in K14D6 keratinocytes. ....	164
Table 4-8. Genes listed as potentially upregulated after CCL3 treatment in K14D6 keratinocytes compared to wild-type keratinocytes after CCL3 treatment. ....	166
Table 4-9. Top 25 ranked genes potentially downregulated in K14D6 keratinocytes treated with CCL3 in comparison to WT keratinocytes treated with CCL3. ....	167
Table 4-10. Expression of D6 in rank product differential expression analysis reports. ....	169
Table 4-11. Potential upregulated functional gene classes in K14D6 keratinocytes compared to wild-type keratinocytes .....	174
Table 4-12. Potential downregulated functional gene classes in K14D6 keratinocytes compared to wild-type keratinocytes. ....	176
Table 4-13. Potential downregulated functional gene classes in Wild-type (WT) keratinocytes after CCL3 treatment compared to wild-type keratinocytes at rest. ....	178

Table 4-14. Potential downregulated functional gene classes in Wild-type (WT) keratinocytes after CCL3 treatment compared to wild-type keratinocytes at rest. ....	179
Table 4-15. List of potential upregulated functional gene classes in K14D6 keratinocytes after CCL3 treatment compared to K14D6 keratinocytes at rest.	182
Table 4-16. Potential downregulated functional gene classes in K14D6 keratinocytes after CCL3 treatment compared to K14D6 keratinocytes at rest.	183
Table 4-17. Potential upregulated functional gene classes in K14D6 keratinocytes after CCL3 treatment compared to Wild-type keratinocytes after CCL3 treatment.....	185
Table 4-18. Potential downregulated functional gene classes in K14D6 keratinocytes after CCL3 treatment compared to Wild-type keratinocytes after CCL3 treatment.....	187
Table 4-19. Genes potentially upregulated only in K14D6 keratinocytes after CCL3 treatment identified for validation. ....	194
Table 4-20. Comparison of data from the rank product reports on six genes identified as potentially differentially expressed in both Wild-type and K14D6 keratinocytes after incubation with CCL3. ....	196
Table 4-21. Genes identified for validation that were potentially upregulated in K14D6 keratinocytes in comparison to wild-type keratinocytes at rest. ....	197
Table 4-22. Calculation of the number of transcripts within each standard for each gene of interest. ....	200

## List of Figures

Figure 1.1 The development of cell subsets during haemopoiesis. ....	23
Figure 1-2. The structure and layers within murine skin. ....	38
Figure 3-1. K14D6 transgene construct.....	126
Figure 3-2. Optimising a method to separate the epidermis from the dermis. .	128
Figure 3-3. Transgenic expression of D6 in the epidermis of K14D6 mice. ....	129
Figure 3-4. Morphology of wild-type and K14D6 epidermal keratinocytes. ....	131
Figure 3-5. Purity of primary epidermal keratinocytes. ....	133
Figure 3-6. D6 transcripts are detected in K14D6 epidermal keratinocytes at high levels. ....	134
Figure 3-7. Optimising an anti-mouse D6 antibody.....	136
Figure 3-8. Expression of chemokine receptors CCR1, CCR3 and CCR5 on primary epidermal keratinocytes.....	139
Figure 3-9. K14D6 keratinocytes are able to bind CCL2 in a D6 dependent manner .....	142
Figure 3-10. Transgenic expression of D6 in epidermal keratinocytes is able to degrade extracellular biotinylated CCL3.....	144
Figure 3-11. Transgenic expression of D6 in murine epidermis limits cutaneous inflammation.....	147
Figure 4-1. Summary of experimental design to characterise transcriptional consequences of D6 ligand binding. ....	151
Figure 4-2. Venn diagram summarising potential upregulated functional gene classes using iGA analysis of four different group comparisons. ....	1
Figure 4-3. Venn diagram summarising the potential downregulated functional gene classes using iGA analysis results of 4 different group comparisons.....	1
Figure 4-4. Venn diagram of genes potentially upregulated after CCL3 treatment in wild-type and K14D6 keratinocytes. ....	193
Figure 4-5. A diagram illustrating the use of different primer sets for QPCR. ..	198
Figure 4-6. Specificity of ‘outer’ primers to generate standards for use in QPCR. ....	199
Figure 4-7. Nested primers used in QPCR were specific. ....	201
Figure 4-8. Validation of gene transcripts potentially upregulated after CCL3 treatment in both wild-type and K14D6 keratinocytes .....	203
Figure 4-9. Repeated QPCR for validation of CCL6 .....	204

Figure 4-10. Repeated QPCR for validation of Laptm5 .....	205
Figure 4-11. Validation of gene transcripts identified as potentially upregulated after CCL3 treatment in K14D6 keratinocytes but not wild-type (WT) keratinocytes.....	207
Figure 4-12. Validation of the transcript levels of three genes potentially upregulated between wild-type (WT) and K14D6 keratinocytes. ....	209
Figure 5-1. D6 transcript levels in human skin. ....	218
Figure 5-2. Haematoxylin and eosin staining in human placenta.....	221
Figure 5-3. Optimisation of D6 antibody on placental sections.....	222
Figure 5-4. Change of antigen retrieval method.....	224
Figure 5-5. Different concentrations of primary antibody on placental sections. ....	225
Figure 5-6. Structure and features of human skin .....	227
Figure 5-7. D6 staining in skin section.....	228
Figure 5-8. Different concentrations of primary antibody on human placenta and skin sections.....	230
Figure 5-9. Optimisation of primary antibody on human placenta and human skin sections using 1:750 and 1:1000 dilutions. ....	232
Figure 5-10. D6 staining within human skin .....	233
Figure 5-11. Comparison using avidin/biotin block during D6 staining on human skin. ....	235
Figure 5-12. Levels of D6 transcripts in peripheral blood from human inflammatory diseases. ....	237
Figure 5-13. Profile of peripheral blood mononuclear cells from a healthy control patient. ....	238
Figure 5-14. Analysis of D6 expression on control human T and B cells. ....	240
Figure 5-15. Analysis of D6 expression on control monocytes. ....	241
Figure 5-16. Analysis of D6 expression on control myeloid and plasmacytoid dendritic cells.....	243
Figure 5-17. Cell profile of peripheral blood mononuclear cells from a rheumatoid arthritis patient using flow cytometry.....	244
Figure 5-18. Analysis of D6 expression on T and B cells from a RA patient. ....	246
Figure 5-19. Analysis of D6 expression on monocytes from a RA patient. ....	247
Figure 5-20. Analysis of D6 expression on myeloid and plasmacytoid dendritic cells from a RA patient. ....	248

Figure 5-21. Analysis of D6 expression on peripheral blood cells in control and RA patients. ....249

Figure 5-22 Copy numbers of GAPDH in control, psoriatic arthritis (PsA), rheumatoid arthritis (RA) and psoriasis patients.....250

## **List of publications arising from this work**

Nibbs R.J., Gilchrist G.S., King V., Ferra A., Forrow S., Hunter K.D. & Graham G.J. (2007) The atypical chemokine receptor D6 suppresses the development of chemically induced skin tumours. *J Clin Invest*, 117, 1184-92.

## Acknowledgements

Throughout my PhD, many people have helped me in many ways to reach this point and I am grateful to all of them. My first and most important acknowledgement is to my mum and dad. Both of you have given me great guidance and encouragement throughout the years as well as supporting decisions I have made.

Many thanks go to my supervisor, Professor Gerry Graham, for his guidance and support throughout my PhD. In particular, his advice and patience during the writing of this thesis has been valuable. I would also like to mention Professor Iain McInnes for allowing me the opportunity to be one of the first students on the Oliver Bird Rheumatism PhD programme here at Glasgow University. I thank Iain for his support and guidance, in particular within the first year, his enthusiasm and for his kind words of encouragement throughout.

On this note, I would like to mention the Nuffield Foundation for their funding and developing the Oliver Bird programme not just at Glasgow University but also at four other universities in the UK. At our annual conferences, I have discussed science with fellow Oliver Bird students and in doing so I have also gained a friend or two for life along the way.

Various people have helped me with several practical aspects of my PhD during my time in the lab. Professor David Greenhalgh taught me how to isolate primary keratinocytes, in which this technique has been a big part of this project and I am grateful to him in doing so. Dr Clive McKimmie has taught me many aspects of molecular biology, in particular real-time PCR. I would also like to thank Dr Alasdair Fraser for his expertise in flow cytometry. Thanks to Dr Derek Gilchrist, Clive and Alasdair for proofreading various parts of this thesis.

I would also like to acknowledge every member, past and present, within the chemokine research group not just for your constructive criticism and questions at group meetings but also for providing a friendly and enjoyable atmosphere within the lab. Quite how conversations, during cups of tea, got from A to D was not always logically via B and C but certainly provided many laughs in the process.

Last of all but not least, Mark, for his support and for ensuring that we kept a balance between 'work and play', especially whilst doing our PhDs and for making sure that this was the case whilst I was writing this thesis.

## **Author's Declaration**

The work presented in this thesis represents original work carried out by the author. This thesis has not been submitted in any form to any other university.

## Abbreviations

AA	arachidonic acid
Ag	antigen
AP-1	activating protein-1
APC	antigen presenting cell
ApoE	apolipoprotein E
ATP	adenosine triphosphate
BCR	B cell receptor
CD	cluster of differentiation
CLA	cutaneous lymphocyte-associated antigen
CLP	common lymphoid progenitor
CMP	common myeloid progenitor
CpG	non-methylated CG dinucleotide
DAMP	damage associated molecular pattern
DC	dendritic cell
ddH <sub>2</sub> O	double distilled water
DEPC	diethylpyrocarbonate
DETC	dendritic epidermal T cell
DNA	deoxyribonucleic acid
DMBA	7,12-dimethylbenz( <i>a</i> )anthracene
EAE	experimental autoimmune encephalomyelitis
EPC	endothelial progenitor cell
FC	fold change
Flt3-L	FMS-related tyrosine kinase 3-ligand
Foxp3	forkhead box p3
GAPDH	glyceraldehyde-3-phosphate dehydrogenase
GDP	guanosine diphosphate
GMP	granulocyte monocyte precursor
gp	glycoprotein
GPCR	G-protein coupled receptor
GTP	guanosine triphosphate
HEV	high endothelial venule
HIV	human immunodeficiency virus
HRP	horseradish peroxidase
HSC	haemopoietic stem cell

ICAM-1	intracellular adhesion molecule-1
ICE	IL-1 $\beta$ converting enzyme
IEL	intraepithelial lymphocyte
IFN	interferon
Ig	immunoglobulin
iGA	iterative group analysis
IGF-1	insulin-like growth factor-1
IL	interleukin
IL-1Ra	interleukin-1 receptor antagonist
iT <sub>reg</sub>	inducible regulatory T lymphocyte
JAM	junction adhesion molecule
KO	knock-out
LFA-1	lymphocyte function associated antigen-1
LPS	lipopolysaccharide
mDC	myeloid dendritic cell
MEP	megakaryocyte erythroid precursor
MHC	major histocompatibility complex
MMP	matrix metalloproteinase
NADPH	nicotinamide adenine dinucleotide phosphate
NF- $\kappa$ B	nuclear factor-kappa B
NK	natural killer
NLR	NOD-like receptor
NOD	nucleotide-binding oligomerization domain
PAMP	pathogen associated molecular pattern
PBMC	peripheral blood mononuclear cell
PCR	polymerase chain reaction
pDC	plasmacytoid dendritic cell
PECAM-1	platelet endothelial cell adhesion molecule-1
PGC	primordial germ cell
PRR	pattern recognition receptor
PsA	psoriatic arthritis
QPCR	quantitative polymerase chain reaction
RA	rheumatoid arthritis
RNA	ribonucleic acid
RP	rank product
S1P	sphingosine 1-phosphate

STAT	signal transducer and activator
TACE	TNF- $\alpha$ converting enzyme
TAM	tissue associated macrophage
Tc	cytotoxic T lymphocyte
TCR	T cell receptor
TGF	transforming growth factor
Th	T helper cell
Th1	T helper cell type 1
Th2	T helper cell type 2
Th9	T helper cell type 9
Th17	T helper cell type 17
TLR	toll-like receptor
TNF	tumour necrosis factor
TNFR	tumour necrosis factor receptor
T <sub>reg</sub>	regulatory T lymphocyte
TPA	phorbol 12-myristate 13-acetate
UV	ultraviolet light
VLA-4	very late antigen-4
WT	wild-type
$\alpha$	alpha
$\beta$	beta
$\delta$	delta
$\gamma$	gamma
$\kappa$	kappa

# **Chapter 1 Introduction**

# 1 Introduction

## 1.1 Haemopoiesis

Within the body, there are many different types of blood cells with various functions. Haemopoiesis is the expansion and development of these blood cells from haemopoietic stem cells (HSCs). The principle site of haemopoiesis varies depending on the developmental stage of the mammal. In the fetus, haemopoiesis initially takes place in the yolk sac then the aortic/gonad/mesonephrous (AGM) region, and finally the liver (Cumano and Godin, 2007). After birth, the major location for haemopoiesis is within specialised niches in the bone marrow (Adams and Scadden, 2006). Haemopoietic stem cells are defined by two main properties, self-renewal and multipotency (Bonnet, 2002). By having the capacity to renew, HSCs have the ability to proliferate and maintain their population. Multi-potency refers to the potential of a single HSC to generate differentiated progenitor (also known as precursor) cells that can become various types of blood cell (Cumano and Godin, 2007).

Haemopoietic stem cells divide and give rise to two common progenitor cells, myeloid and lymphoid progenitors, which are specifically committed to generate myeloid and lymphoid cells respectively. Under normal circumstances, these progenitors do not generate cells belonging to the other pathway (Kondo et al., 1997). A common myeloid progenitor cell (CMP) has the ability to differentiate into a granulocyte monocyte precursor (GMP), a megakaryocyte erythroid precursor (MEP) or an immature precursor that is positive for a cell surface protein known as cluster of differentiation (CD) 34. MEP can differentiate into a megakaryocyte, which gives rise to platelets, or erythroblasts from which erythrocytes are derived. A GMP can differentiate and give rise to granulocytes (eosinophils, neutrophils and basophils), mast cells or monocytes (see 1.2.1.3). Macrophages, osteoclasts and myeloid dendritic cells (mDCs) are cell types, which are differentiated from monocytes (Palucka et al., 1998, Schneider et al., 1986). Two subsets of dendritic cells (DCs), Langerhans cells and interstitial dendritic cells (see 1.2.1.3) are derived from the CD34<sup>+</sup> DC precursor, but Langerhans cells can also be derived from monocytes (Ginhoux et al., 2006). A third type of DC, plasmacytoid dendritic cells (pDCs; see 1.2.1.3) are derived

from common lymphoid progenitor cells that also give rise to either a T cell precursor or a B cell precursor. T lymphocytes (see 1.2.1.4) and natural killer cells are derived from T cell precursors whereas B lymphocytes (see.1.2.1.4) are derived from B cell precursors. The theory that haemopoiesis has two common progenitors cells feeding into distinct pathways is the classical model, however there is evidence that lineage pathways are sufficiently flexible to allow myelo-lymphoid progenitors and myelo-erythroid progenitors to exist (Arinobu et al., 2007). A summary of the classical model of development of the different blood lineages is shown in Figure 1.1.

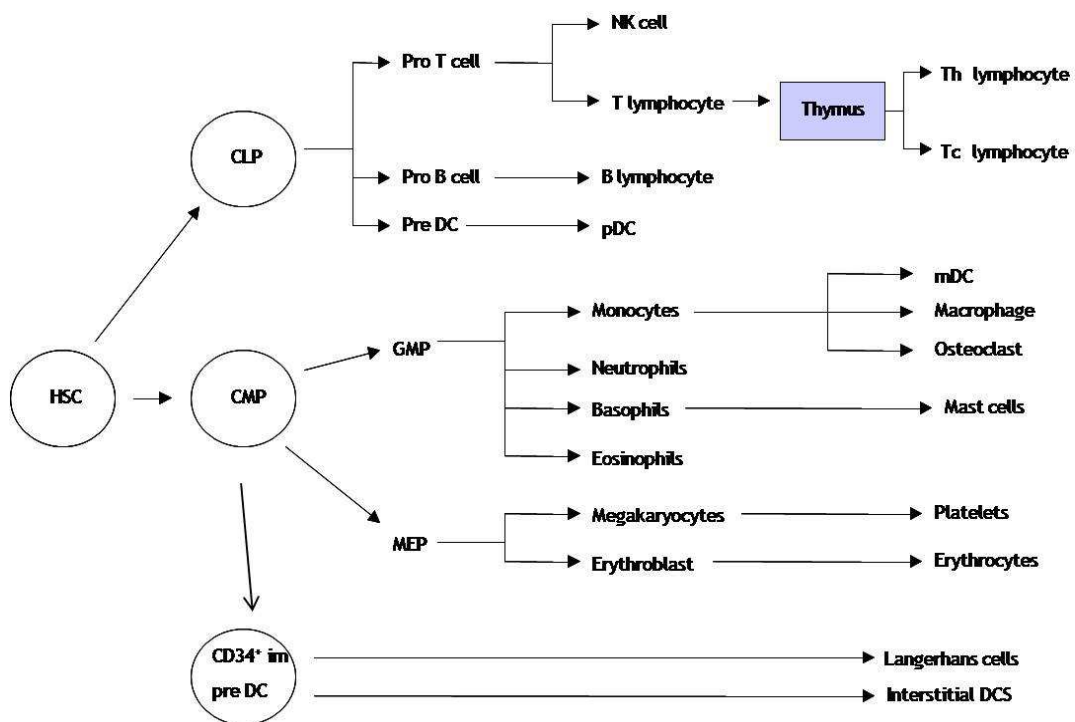


Figure 1.1 The development of cell subsets during haemopoiesis.

Haemopoietic stem cells (HSCs) can differentiate into common myeloid progenitor (CMP) or common lymphoid progenitor (CLP) which give rise to a variety of distinct cells. (GMP) granulocyte monocyte precursor, (MEP) myeloid erythrocyte precursor, (CD34<sup>+</sup> im pre DC) cluster of differentiation 34<sup>+</sup> immature dendritic cell precursor, (pDC) plasmacytoid DC, (mDC) myeloid DC, (NK cell) natural killer cell, (Th lymphocyte) T helper lymphocyte, (Tc lymphocyte) cytotoxic T lymphocyte.

## 1.2 The immune system

The immune system is composed of an organised network of specialised cells, molecules, tissues and organs that play a role in protecting the host from tissue damage or potentially harmful 'foreign' substances that are 'non-self' material. The immune response (see 1.2.1) is the reaction of the immune system to tissue damage or 'foreign' material and consists of two components, the innate- and the adaptive-response.

Viruses, bacteria, fungi, protozoa and worms are foreign substances that can cause infection and damage to the host, if the immune system is unable to detect and neutralise them. Potentially pathogenic material can invade the body through a variety of routes, including across the respiratory or gastrointestinal tracts, or through breaks in the skin. As a result, several lines of defence are in place within the body to prevent invasion and eliminate foreign matter. Areas of the body susceptible to the outside world contain 'tools' to augment physical barriers. For example, cilia and mucus, within the respiratory tract serve to trap and expel pathogens. Whereas chemical barriers, such as peptide antibiotics in the intestine (Ayabe et al., 2000), enzymes in the lungs, (Akinbi et al., 2000) and gastric acid within the stomach (Tennant et al., 2008) are all mechanisms that discourage microorganisms from surviving within the body. However, if a foreign substance does manage to invade or tissue damage occurs, the body responds using specialised cells and proteins of the immune system to eliminate pathogens, limit tissue damage and stimulate tissue repair. A sign of host response to infection or injury is acute inflammation (see 1.4) in which pain, heat, redness and swelling are all classical signals that the process is occurring.

### 1.2.1 *The immune response*

Present and functional from birth, the innate immune system is the first line of defence and responds immediately to pathogens or tissue damage. However, the innate immune response has no immunological 'memory' and cannot 'learn' from previous encounters and upon repeat exposure to the same pathogen, the nature and strength of the innate immune response remains the same throughout life (Ptak and Szczepanik, 1998). In contrast, the adaptive immune response occurs later than the innate immune response but develops as a

specific response to a previously 'seen' molecule, known as an antigen (Ag). Therefore, the adaptive immune response is said to have immunological 'memory'. This results in a quicker and more robust response to an antigen when detected the second or subsequent time.

### **1.2.1.1 Recognition of pathogens in innate immunity**

The innate immune system can respond to various classes of microbes by recognising highly conserved structures, known as Pathogen Associated Molecular Patterns (PAMPs). In bacteria and fungi, PAMPs tend to be components of the cell wall whereas the PAMP within viruses is viral nucleic acid (Medzhitov, 2007). The recognition of PAMPs is mediated by Pattern Recognition Receptors (PRRs), which are encoded within the germline, and are present either on the surface, within cells or may be secreted by them (Janeway and Medzhitov, 2002).

#### **Pathogen recognition receptors**

There are several classes of pathogen recognition receptors and the Toll-like receptors (TLRs) are the most well characterised class. TLRs are cell surface receptors that can recognise components of bacteria, fungi, viruses and parasites (Akira et al., 2006). Discovery of the family began when the Toll gene, encoding a transmembrane receptor within *Drosophila* (Hashimoto et al., 1988) was also found to exist within humans (Medzhitov et al., 1997). Within mammals, at least 11 members of the Toll-like receptor family have been identified and the stimuli for various TLRs are known. Recognition of peptidoglycan and lipoteichoic acid from Gram-positive bacteria is mediated by TLR2 (Schwandner et al., 1999) whilst TLR1 forms a heterodimer with TLR2 to recognise triacylated lipopeptides (Takeuchi et al., 2002). TLR6 can also heterodimerize with TLR2 to recognise diacylated bacterial lipoproteins (Takeuchi et al., 2001). TLR3 binds to double stranded RNA (Alexopoulou et al., 2001) while TLR4 recognises lipopolysaccharide (LPS), which is a major component of the outer membrane of Gram negative bacteria whereas viral single stranded RNA is recognised by TLR7 and TLR8 (Heil et al., 2004, Lund et al., 2004). TLR9 binds bacterial DNA that contains CpG regions (Hemmi et al., 2000) and no endogenous ligand is yet known for TLR10. A ligand known for murine TLR11 is a molecule from a protozoan parasite (Yarovinsky et al., 2005).

In addition, murine TLR11 prevents infection by uropathogenic bacteria (Zhang et al., 2004) however the specific ligand responsible for the infection is not known. In addition to TLRs, there are other cell-surface PRRs, for example, the C-type lectin family. These receptors can bind carbohydrate structures associated with pathogens. One example is Dectin1, which can bind  $\beta$ -glucans and is important in antifungal immunity (Taylor et al., 2007).

In addition to cell-surface PRRs, other PRRs are present within the cytoplasm of the cell and detect PAMPs intracellularly. This includes a family of NOD-like receptors (NLRs), so called because they contain a Nucleotide-binding Oligomerization Domain (NOD) at the carboxy terminus (Fritz et al., 2006). There are two proteins established within the NOD subfamily, known as NOD1 and NOD2, both are known to recognise bacterial lipopolysaccharide resulting in the activation of various genes (Inohara et al., 2001). Other NLRs such as NLRP1 (Nod-like receptor, pyrin domain containing 1) and NLRP3 form multimeric protein complexes known as inflammasomes, which lead to the activation of enzymes involved in the cleavage of certain cytokines (Martinon and Tschopp, 2007). Other types of cytosolic receptors are RNA helicases, such as retinoic-acid-inducible gene 1 and melanoma differentiation-associated gene 5 (Yoneyama et al., 2004, Andrejeva et al., 2004), which detect and unwind double stranded RNA prior to mediating signalling responses important for antiviral immunity.

PRRs are expressed on a variety of immune cells and can influence functions within the innate and the adaptive immune response. Antigen presenting cells (see 1.2.1.3) predominately express cell-surface PRRs, in particular TLRs (Gordon, 2002). Direct interaction of a cell-surface PRR and its ligand can result in the internalisation of the pathogen expressing the ligand (Medzhitov, 2001), in a process known as phagocytosis (see 1.2.1.3). Internalisation of the pathogen is enhanced by the surface of the pathogen being coated in opsonins, which can be antibodies, also known as immunoglobulins (Ig) or proteins involved in the complement cascade. The first discovered complement pathway, so called the classical pathway, involves antibodies forming immune complexes and acting as opsonins. The detection of mannose binding lectin results in activation of the Lectin pathway (Fujita et al., 2004) whereas the alternative pathway is triggered by recognition of the complement protein C3b. All three pathways converge at

the complement protein C3, which can be cleaved to form active proteins C3a, C3b, C4a and C5a. Another complement protein, C5b, induces the formation of a multiple protein complex, known as the membrane attack complex, which forms a pore in the target cell membrane resulting in lysis of the cell and consequently cell death (Walport, 2001).

### **1.2.1.2 Immune response to endogenous danger signals**

In addition, the immune system can detect endogenous molecules associated with tissue damage or stress, therefore act as 'danger signals' and elicit an immune response (Gallucci and Matzinger, 2001). Examples of endogenous 'danger signals', known as Damage Associated Molecular Patterns (DAMPs), include heat shock proteins, high mobility group box 1 and hyaluronic acid (Bianchi, 2007). Some DAMPs can activate the immune response via TLRs, such as TLR4 (Termeer et al., 2002) or the inflammasome (Martinon et al., 2006). Both result in the transcription of many genes involved in the immune response.

### **1.2.1.3 Cells of the innate immune system**

Leukocytes, also known as white blood cells, are involved in the innate immune response. Leukocytes are derived from HSCs (see 1.1) and leukocytes of the innate immune system include basophils, eosinophils, neutrophils, mast cells, monocytes, macrophages, dendritic cells and natural killer cells. All the cells have different morphology and distinct functions.

#### **Granulocytes; neutrophils, eosinophils and basophils**

Granulocytes are white blood cells characterised by the presence of granules within their cytoplasm. They are classified into three types by their histological appearance following staining. Eosinophilic granules stain pink with acidic stains, basophilic granules stain blue with basic reagent and neutrophils contain neutral staining granules.

Neutrophils are the most abundant leukocyte within the human body and normally circulate within the blood. Neutrophils are one of the first cells recruited in an immune response and are a hallmark of acute inflammation (see 1.4). Stimulation of neutrophils results in the release of granules from the

cytoplasm (known as degranulation), which are toxic and help destroy the encountered pathogen. Two main types of granules are contained within the cytoplasm of neutrophils, azurophilic granules and specific granules. Azurophilic granules contain microbicidal substances such as defensins, enzymes such as myeloperoxidase and the proteases, elastase, proteinase-3 and cathepsin G (Faurischou and Borregaard, 2003). Specific granules contain enzymes including properdin, which induces the production of the complement molecule, C5a (Schwaeble and Reid, 1999). In turn, C5a is a chemotactic molecule, which enhances the migration of macrophages, mast cells, dendritic cells and more neutrophils to the site of infection or inflammation (Sozzani et al., 1995).

Eosinophils develop and mature in the bone marrow making up to 5% of the leukocyte population. After maturation, eosinophils circulate in the blood ready to respond to chemokines (see 1.5) and migrate into inflammatory tissues or to the site of a parasitic helminth infection. Activation of eosinophils by interleukin (IL) 5, a cytokine released from Th2 cells (see 1.2.1.4), results in the release of contents from preformed granules containing major basic protein and eosinophil cationic protein (Kita et al., 1992). Upon activation, eosinophils also produce lipid mediators, including prostaglandins and leukotrienes (Bandeira-Melo et al., 2002) which are both instrumental in inflammation. Additionally, eosinophils are widely known for their role in allergic responses, such as atopic asthma, where the immune system overreacts to allergens (Hogan et al., 2008).

Basophils are the least common type of granulocyte, constituting less than 1% of white blood cells within a healthy individual. Basophils are found within the circulation and have the ability to move into tissues. Upon activation, basophils release preformed mediators such as histamine and heparin alongside lipid mediators and cytokines (Galli et al., 1991). Histamine increases vascular permeability, smooth muscle contraction and mucous secretion (Maintz and Novak, 2007) and these effects are augmented by leukotrienes and prostaglandins, which also mediate vasodilatation and increased permeability. All of these substances therefore contribute to the inflammatory process. Notably, basophils are major producers of a cytokine called IL-4 (Min et al., 2004) and this has been linked to their role in chronic allergic inflammation (Mukai et al., 2005). Recent evidence has demonstrated that basophils can also act as antigen presenting cells (see antigen presenting cells below) in response

to protease allergens and helminth parasites (Perrigoue et al., 2009, Sokol et al., 2009).

### **Monocytes and macrophages**

Monocytes constitute 10-15% of leukocytes in humans and enter the circulation from the bone marrow where they patrol the blood. From the bloodstream, monocytes can undergo migration into tissues where they differentiate into macrophages. Human monocytes express CD14 on their surface however they are a heterogeneous population as another subset of monocytes were discovered to be CD14<sup>low</sup> CD16<sup>+</sup> (Passlick et al., 1989, Ziegler-Heitbrock, 2000). A spontaneous null mutation in the coding region of the colony stimulating factor 1 gene in *Csfm<sup>OP</sup>/Csfm<sup>OP</sup>* mice has demonstrated a key role for macrophage-colony stimulating factor in the development and differentiation of macrophages (Marks and Lane, 1976, Yoshida et al., 1990). *Csfm<sup>OP</sup>/Csfm<sup>OP</sup>* mice have excess bone formation resulting in osteopetrosis characterised by dense and brittle bones (Marks and Lane, 1976). *Csfm<sup>OP</sup>/Csfm<sup>OP</sup>* mice also have reduced number of osteoclasts, which are bone resorbing cells, and macrophages within their tissues (Naito et al., 1991).

The presence of infection or inflammation results in the recruitment of monocytes into the tissue, where they may differentiate into macrophages. In response to cytokines, small protein molecules that act as extracellular messengers (see 1.4.1), macrophages are polarised functionally. Macrophages are referred to as M1 (classically activated) if they are induced by cytokines, interferon- $\gamma$  (IFN- $\gamma$ ) and tumour necrosis factor (TNF) or M2 (alternatively activated) macrophages if induced by IL-4 or IL-10 (Gordon, 2003).

Like neutrophils, macrophages are also known as professional phagocytes. Phagocytes are cells that ingest and destroy solid particles by a process called phagocytosis (Allen and Aderem, 1996). Phagocytes express PRRs (see 1.2.1.1) which are able to bind PAMPs, and fragment crystalline  $\gamma$  receptors (Fc $\gamma$ R), which recognise the carboxy-terminal constant region of immunoglobulin isotype G (IgG) on opsonin-coated pathogens (Swanson and Hoppe, 2004). Upon recognition of PAMPs and opsonin-coated pathogens, the cell plasma membrane elongates and extends around the object and internalises the pathogen forming a vesicle

known as a phagosome. The phagosome then fuses with lysosomes, which contain destructive enzymes. Killing of the microbe is mediated by the production of reactive oxygen intermediates converted from oxygen by nicotinamide adenine dinucleotide phosphate (NADPH) oxidase and lysosomal proteases (Roos et al., 2003). Chronic granulomatous disease, caused by defects in the NADPH oxidase enzyme within phagocytic cells, leads to increased susceptibility to infections illustrating the importance of phagocytosis in innate immunity (Rosenzweig, 2008).

Phagocytosis is also a mechanism to remove 'self' cells in the body that are undergoing apoptosis (programmed cell death). Apoptosis alters membrane phospholipid symmetry resulting in exposure of phosphatidylserine, which targets the cell for phagocytosis (Fadok et al., 2001). This mechanism distinguishes healthy 'self' cells from non-healthy 'self' cells and avoids phagocytosis of healthy cells. Phagocytosis of apoptotic cells prevents the surrounding cells and tissues from being exposed to the contents of the apoptotic cell, and in terms of phosphatidylserine actually promotes an anti-inflammatory response (Huynh et al., 2002).

### **Mast cells**

Mast cells are long-lived cells found in various locations. Mast cell precursors are present in the circulation and differentiate into mature mast cells within the tissue in which they reside (Metcalf et al., 1997). Mast cells are present within the skin, mucosal tissues and in close proximity to the blood vessels ready to encounter pathogens. Activation of mast cells results in the secretion of contents, which is similar to that of basophils. Histamine from preformed granules is released, as is newly synthesised lipid mediators and cytokines (Marshall, 2004). Mast cells can function as effector cells in both the innate and the adaptive immune response. These effector functions include the degradation of toxins (Metz et al., 2006) and the killing of pathogens (Dawicki and Marshall, 2007). Mast cells are considered immunomodulatory due to their ability to influence immune cells (Galli et al., 2008). Through the release of a soluble mediator known as tumour necrosis factor (see 1.4.1), mast cells can recruit innate immune cells, such as dendritic cells (Suto et al., 2006) and cells of the adaptive immune response such as T lymphocytes (see 1.2.1.4). Mast cells have

also been described as being able to mediate a negative effect on the immune response by producing IL-10 (Grimbaldeston et al., 2007) but the mechanism by which IL-10 produced by mast cells mediates this effect is unknown (Galli et al., 2008). Mast cells have been implicated in allergy, inflammation and autoimmunity (Lee et al., 2002, Nakae et al., 2007).

### **Dendritic cells**

These cells were discovered and named by Steinman and Cohn in 1973, due to their appearance resulting from branched projections (dendrites) from the cell (Steinman and Cohn, 1973). DCs are a heterogeneous population with several subsets, including plasmacytoid DCs (pDCs), myeloid DCs (mDCs), Langerhans cells (see 1.3.2) and interstitial DCs (Shortman and Liu, 2002). All DCs are capable of acting as antigen presenting cells (see below) but dendritic cell subtypes reside in different locations. The differentiation of DCs is under the influence of FMS-related tyrosine kinase 3-ligand (Flt3-L). Disruption of haemopoiesis occurs in mice that lack Flt3-L and they consequently have low numbers of DCs (McKenna et al., 2000). *In vivo* studies have shown increased numbers of myeloid and plasmacytoid DCs after treatment with recombinant Flt3-L (Karsunky et al., 2003). In addition, DCs can be cultured from blood monocytes in the presence of granulocyte macrophage-colony stimulating factor and the cytokine IL-4 (Sallusto and Lanzavecchia, 1994). However, Langerhans cells are dependent on transforming growth factor- $\beta$  (TGF- $\beta$ ) for their development as mice lacking TGF- $\beta$  do not have Langerhans cells in their skin (Borkowski et al., 1996). DCs are characterised by specific cell surface markers, with different subsets mediating different functions. The main functions of DCs is antigen presentation and they are important in the adaptive response, by providing signals to T lymphocytes which influence the development of T cell clones into distinct subsets (see 1.2.1.4).

### **Antigen presenting cells; linking innate and adaptive immunity**

Antigen presenting cells (APCs), mainly dendritic cells and macrophages, are capable of capturing, processing and presenting pathogen-derived particles known as antigens, on their cell surface to T lymphocytes (see 1.2.1.4). Dendritic cells are the 'professional APC' as these cells are capable of initiating the adaptive response to antigen upon the first exposure. Immature dendritic

cells in peripheral tissues continuously sample the environment ready to detect pathogens or cell damage. Activation of PRRs results in phagocytosis by the DC which then begin to process the pathogenic molecule into peptides, which are presented on the cell surface, by major histocompatibility complex class II molecules (Blander and Medzhitov, 2006). Dendritic cells undergo maturation where they begin to lose the ability to capture antigen and increase their expression of cell surface molecules, such as CD80 and CD86 (Banchereau and Steinman, 1998). At the same time, DCs migrate from their site of activation (i.e. a Langerhans cell in the epidermis) to lymph nodes, which is under the control of the chemokine receptor CCR7. This is discussed in more detail in section 1.5.4. Once in the lymph nodes, DCs can present the antigenic peptide to T lymphocytes (see 1.2.1.4) and generate an adaptive immune response (Jenkins et al., 2001).

#### **1.2.1.4 Cells of adaptive immunity**

##### **Lymphocytes**

Lymphocytes are cells involved in the adaptive immune response and these too are derived from HSCs (see 1.1). Lymphocytes can be classified as T lymphocytes (T cells) or B lymphocytes (B cells) and the functions of both are described below. B lymphocytes develop in the bone marrow and T lymphocytes do too but undergo further selection and development in the thymus (Boehm and Bleul, 2007). Both subsets of lymphocytes have very diverse repertoires of receptors on their surfaces that enable them to recognise specific motifs on any pathogenic material they may encounter. The diversity of these lymphocyte receptors is formed by somatic recombination of V(D)J gene segments during development (Tonegawa, 1983, Bassing et al., 2002). Lymphocytes expressing receptors with high affinity for 'self'-molecules are usually deleted, whereas lymphocytes expressing receptors with high affinity binding to pathogen-associated molecules will survive (Boehm and Bleul, 2007). The antigen specific receptor present on T lymphocytes is known as the T cell receptor (TCR) whereas the antigen specific receptor on B lymphocytes is known as the B cell receptor (BCR).

Naive lymphocytes (those not yet engaged by an antigen for their receptor) move continuously between the bloodstream and lymph nodes, via the

lymphatics, to search for antigens. The chemokine receptor, CCR7 (see 1.5.4) is expressed on naive T cells and is important in mediating their migration (Britschgi et al., 2008).

## T Lymphocytes

Naive T cells continuously search for antigens, being 'presented' on the surface of antigen presenting cells (see 1.2.1.3). The interaction between a TCR and the 'presenting' major histocompatibility complex (MHC) is restricted by the expression of a cell-surface molecule on naive T cells. The expression of CD4 on one type of naive T cells restricts their interaction to being with MHC class II presented antigen whereas CD8 positive (CD4 null) expressing naive T cells may only interact with MHC class I presented antigens, which are generally intracellular pathogens. The interaction between T cells and APCs is focused at a specialised cell-cell junction, known as the immunological synapse (Dustin, 2002). Additionally, during T cell stimulation by APCs, the chemokine receptors CCR5 and CXCR4 (see 1.5.2) are recruited to the immunological synapse (Molon et al., 2005). Recognition of the presented antigen by the TCR with a simultaneous second signal, provided by the interaction of co-stimulatory molecules, results in the proliferation and activation of T cells. The best-characterised co-stimulatory pathway is the B7-1/B7-2-CD28/CTLA4 pathway. For example, CD86 (B7-2), a co-stimulatory molecule present on mature DCs, binds CD28 on the surface of naive T lymphocytes (Caux et al., 1994). This interaction between CD28 and B7-1 or B7-2 results in promotion of T cell survival and the induction of cytokine release, in particular IL-2, which in turn stimulates clonal expansion of the engaged T cell (Carreno and Collins, 2002). Naive T cells then differentiate into effector T cells that perform specific functions according to the type of antigen that activated them. The differentiation of naive T cells is regulated by transcription factors and the cytokine milieu in the environment.

Upon activation and proliferation, CD4<sup>+</sup> naive T cells differentiate into various subsets of effector cells. One effector cell subset is defined as T helper cells due to their ability to help B cells (see below). Upon activation, T helper cells secrete a variety of cytokine combinations, which define T helper cells into three main subtypes. These are T helper cell type 1 (Th1), T helper cell type 2 (Th2) and T helper cell type 17 (Steinman, 2007). In turn, cytokines may be

described by the type of cell that primarily produces them and are classified as Th1- or Th2-associated. IL-1, IL-6, IL-12, tumour necrosis factor (TNF) and IFN- $\gamma$  are Th1-associated cytokines whereas Th2-associated cytokines are IL-4, IL-5 and IL-13 (Abbas et al., 1996).

TCR activation induces low expression of a T box transcription factor, T-bet, which in turn induces the expression of IL-12 $\beta$ 2R and results in the T cell being responsive to IL-12 (Mullen et al., 2001). T-bet is also upregulated by signal transducer and activator 1 (STAT1), which is induced by IFN- $\gamma$  (Afkarian et al., 2002). IL-12 binding results in the upregulation of the transcription factor STAT4 (Thierfelder et al., 1996). Both T-bet expression and the activation of STAT4 result in the production of IFN $\gamma$ . The secretion of IFN $\gamma$  by the T helper cell is very effective in activating macrophages in a classical manner and defines the cell as a Th1 cell.

IL-4 is the predominant cytokine capable of inducing differentiation of naive T cells into Th2 cells by inducing the production of STAT6, which then activates the transcription factor GATA-3 (Kaplan et al., 1996). STAT6 activation induces high levels of GATA-3 (Zhu et al., 2001). As GATA-3 levels rise, this inhibits T-bet and, as a result, this attenuates Th1 development (Ouyang et al., 1998). Moreover, GATA-3 results in the production of cytokines, IL-4, IL-5 and IL-13, which characterise these cells as Th2 (Murphy and Reiner, 2002). These cytokines activate B cells and help in the defence against parasites.

Another subset of T helper cells has been discovered that are distinct from Th1 and Th2. These cells produce IL-17 (Harrington et al., 2005) and are accordingly called Th17 cells. Th17 cells produce IL-17A, IL-17F, IL-6, IL-22 and TNF- $\alpha$ . The differentiation of naive T cells into Th17 cells can be induced by IL-23 (Aggarwal et al., 2003) or IL-6 (see 1.4.1) along with TGF- $\beta$  (Kimura et al., 2007, Mangan et al., 2006). The expression of IL-17 by Th17 cells in response to IL-6 and TGF- $\beta$  requires an orphan nuclear receptor ROR $\gamma$ t and is regulated by STAT3 (Ivanov et al., 2006, Yang et al., 2007). Th17 cells are shown to be present, and play a role in, tissue inflammation and autoimmunity (Hirota et al., 2007a, Park et al., 2005, Pene et al., 2008).

Additionally, a new subset of T helper cells, known as Th9 cells, was recently discovered that produced high levels of IL-9 and IL-10 (Dardalhon et al., 2008, Veldhoen et al., 2008). These cells are similar to Th2 yet they are distinct from Th2 cells as they produce IL-9. However, it remains to be determined whether these cells are functionally different from Th2 cells.

CD4<sup>+</sup> naive T cells can also differentiate into a subset of cells known as regulatory T cells (T<sub>reg</sub> cells). These cells are able to suppress and regulate effector T cell responses and play a role in maintaining peripheral tolerance and prevent autoimmune diseases (Sakaguchi et al., 2006). T<sub>reg</sub> cells are characterised by the expression of the transcription factor, forkhead box P3 (Foxp3) which plays a role in the development of these cells (Hori et al., 2003). Two subsets of Foxp3<sup>+</sup> T<sub>reg</sub> cells have been identified, one subset is the naturally occurring CD4<sup>+</sup>CD25<sup>+</sup> T<sub>reg</sub> (nT<sub>reg</sub>) cells and the second subset is known as inducible T<sub>reg</sub> (iT<sub>reg</sub>) cells. Natural occurring T<sub>reg</sub> cells are derived in the thymus whilst iT<sub>regs</sub> are derived from CD4<sup>+</sup> naive T cells induced to express Foxp3 by TGF-β in the periphery (Chen et al., 2003). *In vivo*, Scurfy mice carry a spontaneous mutation of Foxp3, which results in the development of a fatal autoimmune disease (Brunkow et al., 2001). Foxp3 has also been identified as the defective gene in humans with immunodysregulation polyendocrinopathy and enteropathy, X-linked (IPEX) syndrome (Bennett et al., 2001). These conditions illustrate the importance of T<sub>reg</sub> cells. Although CD4<sup>+</sup> T cells can be classified into functional subsets, there is evidence of functional plasticity in CD4<sup>+</sup> T cell subsets. For example, there is evidence that Th17 cells can convert to Th1 cells (Lee et al., 2009) and regulatory T cells can change to memory T cells (Zhou et al., 2009).

After the activation and proliferation of T cells, these cells migrate to sites of inflammation, a process regulated by many factors including adhesion molecules, chemokines and chemokine receptors (see 1.5.3.1). After the clearance of pathogen, some Ag-specific T cells will remain in the body, known as memory T cells. These cells reside in peripheral tissue and subsequent exposure to the antigen will result in a more rapid response than the initial exposure response (Woodland and Kohlmeier, 2009).

## **B Lymphocytes**

Although B cells are primarily known as antibody producing cells, B cells can also act as antigen presenting cells (Chen and Jensen, 2008). Presentation of Ag on B cells and their recognition by T cells, involves co-stimulatory molecules and the release of cytokines. This triggers B cell proliferation and the secretion of antibodies (Parker, 1993). Cytokines released by the activated T helper cells during this process, feedback to act in an autocrine manner inducing the T cell to proliferate. In addition, B cells also influence T cell differentiation through the secretion of polarising cytokines (Harris et al., 2000).

## **1.3 Cutaneous immune system**

The skin is the largest organ in the body and one of its main functions is to act as a physical barrier to protect the internal organs and tissues within the body. Originally thought as a passive barrier, the skin is highly equipped with immunological mechanisms to be the body's first line of defence against infection and tissue injury (Elias, 2007).

### **1.3.1 *Structure of the skin***

The skin is composed of many epithelial layers and is divided into distinct compartments, which contain various cell types within it. In humans, the skin is composed of three main compartments, the epidermis, the dermis and the hypodermis whereas mice have two main compartments, the epidermis and the dermis. The epidermis is the outer layer of the skin, consisting of many layers of stratified squamous epithelial cells. The epidermis is subdivided into five layers, from the deepest layer to outermost layer, stratum basale (basal cell layer), stratum spinosum (prickle cell layer), stratum granulosum (granular cell layer), stratum lucidum and finally the stratum corneum. It is of note that murine skin contains less cell layers of keratinocytes than human epidermis, resulting in murine skin having a thinner epidermis in comparison to human epidermis. The structure of murine skin is shown in Figure 1.2.

The epidermis of both human and mouse skin constantly renews itself in a process known as tissue homeostasis. This maintenance of tissue homeostasis is

driven by stem cells, which replace cells that are lost through normal differentiation or cell death due to tissue injury (Blanpain et al., 2007). The major cells of the epidermis are keratinocytes, which undergo terminal differentiation regularly to maintain homeostasis. Keratinocytes within the stratum basale, known as basal keratinocytes undergo differentiation whilst gradually moving outwards through each layer, changing shape and the types of structural proteins they express. Within the basal layer, keratinocytes express keratin 5 and keratin 14 (K5 and K14) but as these cells differentiate and enter the spinosum layer, the expression of K5 and K14 is downregulated and other keratin proteins, K1 and K10 are expressed (Blanpain and Fuchs, 2009). Upon reaching the stratum corneum, the cells within this layer are known as corneocytes, which are derived from dead keratinocytes, which begin to shed off the skin surface. The stratum corneum is an important layer as this prevents the skin from dehydration and prevents toxic agents from entering the skin (Proksch et al., 2008). Other cells within the epidermis are melanocytes, which produce melanin responsible for the pigmentation of skin, which are located within the basal layer of the epidermis. Langerhans cells are specialised dendritic cells that reside within the epidermis and merkel cells are associated with sensory nerve endings.

Underneath the epidermis connected by the basement membrane (basal lamina), the dermis consists of connective tissue. The dermis contains many cell types alongside hair follicles, sweat glands, sebaceous glands, blood vessels, lymphatic vessels and sensory nerves. Underlying the dermis in humans is the hypodermis layer, consisting of a layer of subcutaneous fat, helping to insulate the body.

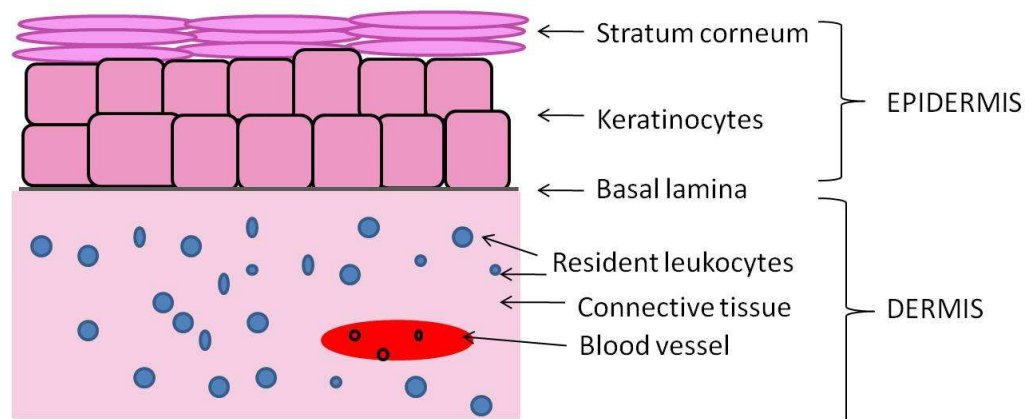


**Figure 1-2. The structure and layers within murine skin.**

The skin is one of the largest organs within the body and contains many layers within it. The outer layer, known as the epidermis, contains cell layers composed of keratinocytes. The compartment underneath the epidermis is the dermis and contains connective tissues and blood vessels.

### **1.3.2 Immune response within the skin**

Bos and Kapsenberg first proposed the concept of the ‘skin immune system’ in 1986, in which both epithelial and immune cells were associated with a role in the cutaneous immune response. The main cells involved are keratinocytes and Langerhans cells within the epidermis, whilst within the dermis, mast cells, dermal dendritic cells and T cells are key players (Bos and Kapsenberg, 1986, Kupper and Fuhlbrigge, 2004). Their main function is to alert the innate immune system when the skin is disturbed by trauma, ultraviolet radiation or pathogens.

Originally, keratinocytes were considered as only being required for the structural component of the skin but are increasingly being considered important participants in the cutaneous immune response. Keratinocytes constitutively produce antibiotic peptides to kill microbial pathogens that enter the skin (Wiedow et al., 1998). Additionally, injury or infection results in the production of  $\beta$ -defensins and cathelicidins, both antimicrobial peptides, by keratinocytes (Harder et al., 1997, Dorschner et al., 2001). Keratinocytes have the ability to recognise PAMPs (see 1.2.1.1) due to their expression of various Toll-like receptors (Kollisch et al., 2005). Keratinocyte TLRs binding to PAMPs results in the production of various immunological agents, including cytokines (see 1.4.1), chemokines (see 1.5) and antimicrobial peptides. TLRs confirmed to be expressed on the human keratinocyte cell surface include TLR1, TLR2, TLR4 and

TLR5 as well as endosomal TLR3 and TLR9 (Lebre et al., 2007). Keratinocytes express NLRs, such as NLRP3, which can recognise PAMPs or DAMPs present in the cytoplasm (Feldmeyer et al., 2007). Various cytokines are released from keratinocytes after stimulation with endotoxin and ultraviolet light, notably TNF $\alpha$ , IL-1 and IL-6 (Kock et al., 1990, Petit-Frere et al., 1998). Indeed, IL-1 $\beta$  secretion from human keratinocytes induced by ultraviolet irradiation is mediated by NLRP3 and activation of the inflammasome complex (Feldmeyer et al., 2007). These cytokines play a role in activating other resident immune cells and upregulate the expression of adhesion molecules on the endothelium, which in turn recruits more leukocytes from the vasculature into the skin (see 1.4.1). Additionally, keratinocytes are capable of stimulating Langerhans cells and T cells of the adaptive immune system. In response to a TLR9 ligand, keratinocytes produce cytokines which enhance the antigen presenting ability of Langerhans cells (Sugita et al., 2007). Another study has suggested that keratinocytes can induce functional responses in memory T cells by processing and presenting peptides to antigen-experienced T cells resulting in T cell cytokine production (Black et al., 2007).

Langerhans cells are the subset of dendritic cells that reside within the epidermis and are characterised by the presence of Birbeck granules (rod-shaped organelles within their cytoplasm) and expression of Langerin in their membrane (Valladeau et al., 2000). Langerhans cells are derived from CD34<sup>+</sup> haematopoietic progenitor cells during haemopoiesis (see 1.1). These DC progenitors then differentiate into either of two alternative DC subsets; one expresses cutaneous lymphocyte-associated antigen (CLA) and subsequently differentiates into a CD11c<sup>+</sup>CD1a<sup>+</sup> cell, the alternative lacks CLA and differentiates into a CD11c<sup>+</sup> CD1a<sup>-</sup> cell (Ito et al., 1999, Strunk et al., 1997). The CD11c<sup>+</sup>CD1a<sup>+</sup> population migrate to the epidermis and become Langerhans cells whilst the CLA<sup>-</sup> population become interstitial DCs, of which a subpopulation of these are dermal DCs found in the dermis of the skin. Langerhans cells express TLR2, TLR4 and TLR5 whereas dermal DCs express TLR3 and TLR4 and as a result they secrete different cytokines in response to specific stimulation (Rozis et al., 2008). Both subsets can capture and process antigen (Nestle et al., 1998). Recent data suggests that dermal DCs and Langerhans cells drain to the lymph nodes but only dermal DCs induce proliferation of T cells (Fukunaga et al., 2008). The migration of DCs from the skin through the afferent lymphatics to the

skin draining lymph nodes is mediated by the surface expression of chemokine receptors including CCR7 (see 1.5.3.2). In the lymph nodes, DCs will present antigen to T and B cells, which will then migrate to the skin and eliminate the trigger causing the response.

Normal healthy skin contains twice as many T cells than there are in the blood and the majority are skin-homing memory T cells (Clark et al., 2006). Within the population of T cells, a subset known as intraepithelial lymphocytes (IELs) are associated with epithelial and mucosal tissues. IELs express TCRs composed of  $\gamma$  and  $\delta$  chains ( $\gamma\delta$  T cells) whereas other T cells express an  $\alpha\beta$  TCR ( $\alpha\beta$  T cells) and these are predominately found in the blood and lymphatics (Girardi and Hayday, 2005). In mice, a proportion of  $\gamma\delta$  IELs are localised in the skin and are termed dendritic epidermal T cells (DETCs). These cells are the first T cells to develop in mice with limited diversity and they express a canonical V $\gamma$ 5V $\delta$ 1 TCR (Asarnow et al., 1988). Although no equivalent population has been found in human skin,  $\gamma\delta$  T cells with limited diversity have been discovered in the human dermis, which are distinct from peripheral blood  $\gamma\delta$  T cell populations (Holtmeier et al., 2001). DETCs can be activated by stressed, damaged or transformed keratinocytes (Havran et al., 1991). Studies have shown that DETCs play a role in keratinocyte homeostasis. DETCs constitutively express insulin like growth factor-1 (IGF-1) but increased levels are released upon stimulation and this in turn promotes keratinocyte survival (Boismenu and Havran, 1994, Sharp et al., 2005). *In vivo*, increased numbers of keratinocytes were found to be undergoing apoptosis in mice lacking DETCs (Sharp et al., 2005). Additionally, by culturing DETCs with skin from TCR $\delta^{-/-}$  mice (lack DETCs), Sharp *et al.*, demonstrated that DETCs can promote keratinocyte survival by the production of IGF-1 (Sharp et al., 2005). A role for IGF-1 in skin homeostasis has been established by the overexpression of IGF-1 *in vivo*, which resulted in epidermal thickening (Bol et al., 1997) whilst mice lacking IGF-1R have a thinner, disrupted epidermis (Liu et al., 1993) as a consequence of decreased proliferation and accelerated rate of differentiation in keratinocytes (Sadagurski et al., 2006). In addition, DETCs play a role in maintaining epidermal integrity and barrier function in response to environmental challenges (Girardi et al., 2006). Other studies have shown that DETCs play a role in promoting wound healing and protecting against inflammatory responses. Wound healing was found to be delayed in TCR $\delta^{-/-}$  mice compared to wild-type controls (Jameson et al., 2002). In the same study, the

delay in wound closure was rescued by activated DETCs or keratinocyte growth factor-1 (Jameson et al., 2002), which had previously been shown to be produced by DETCs *in vitro* upon activation (Boismenu and Havran, 1994). Girardi *et al.*, demonstrated a role for DETCs in regulating the inflammatory response by showing that DETCs can downregulate spontaneous cutaneous inflammation in  $\text{TCR}\delta^{-/-}$  mice (Girardi et al., 2002). Moreover, microarray data showed epidermal cells from  $\text{TCR}\delta^{-/-}$  mice have increased expression of various inflammatory genes, such as IL-1 $\beta$  and chemokines (Girardi et al., 2006). A mechanism for the DETC regulation of cutaneous inflammation is that DETCs induce protein expression of hyaluronan, which allows macrophage infiltration into the damaged tissue to facilitate wound repair (Jameson et al., 2005).

## 1.4 Acute inflammation

Acute inflammation is a normal physiological response triggered by infection or tissue damage. Resident cells within the tissue, such as epithelial cells, macrophages or mast cells, trigger the release of various inflammatory mediators, including cytokines (see 1.4.1), chemokines (see 1.5) and vasodilative amines upon stimulation by agents suggestive of infection or tissue damage. Acute inflammation is characterised by the infiltration of leukocytes controlled by chemokines (discussed in detail in 1.5.3.1), in which initially neutrophils, then 24 to 48hrs later, mononuclear cells dominate (Medzhitov, 2008). Additionally, increased blood flow and vascular permeability, mediated by histamine results in the heat, redness and swelling associated with inflammation (Maintz and Novak, 2007).

### 1.4.1 Cytokines in inflammation

Cytokines allow one cell to mediate effects on cells at a distance, on neighbouring cells, or even on itself. When the immune system is insulted, cells of the innate and adaptive immune system can secrete and detect cytokines, which are involved in many important biological processes, including inflammation (Vilcek and Feldmann, 2004).

## Tumour necrosis factor

One family of cytokines, known as the tumour necrosis factor (TNF) superfamily can mediate various biological responses. One member, TNF $\alpha$ , is mainly produced by activated macrophages but can also be released by other types of leukocytes and it plays an important role in host defence (Medzhitov and Janeway, 2000). TNF $\alpha$  is produced in a pro-form as a 26kDa transmembrane protein arranged as a homotrimer (Kriegler et al., 1988, Tang et al., 1996). This membrane form can be cleaved by TNF- $\alpha$  converting enzyme (TACE) to release soluble TNF (Black et al., 1997). TNF $\alpha$  can bind two membrane receptors, TNFR1 (p55) or TNFR2 (p75), which are members of the TNF receptor superfamily (Locksley et al., 2001). Signalling through TNFR1 and TNFR2 can lead to the activation of transcription factors, NF- $\kappa$ B or activating protein-1 (AP-1), which can promote cell survival and inflammation, or caspase-induced cell death (Baud and Karin, 2001). The inflammatory response is mainly coordinated through NF- $\kappa$ B, resulting in increased transcription of various genes, including those triggering the cytokine cascade by producing IL-1 $\beta$ , IL-6, more TNF $\alpha$ , chemokines (see 1.5) and adhesion molecules (Bonizzi and Karin, 2004).

Tumour necrosis factor is a key mediator in inflammation and its overexpression can result in many chronic inflammatory diseases and autoimmune diseases (Kollias et al., 1999). The interest in pro-inflammatory cytokines started when pro-inflammatory cytokines were detected in biopsy samples from rheumatoid arthritis (RA) patients, which illustrated their importance in joint inflammation (Feldmann and Maini, 1999). Studies using animal models of arthritis indicated TNF $\alpha$  as a key mediator of the disease, as anti-TNF treatment ameliorated collagen-induced arthritis (Piguet et al., 1992, Williams et al., 1992) which is an accepted murine model of RA (see 1.4.3.3). Additionally, it was discovered that overexpression of human TNF $\alpha$  (hTNF $\alpha$ ) in mice resulted in a spontaneous arthritis (Keffer et al., 1991). Butler *et al.*, backcrossed hTNF $\alpha$  transgenic mice onto an arthritis susceptible DBA/1 background and the expected elevated levels of human TNF $\alpha$  were accompanied by increased IL-1 $\beta$  and IL-6 levels in the joints of these mice (Butler et al., 1997). As a result, TNF $\alpha$  in particular and other cytokines have been targeted for therapeutic use in RA and other inflammatory diseases. This is discussed in more detail in 1.4.4.

## IL-1 family

Members of the interleukin-1 (IL-1) family are produced by macrophages, activated Th1 cells, epithelial and endothelial cells. The IL-1 family is composed of 11 members including IL-1 $\alpha$ , IL-1 $\beta$ , IL-1 receptor antagonist (IL-1Ra), IL-33 and several new members, resulting in the proposal of a new terminology, IL-1F1 through to IL-1F11 (Sims et al., 2001). Like TNF, IL-1 $\alpha$  and IL-1 $\beta$  exist in precursor forms and whilst IL-1 $\alpha$  is active in its precursor (Kaplanski et al., 1994) and mature form, IL-1 $\beta$  secretion is dependent on cleavage by IL-1 $\beta$  converting enzyme (ICE) also known as caspase 1 (Thornberry et al., 1992). Notably, for the secretion of IL-1 $\beta$  from monocytes and macrophages, stimulation by adenosine triphosphate (ATP) is required, which then activates the P2x7 receptor (Ferrari et al., 2006) and this subsequently triggers the formation of active caspase 1. Both IL-1 $\alpha$  and IL-1 $\beta$  can bind IL-1 receptor type I (IL-1RI) and IL-1R type II, however only IL-1RI is able to initiate signal transduction (Sims et al., 1993) which requires IL-1R accessory protein in order to do so (Cullinan et al., 1998) whereas IL-1RII acts as a decoy receptor (Colotta et al., 1993).

IL-1 $\beta$  induces endothelial cells to upregulate the expression of adhesion molecules involved in leukocyte binding and so indirectly recruits leukocytes to sites of inflammation (Wang et al., 1995). IL-1 $\beta$ , like TNF, can induce fever by acting on the hypothalamus and it can also induce the synthesis of acute phase proteins, a response impaired in IL-1 $\beta$  deficient mice (Zheng et al., 1995). Additionally, IL-1 results in the production of other cytokines such as IL-6 which is also involved in the inflammatory response (Dinarello, 1996). Membrane IL-1 $\alpha$  has been shown to play a role in lipid-mediated inflammation as IL-1 $\alpha$  deficient mice demonstrated reduced lesion size in an atherogenesis model induced by high cholesterol (Kamari et al., 2007). Within the interleukin-1 family, an endogenous antagonist exists, IL-1Ra can block the action of IL-1 by binding to IL-1RI, therefore preventing the activity of IL-1 (Arend, 1991). Mice deficient in IL-1Ra develop spontaneous diseases such as arthritis (Horai et al., 2000).

## IL-6

IL-6 was originally identified as a substance released by T lymphocytes which induced B lymphocytes to produce antibodies (Hirano et al., 1986). IL-6, is now known to mediate various biological functions including the activation of T and B cells, macrophages, osteoclasts (bone absorbing cells) and the proliferation of keratinocytes as well as having effects on haemopoiesis (Kishimoto, 2005). IL-6 exerts its effects by binding to the IL-6 receptor which then associates with glycoprotein 130 (gp130), a signal transducer protein (Taga et al., 1989). As well as a membrane bound IL-6R, a natural soluble form of IL-6R (sIL-6R) can also be produced by shedding from the cell surface or alternatively from spliced mRNA (Lust et al., 1992, Matthews et al., 2003). Soluble IL-6R along with IL-6 can stimulate cells that express gp130 but do not express membrane bound IL-6R (Mackiewicz et al., 1992) and this process is known as trans-signalling (Rose-John and Heinrich, 1994).

In the context of inflammation, IL-6 plays a role in stimulating endothelial cells to upregulate their expression of the chemokine, CCL2 (see 1.5) and it therefore plays a role in recruiting leukocytes to sites of inflammation (Romano et al., 1997). Illustrating the role of IL-6 in inflammation, IL-6 deficient mice were found to be resistant or to have reduced severity to experimental induced arthritis and collagen induced arthritis respectively (Boe et al., 1999, Sasai et al., 1999). In addition, Nowell *et al.*, demonstrated that in an experimental induced model of arthritis, it is sIL-6R which directs the IL-6 activity and this can be blocked by exogenous soluble glycoprotein 130 (Nowell et al., 2003). Indeed, elevated levels of IL-6 and sIL-6R have been documented in both rheumatoid arthritis and Crohn's disease (Mitsuyama et al., 2006, Robak et al., 1998). This has subsequently led to the therapeutic targeting of IL-6, in which one antibody, Tocilizumab, is currently subject to clinical trials (see 1.4.4).

### **1.4.2 Resolution of inflammation**

Normally the acute inflammatory response is followed by resolution of inflammation and tissue repair, through the removal of leukocytes and debris at the inflamed site, resulting in tissue homeostasis. The mechanisms involved have been described in three phases; 1) leukocytes migrate to the site containing the

stimuli to fight and remove it 2) cell clearance occurs and 3) the site where the inflammatory response took place returns back to its normal state (Serhan et al., 2007). The resolution of inflammation was thought to be a passive process but in recent years, new cellular and molecular mechanisms for the resolution phase of inflammation have been discovered. These mechanisms involve families of lipid mediators, known as lipoxins, resolvins and protectins.

Lipoxins were the first to be discovered and are derived from Arachidonic Acid (AA) present within the cell membrane. It was discovered that during acute inflammation prostaglandins, especially prostaglandin E<sub>2</sub> (PGE<sub>2</sub>), also derived from AA can encourage the conversion of a class of molecules known as leukotrienes to lipoxins, which promote resolution (Levy et al., 2001). Resolvins and protectins are derived from omega-3-polyunsaturated fatty acid, known as Eicosapentanoic Acid and Docosahexanoic acid. Resolvins are split into two groups; the Resolvin E series and Resolvin D series, named according to the fatty acid they are derived from. Resolvin E series are derived from Eicosapentanoic acid and the D series are generated from Docosahexanoic acid. Protectins are also derived from Docosahexanoic acid (Serhan et al., 2002). Lipoxins A<sub>4</sub> and B<sub>4</sub> as well as Resolvin E<sub>1</sub> mediate the first mechanisms involved in resolving inflammation. They are capable of preventing neutrophils from migrating across the vascular endothelium into the tissues (Colgan et al., 1993, Papayianni et al., 1996, Serhan et al., 2000). Lipoxin A<sub>4</sub> and Resolvin E<sub>1</sub> can inhibit IL-12 production from dendritic cells (Aliberti et al., 2002, Arita et al., 2005) therefore preventing activation of T cells in the area. Protectin D<sub>1</sub> inhibits the production of TNF $\alpha$  and IFN $\gamma$  from stimulated T cells and induces T cell apoptosis (Ariel et al., 2005). Consequently, protectin D<sub>1</sub> limits the activation of leukocytes and causes T cell death. Lipoxin A<sub>4</sub>, Resolvin E<sub>1</sub> and Protectin D<sub>1</sub> can stimulate macrophages to take-up neutrophils by phagocytosis (Godson et al., 2000, Schwab et al., 2007) therefore by removing apoptotic cells, cell clearance occurs. Macrophages then leave the site of inflammation via the draining lymph node allowing the tissue to return to normal (Bellingan et al., 1996).

### **1.4.3 Chronic inflammation**

When acute inflammation persists or complete resolution does not occur, the beneficial aspect of inflammation is lost and inflammation becomes chronic. This can last days, months or even years and can result in tissue damage. The cell infiltrate changes, leukocytes accumulate with increased numbers of adaptive immune cells. Chronic inflammation results in the development of a wide variety of inflammatory diseases, influenced by both genetic predisposition and environmental factors.

#### **1.4.3.1 Psoriasis**

Psoriasis is an inflammatory skin disease which is prevalent worldwide and affects 2-3% of the population in the UK (Smith and Barker, 2006). Psoriasis is a disease mediated by components of the immune system with evidence of genetic predisposition to the disease (Bowcock and Krueger, 2005). Clinical symptoms of psoriasis can appear in a variety of ways depending on location, severity and activity of the disease.

##### **Clinical spectrum of psoriasis**

Psoriasis is a recurring inflammatory disease with a wide clinical spectrum including five types of psoriasis, summarised in Table 1.1 (as reviewed by Naldi and Gambini, 2007). Psoriatic lesions are generally characterised by erythematous plaques covered with silvery scales surrounded by a distinct border, and the skin may itch or bleed more easily. The most common type of psoriasis is psoriasis vulgaris, also known as plaque psoriasis. Guttate psoriasis is common in children or young adults after streptococcal infection (Telfer et al., 1992, Gudjonsson et al., 2003). Pustular types of psoriasis are rarer than the non-pustular forms however, both can progress to psoriatic erythroderma, in which active psoriasis involves the whole skin or near total involvement affecting the whole body. In some psoriasis patients, physical trauma to the skin can trigger psoriatic lesions, known as the Koebner phenomenon (Weiss et al., 2002).

<b>Type</b>	<b>Clinical presentation of lesion</b>	<b>Location</b>
<b>Psoriasis Vulgaris</b>	<b>Red sharply defined areas covered by shiny scales</b>	<b>Elbows, knees, lower back and scalp</b>
<b>Guttate Psoriasis</b>	<b>Small lesions</b>	<b>Trunk and extremities</b>
<b>Inverse Psoriasis</b>	<b>Red with shiny plaques with no scales</b>	<b>Scalp, face and neck</b>
<b>Generalised Pustular Psoriasis</b>	<b>Red plaques and small pustules</b>	<b>Various areas</b>
<b>Localised Pustular Psoriasis</b>		
i) <b>Palmoplantar pustulosis</b>	<b>Small pustules</b>	<b>Soles of feet and palms</b>
ii) <b>Acrodermatitis continua</b>	<b>Small pustules</b>	<b>Tips of fingers and toes</b>

Table 1-1. Clinical spectrum of psoriasis

Five different types of psoriasis occur and the location and presentation of the psoriatic lesions vary in each type.

### **Pathological changes in psoriasis**

Within psoriatic skin, pathological changes occur and the lesions contain common histological hallmark features. Within fully developed plaques, hallmark features are; epidermal hyperplasia (increased number of cells within the epidermal compartment), hyperkeratosis, (overgrowth of the corneous layer of the skin), infiltration of immune cells, angiogenesis and epidermal thickening caused by increased keratinocyte proliferation (Murphy et al., 2007).

### **Immunopathogenesis of psoriasis**

Originally, the pathology of psoriasis was proposed to be mediated by keratinocytes, due to abnormalities in keratinocyte proliferation compared to normal skin (Weinstein et al., 1984). By the late 1970's, T cells were assumed to be the main mediators driving the disease. Consistent with this, when cyclosporin A (a drug that inhibits T cell activation) was given to a transplant patient, clearance of the patients psoriasis occurred (Mueller and Herrmann, 1979). Further studies with targeted therapy against activated T cells confirmed the role of T cells in the pathogenesis of psoriasis (Nicolas et al., 1991). Studies examining clonality of the T cell receptor have shown that infiltrating T cells in psoriatic plaques express a highly restricted TCR repertoire indicating oligoclonal expansion (Lin et al., 2001b). This suggests that a common antigen is present that drives the pathogenic T cell response in psoriasis (Prinz et al., 1999). One

such example could be an antigen derived from streptococcal infection which can precede type 1 psoriasis, which is characterised by early manifestation of the disease, i.e., under 40 years of age (Weisenseel et al., 2002). Additionally, a study by Vollmer *et al.*, has shown that the same T cell receptor pattern dominates in repeated flares of psoriasis (Vollmer et al., 2001). Although it has also been suggested that regulatory T cells are dysfunctional resulting in uncontrolled T cell activation (Sugiyama et al., 2005).

Characterisation of T cells within psoriatic lesions shows that they belong to the Th1 subset and produce type 1 cytokines including TNF $\alpha$ , IFN $\gamma$  and IL-2 (Austin et al., 1999, Schlaak et al., 1994). As a result, psoriasis has been classified as Th1-mediated disease (Lew et al., 2004). TNF $\alpha$ , in particular is implicated as an important mediator as it is central to the presentation of spontaneous psoriasis in a murine model (Boyman et al., 2004). Additionally the study by Boyman *et al.*, illustrated that resident populations of T cells and DCs are able to induce psoriasis, shown by grafting non-lesional human skin from psoriasis patients to immunodeficient AGR129 mice (these mice are deficient in both type 1 and type II IFN receptors and for the recombinase activating gene 2).

There is also evidence of the innate immune system being dysregulated in psoriasis (Bos et al., 2005). IFN $\alpha$  released from plasmacytoid DCs (see 1.2.1.3) is able to drive T cell proliferation and development of the disease (Nestle et al., 2005). Plasmacytoid dendritic cells can be activated by environmental TLR agonists (see 1.2.1.1), heat shock proteins produced by damaged cells (see 1.2.1.2) or even anti-microbial peptides produced by keratinocytes (Buchau and Gallo, 2007). In addition, *in vivo* models have implicated macrophages as having a pathogenic role in the disease (Stratis et al., 2006, Wang et al., 2006).

A central role for pro-inflammatory cytokines within psoriasis was proposed over 15 years ago (Nickoloff, 1991). Indeed the levels of IL-6 was discovered to be elevated in psoriatic plaques and was found to promote keratinocyte proliferation *in vitro* (Grossman et al., 1989). Therefore, the altered proliferation of keratinocytes was thought to be a consequence of the inflammatory response driven by cytokines. *In vitro* studies have shown exposure to TNF $\alpha$  and IL-1 $\beta$  induces changes to keratinocytes, which are observed in psoriasis (Wei et al., 1999). More recently described cytokines such as IL-15, IL-

IL-19 and IL-20 are present in psoriatic lesions and play a role in promoting keratinocyte survival and inhibiting keratinocyte apoptosis (Ruckert et al., 2000, Wei et al., 2005). To determine the role of single cytokines, transgenic mice expressing cytokines in basal keratinocytes were studied. In mice overexpressing IL-6, no psoriasis phenotype was seen and no effect on keratinocyte differentiation or proliferation occurred (Turksen et al., 1992). However, when IL-1 $\alpha$  was overexpressed in a similar manner, inflammatory lesions were observed along with hyperkeratosis (Groves et al., 1995). Of the several new IL-1 family members that have been described, one, IL-1F6, when overexpressed in the mouse skin resulted in a phenotype of hyperkeratosis, accumulation of inflammatory cell infiltrate and increased levels of cytokines and chemokines (Blumberg et al., 2007). The same study found that IL-1F5 was antagonistic of the effects and therefore the balance between IL-1F5 and IL-1F6 plays a role in regulating skin inflammation (Blumberg et al., 2007).

Altered signal transduction and transcription pathways in epidermal keratinocytes have been suggested as an explanation for dysregulation of keratinocyte proliferation in psoriasis (McKenzie and Sabin, 2003). Indeed, mice with specific deletion of the I kappa B kinase 2 (IKK2), which is a protein involved in the process of activating NF- $\kappa$ B, in the epidermis developed a psoriasis-like pathology mediated by TNF $\alpha$ , implicating a role for NF- $\kappa$ B in the pathology of the disease (Pasparakis et al., 2002). A study by Zenz *et al.*, targeted in the skin the deletion of specific transcription factors (junB and c-jun proteins) involved in activating transcription factor AP-1, which in turn is involved in the regulation of genes involved in keratinocyte differentiation (Eckert and Welter, 1996). Mice deficient of jun proteins within their keratinocytes demonstrated a psoriasis-like pathology (Zenz et al., 2005). Additionally, when JunB and jun were deleted in keratinocytes of recombinase activating gene 2 deficient mice or TNFR1 deficient mice, it was discovered that involvement of T and B cells, as well as TNF $\alpha$ , were required for development of a psoriasis phenotype (Zenz et al., 2005). Interestingly, this study illustrated that changes within the epidermis can have consequences for distant sites such as joints, as these mice also developed arthritic like lesions (Zenz et al., 2005). Signal transducers and activators of transcription are involved in conveying extracellular signals to the nucleus. One of these, STAT3 was found to be activated in the lesional skin of psoriatic patients (Sano et al., 2005). Transgenic

mice with constitutively active STAT3 expression in the epidermis developed spontaneous psoriatic lesions, which were dependent on activated T cells (Sano et al., 2005). These studies therefore indicate that the pathogenesis of psoriasis is mediated by cross-talk between immune cells and keratinocytes.

Recent emerging data has implicated IL-23 and Th17 cells (see 1.2.1.4) in the pathogenesis of psoriasis. IL-23 was implicated when it was shown that an injection of IL-23 into murine skin resulted in histopathological features similar to psoriasis (Chan et al., 2006). IL-23 is a heterodimeric protein composed of IL-23p19 and a subunit of IL-12, IL-12p40 (Oppmann et al., 2000). IL-23 binds and signals through the IL-23 receptor complex which is composed of IL-12RB1 (IL-12p40) and IL-23R subunits (Parham et al., 2002). In human psoriatic skin lesions, it was discovered that there was elevated mRNA levels of IL-23p19 and IL-12p40 compared to uninvolved skin (Lee et al., 2004). Additionally, it has been shown that polymorphisms in the genes that encode for IL-23R or IL-12p40 can contribute to the psoriasis phenotype and depending on the polymorphism in these genes, they can promote susceptibility or protection from developing psoriasis (Capon et al., 2007, Cargill et al., 2007, Nair et al., 2008). It is of note that STAT3 is the main mediator involved in IL-23 signalling (Yang et al., 2007). IL-23 can induce Th17 cells to produce Th17 cytokines (Aggarwal et al., 2003). Indeed IL-17 mRNA was detected in lesional psoriatic skin but not in uninvolved skin (Teunissen et al., 1998) and cells producing IL-17 have been isolated from the dermis of psoriatic lesions (Lowe et al., 2008). These studies therefore implicate Th17 and IL-17 (see 1.2.1.4) in the pathogenesis of psoriasis. Other Th17-type cytokines have also been implicated such as IL-22. A study by Zheng *et al.*, found that the inflammatory skin reaction induced by injections of IL-23 was dependent on IL-22 (Zheng et al., 2007). Consistent with this, human studies have revealed elevated levels of IL-22 mRNA and protein levels in psoriatic skin (Boniface et al., 2007). It is of note that IL-12, a Th1 cytokine and IL-23, both signal using IL-12p40 subunit and the studies by Chan *et al.*, and Zheng *et al.*, both illustrated that the injection of IL-12 is able to mediate skin inflammation although not to the same extent. Therefore, the studies to date suggest that the pathogenesis of psoriasis seems to involve interactions between keratinocytes and immune cells, which are mediated by Th1 and Th17 pathways.

### **1.4.3.2 Psoriatic arthritis**

Psoriatic arthritis (PsA) is an inflammatory joint disease (arthritis) that is associated with psoriasis. As with all types of arthritis, inflammation of the joints results in swelling, redness and pain. Psoriatic arthritis is recognised as being distinct from rheumatoid arthritis (see 1.4.3.3) by clinical features such as involvement of distal interphalangeal joints, asymmetrical joint distribution, dactylitis (inflammation of the whole digit) and inflammation at the site where the tendon enters the bone, known as enthesitis (Gladman et al., 2005). Diagnosis depends on the presentation pattern of joints affected along with a history of psoriasis in the patient, or the patient's family and can also involve radiographic imaging in which erosion of the joint and bony proliferations are characteristic of PsA (Kleinert et al., 2007).

### **1.4.3.3 Rheumatoid arthritis**

Rheumatoid arthritis (RA) is a chronic inflammatory disease that primarily causes swelling and destruction of joints and their surrounding tissue. RA is a disease where complications occur away from the joint and it is associated with increased mortality (Gabriel, 2008). RA affects approximately 1% of the population in the UK and affects more women than men in a ratio of 3:1 (Symmons et al., 2002). RA is described as an autoimmune condition because the immune system begins to attack host molecules. In many cases of RA, the immune system may produce antibodies that are specific for immunoglobulin class G (IgG) or citrullinated peptides (Schellekens et al., 1998). However, these can be present before the onset of disease. The trigger of clinical onset of disease is not entirely known, although genetic predisposition and environmental components are high risk factors. For example, RA is associated with certain alleles of HLA DR4 and smoking is implicated as an environmental risk factor in these individuals in the development of the disease (Klareskog et al., 2006).

The clinical features of rheumatoid arthritis are presentation with stiffness and inflammation in several joints in a symmetrical pattern. Pathologically, the lining of the synovium becomes inflamed (synovitis) and synovial hyperplasia occurs due to increased numbers of leukocytes, including T and B cells infiltrating the synovium and proliferation of fibroblast-like synoviocytes

(Sweeney and Firestein, 2004). The synovium begins to invade the cartilage and forms a mass of tissue called the pannus. As disease progresses, the pannus begins to cause damage to the cartilage and erosion of the bone which can lead to joint destruction and severe disability (Sweeney and Firestein, 2004). Increased understanding of the mechanisms involved has allowed therapeutics to be developed. The most successful of these so far is anti-TNF therapy (Feldmann, 2002).

#### **1.4.4 Treatment of inflammatory diseases**

Patients with chronic inflammatory diseases suffer a severely reduced quality of life. Fortunately research into understanding the pathogenesis of the diseases, and in particular, how the various immune mechanisms involved in the inflammatory response can cause damage has revealed several therapeutic targets for treatment. New therapies have targeted cytokines as these are thought to be the principle mediators involved in inflammation (see 1.4.1). Therapies that block TNF include Etanercept (a fusion protein), Infliximab (an anti-TNF $\alpha$  chimeric monoclonal antibody) and Adalimumab (a humanised monoclonal antibody against TNF). Targeting IL-1, Anakinra is an IL-1 receptor antagonist. Etanercept, Infliximab and Adalimumab have all been approved for use in psoriasis (Tzu and Kerdel, 2008) and RA. Infliximab is also used to treat Crohns disease (Mouser and Hyams, 1999) whilst use of Anakinra is restricted to treating RA (Bresnihan et al., 1998). A new emerging therapy is Tocilizumab, an anti-IL-6 receptor antibody which, in clinical trials has reduced disease activity in rheumatoid arthritis patients (Genovese et al., 2008). Although these therapies do improve clinical symptoms, one problem is that some patients do not respond well to these treatments. However, increased understanding of how the inflammatory process is mediated has led to targeting small molecules known as chemokines for alternative treatments (Pease and Williams, 2006).

### **1.5 Chemokines**

Chemokines are small peptide molecules (8-12kDa) that belong to a larger family, known as cytokines. This subset of cytokines have the ability to regulate cell migration either for homeostasis (see 1.5.3.2) or to direct leukocytes to sites of inflammation or infection (see 1.5.3.1) and are also known as

'chemotactic cytokines'. Due to their ability to guide the directional movement of leukocytes, chemokines are involved in multiple biological processes including lymphoid organ development, lymphocyte trafficking, angiogenesis and inflammation (Rot and von Andrian, 2004). The functional role of chemokines is discussed in detail in 1.5.3.

To date, approximately 50 chemokines have been discovered with a shared homology of between 20 and 80% in amino acid sequences (Borish and Steinke, 2003). To be classified as a chemokine, the molecule must have a characteristic biochemical hallmark (see 1.5.1) as well as the ability to regulate chemotaxis. Chemokines mediate their biological effects through their own family of chemokine receptors (see 1.5.2), which are part of a larger family of G Protein Coupled Receptors (Murphy et al., 2000). Chemokine ligands are often described as being 'promiscuous' because many bind to multiple different receptors. Usually a member of a certain chemokine family will only bind to members of the relevant chemokine receptor family (i.e., CCLs mostly bind CCRs).

### **1.5.1 Nomenclature**

Originally, upon identification, chemokines were given names reflecting their assumed function. However, due to the large number of chemokines discovered, and to prevent molecules being given multiple names, a systematic nomenclature system was established (Zlotnik and Yoshie, 2000).

The structural motif required to be classified as a chemokine, is a series of cysteine residues. Chemokines are named according to the precise nature of this cysteine sequence, followed by L (for ligand) and a number. The spacing and positioning of the first two N-terminal cysteine residues determines their chemokine classification. Following this classification, chemokines are divided into four subfamilies. A summary of the systematic classification is shown in Table 1-2.

#### **CC chemokine family**

Chemokines assigned to the CC family have the first two N-terminal cysteine residues adjacent to each other (CC). Twenty-eight members, CCL1 to CCL28, currently belong to the CC chemokine family making it the largest of the four

subgroups. The majority of the CC chemokines are regarded as being important in controlling the movement of cells to sites of inflammation. Examples of CC chemokines in this role include CCL3 and CCL5, which are involved in eosinophil, macrophage and mast cell recruitment to sites of inflammation (Conti and DiGiacchino, 2001) whereas CCL2, CCL7, CCL8 and CCL13 are all involved in controlling the migration of monocytes. Other CC chemokines, such as CCL19 and CCL21 function under homeostatic conditions and are important in coordinating the innate and the adaptive immune responses (see 1.5.3.2). CC chemokines tend to bind a subgroup of chemokine receptors referred to as CC chemokine receptors (CCRs; see 1.5.2)

### **CXC chemokine family**

The CXC subfamily, where any amino acid (X) separates the first two adjacent cysteine residues, is the second largest family with 16 members. CXCL8 (IL-8) is an important chemokine that recruits polymorphonuclear cells and is the most potent chemokine for neutrophils. Additionally, CXCL8 can trigger firm adhesion of monocytes to vascular endothelium *in vitro* (Gerszten et al., 1999). Mice however do not express CXCL8 but MIP-2 and KC are homologues of human CXC chemokines and both bind murine CXCR2 (Bozic et al., 1994). Another CXC chemokine, CXCL12, was discovered to have an important role in embryonic development and haemopoiesis (see 1.5.3.3).

Additionally, CXC chemokines can be further subdivided by the presence or absence of a specific motif, known as the ELR motif (see 1.5.3.4). The presence of the motif correlates with the ability of the chemokine to stimulate blood vessel formation, a process known as angiogenesis (see 1.5.3.4).

### **XC and CX3C chemokine family**

The XC subfamily contains the second and fourth conserved cysteine residues whilst in the CX3C subfamily, chemokines contain three amino acids between the first and second cysteine residue. Two members form the XC subfamily (XCL1 and XCL2) whilst the CX3C chemokine family only has one member, CX3CL1, also known as fractalkine (Bazan et al., 1997, Ono et al., 2003). CX3CL1 is one of two

chemokines that is membrane bound, the other is CXCL16 (Matloubian et al., 2000) whereas all the others are secreted.

### **Constitutive versus inflammatory chemokines**

Additionally, chemokines and their receptors can be broadly divided into constitutive or inflammatory subgroups. Homeostatic (constitutive) chemokines are present under normal conditions and have a role in basal leukocyte trafficking and lymphoid organ structure. CCL19, CCL21 and CCL25 are considered constitutive chemokines. Mice which are homozygous for the paucity of lymph node T cell (plt) mutation do not express CCL19 or CCL21 and this consequently results in T lymphocytes and dendritic cells being unable to home to the secondary lymphoid organs (Gunn et al., 1999). CXCR5 is a receptor which only binds one ligand, CXCL13 (Legler et al., 1998). CXCR5 deficient mice have defects in the development of B cell follicles within the spleen (Voigt et al., 2000).

In contrast, inflammatory (inducible) chemokines can be produced at very high levels upon stimulation with inflammatory agents. The genes for human inflammatory chemokines are mostly found on chromosome 17 for CC chemokines and inflammatory CXC chemokines are typically found on chromosome 4 (Murphy et al., 2000). Inflammatory chemokines, such as CCL2, CCL3 and CCL5, are produced by many different cell types and recruit leukocytes to sites of infection, inflammation or tissue injury. The chemokine receptor, CCR2, is regarded as an inflammatory receptor, which binds a subgroup of chemokines, previously named monocyte chemotactic proteins (MCPs 1-4), now known as CCL2, CCL7, CCL8 and CCL13 (Murphy et al., 2000). Inflammatory chemokines and their receptors tend to be more promiscuous than chemokines involved in basal trafficking and homing. However, some chemokines cannot be strictly classified as inflammatory or constitutive as they have the ability to function as both (Moser et al., 2004). A summary of inflammatory and constitutive chemokines is shown in Table 1-2.

### **1.5.2 Chemokine receptors**

Chemokine receptors are seven transmembrane spanning receptors, which are coupled to heterotrimeric GTP binding proteins. Chemokine receptor length

varies between 340 and 370 amino acid and most contain a DRYLAIV motif in the second intracellular loop, which is highly conserved (Murphy et al., 2000). The three dimensional structure of chemokine receptors is not known and current models are based on the three dimensional structure of another G-protein coupled receptor (GPCR) known as rhodopsin (Palczewski et al., 2000).

The chemokine receptors have a systematic classification system (Murphy et al., 2000), in which receptors are named according to the subfamily of chemokines they bind, followed by R (for receptor) and a number. This is summarised in Table 1-2.

### CC chemokine receptors

Currently the CCR subfamily consists of 10 receptors and all bind chemokines within the CC subfamily. CCR1 was the first CC chemokine receptor to be identified and is the receptor for multiple chemokines, which include CCL3, CCL5, CCL7 and CCL14 (Gao et al., 1997). CCR1 is expressed on monocytes, basophils, eosinophils, T and B lymphocytes. In mice lacking CCR1, neutrophils failed to migrate in response to CCL3 (Gao et al., 1997). Additionally, using a model of granuloma formation induced with *Schistosoma mansoni* eggs, the size of lung granuloma formation was reduced in CCR1 deficient mice and was also associated with an imbalance in Th1/Th2 cytokines (Gao et al., 1997). CCR1 knockout mice have also been shown to prolong allograft survival in corneal- and cardiac- transplants (Gao et al., 2000, Hamrah et al., 2007) as well as showing partial resistance to development of experimental autoimmune encephalomyelitis (Rottman et al., 2000).

CCR2 is predominantly expressed on monocytes but is also expressed on T cells and dendritic cells. Based on chemokine receptor expression, monocytes can be subdivided into two subsets, CCR2<sup>hi</sup> CX3CR1<sup>lo</sup> which migrate to sites of inflammation and a CCR2<sup>lo</sup> CX3CR1<sup>hi</sup> homeostatic subset (Geissmann et al., 2003). In a model of experimental peritoneal inflammation, mice lacking CCR2 were unable to recruit monocytes and macrophages to the peritoneum (Kurihara et al., 1997). It was also discovered, when mice deficient in CCR2 were crossed with apolipoprotein E (ApoE) null mice, that lack of CCR2 resulted in reduction of atherosclerotic lesions (Boring et al., 1998). In contrast, CCR2 is thought to be protective in a model of Alzheimer's disease. Mice deficient in CCR2 displayed

accelerated disease progression and reduced accumulation of microglia within the brain (El Khoury et al., 2007).

CCR3 is a chemokine receptor predominately expressed on eosinophils and its ligand CCL11 is a potent chemo-attractant and activator of this cell type (Elsner et al., 1998). Basophils, mast cells and Th2 cell subsets express CCR3 to a lesser extent and other ligands of CCR3 are CCL5, CCL7, CCL13, and CCL26 (Murphy et al., 2000). Due to the expression profile of CCR3 and the association of these cells with allergic disease, in particular asthma, CCR3 was thought to play a key role in these diseases. A study by Humbles *et al.*, showed that after allergen challenge, eosinophils were unable to migrate to the lungs in CCR3 deficient mice (Humbles et al., 2002). It was discovered that large numbers of eosinophils had accumulated beneath the blood vessels in the subendothelial space in CCR3 deficient mice (Humbles et al., 2002). Additionally, in a model of allergic skin inflammation, eosinophils failed to migrate to the skin in CCR3 knockout mice (Ma et al., 2002). Together these data suggest that CCR3 plays a key role in mediating eosinophil migration and subsequently allergic disease.

CCR4 is expressed on distinct subsets of T cells, such as Th2 and skin homing T cells (Bonecchi et al., 1998, Campbell et al., 1999). CCL17 and CCL22 are ligands which bind with high affinity to CCR4 (Imai et al., 1997, Imai et al., 1998). The contribution that CCR4 makes towards Th2 responses in the lung requires clarification since in a model of airway inflammation, which was Th2 dependent, no disrupted effects were seen in mice lacking CCR4 (Chvatchko et al., 2000). CCR4 is required in the homing of T cells to the skin (see 1.5.3.2).

CCL3, CCL4, CCL5 and CCL8 are all ligands for CCR5, which is a major co-receptor for HIV (see 1.5.4.1). Expression of CCR5 can be found on macrophages, dendritic cells and certain T cell subsets. CCR5 knockout mice infected with *Listeria monocytogenes* had reduced efficiency in clearing the infection and had impaired macrophage function (Zhou et al., 1998). CCR5 is also involved in T cell stimulation within the immunological synapse (Contento et al., 2008) and is thought to be protective against West Nile virus (see 1.5.4.1).

To date, only one ligand, CCL20, has been identified, which is able to bind CCR6 (Baba et al., 1997). Various subsets of T cells, in particular Th17 cells and immature dendritic cells express CCR6. Using CCR6 knockout mice, CCR6 was

discovered to be involved in the localisation of DCs, homeostasis of lymphocytes and the immune response within the gut (Cook et al., 2000). CCR6 is involved in controlling the migration of Th17 cells to the intestine and the regulation of effector T cell subsets (Wang et al., 2009). CCR6 has a pathological role in experimental autoimmune encephalomyelitis (EAE) in which CCR6 has been shown to be involved in the initiation of EAE by regulating the entry of Th17 cells into the central nervous system (Reboldi et al., 2009) and by controlling regulatory CD4<sup>+</sup> T cells (Villares et al., 2009).

Studies using CCR7 knockout mice confirmed the importance of CCR7 in lymphoid organ development as well as involvement in co-ordinating the innate and the adaptive immune response (see 1.5.3.2). CCR7 is a receptor for CCL19 and CCL21 and is constitutively expressed on T cells and mature DCs in the lymphoid organs (Forster et al., 1999). CCR7 plays a key role in mediating the trafficking of mature dendritic cells from peripheral tissues to the lymph node and the role of CCR7 is discussed in more detail in 1.5.3.2.

The role of CCR8 is not well-defined as studies involving this receptor are conflicting. CCR8 is the receptor for CCL1 and CCL16 and expression of CCR8 is predominantly on Th2 cells (Roos et al., 1997). A role for CCR8 in the functional Th2 response was implicated in the first study on CCR8 knockout mice. In the study, CCR8 knockout mice displayed a dysfunctional Th2 immune response, in which there was defective Th2 cytokine production and reduced eosinophil recruitment in an ovalbumin induced model of airway inflammation (Chensue et al., 2001). However, other studies have shown that absence of CCR8 did not affect Th2 cytokine response or eosinophilia in a murine model of allergic airway inflammation (Chung et al., 2003). In a model of ovalbumin induced allergic airway disease, CCR8 knockout mice developed pathological disease similar to wild-type mice and the absence of CCR8 did not affect the Th2 response in this model (Goya et al., 2003). Other studies have shown that CCR8 may have a negative impact on the immune response. In septic peritonitis, CCR8 knockout mice displayed an enhanced innate immune response to clear bacteria (Matsukawa et al., 2006). Additionally, in a model of asthma induced by fungal allergens, CCR8 knockout mice were able to clear the fungal material from the lung more rapidly than the wild-type (Buckland et al., 2007). These differences

may reflect the complexity of utilising distinct *in vivo* models to define the role of individual receptors.

CCR9 binds CCL25 which is expressed in the small intestine (Zaballos et al., 1999). Studies utilizing CCR9 deficient mice have demonstrated a role for CCR9 in regulating T cell development within the thymus and migration of  $\gamma\delta$  T cells to the small intestine (Uehara et al., 2002). As a homing receptor for the gut, CCR9 has been implicated in crohns disease (Papadakis et al., 2001) and also cancer (see 1.5.4.2).

Another CC chemokine receptor to which CCL27 and CCL28, have been shown to bind is CCR10 (Homey et al., 2000b, Wang et al., 2000). CCR10 is expressed on a subset of T cells, which home in a CCL27 dependent manner to the skin (see 1.5.3.2) and has been implicated in cutaneous diseases such as psoriasis (see 1.5.4.3) and cancer (see 1.5.4.2). Additionally, CCR10 is involved in directing the migration of IgA producing plasma cells towards CCL28 expressed in mucosal tissue (Kunkel et al., 2003).

### **CXC chemokine receptors**

To date, there are six chemokine receptors which belong to the CXC subfamily and are accordingly named CXCR1 through to CXCR6 (although see 1.6.3 for CXCR7). CXCR1 and CXCR2 are two closely related receptors with 77% homology and bind to CXCL8 in humans with high affinity. Both receptors are predominately expressed on human neutrophils (Doroshenko et al., 2002). CXCR1 can also bind CXCL6 whereas CXCL1 to CXCL7 can all bind to CXCR2. CXCR1 expression on human neutrophils is thought to be important for the clearance of urinary tract infection. Indeed, disease-associated polymorphisms in CXCR1 have been identified in children prone to the most severe form of urinary tract infection known as acute pyelonephritis (Lundstedt et al., 2007). In the same study, reduced expression of CXCR1 was found in the children prone to acute pyelonephritis (Lundstedt et al., 2007). Murine CXCR1 has been identified and shown to be a functional receptor but the exact role of murine CXCR1 is unknown (Fan et al., 2007). CXCR2 deficient mice displayed impaired neutrophil migration and CXCR2 is protective against *Toxoplasma gondii* infection (Del Rio et al., 2001). CXCR2 also plays a role in wound healing (see 1.5.3.4) and deletion

of CXCR2 slowed the progression of atherosclerosis in mice (Boisvert et al., 2000).

CXCR3 is highly expressed on activated lymphocytes, predominantly Th1 lymphocytes and CXCL9, CXCL10 and CXCL11 are ligands for CXCR3. In a model of acute cardiac allograft rejection, CXCR3 deficient mice were resistant to the development of rejection (Hancock et al., 2000) and CXCR3 has also been implicated in atherosclerosis, glomerulonephritis and multiple sclerosis (Lazzeri and Romagnani, 2005).

CXCR4 binds one ligand, CXCL12 (Nagasawa et al., 1999) and in mice, targeted deletion of CXCR4 is perinatally lethal showing an important role for CXCR4 in embryonic development and haemopoiesis (see 1.5.3.3). CXCR4, expressed on T lymphocytes, plays a role in the immunological synapse and is a major co-receptor for human immunodeficiency virus (see 1.5.4.1).

CXCR5, to date, only has one ligand which is CXCL13 (Legler et al., 1998). CXCR5 is expressed on B lymphocytes and plays a role in B cell migration and organisation of secondary lymphoid organs (see 1.5.3.2). The last of the CXC chemokine receptors discovered to date is CXCR6. One ligand, CXCL16, is known to bind CXCR6 which is expressed on T lymphocytes and has been shown to have a minor role in the entry of human immunodeficiency virus (HIV) to T lymphocytes (Matloubian et al., 2000).

### **CX3CR1 and XCR1**

CX3CR1 facilitates peripheral blood leukocyte migration and adhesion. In a model of atherosclerosis, reduced lesion size in ApoE and CX3CR1 double deficient mice was reported and thought to be mediated by CX3CR1 expression on macrophages (Combadiere et al., 2003) however impaired dendritic cell migration has also been reported (Liu et al., 2008).

Neutrophils and B cells express XCR1 which supports chemotaxis towards XCL1 (Huang et al., 2001). XCR1 has been implicated in rheumatoid arthritis as the receptor was found to be upregulated on mononuclear cells infiltrating the synovial tissue from joints of RA patients (Wang et al., 2004a). Within the RA synovium, XCL1 was produced by infiltrating T cells (Blaschke et al., 2003).

## Cell specific chemokine receptors

Each cell type expresses a certain 'set' of chemokine receptors, whose expression can be modulated over time by environmental stimuli. Additionally, chemokine receptors can distinguish between cell subsets, such as T cells. Naive T cells express CCR7 and, depending on the conditions during activation, CD4<sup>+</sup> naive T cells can differentiate into various effector subsets each with their own pattern of receptors. Th1 cells tend to express CXCR3, CXCR6 and CCR5 whilst CCR4 and CCR8 are typically expressed on Th2 cells (Syrbe et al., 1999). Th17 cells express CCR6 (Hirota et al., 2007b). Expression of CCR7 can also differentiate the subsets of memory T cells (Sallusto et al., 1999). Receptor expression can also change on cells under inflammatory conditions, for example on antigen presenting cells. This allows the cells to move from the site of inflammation to the lymph nodes (see 1.5.3.2). In addition, patterns of chemokine receptors also allow cells to home to certain tissues (see 1.5.3.2).

Cells can express various chemokine receptors and chemokines may have multiple target receptors (Mantovani, 1999). This means a single chemokine could enhance the infiltration of multiple cell types whilst other chemokines in the local environment affect different subsets of cells. Additionally, cells may be 'pulled' in opposing directions when surrounded by multiple chemokines. Also by having multiple receptors on cells, if one chemokine receptor or ligand is defective then the biological function can be achieved by other chemokine receptors, therefore creating redundancy within the system.

Systematic name	Chemokine receptor
CCL1	CCR8
CCL2	CCR2
CCL3	CCR1, CCR5
CCL3L1	CCR5
CCL4	CCR5
CCL5	CCR1, CCR3, CCR5
CCL6	
CCL7	CCR1, CCR2, CCR3
CCL8	CCR2, CCR3, CCR5
CCL9	
CCL10	
CCL11	CCR3
CCL12	CCR2
CCL13	CCR2, CCR3
CCL14	CCR1
CCL15	CCR1, CCR3
CCL16	CCR1
CCL17	CCR4
CCL18	
CCL19	CCR7
CCL20	CCR6
CCL21	CCR7
CCL22	CCR4
CCL23	CCR1
CCL24	CCR3
CCL25	CCR9
CCL26	CCR3
CCL27	CCR10
CCL28	CCR3, CCR10
CXCL1	CXCR1, CXCR2
CXCL2	CXCR2
CXCL3	CXCR2
CXCL4	CXCR3
CXCL5	CXCR2
CXCL6	CXCR1, CXCR2
CXCL7	CXCR2
CXCL8	CXCR1, CXCR2
CXCL9	CXCR3
CXCL10	CXCR3
CXCL11	CXCR3
CXCL12	CXCR4
CXCL13	CXCR5
CXCL14	
CXCL15	
CXCL16	CXCR6
CX3CL1	CX3CR1
XCL1	XCR1
XCL2	XCR1

**Table 1-2. Classification of chemokines and their receptors**

Chemokines are classified according to their subfamily, CC, CXC, CX3C or C and the receptors are classified according to the subfamily of chemokines that they bind. Chemokines can also be classified as inflammatory (red), constitutive (blue) or function as both (yellow). The receptors for some chemokines are not known (left blank) or the functions for chemokines are not known (white). Table is adapted from (Moser et al., 2004, Zlotnik and Yoshie, 2000).

### 1.5.2.1 Chemokine receptor signalling

Ligand binding to GPCRs catalyses the exchange of bound guanosine diphosphate (GDP) for guanosine triphosphate (GTP) in the  $\alpha$  subunit of the G-protein. Consequently, the G-protein dissociates into active  $\alpha$  and  $\beta\gamma$  subunits. The  $\alpha$  and  $\beta\gamma$  subunits can subsequently activate downstream intracellular signalling pathways or directly affect functional proteins depending on the  $G\alpha$  subtype, which has four main classes  $G_s$ ,  $G_i$ ,  $G_q/11$ ,  $G_{\alpha 12/13}$  and a recently discovered fifth class, known as  $G_v$  (Oka et al., 2009). Chemokine receptors are predominantly thought to couple to  $G_i$  proteins for chemotaxis as ligand induced signalling was suppressed with pertussis toxin, an inhibitor of  $G_i$  proteins (Thelen, 2001). However, an alternative signalling pathway which is dependent on  $G_i$  proteins and also  $G_q$  proteins is required for dendritic cell migration in response to inflammatory agents (Shi et al., 2007). Additionally, CXCR4 and CCR5 recruited to the immunological synapse of T cells were coupled to  $G_q$  and/or  $G_{11}$  protein and lost their ability to initiate chemotaxis (Molon et al., 2005). An essential step for cell migration is the release of the subunits and the regulation of cell migration is mediated by the  $\beta\gamma$  subunit (Neptune et al., 1999). The  $\beta\gamma$  subunits activate the membrane-associated enzymes phospholipase  $C\beta_2$  and phospholipase  $C\beta_3$  (Barr et al., 2000, Sankaran et al., 1998), which catalyse the cleavage of phosphatidylinositol-4, 5-bisphosphate leading to the formation of inositol-1, 4, 5-trisphosphate ( $IP_3$ ) and diacylglycerol (DAG). Increased levels of  $IP_3$  induce the release of calcium from intracellular vesicles resulting in a transient rise in the levels of free calcium within the cell. DAG activates protein kinase C. The  $\beta\gamma$  subunit also activates phosphatidylinositol 3 kinase  $\gamma$  (Stephens et al., 1994) leading to the activation of protein kinase B (Didichenko et al., 1996), which is important in inducing changes within the cell required for chemotaxis (Li et al., 2000). Signalling is terminated by GTP hydrolysis, allowing re-association of  $\alpha$  with the  $\beta\gamma$  subunit. Signalling results in a variety of cellular responses such as chemotaxis, adhesion, respiratory burst and degranulation depending on the cell type, ligand and the receptor present.

### 1.5.2.2 Chemokine receptor internalisation

Upon ligand binding, chemokine receptors may internalise into the cell in two ways, either by clathrin mediated endocytosis or by lipid raft/caveolae-

dependent internalisation (Venkatesan et al., 2003). Internalisation of a chemokine receptor can affect the response by the cell to chemokines.

In clathrin-mediated endocytosis, ligand binding results in G-protein coupled receptor kinases phosphorylating residues of the carboxy terminus and intracellular loops on chemokine receptors, resulting in the G-protein becoming uncoupled from the receptor (Ferguson, 2001). Phosphorylation allows two adapter molecules, adaptin-2 and  $\beta$ -arrestin to associate with the receptor, recruit clathrin, and form clathrin coated pits (Laporte et al., 1999). These pits form from the cell membrane wrapping round the receptor and pinch off from the membrane. The chemokine receptor is targeted for recycling back to the cell surface (to be exposed to ligand) or for degradation in the late endosomal compartment. Studies have shown that CXCR1 requires both  $\beta$ -arrestins and dynamin for endocytosis (Barlic et al., 1999) while CXCR4 also requires  $\beta$ -arrestin but not dynamin (Cheng et al., 2000).

There are reports that chemokine receptors can mediate receptor internalisation in a mechanism that does not involve clathrin; instead, they use lipid rafts or caveolae, which are cholesterol rich structures. Receptors enter a compartment known as a caveosome upon internalisation and fuse with endosomes which merge with the clathrin coated pathway (Sharma et al., 2003). Studies have shown that CCR5 uses the caveolae pathway by showing its colocalisation with a protein, known as caveolin 1, which is thought to be involved in stabilising the caveolae structure (Nguyen and Taub, 2002). However, CCR5 has also been shown to be dependent on clathrin mediated endocytosis (Signoret et al., 2005).

Regulation of receptor internalisation is controlled by a family of small GTPases, known as Rabs, which cycle between the inactive GDP bound and active GTP bound states. Rab GTPases localise to specific compartments within the cell. Rab4, Rab5 and Rab11 are known to associate with the early endosomal compartment (van der Sluijs et al., 1992, Sonnichsen et al., 2000). Rab11 also associates with the recycling compartment (Ullrich et al., 1996). *In vitro* studies examining internalisation of CXCR2 after stimulation using overexpression of dominant negative mutants of Rab5 and Rab11 prevented receptor internalisation and recycling respectively (Fan et al., 2003). Overall, both cell

type and the regulation process may determine how a cell can respond to subsequent ligand.

### **1.5.3 *Functions of chemokines and their receptors***

Chemokines are described as chemotactic because they are able to elicit directional cell movement, known as chemotaxis. Due to the ability of chemokines to influence cell migration, chemokines are involved in many roles within the immune system.

#### **1.5.3.1 Leukocyte migration**

Leukocyte extravasation is the movement of leukocytes from the circulation through the blood vessel walls into the tissues, which is regulated by the endothelium. In particular, chemokines trigger the arrest of leukocytes whilst rolling along the endothelium (Campbell et al., 1998). Leukocyte extravasation was initially characterised as a three-step cascade, involving leukocyte rolling, activation and arrest (Butcher, 1991) but is now viewed to have the additional steps of adhesion strengthening, intravascular crawling and transmigration (Ley et al., 2007).

The expression of adhesion molecules on endothelial cells, which play an important role in the rolling and arrest of leukocytes, are upregulated by inflammatory stimuli. A family of adhesion molecules known as selectins are involved in the process of leukocyte rolling along the endothelium. Resting endothelial cells store P-selectin within specialised secretory vesicles and activation of endothelial cells by histamine or cytokines results in the expression of P-selectin on the cell surface (Jones et al., 1993, Ley and Reutershan, 2006). In response to inflammatory cytokine binding, such as TNF $\alpha$  or IL-1, transcription occurs within the endothelial cell resulting in the expression of E-selectin (Ley and Reutershan, 2006, Gotsch et al., 1994). The interaction of selectins with their ligands present on leukocytes allows leukocytes to adhere to the endothelium. The speed of leukocyte rolling along the endothelium was found to be faster in mice deficient in E-selectin compared to the speed of leukocytes rolling in wild-type mice and demonstrated that E-selectin was required for slow rolling of leukocytes (Kunkel and Ley, 1996). To support cell adhesion, P-selectin

and L-selectin require shear stress and 'catch' bonds to make the interactions stronger (Lawrence et al., 1997, Yago et al., 2004). A second class of molecules, known as integrins, present on leukocytes also participate in rolling and firm adhesion of leukocytes to the endothelium. Slow rolling *in vivo* was shown to require  $\beta$ 2-integrins as well as E-selectin. A study by Dunne *et al.*, revealed that slow rolling of leukocytes required lymphocyte function associated antigen-1 (LFA-1) and macrophage antigen-1 (Dunne et al., 2002). Slow leukocyte rolling mediated by macrophage antigen-1 (MAC-1) was shown to bind intracellular adhesion molecule-1 (ICAM-1) present on the endothelium in order to do so (Dunne et al., 2003). Additionally recent evidence suggests E-selectin can induce LFA-1 on neutrophils into a structural conformation which has an intermediate affinity (Salas et al., 2004) for its ligand ICAM-1 on endothelial cells and allows for transient binding (Chesnutt et al., 2006). However, chemokines are the dominant activators of integrin-mediated adhesion between leukocytes and the endothelium.

Inflammatory cytokines stimulate endothelial cells to express chemokines on their surface. Additionally, platelets can also deposit CCL5 on the endothelium which then triggers the arrest of monocytes (von Hundelshausen et al., 2001). Most circulating leukocytes express their integrins in a low affinity state (Carman and Springer, 2003) and chemokines are capable of activating integrins into a high affinity state (Laudanna et al., 2002). Evidence from T cells suggest that chemokines, such as CXCL12 and CCL21, can increase the affinity of the LFA-1 integrin (Constantin et al., 2000) by inducing 'inside-out' signalling resulting in conformational changes (Shamri et al., 2005). In human monocytes, increased affinity in very late antigen-4 (VLA-4) binding of vascular cell adhesion molecule-1 involves conformational changes (Chan et al., 2001) and requires phospholipase C mediated calcium signalling to facilitate monocyte arrest (Hyduk et al., 2007). Once firm adhesion of these cells occurs, transmigration can then take place.

Transmigration (diapedesis) is a process where leukocytes cross the vascular wall, which is composed of endothelial cells connected by adhesive junctions, and the endothelial-cell basement membrane. Transmigration can be initiated by chemoattractants and shear stress signals (Cinamon et al., 2004). There is evidence that crawling along the endothelium is required for transmigration.

This has been shown for monocytes and neutrophils which are dependent on ICAM1 and MAC-1 present on the leukocyte (Schenkel et al., 2004, Phillipson et al., 2006). Diapedesis can occur in two ways, the paracellular route, which is the route most commonly used where the cells migrate between endothelial cells at their junctions, or transcellular where leukocytes go directly through a cell (Engelhardt and Wolburg, 2004).

Leukocytes transmigrating by the paracellular route require an increase in intracellular calcium levels within endothelial cells which has been proposed to be activated by crosslinking signals, such as ICAM-1 or soluble proteins from activated leukocytes (Etienne-Manneville et al., 2000, Muller, 2003). Increased intracellular levels of calcium results in the activation of myosin light chain kinase resulting in a conformational change in myosin II regulatory light chain and subsequently leading to the retraction of endothelial cells that might facilitate leukocyte passage (Hixenbaugh et al., 1997). Myosin light chain kinase mediates vascular permeability and was required for neutrophil transmigration in the lung (Xu et al., 2008). Proteins involved in the transmigration of leukocytes are platelet endothelial cell adhesion molecule 1 (Muller et al., 1993), CD99 (Schenkel et al., 2002), and a family of proteins known as junction adhesion molecules (JAMs), which are also members of the immunoglobulin superfamily (Bazzoni, 2003). Platelet endothelial cell adhesion molecule 1 (PECAM-1), CD99 and JAMs have homophilic interactions but additionally JAMs can also interact with integrins to facilitate leukocyte transmigration (Ostermann et al., 2002). PECAM-1 can translocate from intracellular vesicles within endothelial cells to endothelial junctions (Mamdouh et al., 2003). Blocking PECAM-1 with a soluble form of PECAM-1, which acts as a competitive inhibitor, has been shown to reduce transmigration by 90%, *in vivo* (Liao et al., 1997). To add to this, PECAM-1 deficient mice are still able to recruit leukocytes to sites of inflammation and additionally demonstrate there are PECAM-1 independent mechanisms for leukocyte transmigration (Duncan et al., 1999). Blocking CD99 reduced diapedesis of monocytes and neutrophils whilst blocking both CD99 and PECAM-1 resulted in an additive effect on monocytes and leukocyte migration (Lou et al., 2007, Schenkel et al., 2002). Junction adhesion molecules are present on epithelial cells and endothelial cells localised in the tight junction of cells and are present on various leukocytes. The first evidence for a functional role for JAMs *in vivo* was shown in an air pouch model of skin

inflammation (Martin-Padura et al., 1998). By blocking JAM-A with a monoclonal antibody, monocytes and neutrophil transmigration was reduced (Martin-Padura et al., 1998). Subsequent studies have found that JAM-A can bind in a homophilic manner between JAM-A on leukocytes and endothelial cells (Bazzoni et al., 2000). Additionally, JAM-A is also able to bind leukocyte integrin LFA-1 and this interaction was required for diapedesis of T cells and neutrophils (Ostermann et al., 2002). *In vitro* studies have revealed JAM-A is able to relocate from intracellular junctions to the surface of endothelial cells in response to stimulation with TNF $\alpha$  and IFN $\gamma$  (Ozaki et al., 1999). In addition to this, it has been shown at endothelial junctions that JAM-A co-localises with LFA-1 on projections of the neutrophil membrane, known as pseudopods (Shaw et al., 2004). JAM-B is able to bind VLA-4 but in order to do so, JAM-B has to bind to JAM-C present on the leukocyte first (Cunningham et al., 2002). JAM-B has been implicated in lymphocyte transmigration across high endothelial venules (HEV) where it is highly expressed (Johnson-Leger et al., 2002). As well as binding to JAM-B, JAM-C can bind leukocyte integrin MAC1 (Santoso et al., 2002). Overexpression of JAM-C in endothelial cells *in vivo* resulted in an influx of monocytes and granulocytes in a lung inflammation model and a specific JAM-C antibody blocked the increase in recruitment of cells (Aurrand-Lions et al., 2005) illustrating a role for JAM-C in the transmigration process.

The ability of leukocytes to penetrate endothelial cells by the transcellular route was first shown by neutrophils (Feng et al., 1998). Leukocytes travelling by the transcellular route also extend protrusive structures, termed podosomes, to break and invade the endothelial surface (Carman et al., 2007). The transcellular pathway is mediated by caveolin, a protein involved in endocytosis, and F-actin, a structural filament protein. It has been proposed that ligation of ICAM-1 leads to the translocation of ICAM-1 to caveolin and F-actin rich areas (Millan et al., 2006). Other endothelial membrane structures such as vesiculo-vacuolar organelles (Dvorak and Feng, 2001) may also be involved in forming a transmembrane pore and allowing leukocytes to migrate through the cell.

Upon migration into the surrounding tissues, leukocytes are guided by local sources of chemokines to move towards the area of infection or inflammation. Leukocytes are then activated either by cytokines released by resident cells within the tissue or by direct contact through recognition of pathogen.

### 1.5.3.2 Cell trafficking and surveillance

During homeostasis, naive T lymphocytes (see 1.2.1.4) search for antigens by recirculating between the blood and the secondary lymphoid organs. In doing so, naive T cells exit the blood and enter the lymph nodes via high endothelial venules (von Andrian and Mempel, 2003). Two homeostatic chemokines, CCL19 and CCL21 and the shared receptor for these chemokines, CCR7, are required for the migration of lymphocytes across the high endothelial venules (HEVs) into the lymph nodes. Naive lymphocytes, T<sub>regs</sub> and a subpopulation of memory T cells, known as central memory T cells (T<sub>CM</sub> cells), all express CCR7 (Reif et al., 2002, Sallusto et al., 1999, Szanya et al., 2002). CCR7 expressing cells home towards the ligands, CCL19 and CCL21, which are displayed on HEVs. CCL21 is constitutively expressed by HEVs (Gunn et al., 1998) whereas CCL19 is transcytosed across the endothelial barrier and displayed on the lumen of HEV (Baekkevold et al., 2001). The importance of CCR7 and its ligands in mediating T cell entry into the lymph nodes was demonstrated in mice deficient in CCR7 (Forster et al., 1999) and in mice unable to produce CCL19 and CCL21 due to a spontaneous *plt* mutation (Gunn et al., 1999). In both strains of mice, there are reduced numbers of naive T cells present in the lymph nodes. Once in the lymph node, and in the absence of antigen stimulation, T cells resensitise to sphingosine 1-phosphate (S1P), which binds the S1P receptor 1 expressed on T cells and mediates lymph node egress to the bloodstream via the efferent lymphatics (Schwab and Cyster, 2007).

Antigen presenting cells (see 1.2.1.3), such as monocytes and dendritic cells patrol the blood and migrate to the tissues to scavenge for pathogens. During this process, monocytes and immature DCs express inflammatory chemokine receptors such as CCR1, CCR2 and CCR5 (Martín-Fontecha et al., 2003). After antigen capture and maturation, macrophages and dendritic cells downregulate the inflammatory receptors and upregulate the expression of CCR7 (Yanagihara et al., 1998). CCR7 on 'mature' DCs mediates their exit from the tissues, such as the skin and intestine, into the draining and mesenteric lymph nodes respectively (Jang et al., 2006, Martín-Fontecha et al., 2003).

Once in the lymph nodes, DCs can activate naive lymphocytes to form effector T cells. Within the lymph node, CCR7 expressing cells are recruited to the T cell

area (the paracortex) which expresses CCL19 (Gunn et al., 1998) whereas CXCL13 is produced in the follicular compartment enriched with B cells (Schaerli et al., 2000). Indeed, (as mentioned above in 1.5.1) the structure of the follicular compartments within the spleen and lymph nodes are disrupted in CXCR5 deficient mice (Gunn et al., 1999). CXCR5 deficient mice displayed disorganisation of B cell follicles, and lymphocytes lacking CXCR5 were unable to migrate to B cell follicles (Forster et al., 1996). Additionally, CCR7 is also involved in secondary lymphoid organ development in coordination with CXCR5, as shown using mice double deficient in CXCR5 and CCR7 which lacked peripheral lymph nodes (Ohl et al., 2003). Following activation in the lymph node, follicular B cells upregulate CCR7 and downregulate CXCR5 which directs them to the T cell zone to receive help from CD4<sup>+</sup> T helper cells (Reif et al., 2002). Additionally, activated CD4<sup>+</sup> T cells transiently express CXCR5 upon stimulation (Schaerli et al., 2000). During this process, a subset of T helper cells are generated, known as follicular Th cells, which express CD4 and stable expression of CXCR5 along with low levels of CCR7. These cells migrate towards the B cell area and co-localise with B cells providing help for antibody production (Hardtke et al., 2005).

Upon encounter with antigen, lymphocytes upregulate their expression of adhesion molecules and chemokine receptors during differentiation, which allows them to migrate into distinct peripheral tissues, such as the skin or the intestine. The mechanism that drives the pattern of molecule expression is known as 'imprinting', which is mediated by DCs and the lymph node environment (Sigmundsdottir and Butcher, 2008). There is evidence that naive T lymphocytes are 'reprogrammed' during activation and the lymph node environment can influence this process. This was demonstrated in mice using naive transgenic T cells. Molecules important in intestinal homing were upregulated on the T cells when activated in the mesenteric lymph nodes yet when the cells were activated in the skin draining lymph nodes, molecules associated with trafficking to the peripheral tissues were upregulated (Campbell and Butcher, 2002).

Indeed, environmental stimuli have been implicated in influencing the homing properties of antigen experienced memory or effector T cells, in which DCs process both the antigen present and the stimuli from the environment and

present them to T cells in the lymph node. For example, vitamin D3 which can be generated in the skin after exposure to sunlight, can increase the expression of CCR10 on proliferating T cells (Sigmundsdottir et al., 2007). Keratinocytes and DCs also express enzymes which are involved in vitamin D3 metabolism (Sigmundsdottir et al., 2007). Another example is retinoic acid, which is derived from the diet in the form of vitamin A. Retinoic acid has been shown *in vitro* to upregulate  $\alpha 4\beta 7$  integrin and CCR9 on T cells, which are both homing receptors for the gut and bind mucosal vascular addressin cell adhesion molecule 1 and CCL25 respectively (Iwata et al., 2004).

A subset of T lymphocytes express cutaneous lymphocyte-associated antigen (CLA) and are capable of homing to the skin (Sigmundsdottir and Butcher, 2008). CLA<sup>+</sup> T lymphocytes are able to transmigrate through the blood vessel into the skin by binding E selectin (Fuhlbrigge et al., 1997). Chemokine receptors implicated in T cell homing to the skin are CCR4 and CCR10. Circulating CLA<sup>+</sup> CD4<sup>+</sup> T cells express CCR4 (Campbell et al., 1999) and a subset of these cells also express CCR10 (Hudak et al., 2002). Both have been shown to be important in recruiting T cells to inflamed skin (Reiss et al., 2001). Cells expressing CCR4 migrate towards its ligand, CCL17, which is produced by keratinocytes and dendritic cells within the skin (Campbell et al., 1999). Epidermal keratinocytes constitutively and inducibly express CCL27, a ligand for CCR10 (Morales et al., 1999).

### 1.5.3.3 Haemopoiesis

Chemokines not only play a role within the immune system but also play a role in development and migration of stem cells and haemopoiesis (see 1.1). CXCL12, also known as stromal derived factor 1, is a constitutive chemokine, which binds CXCR4 (Nagasawa et al., 1999). Mice deficient in either CXCR4 or CXCL12 show problems with heart, brain and blood cell development and ultimately the deletions are perinatally lethal (Nagasawa et al., 1996, Zou et al., 1998). The phenotype of the CXCR4 and CXCL12 deficient mice are very similar and this was thought to be due to the monogamous relationship between the ligand and its receptor. However, it is of note that another chemokine receptor, CXCR7 (see 1.6.3) was recently shown to bind CXCL12 (Balabanian et al., 2005). Additional defects described in CXCR4 and CXCL12 deficient mice were problems with

myelopoiesis and B lymphocyte development (Nagasawa et al., 1996, Zou et al., 1998).

A role for CXCL12 and CXCR4 was demonstrated in the movement of haemopoietic stem cells (HSCs). HSC in CXCR4 deficient mice were able to move to the fetal liver but not from the liver to the bone marrow (Ma et al., 1999, Zou et al., 1998). CXCR4 has been found to be expressed on various tissue progenitor cells (Ratajczak et al., 2006) as well as haemopoietic stem cells (Rosu-Myles et al., 2000). Similarly, CXCL12 is expressed in many different tissues and organs within the body, such as within the bone marrow, lymph node and muscle derived fibroblasts (Ratajczak et al., 2003, Zou et al., 1998). HSCs are retained within the bone marrow of adult mice, and this is mediated by CXCL12. Inactivation of CXCL12 by neutrophil derived proteases allows mobilisation of HSCs into the blood (McQuibban et al., 2001). Indeed, this process has been targeted for stem cell mobilisation to increase numbers of HSC in the blood to harvest for use in stem cell transplants. In addition, engraftment of HSCs after transplantation induced homing to the bone marrow also requires CXCL12 and CXCR4. CXCL12 can stimulate the arrest of CD34<sup>+</sup> cells mediated by integrins (Peled et al., 1999) and proteoglycans can present immobilised CXCL12 on bone marrow endothelial cells which can induce CD34<sup>+</sup> cell adhesion (Netelenbos et al., 2002). The CXCR4 antagonist, AMD3100 can also stimulate rapid mobilisation of HSCs from the bone marrow (Broxmeyer et al., 2005). Evidence suggests that mobilisation and homing of HSCs depend on opposing expression levels of chemokine receptors and adhesion molecules on HSCs and it is the balance that determines whether stem cells home to the bone marrow or are mobilised into the bloodstream (Gazitt, 2004).

#### **1.5.3.4 Angiogenesis**

The formation of new blood vessels, known as angiogenesis, is an important physiological mechanism required after tissue damage for wound repair and has been implicated in tumour growth and many chronic inflammatory diseases (Carmeliet, 2005). Angiogenesis is a process balanced by angiogenic and angiostatic factors, which promote or inhibit the formation of new blood vessels respectively. In order to form new vessel walls, the production of new

endothelial cells are required. Chemokines regulate this process by recruiting endothelial progenitor cells (EPCs) and inducing their proliferation.

EPCs are a subtype of progenitor cells present within the bone marrow, which are able to migrate to the circulation and differentiate into mature endothelial cells. EPCs were initially isolated from adult peripheral blood (Asahara et al., 1997) and subsequent characterisation of the phenotype of these cells revealed the expression of CD133, CD34 and vascular endothelial growth factor receptor-2 (Peichev et al., 2000). One of the markers, CD133 (originally termed AC133) is a marker for haemopoietic stem and progenitor cells from human bone marrow and peripheral blood (Yin et al., 1997). Subsequently, it was discovered that a bone marrow derived population of CD133<sup>+</sup> cells could also be differentiated and expanded into endothelial progenitor cells (Quirici et al., 2001). Additionally, a CD34 negative population of cells isolated from peripheral blood can also give rise to EPCs and this population of cells is a subset of CD14<sup>+</sup> monocytes that are able to transdifferentiate into endothelial cells (Harrasz et al., 2001). As a result, the exact definitions of EPCs remain controversial due to the different populations of cells within the blood that can acquire an endothelial phenotype.

Like haemopoietic stem cells, EPCs are mobilised from the bone marrow stromal niche to the vascular compartment of the bone marrow and this process is initiated by the matrix metalloproteinase 9 (Heissig et al., 2002). An important trigger for the mobilisation of EPCs is the interaction between CXCL12 and CXCR4. Not only is CXCL12 expressed on bone marrow stromal cells but also on endothelial cells (Petit et al., 2007). CXCL12 gene expression is regulated by the transcription factor, hypoxia inducible factor-1 $\alpha$  which is upregulated in hypoxic tissue (Ceradini et al., 2004) and in damaged arteries (Karshovska et al., 2007) which in turn recruits CXCR4<sup>+</sup> progenitor cells. Once mobilised, EPCs can then home to sites of endothelial injury and ischaemia, a process regulated by chemokines, and contribute to endothelial regeneration and repair.

The CXC subfamily of chemokines can regulate angiogenesis and within this family there are angiogenic and angiostatic members (Strieter et al., 2005). The CXC chemokines have an additional structural motif near the first N- terminal cysteine residue that determines their angiogenic or angiostatic properties. This motif consists of three amino acids, which are glutamic acid, leucine and

arginine, known as the ELR motif (Strieter et al., 1995). Members that contain this motif tend to be angiogenic whereas members that lack the ELR motif tend to be angiostatic. CXCL1, CXCL2, CXCL3, CXCL5, CXCL6, CXCL7 and CXCL8 are all angiogenic factors that mediate their effects through CXCR2 (Addison et al., 2000). Moreover, by mutating the ELR motif in CXCL8, it was no longer angiogenic but in fact angiostatic (Strieter et al., 1995). Angiostatic factors include CXCL9 and CXCL10 (Angiolillo et al., 1995, Arenberg et al., 1996). There is an exception to the rule of ELR correlation within the CXC subfamily and that is CXCL12 which lacks the ELR motif but is angiogenic (Strieter et al., 2005). However, angiogenic properties are not just restricted to the CXC chemokines or the presence of an ELR motif. CCL11 and CX3CL1 are examples of chemokines outwith the CXC subfamily that are angiogenic (Lee et al., 2006, Salcedo et al., 2001) and evidence has shown that CCL21 is angiostatic (Vicari et al., 2000).

All of the ELR<sup>+</sup> CXC chemokines bind to CXCR2, which is expressed on EPCs (Addison et al., 2000). Mice lacking CXCR2 displayed delayed wound healing (Devalaraja et al., 2000), illustrating that CXCR2 is a key receptor to the process of angiogenesis. In another study, blocking keratinocyte derived chemokine (KC/CXCL1), a ligand of CXCR2, after arterial injury in ApoE deficient mice, resulted in inhibition of endothelial recovery (Liehn et al., 2004). The receptor through which CXC chemokines are thought to mediate their angiostatic effect is CXCR3. Ligands that can bind CXCR3 present on endothelial cells were found to mediate angiostatic activity (Romagnani et al., 2001). CXCR3 exists as two splice variants and one variant, CXCR3B was found to mediate the angiostatic activity of CXCL4, CXCL9 and CXCL10 (Lasagni et al., 2003) and binding to CXCR3B by CXCL4 and CXCL10 has been shown to activate the p38 (MAPK) pathway (Petrai et al., 2008). A role for CCR2 and CCL2 in the homing of EPCs after endothelial injury has also been shown. Inflamed endothelial cells have been shown to express CCR2 (Weber et al., 1999). Indeed, bone marrow derived myeloid cells overexpressing CCL2 were infused *in vivo* after arterial injury and resulted in accelerated healing of the endothelium (Fujiyama et al., 2003).

#### **1.5.4 Role of chemokines and their receptors in disease**

The process of inflammation is a delicate balancing act. Acute inflammation is beneficial to host defence against infection and for tissue repair. However, if

inflammation persists and does not resolve, this leads to chronic inflammation (see 1.4.3). Central in many inflammatory diseases is the infiltration and recruitment of leukocytes mediated by chemokines. As a result, chemokines and their receptors have been implicated in the pathogenesis of a wide range of diseases from autoimmune diseases, for example multiple sclerosis, to inflammatory and vascular diseases such as atherosclerosis, and even tumours (Gerard and Rollins, 2001).

#### **1.5.4.1 Human immunodeficiency virus**

Human immunodeficiency virus (HIV) was identified in 1983 as a retrovirus, which caused acquired immunodeficiency syndrome (Gallo and Montagnier, 2003). A clinical characteristic of advanced HIV-mediated disease is a fall in the number of circulating CD4<sup>+</sup> T cells. It was later discovered that envelope proteins, mainly glycoprotein 120 (gp120) present on the surface of HIV could bind to CD4 (Dalglish et al., 1984). This explained why the virus tended to infect cells expressing CD4, predominately CD4<sup>+</sup> T cells. The entry of HIV into cells was demonstrated to be facilitated by chemokine receptors, CCR5 and CXCR4 (Deng et al., 1996, Dragic et al., 1996). Binding of gp120 to CD4 results in conformation changes in gp120, which in turn is then able to bind to the chemokine receptor (Wu et al., 1996). This subsequently results in membrane fusion and expulsion of viral contents into the cell.

Originally, HIV strains were classified according to the target cellular tropism. M-tropic strains of HIV replicated in macrophages whilst T-tropic strains infected T-cells. T-tropic strains preferentially use CXCR4 and M-tropic use CCR5 to gain entry to the cells (Lusso, 2006). Subsequently, the HIV strains were designated according to the coreceptor used. For example X4 strains are CXCR4 specific, R5 strains are CCR5 specific and R5/X4 strains are dual tropic and can use either CXCR4 and CCR5 to enter their target cells (Berger et al., 1998). Other chemokine receptors, such as CCR2B, CCR3, CCR8 and CX3CR1 have been shown to be used by certain HIV strains for cell entry *in vitro* (Lusso, 2006). Chemokines also play a role in HIV pathogenesis. CD8<sup>+</sup> T cells produced chemokines which were able to suppress replication of HIV in CD4<sup>+</sup> T cells (Levy et al., 1996). These chemokines were CCL3, CCL4 and CCL5, which are all capable of binding to CCR5 and therefore were reducing the ability of HIV to

bind to CCR5 (Cocchi et al., 1995). Indeed high levels of CCR5 binding chemokines are associated with slower disease progression (Ullum et al., 1998). Additionally, CCL3L1, a potent ligand for CCR5, has variable copy numbers in individuals due to duplicated isoforms of the gene which encodes CCL3 (Townson et al., 2002). Subsequently, low CCL3L1 copy numbers was discovered to be associated with increased susceptibility to HIV (Gonzalez et al., 2005).

Interest in targeting chemokine receptors in HIV has arisen from evidence of a genetic polymorphism associated with the disease. A 32 base pair deletion in the gene encoding CCR5 results in a loss of function receptor and individuals homozygous for this deletion (known as CCR5 $\Delta$ 32), which occurs in 1% of the Caucasian population, are resistant to HIV infection (Liu et al., 1996). However, 20% of the Caucasian population are heterozygous for the CCR5 $\Delta$ 32 mutation and in those that do get HIV, the rate of progression is slower (de Roda Husman et al., 1997). Other polymorphisms in CCR2, CX3CR1, CXCL12, CCL5 and CCL3 genes have been discovered and have been associated with host resistance or susceptibility to HIV and disease progression (Reiche et al., 2007).

Since individuals with the CCR5 $\Delta$ 32 mutation developed normally and seemed healthy, this led to targeting CCR5 for HIV therapy. Indeed, one drug known as Maraviroc has been approved for clinical use in HIV. Maraviroc is a CCR5 antagonist, which blocks the entry of HIV into CCR5 expressing cells by preventing the interaction between CCR5 and gp120 (Dorr et al., 2005). Another drug, AMD3100 was also able to inhibit HIV activity, in particular T-tropic strains by acting as a CXCR4 antagonist (Schols et al., 1997). During clinical trials for AMD3100, it was discovered that AMD3100 resulted in an increase in circulating CD34<sup>+</sup> haemopoietic stem cells (Liles et al., 2003). As a result, AMD3100, is a drug currently approved for use to enhance the mobilisation of stem cells into the blood for collection and use in autologous transplantation in patients with haematological malignancies (Devine et al., 2004).

Recent evidence suggests that CCR5 does play a role within host defence. CCR5 has been shown to play a key role in the survival of mice infected with West Nile virus (Glass et al., 2005). West Nile virus is a virus transmitted by mosquitoes which can infect humans and manifests clinically with fever and sometimes neurological problems, such as meningitis and encephalitis (Hayes and Gubler,

2006). Mice infected with West Nile virus showed increased expression of chemokines, in particular CCR5 ligands such as CCL3, CCL4 and CCL5, within the brain (Shirato et al., 2004). CCR5 was shown to be involved in mediating leukocyte trafficking to the brain and was crucial in eliminating the virus from the brain (Glass et al., 2005). Subsequently, a role for CCR5 was examined in humans displaying symptoms of West Nile virus infection and the frequency of CCR5 $\Delta$ 32 within the cohort. It was concluded that individuals homozygous for CCR5 $\Delta$ 32 were at increased risk of West Nile virus infection and that CCR5 was indeed protective (Glass et al., 2006).

#### **1.5.4.2 Cancer**

Uncontrollable cell growth can ultimately result in cancer, which involves many steps. Primary tumour development requires signals which allow the tumour to grow and escape detection from the immune system (Hanahan and Weinberg, 2000). The formation of secondary tumours in organs at a distant site from the original tumour is known as metastasis. For metastasis to occur, tumours must invade vascular or lymphatic vessels, home to other organs, promote growth and survival in the new environment (Gupta and Massague, 2006). Roles for chemokines and their receptors in cancer have been established and play a role in directing cells during metastasis as well as tumour cell growth, survival and angiogenesis (Balkwill, 2003).

Tumours do not only consist of cancerous cells but also contain leukocytes which influence the tumour microenvironment (Balkwill and Mantovani, 2001). There is evidence that chemokines associated with tumour cells can help evade the immune response and prevent rejection of the tumour (Coussens and Werb, 2002). For example, ovarian cancer produces CCL2 and CCL5 (Negus et al., 1995, Negus et al., 1997) and their levels of expression were found to correlate with the numbers of macrophages and lymphocytes localised within the area of chemokine production respectively (Negus et al., 1997). Tumour cells can also promote an environment that helps them to survive by producing chemokines that preferentially select Th2 lymphocytes and evade the immune response against tumours (Balkwill and Mantovani, 2001). In Kaposi sarcoma, three chemokines, which can attract Th2 cells, are encoded by the human kaposi sarcoma-associated herpes virus (Sozzani et al., 1998). There is evidence that

tumour associated macrophages (TAMs) are M2 polarised macrophages (Mantovani et al., 2004) and can release IL-10 which is immunosuppressive (Sica et al., 2000). TAMs also play a role in tumour progression, metastasis and angiogenesis (Bingle et al., 2002, Lin and Pollard, 2007). Additionally infiltrating leukocytes and stromal cells are thought to promote tumour progression by producing matrix metalloproteinases (Giraudo et al., 2004). Indeed, CCL2, CCL4 and CCL5 can induce MMP-9 in macrophages (Robinson et al., 2002).

Chemokines also contribute to tumour growth and the best-characterised chemokines for this role are CXCL1, CXCL2 and CXCL3 (also known as the growth-related oncogene (GRO) family of chemokines). These chemokines act as autocrine growth factors in various cancers (Luan et al., 1997). CXCL1, CXCL2, CXCL3 and CXCL12 can all activate the phosphatidylinositol 3-kinase AKT pathway (Curnock et al., 2002) which promotes cell proliferation and survival in cancerous cells (Vivanco and Sawyers, 2002). Additionally, chemokines can either promote or inhibit angiogenesis (see 1.5.3.4). The expansion of a solid tumour mass requires angiogenesis as new blood vessels are required to supply the cancerous tissue with oxygen and nutrients from the blood to survive (Hanahan and Weinberg, 2000).

Metastasis is not a random process but is actually an ordered and specific process (Gupta and Massague, 2006). For example, secondary tumours that metastasize from breast cancer tend to be found in bone marrow, lymph nodes, lung and liver directed by chemokines and their receptors (Muller et al., 2001). Indeed, in many types of cancer, malignant cells express increased levels of chemokine receptors, with the most widely expressed receptors being CXCR4 and CCR7, although CCR9 and CCR10 are also expressed. Human breast cancer and melanoma cell lines were discovered to express chemokine receptors that may be characteristic for each type of cancer. CXCR4 was found to be the dominant chemokine receptor on metastasising breast cancer cells whilst CCR10 was typically the highest expressed on the metastatic melanoma cell lines (Muller et al., 2001). Therefore, tumour cells expressing chemokine receptors may migrate and metastasise to sites where the ligands are expressed. Expression of CCR7 has been found in various cancers, including breast cancer (Muller et al., 2001), non-small lung cancer (Takanami, 2003) and oesophageal squamous cancer (Ding et al., 2003) in which expression of CCR7 was associated

with lymph node metastasis and correlated with poor clinical outcome. Transfection of B16 murine melanoma cells with CCR7, which resulted in CCR7 being expressed higher than CCR10, resulted in the melanoma cell metastasising more efficiently to the lymph nodes (Wiley et al., 2001). Furthermore, metastasis to the lymph nodes was blocked with anti-CCL21 antibody (Wiley et al., 2001). The skin is a common site of metastasis for melanoma cancer cells, which highly express CCR10 and bind CCL27, which is also highly expressed in the skin (Murakami et al., 2003). Moreover, a form of T cell lymphoma known as cutaneous T cell-lymphoma, forms tumours within the skin and also expresses CCR10 (Notohamiprodjo et al., 2005). Another chemokine receptor, CCR9 is expressed in melanoma and prostate cancer cells (Hwang, 2004, Singh et al., 2004) and CCR9 expression is correlated with metastasis to the small intestine (Letsch et al., 2004) where its ligand, CCL25 is expressed (Zaballos et al., 1999).

#### **1.5.4.3 Psoriasis**

As well as dysregulation in keratinocyte proliferation, altered activity of immune cells within the skin also occurs in psoriasis (see 1.4.3.1). There is increasing evidence of the involvement of chemokines and their receptors in this dysregulation of immune cells.

CXCL8 was one of the first chemokines to be associated with psoriasis (Schroder and Christophers, 1986), however CXCL1 is another chemokine that is increased in the lesions of psoriatic skin, interestingly it colocalises with CXCL8 (Gillitzer et al., 1996). Both CXCL1 and CXCL8 can bind CXCR1 and CXCR2, which are both predominantly expressed on neutrophils (Morohashi et al., 1995). Indeed, within the epidermis of psoriatic skin, overexpression of CXCR2 has been attributed to infiltrating neutrophils, but also keratinocytes (Kulke et al., 1998).

Keratinocytes are capable of producing CCL2 and CCL5 upon stimulation with  $\text{TNF}\alpha$  and  $\text{IFN}\gamma$  (Li et al., 1996). Expression of CCL2 mRNA is present within psoriatic lesions (Gillitzer et al., 1993) and CCL2 protein expression has been located to cells within the epidermis of normal and psoriatic skin (Deleuran et al., 1996). CCL2 can bind CCR2, a receptor that is expressed on monocytes and macrophages. Monocytes from peripheral blood of psoriatic patients were found

to have elevated levels of CCR2 expression compared to controls and CCR2 positive cells were present in psoriatic skin biopsies (Vestergaard et al., 2004).

T lymphocytes have been implicated in the pathogenesis of psoriasis and studies indicate that CCL27, CCL20, CCR10 and CCR6 play a role in recruiting T lymphocytes to the skin. In inflammatory skin diseases such as psoriasis and atopic dermatitis, the majority of T lymphocytes infiltrating the skin express CCR10 (Homey et al., 2002). As mentioned in 1.5.3.2, CCL27 is produced by epidermal keratinocytes (Morales et al., 1999). Consistent with this, the interaction between CCL27 and CCR10 regulates T cell recruitment to normal skin as well as inflamed skin (Homey et al., 2002). Additionally skin homing T cells also express CCR4 (Campbell et al., 1999). Blocking CCR4 or CCL27 in mice prevented the migration of lymphocytes to inflamed skin (Reiss et al., 2001). CCL20 is another chemokine that has been shown to be associated with psoriasis. Homey *et al.*, have shown that CCL20 and its receptor, CCR6 are upregulated in psoriatic skin (Homey et al., 2000a). In addition, this study showed that keratinocytes expressing CCL20 colocalised with skin infiltrating T lymphocytes and high levels of CCR6 were expressed on skin homing T lymphocytes (Homey et al., 2000a). Another receptor with a potential role in psoriasis is CXCR3, which is expressed on dermal lymphocytes and the ligands for CXCR3, CXCL9 and CXCL10, were upregulated in lesions of psoriatic skin (Rottman et al., 2001).

#### **1.5.4.4 Rheumatoid arthritis**

Rheumatoid arthritis (RA) is a debilitating chronic inflammatory disease (see 1.4.3.3). Within the synovium of rheumatoid arthritis patients, the inflammatory infiltrate consists of a mixture of cells including macrophages, T cells, B cells, neutrophils, mast cells and dendritic cells. The recruitment of inflammatory cells to the synovial tissue is mediated by chemokines and their receptors, of which several have been identified in situ. The cellular infiltrate within the synovial tissue of rheumatic joints expresses chemokine receptors including CCR5, CCR2, CCR3, CXCR3 and CXCR2 (Szekanecz et al., 2003).

Studies have shown that synovial fluid and tissues from rheumatoid arthritis patients express high levels of CCL2 (Koch et al., 1992). CCL2 is a chemokine that can attract T lymphocytes in addition to monocytes. CCL2 can also

stimulate cells within cartilage (chondrocytes) to produce MMP-3 which degrades the extracellular matrix (Borzi et al., 2000). Additionally, CCL2 and other chemokines such as CXCL10 and CCL13 are able to increase the proliferation of fibroblast like synoviocytes resulting in synovial hyperplasia (Garcia-Vicuna et al., 2004). Targeting CCL2 in mice resulted in a reduction in macrophage infiltration and reduced disease severity of arthritis (Gong et al., 1997). In a collagen induced arthritis model, CCR2 null mice displayed enhanced T cell production and accumulation of macrophages within the joint (Quinones et al., 2004).

Additionally, CCL5 is another chemokine implicated in the pathogenesis of the disease. Expression of CCL5 is seen in the synovial lining of rheumatoid joints and is produced by synovial T cells (Robinson et al., 1995). In an adjuvant induced arthritis model in rats, blocking CCL5 was shown to ameliorate the disease (Barnes et al., 1998). Small molecule antagonist blocking CCR5, a receptor for CCL5, in a collagen induced arthritis model resulted in inhibition of T cell migration and reduction in disease severity (Yang et al., 2002).

Elevated levels of CCL20 were discovered in the rheumatoid joint along with expression of its receptor CCR6. It was found that expression of CCL20 in the joint resulted in the recruitment of cells expressing CCR6 (Matsui et al., 2001). Th17 cells express CCR6 and have been shown to be recruited to the joint in a murine model of arthritis (Hirota et al., 2007b).

In addition, synovial fluid from RA patients contains elevated levels of CXCL8 and the production of CXCL8 in synovial tissues is mediated by macrophages (Koch et al., 1991). Ligands of CXCR3, CXCL9 and CXCL10 are both upregulated in RA synovial tissue and synovial fluid (Patel et al., 2001). As well as being involved in the recruitment of macrophages, both are able to enhance proliferation of fibroblast-like synoviocytes (Garcia-Vicuna et al., 2004). Increased levels of XCL1 and CX3CL1 are also present within synovial fluid of rheumatoid arthritis patients (Volin et al., 2001, Wang et al., 2004a) as well as increased expression of XCR1 on mononuclear cells in synovial tissue (Wang et al., 2004a). CX3CL1 is thought to be one chemokine involved in mediating angiogenesis in rheumatoid arthritis (Volin et al., 2001).

These studies show chemokines and their receptors play a pathological role in chronic inflammatory diseases such as psoriasis and rheumatoid arthritis. Targeting chemokines and their receptors within these diseases may provide potential therapies.

## 1.6 Atypical chemokine receptors

In recent years, there has been the discovery of atypical chemokine receptors (Nibbs et al., 2003), which are officially chemokine binding proteins according to the international union of pharmacology (IUPHAR) classification system (Murphy et al., 2000). These seven transmembrane spanning proteins share homology with true chemokine receptors and bind chemokines, but these receptors do not seem to signal upon ligand binding, at least not using the classical signalling pathways used by GPCRs (see 1.5.2.1). With no evidence of signalling, the atypical receptors do not receive a classical chemokine receptor name and are classified as chemokine binding proteins. Within this group, is the Duffy Antigen Receptor for Chemokines (DARC), D6 and CCX-CKR, which are alternatively labelled as 'silent' receptors (Graham, 2009). Another receptor beginning to emerge as a silent receptor is CXCR7. Although DARC, D6 and CCX-CKR may not be able to signal and induce chemotaxis, studies show that these receptors have an important role within immunity and inflammation (Graham, 2009).

### 1.6.1 DARC

DARC was originally known as the Duffy blood group antigen, which was found to be present on red blood cells and forms a blood group system (Hadley and Peiper, 1997). However, it was later discovered that the Duffy antigen allowed entry of parasites responsible for malaria, such as *Plasmodium vivax* (Horuk et al., 1993). Individuals who lack DARC on red blood cells, due to a polymorphism in the promoter which prevents the transcription factor GATA-1 from binding thus blocking expression of DARC on red blood cells, are resistant to malaria (Tournamille et al., 1995). It is thought that this mutation may have emerged due to selective pressure to prevent malaria infection.

Following cloning, DARC was originally thought to be a nine transmembrane receptor (Chaudhuri et al., 1993) but was later proposed to be a seven

transmembrane spanning structure similar to the chemokine receptor family. DARC lacks the conserved DRYLAIV motif and shows no increase in intracellular calcium subsequent to ligand binding (Neote et al., 1994). However, DARC can bind 11 ligands, including those from the CC and CXC family with preference for the inflammatory subset within both families (Gardner et al., 2004). Chemokine binding to DARC is localised to the amino terminal domain of the receptor (Lu et al., 1995) and requires a disulphide bridge between the first and fourth cysteine suggesting that sequences within the pocket caused by the disulphide bond are important (Tournamille et al., 1997). As well as being expressed on erythrocytes, DARC is also expressed on vascular endothelial cells in various organs and within the cerebellum (Hadley et al., 1994, Horuk et al., 1996). Individuals who lack DARC on red blood cells still express DARC on vascular endothelial cells (Peiper et al., 1995) leading to suggestions that DARC may play an important role within this location.

DARC on erythrocytes, may function as a 'chemokine sink' (Darbonne et al., 1991) and as a result may prevent activation of circulating leukocytes. Indeed, DARC deficient mice also show an exaggerated response to LPS and within the lungs and liver of these mice, increased numbers of polymorphonuclear cells were found (Dawson et al., 2000). It has been suggested that DARC on erythrocytes plays a role in maintaining the concentration of chemokines in plasma. Chemokines injected intravenously were more rapidly removed from the circulation in DARC deficient mice compared with wild-type mice (Fukuma et al., 2003). In another study, DARC deficient mice displayed larger tumours in a model of prostate cancer compared to the tumours in wild-type mice (Shen et al., 2006). Individuals lacking DARC on erythrocytes are at increased risk and mortality of various malignant diseases, including prostate cancer (Lentsch, 2002).

DARC is also expressed on endothelial cells and is proposed to play a role in transporting chemokines across the endothelium, a process known as transcytosis. CXCL8 transportation across the endothelium occurs through DARC (Middleton et al., 2002, Lee et al., 2003b) and DARC has been found associated with caveolae (see 1.5.2.2) within endothelial cells (Chaudhuri et al., 1997). DARC has also been shown to play a role in chemokine-induced angiogenesis *in vivo* using DARC transgenic mice (Du et al., 2002). Overexpression of DARC on

endothelial cells within these mice resulted in a reduced angiogenic response (Du et al., 2002). To contrast this, endothelial DARC was able to transcytose chemokines *in vitro* and using a model of contact hypersensitivity, leukocyte migration across the endothelium was enhanced in DARC transgenic mice compared to wild-type (Pruenster et al., 2009).

Expression of DARC has been found to be present in a variety of diseases including renal disease and within rheumatoid arthritis synovium (Liu et al., 1999, Patterson et al., 2002). Indeed, upregulation of DARC on the endothelium has been found to take place during renal transplant rejection, pneumonia and in the early stages of rheumatoid arthritis (Gardner et al., 2006, Lee et al., 2003a, Segerer et al., 2000). The role of DARC in acute renal injury was investigated using two neutrophil dependent models. In both models, DARC deficient mice were protected from renal injury. In the ischaemic perfusion model, the number of neutrophils recruited to the kidney was reduced (Zarbock et al., 2007). However, in a chronic model of renal inflammation characterised by the accumulation of macrophages and T cells, renal recruitment of macrophages and T cells still occurred in DARC deficient mice (Vielhauer et al., 2009). These studies suggest that DARC does not play a role in monocyte and T cell recruitment in prolonged renal inflammation. In an LPS induced acute lung injury model, erythrocyte DARC was shown to limit polymorphonuclear cell infiltration into the lung by acting as a chemokine sink and endothelial DARC was shown to play a minor role in promoting leukocyte transmigration through the pulmonary endothelium (Reutershan et al., 2009).

### **1.6.2 CCX-CKR**

CCX-CKR (ChemoCentryx chemokine receptor) has previously been named as CCR11 and CCRL1 (Gosling et al., 2000, Khoja et al., 2000, Schweickart et al., 2000). Human CCX-CKR can bind CCL19, CCL21 and CCL25 (Gosling et al., 2000) with high affinity. These chemokines are regarded as homeostatic and are involved in directing cells to tissues and secondary lymphoid compartments. CCL19 and CCL21 are ligands for CCR7 and CCL25 was previously thought to bind only CCR9. CCX-CKR has structural similarities to CCR7 and CCR9 and displays 29-35% amino acid homology with the general chemokine receptor family (Gosling et al., 2000). However, like DARC, this receptor was not given an official

chemokine receptor name because there was no evidence of signalling (Murphy, 2002). This was later confirmed following characterisation of mouse CCX-CKR which showed that murine CCX-CKR in transfected cells could bind CCL19, CCL21 and CCL25 yet did not give any signs of signalling as calcium flux did not occur (Townson and Nibbs, 2002). This has led to the inclusion of CCX-CKR in the atypical chemokine receptor family.

Mouse CCX-CKR is highly expressed in the heart and lungs and is expressed at lower levels in all tissues (Townson and Nibbs, 2002). However human CCX-CKR was found to be highly expressed in the heart, lung and small intestine as well as weak expression in the brain and skeletal muscles (Gosling et al., 2000, Townson and Nibbs, 2002). Although CCX-CKR does not seem to signal, the biochemical and trafficking properties of the receptor have been defined (Comerford et al., 2006). This study showed that human CCX-CKR was able to internalise and degrade ligand more efficiently than CCR7 and was able to continue internalising CCL19 when CCR7 was not. Internalisation of chemokine and receptor did not require components of the clathrin coated mediated endocytosis pathway, such as  $\beta$ -arrestin and clathrin coated vesicles but did require dynamin and is suggested to require caveolae (Comerford et al., 2006).

CCX-CKR has been proposed to act as a scavenging receptor (Comerford et al., 2006). In a study by Heinzl *et al.*, CCX-CKR was shown to be involved DC homing via the afferent lymphatics under homeostatic conditions. Reduced numbers of CD11c<sup>+</sup> MHCII<sup>high</sup> DCs were found in the skin draining lymph nodes of CCX-CKR deficient mice (Heinzl et al., 2007). Additionally, overexpression of CCX-CKR in thymic epithelial cells resulted in impaired migration of haemopoietic thymic precursors to the embryonic analage therefore further implicating a role for CCX-CKR in leukocyte migration under homeostatic conditions (Heinzl et al., 2007).

In pulmonary sarcoidosis, CCX-CKR transcripts are upregulated in bronchoalveolar cells and transcript levels correlated with disease severity alongside an increase in CCL19 levels in pulmonary sarcoidosis (Kriegova et al., 2006). However, the exact role of CCX-CKR in this disease has not yet been defined.

### **1.6.3 CXCR7**

Formally known as RDC1, this receptor was cloned and characterised from mouse genomic DNA where it was found to show 88% amino acid similarity to the human RDC1 receptor. Mouse RDC1 was discovered to share 43% amino acid similarity to mouse CXCR2 and the RDC1 gene was localised to chromosome 1 where the genes for CXCR2 and CXCR4 are also located (Heesen et al., 1998). This led to the suggestion that RDC1 was an orphan CXC chemokine receptor.

It was then reported that RDC1 binds to CXCL12 and CXCL11 (Balabanian et al., 2005, Burns et al., 2006). CXCL12 binding to RDC1 in transfected cells resulted in calcium mobilisation and cell migration therefore it was proposed to rename it CXCR7 (Balabanian et al., 2005). However, another study reported that there was no calcium flux or cell migration after ligand binding to CXCR7/RDC1 yet CXCR7/RDC1 expression increased cell survival and adhesion (Burns et al., 2006). More recently CXCR7/RDC1 has been implicated in promoting tumour growth in breast, lung and prostate cancer (Miao et al., 2007, Wang et al., 2008). In the study by Wang et al, CXCR7/RDC1 was shown to signal via a downstream signalling pathway, known as the AKT pathway, which contradicted previous results. However, the contrasting results may be due to the use of different tumour cell lines and it was not ruled out that CXCL12 may have mediated signalling through CXCR4 heterodimerisation with CXCR7/RDC1 (Sierro et al., 2007). Indeed, when CXCR7 and CXCR4 are coexpressed, CXCR7/CXCR4 heterodimer formed as efficiently as receptor homodimers and it has been suggested that CXCR4/CXCR7 heterodimers in T cells may regulate CXCL12 mediated chemotaxis (Levoye et al., 2009). Therefore, more studies are required before this chemokine receptor is either officially designated into the CXCR subfamily or to confirm its membership in the atypical chemokine family.

CXCR7 was found to be highly expressed on monocytes and B cells (Infantino et al., 2006). Indeed the ability of B cells to differentiate into plasma cells capable of secreting antibodies correlated with CXCR7 expression levels (Infantino et al., 2006). Additionally, a ligand produced from mature plasmacytoid dendritic cells, was found to be different from CXCL12 and CXCL11 but was able to induce CXCR7 internalisation on primary B cells (Infantino et al., 2006).

Disruption of CXCR7 in mice was lethal which illustrated a role for the receptor in vascular development (Sierro et al., 2007). The defects in CXCR7 null mice were due to defects in the heart and not due to haemopoietic problems (Sierro et al., 2007). Additionally expression of CXCR7 has been shown in the neurons of developing, and adult, rat brains although the exact role for CXCR7 at this site is not known (Schonemeier et al., 2008).

In zebrafish, the migration of primordial germ cells (PGCs) was primarily known to be guided by CXCL12 and its receptor CXCR4 (Doitsidou et al., 2002, Knaut et al., 2003). Initial studies suggested that there was regulated expression of chemokine receptors CXCR4 and CXCR7 at the leading and trailing edge of the migrating primordium (Dambly-Chaudiere et al., 2007). A recent study has shown that CXCR7 is expressed in the somatic environment and plays a role in the migration of PGCs (Boldajipour et al., 2008). The authors conclude that CXCR7 acts as a decoy receptor and is involved in PGC migration by controlling the levels of the chemokine CXCL12 (Boldajipour et al., 2008).

#### **1.6.4 D6**

The atypical chemokine receptor, D6, was originally identified in the mouse (Nibbs et al., 1997a). It encodes a protein of 378 amino acids containing seven transmembrane spanning domains with 30% identity and 60% homology to the murine CCR family. However, the amino acid sequence in the second intracellular domain, which is highly conserved among chemokine receptors, was found to contain the sequence DKYLEIV and not DRYLAIV. The DRYLAIV motif is important for G-protein coupling and chemokine receptor signalling. Human D6 was also cloned and was discovered to be 71% identical to murine D6 and also contained the DKYLEIV motif (Nibbs et al., 1997b). Purification of the human D6 protein revealed that D6 has a molecular mass of 49kDa and was sulphated and glycosylated at the N-terminus (Blackburn et al., 2004).

Mouse expression of D6 is high in lung, liver and spleen and is expressed in the heart, brain, thymus, ovary, muscle, liver and kidney as well as the skin (Nibbs et al., 1997a). D6 is present on astrocytes within the brain (Neil et al., 2005). Expression of D6 is found within the placenta on trophoblasts, skin, lungs, on

endothelial cells lining the lymphatics within humans (Nibbs et al., 2001) and leukocytes, in particular, B cells and dendritic cells (McKimmie et al., 2008).

D6 displays high affinity binding to a large number of inflammatory chemokines within the CC chemokine subfamily including CCL2, CCL3, CCL4, CCL5, CCL7, CCL8, CCL11, CCL13, CCL14 (Nibbs et al., 1997b), CCL17 and CCL22. D6 does not bind CCL19 or CCL20, which are considered to be homeostatic chemokines (Bonecchi et al., 2004). Nibbs *et al.* also demonstrated enhanced binding of an isoform of human CCL3, known as CCL3L1, to D6. The enhanced binding was found to be due to a proline residue at position 2 (Nibbs et al., 1999). In addition, D6 can bind the full length CCL22 but not a truncated form of CCL22 where the first two amino acids have been cleaved by an enzyme, CD26 (Bonecchi et al., 2004). CD26 is a serine protease expressed by many cells and is selective for substrates with a proline or alanine residues at position 2 of the NH2 terminus (Struyf et al., 2003). Upon ligand binding, D6 does not induce calcium fluxes or mediate chemotaxis, signs of classical G-protein signalling (Nibbs et al., 1997b) and therefore has not been given a CCR name. However, ligand binding to D6 results in internalisation and degradation of the ligand leading to the proposal that D6 may act as a 'scavenging' or 'decoy' receptor for inflammatory CC chemokines (Fra et al., 2003). Therefore D6 may be 'mopping up' CC chemokines regulating the levels available, and limiting the numbers of leukocytes within an inflamed area.

Various properties and mechanisms allow D6 to internalise CC chemokines. In the absence of ligand, D6 is phosphorylated and is therefore constantly 'switched on' and has the ability to internalise (Blackburn et al., 2004). Another feature is that only 5% of D6 is present on the cell surface and the rest is within the cell in intracellular vesicles (Blackburn et al., 2004). Subsequently, D6 was found to move to and from the cell surface in the absence of ligand binding without any reduction in total cell surface levels (Weber et al., 2004). D6 recycling in absence of ligand requires Rab4 and Rab11 (Bonecchi et al., 2008). In addition, D6 requires Rab5 and dynamin I to be able to internalise ligand (Weber et al., 2004) and is dependent on  $\beta$ -arrestin (Galliera et al., 2004), all components of the clathrin coated endocytosis pathway. An amino acid sequence in the C terminus of D6 is not homologous to other chemokine receptors and is conserved through various species. This region contains a serine cluster that controls the

stability, constitutive phosphorylation and trafficking of D6. The C terminus does not control internalisation of chemokine but does prevent subsequent progressive scavenging of the ligand (McCulloch et al., 2008). Ligand binding to D6 has been shown to increase D6 scavenging using Rab11 and increases D6 expression on the cell membrane (Bonecchi et al., 2008). In addition, LPS can downregulate D6 mRNA levels whereas TGF- $\beta$  can upregulate D6 mRNA levels in myeloid cells and D6 expression within dendritic cells was GATA-1 dependent (McKimmie et al., 2008). Other evidence has shown IL-1 $\beta$  and TNF $\alpha$  can upregulate D6 mRNA expression in human breast cancer cell lines (Wu et al., 2008).

The role of D6 *in vivo* was examined using D6 null mice to investigate the hypothesis that D6 may regulate the level of inflammatory chemokines. Jamieson *et al.* used a model of cutaneous inflammation induced by phorbol 12-myristate 13-acetate (TPA) application to murine dorsal skin on three consecutive days. It was found that D6 null mice could not clear inflammatory CC chemokines as effectively as the wild-type mice after 24 hours resulting in development of a pathology similar to human psoriasis. The pathology that developed in D6 null mice was characterised by an accumulation of T cells within the epidermis, mast cells in the dermis and was dependent on TNF $\alpha$  (Jamieson et al., 2005). Another study used a model of skin inflammation induced by injection of complete Freund's adjuvant. In this instance, D6 null mice displayed an increased inflammatory response with increased numbers of leukocytes, angiogenesis and areas of necrosis as well as increased cellularity in lymph nodes (Martinez de la Torre et al., 2005). Therefore, these studies suggest that, *in vivo*, D6 plays a role in the resolution of inflammation.

Further studies have investigated the role of D6 expression in other tissues. D6 within the placenta plays a role in reducing fetal loss in two separate models induced either by systemic inflammation or anti-phospholipid antibodies (Martinez de la Torre et al., 2007). In a model of allergic pulmonary inflammation, D6 null and wild-type mice were sensitised to ovalbumin and then exposed to ovalbumin aerosol on a single occasion or consecutively for seven days (Whitehead et al., 2007). D6 was shown to scavenge certain chemokines in the lung in a concentration dependent way and the lungs of D6 null mice had increased levels of T cells, dendritic cells and eosinophils. Confusingly, despite

the increase in leukocyte numbers, the absence of D6 also resulted in reduced reactivity of the airway leading to the proposal that inhibition of D6 may help allergen induced asthmatic patients (Whitehead et al., 2007).

D6 has also been shown to play a role in the development of skin tumours. A chemically induced skin tumour model was used in which a cutaneous application of 7, 12-dimethylbenz(*a*)anthracene (DMBA) followed by 12 2-week cycles of phorbol 12-myristate 13-acetate (TPA) was applied to murine skin. Deletion of D6 made an otherwise resistant strain susceptible to tumour development, which correlated with prolonged skin inflammation, including infiltration of epidermal T cells and dermal mast cells (Nibbs et al., 2007). In a tumour susceptible mouse strain, deletion of D6 resulted in enhanced susceptibility to papilloma formation (Nibbs et al., 2007). After discontinuing TPA use, which was used as a tumour promoting agent to drive tumour emergence after mutagenesis by DMBA, D6 deficient mice developed enlarged papillomas whereas papilloma size in wild-type mice did not increase (Nibbs et al., 2007). In a model of liver injury induced by carbon tetrachloride, D6 deficient mice displayed prolonged liver damage with increased levels of CCL2, CCL3 and CCL5 after 48 hours (Berres et al., 2009). Additionally, increased numbers of leukocytes, in particular T cells and NK cells was found in the liver of D6 deficient mice compared to wild-type (Berres et al., 2009). In a model of colitis induced by dextran sodium sulphate, D6 deficient mice were less susceptible to colitis (Bordon et al., 2009). There was no difference in the level of pro-inflammatory chemokines released from colon explants or leukocytes recruited to the colon in D6 deficient mice compared to wild-type. However, D6 deficient mice displayed higher levels of IL-17A and increased numbers of IL-17A  $\gamma\delta$  T cells suggesting that D6 plays a role in regulating IL-17A secretion by  $\gamma\delta$  T cells in the colon (Bordon et al., 2009). Another study examining D6 in experimental colitis induced by dextran sodium sulphate found that D6 deficient mice were more susceptible to colitis with higher levels of pro-inflammatory chemokines and increased leukocyte infiltration (Vetrano et al., 2009). Additionally, using chimeric mice, the ability of D6 to control intestinal inflammation was located to D6 expression in the stromal/lymphatic area, i.e. on lymphatic vessels (Vetrano et al., 2009). Also in the same study, D6 deficient mice were more susceptible to chronic colitis associated cancer than wild-type mice.

Other roles for D6 have been suggested. D6 null mice are relatively resistant to EAE due to an impaired adaptive immune response (Liu et al., 2006). In addition, the role of D6 in the immune response to *Mycobacterium tuberculosis* has been examined and D6 null mice were more susceptible to mortality after infection by *Mycobacterium tuberculosis* (Di Liberto et al., 2008). Mortality was associated with increased local and systemic inflammation, increased CC chemokine levels as well as infiltration of macrophages and T cells to the lungs. However blocking CC chemokines in D6 deficient mice resulted in prolonged survival yet uncontrollable growth of *Mycobacterium tuberculosis* within the lung (Di Liberto et al., 2008).

Studies involving D6 in human diseases are emerging. D6 is expressed in atopic dermatitis and rheumatoid arthritis synovium as well as kaposi sarcoma, a form of malignant vascular tumour (McKimmie et al., 2008, Nibbs et al., 2001). D6 is also expressed in human breast cancer cell lines and tissues. Overexpression of D6 in breast cancer cell lines was found to inhibit proliferation and invasion ability of the tumour *in vitro*. D6 protein expression in human tissues was correlated positively with disease free survival (Wu et al., 2008). One study has shown that genetic variation in the D6 receptor correlates with the grade of liver inflammation in hepatitis C (Wiederholt et al., 2008). Additionally, patients with high levels of liver inflammation expressed lower levels of D6 mRNA (Wiederholt et al., 2008). To add to this, expression levels of D6 mRNA varied widely in control human hepatocytes suggesting that variation in D6 levels may be due to certain genotype variations in the D6 receptor (Wiederholt et al., 2008). Increased expression of D6 has also been found on lymphatic vessels and leukocytes within ulcerative colitis, crohns disease and colon cancer compared to normal colon mucosa (Vetrano et al., 2009).

These studies show that D6 is a key chemokine receptor involved in the regulation of inflammation and the immune response. However, the precise role and mechanisms of D6 function in inflammation and chronic inflammatory diseases are still poorly understood and further work is required to clarify the function of D6 in these processes.

## 1.7 Aims

The overall aim of the work within this thesis was to determine whether the manipulation of the expression of the atypical chemokine receptor, D6, has the potential to be of future therapeutic value.

D6 was reported to play an important role in the resolution of the cutaneous inflammatory response in mice. Therefore, we hypothesised that increased expression of D6 would be able to limit inflammation *in vivo*.

To test our hypothesis, K14D6 transgenic mice were generated to allow ectopic expression of D6 to be targeted to the epidermis. Characterisation of the K14D6 transgenic mice was required to ensure the D6 transgene was transcribed, expressed at the protein level and was functional. To test whether increased expression of D6 within K14D6 mice could limit inflammation, a well-characterised model of skin inflammation was used.

Using a microarray approach, the transcriptional consequences of ligand binding to D6 and basal expression of D6 were examined. Primary murine keratinocytes from wild-type and K14D6 mice were isolated, cultured and incubated with either PBS or CCL3. By examining changes in the cellular transcriptome after ligand binding to D6, it was hoped that this would give an insight into cellular functions mediated by D6.

The final aim of this thesis was to determine whether there is a correlation between D6 expression levels and cutaneous inflammatory diseases, in particular psoriasis. This was assessed by analysing D6 expression in peripheral blood and skin biopsies collected from psoriatic patients. Other inflammatory diseases such as atopic dermatitis, psoriatic arthritis and rheumatoid arthritis were also examined for D6 expression.

## **Chapter 2**

## **Materials and Methods**

## 2 Materials and Methods

### 2.1 Materials

#### 2.1.1 *Antibodies*

Abcam (Cambridge, UK)	fluorescein isothiocyanate (FITC)-conjugated mouse anti-pan cytokeratin
BD Pharmingen (Oxford, UK)	FITC-conjugated mouse IgG1 (isotype control)
	Allophycocyanin (APC)-conjugated mouse anti-human CD3
	phycoerythrin (PE)-conjugated mouse anti-human CD14
	PE-conjugated mouse anti-human CD20
	Viaprobe
Chemicon (Harrow, UK)	HRP-conjugated donkey anti-chicken IgY
DAKO UK (Ely, UK)	Mouse IgG2a (isotype control)
	Mouse IgG1
In house	Mouse anti-human D6
Miltenyi Ltd (Surrey, UK)	APC-conjugated mouse anti-human CD1c
	APC-conjugated mouse anti-human CD304 (BDCA)
Sigma (Poole, UK)	FITC-conjugated goat anti-mouse IgG (Fc specific) F(ab') <sub>2</sub> fragment
Vector Laboratories (Peterborough, UK)	Biotinylated anti-mouse IgG

### **2.1.2 Chemicals, reagents and solutions**

<b>Ambion (Warrington, UK)</b>	Nuclease free water
	RNase Zap
<b>Biogenesis (Poole, UK)</b>	Normal Human serum
<b>Bioline (London, UK)</b>	5x DNA Loading Buffer
	Hyperladder I
	Hyperladder IV
<b>BDH (Letterworth, UK)</b>	DPX mounting solution
	Hydrogen Peroxide 30% Solution
	Sodium Chloride (NaCl)
<b>Cell Path (Newtown, UK)</b>	Haematoxylin Z
	Putts Eosin
	Scotts tap water solution
<b>Fisher scientific (Loughborough, UK)</b>	Chloroform
	Citric Acid
	Diaminoethanetetra-acetic acid (EDTA) disodium salt
	Ethanol
	Sodium dodecyl sulfete (SDS)
<b>Gibco (Invitrogen, Paisley, UK)</b>	Phosphate buffered Saline (PBS)
<b>Invitrogen (Paisley, UK)</b>	Ethidium Bromide
	MES running buffer
	Multimark multicolour standard
	Nitrocellulose transfer membrane
	NuPage 4-12% Bis-tris gel
	NuPage Transfer Buffer
	Trizol

**Melford (Ipswich, UK)**

Tris Hydrochloric acid (HCl)

**Sigma (Poole, UK)**

Ammonium Thiocyanate

Bovine serum albumin (BSA)

Dithiothreitol (DTT)

Fibronectin

Histopaque 1077

Cell lytic-M mammalian cell lysis buffer

2-Mercaptoethanol

Phorbol 12-Myristate 13-Acetate

Sample buffer Laemmli 2x concentrate

Tween 20

**Surgipath (Peterborough, UK)**

Neutral buffered formalin

**Thermo Scientific  
(Loughborough, UK)**

Xylene

**Vector Laboratories  
(Peterborough, UK)**

Normal Horse Serum

### **2.1.3 Chemokines**

**Almac sciences (Gladsmuir, UK)**

Biotinylated CCL3

CCL2 conjugated to Alexa-647

CCL3

**Peprtech (London, UK)**

CCL22

### **2.1.4 Enzymes, kits and PCR master mix**

<b>Abgene (Epsom, UK)</b>	Pre-aliquoted ReddyMix PCR master mix
<b>Ambion (Warrington, UK)</b>	RNase free DNase kit
<b>Applied Biosystems (Foster City, CA)</b>	Power SYBR Green PCR master mix
<b>BD Pharmingen (Oxford, UK)</b>	Standard Fix-Permabilisation kit
<b>BIOS Europe Ltd (Skelmersdale, UK)</b>	RAPI-DIFF II kit
<b>Invitrogen (Paisley, UK)</b>	Superscript First strand synthesis system for RT-PCR kit
<b>Perbio science Ltd (Cramlington, UK)</b>	bicinchoninic acid (BCA) protein assay
	Supersignal West Femto chemiluminescent substrate
	Supersignal West Pico chemiluminescent substrate
<b>Qiagen (Crawley, UK)</b>	QIA quick PCR purification kit
	RNase free DNase I
	RNeasy mini kit
<b>Sigma (Poole, UK)</b>	Proteinase K
<b>Vector Laboratories (Peterborough, UK)</b>	Avidin/biotin blocking kit
	DAB Substrate Kit, 3,3'-diaminobenzidine
	Standard Vectastain ABC kit

## 2.1.5 Primers

VH Bio (Gateshead, UK)

Primers

PRIMER NAME		SEQUENCES
mD6	Forward	5' AGCTTTACCTGCTGAACCTGG 3'
	Reverse	5' AAGAAGATCATGGCCAAGAGTG 3'
K14mD6 Forward	Forward	5' ATGACAAGCTCCAAAGAGATG 3'
	Reverse	5' CTCTTCACTGATCTCCCTCCAC 3'
$\beta$ -Actin	Forward	5' TGAACCCTAAGGCCAACCGTG 3'
	Reverse	5' GCTCATAGCTCTTCTCCAGGG 3'
CCR1	Forward	5' GCGCTCATTTCCCCTACAA 3'
	Reverse	5' CGGCTTTGACCTTCTTCTCA 3'
CCR2	Forward	5' TGGGACAGAGGAAGTGGTGT 3'
	Reverse	5' TGAGGAGGCAGAAAATAGCAG 3'
CCR3	Forward	5' GCAGGTGACTGAGGTGATTG 3'
	Reverse	5' CTGTGGAAAAGAGCCGAAG 3'
CCR4	Forward	5' CTCGCCTTGTTTCAGTCA 3'
	Reverse	5' GATTTCCCTCCACCCAGCA 3'
CCR5	Forward	5' TTTGTTCTGCCTTCAGACC 3'
	Reverse	5' TTGGTGCTCTGTTCCCTCATCTC 3'
Col3a1 outer	Forward	5' GGGTATCAAGGGTGAAAGTGG 3'
	Reverse	5' AACTCCAACAATGGCAGCA 3'
Lzp-s outer	Forward	5' AGACCGAAGCACCGACTATG 3'
	Reverse	5' TCCTGGCTGAAGAACTGACC 3'
Ptx3 outer	Forward	5' TTGGGTCAAAGCCACAGA 3'
	Reverse	5' AATGAACAATGGGCAACAGAG 3'
Laptm5 outer	Forward	5' CGCAGCCATAGGAAGTTAGG 3'
	Reverse	5' CGGCGAGACTGTTGGACT 3'
CCL6 outer	Forward	5' CTTTATCAGCAGGAGGGGAAC 3'
	Reverse	5' CCCAAGAGCCCAGTTTCAG 3'
Npm3 outer	Forward	5' ACACCCGCTCCTTCACTTT 3'
	Reverse	5' TCCCACCCCTATTCTCTTC 3'

<b>STEAP4 outer</b>	Forward	5' AAAGCAGCACTCGGCATACT 3'
	Reverse	5' AGAAAGCACACCACCACTCC 3'
<b>Slc6a14 outer</b>	Forward	5' TGGAGGATTTTGCCACTGTT 3'
	Reverse	5' ATGAGCCAAGCCAGAAGAAG 3'
<b>Lcn2 outer</b>	Forward	5' CCCTGTATGGAAGAACCAAGG 3'
	Reverse	5' AGGTGGATGGGGAGTGCT 3'
<b>ApoE outer</b>	Forward	5' GTGCTGTTGGTCACATTGCT 3'
	Reverse	5' GCGTATTTGCTGGGTCTGTT 3'
<b>Aldh1a7 outer</b>	Forward	5' TCAAGCCAGCAGAGCAAAC 3'
	Reverse	5' GGACAGGGACAGCCAAATAG 3'
<b>Dkk2 outer</b>	Forward	5' TCTTCCAAAGCCAGACTCCA 3'
	Reverse	5' TTCCCTGTTCTTCAGCGTTC 3'
<b>Nrk outer</b>	Forward	5' CAGATTCAAGTCGTGGAGCA 3'
	Reverse	5' GAACCAACAGCCAGGTCAA 3'
<b>Bcat1 outer</b>	Forward	5' GGATGCTGGGGTGATTGA 3'
	Reverse	5' TTCTTCCAAGTACTGTGCTG 3'
<b>Col3a1 QPCR</b>	Forward	5' AGGTTCTCCTGGTGCTGCT 3'
	Reverse	5' TGCCCACTTGTTCCATCTTT 3'
<b>Lzp-s QPCR</b>	Forward	5' GCCCATTCTGTCTCTTTCTCAC 3'
	Reverse	5' TGTTTTGCCCTGTTTCTGCT 3'
<b>Ptx3 QPCR</b>	Forward	5' ACGGAGGAGCCCAGTATGTT 3'
	Reverse	5' TCGTCTATTACGCACCGAAGT 3'
<b>Laptm5 QPCR</b>	Forward	5' GATTGTGGTGCCCGTTTG 3'
	Reverse	5' CTCCGTTTCTATTTCTTTTTCTCCT 3'
<b>CCL6 QPCR</b>	Forward	5' CCTAAGCACCCCTGAAGCAAG 3'
	Reverse	5' GGTCCTGGGGAAGACAGAA 3'
<b>Npm3 QPCR</b>	Forward	5' CGGACGAGTGTAATGTGGTG 3'
	Reverse	5' CAGGTGGTTGGAGTTGGAAA 3'
<b>STEAP4 QPCR</b>	Forward	5' GGAGAAAAGCCCCAAATGA 3'
	Reverse	5' ACCCAAATACCCCAGA 3'
<b>Slc6a14 QPCR</b>	Forward	5' TCTTGGGCAGACGAAAAGT 3'
	Reverse	5' GCAGGTGAGATTGCTGGTATTT 3'
<b>Lcn2 QPCR</b>	Forward	5' CTGAATGGGTGGTGAGTGTG 3'
	Reverse	5' CTTGGTATGGTGGCTGGTG 3'
<b>ApoE QPCR</b>	Forward	5' GTGGCAAAGCAACCAACC 3'
	Reverse	5' TCCGTCATAGTGCCTCCATC 3'

<b>Aldh1a7 QPCR</b>	Forward	5' CAGATGCCGACTTGGACAG 3'
	Reverse	5' TCCTCAACAAAAAGCCTGGA 3'
<b>Dkk2 QPCR</b>	Forward	5' TTGGAATGCGGAAGAATGAG 3'
	Reverse	5' GAGGCACATAACGGAAGCAC 3'
<b>Nrk QPCR</b>	Forward	5' GCGATGAGGAAGAAAGAGGA 3'
	Reverse	5' CACAGCAACCGCAATGTATG 3'
<b>Bcat1 QPCR</b>	Forward	5' AGGTGTCTGAGGCTGGTTGT 3'
	Reverse	5' CTATGTGCTGGGCTTTGAGG 3'
<b>Mouse D6 QPCR</b>	Forward	5' TTCTCCCACTGCTGCTTCAC 3'
	Reverse	5' TTCCATCTCAACATCACAGA 3'
<b>Mouse GAPDH QPCR</b>	Forward	5' CAGCAAGGACACTGAGCAAG 3'
	Reverse	5' TATTATGGGGGTCTGGGATG 3'
<b>Human D6 QPCR</b>	Forward	5' AGGAAGGATGCAGTGGTGTC 3'
	Reverse	5' CGGAGCAAGACGATGAGAAG 3'
<b>Human GAPDH QPCR</b>	Forward	5' CAAGGCTGAGAACGGGAAG 3'
	Reverse	5' GGTGGTGACGCCGCCAGT 3'

### **2.1.6 Tissue culture media and reagents**

**Gibco (Invitrogen, Paisley, UK)**

Dulbecco's modified Eagle's Medium (DMEM)

Fetal Calf Serum (FCS)

Glutamine

Streptomycin/Penicillin

Trypsin (0.25%)

**Cambrex (Walkersville, MD)**

Keratinocyte bullet kit (keratinocyte growth media and supplements)

## **2.2 Methods**

### **2.2.1 *Molecular Biology***

#### **2.2.1.1 Preparation of genomic DNA from tail tips**

Tail tips from weaned mice were digested in screwcap eppendorfs with 100µl lysis buffer (100mM TrisHCl, 5mM EDTA, 0.2% SDS, 200mM NaCl) and 1µl (10mg/ml) proteinase K in a water bath at 55°C overnight. The tubes were heated for 5 minutes in a heating block at 96°C then each sample was diluted with 500µl of double distilled water (ddH<sub>2</sub>O). The tubes were centrifuged at 12,000x g and stored at 4°C. For neonates, the tail tips were only incubated for 6 hours in the water bath and were then processed as described above.

#### **2.2.1.2 RNA extraction using Trizol**

Trizol was used for RNA extraction from tissues following manufacturer's instructions. Tissues were 'snap frozen' with liquid nitrogen and ground with a mortar and pestle. For homogenisation, 1ml Trizol was added per 50-100mg tissue, thoroughly mixed and left for 5 minutes to dissociate complexes. Chloroform, 0.2ml per ml Trizol, was added and the tubes inverted 15 times before incubation at room temperature for 2 minutes. The tubes were centrifuged (12,000x g, 15 minutes, 2-8°C) and the RNA layer (colourless aqueous layer) was transferred to a fresh RNase free tube. RNA was precipitated from the aqueous layer with isopropyl alcohol (0.5ml/1ml trizol) and incubated for 10 minutes at room temperature, centrifuged (10 minutes, 12,000 x g) and the supernatant carefully removed. The pellet was washed with 75% ethanol, centrifuged (7,500x g, 5 minutes, 2-8°C), supernatant removed and the RNA pellet left to dry. The pellet was resuspended in 100µl RNase free water. RNA concentration was measured using a spectrophotometer.

RNA was DNase-treated, to remove any DNA present, using the RNase-free DNase kit according to manufacturer's instructions. 10x DNA buffer (5µl) was added to 5µg RNA sample along with 1µl DNase and made up to 50µl with diethylpyrocarbonate (DEPC) treated water and incubated at 37°C for 30

minutes. DNase inactivating reagent (5 $\mu$ l) was added and mixed thoroughly for two minutes at room temperature then spun at 12,000x g at 4°C for 2 minutes. The DNase free RNA was transferred to a fresh clean tube. However, most of the RNA was DNase treated using RNeasy mini columns and on-column DNase treatment (see 2.2.1.4).

### **2.2.1.3 RNA extraction using RNeasy Mini Kit**

The RNeasy kit technology involves the lysis of tissue or cells by using a buffer containing guanidinium-isothiocyanate (buffer RLT), which will denature any RNase enzymes present, preventing RNA from being destroyed. The kit also contains silica-gel-membrane columns, which allow RNA to bind, in ideal binding conditions with the use of ethanol, and any contaminants present are removed by washing and centrifuging the columns.

Extraction of RNA from cells was performed following manufacturer's instructions. In brief, cells were disrupted with either 350 $\mu$ l or 600 $\mu$ l buffer RLT containing 2-mercaptoethanol, depending on the number of cells. This process lyses the cells and inactivates any RNases present by denaturing them. The cells were then homogenised by passing the lysate through a 20-gauge needle at least five times. One volume of 70% ethanol was added to the lysate, and mixed thoroughly before applying to the RNeasy spin column. The columns were centrifuged for 15 seconds at 8,000 x g and the flow through discarded. Wash buffer, RW1, (350 $\mu$ l) was then applied to the column, centrifuged (15 seconds, 8,000x g) and the flow through discarded followed by a 15 minute incubation with DNase1 at room temperature. The columns were washed with 350 $\mu$ l of wash buffer RW1, centrifuged and the flow through was discarded. Buffer RPE (500 $\mu$ l) was applied to the column, which was then centrifuged at 8,000x g. A second volume of RPE was added, to ensure all contaminants were removed, and the column was centrifuged at 8,000x g for 2 minutes. RNA was eluted in RNase-free water and centrifuged at 8,000x g for 1 minute before the concentration of RNA was measured using a spectrophotometer.

#### **2.2.1.4 RNA clean up**

This method was applied to RNA extracted from tissues, which was required for quantitative PCR (QPCR). The RNA clean up method involved DNase treatment using the RNeasy mini kit to remove any contaminating DNA. In brief, no more than 100µg RNA was loaded onto an RNeasy mini column. The sample was adjusted to a volume of 100µl, if required, with RNase free water. Buffer RLT (350µl) was added to the RNA sample and mixed thoroughly before addition of 250µl ethanol and was applied to the RNeasy mini column. From this point on, the method followed was the same as in 2.2.1.3

#### **2.2.1.5 RNA quality test**

Once RNA was isolated from tissues or cells and had been DNase treated, a small sample was tested to check the quality of RNA and to ensure no degradation had occurred. RNA (1µl) was mixed with 3µl ddH<sub>2</sub>O and 1µl 5x loading dye and electrophoresed on a 1% agarose gel (see 2.2.1.8) for 20 minutes at 120V and visualised under a ultraviolet (UV) light for the presence of the 28s and 18s ribosomal bands of RNA. Intact RNA displays 2 clear and sharp bands which correspond to the 28s and 18s bands, with the 28s band being twice as intense as the 18s band. If no distinct bands but a smear appeared, this indicated that the RNA was degraded and was of no use.

The quality of RNA can also be checked when quantifying RNA using a spectrophotometer. The absorbance of the RNA is measured at 260 and 280nm and the ratio of these readings give an indication of the quality of the RNA and whether there are any contaminants such as protein or phenol. A ratio of 1.8 to 2.1 indicates that the RNA is good quality and has limited contamination.

#### **2.2.1.6 cDNA synthesis from RNA**

cDNA was transcribed from RNA using Superscript first strand cDNA synthesis kit following manufacturer's instructions. For each sample, a minus reverse transcriptase (RT) reaction was performed as a control. In brief, 1µg RNA was placed in an RNase free tube with 1µl dNTP and 1µl Oligo (dT) and made up to a final volume of 10µl in DEPC treated water, incubated at 65°C for 5 minutes and

placed on ice for 1 minute. An RT master mix was made up per reaction to contain 2 $\mu$ l 10xRT buffer, 4 $\mu$ l 25mM MgCl<sub>2</sub>, 2 $\mu$ l 0.1M DTT and 1 $\mu$ l RNase OUT recombinase inhibitor. Master mix (9 $\mu$ l) was added to each denatured RNA sample and incubated for 2 minutes at 42°C. Superscript II RT (1 $\mu$ l) or DEPC-treated water (1 $\mu$ l) was added to the +RT and -RT samples respectively. All samples were incubated at 42°C for 50 minutes followed by a 15-minute incubation at 70°C to inactivate the reaction and then chilled on ice. RNase H (1 $\mu$ l) was added and the samples were incubated for 20 minutes at 37°C. The first strand cDNA could then be amplified by polymerase chain reaction (PCR) or diluted 1:5 in nuclease free water for quantitative polymerase chain reaction (QPCR).

### **2.2.1.7 Polymerase chain reaction**

Polymerase chain reaction is a method that amplifies DNA, in which one PCR cycle ideally doubles the amount of the targeted sequence. Each PCR cycle consists of three steps, a denaturing step, an annealing step and a primer extension step. The denaturing step is first where the temperature is high to separate double stranded DNA into single strands. The annealing step involves a decrease in temperature and allows the primers to bind (or anneal) to the target DNA template. The temperature is increased in the primer extension step, to an optimum temperature that will allow DNA polymerase to bind and elongate the primers generating new DNA and the cycle starts again. After 25 to 35 cycles, the amplified product can be analysed.

ReddyMix PCR master mix tubes were used for PCR applications. 1 $\mu$ l (or 0.4 $\mu$ l for genotyping) of each of the appropriate forward and reverse primers at a concentration of 10 $\mu$ M (20 $\mu$ M for murine D6) were normally used. When the DNA template concentration was not known, 2 $\mu$ l was used unless it was for genotyping of primary keratinocytes where 3.75 $\mu$ l was added. The tubes were incubated in a PCR thermocycler. Primer sequences used are detailed in section 2.1.5.

The PCR programmes were as follows;

**WT/K14mD6 genotyping:** 96°C for 5 minutes, (96°C for 15 seconds, 55°C for 15 seconds, 68°C for 30 seconds) x 35 cycles, 68°C for 10 minutes, using K14mD6 primers.

**Primary keratinocyte genotyping:** same as WT/ K14mD6 genotyping.

**Detection of murine D6:** 94°C for 2 minutes, (92°C for 15 seconds, 55°C for 15 seconds, 72°C for 30 seconds) x 30 cycles, 68°C for 10 minutes, using 20µM mD6 primers.

**Detection of CCR1, 3 and 5:** 94°C for 10 minutes, (94°C for 15 seconds, 59°C for 30 seconds, 72°C for 30 seconds) x 35 cycles, 72°C for 10 minutes.

**Detection of CCR2 and 4:** 94°C for 10 minutes, (94°C for 15 seconds, 61°C for 30 seconds, 72°C) x 35 cycles, 72°C for 10 minutes.

**β-Actin:** 94°C for 2 minutes, (92°C for 15 seconds, 55°C for 15 seconds, 72°C for 30 seconds) x 30 cycles, 68°C for 10 minutes.

### **2.2.1.8 Agarose gel electrophoresis**

Electrophoresis grade agarose was dissolved in 1x tris-acetate EDTA (TAE) buffer by heating. Ethidium bromide was added to the cooled gel to give a final concentration of 0.05µg/ml and then the gel was poured to set in a flat cassette apparatus at room temperature. Samples were run alongside a DNA ladder marker and, unless otherwise stated, all gels were run at 90V in 1xTAE buffer. DNA was visualised under UV light and the gel image captured using an Alpha Imager gel documentation system.

### **2.2.1.9 Quantitative polymerase chain reaction**

Standard PCR gives an indication of the presence of transcripts however; it is not accurate in assessing quantitatively if one sample contains more transcripts than another sample. To do this, requires a method known as quantitative PCR or

real-time PCR. This QPCR protocol determined transcript number utilising a methodology based on a SYBR Green master mix, which contains SYBR Green I dye that binds double stranded DNA resulting in a fluorescent signal being emitted (Morrison et al., 1998). Therefore, as SYBR Green detects new copies of double stranded DNA formed during the PCR reaction, the fluorescent intensity increases. This method involved using a standard curve, which required the generation and isolation of standards for the gene of interest as well as designing and validating primers to use in the QPCR machine.

### *Designing primers*

Two sets of primers were required for each gene of interest in SYBR Green based QPCR. One is a set of 'inner' (nested) primers for use in the QPCR machine and the second set, 'outer' primers were designed to generate PCR products of the gene of interest to act as standard templates. Therefore, standard templates are generated by PCR using outer primers to amplify a specific part of DNA in which the inner primers bind.

All primers were designed using Primer3 software and the nucleotide sequence of the gene of interest. Primer3 software is available at; ([http://www.broad.mit.edu/cgi-bin/primer/primer3\\_www.cgi/](http://www.broad.mit.edu/cgi-bin/primer/primer3_www.cgi/)). Primers were designed with QPCR specification, which are more stringent than required for standard PCR primers, such as optimal melting temperature of the primers ( $T_m$ ), maximum self-complementarity and maximum 3' self-complementarity. The maximum self-complementarity determines the alignment and self-complementarity of a single primer as well as a maximum alignment score for the complementarity between the left and right primers as a pair. Maximum 3' self-complementarity is the maximum alignment score allowed when testing a single primer for self-complementarity and for the complementarity between the 3' of the left and right primers. Maximum 3' self-complementarity score between primers gives an indication of the likelihood of primer-dimers occurring during PCR. The specifications of the primers were designed to the conditions of;

- between 18 and 23 base pair (bp) in length
- between 40 and 65% GC content,

- melting temperature of the primers should be between 59.5°C and 61.5°C with an optimal  $T_m$  of 60°C,
- product size should be between 100 and 180bp,
- maximum self-complementarity : 2
- maximum 3' self-complementarity: 1
- avoid stretches of 4 G or C bases in a row.

Primers were designed to bind within the last 1500bp of the 3' end of the mRNA. Using these specifications, primers were usually generated however if no primers were suggested by Primer3, some conditions were relaxed until primers were suggested. These conditions were increasing maximum self-complementarity from 2 to 3, decrease the optimal melting temperature of the primers to 59°C or examine more of the 5' sequence on the template until suitable primers are found. One condition that was not relaxed was the maximum 3' self-complementarity, which remained at 1. These specifications were used to design 'inner' QPCR primers. Once these were designed, outer primers were designed to amplify the region in which inner QPCR primers would bind. The 'outer' primers were designed using the same software and similar parameters however, they were allowed to have higher self-complementarity and generate a larger product size.

### *Validation of primers*

Both sets of primers were tested for specificity by standard PCR using cDNA prepared from RNA isolated from tissue or cells known to express the gene of interest. In general, 2µl of cDNA and 1µl of the forward and reverse primer were added to Reddy mix tubes. The PCR programme was 95°C for 3 minutes, (95°C for 15 seconds, 59°C for 20 seconds, 72°C for 20 seconds) x35 cycles, 72°C for 10 minutes. PCR products were separated using electrophoresis on an agarose gel (1% for PCR products containing standards and 2% for PCR products generated using inner QPCR primers) and visualised using ethidium bromide under a UV light. Inner QPCR primers were suitable for QPCR if a single, clear and distinct band of the correct size occurred, therefore indicating specificity. However if multiple bands occurred, this suggested that the inner QPCR primers were

unsuitable for QPCR. However, if primer-dimer or low molecular weight bands occurred, then altering PCR conditions, such as increasing annealing temperature or decreasing primer concentration or both, could correct for these. On the other hand, if no product was visible, then increasing primer concentration and/or decreasing annealing temperature helped primers to produce a specific product.

### *Generating standards for QPCR*

To quantify the levels of the gene of interest in unknown samples, the generation of a standard curve was required. A PCR product using the outer primers generated a standard DNA template for each gene of interest. The product generated was required to be a clear distinct band of the predicted size. If this was the case, the PCR product was purified using a PCR purification column following manufacturer's instructions (Qiagen QIAquick PCR purification kit). In brief, 5 volumes of binding buffer PB were added to 1 volume of PCR sample and mixed. A yellow coloured sample indicated the pH was less than or equal to 7.5, which is optimal for DNA adsorption. The sample was applied to the QIAquick column and centrifuged for 30 seconds to allow binding of DNA. The flow through was discarded and 0.75ml Buffer PE was added to the column and centrifuged for 30 seconds to wash impurities through the column. The flow through was discarded and the column was centrifuged for a further 30 seconds to remove any ethanol residue then the QIAquick column was placed in a clean eppendorf tube. Buffer EB (50µl) was added to the centre of the QIAquick membrane and the column was centrifuged for 1 minute to elute DNA. The purified PCR products were diluted in nuclease free water to generate serial dilutions, each being 10 fold more dilute than the previous. The range of standards was from  $1 \times 10^{-4}$  fold dilution to  $1 \times 10^{-9}$  fold dilution to generate a good standard curve. Each of these standards was used as a template for QPCR using the inner QPCR primers for amplification. Using standards where different levels of template are present gives an indication of the range and sensitivity of the assay. The use of standards allows relative or absolute quantification of unknown transcript levels.

### *Calculating transcript numbers*

Relative quantification was used to determine relative differences of gene transcript levels between samples and was expressed as fold change. For relative quantification, arbitrary values were given to the standards. For example,  $1 \times 10^{-4}$  fold dilution was given the arbitrary value of 10,000,000 copies and  $1 \times 10^{-9}$  fold dilution standard was given the arbitrary value of 100 copies.

To quantify the absolute level of transcripts, the number of copies of PCR products within each standard was determined. To do this,  $3 \mu\text{l}$  of each standard PCR product, after purification, was mixed with  $1 \mu\text{l}$  ddH<sub>2</sub>O and  $1 \mu\text{l}$  5x loading dye and run on a 1% agarose gel alongside  $5 \mu\text{l}$  Hyperladder I marker, where the mass of each band is known. The intensity of the bands in Hyperladder I and standard PCR products were quantified by densitometric analysis using software on the Alpha Imager gel documentation system. A standard curve was generated using the known mass of the Hyperladder band and the band's intensity. Therefore using the intensity of the standard PCR product, the mass per  $\mu\text{l}$  was determined using the standard curve. Transcript copy numbers within each standard was calculated using a series of formulae and facts as follows.

Firstly, the molecular weight of the standard was calculated;

- Average molecular weight for double stranded nucleotide = 660 Daltons
- Molecular weight of double stranded DNA = 660 Daltons x bp length

The number of moles/ $\mu\text{l}$  was calculated;

- Moles of standard = (mass/ $\mu\text{l}$ )/(molecular weight DNA)

Then to convert moles into copy number, the number of molecules per mole is  $6.023 \times 10^{23}$  copies (Avogadro's constant)

- Copies DNA per  $\mu\text{l}$  = Avogadro's Constant x moles

The known value of copies of DNA per  $\mu\text{l}$  was used to calculate the number of copies in each of the diluted standards.

### *Setting up SYBR green based QPCR*

Before starting, a plan was made of the 96 well QPCR plate, and a master mix was made to cover all reactions within the QPCR plate. For each reaction, 7.5µl of Power SYBR Green master mix, 0.6µl of primer mix and 5.4µl of nuclease free water were mixed together.

Standard or sample cDNA (4.5µl) was placed in a mixing well, along with 40.5µl master-mix and was mixed thoroughly and carefully by pipetting up and down three times. Of this, 15µl was placed in three of the wells on the QPCR plate (each sample was applied in triplicate). A non-template control (NTC) was also included to determine the level of contamination and the detection limit of the assay. The plate was spun for 20 seconds at 400x g before being placed in the QPCR machine (Applied Biosystems 7900HT Real time PCR system). In general, the QPCR conditions were; 94°C for 10 minutes, (94°C for 3 seconds, 60°C for 30 seconds) x 40 cycles followed by a dissociation stage. A dissociation stage for SYBR Green based QPCR is important, as a melt curve analysis can be determined at the end, which allows determination of the specificity of the PCR reaction.

The software on the QPCR machine automatically works out the level of fluorescence that indicates exponential PCR amplification and the cycle number at which each well crosses the threshold. This is known as the Ct value. By using arbitrary or absolute copy numbers, the software can then use the Ct value to calculate the copy numbers in each sample taken from the standard curve. However, before using these values, certain analysis of the data is required. The standard curve should have a correlation of  $r^2 > 0.97$  and a slope of approximately 3.3 (this means the PCR product has amplified 10-fold every 3.3 cycles and indicates the reaction was 100% efficient). The Ct value generated the NTC sample was noted as this signifies the sensitivity level of the assay. Examination of the dissociation curve should reveal one peak indicating the reaction was specific and no primer-dimer occurred.

### *Normalising QPCR data*

All QPCR data was normalised using a housekeeping gene. To allow comparison of gene levels between samples, the amount of housekeeping gene within all

samples was assessed. The housekeeping gene used was glyceraldehyde-3-phosphate dehydrogenase (GAPDH). The GAPDH gene codes for an enzyme (catalyses the oxidative phosphorylation of glyceraldehyde -3-phosphate to 1, 3-diphosphoglycerate) involved in cell metabolism. The amount of transcripts of the gene of interest is normalised using the housekeeping gene to control for varying amounts of cDNA between samples due to differential rates of RNA degradation, varying efficiency during the RNA extraction procedure and the efficiency of the reverse transcription reaction.

To calculate absolute transcript levels for the gene of interest, the data was normalised to GAPDH using the following calculation:

- $\text{Copy number of gene of interest} / \text{copy number of GAPDH gene} \times 10^5$

This gives the copy number of the gene of interest per 10,000 copies of GAPDH

When calculating relative levels for the gene of interest, each sample was allocated a ratio of its GAPDH content compared to the 75<sup>th</sup> percentile of the GAPDH levels of all the samples. The levels of the gene of interest were then normalised by dividing by the GAPDH ratio. An example is shown below:

Sample	Gene of interest (copy number)	GAPDH (copy number)	GAPDH ratio	Corrected level of gene of interest
skin	40	14	0.86	46.4
skin + x	40	17	1.04	38.2
	<b>75<sup>th</sup> percentile</b>	<b>16.25</b>		
WT keratinocyte	88	36	1.10	39.7
WT keratinocyte + x	44	22	0.67	32.5
	<b>75<sup>th</sup> percentile</b>	<b>32.5</b>		

**Table 2-1. Example of normalisation of QPCR data using a housekeeping gene to determine levels of 'gene of interest'.**

In the first example, skin and skin + x appear to express a similar level of the 'gene of interest'. Once the data has been normalised, skin actually has higher levels of 'gene of interest' than skin+x. This was because the skin expressed a lower level of GAPDH (14 copies) than skin+ x (17 copies). In the second example, initially the level of the 'gene of interest' in WT keratinocytes appears to be 2-fold higher than WT keratinocyte+x. Once normalised, it can be seen that the difference in the levels of the 'gene of interest' between WT keratinocytes and WT keratinocytes+X is actually less.

## **2.2.2 *In vivo analysis***

### **2.2.2.1 Maintenance of mice**

Mice were housed within the animal facility at the Central Research Facility at Glasgow University. All procedures performed on mice were in accordance with United Kingdom Home Office guidelines as well as under appropriate project and personal licences.

### **2.2.2.2 Genotyping of mice**

A K14D6 mouse colony was maintained by crossing of K14D6 x FVB/N wild-type mice resulting in littermates being either K14D6 or wild-type. Weaned mice and neonates were tail tipped and DNA was extracted (see 2.2.1.1). Genotype was determined by PCR. DNA (2 $\mu$ l) and 0.4 $\mu$ l of 10 $\mu$ M K14mD6 primers were added to pre-aliquoted redy master mix tubes. PCR conditions were 96°C for 5 minutes, (96°C for 15 seconds, 55°C for 15 seconds, 68°C for 30 seconds) x 35 cycles and 68°C for 10 minutes. PCR products were electrophoresed on a 1% agarose gel containing ethidium bromide. A band of approximately 400bp size indicated K14D6 transgenic and no band indicated D6 wild-type littermate.

### **2.2.2.3 Epidermal sheet preparation**

Two methods were tested to determine the best method to isolate epidermal sheets from mouse skin. Subcutaneous fat was removed from dorsal skin and the skin was cut into small sections. One method involved incubating the skin, dermal side down, in 0.5M ammonium thiocyanate in PBS for 10 and 20 minutes at 37°C. The second method involved incubating the skin, dermal side down, in 0.025M EDTA for 2 hours at 37°C. Dermal and epidermal sections were separated carefully and were fixed in formalin to be stained with haematoxylin and eosin or were 'snap-frozen' in liquid nitrogen for RNA extraction following the method described in 2.2.1.2.

#### **2.2.2.4 Harvesting of primary keratinocytes**

Neonates (from K14D6 x WT crosses) were sacrificed, placed into 70% ethanol and tail tipped for genotyping using K14mD6 primers (see 2.2.1.1 and 2.2.2.2). A clean cut of the skin was made from the tail to the head and the body was separated from the skin. The skin was placed dermal side down, stretched on the tissue culture dish with forceps and left for 20 minutes to dry before the skin was placed dermal side down in 0.25% trypsin overnight at 4°C. The epidermis was carefully peeled apart from the dermis, placed into 15ml tubes containing DMEM/10% FCS, and shaken for 20 minutes. The suspension was filtered through a gauze swab, centrifuged (1000x g for 5 minutes) and the supernatant carefully discarded (Yao et al., 2006). The pellet was resuspended in 1ml supplemented keratinocyte growth media (KGM) per skin containing 0.05mM calcium ready to seed and be cultured for five days for either RNA isolation, western blotting or flow cytometry.

#### **2.2.2.5 Staining of primary keratinocytes**

Keratinocytes were harvested and resuspended before seeding 500µl into chambered slides coated with fibronectin. The cells were fed every two days with fresh keratinocyte growth media. On day 5, the media was aspirated and the slides were allowed to dry before the sides of the chambered slides were broken off. Cells were fixed in methanol for 10 minutes and allowed to air dry. The cells were incubated in the red stain from the RAPI-Diff II kit, which is a staining kit similar to giemsa, for 3 minutes and 30 seconds then put into the blue stain for 10 seconds and rinsed in ddH<sub>2</sub>O and allowed to air dry. A coverslip was applied, mounted with DPX solution and dried for 24 hours. Pictures were taken with Axiovision software and microscope.

#### **2.2.2.6 Assessment of keratinocyte purity**

Keratinocytes from individual neonates were isolated and cultured for five days to be assessed for purity by flow cytometry. At the stage of isolation, keratinocytes were resuspended in 1ml KGM. 200µl of keratinocytes was aliquoted into wells in 24 well plate and cultured for five days. Keratinocytes were trypsinised in 1ml 0.25% trypsin for 5 minutes at 37°C and washed with

PBS/2mM EDTA/0.1% FCS (PEF) then permeabilised using a standard fix-permeabilisation kit, which permeabilises cells. Keratinocytes were labelled for 10 minutes at room temperature with 1.5µg/ml FITC-conjugated mouse anti-cytokeratin (pan) antibody or FITC-conjugated mouse IgG1 antibody (isotype control). Keratinocytes were washed and analysed by flow cytometry using a FACS Calibur machine, in which cytokeratin expression was measured and compared to the isotype control.

### **2.2.2.7 Incubation of keratinocytes with biotinylated CCL3**

Keratinocytes from individual neonates were isolated and cultured in 6cm plates. On day 5, media was aspirated from primary keratinocytes, washed with PBS and 1ml of fresh KGM containing 1% BSA was added. To each plate of  $2.5 \times 10^5$  cells, 10nM biotinylated CCL3 (BioCCL3) was added and incubated at 37°C. Media was sampled from the plates at various timepoints for western blotting. To ensure the result was D6 specific, keratinocytes were incubated with 10nM BioCCL3 and 100nM CCL22. Both are D6 ligands and therefore this is a D6-specific competition assay. Media was also sampled at various time points for western blotting.

### **2.2.2.8 Detection of biotinylated CCL3 by western blotting**

15µl of KGM media sampled from keratinocytes incubated with BioCCL3 were mixed with 15µl 2x Laemmli buffer and heated at 90°C for 5 minutes. Samples were added to a well in a 4-12% NuPage Bis-Tris gel alongside a multicolor multicolour standard, in the inner chamber of the tank containing MES running buffer with 0.1M DTT. The outer chamber of the tank was filled with MES running buffer and the gel set to run at 120V for one and a half hours or until the bromophenol blue marker was approximately  $\frac{3}{4}$  of the way down the gel. The gel was then placed onto a nitrocellulose transfer membrane in a blot module with transfer buffer and run at 150mV for approximately two hours. The transfer membrane was left overnight in 10% powdered milk in PBS at 4°C. The membrane was washed several times with PBS/0.1% Tween 20 for approximately half an hour. The detection agent, streptavidin labelled horseradish peroxidase (HRP) was diluted 1:2000 and incubated with the transfer membrane for 1 hour before thoroughly washing with PBS/0.1% Tween 20. The chemiluminescent

substrate for HRP was detected by 'west femto' and the membrane was drained, exposed to x-ray film, which was then placed through a film developer.

### **2.2.2.9 Assessment of CCL2 binding by keratinocytes using flow cytometry**

Individual keratinocytes were isolated and cultured for five days to be assessed in their ability to bind CCL2 by flow cytometry. At the stage of isolation, keratinocytes were resuspended in 1ml KGM. 200µl of keratinocytes were aliquoted into wells in 24 well plates and cultured for five days. On day 5, 250µl fresh media containing 1% BSA was added to the cells. Keratinocytes were incubated with either PBS, 25nM CCL2 conjugated to Alexa 647 (CCL2-alexa 647) or 25nM CCL2-alexa 647 and 250nM CCL3 for 100 minutes at 37°C. Keratinocytes were trypsinised in 1ml 0.25% trypsin for 5 minutes at 37°C and washed twice with PEF (PBS/2mM EDTA/0.1% FCS). Keratinocytes were then analysed for binding of CCL2-alexa 647 using the FACS Calibur flow cytometry.

### **2.2.2.10 Testing an anti-mouse D6 antibody**

A polyclonal antibody raised in chicken against murine D6 became available. It was not known whether this antibody would be specific for D6 and therefore the antibody was required to be tested and optimised. It was decided to test the antibody on cells known to express murine D6 using western blotting. A stable transfected cell line (Human Embryonic Kidney cells (HEKs)) expressing murine D6 had been made and used within our lab previously known as HEKmd6. HEKs and HEKmd6 were cultured in complete DMEM (containing 10% fetal calf serum, 4mM L-glutamine, penicillin and streptomycin). Once the cells were confluent, the cells were trypsinised, centrifuged for 5 minutes and the cell pellet resuspended in 5 ml of media. The cells were counted and  $2 \times 10^6$  cells were aliquoted and centrifuged again for 5 minutes. The cell pellet was lysed in 500µl of cell lytic-M mammalian cell lysis buffer and placed on ice for 15 minutes. The lysed cells were then centrifuged and the supernatant was carefully taken off. Total protein levels within the supernatants were measured using a bicinchoninic acid (BCA) protein assay following manufacturer's instructions. In brief, 25µl sample or standard was added in duplicate to a 96 well plate and 200µl of reagent was added to each well. The plate was mixed thoroughly on a plate

shaker for 30 seconds and incubated at 37°C for 30 minutes before absorbance was measured at 562nm in a plate reader. For the western blot, 15µl of supernatant contained a total of 10µg protein and was mixed with 15µl HU buffer (8M urea, 5% SDS, 200mM Tris-HCl pH8.0, 0.1mM EDTA, 0.5% bromophenol blue, 100mM DTT). The gel and transfer membrane were run as described in 2.2.2.8. The primary antibody, anti-mouse D6 antibody, was diluted and incubated with the transfer membrane for 1 hour at room temperature before thoroughly rinsing with PBS/0.1% Tween 20. The secondary antibody, donkey anti-chicken conjugated to HRP, was diluted 1:5000 and added to the membrane for 1 hour before washing with PBS/0.1% Tween. The chemiluminescent substrate for HRP was detected by incubation with 'west pico' for 5 minutes and then membrane was drained, exposed to x-ray film, which was then placed through a film developer.

#### **2.2.2.11 Cutaneous skin inflammation model**

The dorsal skin of mice was shaved and two days later 150µl of a 50µM solution of Phorbol 12-Myristate 13-Acetate, (PMA, also known as TPA) was applied to the dorsal skin of each mouse on three consecutive days to induce inflammation.

#### **2.2.2.12 Haematoxylin staining**

Mouse dorsal skin was placed into 10% neutral buffered formalin and transported to the University of Glasgow Veterinary School, where the sections were cut and stained with haematoxylin and eosin.

#### **2.2.2.13 Measuring skin thickness**

Haematoxylin and eosin skin sections were analysed for skin thickness, in particular epidermal and dermal thickness. A specialised eyepiece containing a grid was used in the microscope. Thickness was assessed by counting the number of squares the skin filled, which was then multiplied by 50 to convert the thickness to microns.

### **2.2.3 Keratinocyte microarray**

Microarrays allow the analysis of expression of thousands of genes in one assay. Microarray platforms are chips with a solid matrix consisting of fixed DNA sequences (probes) that correspond to specific genes, in a known order. RNA is harvested from the cells or tissues of interest and labelled. The labelled targets are hybridised to the probes, which then provides a quantitative measure of the abundance of RNA sequences within the target population. In this project, an oligonucleotide microarray was used (Affymetrix GeneChip). These chips contain thousands of oligonucleotides, which are single stranded probes made based on sequence information in databases, on a glass surface. Target RNA is biotinylated and added to the GeneChip. A streptavidin-phycoerythrin conjugate recognises any hybridised probes and fluorescent signals emitted are then detected.

#### **2.2.3.1 Keratinocyte incubation and RNA extraction**

Keratinocytes were isolated from 1 neonate skin, pooled into groups of three and seeded into T75 flasks and cultured for 5 days. On day 5, media was removed and 5ml fresh KGM was added along with PBS or 10nM CCL3 in PBS and incubated for 6 hours at 37°C. Media was removed and RNA was extracted from cells using RNeasy mini kit (see 2.2.1.3). Samples were transferred to the Sir Henry Wellcome Functional Genomics Facility (University of Glasgow) where further processing of samples was carried out and the microarray analysis performed. RNA quantity and quality was assessed using a Nanodrop 1000 and the Bioanalyser 2100 respectively. Each sample was subject to linear amplification before being converted to biotinylated cRNA and applied to Affymetrix GeneChip Mouse genome 430 2.0 Array for generation and analysis of data.

#### **2.2.3.2 Microarray analysis**

The data from the Affymetrix gene chips were analysed using combinations of Rank Products (RP) and Iterative Group Analysis (iGA). Rank Products generates lists of differentially expressed genes and determines statistical significance to each gene. Rank products are more reliable and consistent, when datasets contain low sample numbers or noisy datasets, than the popular method,

significance analysis of microarrays (SAM) for differential gene expression analysis (Jeffrey IB et al. 2006). The lists of genes produced by Rank products are processed using Iterative group analysis (iGA), which identifies functional changed groups of genes, assigned according to Gene Ontology (<http://www.geneontology.org>). Iterative group analysis combines the relative position of the genes in RP list and the number of changed genes within the group to determine the strength of changes within the group statistically. An important feature is that experimental replicates are not required because statistical significance can be determined by using group members as internal replicates. Terminology used by this software can be found in Appendix One. Full microarray data using Rank Products and iGA analysis can be found in Appendix Two and Three respectively. Validation of microarray data was performed by quantitative PCR.

## **2.2.4 Human analysis**

### **2.2.4.1 Collection of human psoriasis skin biopsies**

Skin biopsies were obtained from control, psoriasis and eczema patients and stored in 10% neutral buffered formalin by a dermatologist, Anne Sergeant, from clinics at Glasgow Royal Infirmary. Some of the samples were processed and made into cDNA (see 2.2.1.2 and 2.2.1.6) and analysed for D6 transcripts using quantitative PCR. Other skin biopsies were kept for embedding into paraffin blocks to use for immunohistochemistry.

#### ***Embedding of human tissue***

Skin biopsy samples were placed in trays and placed in an embedding machine (Thermo) to be embedded in paraffin wax blocks. Samples were placed in 10% neutral buffered formalin for 30 minutes, 70% alcohol for 1 hour, 90% alcohol for 1 hour, 95% alcohol for 1 hour then 5.5 hours in 100% alcohol, 3.5 hours in xylene and 9 hours in wax. The samples were placed in a known orientation and allowed to set in wax ready for sections to be cut onto poly-lysine coated slides.

### ***Haematoxylin and eosin staining***

Sections were placed in xylene for 3 minutes, 10 dips in 100% alcohol, 10 dips in 70% alcohol, washed in running water and placed in haematoxylin Z for 7 minutes. The sections were then washed in running water followed by 12 dips in 1% acid alcohol, rinsed in running water, placed in Scotts tap water solution for 2 minutes and the sections were checked for staining microscopically. Once staining occurred, the sections were washed in running water and then placed in Putts eosin (diluted 1:2 with water) before being washed again in running water for 2 minutes. The sections were dehydrated in 70% alcohol, two sets of 100% alcohol and three sets of xylene for 1 minute each. The sections were mounted with coverslips using DPX mounting solution and allowed to air dry.

### ***Immunohistochemistry using anti-human D6 antibody***

A monoclonal anti-human D6 antibody had previously been optimised for use on human placenta. However, none of this clone was available and therefore a different clone of antibody was used and required testing on human placenta and optimisation on human skin sections. Once optimised the protocol was as follows; Slides were heated in an oven at 60°C for 35 minutes, dewaxed in xylene for 10 minutes before being rehydrated in 100% ethanol (2x 5 minutes), 95% ethanol (2x 5 minutes), 70% ethanol (5 minutes), PBS (5 minutes). Endogenous peroxidase activity was blocked by immersing slides in freshly prepared 0.5% hydrogen peroxide in methanol for 30 minutes then the slides were washed in PBS twice each for 5 minutes. To retrieve antigens, slides were immersed in 1mM citrate buffer (pH 6.0) and boiled in the microwave for 3x 5 minutes. The slides were left to cool for 20 minutes before being washed in double distilled water for 5 minutes and then PBS (2x 5 minutes). Sections were blocked with 20% horse/20% human serum in PBS containing diluent of avidin D (from Avidin/Biotin blocking kit) for 30 minutes at room temperature in a humidified box. Blocking serum was tapped off and sections were incubated, in mouse anti-human D6 or mouse IgG2a isotype control (diluted 1:1000 to give final concentration 0.1µg/ml) in 2% horse serum with 4 drops/ml of Biotin (from Avidin/Biotin blocking kit), overnight at 4°C in a humidified box. Sections were washed in PBS (2x 5 minutes) and incubated for 30 minutes in biotinylated anti-mouse IgG (diluted 1:200) in PBS containing 2% horse serum and 5% human serum at room temperature. An avidin biotin enzyme complex (with peroxidase as the

enzyme) was made (2 drops of solution A into 5mls PBS mixed followed by 2 drops solution B, from Standard Vectastain ABC kit) and applied to the sections, which were then incubated at room temperature for 30 minutes. The slides were washed in PBS (2x 5 minutes). The substrate, DAB 3,3'-diaminobenzidine was made following manufacturer's instructions (5mls distilled water, add 2 drops buffer, 4 drops DAB and 2 drops hydrogen peroxide and mix) and incubated on sections until appropriate staining was seen under the microscope. Sections were washed in water for 5 minutes, stained in haematoxylin for 15 seconds then washed in water. The sections were then dehydrated through the alcohols (70% alcohol, 95% alcohol, 100% alcohol) then in xylene and finally mounting sections with DPX and allowing to air dry before analysis. Pictures of sections were taken using a microscope and Axiovision software.

#### **2.2.4.2 Collection of peripheral blood samples**

Peripheral blood samples were collected from control, psoriasis, psoriatic arthritis and rheumatoid arthritis patients at various clinics. Axel Hueber, a rheumatologist at Glasgow Royal Infirmary and Clinical Research Fellow within the department, collected samples from psoriatic arthritis patients and controls. Hilary Wilson, a consultant at Glasgow Stobhill Hospital sent us rheumatoid arthritis peripheral blood samples from her clinic. Psoriasis blood samples were collected mainly by David Burden, a consultant dermatologist at Glasgow Western Infirmary as well as samples from a clinic run by Susan Holmes, a consultant dermatologist at Glasgow Royal Infirmary. All 10ml samples were collected into lithium heparin vacuettes.

##### ***Isolation of peripheral blood mononuclear cells***

Blood samples were placed into sterile 50ml centrifuge tubes and an equal volume of PBS added and thoroughly mixed. The blood was slowly applied using a sterile pasteur pipette onto 4ml Histopaque 1077 in a 15ml centrifuge tube (2 for each sample). The samples were spun at 400x g for 20 minutes, which separates the blood samples into different layers. The very bottom layer is red blood cells then histopaque, followed by a white ring layer, which is the peripheral blood mononuclear cell (PBMC) layer. The PBMC layer was carefully taken up into a pasteur pipette and transferred to a new 15ml tube and placed on ice. The PBMCs were mixed with PBS to wash the PBMC layer, placed in a 4°C

centrifuge and spun at 300x g for 5 minutes. The supernatant was carefully taken off, and the pellet was composed of T and B-lymphocytes, monocytes and dendritic cells. The PBMCs were either counted for cell surface analysis by FACS or RNA was extracted from them using 350µl buffer RLT containing 2-mercaptoethanol.

*Detection of D6 surface levels on specific PBMCs by flow cytometry.*

PBMCs were isolated from peripheral blood and cell numbers counted. No more than half a million cells were placed into various tubes to stain specific lineage markers for monocytes, T and B lymphocytes and myeloid and plasmacytoid dendritic cells. Anti-human D6 antibody or anti-human IgG2a (both 1.5µg/ml) were added to the appropriate tubes containing 500,000 cells and incubated with the cells for 10 minutes at room temperature. The cells were washed with PEF (PBS/2mM EDTA/0.1% FCS) and spun at 300x g for 5 minutes. The supernatant was removed and the cell pellets dispersed. The secondary antibody, FITC-conjugated goat anti-mouse IgG antibody F(ab)2 fragment, was added to all tubes, incubated for 10 minutes at 4°C, washed and spun (300x g, 5 minutes). Unlabelled mouse IgG1 was added to all tubes, to block the remaining active sites of the secondary antibody to prevent non-specific binding, incubated for 10 minutes at 4°C and washed as previously stated. The next step was lineage specific antibodies, where four separate antibody cocktails were made. An APC-conjugated anti-human CD3 antibody was used for T cells, PE-conjugated anti-human CD20 antibody for B cells and for monocytes, a PE-conjugated anti-human CD14 antibody was used. For myeloid and plasmacytoid DCs, antibodies against markers on monocytes and B cells are required as these cells can also contain a myeloid DC marker (CD1c) and plasmacytoid DC marker (CD304) and therefore need to be excluded when analysing DC population for D6 staining. The lineage specific antibodies were added to the appropriate tubes, incubated for 10 minutes at 4°C. The tubes were washed with PEF and centrifuge (300x g, 5 minutes). Before samples were run through the FACs Calibur machine, 5µl viaprobe was added to detect any dead cells present.

### **2.2.5 Statistical Analysis**

All graphs and statistical analysis were performed using Graphpad Prism version 4.0. Graphs were mean  $\pm$  standard error mean (SEM). Statistics used in this thesis were unpaired student's t-test, a Kruskal Wallis test with Dunn's multiple comparison test (Figure 3-11A), two way ANOVA with Bonferroni post test (Figure 3-9, Figure 4-8, Figure 4-9, Figure 4-10, Figure 4-11 and Figure 4-12) and one way ANOVA with Bonferroni post test (Figure 5-1A, Figure 5-12 and Figure 5-22). A 'p-value' of less than or equal to 0.05 was determined statistically significant.

## **Chapter 3    Characterisation of K14D6 Mice**

## 3 Characterisation of K14D6 mice

### 3.1 Introduction

Inflammation is the host's natural response to infection and helps restore damaged tissue. The initiation of inflammation, which is well characterised, is mediated by pro-inflammatory mediators, such as chemokines and cytokines, involved in controlling the migration and behaviour of leukocytes in tissues. The resolution of inflammation occurs naturally but little is known about the mechanisms involved.

D6 is an atypical chemokine receptor with high affinity for 12 pro-inflammatory CC chemokines (Fra et al., 2003, Nibbs et al., 1997a). *In vitro* studies have shown that D6 can reduce extracellular CC chemokines by constitutively recycling to and from the cell surface (Weber et al., 2004). Surface D6 binds and internalises ligand, targeting it for degradation within the cell (Weber et al., 2004). *In vivo* studies, using a model of skin inflammation involving topical applications of TPA, have shown that D6 null mice demonstrate a prolonged and exaggerated cutaneous inflammatory response (Jamieson et al., 2005). As a consequence, D6 null mice demonstrated a psoriasis-like pathology, characterised by a large influx of mast cells into the dermis and CD3<sup>+</sup> T cells into the epidermis (Jamieson et al., 2005). One mechanism proposed for the exaggerated inflammatory response was that D6 null mice were less effective at clearing bioavailable CC chemokines (Jamieson et al., 2005). As a result of the *in vivo* studies, D6 was proposed to play an important role in aiding the resolution of the inflammatory response.

We hypothesised that if the absence of D6 results in exaggerated inflammation, then increased expression of D6 would suppress the inflammatory response. Therefore, the aim was to determine whether increased expression of D6 within murine skin, using epidermis-specific D6 transgene, would suppress the cutaneous inflammatory response in a skin inflammation model. This study, as a result, would give an indication of the therapeutic potential of D6.

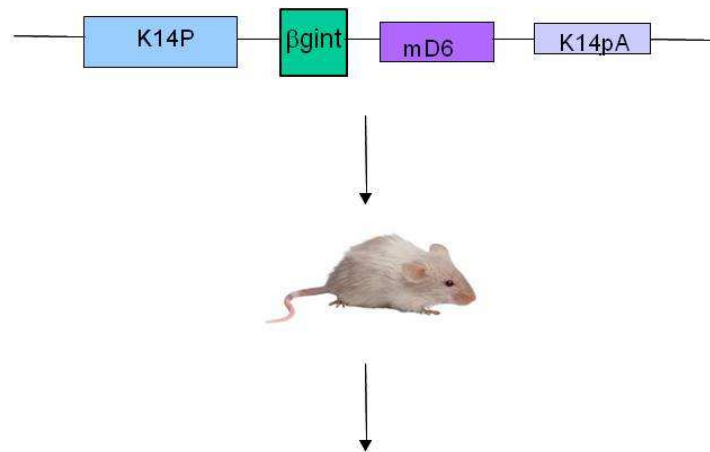
Scientific advances in genetic engineering have resulted in the production of genetically modified organisms in which the overexpression of molecules in

animals (transgenic) can now give us a better understanding of the function of these proteins. Within this chapter, details of how D6 transgenic mice were generated and the characterisation of these mice will be described. Validation of these mice was performed to ensure that the transgene is specifically transcribed where expected, that the resulting protein is functional and plays the biological role hypothesised.

### **3.2 Generation of K14D6 transgenic mice**

D6 null mice used in the skin inflammation model were generated on a C57BL/6 background (Jamieson et al., 2005). In addition, D6 null mice had also been backcrossed on to an FVB/N background, to use for a cancer model within our laboratory (Nibbs et al., 2007). As D6 transgenic mice were required for both the cancer and skin inflammation models, transgenic mice were generated on an FVB/N background.

To examine the role of increased D6 expression in the skin, a well-characterised keratin 14 (K14) promoter (Vassar et al., 1989) was used to drive expression of D6 in the basal keratinocyte layer within the skin. Murine D6 was cloned into an expression vector (pG32.K14 vector, gift of E.Fuchs) containing the human keratin 14 promoter, rabbit  $\beta$ -globin intron, the human K14 3' untranslated region and poly adenylation signal (K14pA). Figure 3.1 illustrates the construct used to express D6 in K14D6 transgenic mice (D.S.Gilchrist and S.Forrow generated these mice). The transgene construct was introduced into FVB/N embryos by pronuclear injection and surviving embryos were then transferred into pseudopregnant foster mice. Two founders were generated, known as Transgenic (K14mD6)1 and Transgenic (K14mD6)2. Offspring carrying the transgene were identified by PCR using tail tip DNA (see 2.2.1.1 and 2.2.1.7). Female offspring from the two founders were assessed for susceptibility to skin inflammation and papilloma formation. Transgenic offspring from both founders were protected in comparison to their wild-type littermates (Nibbs et al., 2007). Subsequent experiments were performed using female offspring from Transgenic (K14mD6)1 founder.



Drives expression of D6 in basal keratinocytes within the epidermis

Figure 3-1. K14D6 transgene construct.

The K14D6 transgene was constructed by cloning the open reading frame of murine D6 (mD6) into an expression vector containing the human K14 promoter (K14P), the rabbit B globin intron ( $\beta$ gint), (K14pA) the human keratin 14 3' untranslated region and polyadenylation signal (Vassar et al., 1989). Transgenic mice were generated on an FVB/N background in which murine D6 transgene is expressed by keratin 14 promoter in basal keratinocytes within the epidermis.

### 3.3 The D6 transgene is expressed in the epidermis in K14D6 mice

To confirm that the transgene expression was directed to the epidermis, a method of separating the murine epidermis from the dermis was required before reverse transcription (RT)-PCR on epidermal sheets could be performed. Two methods of separating the epidermis were compared.

Dorsal skin was dissected and subcutaneous fat was removed before cutting the skin into thin sections. Skin was placed dermal side down in either 0.5M ammonium thiocyanate for 10 minutes at 37°C, 0.5M ammonium thiocyanate for 20 minutes at 37°C or 25mM EDTA for 2 hours at 37°C (Komatsu et al., 1996, Ratzinger et al., 2002). After incubation, the epidermis was separated from the dermis. Sections were fixed in 10% neutral buffered formalin and sent to Glasgow Veterinary School for sections to be paraffin embedded, cut and stained with haematoxylin and eosin (Figure 3-2).

The epidermis is only 1-2 cell layers thick, which consists mainly of keratinocytes, whilst the dermis is thicker and contains both blood and lymphatic vessels. By incubating the skin in ammonium thiocyanate for 10 minutes, staining showed that separation of the skin layers was incomplete (Figure 3-2A). The epidermal section showed parts of the dermis were still present in epidermal sections (Figure 3-2A). Similarly, within the dermal sections, parts of the epidermis were also still attached (Figure 3-2B). By increasing the incubation time of the skin in ammonium thiocyanate, there were fewer traces of the dermis in epidermal sections (Figure 3-2C). However, within the dermal sheet section, no epidermis remained (Figure 3-2D). Additionally, when using ammonium thiocyanate, it was difficult to separate the skin epidermal and dermal sheets in one piece.

When the skin was incubated in EDTA for two hours, the epidermis was easier to separate from the dermis and came apart in a single piece. Analysis of epidermal sections showed the separation looked cleaner with little evidence of the dermis being present (Figure 3-2E). In the dermis, there are many nucleated cells present (stained in blue) with no evidence of epidermis present at the surface (Figure 3-2F).

It was therefore concluded that separation of skin layers was best achieved by incubating sections in 25mM EDTA for 2 hours.

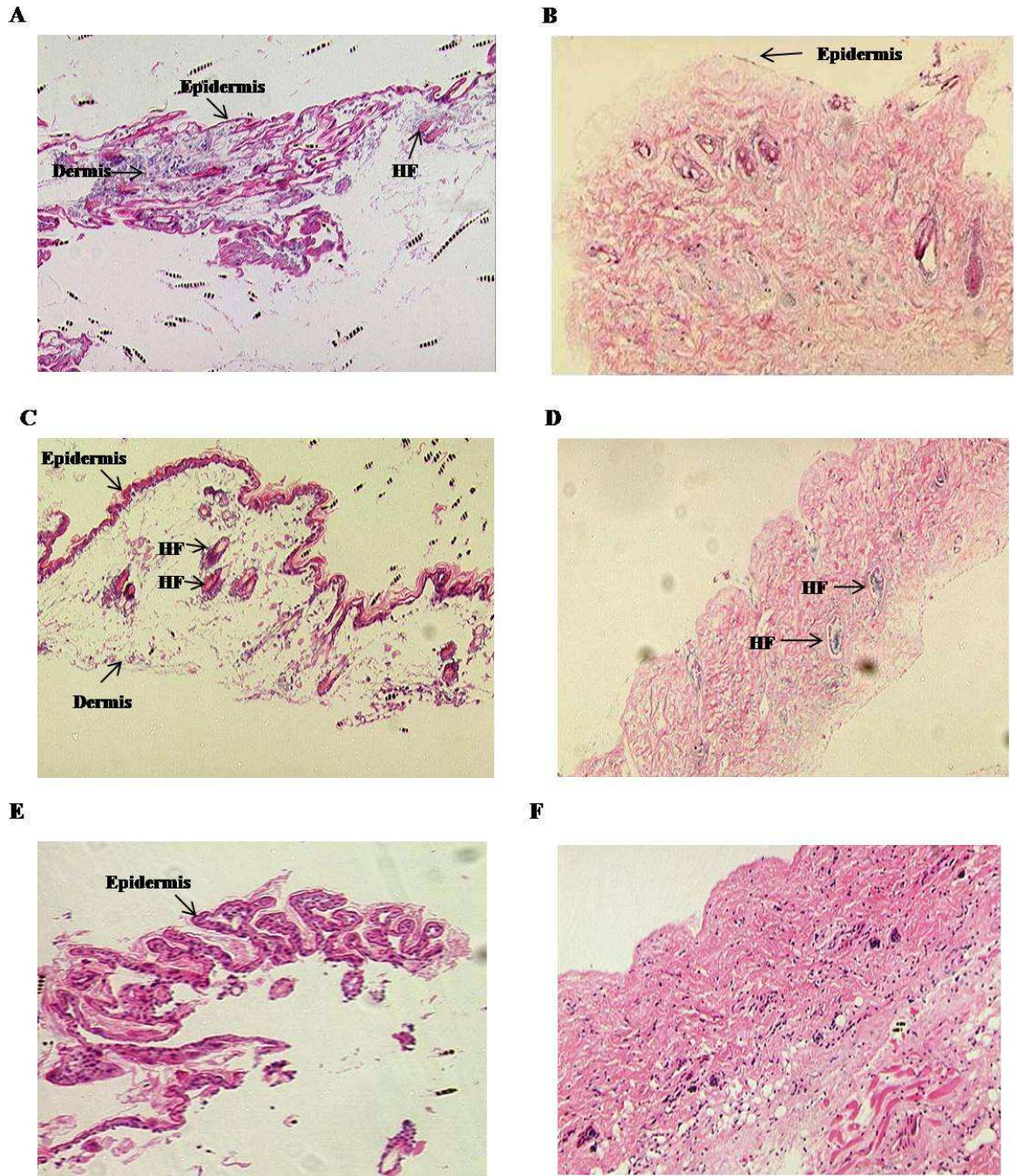


**Figure 3-2.** Optimising a method to separate the epidermis from the dermis.

Dorsal skin was dissected, subcutaneous fat removed and cut into thin sections. Skin was placed dermal side down in either (A&B), 0.5M ammonium thiocyanate at 37°C for 10 minutes at 37°C (C&D), 0.5M ammonium thiocyanate for 20 minutes at 37°C or (E&F), 25mM EDTA for 2 hours at 37°C. Epidermal sheets were separated from the dermis, fixed in formalin and stained in haematoxylin and eosin. Images of epidermal sections are shown in A, C and E while dermal sections are shown in B, D and F. HF indicates hair follicle. Magnification 100x.

Having decided on the best method to use, RNA was isolated from the epidermal sheets of wild-type and K14D6 transgenic mice and converted to cDNA to analyse for the expression of D6 transcripts. This was to confirm that within the K14D6 mice, the D6 transgene was being expressed within the epidermis as anticipated.

Using RT-PCR, D6 was detected in the epidermis of K14D6 mice whilst being absent from wild-type epidermis (Figure 3-3). D6 is known to be expressed within the skin, specifically on lymphatic endothelial cells present within the dermis (Nibbs et al., 2001). Extraction of RNA was attempted from dermal sheets, which were separated from the epidermis using 25mM EDTA however, obtaining intact RNA proved extremely difficult. One possible reason for this failure may be that as the skin sections were dermal side down in the solutions, RNA was degraded during processing.

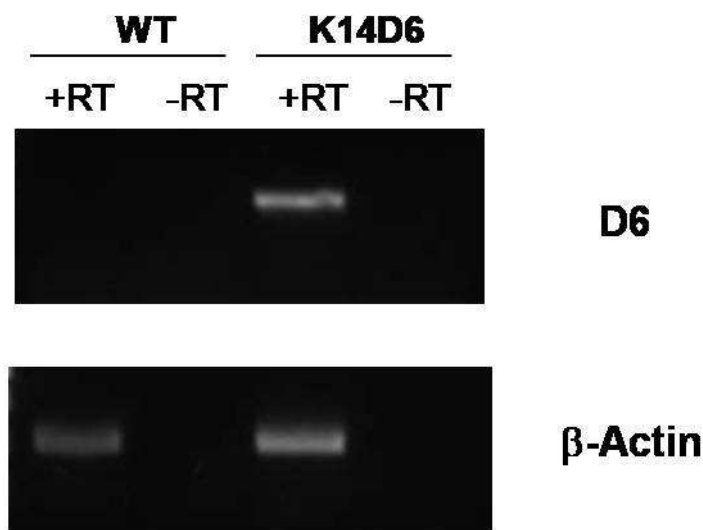


Figure 3-3. Transgenic expression of D6 in the epidermis of K14D6 mice.

RNA was extracted from the epidermis of dorsal skin separated by 25mM EDTA in PBS (37°C for 2 hours) from wild-type (WT) and K14D6 mice. RT-PCR was performed (+/- reverse transcriptase (RT)) to detect mouse D6 and  $\beta$ -actin. Products were run on a 1% agarose gel and visualised by UV light.

### **3.4 The D6 transgene is expressed by K14D6 epidermal keratinocytes**

The next step was to confirm that D6 transgene expression was targeted specifically to proliferative epidermal keratinocytes within the K14D6 transgenic mice, which in turn would allow the functional ability of the D6 transgene to be assessed.

Primary epidermal keratinocytes were isolated and cultured from the skins of 12-24hr old neonates (Yao et al., 2006) and examined for D6 expression. Neonates were from K14D6 x FVB/N crosses therefore neonatal tail tips were obtained in which DNA was extracted and used for genotyping to determine wild-type and K14D6 mice within the litter. Skin was taken from neonates and placed into individual plates dermal side down in 0.25% trypsin overnight at 4°C. The epidermis was carefully separated from the dermis and either placed, individually or pooled, in DMEM containing 10% FCS solution, shaken for 20 minutes, then filtered and centrifuged. The keratinocyte cell pellet was resuspended in keratinocyte growth media and cultured for 5 days. With very efficient technique, one skin can yield initially approximately 2.5 million keratinocytes with a plating efficiency of 40%. To determine how successful the method was, the morphology and purity of the keratinocytes cultures was assessed by RAPI-DIFFII staining.

Prior to staining, keratinocytes from individual neonates were resuspended in 1ml of keratinocyte growth media and 500µl plated into chambered slides and cultured. On day 5, the media was aspirated and the cells were stained using RAPI-DIFFII. Staining of wild-type and K14D6 keratinocytes showed the morphology of K14D6 keratinocytes to be phenotypically similar to wild-type keratinocytes (Figure 3-4). Within both sets of cultured keratinocytes, the majority of the cells were round and small, features typical of keratinocytes (examples shown within red circle in Figure 3-4). However, there were occasional larger cells within both populations, which could have been fibroblasts (examples shown in black circle in Figure 3-4).

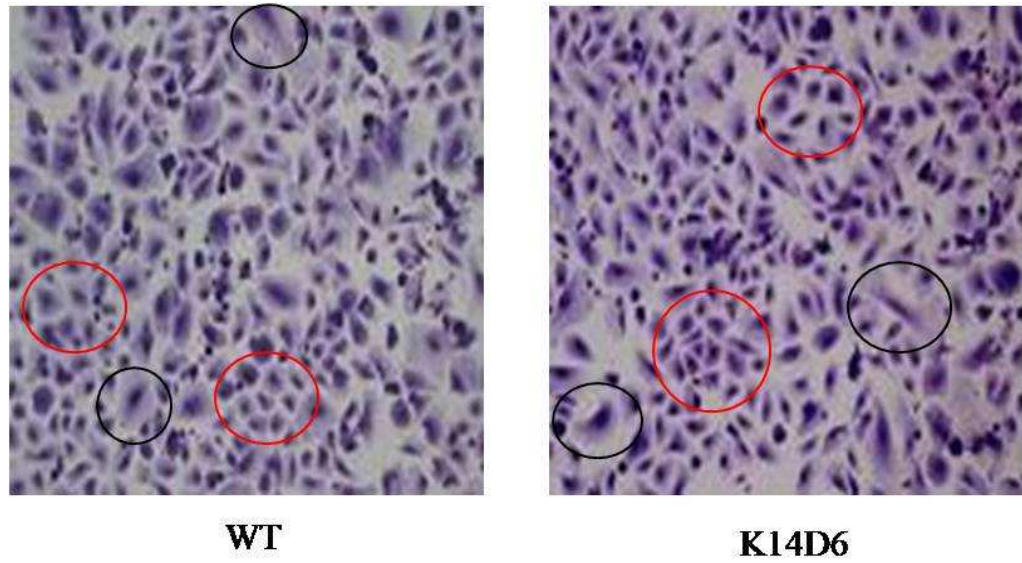


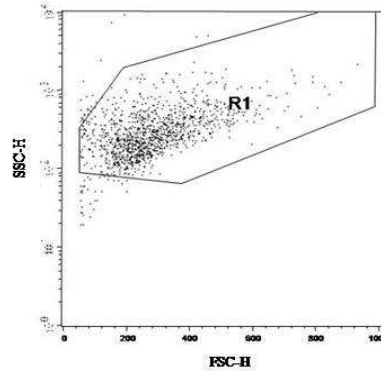
**Figure 3-4. Morphology of wild-type and K14D6 epidermal keratinocytes.**

WT and K14D6 keratinocytes were harvested and cultured in chamber slides for 5 days, before cells were fixed with methanol then stained with RAPI-DIFFII. Magnification is 200x. Red circles denote keratinocytes and black circles denote fibroblasts.

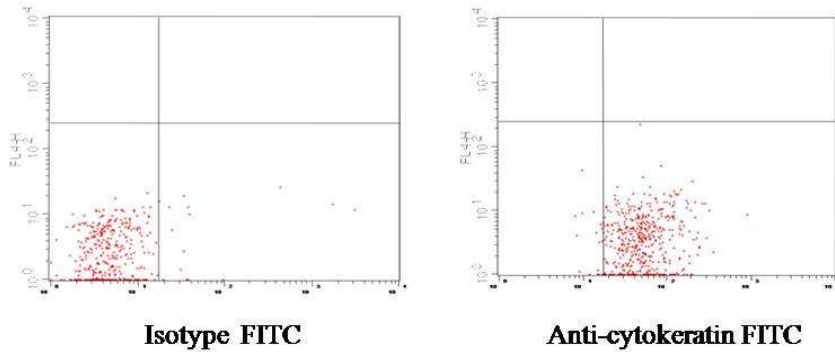
To further assess the purity of the keratinocytes cultures, flow cytometric analysis was performed on cells stained with the keratinocyte-specific anti-cytokeratin antibody. Keratinocytes were isolated from individual neonates (wild-type and K14D6), trypsinised, washed, permeabilised and stained with either FITC-conjugated mouse anti-cytokeratin (pan) antibody or FITC-conjugated matched isotype antibody and the cell populations analysed by flow cytometry.

Figure 3-5A shows the whole cell population using forward and side scatter detectors indicating size and granularity of the cells respectively. The majority of the cells are of the same size, within log 2 and 3, and the majority of the cells are of similar granularity, between 200 and 400 on the forward scatter. The keratinocyte population was gated, R1 shown in Figure 3-5A and cells within this gate were then analysed for antibody staining. Figure 3-5B shows in the left hand plot, the cell population gated by R1, stained with FITC-conjugated isotype control to detect non-specific binding and the baseline was set just to the right of log 1. The percentage of R1 gated cells stained with the FITC-conjugated isotype antibody, detected in the lower left quadrant, was 95.65%. The right plot in Figure 3-5B shows cells gated through R1 that have stained positively with FITC-conjugated anti-cytokeratin antibody, shown in the lower right quadrant indicating that the population was 96% pure epidermal keratinocytes. A representative overlay plot of a population of wild-type and K14D6 keratinocytes shows a log shift in positively stained anti-cytokeratin cells compared to isotype (Figure 3-5C) and therefore shows that the isolation method yields a highly pure keratinocyte population for wild-type and K14D6 keratinocytes. Anti-cytokeratin staining showed epidermal keratinocytes that were isolated to be 96% pure populations.

**A**



**B**



Quadrant	Events	% Gated
UL	1	0.08
UR	0	0.00
LL	1028	95.65
LR	54	4.28

Quadrant	Events	% Gated
UL	0	0.00
UR	0	0.00
LL	67	4.00
LR	1607	96.00

**C**

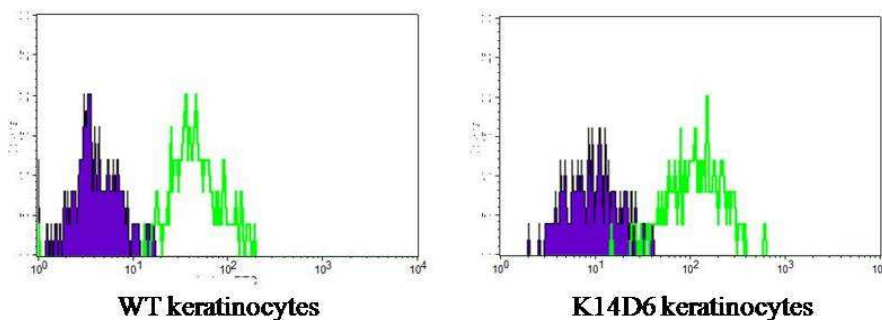


**Figure 3-5. Purity of primary epidermal keratinocytes.**

Keratinocytes from wild-type (WT) and K14D6 mice were isolated, cultured and stained for intracellular cytokeratin analysed by flow cytometry. (A) Keratinocyte population was gated using forward and side scatter (B) The left hand plot shows keratinocytes stained with isotype antibody whereas the right hand plot shows keratinocytes from the same population stained with anti-cytokeratin. The box below shows the number of events and % gated cells with positive anti-cytokeratin cells appearing in lower right quadrant of plot. (C) A histogram plot of isotype (blue) and anti-cytokeratin (green) positive keratinocytes in WT and K14D6 population. These are all representative examples and n=3/group.

To confirm the D6 transgene was targeted to proliferative epidermal keratinocytes within K14D6 mice, RNA was extracted from keratinocytes and assessed for D6 transcripts. For RNA extraction, the epidermis from 3 neonates were pooled together after genotype was determined and the cell pellet was resuspended in 3ml keratinocyte growth media and cultured for five days in a T75 flask.

Using RT-PCR, D6 transcripts were detected in K14D6 epidermal keratinocytes but not in wild-type keratinocytes (Figure 3-6A). Quantitative PCR (QPCR) showed D6 transcripts were present at high levels in K14D6 compared to wild-type epidermal keratinocytes ( $p < 0.001$ ), which had no detectable D6 transcripts above background levels (Figure 3-6B). This confirms that D6 is ectopically expressed in K14D6 epidermal keratinocytes, after explant and culture, at a high level.

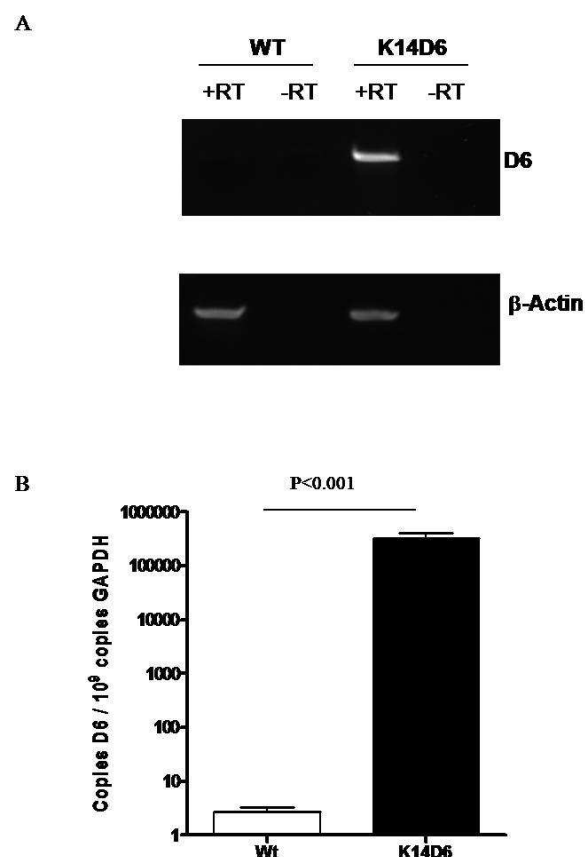


**Figure 3-6.** D6 transcripts are detected in K14D6 epidermal keratinocytes at high levels.

RNA was extracted from epidermal keratinocytes isolated and cultured from wild-type and K14D6 mice. (A) RT-PCR was performed (+/- reverse transcriptase (RT)) to detect mouse D6 and  $\beta$ -actin. Products were run on a 1% agarose gel and visualised using ethidium bromide under a UV light. (B) RNA from epidermal keratinocytes from WT and K14D6 mice was converted to cDNA and diluted with nuclease free water. Levels of D6 transcripts in epidermal keratinocytes were assessed by quantitative PCR using SYBR green. Levels were normalised using a 'housekeeping' gene, GAPDH ( $n=3$ /group, bars show mean  $\pm$  SEM).

In this study, D6 is under the transcriptional control of the human K14 promoter. This promoter is able to drive expression in epithelial cells within the skin as well as within the thymus, tongue and oesophagus (Wang et al., 1997). Expression of D6 in the tongue, thymus and oesophagus is unlikely to contribute to skin pathology. However, thymus from K14D6 mice have been analysed by Professor G. Anderson and the architecture of the thymus was considered normal.

### **3.5 Detection of mouse D6 protein**

The next step was to examine the presence of the D6 protein in K14D6 transgenic mice either by immunohistochemistry or by western blotting. However, no antibody to mouse D6 was available. During this project, an anti-mouse D6 antibody (raised in chicken) was made through collaborations. The antibody was required to be tested and optimised to determine whether it was D6 specific.

The antibody was tested by western blotting using human embryonic kidney cells 293 (HEK) that had been stably transfected with murine D6 (HEK<sub>m</sub>D6) and untransfected HEK cells as a negative control. The cells were cultured and  $2 \times 10^6$  cells were lysed in mammalian cell lysis buffer, centrifuged and the supernatant was retained. Total protein within the supernatant was analysed by a BCA protein assay following manufacturer's instructions. A total of 10 $\mu$ g protein from HEK and HEK<sub>m</sub>D6 was loaded into the wells of a NuPAGE 4-12% Bis-tris gel alongside a multimeric colour molecular weight standard. The gel was electrophoresed and transferred to membrane using a semi-dry transfer system before being incubated in different concentrations of the chicken anti-mouse D6 antibody for 1 hour at room temperature. Primary antibody dilutions tested were 1:50, 1:250 and 1:1000. The secondary antibody, donkey anti-chicken IgY conjugated to horseradish peroxidase was used at 1:5000 dilution. Horseradish peroxidase was detected by chemiluminescent substrate 'west pico' (Pierce).

The concentration of the primary antibody at 1:50 and 1:100 was too high as no specific bands could be determined in the blot due to high background staining (data not shown). However, bands were easily detected using the 1:1000 dilution. A band of 52kDa, the approximate molecular weight of D6 was detected

in both HEKmd6 and the HEK negative control (Figure 3-7A). Additionally a band of approximately 98kDa was also detected in both HEKs and HEKmd6 (Figure 3-7A). The experiment was repeated three times using fresh cells with the same result, indicating non-specific binding. To try to eliminate non-specific binding, the experiment was repeated with the antibodies diluted in 5% milk. A band appeared at approximately 52kDa and 98kDa in extracts of both HEK and HEKmd6 cells (Figure 3-7B). Therefore, it was concluded that the antibody was actually detecting some non-specific proteins and was not specific for murine D6. As a result, the chicken anti-mouse D6 antibody could not be used for further studies.

Since the antibody was not specific, another assay was required to determine the presence of the D6 protein within K14D6 keratinocytes. A ligand-binding assay was used to determine D6 receptor expression in K14D6 transgenics.

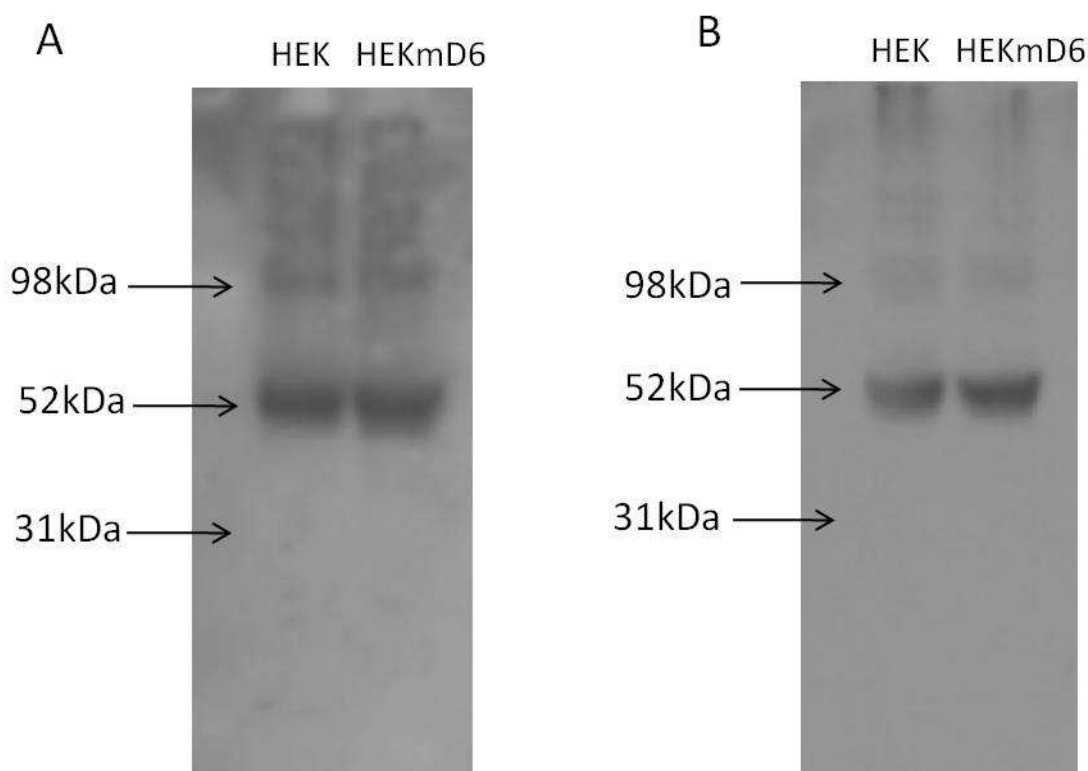


**Figure 3-7. Optimising an anti-mouse D6 antibody**

Protein was extracted from human embryonic kidney (HEK) cells and HEKmd6 (HEK stably transfected with murine D6) and 10 $\mu$ g total protein was used in western blotting. The primary antibody, chicken anti-mouse D6 antibody, was used at 1:1000 dilution and the secondary antibody conjugated to horseradish peroxidase (HRP) was used at 1:5000. HRP was detected using West Pico. (A) Antibodies are diluted in PBS/0.1% Tween 20 (PBST) (B) Antibodies were diluted in 5% milk in PBST. Images are a representative of three replicate experiments.

### **3.6 Characterisation of chemokine receptor transcripts in primary keratinocytes**

Although there was no antibody against mouse D6 available to detect the presence of the protein, D6 transcripts were present in the transgenic keratinocytes and therefore the functional ability of D6 to bind and internalise a D6 specific ligand was assessed (McKimmie et al., 2008, McKimmie and Graham, 2006). To examine the functional ability of D6, fluorescently labelled chemokines or biotinylated chemokines were used. Ligand binding to cells can be detected by flow cytometry using fluorescently labelled chemokines. A biotinylated chemokine, which could be detected by western blotting using streptavidin conjugated to HRP, was used to determine the capability of the D6 transgene to internalise and degrade chemokines.

However, before going on to examine the functional ability of D6, it was important to determine which chemokine receptors were present on primary keratinocytes, as this would help determine the most suitable ligand to use to assess D6 function because all D6 ligands bind other chemokine receptors. D6 can bind many inflammatory CC chemokines, which are also capable of binding to other chemokine receptors, mainly CCR1, CCR2, CCR3, CCR4 and CCR5 (summarised in Table 3-1.) It is of note that murine CCR3 is able to bind CCL3 whilst human CCR3 is not able to (Menten et al., 2002). Studies have shown that CCR1 and CCR5 are present in a human keratinocyte cell line (HaCaT) and primary human keratinocytes express CCR3 (Petering et al., 2001, Szabo et al., 2001). These studies indicated the possibility of the presence of CCR1, CCR3 and CCR5 on murine keratinocytes.

Chemokine receptor	D6 Ligands											
	CCL2	CCL3	CCL3L1	CCL4	CCL5	CCL7	CCL8	CCL11	CCL13	CCL14	CCL17	CCL22
D6												
CCR1												
CCR2												
CCR3												
CCR4												
CCR5												

**Table 3-1. Summary of D6 ligands, which CCR1, CCR2, CCR3, CCR4 and CCR5 can bind.**

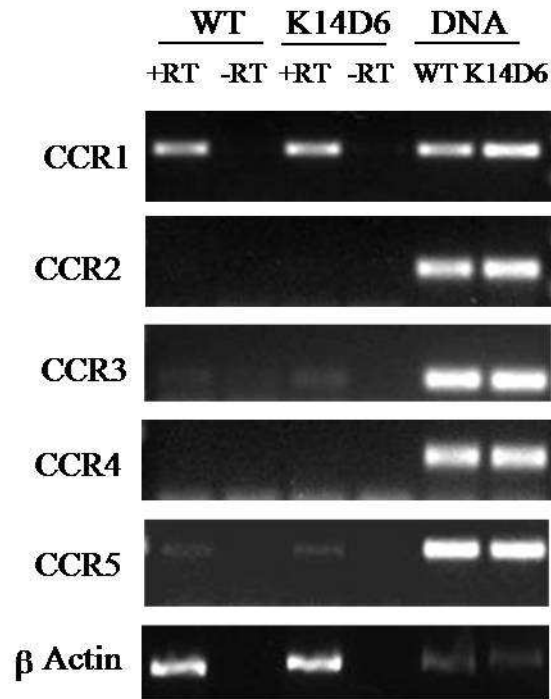
D6 can bind 12 pro-inflammatory chemokines as listed. CCR1, CCR2, CCR3, CCR4 and CCR5 can bind several D6 ligands (indicated by grey shaded box). Murine CCR3 can bind CCL3 whereas human CCR3 does not (indicated by black shaded box).

Wild-type and K14D6 keratinocytes were isolated and cultured in T75 flasks for 5 days before RNA was extracted using the RNeasy mini kit. To determine a suitable ligand to use to test D6 function, cDNA was synthesised from 1µg RNA and examined for the expression of chemokine receptors CCR1-CCR5 using RT-PCR.

Strong expression of CCR1 transcripts was seen in the wild-type and K14D6 keratinocytes as well as weak expression of CCR3 and CCR5 transcripts. Conversely, CCR2 and CCR4 transcripts were absent from both wild-type and K14D6 keratinocytes (Figure 3-8A). DNA from tail tips of wild-type and K14D6 mice were used as a positive control to ensure that the primers and PCR worked. CCR1, CCR3 and CCR5 transcripts were quantified by quantitative PCR. There was no significant difference in the transcript levels of CCR1, CCR3 or CCR5 between wild-type and K14D6 epidermal keratinocytes. This indicates that ectopic expression of D6 in resting epidermal keratinocytes does not affect the transcript levels of CCR1, CCR3 or CCR5 (Figure 3-8B).

Therefore, to test the ability of transgenically expressed D6 to bind ligands, any ligand that binds CCR1, CCR3 and CCR5 were not suitable. The most suitable ligands would be chemokines that only bind D6 and CCR2 or CCR4, such as CCL2, CCL17 or CCL22.

A



B

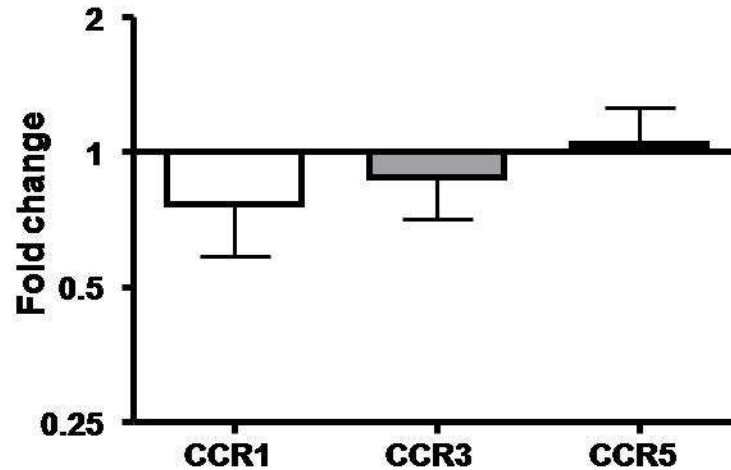


Figure 3-8. Expression of chemokine receptors CCR1, CCR3 and CCR5 on primary epidermal keratinocytes.

(A) RNA was extracted from WT and K14D6 epidermal keratinocytes and subjected to RT-PCR (+/- reverse transcriptase (RT)) for chemokine receptors CCR1-5 and  $\beta$ -actin. DNA was extracted from tail tips as a positive control. Products were electrophoresed on a 1.5% agarose gel and visualised with ethidium bromide by UV light. (B) RNA from epidermal keratinocytes from WT and K14D6 mice were converted to cDNA and diluted with nuclease free water. Levels of CCR1, CCR3 and CCR5 transcripts in epidermal keratinocytes were examined by quantitative PCR using SYBR Green. Levels were normalised against a 'house keeping' gene, GAPDH and represented as fold change in transcript level of CCR1, CCR3 and CCR5 in K14D6 keratinocytes compared to transcript levels in WT keratinocytes respectively (n=3/group, bars are mean  $\pm$  SEM).

### **3.7 The function of D6 in K14D6 epidermal keratinocytes**

D6 is capable of binding many inflammatory chemokines and has been proposed to function as a scavenging receptor (Fra et al., 2003), internalising and targeting chemokines for degradation (Weber et al., 2004), thereby removing CC chemokines from its surroundings. Therefore, the ability of D6 in K14D6 keratinocytes to function was assessed in two ways. One was to examine the ability of D6 in K14D6 keratinocytes to bind a D6 ligand and the second was to assess the ability of D6 in K14D6 keratinocytes to remove chemokines from its surroundings.

#### **3.7.1 *K14D6 keratinocytes can bind CCL2, a D6 ligand.***

To assess whether D6 from K14D6 keratinocytes was functional, the ability of these cells to bind a fluorescent-labelled CCL2 (CCL2-Alexa 647) was examined. CCL2 is a ligand for D6 (Nibbs et al., 1997a) which can also bind CCR2. To determine whether any binding of CCL2 by keratinocytes was specifically due to D6, a competition assay was set up using a 10-fold excess of CCL3, another D6 ligand (Nibbs et al., 1997a). In this assay, it is only binding of CCL2 by D6 that can be outcompeted by CCL3.

Individual populations of epidermal keratinocytes were isolated from wild-type and K14D6 mice, resuspended in 1ml of keratinocyte growth media and 200 $\mu$ l was seeded in triplicate into 24 well plates and cultured for five days. Fresh keratinocyte media was added (250 $\mu$ l) and cells were treated with either PBS, 25nM fluorescent-labelled CCL2, or 25nM fluorescent-labelled CCL2 and 250nM CCL3, and incubated for 100 minutes at 37°C. Keratinocytes were washed, trypsinised, resuspended and labelled, CCL2 binding was assessed by flow cytometry.

Keratinocytes were gated (R1) using forward and side scatter (Figure 3-9A) before going on to analyse non-specific and specific fluorescent-labelled CCL2 binding. Figure 3-9B shows keratinocytes that have been gated through R1 and shows cells treated with PBS (left panel), keratinocytes stained with fluorescent-labelled CCL2 (middle panel) and keratinocytes stained with fluorescent-labelled CCL2 in the presence of excess CCL3 (right panel). The top panel in Figure 3-9B

illustrates an example of a wild-type keratinocyte population and the bottom panel shows an example of K14D6 keratinocyte population. Non-specific binding was determined and set within the lower left quadrant of the plot for wild-type and K14D6 keratinocytes. In the presence of fluorescently labelled CCL2, a number of cells were seen to shift from the lower left quadrant to the lower right quadrant in K14D6 keratinocytes but not in the wild-type, indicating K14D6 keratinocytes are positive for CCL2 binding (Figure 3-9B middle panel). In the presence of CCL2 and excess CCL3, wild-type keratinocytes remained within the lower left quadrant whereas K14D6 keratinocytes shifted from the lower right quadrant to the lower left quadrant (Figure 3-9B right panel). This data indicates that CCL2 binding in K14D6 keratinocytes was outcompeted by CCL3. Figure 3-9C shows an overlay plot of K14D6 keratinocytes treated with PBS, fluorescently labelled CCL2 and labelled CCL2 in the presence of excess CCL3 (blue, pink and green respectively). Figure 3-9C illustrates that K14D6 keratinocytes can bind the fluorescently labelled CCL2, shown by a shift in the green line compared to the control (blue line), yet in the presence of excess CCL3 this binding is inhibited, illustrated by the pink line being similar to control (blue). The data were quantified using the mean percentage of keratinocytes that were positively labelled for CCL2 under the different conditions using the percentage of cells gated by R1 present in the lower right quadrant. In the wild-type population, the percentage of keratinocytes positively labelled with CCL2 was found to be lower than 1% and there was no significant difference between wild-type keratinocytes treated with PBS, fluorescent-labelled CCL2 or fluorescent-labelled CCL2 and excess CCL3 (Figure 3-9D). Whereas in the K14D6 population, the percentage of cells positive for fluorescent-labelled CCL2 in the PBS treated group was significantly increased to approximately 45% in keratinocytes treated with fluorescently labelled CCL2 ( $p < 0.001$ ). In the presence of excess CCL3, the percentage of K14D6 keratinocytes labelled with CCL2 was significantly reduced from 45% to 2% ( $p < 0.001$ ; shown in Figure 3-9D).

In summary, binding of CCL2 occurred in K14D6 keratinocytes but not in wild-type keratinocytes, indicating that CCL2 binding by K14D6 keratinocytes was due to D6. These data further confirmed the absence of CCR2 on primary epidermal keratinocytes.

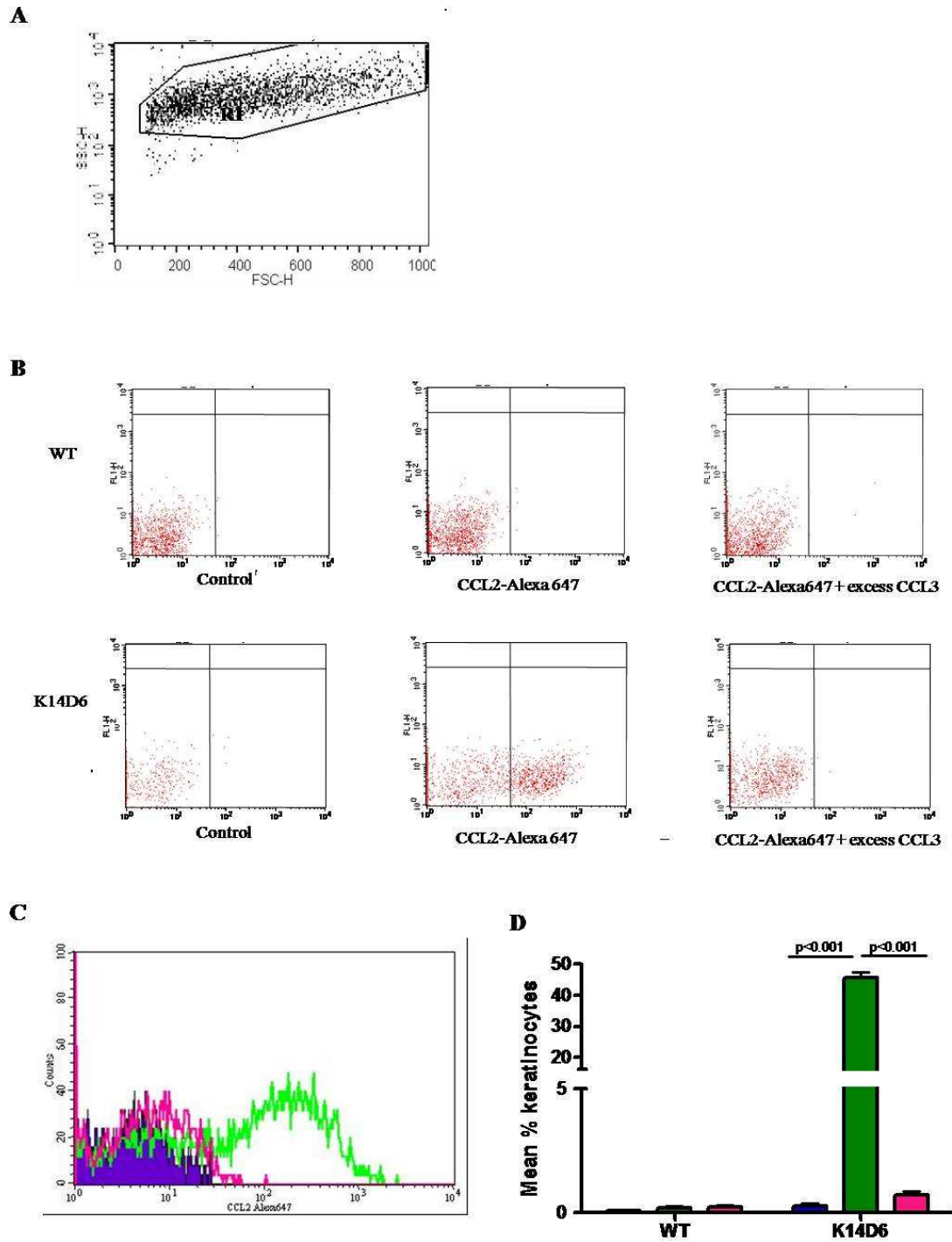


Figure 3-9. K14D6 keratinocytes are able to bind CCL2 in a D6 dependent manner

Keratinocytes were cultured from individual WT and K14D6 mice in 250 $\mu$ l KGM with 1% BSA and incubated with (i) PBS (ii) 25nM CCL2-alexa 647 or (iii) 25nM CCL2-alexa 647 with 250nM CCL3 for 100 minutes at 37°C. Keratinocytes were trypsinised and resuspended in PBS/2mM EDTA/0.1%FCS and samples analysed by FACS. (A) Representative plots of WT and K14D6 keratinocytes stained with CCL2-alexa 647 under the different conditions. (B) A representative histogram plot of K14D6 keratinocytes showing uptake of CCL2 in untreated cells (blue), cells treated with CCL2 (green) and cells treated with CCL3 and CCL2 (pink). (C) The mean % of WT and K14D6 keratinocytes labelled with CCL2-Alexa 647; n=3/group and columns are mean  $\pm$  SEM.

### **3.7.2 *K14D6 keratinocytes can remove extracellular CCL3 from the media.***

D6 in K14D6 keratinocytes was able to bind CCL2 and therefore the next step was to determine whether D6 from the transgene was able to internalise and degrade ligands. D6 activity in K14D6 keratinocytes was assessed by its ability to deplete extracellular biotinylated CCL3, a D6 ligand. Keratinocytes were individually isolated and seeded into 6ml plates with 5ml of keratinocytes growth media. After five days, the number of keratinocytes within the plates was  $2.5 \times 10^5$  cells. Wild-type and K14D6 keratinocytes were treated with 10nM biotinylated CCL3 and samples of supernatant were taken at various timepoints over 24 hours. Any remaining biotinylated CCL3 in the media was detected using streptavidin labelled with HRP on a western blot (McCulloch et al., 2008).

Wild-type keratinocytes did not deplete biotinylated CCL3 from the surrounding media as there was no decrease in the amount of biotinylated CCL3 detected at 0 hours from 2, 4, 6, 8, 12 and 24 hours whereas by 4 hours in the presence of K14D6 keratinocytes, less biotinylated CCL3 was detected than was present at 0hrs (Figure 3-10A). By 12 hours, the levels of biotinylated CCL3 in the media in the presence of K14D6 keratinocytes was markedly less and very little biotinylated CCL3 remained after 24 hours (Figure 3-10A). Therefore, K14D6 keratinocytes were able to remove extracellular CCL3 from the media progressively whereas wild-type keratinocytes did not.

To ensure that the progressive removal of CCL3 was D6 dependent in K14D6 keratinocytes, a competition assay was set up, with 10nM biotinylated CCL3 added along with a 10-fold molar excess of CCL22, a high affinity D6 ligand (Bonecchi et al., 2004). An excess of CCL22 should bind all D6 receptors and prevent binding of biotinylated CCL3 to D6. As a result, excess CCL22 prevented depletion of biotinylated CCL3 by K14D6 keratinocytes as the levels of biotinylated CCL3 remained the same at 0, 2, 4, 6, 8, 12 and 24 hours, indicating that depletion of biotinylated CCL3 is D6 dependent (Figure 3-10B). Therefore, D6 in K14D6 keratinocytes is functional.

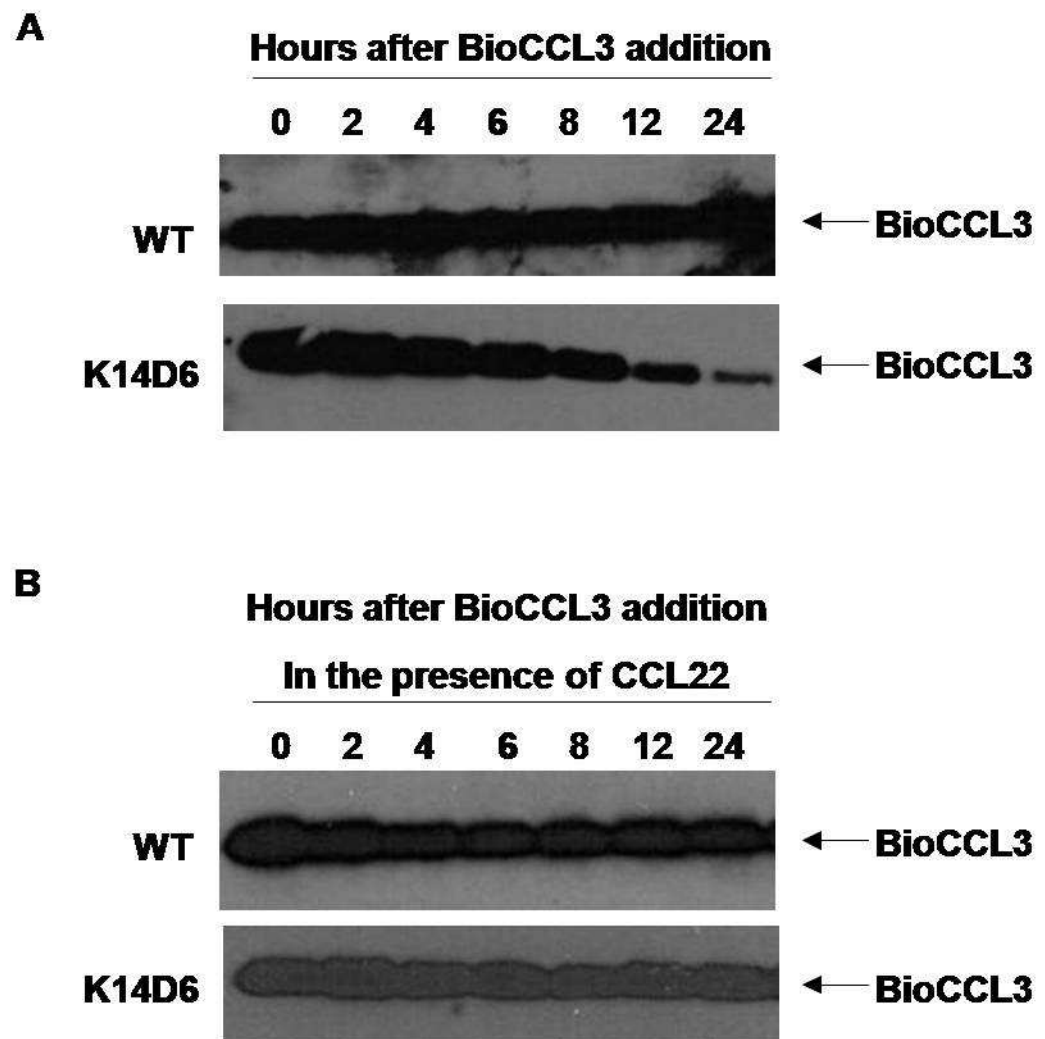


Figure 3-10. Transgenic expression of D6 in epidermal keratinocytes is able to degrade extracellular biotinylated CCL3.

Keratinocytes from neonatal wild-type (WT) or K14D6 mice were cultured in 1ml keratinocyte growth media containing (A) 10nM biotinylated CCL3 (BioCCL3) or (B) 10nM BioCCL3 in competition with 100nM CCL22. The remaining BioCCL3 was detected by western blotting using streptavidin conjugated to HRP at the timepoints indicated. Data shown is representative of three experiments.

### **3.8 Transgenic expression of D6 dampens cutaneous inflammation.**

To assess the ability of the K14D6 transgene to dampen down inflammation *in vivo*, a well-characterised cutaneous inflammation model was used involving application of 12-O-tetradecanoyl-phorbol-13-acetate, also known as TPA (Stanley et al., 1991) to the skin of FVB/N wild-type and K14D6 transgenic mice. In this model, the lower dorsal skin of the mice was shaved two days before starting the TPA application. TPA was applied to the dorsal skin of the mice once on three consecutive days. TPA is a tumour promoter, which activates protein kinase C and application of the chemical on three consecutive days results in acute inflammation, which eventually resolves (Jamieson et al., 2005).

This model was used previously with D6 null mice, on a C57BL/6 background, in which these mice demonstrated a prolonged and exaggerated inflammatory response (Jamieson et al., 2005). These studies showed that in comparison to wild-type mice, D6 null mice were unable to clear CCL5 and CCL3, both D6 ligands, from the site of skin inflammation 24 hours after TPA application. These data suggested that D6 was involved in regulating chemokine levels at sites of inflammation by playing a role in chemokine removal. Histological analysis of the skin after TPA induced inflammation revealed D6 null mice demonstrated increased skin thickening, hyperkeratosis, epidermal hyperplasia, increased angiogenesis and increased infiltration of inflammatory cells, in particular epidermal T cells and dermal mast cells (Jamieson et al., 2005). The exaggerated inflammatory response was shown to be TNF-dependent, and histological changes within D6 null mice skin showed similar characteristics to those found in human psoriasis. Therefore, since absence of D6 resulted in an exaggerated cutaneous inflammatory response, we examined whether increased expression of D6 within the epidermis would suppress the inflammatory response.

Four days after the final application of TPA, mice were sacrificed and the dorsal skin was harvested, fixed in 10% neutral buffered formalin for haematoxylin and eosin staining as well as for CD3 staining and astra blue staining to identify T cells and mast cells respectively. Skin sections were analysed for skin thickness

by counting the number of squares the skin filled within the grid in the eyepiece in which twenty random points per skin section were counted.

There was no significant difference in skin thickness between untreated D6 null mice, wild-type and K14D6 mice (Figure 3-11A). Four days after the final application of TPA, D6 null mice demonstrated a significant increase in skin thickness compared to resting skin thickness ( $p < 0.001$ ; Figure 3-11A). Wild-type mice also demonstrated a significant increase in skin thickness after four days compared to resting skin thickness ( $p < 0.001$ ; Figure 3-11A). However, K14D6 mice showed no significant difference in skin thickness four days after the final application of TPA compared to resting skin thickness (Figure 3-11A). This data illustrated that D6 null mice on a different background also demonstrated an exaggerated inflammatory response within the skin to TPA. Four days after the final application of TPA, K14D6 mice contained fewer T cells in the epidermis in comparison to wild-type mice ( $p < 0.001$ ; Figure 3-11B). K14D6 mice also demonstrated a significant reduction in the number of mast cells present within the skin in comparison to wild-type mice ( $p < 0.001$ ; Figure 3-11C).

These data confirm D6 null mice demonstrate an exaggerated inflammatory response to TPA in comparison to wild-type mice and indicate that K14D6 mice can suppress *in vivo* inflammation due to the increased expression of D6.

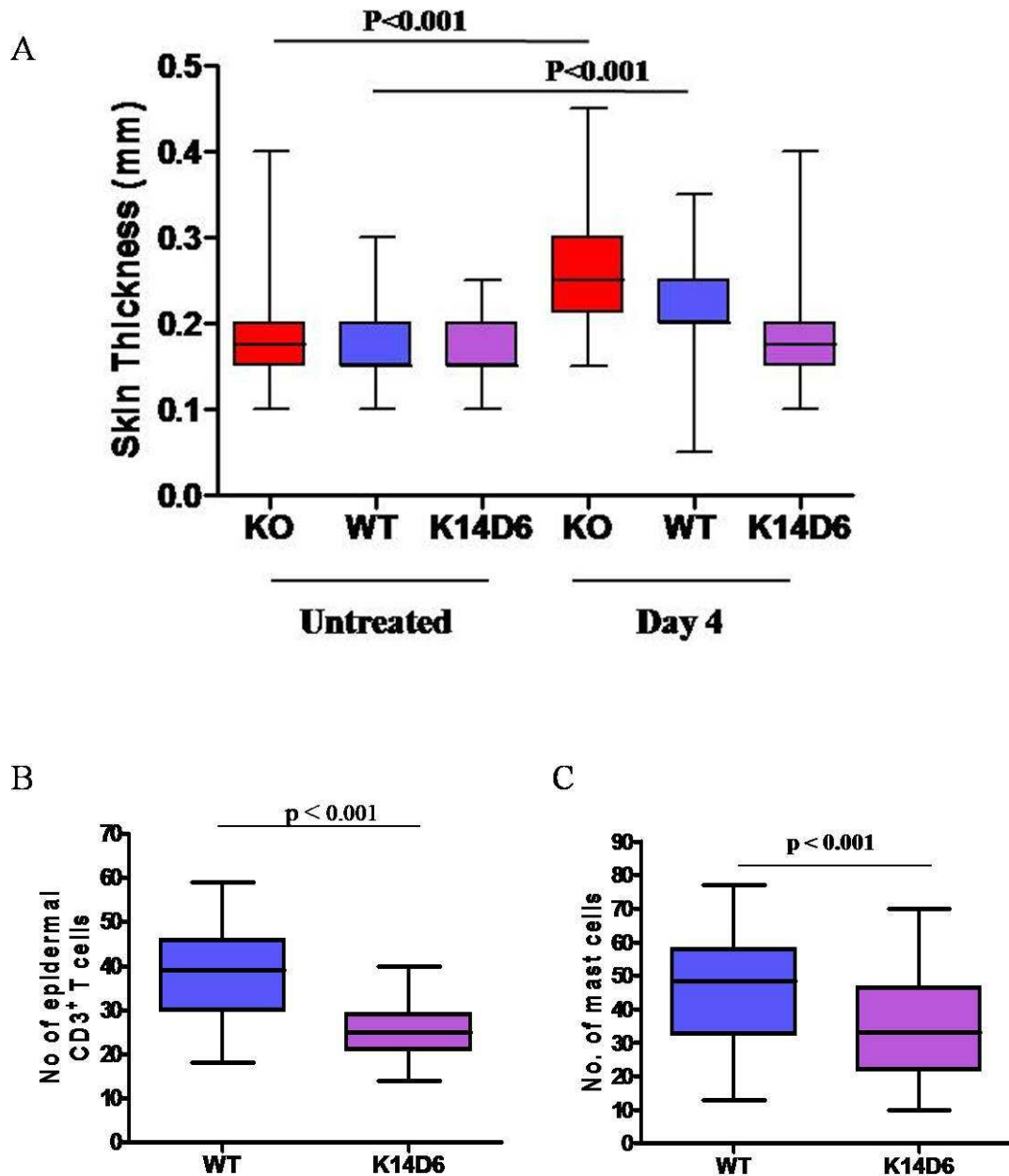


Figure 3-11. Transgenic expression of D6 in murine epidermis limits cutaneous inflammation.

(A) D6 null mice (KO), Wild-type (WT) and K14D6 mice ( $n=5$ /group) received an application of TPA on the dorsal skin on three consecutive days. Four days later, the skin was harvested. Dorsal skin from untreated mice ( $n=5$ /group) was harvested immediately. Skin sections were scored for epidermal thickness. (B) Skin sections from WT and K14D6 mice four days after the final application of TPA were stained with an anti-mouse CD3 antibody to identify T cells. The number of T cells within the epidermis was counted using 20 random points per skin section. (C) Mast cells were stained with astra blue in WT and K14D6 skin and the number of mast cells were counted in 20 random fields per section.

### 3.9 Summary of Chapter 3

D6 was proposed to play a role within the resolution phase of inflammation and the main aim of this chapter was to test the hypothesis that increased expression of D6 would suppress inflammation. To test this hypothesis, transgenic mice were generated where D6 expression would be increased ectopically. Since the biological role of D6 was hypothesised using a skin inflammation model, it was decided to transgenically express D6 within the skin so that the skin inflammation model could be used to test the hypothesis. Therefore, K14D6 mice were generated so that increased expression of D6 would be targeted to the epidermal layer of murine skin under the control of the human K14 promoter. Therefore, the work in this chapter was to characterise and validate the K14D6 transgenic mice.

In summary, K14D6 mice express D6 transcripts within the epidermis, more specifically within epidermal keratinocytes after explant and culture, and such transcripts are absent from wild-type mice. Ectopic expression of D6 within K14D6 keratinocytes does not change the morphology in comparison to wild-type keratinocytes. CCR1, CCR3 and CCR5 transcripts are present in primary murine keratinocytes and ectopic expression of D6 in K14D6 keratinocytes does not affect CCR1, CCR3 or CCR5 transcript levels. K14D6 keratinocytes are able to bind CCL2, a D6-specific ligand, whereas wild-type keratinocytes are not able to. K14D6 keratinocytes are able to progressively deplete extracellular CCL3 whereas wild-type keratinocytes do not and therefore the K14D6 transgene is functional. In terms of skin inflammation, K14D6 mice were able to suppress inflammation in response to a topical application of a skin irritant whereas D6 null and wild-type could not. Therefore, D6 can suppress skin inflammation and has the potential to be of therapeutic use.

## **Chapter 4    Characterisation of the transcriptional consequences of D6 ligand binding**

## 4 Characterisation of the transcriptional consequences of D6 ligand binding

### 4.1 Introduction

Many members of the chemokine receptor family signal through the activation of G-proteins as they belong to the family of G-protein coupled receptors (Murphy et al., 2000). Conversely, there are four chemokine receptors, DARC, D6, CCX CKR and CXCR7, which are unconventional because there does not seem to be any signalling activity after high affinity ligand binding (Graham, 2009). *In vitro* studies have examined ligand dependent functional responses, such as calcium fluxes and chemotaxis, for both human and murine D6 and have shown that ligand binding to D6 does not trigger these responses (Fra et al., 2003, Nibbs et al., 1997a). However, the possibility that D6 may signal via a different mechanism other than G-protein coupling has not been investigated. Human lymphatic endothelial cells are known to express D6 by immunohistochemistry (Nibbs et al., 2001, Vetrano et al., 2009). However, D6 was not expressed on isolated human lymphatic endothelial cells indicating that D6 had been transcriptionally silenced (Amatschek et al., 2007). Within our laboratory, we had D6 transgenic mice (K14D6), where ectopic expression of D6 was targeted to epidermal keratinocytes. In the previous chapter, a method of isolating primary keratinocytes was utilised to characterise the level of D6 transcripts and the functional activity of D6 in wild-type and K14D6 mice. D6 transcripts were only expressed and functional in K14D6 epidermal keratinocytes (see Chapter 3). As a result, epidermal keratinocytes from K14D6 mice are a primary cell type that can be isolated and cultured whilst still expressing D6. Therefore, the aim of this work was, using a microarray approach, to determine any transcriptional consequences of ligand binding to D6. By assessing the transcriptional consequences, this would give an indication into cell functions mediated through D6 *in vivo*.

The work described in this chapter exploits microarray technology to characterise the changes to the cellular transcriptome after ligand binding to D6 using primary keratinocytes isolated from wild-type and K14D6 mice. It was hoped that the microarray analysis would yield information on altered gene

expression after ligand binding to D6. A second aspect was to determine if there were any transcriptional consequences induced by basal D6 expression, independent of ligand, within K14D6 keratinocytes.

## 4.2 Experimental details

Primary keratinocytes were isolated from neonatal mice and after genotyping; keratinocytes were pooled from three mice of the same genotype and cultured for 5 days in a T75 flask. On day 5, wild-type and K14D6 keratinocytes were incubated with 10nM CCL3, a high affinity D6 ligand, or PBS for 6 hours at 37°C. Keratinocytes were incubated for 6 hours since transcriptional changes through ligand binding to chemokine receptors can occur between 2 and 8 hours (Valerio et al., 2004). RNA was isolated from primary keratinocytes, transcribed into biotinylated cRNA and applied to an Affymetrix Mouse genome 430 2.0 Array Gene Chip (<http://www.affymetrix.com/>). The data generated was analysed using rank products (Breitling et al., 2004b) and iterative group analysis (iGA) methods (Breitling et al., 2004a). The experimental design is summarised in Figure 4-1.

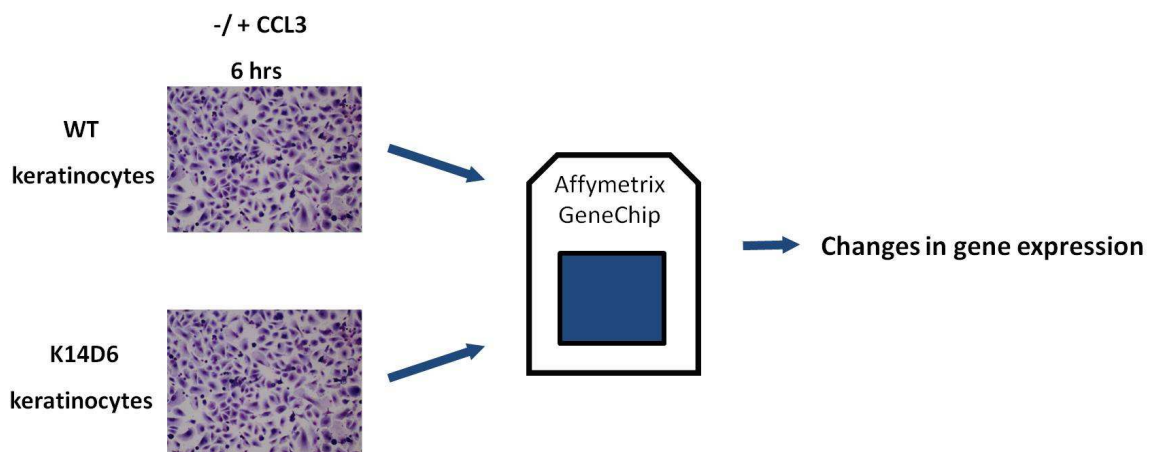


**Figure 4-1. Summary of experimental design to characterise transcriptional consequences of D6 ligand binding.**

**Primary wild-type (WT) and K14D6 keratinocytes were isolated and cultured from neonatal mice. Keratinocytes were incubated with PBS or 10nM CCL3 for 6hrs. RNA was isolated from primary keratinocytes and prepared for application to an Affymetrix gene chip to measure changes in gene transcription.**

### 4.3 Generation and validation of RNA for microarray application

RNA was extracted from the samples and subsequently processed by staff at the Sir Henry Wellcome Functional Genomics Facility at the University of Glasgow (<http://www.gla.ac.uk/faculties/fbls/functionalgenomicsfacility/>) where the microarray analyses were performed. The RNA samples were assessed for quantity, using a Nanodrop ND-1000, in which 1 $\mu$ l of each sample was analysed (Table 4-1). The quality of RNA was assessed using an Agilent 2100 Bioanalyser. Each experimental condition was repeated in triplicate for statistical analysis.

The concentration of the samples varied from 38.1ng/ $\mu$ l to 1742.4ng/ $\mu$ l (Table 4-1). One sample, wild-type control 2, was below the recommended level of 2 $\mu$ g total RNA required for the microarray (Table 4-1). Therefore all samples prior to being transcribed into biotinylated cRNA underwent linear amplification (Phillips and Eberwine, 1996). If only one sample underwent linear amplification this would skew the data, therefore all the samples were amplified to give a fair comparison. The cRNA was then applied to Affymetrix GeneChip Mouse genome 430 2.0 Array for generation and analysis of data.

Sample	Concentration of RNA (ng/ $\mu$ l)	Total yield RNA ( $\mu$ g)
WT control 1	1742.4	52.3
WT control 2	38.1	1.1
WT control 3	269.9	8.1
WT + CCL3 1	1566.5	47.0
WT + CCL3 2	402.5	12.1
WT + CCL3 3	421.7	12.7
K14D6 control 1	1020.8	30.6
K14D6 control 2	304.9	9.1
K14D6 control 3	482.1	14.5
K14D6 + CCL3 1	857.9	25.7
K14D6 + CCL3 2	717.8	21.5
K14D6 + CCL3 3	799.7	24.0

**Table 4-1. Concentration and total yield of RNA extracted from keratinocytes analysed by a Nanodrop ND-1000.**

Primary keratinocytes were isolated and cultured for 5 days before addition of PBS or 10nM CCL3 for 6 hours at 37°C. RNA was isolated and 1 $\mu$ l of each sample was analysed for quantity using a Nanodrop ND-1000 by staff at the Functional Genomics Facility. n=3/group and each sample consisted of keratinocytes from 3 neonatal mice.

## 4.4 Analysis of microarray Data

The analysis of the microarray was carried out in the Sir Henry Wellcome Functional Genomics Facility, where the data were generated and automatically analysed by FunAlyse, in-house microarray data analysis software. This software generates a directory for each project and data is normalised using the robust multichip average (RMA) method (Irizarry et al., 2003). The software performs two different sets of analysis producing two reports. These are known as the rank product (RP) report (Breitling et al., 2004b) and the iterative group analysis report (Breitling et al., 2004a). The iGA report is generated using the list of genes produced by the rank product analysis and identifies functional changed groups of genes. Terminology used by this software can be found in Appendix One. All data generated by the microarray can be found in Appendices Two and Three. The comparisons made were:

- 1) WT control (baseline) versus K14D6 control
- 2) WT control (baseline) versus WT + CCL3
- 3) K14D6 control (baseline) versus K14D6 + CCL3
- 4) WT + CCL3 (baseline) versus K14D6 + CCL3

### 4.4.1 *Rank product differential expression analysis reports*

The rank products analysis report lists genes sorted according to a measure of differential expression calculated using the rank product method. The rank products method is a non parametric statistical test where the RP score is a measure of differential expression based on ranks of fold changes (Breitling et al., 2004b). It is a biologically motivated test based on the idea that a gene is highly up or downregulated in one experiment but if the same gene is at the top of a list in a replicate experiment then it is likely that this gene is actually changed. Therefore rank product values are calculated using the position of the gene (the most strongly upregulated or downregulated gene is assigned a value of 1) in each of the replicate experiments sorted by increasing or decreasing fold change. The smaller the RP score is, the higher the likelihood the gene is up or downregulated. The FunAlyse software cuts the list of differentially expressed genes at a level of 50% false discovery rate (FDR), which is the expected

percentage of false positives, or the software lists the top 100 genes according to their rank product score, regardless of their FDR, depending on the list that is longer. The full rank product differential expression analysis reports can be found in Appendix Two.

#### **4.4.1.1 WT keratinocytes versus K14D6 keratinocytes**

To investigate basal differences in transcription upon D6 expression, a comparison between resting K14D6 keratinocytes and wild-type keratinocytes was made.

##### **i) Potential upregulated genes**

The software generated a list of the top 100 genes according to rank product score (The full list can be found in Appendix Two) however, only six genes were potentially upregulated with less than 50% false discovery rate (Table 4-2).

Out of the six genes, only 2, chemokine binding protein 2 (Ccbp2, which is also known as D6) and dickkopf homolog 2 (Dkk2), changed more than 2-fold, which was identified as an arbitrary cut off (Table 4-2). Of the six potentially upregulated genes, the rank product (RP) score varied from 1.00, which was the highest ranked gene (Ccbp2) to an RP score of 470.76 for the lowest ranked gene with an FDR of less than 50%, which was tissue factor pathway inhibitor 2 (Tfpi2). The fold change (FC), varied from 49.59 to 1.48 (Ccbp2 and branched chain aminotransferase 1 (Bcat1) respectively) within the top six genes shown to be expressed at higher levels in resting K14D6 keratinocytes by the microarray (Table 4-2). One gene, Ccbp2, within this comparison was found to have an RP score of 1.00, which is the smallest RP value that can be achieved and was found to be expressed at higher levels (49.59 fold change), in K14D6 keratinocytes compared to wild-type keratinocytes and also had a 0% false discovery rate.

This data indicates that the gene, Ccbp2, is potentially upregulated by 49.52 fold in K14D6 keratinocytes compared to wild-type keratinocytes. In chapter 3, the levels of D6 transcripts were shown to be significantly higher in K14D6 keratinocytes compared to WT keratinocytes (see Figure 3-6). Therefore, these data confirm that the K14D6 transgene is expressed within K14D6 keratinocytes.

RP score	FDR (%)	FC	Gene Symbol	Gene Title
1.00	0.00	49.59	Ccbp2	Chemokine binding protein 2
206.84	15.50	2.66	Dkk2	Dickkopf homolog 2 ( <i>Xenopus laevis</i> )
348.58	43.33	1.81	Nrk	Nik related kinase
359.51	34.50	1.48	Bcat1	Branched chain aminotransferase 1, cytosolic
389.02	32.50	1.56	Stc2	Stannocalcin 2
470.76	47.67	1.62	Tfpi2	Tissue factor pathway inhibitor 2

**Table 4-2. The top 6 genes listed by RP score as potentially upregulated genes in K14D6 keratinocytes compared to wild-type keratinocytes.**

Potentially upregulated genes were listed in order of rank product score (RP score) with details of % false discovery rate (FDR) and fold change (FC).

## ii) Potential downregulated genes

A list of 100 potentially downregulated genes was generated by the analysis software according to RP scores in the comparison between K14D6 keratinocytes and wild-type keratinocytes; however only 81 of these genes had an FDR of less than 50% (Full list can be found in Appendix Two). Of the 81 genes, the RP score varied from 80.91 to 1158.63 with fold change varying between -2.92 and -1.02 (Appendix Two). The top 25 potentially downregulated genes listed in the RP report are summarised in Table 4-3.

Of the top 25 genes listed, only 24 genes were potentially downregulated as P lysozyme structural (Lzp-s) appeared twice in the RP report (Table 4-3). Of the 24 genes, only 4 changed more than 2-fold and these were within the top 5 ranked genes shown in Table 4-3. Lzp-s had the lowest RP score of 80.91, an FDR of 0% and a fold change of -2.92. Additionally, Lzp-s was third in the list with an RP score of 119.46, an FDR of 1.67 and a fold change of -2.73. Cathepsin S (Ctss) was second in the list with an RP score of 99.49 and changed by -2.81 fold. The other two genes found to be potentially downregulated more than 2-fold were C-type lectin domain family member n (Clec4n) and lysosomal associated protein transmembrane 5 (Lptm5) which were placed 4<sup>th</sup> and 5<sup>th</sup> in the RP report with 5.75% and 8.20% FDR respectively. This data indicates that ectopic expression of D6 may have a negative impact on the transcription of Lzp-s, Ctss, Clec4n and Lptm5.

RP score	FDR (%)	FC	Gene Symbol	Gene Title
80.91	0.00	-2.92	Lzp-s	P lysozyme structural
99.49	0.50	-2.81	Ctss	Cathepsin S
119.46	1.67	-2.73	Lzp-s	P lysozyme structural
204.14	5.75	-2.04	Clec4n	C-type lectin domain family, member n
241.21	8.20	-2.02	Laptm5	Lysosomal associated protein transmembrane 5
288.72	11.17	-1.84	Clec4d	C-type lectin domain family 4, member d
314.02	13.14	-1.94	1110014K05Rik	RIKEN cDNA 1110014K05 gene
349.82	16.00	-1.84	Fcgr3	Fc receptor, IgG, low affinity III
391.54	19.33	-1.96	A030004J04Rik	RIKEN cDNA A030004J04 gene
395.41	17.70	-1.88	Lyzs	Lysozyme
395.62	16.09	-1.74	Ms4a11	Membrane-spanning 4-domains, subfamily A, member 11
412.07	17.00	-1.79	Apoe	Apolipoprotein E
436.82	18.77	-1.76	Jarid1d	Jumonji, AT rich interactive domain 1D (Rbp2 like)
458.61	20.36	-1.75	Sepp1	Selenoprotein P, plasma, 1
463.19	19.87	-1.87	2310002A05Rik	RIKEN cDNA 2310002A05 gene
464.93	19.06	-1.73	Gp49a /// Lilrb4	Glycoprotein 49A /// leukocyte immunoglobulin-like receptor, subfamily B, member 4
529.00	26.29	-1.75	Sprr15	Small proline rich-like 5
530.23	24.89	-1.86	Lce5a	Late cornified envelope 5A
533.51	23.89	-1.78	Sprr17	Small proline rich-like 7
577.80	28.95	-1.73	1110055J05Rik	RIKEN cDNA 1110055J05 gene
601.17	30.43	-1.73	1110001M24Rik	RIKEN cDNA 1110001M24 gene
626.85	32.00	-1.60	Ddx3y	DEAD (Asp-Glu-Ala-Asp) box polypeptide 3, Y-linked
639.19	32.13	-1.32	Cxcl4	Chemokine (C-X-C motif) ligand 4
646.43	31.58	-1.56	Rbm5	RNA binding motif protein 5
648.49	30.68	-1.72	Sprr12	Small proline rich-like 2

**Table 4-3. Twenty-five top genes potentially downregulated in K14D6 keratinocytes compared to wild-type keratinocytes.**

**Genes were listed in order of rank product score (RP score) with details of % false discovery rate (FDR) and fold change (FC).**

#### **4.4.1.2 WT keratinocytes versus WT keratinocytes + CCL3**

Wild-type keratinocytes at rest and after ligand binding were compared to assess the basic differences in transcripts induced after ligand binding through chemokine receptors CCR1, CCR3 and CCR5.

##### **i) Potential upregulated genes**

The microarray showed higher levels of 217 genes, with an FDR of less than 50%, in wild-type keratinocytes incubated with CCL3 compared to control WT keratinocytes. The RP score varied from 145.79 to 1681.26 and the FC ranged from 3.72 to 1.3 (The full list can be found in Appendix Two). Of the 217 genes potentially upregulated using the rank product score, 71 genes demonstrated a 2-fold change with 9 of these changing more than 3-fold (Appendix Two). Table 4-4 lists the top 25 genes found to be potentially upregulated by CCL3 in wild-type keratinocytes using the rank product method.

The first five genes listed as potentially upregulated by RP score were membrane spanning 4-domain subfamily A member 7 (Ms4a7), chemokine (C-X-C motif) ligand 4 (CXCL4) also known as platelet derived factor 4, pleckstrin (Plek), procollagen type III alpha 1 (Col3a1) and dickkopf homolog 2 (Dkk2). Ms4a7 had an RP score of 145.79, a 14% FDR and a fold change of 2.46 whereas CXCL4 had an RP score of 171.94, a FDR of 9.5% and fold change of 2.10. Plek was ranked third in the list with an RP score of 189.97, an FDR of 8.33% and was expressed at higher levels by 2.61-fold. The fourth ranked gene was Col3a1 with an RP score of 224.73, a FDR of 10.25% and a fold change of 3.72 whereas the fifth ranked gene with an RP score of 228.64, an 8.2% FDR and changed by more than 3-fold was Dkk2.

RP score	FDR (%)	FC	Gene Symbol	Gene Title
145.79	14.00	2.46	Ms4a7	Membrane-spanning 4-domains, subfamily A, member 7
171.94	9.50	2.10	Cxcl4	Chemokine (C-X-C motif) ligand 4
189.97	8.33	2.61	Plek	Pleckstrin
224.73	10.25	3.72	Col3a1	Procollagen, type III, alpha 1
228.64	8.20	3.50	Dkk2	Dickkopf homolog 2 ( <i>Xenopus laevis</i> )
236.57	7.00	3.11	Tfpi2	Tissue factor pathway inhibitor 2
287.28	9.86	3.29	Lum	Lumican
288.57	8.75	2.86	Thbs2	Thrombospondin 2
288.84	7.78	2.48	B130021B11Rik	RIKEN cDNA B130021B11 gene
269.29	7.20	2.71	Mmp2	Matrix metalloproteinase 2
303.38	7.55	3.20	Pdgfrb	Platelet derived growth factor receptor, beta polypeptide
314.50	7.50	3.25	Col6a1	Procollagen, type VI, alpha 1
319.04	7.15	2.86	Crabp1	Cellular retinoic acid binding protein 1
322.66	7.00	2.96	Col6a2	Procollagen, type VI, alpha 2
329.93	7.00	2.13	C1qa	Complement component 1, q subcomponent, alpha polypeptide
335.60	6.88	2.65	Mmp2	Matrix metalloproteinase 2
339.17	6.71	2.78	Il1rl1	Interleukin 1 receptor-like 1
373.12	8.39	2.55	Dpep1	Dipeptidase 1 (renal)
394.70	9.68	2.21	Col11a1	Procollagen, type XI, alpha 1
397.90	9.35	2.16	Ms4a6d	Membrane-spanning 4-domains, subfamily A, member 6D
415.35	9.67	1.88	Laptn5	Lysosomal-associated protein transmembrane 5
417.60	9.32	2.82	Postn	Periostin, osteoblast specific factor
421.55	9.22	2.10	Nr2f1	Nuclear receptor subfamily 2, group F, member 1
437.53	10.04	2.56	Cdh11	Cadherin 11
439.43	9.72	1.97	F13a1	Coagulation factor XIII, A1 subunit

**Table 4-4. The first 25 genes listed as potentially upregulated by CCL3 in wild-type keratinocytes.**

**Genes were listed in order of rank product score (RP score) with details of % false discovery rate (FDR) and fold change (FC).**

**ii) Potential downregulated genes**

Addition of CCL3 to wild-type keratinocytes resulted in the potential downregulation of 13 genes with an FDR of less than 50%, as summarised in Table 4-5. The RP score varied from 228.87 to 574.12 and the FC, -4.27 to -1.47, for the highest ranked gene and 15<sup>th</sup> ranked gene respectively (one gene, *Ddx3y*, appeared in the list three times). Of the 13 listed genes, one gene was expressed more than 4 fold lower, which was DEAD box polypeptide (*Ddx3y*). Eukaryotic translation initiation factor 2 (*Eif2s3y*) was potentially downregulated more than 3 fold. Genes potentially downregulated more than 2 fold were jumonji (*Jarid1d*) and *Ddxy3* (Table 4-5). All three of these genes are linked to the Y chromosome (Isensee and Ruiz Noppinger, 2007). One explanation could be that the population of keratinocytes treated with CCL3 were isolated, coincidentally, from more females than males in comparison to the keratinocyte population used as resting wild-type keratinocytes.

RP score	FDR (%)	FC	Gene Symbol	Gene Title
228.87	45.00	-4.27	Ddx3y	DEAD (Asp-Glu-Ala-Asp) box polypeptide 3, Y linked
263.41	32.50	-1.59	1110014K05Rik	RIKEN cDNA 1110014K05 gene
265.52	22.00	-1.79	Hnr	Hornerin
302.93	23.50	-2.63	Ddx3y	DEAD (Asp-Glu-Ala-Asp) box polypeptide 3, Y linked
319.33	21.20	-3.57	Eif2s3y	Eukaryotic translation initiation factor 2, subunit 3, structural gene Y-linked
332.57	19.83	-1.63	Spr15	Small proline rich-like 5
387.48	28.00	-1.55	Lce5a	Late cornified envelope 5A
415.16	30.12	-1.58	Rptn	Repetin
443.01	32.11	-2.14	Jarid1d	Jumonji, AT rich interactive domain 1D (Rbp2 like)
453.86	30.90	-1.49	Spr17	Small proline rich-like 7
494.01	36.36	-1.51	---	---
506.99	35.75	-1.84	Uty /// LOC546404 /// LOC546411	Ubiquitously transcribed tetratricopeptide repeat gene, Y chromosome /// similar to male-specific histocompatibility antigen H-YDb /// similar to male-specific histocompatibility antigen H-YDb
508.76	33.62	-1.53	LOC433621 /// LOC545581	Similar to Acidic ribosomal phosphoprotein P0 /// similar to Acidic ribosomal phosphoprotein P0
544.39	36.79	-1.98	Ddx3y	DEAD (Asp-Glu-Ala-Asp) box polypeptide 3, Y linked
574.12	38.80	-1.47	1110001M24Rik	RIKEN cDNA 1110001M24 gene

**Table 4-5. Top 15 genes potentially downregulated gene by CCL3 in wild-type keratinocytes.**

**Genes were listed in order of rank product score (RP score) with details of % false discovery rate (FDR) and fold change (FC).**

### 4.4.1.3 K14D6 keratinocytes versus K14D6 + CCL3

To assess the transcriptional consequences of ligand binding to D6, a comparison between resting K14D6 keratinocytes and K14D6 keratinocytes after ligand binding was made.

#### i) Potential upregulated genes

The microarray showed higher levels of 171 genes in K14D6 keratinocytes incubated with CCL3 compared to K14D6 keratinocytes at rest (see full list in Appendix Two). The RP score of the 171 genes varied from 97.20 to 1538.85 and the FC ranged from 3.31 to 1.24. Out of 171 genes, 11 genes were potentially differentially expressed more than 2 fold and all were within the first top 25 genes summarised in Table 4-6. It is of note that Table 4-6 lists the top 25 potentially upregulated genes as listed in the RP report; however only 24 genes are potentially upregulated as Lzp-s appears twice.

One gene potentially differentially expressed by more than 3 fold was aldehyde dehydrogenase family 1 (Aldh1a7), which was also the first gene on the rank product list with an RP score of 97.20 and a 3% false discovery rate (Table 4-6). P lysozyme structural (Lzp-s) was ranked 2<sup>nd</sup> and 4<sup>th</sup> in the RP report with RP scores of 106.48 and 132.50 respectively, both times with an FDR of 1.5% and a fold change of 2.47 and 2.33 respectively. Cathepsin S (Ctss) was listed 3<sup>rd</sup> with an RP score of 110.66, an FDR of 1.33% and was changed by 2.33 fold. Nucleoplasmin 3 (Npm3) was listed 5<sup>th</sup> with an RP score of 147.22, an FDR of 1.4% and was potentially upregulated by 2.11 fold. Selenoprotein P plasma 1 (Sepp1) was listed 6<sup>th</sup> with an RP score of 162.85 and was potentially differentially expressed by 2.31 fold, followed by pentraxin related gene 3 (Ptx3) with an RP score of 199.63, potentially upregulated by 2.18 fold and an FDR of 2.71%. Aldehyde dehydrogenase family 1 subfamily A1 (Aldh1a1) had an RP score of 210.40 and changed by 2.31 fold whereas lysosomal-associated protein transmembrane 5 (Laptm5) and Fc receptor IgG low affinity III (Fcrg3) had an RP score of 234.4 and 242.06 respectively (listed 9<sup>th</sup> and 10<sup>th</sup>) and changed by 1.89 and 1.97 fold respectively.

Within the top 25 genes listed, seven genes expressed at higher levels by CCL3 in K14D6 keratinocytes were found to be expressed at lower levels in resting K14D6

keratinocytes compared to wild-type keratinocytes (Table 4-6 and 4-3 respectively). These genes were *Lzp-s*, *Ctss*, *Laptm5*, *Fcgr3*, Lysozyme (*Lyzs*), apolipoprotein E (*Apoe*) and *Sepp1*. This suggests that in absence of ligand, basal D6 may have a negative impact on the transcription of these genes but CCL3 binding may be able to induce transcription of these genes.

RP score	FDR (%)	FC	Gene Symbol	Gene Title
97.20	3.00	3.31	<i>Aldh1a7</i>	Aldehyde dehydrogenase family1, subfamily A7
106.48	1.50	2.47	<i>Lzp-s</i>	P lysozyme structural
110.66	1.33	2.33	<i>Ctss</i>	Cathepsin S
132.50	1.50	2.33	<i>Lzp-s</i>	P lysozyme structural
147.22	1.40	2.11	<i>Npm3</i>	Nucleoplasmin 3
162.85	1.50	2.31	<i>Sepp1</i>	Selenoprotein P, plasma, 1
199.63	2.71	2.18	<i>Ptx3</i>	Pentraxin related gene
210.40	2.75	2.31	<i>Aldh1a1</i>	Aldehyde dehydrogenase family 1, subfamily A1
234.40	3.67	1.89	<i>Laptm5</i>	Lysosomal- associated protein transmembrane 5
242.06	3.90	1.97	<i>Fcgr3</i>	Fc receptor, IgG, low affinity III
254.35	4.27	2.18	<i>Col3a1</i>	Procollagen, type III, alpha 1
279.37	5.17	2.22	<i>Steap4</i>	STEAP family member 4
296.41	6.38	1.61	<i>Slc6a14</i>	Solute carrier family 6 (neurotransmitter transporter), member 14
302.93	6.14	2.05	2610001E17Rik	RIKEN cDNA 2610001E17 gene
305.98	5.87	1.79	<i>Lcn2</i>	Lipocalin 2
313.90	5.94	1.92	<i>Apoe</i>	Apolipoprotein E
373.00	9.29	1.82	<i>Ccl9</i>	Chemokine (C-C motif) ligand 9
398.97	11.22	1.98	<i>Gpm6b</i>	Glycoprotein m6b
423.63	12.68	2.11	<i>Gtl2 /// Lphn1</i>	GTL2, imprinted maternally expressed untranslated mRNA /// latrophilin 1
427.48	12.40	1.68	<i>Sprr2f</i>	Small proline-rich protein 2F
430.38	12.24	1.86	<i>Ccl6</i>	Chemokine (C-C motif) ligand 6
435.11	12.23	1.60	2310003F16Rik	RIKEN cDNA 2310003F16 gene
446.67	12.52	1.92	<i>Gp49a /// Lilrb4</i>	Glycoprotein 49 A /// leukocyte immunoglobulin-like receptor, subfamily B, member 4
463.36	13.08	1.86	<i>Col1a1</i>	Procollagen, type I, alpha 1
464.59	12.56	1.85	<i>Lyzs</i>	Lysozyme

**Table 4-6. Top 25 genes potentially upregulated by CCL3 in K14D6 keratinocytes.**

**Genes were listed in order of rank product score (RP score) with details of % false discovery rate (FDR) and fold change (FC).**

***Genes potentially upregulated by CCL3 in both WT and K14D6 keratinocytes***

The microarray showed that CCL3 binding to K14D6 keratinocytes resulted in the potential upregulation of 171 genes with an FDR of less than 50%, however CCL3 ligand binding in wild-type keratinocytes resulted in the potential upregulation of 217 genes (Full results in Appendix Two). Eighty seven genes expressed at higher levels in K14D6 keratinocytes as a result of ligand binding were also expressed at higher levels in wild-type keratinocytes after ligand binding, accounting for 99 of the 217 genes listed within the wild-type + CCL3 RP report (some genes were listed twice).

Comparing the first 25 ranked genes potentially upregulated by CCL3 in the wild-type and K14D6 keratinocytes (Table 4-4 and Table 4-6 respectively), only two genes appear in the top 25 of both lists. The two genes are *Laptm5*, which is listed 9<sup>th</sup> in K14D6 keratinocytes (Table 4-6) and is listed 21<sup>st</sup> in wild-type keratinocytes (Table 4-4). The second gene is procollagen type III (*Col3a1*), found to be potentially differentially expressed by CCL3 binding in both K14D6 and wild-type keratinocytes, was listed 11<sup>th</sup> and 4<sup>th</sup> respectively (Table 4-6 and Table 4-4). Other genes were potentially upregulated after CCL3 binding in both K14D6 keratinocytes and wild-type keratinocytes (although these genes are not shown in Table 4-4 but are listed in Appendix Two). These genes were, *Aldh1a7*, *Lzp-s*, *Ctss*, *Sepp1*, *Ptx3*, *Aldh1a1*, *Fcgr3*, *Col3a1*, Riken cDNA 2610001E17 gene, *ApoE*, *CCL9*, *Gtl2*, *CCL6*, glycoprotein 49a (*Gp49a*), *Col1a1* and *Lyzs*. Genes potentially upregulated in both wild-type and K14D6 keratinocytes after ligand binding suggest that these may be transcriptional consequences induced through ligand binding to CCR1, CCR3 or CCR5.

Genes found only to be potentially upregulated in K14D6 keratinocytes were *Npm3*, *STEAP4*, solute carrier family 6 member 14 (*Slc6a14*), lipocalin 2 (*Lcn2*), glycoprotein m6b (*Gpm6b*), small proline-rich protein 2F (*Sprr2f*) and Riken cDNA 2310003F16 gene (Table 4-6). This suggests the possibility that these genes are affected by CCL3 binding to D6. Genes found only to be potentially upregulated, within the first 25 listed in Table 4-4, in wild-type keratinocytes after CCL3 binding were *Dkk2*, *Tfpi2*, Riken cDNA B130021B11 gene, complement component 1 q subcomponent (*C1qa*), nuclear receptor subfamily 2 (*Nr2f1*) and coagulation factor XIII (*F13a1*). These genes were not expressed at higher levels

after CCL3 binding in K14D6 keratinocytes. This suggests the possibility that the presence of D6 on K14D6 keratinocytes may limit the induction of Dkk2, Tfp12, RIKEN cDNA B130021B11 gene, C1qa, Nr2f1 and F13a1.

## ii) Potential downregulated genes

The microarray showed lower levels of only four genes, with an FDR of less than 50%, in the comparison between resting K14D6 keratinocytes and K14D6 keratinocytes after addition of CCL3 (Table 4-7). The RP score varied from 123.91 to 369.64 for these four genes and the FC varied from -1.85 to -1.44 (Table 4-7). Two genes were not given a gene symbol or title but the rank product report has hyperlinks for each differentially expressed gene to a database, the Stanford Online Universal Resource for Clones and Ests (SOURCE). Using this hyperlink, these genes were identified as adapter related protein complex 2 beta 1 subunit (Ap2b1) and cannabinoid receptor 1 (Cbp1). The first gene, Ap2b1, had an RP score of 123.91, a 2% false discovery rate and was potentially downregulated by 1.85 fold. The second gene expressed at lower levels was sulfatase 1 with an RP score of 254.52, changed by 1.62 fold with an FDR of 29%. The third gene was uroplakin 1B with an RP score of 294.66, an FDR of 26.67% and was potentially downregulated by 1.6 fold. The fourth gene listed was cannabinoid receptor 1 with an RP score of 369.64 and a false discovery rate of 34%.

RP score	FDR (%)	FC	Gene Symbol	Gene Title
123.91	2.00	-1.85	Ap2b1	Adapter related protein complex 2 beta 1 subunit
264.52	29.00	-1.62	Sulf1	Sulfatase 1
294.66	26.67	-1.60	Upk1b	Uroplakin 1B
369.64	34.00	-1.44	Cbp1	Cannabinoid receptor 1

**Table 4-7. Top 4 genes listed as potentially downregulated after CCL3 treatment in K14D6 keratinocytes.**

**Genes were listed in order of rank product score (RP score) with details of % false discovery rate (FDR) and fold change (FC).**

***Genes potentially downregulated by CCL3 binding in both WT and K14D6  
keratinocytes***

CCL3 ligand binding in wild-type keratinocytes resulted in the potential downregulation of 13 genes (Table 4-5) whereas CCL3 treatment on K14D6 keratinocytes resulted the potential downregulation of 4 genes (Table 4-7). All the genes expressed at lower levels in wild-type keratinocytes by CCL3 were different from the genes expressed at lower levels by CCL3 in K14D6 keratinocytes. This suggests that CCL3 binding may have a negative impact on the gene transcripts via different mechanisms in wild-type and K14D6 keratinocytes.

#### **4.4.1.4 WT + CCL3 versus K14D6 + CCL3**

This comparison would give an understanding of the genes that are potentially up- or downregulated after CCL3 binding in K14D6 keratinocytes compared to wild-type keratinocytes.

##### **i) Potential upregulated genes**

Seven genes, with less than 50% FDR, were expressed at higher levels after CCL3 treatment in K14D6 keratinocytes compared to wild-type keratinocytes (Table 4-8). The RP score varied from 1.28 to 423.42 with fold change of between 35.02 and 1.52. Of the seven genes, 3 genes were potentially differentially expressed more than 2 fold. The gene with the smallest RP score of 1.28 was *Ccbp2* (D6). This gene was potentially upregulated by 35 fold in K14D6 keratinocytes after incubation with CCL3 compared to wild-type keratinocytes incubated with CCL3. Of the seven genes potentially upregulated, three were Y-linked meaning these are genes encoded within the Y-chromosome. The genes were *Ddx3y*, which was ranked 2<sup>nd</sup> and 4<sup>th</sup>, *Eif2s3y* and *Uty* (Table 4-8). As these are Y-linked genes (Isensee and Ruiz Noppinger, 2007), this data suggests that the keratinocyte population used within the K14D6 + CCL3 group were isolated from more male neonates than the wild-type + CCL3 group.

RP score	FDR (%)	FC	Gene Symbol	Gene Title
1.28	0.00	35.02	Ccbp2	Chemokine binding protein 2
90.60	12.00	3.97	Ddx3y	DEAD (Asp-Glu-Ala-Asp) box polypeptide 3, Y-linked
186.44	9.00	3.73	Eif2s3y	Eukaryotic translation initiation factor 2, subunit 3, structural gene Y-linked
280.18	21.25	2.31	Ddx3y	DEAD (Asp-Glu-Ala-Asp) box polypeptide 3, Y-linked
335.66	27.20	1.55	Slc6a14	Solute carrier family 6(neurotransmitter transporter), member 14
396.73	33.67	1.58	Uty /// LOC546404 /// LOC546411	Ubiquitously transcribed tetratricopeptide repeat gene, Y chromosome /// similar to male-specific histocompatibility antigen H-YDb /// similar to male-specific histocompatibility antigen H-YDb
407.62	31.86	1.92	Jarid1d	Jumonji, AT rich interactive domain 1D (Rbp2 like)
423.42	32.00	1.52	Slc7a3	Solute carrier family 7 (cationic amino acid transporter, y+ system), member 3

**Table 4-8. Genes listed as potentially upregulated after CCL3 treatment in K14D6 keratinocytes compared to wild-type keratinocytes after CCL3 treatment.**

Genes were listed in order of rank product score (RP score) with details of % false discovery rate (FDR) and fold change (FC).

#### *Genes potentially upregulated due to ectopic expression of D6*

Ccbp2 was potentially upregulated, with an RP score of 1.28, in the wild-type + CCL3 versus K14D6 + CCL3 comparison (Table 4-8). However, Ccbp2 was also potentially upregulated and ranked 1<sup>st</sup> with an RP score of 1.00 in the WT versus K14D6 keratinocytes comparison (Table 4-2). Therefore, these data confirm that there are higher levels of D6 within K14D6 keratinocytes confirming that the D6 transgene is expressed within K14D6 keratinocytes.

It was noted that three Y-linked genes, Ddx3y, Eif2s3y and Uty, were potentially upregulated in K14D6 keratinocytes after ligand binding in comparison to wild-type keratinocytes after CCL3 binding (Table 4-8). Ddx3y and Eif2s3y were also potentially downregulated in wild-type keratinocytes after CCL3 binding compared to wild-type keratinocytes at rest (Table 4-5). This comparison supports evidence that the keratinocyte population used in the wild-type + CCL3 samples were derived from more female neonates than males.

## ii) Potential downregulated genes

Twenty three genes, with less than 50% FDR, were found to be potentially downregulated with an RP score range of 145.03 to 754.73 and fold change of -2.12 to -1.39 (Table 4-9 lists top 25 ranked genes as Lzp-s and Clec4n appear twice). Four genes were found to change more than 2-fold, which were lysosomal associated protein transmembrane 5 (Laptm5), P-lysosome structural (Lzp-s), C-type lectin domain family 4 member d (Clec4d) and C-type lectin family 4 member n (Clec4n), in which three of these were listed within the top four in terms of RP score (Table 4-9).

RP score	FDR (%)	FC	Gene Symbol	Gene Title
145.03	10.00	-2.01	Laptm5	Lysosomal-associated protein transmembrane 5
154.19	5.50	-1.96	Lzp-s	P lysozyme structural
163.17	3.67	-2.04	Lzp-s	P lysozyme structural
186.83	4.50	-2.12	Clec4d	C-type lectin domain family 4, member d
204.23	4.60	-1.93	Ctss	Cathepsin S
236.28	6.33	-1.96	Plek	Pleckstrin
377.58	22.14	-1.93	Ms4a7	Membrane-spanning 4-domains, subfamily A, member 7
378.78	19.62	-1.69	Cxcl4	Chemokine (C-X-C motif) ligand 4
381.87	17.89	-1.70	Tfpi2	Tissue factor pathway inhibitor 2
407.64	20.70	-1.82	F13a1	Coagulation factor XIII, A1 subunit
418.00	20.82	-1.74	Ms4a11	Membrane-spanning 4-domains, subfamily A, member 11
418.30	19.08	-1.77	Mrc1	Mannose receptor, C type 1
421.12	17.92	-1.73	Ccl6	Chemokine (C-C motif) ligand 6
421.60	16.86	-1.56	B130021B11Rik	RIKEN cDNA B130021B11 gene
427.86	16.67	-2.06	Clec4n	C-type lectin domain family 4, member n
462.57	19.31	-1.86	Fcgr2b	Fc receptor, IgG, low affinity IIb
502.33	23.24	-1.83	Ms4a6d	Membrane-spanning 4-domains, subfamily A, member 6D
562.57	31.33	-1.66	Lyzs	Lysozyme
565.86	30.11	-1.82	C1qa	Complement component 1, q subcomponent, alpha polypeptide
572.64	29.65	-1.78	Clec4n	C-type lectin domain family 4, member n
640.21	37.48	-1.75	Spp1	Secreted phosphoprotein 1
646.39	36.95	-1.39	Dcn	Decorin
694.46	43.87	-1.75	C3ar1	Complement component 3a receptor 1
698.40	42.71	-1.63	Cck	Cholecystokinin
730.34	46.00	-1.64	Fcgr3	Fc receptor, IgG, low affinity III

**Table 4-9. Top 25 ranked genes potentially downregulated in K14D6 keratinocytes treated with CCL3 in comparison to WT keratinocytes treated with CCL3.**

Genes were listed in order of rank product score (RP score) with details of % false discovery rate (FDR) and fold change (FC).

***Genes potentially downregulated due to ectopic expression of D6***

Twelve of the potentially downregulated genes, summarised in Table 4-9, were also potentially downregulated in resting K14D6 keratinocytes in comparison to resting wild-type keratinocytes. Nine of the 12 genes are within the top 25 genes of both tables (Table 4-9 and 4-3 respectively). These were Laptm5, Lzp-s (listed twice), Clec4d, Ctss, CXCL4, Ms4a11, Lyzs, Clec4n and Fcgr3. The other three genes were mannose receptor c-type 1 (Mrc1), CCL6 and Fc receptor IgG low affinity IIb (Fcgr2b), listed as potentially downregulated after ligand binding in K14D6 keratinocytes compared to wild-type (Table 4-9). Mrc1, CCL6 and Fcgr2b are ranked 66<sup>th</sup>, 64<sup>th</sup> and 44<sup>th</sup> respectively in the potentially downregulated gene comparison between resting K14D6 and wild-type keratinocytes (Full list in Appendix Two). This would suggest that ectopic expression of D6 might affect the levels of these genes at rest. To determine a possible explanation as to why these genes were potentially downregulated with resting levels of D6, it was discovered that four of the genes, Ctss, Lyzs, Lzp-s and Laptm5 were associated with the lysosome. Ctss, Lzp-s and Lyz are all lysosomal proteins whereas Laptm5 is a transmembrane spanning protein present in the lysosome (Adra et al., 1996). However, only Lzp-s and Lyz were genes encoded within the same chromosome. This ruled out the possibility that basal D6 in absence of ligand was affecting the transcription of genes encoded within the same chromosome.

However, some of these genes, Laptm5, Lzp-s, Ctss, CCL6 and Fcgr3 were potentially upregulated by CCL3 in K14D6 keratinocytes (Table 4-6). This suggests CCL3 binding in K14D6 keratinocytes may be able to induce these genes. However, it was noted that the potential downregulation of Laptm5, Lzp-s, Ctss, CCL6 and Fcgr3 in K14D6 keratinocytes after ligand binding compared to wild-type might be due to lower levels of gene expression in resting K14D6 keratinocytes.

#### 4.4.1.5 Summary of rank product differential analysis reports

From the list of potentially differentially expressed genes using the rank product method, the conditions under which the largest number of genes were potentially differentially expressed and with a false discovery rate of less than 50% was after keratinocytes were incubated with CCL3. Two hundred and seventeen genes were potentially upregulated in wild-type keratinocytes and 171 genes were potentially upregulated in K14D6 keratinocytes. The largest number of genes potentially downregulated was in K14D6 keratinocytes at rest compared to wild-type keratinocytes at rest, with 81 genes potentially differentially expressed.

One gene in this analysis stood out from the rest and this was *Ccbp2* (D6) with an RP score of 1. *Ccbp2* was listed in two rank product differential expression analysis reports with the two smallest rank product score values in the full microarray analysis, along with the highest fold change and 0% false discovery rate (summarised in Table 4-10). These data confirm there is upregulation of D6 with a 49.59 fold change in resting K14D6 keratinocytes compared to the wild-type. D6 was also expressed at higher levels, with a 35.02 fold change, in K14D6 keratinocytes compared to wild-type keratinocytes after ligand binding, however CCL3 does not affect the levels of D6, as the gene was not found to be differentially expressed in comparison to K14D6 keratinocytes not treated with CCL3.

Comparison	Gene	RP score	FDR (%)	FC
WT control v K14D6 control	<i>Ccbp2</i>	1.00	0.00	49.59
WT + CCL3 v K14D6 +CCL3	<i>Ccbp2</i>	1.28	0.00	35.02

**Table 4-10. Expression of D6 in rank product differential expression analysis reports.**

**D6 (*Ccbp2*) was potentially upregulated in K14D6 keratinocytes at rest compared to wild-type (WT) control keratinocytes and in K14D6 keratinocytes after incubation with CCL3 compared to wild-type keratinocytes after CCL3 incubation. RP score is rank product score, FDR is the false discovery rate and FC is the fold change in the gene.**

### ***Transcriptional changes due to ectopic expression of D6***

The microarray showed that only six genes were expressed at higher levels in K14D6 keratinocytes in comparison to wild-type keratinocytes. These were Ccbp2 (D6), Dkk2, Nr1, Bcat1, Stc2 and Tfpi2 (Table 4-2). Ccbp2 was the only gene with an RP score of 1 and confirmed that there is increased expression of D6 within K14D6 keratinocytes.

Eighty one genes were potentially downregulated, with an FDR of less than 50%, in untreated K14D6 keratinocytes compared to wild-type keratinocytes suggesting transcriptional changes may have occurred through D6 in a ligand independent manner. Within this group, the 1<sup>st</sup> ranked gene potentially differentially expressed was Lzp-s, which had the third smallest RP score of 80.91 in the microarray (after D6 with an RP score of 1 and 1.28).

### ***Effect of CCL3 binding on keratinocytes***

The largest number of genes potentially upregulated was after ligand binding with CCL3 in keratinocytes. CCL3 binding in wild-type keratinocytes resulted in 217 potentially differentially expressed genes whereas 181 genes were potentially differentially expressed in K14D6 keratinocytes.

When comparing both RP differential expression reports, 87 genes potentially upregulated in K14D6 keratinocytes by CCL3 binding were also potentially upregulated in wild-type keratinocytes after CCL3 binding. Two genes, Lzp-s and Col3a1, were listed within the top twenty five genes expressed at higher levels by CCL3 binding in both wild-type and K14D6 keratinocytes. Genes potentially upregulated in both wild-type and K14D6 keratinocytes suggests that these genes may be induced through CCL3 binding to common receptors, such as CCR1, CCR3 and CCR5, shown to be present on wild-type and K14D6 keratinocytes previously within Chapter 3.

The microarray showed lower levels of 13 genes in wild-type keratinocytes and lower levels of 4 genes in K14D6 keratinocytes after CCL3 binding. None of the genes potentially downregulated in wild-type and K14D6 keratinocytes were the same. Many of the genes potentially downregulated in wild-type keratinocytes after CCL3 binding were Y-linked genes and may have been due to the

keratinocyte populations used being isolated from more female neonates coincidentally than the keratinocyte population used as resting wild-type.

### ***Differential expression of genes after CCL3 binding between WT and K14D6 keratinocytes***

Differences in gene expression after ligand binding between wild-type and K14D6 keratinocytes were analysed in the WT + CCL3 v K14D6 + CCL3 rank product report. Differential gene expression would give an indication into the effect the presence of D6 in K14D6 keratinocytes has on the cell transcriptome after CCL3 binding. Only seven genes were potentially upregulated in K14D6 keratinocytes compared to the wild-type. One gene potentially upregulated was *Ccbp2* (D6) as discussed above and summarised in Table 4-10. Three of the seven genes potentially upregulated within K14D6 keratinocytes were Y-linked genes. One possibility may be that the keratinocytes used for the WT + CCL3 population were isolated from fewer males than the K14D6 + CCL3 population. This also correlates with Y-linked genes being potentially downregulated in WT v WT + CCL3 comparison. The other two genes potentially differentially expressed were both solute carrier family genes, *Slc6a14* and *Slc7a3*. These two genes were not potentially differentially upregulated in K14D6 keratinocytes at rest compared to wild-type and therefore the potential upregulation could not be explained by an initial higher level of gene expression in resting K14D6 keratinocytes.

Twelve genes were potentially downregulated at rest and after ligand binding in K14D6 keratinocytes compared to wild-type keratinocytes (Table 4-3 and Table 4-9 respectively). Nine out of the twelve genes were listed within the top 25 genes in both comparisons. These genes were *Lptm5*, *Lzp-s*, *Clec4d*, *Ctss*, *CXCL4*, *Ms4a11*, *Clec4n*, *Lyzs* and *Fcgr3*. The nine genes listed were also potentially upregulated by CCL3 in K14D6 keratinocytes. This suggests that the differential expression of these genes after ligand binding between wild-type and K14D6 keratinocytes is due to K14D6 keratinocytes having a lower expression of these genes at rest than wild-type keratinocytes.

Eleven genes potentially downregulated after ligand binding in K14D6 keratinocytes compared to wild-type were not potentially downregulated in resting K14D6 keratinocytes. These were *Plek*, *Ms4a7*, *Tfpi2*, *Fl3a1*, *B130021B11Rik*, *Ms4a6d*, *C1qa*, *Spp1*, decorin (*Dcn*), *C3ar1* and cholecystokinin

(Cck). This result indicates that the difference was potentially due to ectopic expression of D6 affecting the transcriptional consequence of CCL3 by inhibiting gene expression.

#### **4.4.2 Iterative group analysis**

The lists of genes produced by rank products are further processed using iterative group analysis (iGA), which identifies functional changed groups of genes, where each gene is assigned to a functional class according to Gene Ontology (<http://www.geneontology.org>). Iterative group analysis combines the relative position of the genes in the RP list and the number of changed genes within the group to statistically determine the strength of changes within the group. This analysis was performed using various steps, firstly sorting the genes according to a differential expression method, in this case by RP score, either by increasing or decreasing order. The second step was to count the members of each functional class of interest and then for each functional class member determine the probability of change (p-value) for the gene member to be in that position by chance (Breitling et al., 2004a). The p-value for each member was plotted against the position of each class member within a functional group. The position with the smallest p-value was assigned as the 'cut off' point for each functional group. Therefore, all gene members above this position were determined as potentially differentially expressed and the smallest p-value was assigned the p value changed for the group. This was performed for all the functional gene classes, which were then sorted according to their p-value changed. The threshold of the p value changed was  $1.2 \times 10^{-4}$  and therefore classes with the smallest P value changed (below  $1.2 \times 10^{-4}$ ) were the most significantly changed. An advantage of iGA analysis is that it does not require all members of the group change. Another important feature is that experimental replicates are not required because statistical significance can be determined by using group members as internal replicates. Full details of four iGA reports can be found in Appendix Three.

To identify functional changed groups of genes, four comparisons were made:

- 1) WT control (baseline) Versus K14D6 control
- 2) WT control (baseline) Versus WT + CCL3
- 3) K14D6 control (baseline) Versus K14D6 + CCL3
- 4) WT + CCL3 (baseline) Versus K14D6 + CCL3

#### 4.4.2.1 WT control v K14D6 control keratinocytes

##### i) Potential upregulated functional genes classes

Ectopically expressing D6 within keratinocytes resulted in 9 classes of genes, which involved 18 distinct gene members, being potentially upregulated in K14D6 keratinocytes compared to wild-type keratinocytes at rest (Table 4-11).

Four of these groups included genes associated with cell structure, which were collagen, extracellular matrix structural constituent conferring tensile strength, collagen triple helix repeat and extracellular matrix structural constituent. All of these groups involved the procollagen family of genes, which are also all involved in the phosphate transport group listed. Other functional gene classes potentially differentially expressed were transmembrane receptor protein tyrosine kinase signalling pathway, cadherin cytoplasmic region, intracellular calcium activated chloride channel activity and prostaglandin biosynthesis.

WT control V K14D6 control	Group members	Changed members	P-value Changed
5581- collagen	34	5	1.9e-07
7169- transmembrane receptor protein tyrosine kinase signalling pathway	76	6	4.3e-06
30020- extracellular matrix structural constituent conferring tensile strength	29	4	4.5e-06
IPR008160- Collagen triple helix	65	5	5.1e-06
IPR000233- Cadherin cytoplasmic region	12	3	7.8e-06
6817- phosphate transport	84	5	1.8e-05
1516- prostaglandin synthesis	9	2	2.9e-05
5201- extracellular matrix structural constituent	47	4	3.2e-05
5229- intracellular calcium activated chloride channel activity	3	3	1.0e-04

**Table 4-11. Potential upregulated functional gene classes in K14D6 keratinocytes compared to wild-type keratinocytes**

### ***Comparison with WT control V K14D6 control RP report***

Only six genes with an FDR of less than 50% were potentially upregulated in resting K14D6 keratinocytes in comparison to wild-type, using RP score (Table 4-2). None of the genes were listed as changed members within the top changed groups in the iGA analysis report. However, genes ranked 9<sup>th</sup> and 15<sup>th</sup> in the RP report, prostaglandin I2 synthase and prostaglandin-endoperoxidase synthase, were the two changed members within the prostaglandin synthesis group, which was statistically determined as potentially upregulated. Five procollagen genes are members within 5 of the top 9 changed groups in the iGA report. All 5 genes were ranked between 32 and 62 in the RP report and all had a false discovery of more than 50%.

#### **ii) Potential downregulated functional gene classes**

Gene classes found to be potentially downregulated in K14D6 keratinocytes compared to wild-type keratinocytes at rest included 11 groups of genes classes involving 21 distinct genes (Table 4-12).

The top changed group involved the functional class of cornified envelope, followed by keratinisation. Other groups such as glycoside hydrolase, lysozyme activity, cell wall catabolism and cytolysis involved the same two members changing, which were P lysozyme structural (Lzp-s) and lysozyme (Lyzs). Three groups involving chemokines were potentially downregulated, in which four chemokines were consistently changed across all three groups; these were CXCL4, CCL9, CCL6 and CXCL2. The fifth changed member within the chemotaxis group was complement component 3a receptor 1 (C3ar1). The other top changed groups were involved in IgG binding and tyrosinase. This suggests that the possibility that the presence of D6 within K14D6 keratinocytes may inhibit the expression levels of genes within these functional gene classes.

WT control V K14D6 control	Group members	Changed members	P-value Changed
1533- cornified envelope	14	7	9.3e-13
31424 – keratinisation	23	4	4.1e-06
IPR001916- Glycoside hydrolase, family 22	8	2	4.6e-06
3796- lysozyme activity	10	2	7.4e-06
16998- cell wall catabolism	16	2	2.0e-05
IPR001811- Small chemokine, interleukin-8 like	31	4	2.2e-05
19835- cytolysis	20	2	3.1e-05
19864 – IgG binding	5	2	4.1e-05
8009- chemokine activity	38	4	5.0e-05
6935- chemotaxis	87	5	1.1e-04
IPR002227- Tyrosinase	3	3	1.2e-04

**Table 4-12. Potential downregulated functional gene classes in K14D6 keratinocytes compared to wild-type keratinocytes.**

### *Comparison with the RP report*

P-lysozyme structural and lysozyme were two members that changed consistently across 4 top changed groups in the iGA analysis and these were genes that were also potentially differentially expressed within the top twenty five genes listed in the RP report (Table 4-3). Three of the top changed groups contained four chemokines that changed consistently in the iGA analysis and three of these chemokines (CXCL4, CCL9 and CCL6) were potentially differentially expressed in the rank product report. Changed members within the cornified envelope and keratinisation group were listed within the rank product report. Fcgr3 was a changed member within the IgG binding group, which was potentially differentially expressed in the RP report. Tyrosinase was the 11<sup>th</sup> top changed group in the iGA analysis report yet none of the three changed members, dopachrome tautomerase, tyrosinase-related protein 1 and tyrosinase, were listed as potentially differentially expressed within the 100 genes listed in the RP report.

#### 4.4.2.2 WT control v WT control + CCL3

##### i) Potential upregulated functional gene classes

CCL3 ligand binding to wild-type keratinocytes resulted in the potential upregulation of 22 functional gene classes in comparison to wild-type keratinocytes at rest. These 22 groups consisted of 42 distinct genes (Table 4-13).

The top three groups had the highest numbers of changed members. The 8 changed members within the top changed group of collagen triple helix repeat were also seven of the members that change within the second listed changed gene group involved in phosphate transport. The third top changed group involved in extracellular matrix structural constituent contains five changed members that were also classified within the collagen triple helix repeat class of genes. Eight of the top 23 changed groups are all involved in structural support involving collagen and the extracellular matrix. Three groups identified involved chemokines, with the changed members identified as CXCL2, CXCL4, CXCL5, CCL2, CCL6 and CCL9. Of note, CXCL2, CXCL4, CCL6 and CCL9 were members of functional groups that were potentially downregulated in resting K14D6 keratinocytes compared to wild-type keratinocytes (Table 4-12). Other gene class groups potentially differentially expressed in wild-type keratinocytes by CCL3 were phosphate transport, transmembrane receptor protein tyrosine kinase pathway, CD20/IgE Fc receptor beta subunit, cysteine-rich flanking region, heparin binding, inflammatory response pathway, eicosanoid synthesis, von willebrand factor, lysyl oxidase, intracellular calcium activated chloride channel activity and positive regulation of phagocytosis. (Table 4-13).

WT control V WT + CCL3	Group members	Changed members	P-value changed
IPR008160- Collagen triple helix repeat	71	8	7.6e-11
6817- phosphate transport	84	7	1.3e-10
5201- extracellular matrix structural constituent	48	8	4.3e-10
30020- extracellular matrix structural constituent conferring tensile strength	29	5	1.1e-09
5581- collagen	35	5	2.9e-09
IPR000885- Fibrillar collagen, C-terminal	11	5	3.2e-09
IPR-001811- small chemokine, interleukin-8 like	31	6	1.8e-08
8009- chemokine activity	38	6	6.4e-08
7169- transmembrane receptor protein tyrosine kinase signalling pathway	76	6	4.7e-07
IPR007237- CD20/Ig E Fc receptor beta subunit	15	4	5.5e-07
IPR000372- Cysteine-rich flanking region, N-terminal	39	5	2.2e-06
1527-microfibril	6	3	3.8e-06
30023- extracellular matrix constituent conferring elasticity	2	2	4.9e-06
6935- chemotaxis	87	6	9.4e-06
8201- heparin binding	57	5	2.3e-05
Inflammatory_Response_Pathway-GenMAPP	40	3	4.1e-05
Eicosanoid_Synthesis- GenMAPP	21	3	4.6e-05
IPR001007- von Willebrand factor, type C	22	2	5.0e-05
IPR001695- Lysyl oxidase	4	2	7.2e-05
5229- intracellular calcium activated chloride channel activity	3	3	9.8e-05
50766- positive regulation of phagocytosis	21	3	1.1e-04
5588- collagen type V	3	3	1.2e-04

**Table 4-13. Potential downregulated functional gene classes in Wild-type (WT) keratinocytes after CCL3 treatment compared to wild-type keratinocytes at rest.**

### *Comparison with the RP report*

Seven of the top changed functional groups induced by CCL3 in wild-type keratinocytes, reported in the iGA report, consisted of the same changed gene members (Full list in Appendix Three). These were Col3a1, Col6a1, Col6a2, C1qa, Col11a1, Col1a2 and Emilin 1. Five of these, Col3a1, Col6a1, Col6a2, C1qa and Col11a1, were listed within the top 25 genes in the RP report (Table 4-4). The other two were ranked 29<sup>th</sup> and 36<sup>th</sup> in the RP report (Full list in Appendix Two). Three of the top changed groups involved chemokines and these were all present in the RP report, CXCL4 was listed 2<sup>nd</sup>, CXCL5 was listed 39<sup>th</sup>, CCL2 was listed 50<sup>th</sup>, CCL6 was listed 79<sup>th</sup>, CCL9 was listed 109<sup>th</sup> and CXCL2 was 112<sup>th</sup>, all had an FDR of less than 50% (Full report in Appendix Two).

## ii) Potential downregulated functional gene classes

After CCL3 binding to wild-type keratinocytes, 14 functional gene classes involving 22 distinct genes, were potentially downregulated in comparison to wild-type keratinocytes at rest (Table 4-14). The top changed group is the cornified envelope and has four changed members (The full iGA analysis report is in Appendix Three). Members within this group are also found to be changed within the functional gene classes of calcium binding protein, keratinisation and one gene is found to be changed within the functional gene class of structural constituent of cytoskeleton. Four genes were found to be changed within the melanosome class and these genes were also classified as changed within the melanin biosynthesis from tyrosine and tyrosinase group. Members within the intermediate filament group are also the same members that have changed within intermediate filament protein group, sarcolemma and structural constituent of cytoskeleton group. Another three groups potentially differentially expressed with the same changed members are calcium-independent cell-cell adhesion group, identical protein binding and the PMP-22/EMP20 and claudin family. Another functional group potentially downregulated was transcription factor jumonji (Takeuchi et al., 2006), which involved gene members that are encoded within the Y-chromosome.

WT control V WT + CCL3	Group members	Changed members	P-value Changed
1533- cornified envelope	14	4	8.0e-11
42470- melanosome	7	4	4.6e-08
IPR003347- Transcription factor jumonji, jmjC	18	3	6.7e-08
5882- intermediate filament	93	8	9.3e-08
IPR001664 – Intermediate filament protein	57	6	4.5e-07
6583- melanin biosynthesis from tyrosine	6	3	4.4e-06
IPR001751- Calcium binding protein, S-100/ IcaBP type	14	2	7.1e-06
IPR002227- Tyrosinase	2	2	2.5e-05
16338- calcium-independent cell-cell adhesion	22	3	2.5e-05
42383- sarcolemma	14	3	4.6e-05
42802- identical protein binding	81	4	6.0e-05
IPR004031- PMP-22/EMP/MP20 and claudin family	30	3	6.5e-05
31424 – keratinisation	23	2	8.9e-05
5200- structural constituent of cytoskeleton	91	5	1.0e-04

**Table 4-14. Potential downregulated functional gene classes in Wild-type (WT) keratinocytes after CCL3 treatment compared to wild-type keratinocytes at rest.**

### ***Comparison with the RP report***

In the RP report, 13 genes were potentially downregulated with an FDR of less than 50% in wild-type keratinocytes after CCL3 binding compared to resting wild-type keratinocytes (Table 4-5). Seven genes potentially differentially expressed in the RP report were also listed as changed gene members in the iGA analysis report. The seven genes were LOC433621, hornerin (Hrnr), repetin (Rptn), DEAD3y, Jarid1a, Uty and Lce5a. LOC433621, Hrnr and Rptn were the three changed members within the cornified envelope group. Of these three, Hrnr and Rptn were also changed members within the calcium binding and keratinisation group. DEAD3y, Jarid1a and Uty are all gene members within transcription factor, jumonji (Takeuchi et al., 2006). Other groups in Table 4-14, such as calcium independent cell-cell adhesion, all contain changed gene members that were listed in the RP report but with an FDR of more than 50%.

#### **4.4.2.3 K14D6 control v K14D6 + CCL3**

##### **i) Potential upregulated functional gene classes**

Twenty-two functional gene classes were potentially upregulated after CCL3 ligation in K14D6 keratinocytes compared to K14D6 keratinocytes at rest. These 22 groups consisted of 39 distinct genes (Table 4-15). The top changed group was extracellular matrix structural constituent conferring tensile strength, in which seven members within this group changed. These were also the seven members that changed within the second top changed group of collagen and the fourth to seventh top changed groups which were extracellular matrix structural constituent, fibrillar collagen, collagen triple helix repeat and the phosphate transport group (Full list is in Appendix Three). Within this comparison, 7 genes involved in chemotaxis were found to be potentially upregulated after CCL3 binding. Five of the members were also found to be changed within the gene class of small chemokine interleukin-8 like and chemokine activity, which involved CCL9, CCL6, CXCL4, CXCL2 and CCL7. CCL9, CCL6, CXCL2 and CXCL4 were also potentially upregulated gene members within top changed groups after ligand binding in wild-type keratinocytes (Table 4-13). CCL3 binding to K14D6 keratinocytes resulted potential upregulation of genes involved in the positive regulation of phagocytosis, IgG binding and mast cell activation. Other

groups differentially expressed were glycosidase hydrolase family 22 and lysozyme activity involving the same two changed members and some members within the intracellular activated chloride channel activity group were also involved in the functional gene class of Von Willebrand factor. Other potentially differentially expressed gene classes were heparin binding, myelin proteolipid protein PLP, CD20/IgE Fc receptor subunit, aldehyde dehydrogenase, calcium binding protein and tyrosinase.

Thirteen functional gene classes were expressed at higher levels after CCL3 binding in both wild-type and K14D6 keratinocytes (Table 4-13 and Table 4-15 respectively). These were three functional groups involving collagen (collagen, fibrillar collagen, collagen triple helix repeat) and two involved the extracellular matrix (extracellular matrix structural constituent conferring tensile strength and extracellular matrix structural constituent). The other functional groups were heparin binding, CD20/IgE Fc receptor subunit, intracellular calcium activated chloride channel activity, phosphate transport and three involved chemokines (chemotaxis, small chemokine interleukin-8 like and chemokine activity). Von willebrand factor was potentially upregulated in both, although in wild-type this was type C whilst in K14D6 keratinocytes this was type A.

<b>K14D6 control V K14D6 + CCL3</b>	<b>Group members</b>	<b>Changed members</b>	<b>P-value changed</b>
30020- extracellular matrix structural constituent conferring tensile strength	29	7	1.9e-10
55871- collagen	35	7	6.9e-10
82017- heparin binding	57	8	1.7e-09
5201- extracellular matrix structural constituent	48	7	6.8e-09
IPR000885- Fibrillar collagen, C-terminal	10	4	2.4e-08
IPR008160- Collagen triple helix repeat	72	6	1.5e-07
6871- phosphate transport	85	7	3.9e-07
6935- chemotaxis	87	7	3.9e-07
IPR001811- Small chemokine, interleukin-8 like	31	5	5.7e-07
8009- chemokine activity	38	5	1.6e-06
50766-positive regulation of phagocytosis	21	3	3.9e-06
19864 – IgG binding	5	2	2.2e-05
IPR-001614 –Myelin proteolipid protein PLP	3	2	3.1e-05
IPR007237- CD20/IgE Fc receptor beta subunit	14	3	3.8e-05
IPR001916- Glycoside hydrolase, family 22	8	2	5.0e-05
IPR002086- Aldehyde dehydrogenase	26	2	5.3e-05
45576- mast cell activation	9	2	7.7e-05
3796- lysozyme activity	10	2	8.1e-05
IPR001571- Calcium binding protein, S-100/ICaBP type	15	3	9.3e-05
5229- intracellular calcium activated chloride channel activity	3	3	9.4e-05
IPR002227- Tyrosinase	3	3	9.8e-05
IPR002035- von Willebrand factor, type A	44	4	1.1e-04

**Table 4-15. List of potential upregulated functional gene classes in K14D6 keratinocytes after CCL3 treatment compared to K14D6 keratinocytes at rest.**

### *Comparison to RP report*

In the RP report, 171 genes were potentially upregulated in K14D6 keratinocytes after ligand binding (For full list see Appendix Two). Thirty six genes listed as potentially differentially expressed within the RP report were members within the top changed groups (Table 4-15). Of the top 25 genes listed within the RP report (see Table 4-6), 12 genes were found to be changed members within the top changed groups in Table 4-15. Genes potentially upregulated were Aldh1a7 and Aldh1a1, both changed members within the aldehyde dehydrogenase group. Col3a1 and col1a1, listed as 11<sup>th</sup> and 24<sup>th</sup> in Table 4-6, are changed members within six functional gene groups. CCL9 and CCL6 were potentially upregulated in Table 4-6 and were changed members within the chemotaxis group. Ptx3 and Fcgr3 are changed members within the functional group positive regulation of phagocytosis, which were also listed in the top 25 genes in the RP report (Table 4-6). Lzp-s and Lyzs were listed 2<sup>nd</sup> and 25<sup>th</sup> in the RP report (Table 4-6) in which both were changed members within the glycoside hydrolase group.

## ii) Potential downregulated functional gene classes

CCL3 binding in K14D6 keratinocytes resulted in 7 potentially downregulated functional gene classes (Table 4-16). The top changed group was plectin repeat with a p-value change of  $3.8 \times 10^{-08}$  in which 4 members of the group changed. The second top changed group with a p-value changed of  $6.1 \times 10^{-07}$  was sarcolemma, in which 3 members changed and are also the 3 members that changed within the changed groups of Z disc, response to pest pathogen or parasite and the intermediate filament protein group with p-value changed of  $4.8 \times 10^{-06}$ ,  $7.4 \times 10^{-06}$  and  $3.7 \times 10^{-05}$  respectively. Other changed groups were muscle maintenance and spectrin repeat with 2 and 3 members changed respectively.

CCL3 binding resulted in potential downregulation of 14 functional gene classes in wild-type keratinocytes whereas in K14D6 keratinocytes, only 7 functional groups were potentially downregulated (Table 4-14 and 4-16 respectively). Only two functional gene classes were expressed at lower levels after ligand binding in both wild-type keratinocytes and K14D6 keratinocytes, which were sarcolemma and intermediate filament protein (Table 4-14 and Table 4-16 respectively).

K14D6 control V K14D6 + CCL3	Group members	Changed members	P-value changed
IPR001101- Plectin repeat	8	4	3.8e-08
42383- sarcolemma	14	3	6.1e-07
30018- Z disc	27	3	4.8e-06
9613- response to pest, pathogen or parasite	31	3	7.4e-06
IPR001664 – Intermediate filament protein	59	4	3.7e-05
46716-muscle maintenance	4	2	5.7e-05
IPR002017- Spectrin repeat	19	3	1.1e-04

**Table 4-16. Potential downregulated functional gene classes in K14D6 keratinocytes after CCL3 treatment compared to K14D6 keratinocytes at rest.**

### *Comparison to the RP report*

In the RP report, only four genes were potentially downregulated with an FDR of less than 50% after CCL3 binding in K14D6 keratinocytes (Table 4-7). None of the four genes listed were the changed members in any of the 7 top changed groups in the respective iGA analysis report.

#### 4.4.2.4 WT + CCL3 v K14D6 + CCL3

To determine the transcriptional consequences of D6 in K14D6 keratinocytes after ligand binding, functional gene classes were analysed for differential expression in a positive or negative direction in comparison to wild-type keratinocytes after CCL3 ligand binding.

##### i) Potential upregulated functional gene classes

Seven gene classes, which consisted of 14 distinct genes, were expressed at higher levels in K14D6 keratinocytes after ligand binding (Table 4-17). Four members changed within the top changed group of melanin biosynthesis. Within this group, 3 of the members were also changed members in the functional class involved in melanosome and 2 were changed members within the tyrosinase group. The second functional gene class group was involved in the cornified envelope, involving 5 changed members. Of these, three were members that changed within the keratinisation functional gene class. The third top changed group was transcription factor jumonji in which 3 members changed and 2 members changed within the amino acid transporter activity group.

None of the top changed groups in K14D6 keratinocytes after ligand binding (Table 4-17) were the same as the top changed groups potentially upregulated in resting K14D6 keratinocytes compared to wild-type keratinocytes (Table 4-11). It was noted that 6 of the 7 top changed groups in Table 4-17 were expressed at lower levels in wild-type keratinocytes after ligand binding compared to resting wild-type keratinocytes (Table 4-14). Therefore, CCL3 potentially induced the downregulation of these groups in wild-type keratinocytes but not in K14D6 keratinocytes, this could explain why these groups are the top groups potentially upregulated in K14D6 keratinocytes compared to wild-type keratinocytes after ligand binding.

WT + CCL3 v K14D6 + CCL3	Group members	Changed members	P-value changed
6583- melanin biosynthesis from tyrosine	6	4	3.4e-11
1533- cornified envelope	14	5	1.2e-08
IPR003347- Transcription factor jumonji, jmjC	21	3	3.9e-08
42470- melanosome	7	3	6.8e-08
IPR002227- Tyrosinase	2	2	1.6e-06
15171- amino acid transporter activity	18	2	2.5e-05
31424 – keratinisation	23	3	4.3e-05

**Table 4-17. Potential upregulated functional gene classes in K14D6 keratinocytes after CCL3 treatment compared to Wild-type keratinocytes after CCL3 treatment.**

### *Comparison to the RP report*

Only eight genes were potentially upregulated in K14D6 keratinocytes compared to wild-type keratinocytes after ligand binding in the RP report (Table 4-8). Three genes expressed at higher levels in the RP report, *Ddx3y*, *Uty* and *Jarid1d*, are the three gene members that changed within the transcription factor jumonji functional gene class (Table 4-17). *Slc6a14* and *Slc7a3* were two genes listed in the RP report, which were the two changed gene members within the amino acid transporter activity group. Genes involved in melanin biosynthesis, cornified envelope, melanosome group, tyrosinase and keratinisation were not potentially upregulated, with an FDR of less than 50%, in the RP report.

## ii) Potential downregulated functional gene classes

Twelve functional gene classes were potentially downregulated involving 21 distinct genes in K14D6 keratinocytes compared to wild-type keratinocytes after ligand binding by CCL3 (Table 4-18). The top changed group was CD20/IgE Fc receptor beta subunit in which 4 members out of 15 changed. The next three changed groups all involved chemokines. The second changed group was small chemokine interleukin-8 like with four changed members, which were also within the chemotaxis group and the chemokine activity group, all involving CXCL4, CCL6, CXCL5 and CCL9. Chemokines were also potentially downregulated in K14D6 at rest compared to wild-type keratinocytes, which were CCL9, CCL6, CXCL4, and CXCL2 (Table 4-12). Another group that changed was immune cell chemotaxis, involving CXCL4 and CCR1 as two of the changed group members. IgG binding and mast cell activation are two other top changed groups with p-value changed of  $1.8 \times 10^{-05}$  and  $6.5 \times 10^{-05}$ , with only two changed members which are the same, Fc receptor IgG low affinity IIb and Fc receptor IgG low affinity III. Two changed members occurred in the glycosidase hydrolase family 22 group and were also the two changed members within the cell wall catabolism group and lysozyme activity. Other functional gene classes potentially differentially expressed were sarcolemma and C-type lectin.

Several functional gene classes potentially downregulated after ligand binding in K14D6 compared to wild-type keratinocytes were also expressed at lower levels in resting K14D6 keratinocytes compared to resting wild-type keratinocytes (Table 4-18 and 4-12 respectively). These were three groups involving chemokines, which were small chemokine interleukin-8 like, chemotaxis and chemokine activity. The other three groups potentially downregulated in both comparisons were glycosidase hydrolase, lysozyme activity and cell wall catabolism. This suggests that D6 may have a negative impact on genes associated with these functional groups.

WT + CCL3 v K14D6 + CCL3	Group members	Changed members	P-value changed
IPR007237 – CD20/IgE Fc receptor beta subunit	15	4	8.0e-08
IPR001811- Small chemokine, interleukin-8 like	31	4	1.4e-07
6935- chemotaxis	87	5	2.1e-07
8009- chemokine activity	38	4	3.3e-07
30595- immune cell chemotaxis	5	3	3.4e-07
19864 – IgG binding	5	2	1.8e-05
IPR001916- Glycoside hydrolase, family 22	8	2	2.6e-05
3796- lysozyme activity	10	2	4.2e-05
42383- sarcolemma	14	3	5.4e-05
IPR001304- C-type lectin	99	3	6.3e-05
45576- mast cell activation	9	2	6.5e-05
16988- cell wall catabolism	16	2	1.1e-04

**Table 4-18. Potential downregulated functional gene classes in K14D6 keratinocytes after CCL3 treatment compared to Wild-type keratinocytes after CCL3 treatment.**

### *Comparison with RP report*

Twenty-seven genes were expressed at lower levels in K14D6 keratinocytes after ligand binding in comparison to wild-type keratinocytes after ligand binding in the RP report (Table 4-9). Three of the changed members within the top changed CD20/IgE Fc receptor subunit group were potentially downregulated in the RP report. CXCL4 and CCL6 were chemokines potentially differentially expressed in the RP report and were found to be potentially downregulated in the iGA analysis as they are members within the small chemokine, chemotaxis and chemokine activity group. Fcg2rb and Fcgr3 are two genes potentially downregulated in the RP report (Table 4-9) that are also listed as changed members within the IgG binding and mast cell activation groups. P lysozyme structural (Lzp-s) and lysozyme are genes potentially downregulated in the RP report, which were changed members of the glycoside hydrolase, lysozyme activity and cell wall catabolism group in Table 4-18. Clec4d, Mrc1 and Clec4n are genes potentially downregulated in the RP report and are the changed members within the C-type lectin group.

#### 4.4.2.5 Summary of iGA analysis

To gain a better understanding of the data generated using the iGA analysis, the functional gene classes potentially differentially expressed between all comparisons were summarised in a Venn diagram for potential up- and downregulated changes (Figure 4-2 and Figure 4-3 respectively).

Ectopically expressing D6 within keratinocytes resulted in 9 potentially upregulated functional gene classes, in which two classes were unique to this comparison; these were cadherin cytoplasmic region and prostaglandin synthesis (Figure 4-2). Genes involved in transmembrane receptor protein tyrosine kinase signalling and extracellular matrix structural constituent conferring tensile strength were also potentially upregulated by CCL3 in wild-type keratinocytes whereas another five functional gene classes were potentially upregulated by CCL3 in both K14D6 keratinocytes and wild-type keratinocytes. This suggests that basal D6 expression, independent of ligand within K14D6 keratinocytes may affect gene transcription.

The Venn diagram illustrates that several classes of genes are induced by CCL3 in both wild-type and K14D6 keratinocytes demonstrating the effect of CCL3 through receptors present on both wild-type and K14D6 keratinocytes such as CCR1, CCR3 and CCR5. These include 3 functional classes of genes involved in cell movement, CD20/IgE Fc receptor beta subunit, positive regulation of phagocytosis, heparin binding and fibrillar collagen group (Figure 4-2).

Eight functional gene classes were expressed at higher levels only in K14D6 keratinocytes after CCL3 binding in comparison to control K14D6 thus illustrating that genes were potentially differentially expressed because of CCL3 binding to D6. These were the functional gene classes of IgG binding, myelin proteolipid protein PLP, glycoside hydrolase family 22, aldehyde dehydrogenase, mast cell activation, lysozyme activity, calcium binding protein and Von Willebrand factor type A (Figure 4-2).

Ectopically expressing D6 within keratinocytes resulted in the potential downregulation of 11 functional genes classes (Figure 4-3). Only one class of genes to do with cytolysis was specifically found in the comparison between wild-type and K14D6 keratinocytes at rest. Three groups found to be potentially

downregulated due to the presence of non-ligated D6 were also found to be potentially downregulated in the wild-type keratinocytes incubated with CCL3. Seven functional gene classes were potentially downregulated in the presence of non-ligated D6 as well as being potentially downregulated in K14D6 keratinocytes after CCL3 treatment in comparison to wild-type. Three of these groups involved chemokines and the other four functional groups were IgG binding, glycoside hydrolase family 22, lysozyme activity and cell wall catabolism.

Using the Venn diagram, 15 functional classes of genes were shown to be present in both the positive and negative differential expression analysis, illustrated in blue in Figure 4-2 and Figure 4-3 respectively. Three of these groups involving chemokines were found to be expressed at higher levels by CCL3 in both wild-type and K14D6 keratinocytes indicating that CCL3 is able to induce changes in the gene transcripts of chemokines in both wild-type and K14D6 keratinocytes. However, at rest, the chemokine groups were potentially downregulated in K14D6 keratinocytes compared to wild-type indicating that the presence of D6 may affect the transcription of chemokines. In addition, after ligand binding, the chemokine groups were potentially downregulated in K14D6 keratinocytes compared to wild-type. This indicates the possibility that CCL3 may be able to induce the transcription of genes through chemokine receptors CCR1, CCR3 and CCR5. However, the presence of ectopically expressed D6 within K14D6 keratinocytes may be able to limit the transcription levels of these genes.

Figure 4-2. Venn diagram summarising potential upregulated functional gene classes using iGA analysis of four different group comparisons.

Potential upregulated gene classes in each of the comparisons are represented in a corresponding circle. Functional gene classes found in overlapping regions show gene classes potentially upregulated in the other groups. Gene classes highlighted in blue are groups that are also found to be potentially downregulated.

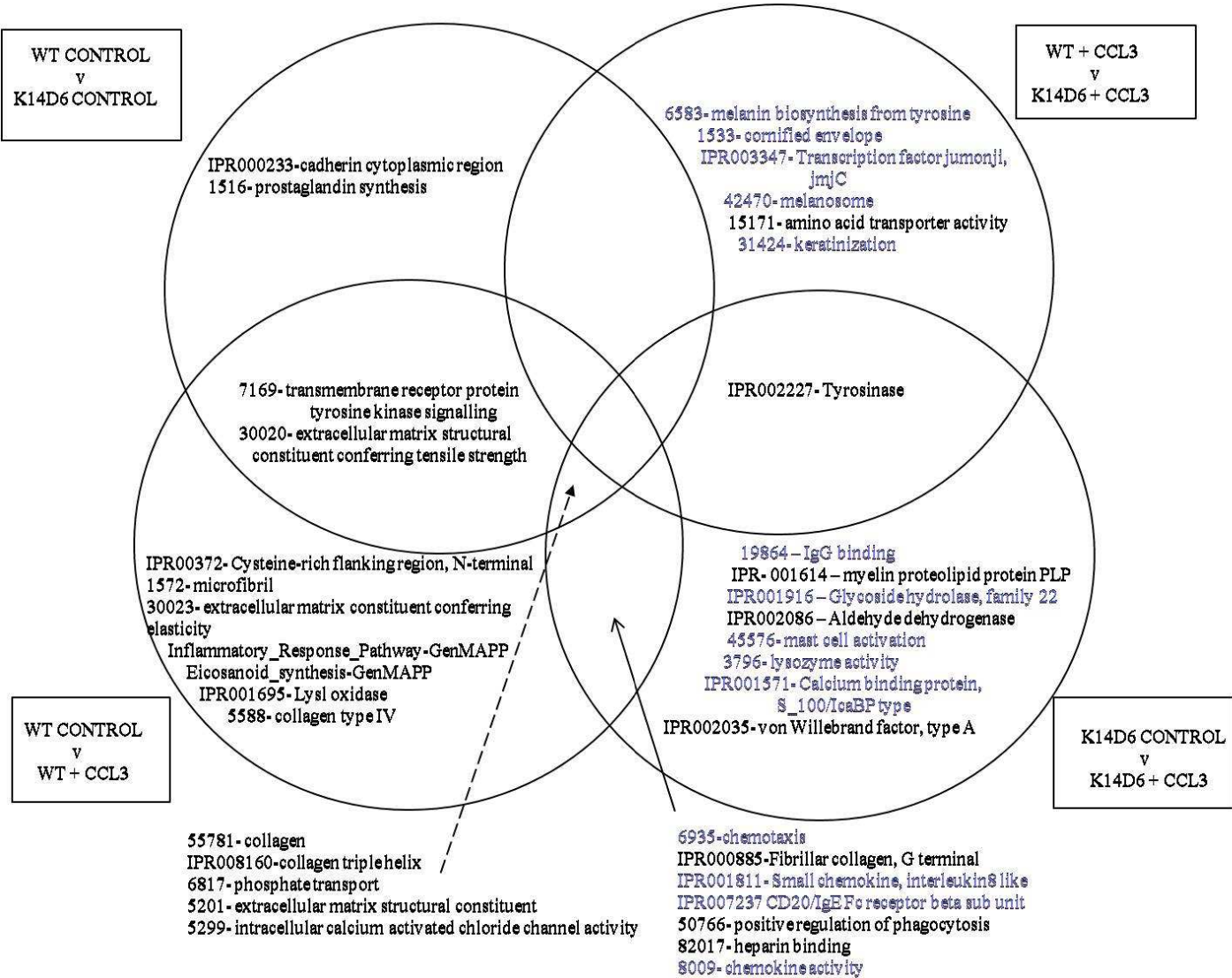
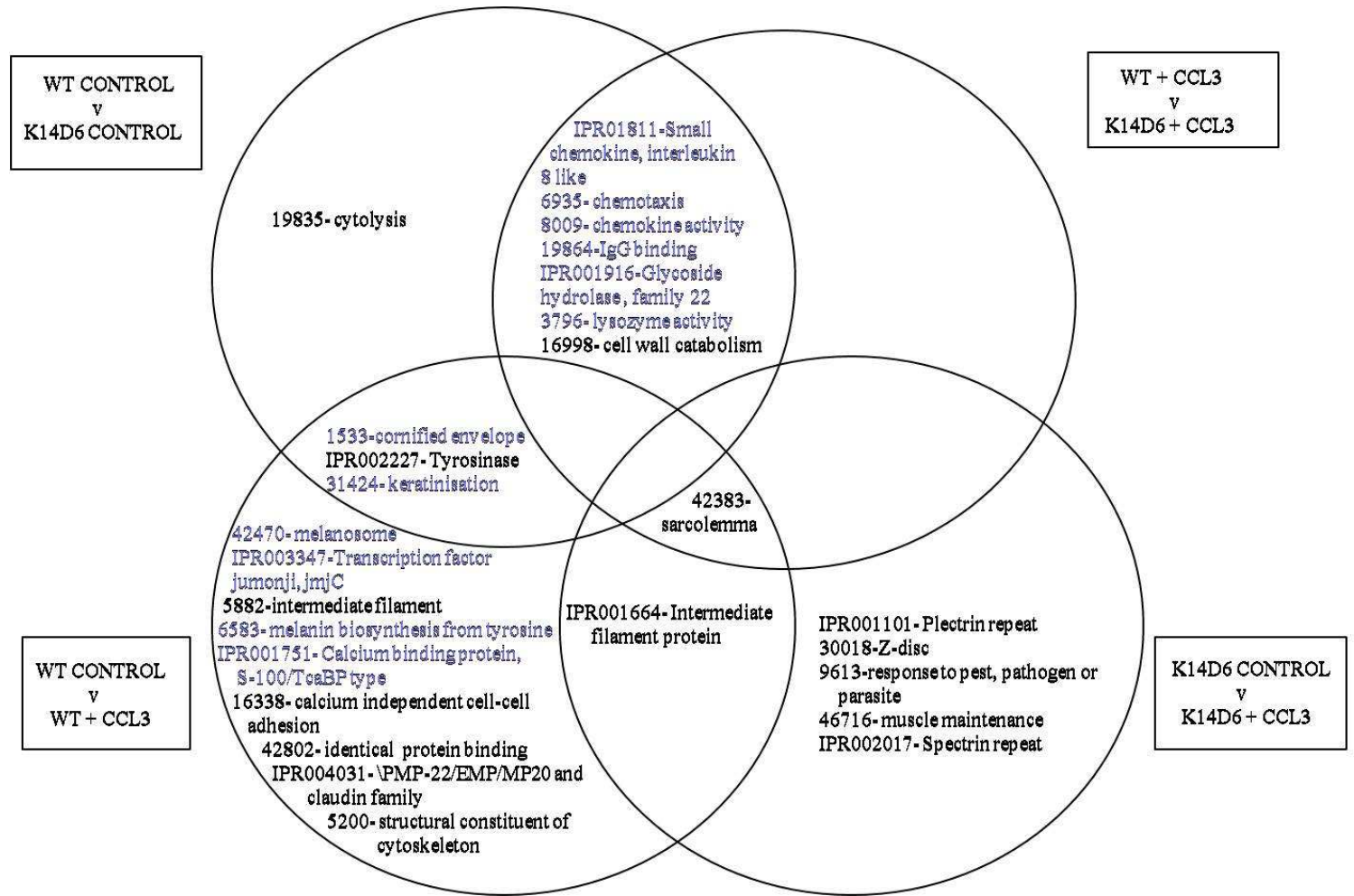


Figure 4-3. Venn diagram summarising the potential downregulated functional gene classes using iGA analysis results of 4 different group comparisons.

Potential downregulated gene classes in each of the comparisons are represented in a corresponding circle. Potential functional gene classes found in overlapping regions show gene classes potentially downregulated in the other groups. Functional gene classes shown in blue are groups which are also found to be potentially upregulated.



## 4.5 Validation of microarray data by QPCR

Validation of the microarray was required to determine if the potentially differentially expressed genes reported in the rank product reports were reproducibly differentially expressed. This was performed using QPCR to measure changes in gene transcript levels. The main objective was to determine whether any transcriptional changes reported in the microarray could be revalidated. Therefore, genes were identified from the microarray data to be validated, primers were designed and validated to generate standards for each gene and for use in QPCR using the SYBR green based method (Morrison et al., 1998). Fresh sets of wild-type and K14D6 primary keratinocytes were isolated (n=3/group in which 3 neonates were pooled to generate 1 sample), cultured and treated with either PBS or CCL3 as previously described for the microarray. RNA was extracted, quantified, converted to cDNA for QPCR.

### 4.5.1 *Identifying potentially upregulated genes to validate by QPCR*

The main objective of the microarray was to determine whether there were transcriptional consequences of ligand binding through D6. To obtain an overview of the data obtained from the microarray, genes potentially upregulated by CCL3 in wild-type and K14D6 keratinocytes with less than 25% FDR in the rank product report were summarised in a Venn diagram (Figure 4-4). The left hand circle shows genes that were potentially upregulated by CCL3 in wild-type keratinocytes and the right circle lists genes potentially upregulated by CCL3 in K14D6 keratinocytes. Genes listed in the overlapping region illustrates genes that were found to be potentially upregulated in both wild-type and K14D6 keratinocytes and suggests that these genes may be induced through CCL3 binding to receptors common to both wild-type and K14D6 keratinocytes, such as CCR1, CCR3 and CCR5. Genes not found in the overlapping region are genes that were found to be specifically potentially upregulated after CCL3 binding in either wild-type or K14D6 keratinocytes.

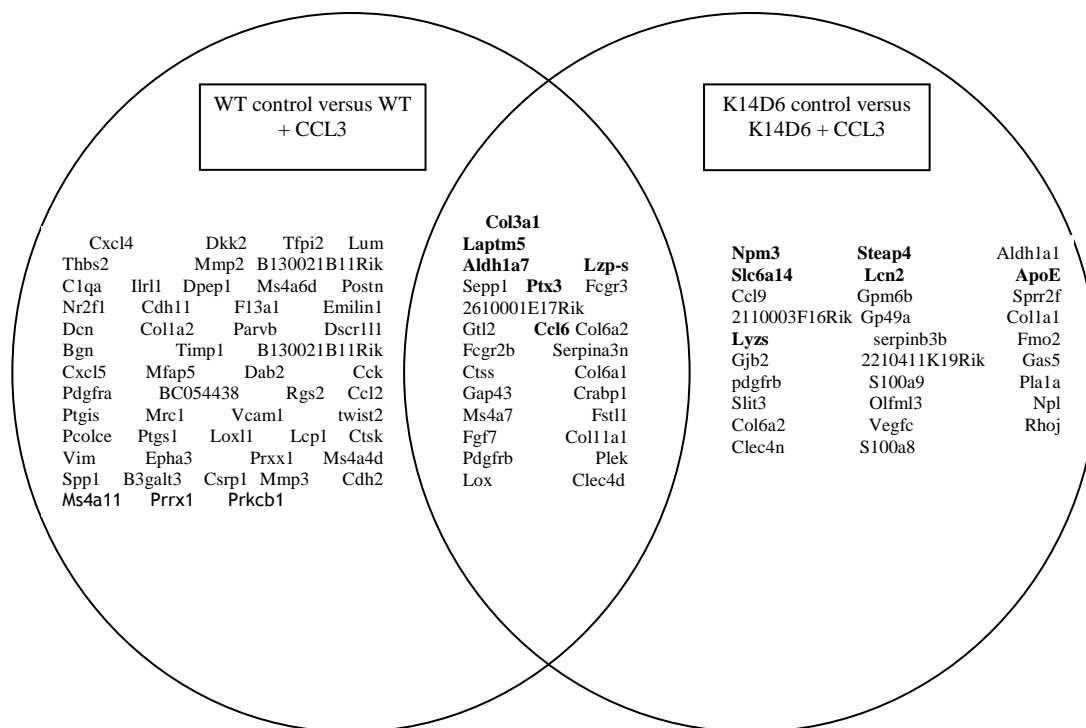


**Figure 4-4. Venn diagram of genes potentially upregulated after CCL3 treatment in wild-type and K14D6 keratinocytes.**

**The genes indicated in bold are genes identified for validation by QPCR.**

### i) Genes identified only in K14D6 keratinocytes after CCL3 binding

Using the Venn diagram (Figure 4-4) and by identifying genes listed at a high ranking in the RP report (Table 4-6), six genes potentially upregulated only in K14D6 keratinocytes after CCL3 treatment were identified for validation. Genes found only to be potentially upregulated in K14D6 after CCL3 treatment and therefore potentially D6 mediated, were identified as:

Nucleoplasmin 3 (Npm3)

STEAP family member 4 (Steap4)

Solute carrier family 6-member 14 (Slc6a14)

Lipocalin 2 (Lcn2)

Apolipoprotein E (ApoE)

Nucleoplasmin 3 was the highest ranked gene, which was only potentially upregulated in K14D6 keratinocytes after CCL3 treatment with an RP score of 147.22, fold change of 2.11 and a false discovery rate of 1.4% (Table 4-19). STEAP4 was the 11<sup>th</sup> gene listed on the RP report, with an RP score of 279.37, fold change of 2.22 and a false discovery rate of 5.17% (Table 4-19). Slc6a14 has an RP score of 296.41, a false discovery rate of 6.38% and a fold change of 1.61 (Table 4-19). Lipocalin 2 has an RP score of 305.98, a 5.87% FDR and a 1.79 fold change (Table 4-19). The last gene identified for validation was apolipoprotein E, with an RP score of 313.19, 5.94% FDR and changed by a fold of 1.92 (Table 4-19).

Gene	RP score	FDR (%)	FC
Npm3	147.22	1.40	2.11
STEAP4	279.37	5.17	2.22
Slc6a14	296.41	6.38	1.61
Lcn2	305.98	5.87	1.79
ApoE	313.90	5.94	1.92

**Table 4-19. Genes potentially upregulated only in K14D6 keratinocytes after CCL3 treatment identified for validation.**

Genes were listed in order of Rank Product score (RP score) with details of % false discovery rate (FDR) and fold change (FC). Data obtained from the RP report as summarised in Table 4-6.

**ii) Genes identified in WT and K14D6 keratinocytes after CCL3 binding**

Genes identified for validation that were potentially upregulated in both WT and K14D6 keratinocytes after CCL3 ligand binding are summarised within the overlapping circles in the Venn diagram (Figure 4-4). Using the list of genes from the Venn diagram, genes were identified for validation using the highest ranked genes in the K14D6 + CCL3 rank product report and were identified as:

Aldehyde dehydrogenase family 1, subfamily A7 (Aldh1a7)

P lysozyme structural (Lzp-s)

Pentraxin related gene (Ptx3)

Lysosomal-associated protein transmembrane 5 (Laptm5)

Procollagen, type III, alpha 1 (Col3a1)

Chemokine (C-C motif) ligand 6 (CCL6)

Aldehyde dehydrogenase was the first gene listed in the RP report as potentially differentially expressed in the comparison between K14D6 keratinocytes at rest and after CCL3 treatment. The RP score of Aldh1a7 was 97.2, with a fold change of 3.31 and a 3% false discovery rate (Table 4-20). The same gene was also potentially upregulated in wild-type keratinocytes after CCL3 treatment, with an RP score of 711.64, a 3.17 fold change and 15.65% false discovery rate (Table 4-20). Lzp-s was potentially differentially expressed in K14D6 keratinocytes by a fold change of 2.7, an FDR of 1.5% and an RP score of 106.48 whereas in the wild-type, Lzp-s had an RP score of 740.13, an FDR of 17.28% and an FC of 1.74 (Table 4-20). Pentraxin related gene was potentially differentially expressed by 2.18 fold in K14D6 keratinocytes after incubation with CCL3, an RP score of 199.63 and an FDR of 2.71%, whereas Ptx3 was potentially upregulated by 1.75 fold in wild-type keratinocytes after CCL3 stimulation, with an RP score of 506.88 and a 10.20% false discovery rate (Table 4-20). The fifth gene identified was Col3a1, which in K14D6 keratinocytes had an RP score of 254.35, a 4.27% FDR and increased by 2.18 fold whereas within wild-type keratinocytes, CCL3 binding resulted in Col3a1 being potentially differentially expressed by 3.72 fold, with a 10.25% false discovery rate and an RP score of 224.73 (Table 4-20). The last gene picked for validation was CCL6. CCL6 had an RP score of 430.38, a 12.24% FDR and changed by 1.86 fold in K14D6 keratinocytes after CCL3. CCL6

was also potentially upregulated by CCL3 in wild-type keratinocytes by 1.87 fold, an RP score of 868.30 and an FDR of 22.85% (Table 4-20).

Gene	WT			K14D6		
	RP score	FDR (%)	FC	RP score	FDR (%)	FC
Aldh1a7	711.64	15.65	3.17	97.2	3.00	3.31
Lzp-s	740.13	17.28	1.74	106.48	1.50	2.47
Ptx3	506.88	10.20	1.75	199.63	2.71	2.18
Laptn5	415.35	9.67	1.88	234.40	3.67	1.89
Col3a1	224.73	10.25	3.72	254.35	4.27	2.18
CCl6	868.30	22.85	1.87	430.38	12.24	1.86

**Table 4-20. Comparison of data from the rank product reports on six genes identified as potentially differentially expressed in both Wild-type and K14D6 keratinocytes after incubation with CCL3.**

### iii) Genes identified in resting K14D6 keratinocytes

It was also decided to validate three genes that were potentially upregulated in resting K14D6 keratinocytes compared to resting wild-type keratinocytes. In the RP analysis, only 6 genes were potentially upregulated in K14D6 keratinocytes compared to wild-type keratinocytes (Table 4-2).

CCbp2 (D6) had a rank product score of 1, the smallest value that can be achieved using the rank product method, which indicates that the gene is significantly differentially expressed. Ccbp2 was chosen not to be validated because the microarray data confirmed that the D6 transgene was present in K14D6 keratinocytes at higher levels than wild-type confirming PCR and QPCR data in chapter 3. Therefore, it was decided to validate three of the genes listed after D6 in the RP report. These were dickkopf homolog 2 (Dkk2), nik related kinase (NrK) and branched chain aminotransferase 1 (Bcat1; Table 4-21). The RP scores for these genes are much larger than one, being 206.84, 348.58 and 359.51 for Dkk2, NrK and Bcat1 respectively, suggesting these genes may not be significantly differentially expressed.

Gene	RP score	FDR %	FC
Ccbp2	1.00	0.00	49.59
Dkk2	206.84	15.50	2.66
Nrk	348.58	43.33	1.81
Bcat1	359.51	34.50	1.48

**Table 4-21. Genes identified for validation that were potentially upregulated in K14D6 keratinocytes in comparison to wild-type keratinocytes at rest.**

#### **4.5.2 Identifying potentially downregulated genes to validate**

Overall, in the RP report, the number of genes potentially downregulated was far less than the number of genes potentially upregulated. None of the potential downregulated genes stood out with their RP score and therefore no potential downregulated genes were identified specifically for validation. However, several genes identified for validation, as potential upregulated genes induced by CCL3, were also present as potentially downregulated genes, for example, Laptm5 and Lzp-s. These two genes were potentially downregulated in two RP reports, one was resting K14D6 keratinocytes compared to wild-type and the second was K14D6 keratinocytes compared to wild-type after CCL3 binding (Table 4-3 and 4-9 respectively). In addition, CCL6 was a gene identified for validation as being potentially upregulated in both wild-type and K14D6 keratinocytes after CCL3 binding, but was potentially downregulated in K14D6 keratinocytes compared to wild-type keratinocytes after ligand binding (Table 4-9). Another gene identified for validation was ApoE, which was potentially upregulated in K14D6 keratinocytes after ligand binding but was potentially downregulated in resting K14D6 keratinocytes compared to wild-type keratinocytes (Table 4-3). As a result, these genes could be analysed for potential up- or downregulation of transcripts between the different groups at the same time.

### 4.5.3 Design and validation of primers

Primers were designed according to the specifications described previously in Chapter Two for use in QPCR. Transcript levels were quantified using a standard DNA template alongside samples of interest. Each specific standard DNA template was generated using standard PCR with 'outer' primers that incorporated the region amplified by the 'nested' primers, as illustrated in Figure 4-5. The number of transcript copies in each standard DNA template was calculated (See 2.2.1.9 for details) and used to determine the absolute number of copies of transcript in each sample of interest.

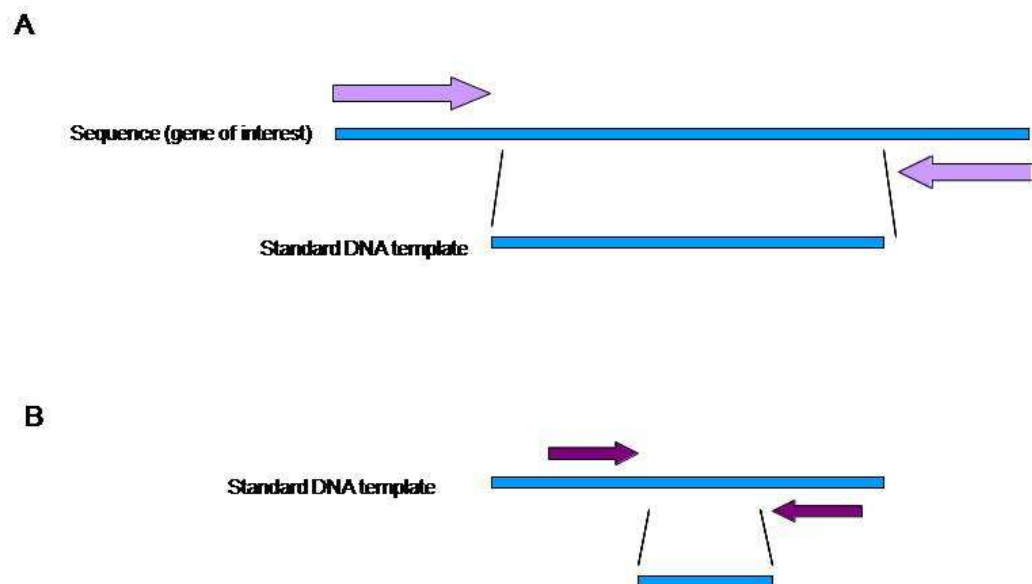
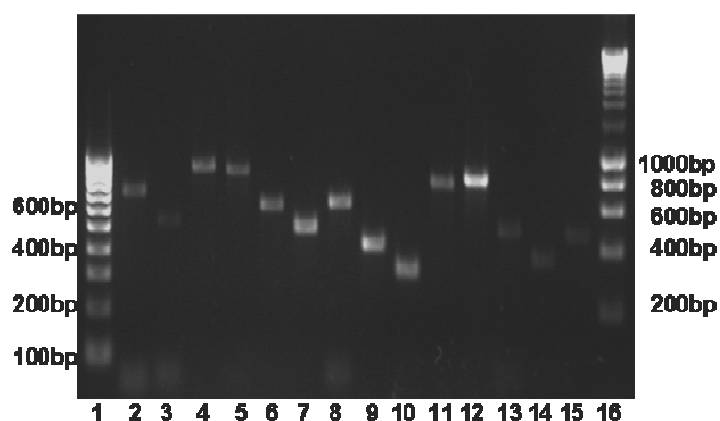


Figure 4-5. A diagram illustrating the use of different primer sets for QPCR.

(A) 'Outer' primers (arrows) were designed to generate a PCR product of the gene of interest for use in QPCR as standard DNA template. (B) The standard DNA template generated using the 'outer' primers would encode the region that would be amplified by the 'nested' primers (arrows) in QPCR.

#### 4.5.4 Validation of outer primers

The 'outer' primers were designed and used to generate a standard DNA template for each gene of interest by PCR. The 'outer' primers were optimised to produce a clear PCR product of the expected size as shown in Figure 4-6. Most 'outer' primers generated a clear band using an annealing temperature of 60°C except for Lzp-s primers, which were required to have an annealing temperature of 61°C. The intensity of the bands varied, with Aldh1a7 being the most intense band under ultraviolet light (Figure 4-6).



Lane	Gene	Expected product Size (bp)
2	Col3a1	700
3	Lzp-s	520
4	Ptx3	903
5	Laptm5	867
6	CCl6	612
7	Npm3	491
8	STEAP4	630
9	Slc6a14	413
10	Lcn2	307
11	ApoE	765
12	Aldh1a7	813
13	Dkk2	487
14	Nrk	359
15	Bcat1	458

Figure 4-6. Specificity of 'outer' primers to generate standards for use in QPCR.

PCR products were amplified from mixed WT and K14D6 keratinocytes cDNA using 'outer' primers and visualised under UV light on a 1% agarose gel. The single bands indicate the specificity of the primers and the specific product sizes expected are listed above. The products were used as reference standards in QPCR. Lane 1, Hyperladder IV; lane 2, Col3a1; lane 3, Lzp-s; lane 4, Ptx3; lane 5, Laptm5; lane 6, ccl6; lane 7, Npm3; lane 8, STEAP4; lane 9, slc6a14; lane 10, Lcn2; lane 11, Apoe; lane 12, Aldh1a7; lane 13, Dkk2; lane 14, NrK; lane 15, Bcat1; lane 16, Hyperladder 1.

#### 4.5.4.1 Calculation of gene transcripts numbers within standards

The bands within the DNA ladder were of a known mass (supplied by the manufacturer Bioline). Therefore, the intensity of the bands under UV light were measured using densitometric analysis. A standard curve was generated using the known mass of the Hyperladder band and the bands intensity. The intensity of each standard DNA template was measured and the mass of the DNA template for each gene was calculated, using the formula generated from the standard curve. The calculated mass for the standard DNA template was then used to calculate the absolute copy numbers of transcripts within the template (Table 4-22), using a series of equations (see 2.2.1.9 for details). Using the known value of copy numbers of transcript in each standard, the number of copies in each of the diluted standards was calculated.

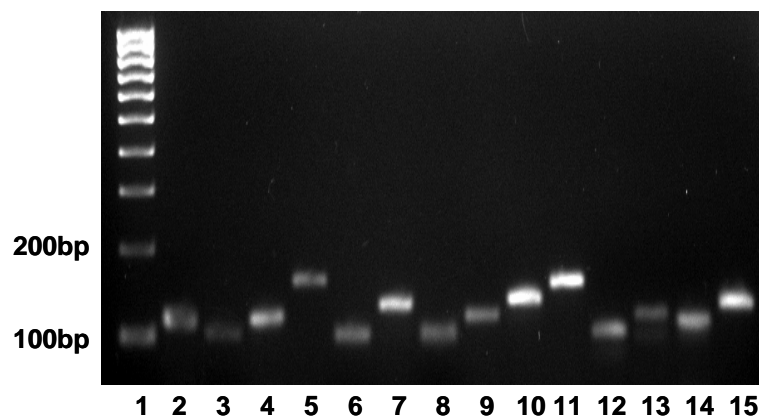
Gene	Mass of Product (ng/ $\mu$ l)	Calculated Copies of product/ $\mu$ l
Col3a1	9.84	12,831,597,359
Lzp-s	3.54	6,212,534,965
Ptx3	13.38	13,485,841,751
Laptn5	10.49	10,946,698,822
Ccl6	14.64	21,770,598,138
Npm3	26.96	49,996,512,991
STEAP4	23.23	33,605,964,406
Slc6a14	30.39	66,951,683,909
Lcn2	27.70	82,339,897,345
ApoE	13.38	15,865,696,177
Aldh1a7	40.92	45,909,407,730
Dkk2	7.73	14,485,032,045
Nrk	5.32	13,523,406,770
Bcat1	4.22	8,408,449,120

**Table 4-22. Calculation of the number of transcripts within each standard for each gene of interest.**

For each standard, the mass was calculated using the formula from the standard curve. Using a series of equations, the number of gene transcripts within each standard was calculated from the mass.

### 4.5.5 Optimisation of 'nested' primers

The 'nested' primers designed for use in QPCR were tested using keratinocyte cDNA (mixed WT and K14D6) to ensure they generated the correct size of product and were specific. All the 'nested' primers were specific and generated PCR products of the expected size (Figure 4-7). All QPCR assays involved SYBR green and a dissociation melting curve analysis was used to ensure there was no primer dimer formation during the reaction.



Lane	Gene	Expected product Size (bp)
2	Col3a1	114
3	Lzp-s	104
4	Ptx3	117
5	Laptm5	160
6	CCl6	102
7	Npm3	132
8	Steap4	103
9	Slc6a14	117
10	Lcn2	133
11	ApoE	153
12	Aldh1a7	100
13	Dkk2	115
14	Nrk	108
15	Bcat1	127

Figure 4-7. Nested primers used in QPCR were specific.

PCR products were generated by amplifying mixed Wt and K14D6 keratinocyte cDNA. The products were electrophoresed on a 2% agarose gel and visualised under a UV light. Lane 1, Hyperladder IV; lane 2, Col3a1; lane 3, Lzp-s; lane 4, Ptx3; lane 5, Laptm5; lane 6, ccl6; lane 7, Npm3; lane 8, STEAP4; lane 9, slc6a14; lane 10, Lcn2; lane 11, Apoe; lane 12, Aldh1a7; lane 13, Dkk2; lane 14, Nrk; lane 15, Bcat1. A single band demonstrates the specificity of each primer pair. The PCR product sizes expected are summarised in the table.

## **4.5.6 QPCR results**

### **4.5.6.1 Validation of genes potentially induced by CCL3 in both wild-type and K14D6 transgenic keratinocytes.**

Six genes, *Aldh1a7*, *Col3a1*, *Laptm5*, *Lzp-s*, *Ptx3* and *CCL6* were identified for validation as being potentially upregulated in both wild-type and K14D6 keratinocytes after CCL3 treatment, suggesting that CCL3 may be regulating gene transcript levels through other chemokine receptors, such as CCR1.

CCL3 treatment had no effect on the transcript levels of *Col3a1* within wild-type or K14D6 keratinocytes (Figure 4-8A; Two-way ANOVA, WT v WT+CCL3  $p>0.05$ , K14D6 v K14D6+CCL3  $p>0.05$ ). CCL3 had no significant effect on *Lzp-s* transcripts in wild-type keratinocytes or K14D6 keratinocytes (Figure 4-8B; Two-way ANOVA, WT v WT+CCL3  $p>0.05$ , K14D6 v K14D6+CCL3  $p>0.05$ ). In wild-type keratinocytes, CCL3 did not induce any significant changes in the transcript levels of *Ptx3* and CCL3 had no effect on the transcript levels of *Ptx3* within K14D6 keratinocytes (Figure 4-8C; Two-way ANOVA, WT v WT+CCL3  $p>0.05$ , K14D6 v K14D6+CCL3  $p>0.05$ ). CCL3 had no significant effect on the transcript levels of *Laptm5* within wild-type keratinocytes or within K14D6 keratinocytes (Figure 4-8D; Two-way ANOVA, WT v WT+CCL3  $p>0.05$ , K14D6 v K14D6+CCL3  $p>0.05$ ). CCL3 had no significant effect on *CCL6* transcript levels in wild-type or K14D6 keratinocytes (Figure 4-8E; Two-way ANOVA, WT v WT+CCL3  $p>0.05$ , K14D6 v K14D6+CCL3  $p>0.05$ ). CCL3 had no effect on the transcript levels of *Aldh1a7* in either wild-type or K14D6 keratinocytes (Figure 4-8F; Two-way ANOVA, WT v WT+CCL3  $p>0.05$ , K14D6 v K14D6+CCL3  $p>0.05$ ). In the microarray, *Laptm5* was listed as potentially downregulated in resting K14D6 keratinocytes compared to WT keratinocytes and was identified as a gene to validate by QPCR. However, there was no significant difference in *Laptm5* transcript levels in resting K14D6 keratinocytes compared to control WT keratinocytes (Figure 4-8D, unpaired students t-test,  $p=0.1459$ ).

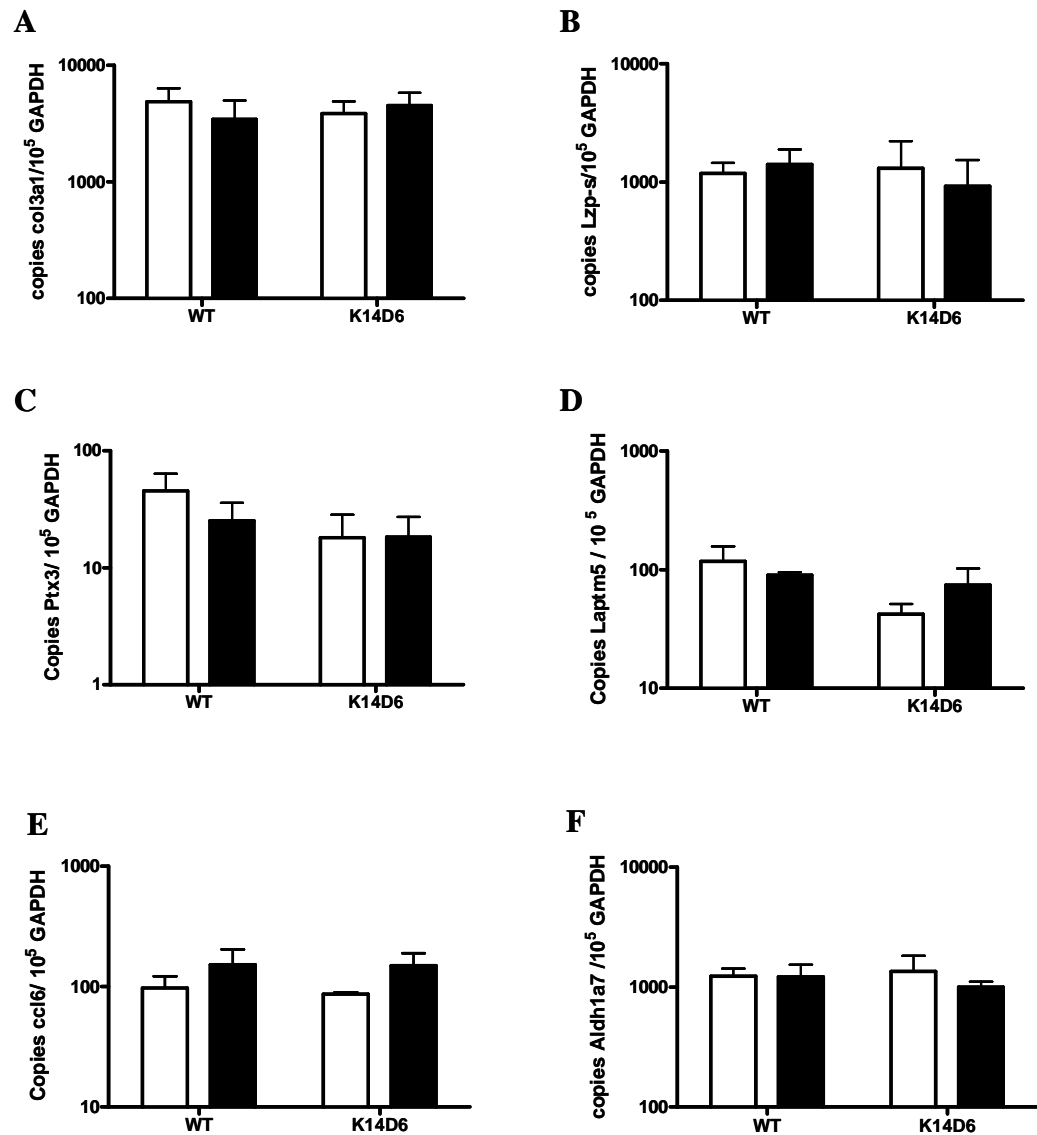
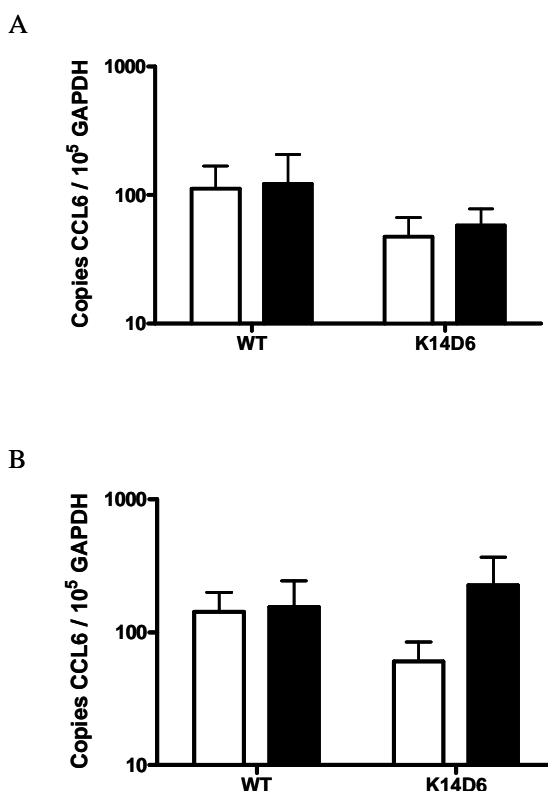


Figure 4-8. Validation of gene transcripts potentially upregulated after CCL3 treatment in both wild-type and K14D6 keratinocytes.

Six genes that were found to be potentially upregulated after CCL3 treatment in both wild-type (WT) and K14D6 keratinocytes were identified for validation by QPCR. The copy numbers of each gene is normalised to  $1 \times 10^5$  copies of GAPDH. (A) Col3a1, (B) Lzp-s, (C) Ptx3, (D) Laptm5, (E) CCL6 and (F) Aldh1a7. White column is control keratinocytes; Black column is keratinocytes treated with 10nM CCL3 for 6hrs at 37°C. Each column is mean  $\pm$  SEM, n=3/group.

Although the data was not significant, the CCL6 and Laptm5 QPCR were repeated with more samples by including RNA from two sets of keratinocytes used in the microarray. The assay was also repeated on fresh sets (n=3/group with 3 neonates pooled per sample) of keratinocytes using 30nM concentration of CCL3 instead of 10nM.

By including keratinocyte samples that were involved in the microarray, sample size was increased from three to five and the QPCR was repeated. In the increased sample group, CCL3 had no significant effect on CCL6 transcript levels in both wild-type and K14D6 keratinocytes (Figure 4-9A; Two-way ANOVA, WT v WT+CCL3  $p>0.05$ , K14D6 v K14D6+CCL3  $p>0.05$ ). Increasing the concentration of CCL3 to 30nM also had no effect on CCL6 transcripts within wild-type keratinocytes or K14D6 keratinocytes (Figure 4-9B; Two-way ANOVA, WT v WT+CCL3  $p>0.05$ , K14D6 v K14D6+CCL3  $p>0.05$ ). These data suggest that CCL3 binding did not have an impact on CCL6 transcript levels in wild-type or K14D6 keratinocytes.



**Figure 4-9. Repeated QPCR for validation of CCL6**

Wild-type (WT) and K14D6 keratinocytes were treated with either PBS (white) or CCL3 (black) for 6hrs at 37°C. QPCR measuring absolute copy numbers was performed. The copy numbers of each gene is normalised to  $1 \times 10^5$  copies of GAPDH. (A) 10nM CCL3 was used, n=5/group (B) The concentration of CCL3 was increased to 30nM n=3/group. Each column is mean  $\pm$  SEM.

Transcript levels of *Lap<sup>tm</sup>5* were re-examined with increased sample size by including samples used within the microarray. CCL3 did not induce any transcriptional changes in *Lap<sup>tm</sup>5* in wild-type keratinocytes or K14D6 keratinocytes (Figure 4-10A; Two-way ANOVA, WT v WT+CCL3  $p > 0.05$ , K14D6 v K14D6+CCL3  $p > 0.05$ ). Additionally, there was no significant difference in the transcript levels of *Lap<sup>tm</sup>5* in resting K14D6 keratinocytes compared to wild-type (Figure 4-10A; unpaired student's t-test,  $p = 0.22$ ). Increasing the concentration of CCL3 to 30nM did not have any significant effect on *Lap<sup>tm</sup>5* transcripts within WT or K14D6 keratinocytes (Figure 4-10B, Two-way ANOVA WT v WT+CCL3  $p > 0.05$ , K14D6 v K14D6+CCL3  $p > 0.05$ ). There was no difference in transcripts levels of *Lap<sup>tm</sup>5* in resting wild-type or K14D6 keratinocytes (Figure 4-10B; unpaired students t-test,  $p = 0.41$ ).

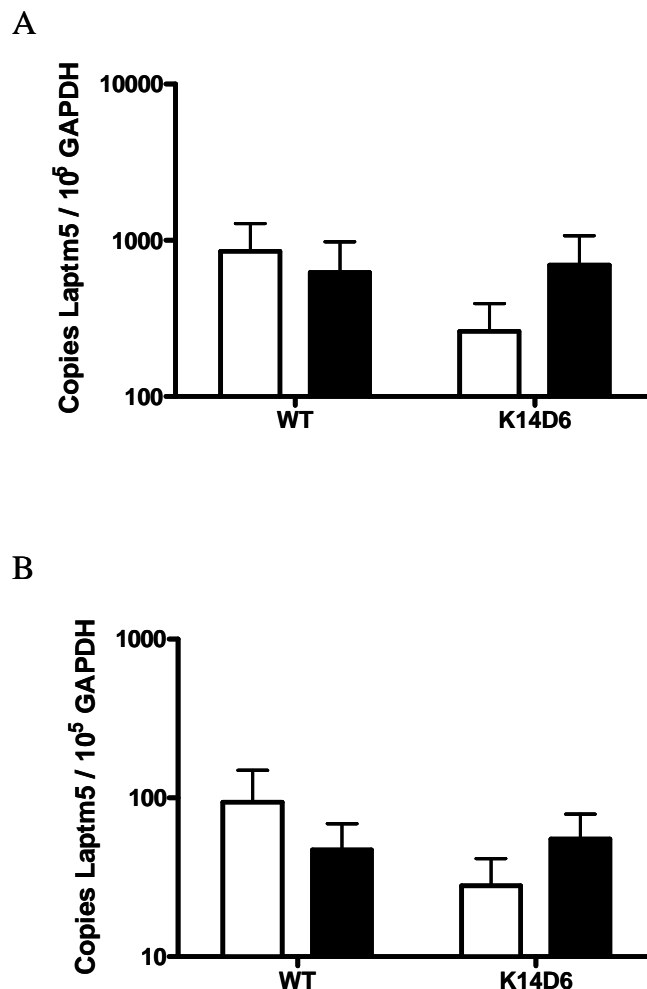


**Figure 4-10. Repeated QPCR for validation of *Lap<sup>tm</sup>5***

Wild-type (WT) and K14D6 keratinocytes were treated with either PBS (white) or CCL3 (black) for 6hrs at 37°C. QPCR measuring absolute copy numbers was performed. The copy numbers of each gene is normalised to  $1 \times 10^5$  copies of GAPDH. (A) 10nM CCL3 was used,  $n = 5/\text{group}$ . (B) The concentration of CCL3 was increased to 30nM,  $n = 3/\text{group}$ . Each column is mean  $\pm$  SEM.

At rest, there was no significant difference in the transcript levels of Col3a1, Lzp-s, Ptx3, Laptm5, CCL6 or Aldh1a7 transcript levels between wild-type and K14D6 keratinocytes (Figure 4-8A, B, C, D, E and F respectively; students t-test, all  $p > 0.05$ ), illustrating that ectopic expression of D6 did not affect the expression levels of these genes.

#### **4.5.6.2 Validation of genes potentially induced by CCL3 only in K14D6 keratinocytes**

Potential upregulation of gene transcript levels through D6 was investigated by identifying five genes from the microarray that were potentially upregulated in only K14D6 keratinocytes after CCL3 treatment. These genes were Npm3, STEAP4, slc6a14, Lcn2 and ApoE. CCL3 treatment caused no significant effect on the transcript levels of Npm3, STEAP4, Lcn2, Apoe or Slc6a14 in K14D6 keratinocytes or wild-type keratinocytes (Figure 4-11A, B, C, D and E respectively; Two-way ANOVA, WT v WT+CCL3  $p > 0.05$ , K14D6 v K14D6+CCL3  $p > 0.05$  for all genes). Additionally, there were also no significant differences in the transcript levels of Npm3, STEAP4, Slc6a14, Lcn2 or ApoE between wild-type and K14D6 keratinocytes at rest (Figure 4-11, student's t-test,  $p > 0.05$ ). These QPCR data would suggest that CCL3 binding to D6 in K14D6 keratinocytes does not have an impact on the transcription of these genes.

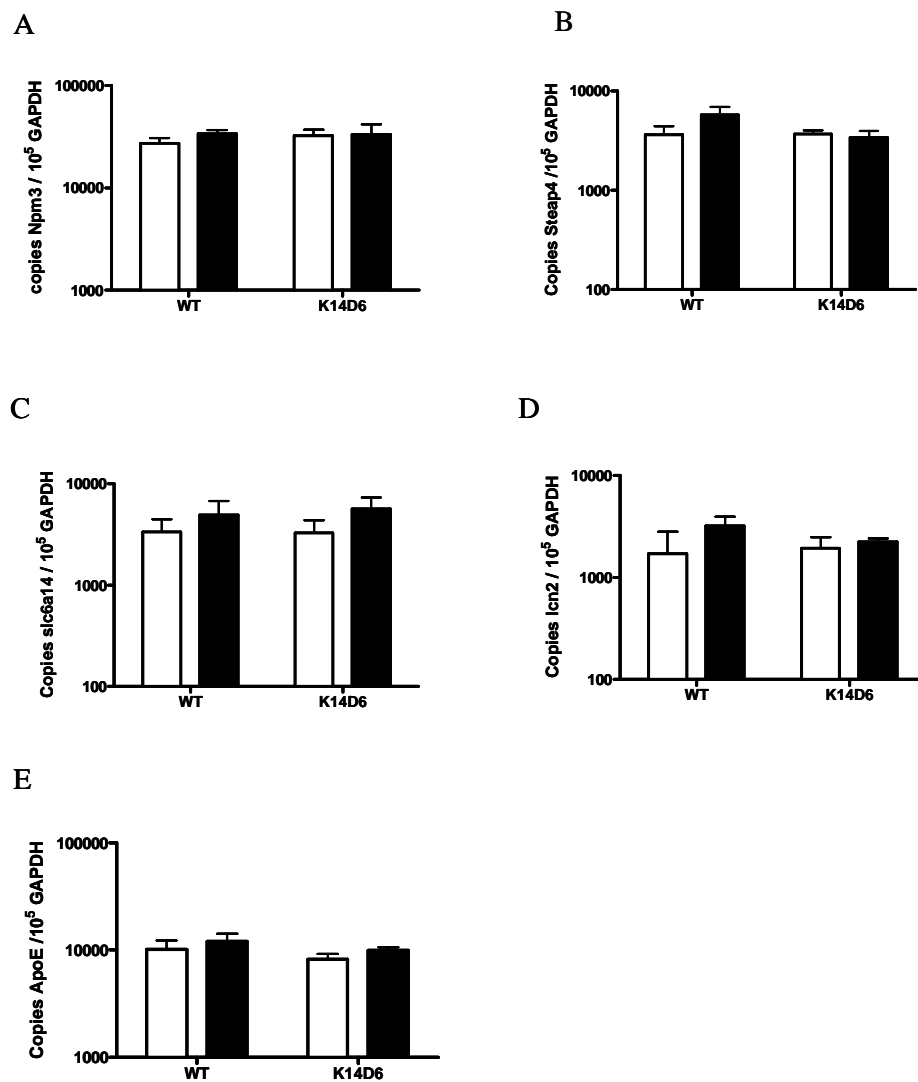


**Figure 4-11. Validation of gene transcripts identified as potentially upregulated after CCL3 treatment in K14D6 keratinocytes but not wild-type (WT) keratinocytes.**

Five genes that were found to be potentially upregulated after CCL3 treatment in K14D6 keratinocytes only were identified for validation. QPCR measuring absolute copy numbers was performed. The copy numbers of each gene is normalised to  $1 \times 10^5$  copies of GAPDH. (A) Npm3, (B) Steap4, (C) slc6a14, (D) Lcn2, (E) ApoE. White column is control keratinocytes; Black column is keratinocytes treated with 10nM CCL3 for 6hrs at 37°C. Each column is mean of three samples  $\pm$  SEM, n=3/group.

### **4.5.6.3 Validation of genes potentially upregulated between wild-type and K14D6 keratinocytes at rest**

To determine whether transgenic overexpression of D6 had any effect on keratinocytes at rest, the transcript levels of the top three genes after D6 reported in the microarray were validated. Out of the three genes identified for validation, *Dkk2* had a fold change above 2, however the RP score varied from 206.84 to 359.51 with FDR between 15.5 and 43.3% (Table 4-2). The QPCR data showed there was no significant difference in the transcript levels of *Dkk2* in K14D6 keratinocytes compared to wild-type keratinocytes at rest (Figure 4-12A, student's t-test,  $p=0.122$ ). There was a non-significant difference in the transcript levels of *Bcat1* between wild-type and K14D6 keratinocytes at rest (Figure 4-12B, student's t-test,  $p=0.119$ ). The transcript levels of *Nrk* were not significantly different in K14D6 keratinocytes compared to wild-type keratinocytes (Figure 4-12C; student's t-test,  $p=0.159$ ). Additionally, treatment of wild-type and K14D6 keratinocytes with CCL3 had no effect on the transcriptional levels of *Dkk2*, *Nrk* and *Bcat1* in comparison to the control keratinocytes (Figure 4-12; Two-way ANOVA, WT v WT+CCL3  $p>0.05$ , K14D6 v K14D6+CCL3  $p>0.05$ ). These QPCR data would suggest that transgenic expression in absence of ligand had no impact on the level of transcription of *Dkk2*, *Nrk* and *Bcat1*.

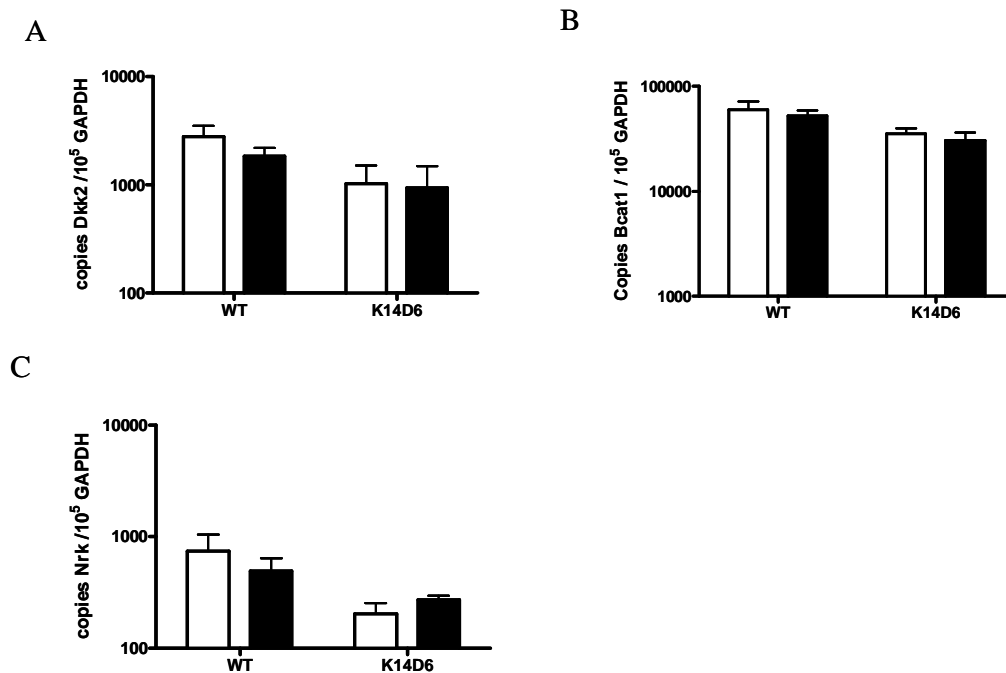


**Figure 4-12. Validation of the transcript levels of three genes potentially upregulated between wild-type (WT) and K14D6 keratinocytes.**

Three genes potentially upregulated in K14D6 keratinocytes compared to wild-type in the microarray data were validated by QPCR. Copy numbers of each gene is normalised to  $1 \times 10^5$  copies of GAPDH, a housekeeping gene. (A) DKK2 (B), Nrk (C) Bcat1. White columns are control keratinocytes. Black columns are keratinocytes treated with 10nM CCL3 for 6 hrs at 37°C. Each column is mean  $\pm$  SEM, n=3/group.

### **4.5.7 Summary of quantitative PCR results**

Various genes were identified from the microarray using the rank products method to validate by QPCR. Six genes were identified that were listed as potentially upregulated in both wild-type and K14D6 keratinocytes after ligand binding. However, by QPCR, none of the genes identified showed any significant changes in gene expression due to CCL3 ligand binding (Figure 4-8). By QPCR, CCL3 did not significantly upregulate any of the genes identified for validation that were identified as potentially upregulated only in K14D6 after ligand binding in the microarray (Figure 4-11). Resting K14D6 keratinocytes did not show any significant upregulation of Dkk2, Nrk or Bcat transcript levels, which were three genes identified for validation from the RP report (Figure 4-12). In the microarray, Lptm5 was potentially downregulated in resting K14D6 keratinocytes compared to wild-type keratinocytes. However, there was no difference in Lptm5 transcript levels between WT and K14D6 keratinocytes by QPCR (Figure 4-10).

No significant differences were found in any of the individual genes validated by QPCR and this correlates with the microarray results. One of the methods for the analysis of microarray data was rank products, in which the smaller the RP value the more likely the gene is up- or downregulated (Breitling et al., 2004b). Many of the genes identified for validation had high RP scores, for example, the smallest RP score (excluding D6) was 97.2 and increased to 868, which suggests the likelihood that these genes were not actually differentially expressed in the microarray.

## 4.6 Discussion of Chapter 4

To date, *in vitro* studies have determined that D6 does not seem to signal by analysing functional responses after ligand binding using cell lines (Nibbs RJ et al., 1997; Fra AM et al., 2003). In this study, we have taken the approach one step further in that we are using primary cells, which contain high levels of ectopically expressed D6. These cells are keratinocytes from wild-type or K14D6 transgenic mice. By analysing the transcriptional consequences of ligand binding in wild-type and K14D6 keratinocytes, it was hoped that this would give an insight into any altered gene expression after ligand binding to D6. In addition, information would also be gained on the transcriptional consequences induced through D6 in a ligand independent manner by comparing the cell transcriptome in resting wild-type and K14D6 keratinocytes.

Examination of the transcriptional data generated using the rank product differential analysis method revealed that the largest number of genes potentially upregulated was after ligand binding in both wild-type and K14D6 keratinocytes. Conversely, the largest number of genes potentially downregulated occurred in resting K14D6 keratinocytes. Of note, the most strongly differentially expressed gene in the microarray was D6 in K14D6 keratinocytes compared to wild-type. These data confirm that D6 is expressed from the transgene driven by the keratin 14 promoter in K14D6 keratinocytes. Within the RP report, many Y-linked genes were listed when a certain population of keratinocytes was used (WT+CCL3). This result added an extra complication to the analysis of the microarray data and therefore an improvement to the design of the experiment would be to ensure that the keratinocytes populations used were all isolated from the same ratio of male to female neonates.

Analysis of the transcriptional data generated using the iGA analysis provided a number of insights into the functional differences induced by non-ligated D6 and ligand binding through D6. CCL3 binding in both wild-type and K14D6 keratinocytes resulted in the potential upregulation of genes encoding chemokines, genes involved in CD20/IgE Fc receptor subunit, positive regulation of phagocytosis and intracellular calcium activated chloride channel activity. This suggests the possibility that CCL3 exerts these effects through common receptors on both wild-type and K14D6 keratinocytes.

It was noted that in wild-type keratinocytes, other genes potentially upregulated by CCL3 were genes involved in transmembrane receptor protein kinase signalling pathway, genes involved in the inflammatory response pathway and eicosanoid synthesis pathways. This suggests the possibility that CCL3 in wild-type keratinocytes activated chemokine receptors capable of signalling and induced genes involved in inflammation. Since these groups were not potentially upregulated in K14D6 keratinocytes, this suggests that ectopic expression of D6 has prevented these genes from being activated. One mechanism may be that D6 removed CCL3 from its surroundings and targeted it for degradation. In turn, this may prevent the ligand binding to chemokine receptors, which would activate the genes involved in the inflammatory response. In addition to this, genes involved in chemokines and CD20/IgE Fc receptor subunit was in fact found to be potentially downregulated in K14D6 keratinocytes compared to wild-type keratinocytes after ligand binding suggesting that ectopic expression of D6 may be able to limit transcriptional consequences of CCL3 binding.

Analysis of the transcriptional consequences of non-ligated D6 revealed potential upregulation of genes involved with transmembrane receptor protein tyrosine kinase receptor pathway, as well as phosphate transport and intracellular calcium activated chloride channel activity. Interestingly, non-ligated D6 in K14D6 keratinocytes resulted in the potential downregulation of functional genes classes involving chemokines.

Although this microarray has given an insight and indication of the transcriptional consequences of D6 after ligand binding, it has to be kept in mind that D6 is ectopically expressed within these keratinocytes. Therefore, these results may be specific to this cell type and whether the same transcriptional consequences occur in a cell that naturally expresses D6 remains to be seen. Another point is that only one ligand was used within this study and does not take into account that *in vivo* many different chemokines are within the local proximity of D6 that may affect the transcriptional consequences of ligand binding. However, this study is one step forward in analysing the functional response of D6 *in vitro*.

## 4.7 Conclusion of Chapter 4

In summary, the main aim of the work within this chapter was to characterise the transcriptional consequences of ligand binding through D6 in ectopically expressed primary keratinocytes. A second aim was to determine if there was any transcriptional consequence of ectopic expression of D6 within K14D6 keratinocytes. The microarray results suggested that CCL3 induced the largest transcriptional changes in both wild-type and K14D6 keratinocytes mediated through common chemokine receptors such as CCR1. However, at the individual gene expression level, one conclusion was D6 is expressed at higher levels in K14D6 keratinocytes compared to wild-type keratinocytes. As a whole, there did not seem to be any significant transcriptional consequences of ligand binding through D6 at the individual gene level, however by analysing functional gene classes, data suggests the possibility that non-ligated D6 and ligated D6 is able to downregulate the gene expression level of chemokines. Therefore, these data suggests that D6 within keratinocytes does not seem to affect the cellular transcriptome as there was no significant upregulation of gene transcripts after ligand binding yet D6 may play a role in limiting the expression levels of genes. In the presence of ligand, D6 may reduce these levels by removal of the ligand leaving less ligand available to bind to other chemokine receptors.

## **Chapter 5 D6 in human psoriasis**

## 5 D6 in human psoriasis

### 5.1 Introduction

Psoriasis is a common inflammatory relapsing skin disease, which varies in location and severity (Naldi and Gambini, 2007). Clinical symptoms of psoriasis appear as lesions on the skin, which in the most common form of psoriasis, generally appear as red plaques. Pathological and histological changes occur within psoriatic lesions and these make up the hallmark features of the disease. Psoriasis has characteristic features that consist of epidermal thickening caused by the increased proliferation of keratinocytes, hyperkeratosis, epidermal hyperplasia, angiogenesis and an influx of leukocytes (Murphy et al., 2007). In addition, patients with psoriasis can also develop inflammatory joint disease (arthritis), known as psoriatic arthritis (Kleinert et al., 2007). Although the trigger of psoriasis is unknown, the key mediators currently thought to drive psoriasis are T cells (Austin et al., 1999) in particular Th1 and Th17 cells (Lowe et al., 2008), cytokines such as  $TNF\alpha$ ,  $IFN\gamma$ , IL-23 (Chan et al., 2006) and keratinocytes (Zenz et al., 2005).

Pathology similar to human psoriasis was demonstrated in mice lacking the atypical chemokine receptor, D6 (Jamieson et al., 2005). In the study, by Jamieson *et al.*, D6 null mice demonstrated an exaggerated inflammatory response within the skin in response to a chemical irritant, TPA, although skin inflammation in D6 null mice did eventually resolve. Histological analysis of skin from D6 null mice revealed several characteristics similar to human psoriasis, such as hyperkeratosis, epidermal hyperproliferation and increased angiogenesis (Jamieson et al., 2005). The pathology displayed in D6 null mice was dependent on TNF (Jamieson et al., 2005) as well as IL-15 and IL-17 (personal communication Professor G.J.Graham), which are all hallmarks of human psoriasis. Thus, D6 null mice displayed psoriasis-like pathology suggesting possible involvement of D6-dysfunction, as a contributing factor in the pathogenesis of the disease.

The aim of the work in this chapter was to determine whether there was any correlation between D6 expression levels and cutaneous disease development. D6 expression levels were examined in human skin biopsies from control

subjects, atopic dermatitis patients and patients with psoriasis. In psoriasis patients, skin biopsies from psoriatic lesions and uninvolved skin from the same patient were also examined. Samples were taken from atopic dermatitis patients because atopic dermatitis is another chronic inflammatory disease of the skin. Diagnosis of atopic dermatitis is based on presentation of skin lesions that are dry (eczema), very itchy (pruritus) and chronic lesions display lichenification of the skin (Beltrani, 1999). Atopic dermatitis is thought to be induced by the skin in individuals who are hypersensitive to allergens, resulting in increased Th2 type cytokines, increased serum IgE levels and eosinophilia (Leung, 1995).

Specifically, the levels of D6 transcripts were examined by quantitative PCR. The presence and location of D6 within the human skin biopsies was examined by immunohistochemistry using an antibody available for human D6 (Nibbs et al., 2001). The main aim of this work was to gain further understanding of the role for D6 in the pathogenesis of human cutaneous inflammatory disorders.

## **5.2 Collection of human skin samples**

To examine the association of D6 with human psoriasis, patient samples were required. Skin samples were taken from volunteers at a Dermatology clinic in Glasgow Royal Infirmary. Skin biopsies were taken from various parts of the body from psoriatic, atopic dermatitis patients and controls. Control samples were obtained from various types of patients, such as patients having a naevus removed, patients with atypical fibroxanthoma or patients with basal cell carcinoma. These skin samples are considered normal by dermatologists. Psoriasis patients had a skin biopsy taken from the centre of a psoriatic lesion and a biopsy taken from uninvolved skin (non-lesional) from the same part of the body. Skin samples were either 'snap frozen' and RNA was extracted from the biopsies for quantitative PCR or samples were placed in 10% neutral buffered formalin and embedded in paraffin wax blocks for immunohistochemistry.

### 5.3 D6 transcripts in human skin

RNA was extracted from human skin biopsies using Trizol and was DNase treated, (see 2.2.1.2 and 2.2.1.4). RNA was obtained from 9 control samples, 9 atopic dermatitis samples, 10 uninvolved psoriatic samples and 13 lesional psoriatic samples. RNA was transcribed into cDNA (by a dermatologist, Anne Sergeant) and used for QPCR. Using QPCR, human skin samples were examined for D6 transcript levels to determine any correlation between presence of disease and D6 expression.

There was no significant difference in D6 transcripts levels between atopic dermatitis samples and control samples or between psoriatic lesions and control. However, D6 transcript levels in uninvolved skin from psoriatic patients were significantly higher than control, atopic dermatitis and psoriatic lesional skin (Figure 5.1A). Uninvolved skin from psoriasis patients contained an 8-fold increase in D6 transcript levels in comparison to control skin (Figure 5-1A). D6 transcript levels were also 8-fold higher in uninvolved skin from psoriasis patients compared to lesional skin of psoriasis patients (Figure 5-1A). In individual psoriasis patients (where matching samples were obtained), 9 out of the 10 patients had higher D6 levels in uninvolved skin than within psoriatic lesions (Figure 5-1B). Conversely, one patient (patient 25) had higher D6 transcript levels in psoriatic lesions than in uninvolved skin, illustrated by the red dotted box in Figure 5-1B. In addition, patient 29 only had slightly higher levels of D6 transcripts within non-lesional skin compared to lesional skin (Figure 5.1B). These results indicate a consistent pattern of expression within psoriasis patients suggesting that D6 is abnormally expressed within uninvolved skin (non-lesional) of psoriasis patients.

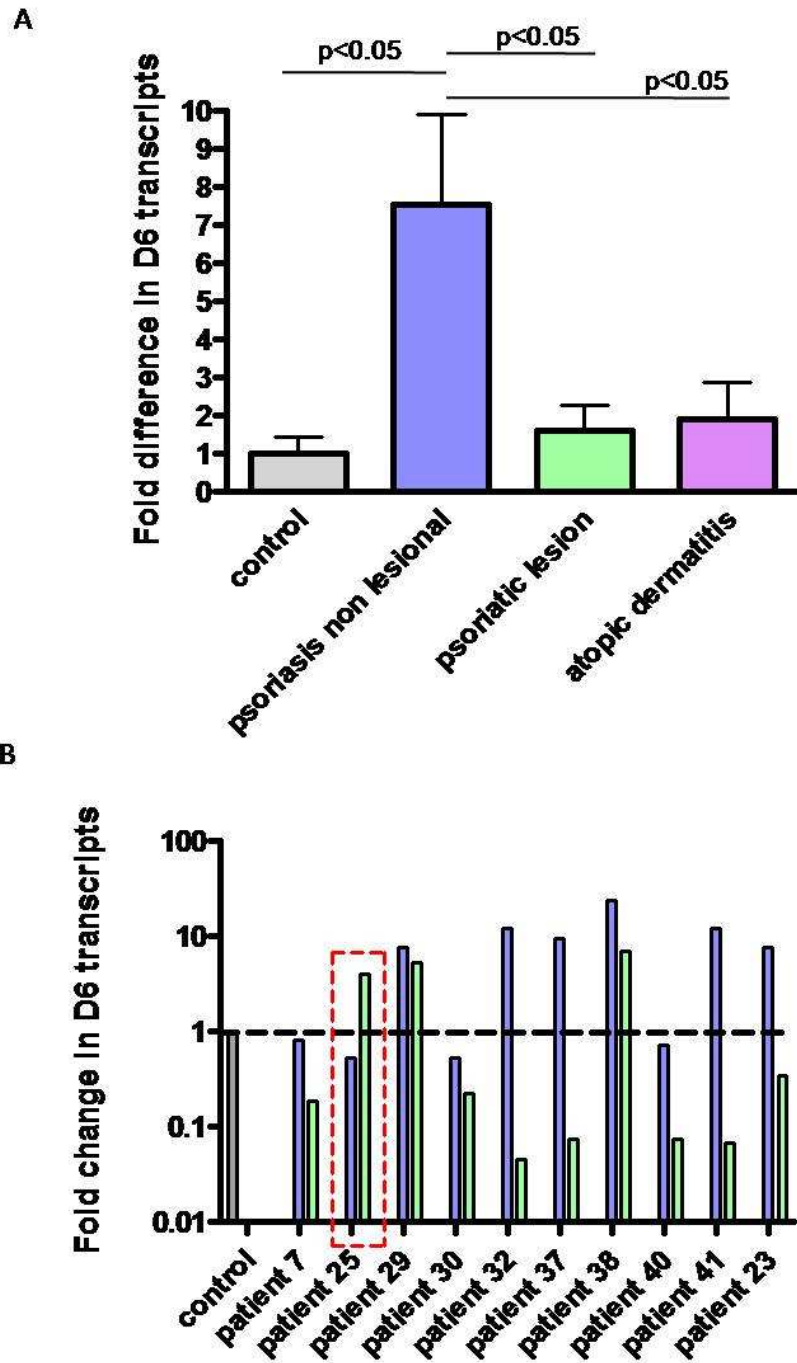


Figure 5-1. D6 transcript levels in human skin.

Levels of D6 transcripts were examined in human skin biopsies from control individuals, atopic dermatitis patients and psoriasis patients (lesions and uninvolved skin). (A) Levels of D6 transcripts are normalised to GAPDH, a housekeeping gene, and expressed as fold change in D6 transcripts compared to control samples. Control n=9, psoriasis non-lesional n=10, psoriatic lesional n=13 and atopic dermatitis n=9, columns show mean  $\pm$  SEM. (B) The individual transcript levels of D6 in non-lesional skin and lesion of each patient. Transcript levels were normalised to GAPDH and expressed as fold change normalised to control samples with a fold change of 1 (shown by black dotted line). Blue column is psoriatic non-lesional and green column is psoriatic lesional skin.

## 5.4 D6 protein in human skin

Within our laboratory, monoclonal antibodies to human D6 had been generated (Nibbs et al., 2001). In brief, human D6 was transfected into a murine cell line (L1.2) and used to immunise C57BL/6 mice. Spleen cells from the immunised mice were fused with myeloma SP2/0 cells to generate hybridomas. Supernatants from the hybridomas were screened and several clones that specifically stained for D6 were further subcloned, expanded and the supernatant collected.

As anti-human D6 antibodies were available for use, human skin biopsies were obtained to stain for the presence of D6 in control human skin and psoriatic skin (within lesions and uninvolved skin). Staining for D6, using immunohistochemistry would allow us to determine the location of D6 within the skin. Human placental samples were used as a positive control as D6 is highly expressed within human placenta, specifically on syncytiotrophoblasts (Martinez de la Torre et al., 2007). Previous studies using one of the monoclonal antibodies generated revealed the presence of D6 on lymphatic endothelial cells by immunohistochemistry (Nibbs et al., 2001). This study used a new clone of antibody and as a result required optimisation for use in immunohistochemistry.

Human skin biopsy samples were obtained from patients and collected into 10% neutral buffered formalin. Samples were processed, embedded in paraffin wax blocks and cut into 4-micron sections to stain either with haematoxylin and eosin or with the anti-human D6 antibody. In sections stained with the anti-human D6 antibody (or isotype control), a biotinylated secondary antibody was used. Bound antibodies were detected using the avidin-biotin-horseradish peroxidase method (Vector Laboratories) and DAB substrate, which results in brown staining. Sections of placenta were used to test the clone of anti-human D6 antibody, initially following the previously optimised protocol.

Firstly, placental sections were cut and then to enable identification of placental structure, sections were stained with haematoxylin and eosin. Figure 5-2 illustrates aspects of the placental structure, which consists of chorionic villi surrounded by maternal blood in the intervillous space. The villus area consists mainly of connective tissue and contains umbilical blood vessels linked to the

fetus. The outer lining of the villus is lined with syncytiotrophoblasts, which are the interface between the mother and the fetus.

To test the clone of antibody, placental sections were stained with high concentrations of the primary antibody using dilutions of 1:10 and 1:50 (stock concentration was 100µg/ml). No brown staining was seen anywhere within the placental sections using 1:10 or 1:50 dilutions of either IgG2a antibody or anti-human D6 antibody (Figure 5-3). This suggested that the conditions used for staining the placental sections were not optimal.

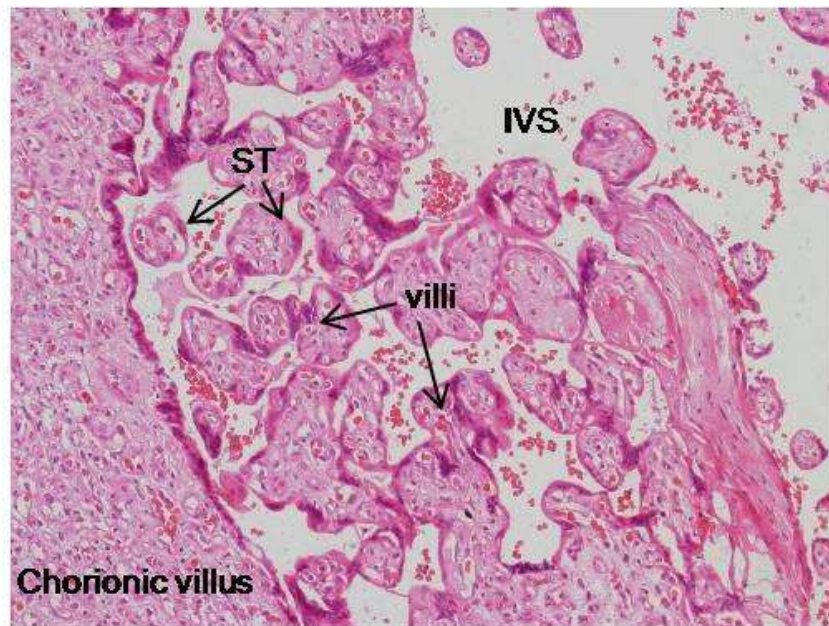


**Figure 5-2. Haematoxylin and eosin staining in human placenta**

Placental sections were processed and sections cut for staining with haematoxylin and eosin to identify placental features, such as chorionic villus, intervillous space (IVS) and syncytiotrophoblasts (ST) lining the villi. Magnification is 100x.

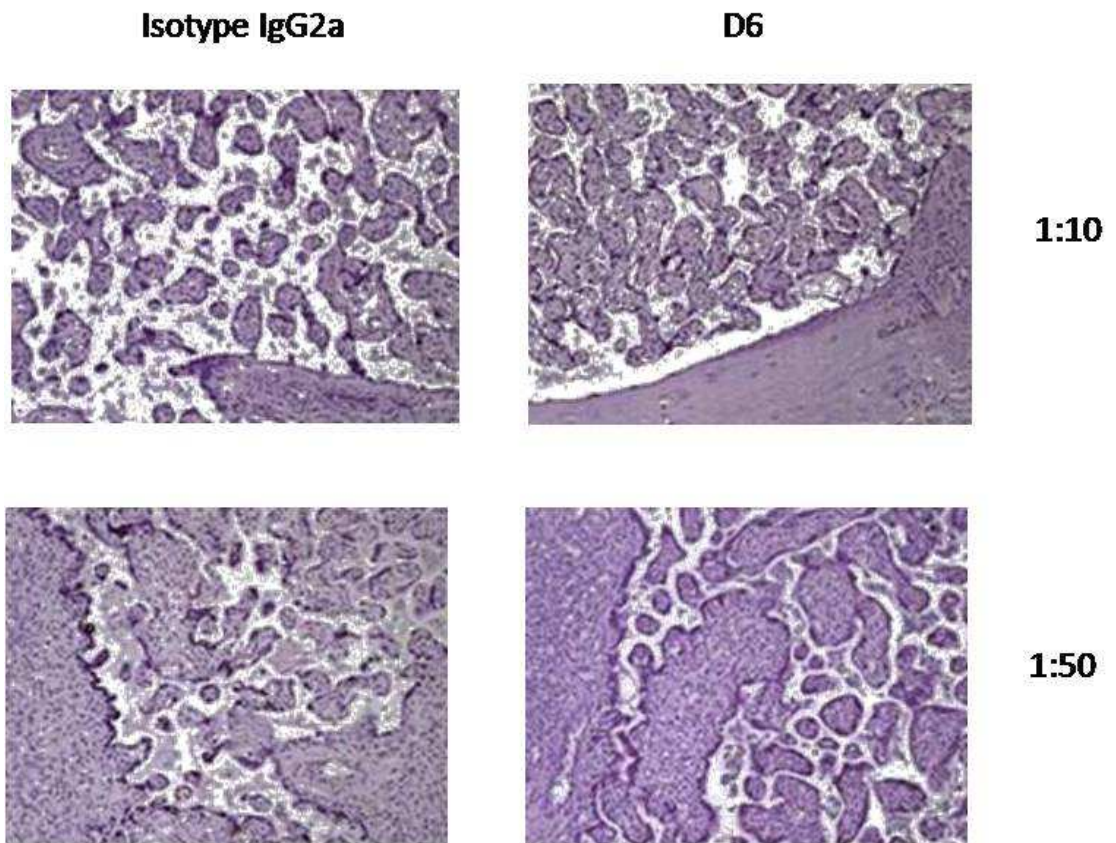


**Figure 5-3. Optimisation of D6 antibody on placental sections.**

Placental sections were stained with either anti-human D6 antibody (4a5) or Isotype IgG2a using either 1:50 or 1:10 dilutions. Magnification is 100x.

There are many factors, which can contribute to staining not occurring in immunohistochemistry, and it was decided to try a different antigen retrieval step. In the next set of staining, the antigen retrieval step was changed from EDTA pH 8 to 1mM citrate buffer pH 6. As a result, brown staining was present in the placental section stained with the anti-human D6 antibody (Figure 5-4). This was evident in the connective tissue within the villus as well as the syncytiotrophoblast layer (Figure 5-4). However, placenta stained with the isotype IgG2a antibody, as a negative control, also displayed brown staining within the villi as well as within syncytiotrophoblasts, indicating high non-specific staining (Figure 5-4).

To reduce background staining, the primary antibody concentration was reduced. Using a 1:50 dilution of the anti-human D6 antibody, brown staining was present in the connective tissue of the villus as well as in the outer layer of the villus (Figure 5-5). However, within the negative control section using an isotype antibody, the connective tissue of the villi and the syncytiotrophoblast layer also stained brown, illustrating high non-specific binding had occurred (Figure 5-5). As a result, a 1:250 dilution of primary antibody was tested and resulted in strong specific D6 staining within syncytiotrophoblast cells in the placenta, as the isotype stained section contained no brown staining within the syncytiotrophoblast layer (Figure 5-5). Since the syncytiotrophoblast layer was only brown in sections stained with the anti-human D6 antibody and was not seen using the isotype control, this suggested that the anti-human D6 antibody (4a5 clone) was working and was specific for D6. This staining confirmed that D6 is expressed on syncytiotrophoblasts within the placenta.

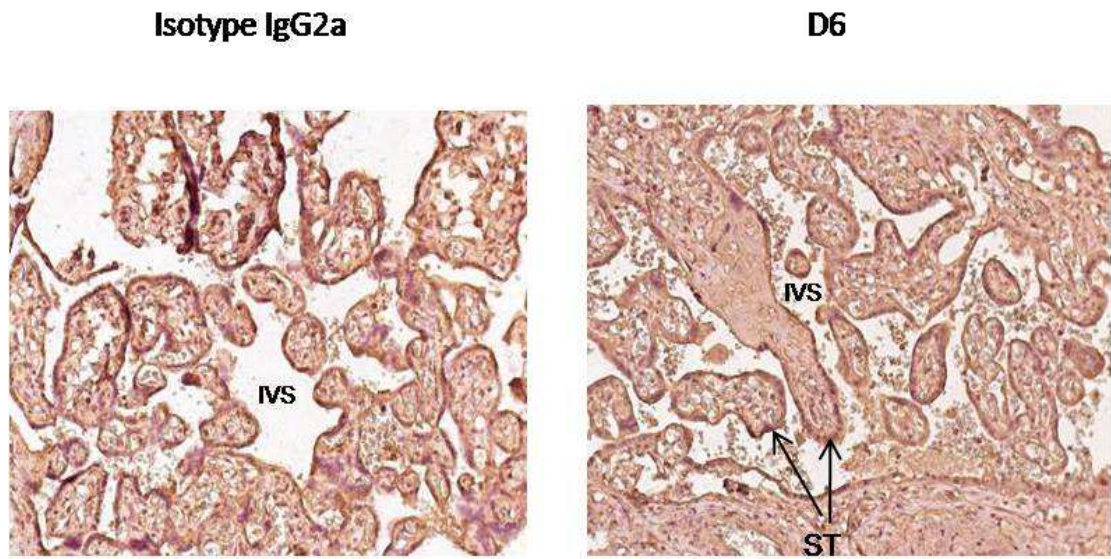


**Figure 5-4. Change of antigen retrieval method.**

Placental sections were stained with either anti-human D6 antibody (4a5) or Isotype IgG2a using 1:10 dilutions. IVS; intervillous space, ST; syncytiotrophoblasts, Magnification 100x.

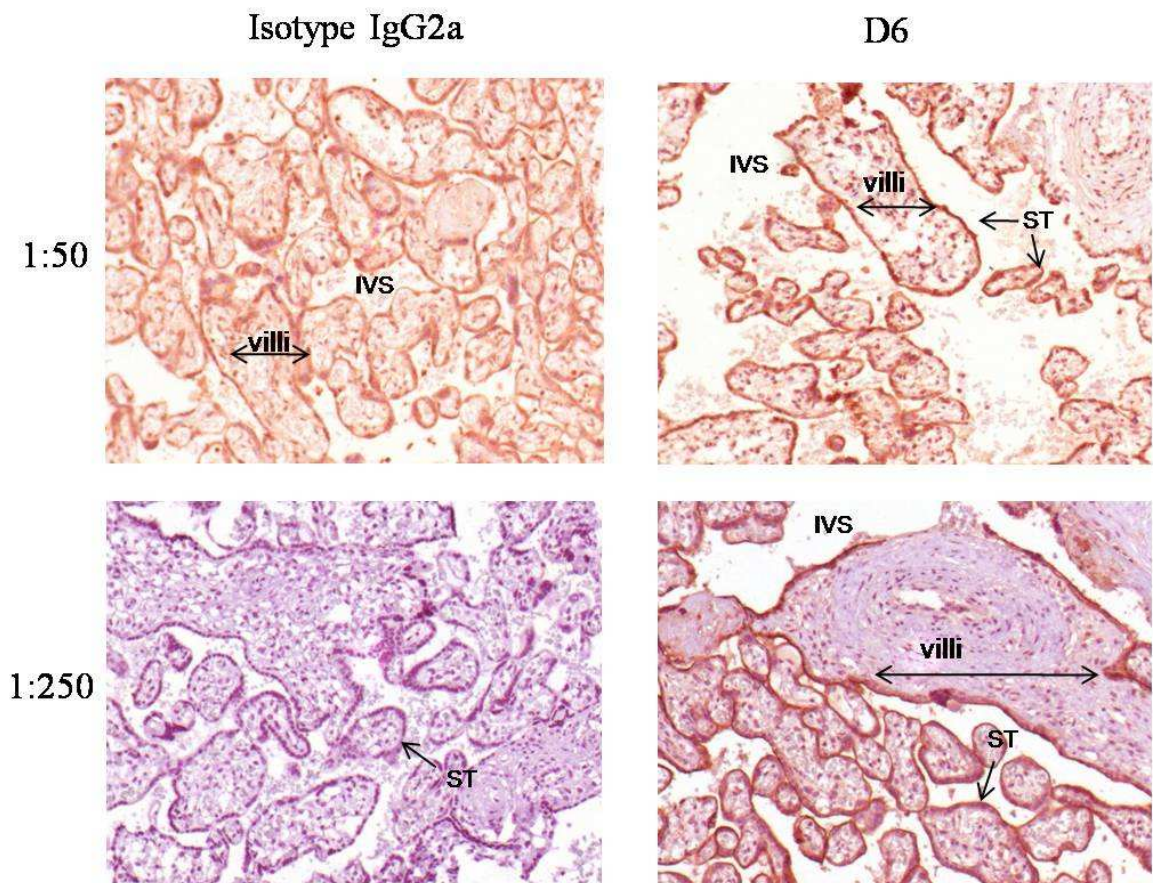
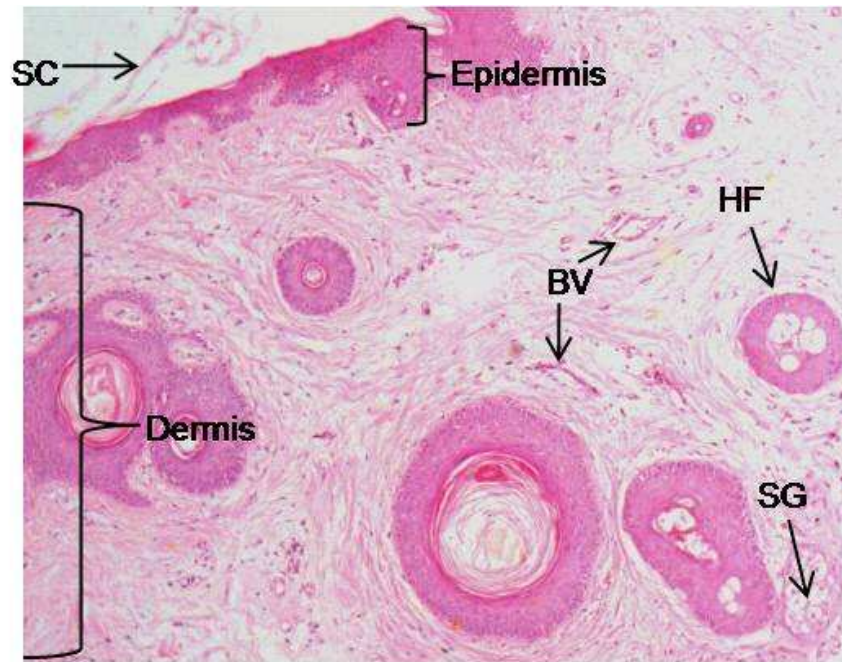


Figure 5-5. Different concentrations of primary antibody on placental sections.

Sections were stained with either 1:50 or 1:250 dilution of isotype IgG2a or anti-human D6 antibody. IVS; intervillous space, ST; syncytiotrophoblasts. Magnification x100.

Since the anti-human D6 antibody was shown to be specific for D6 in the placenta, it was decided to stain human skin sections and use placental sections as a positive control. First, skin sections were cut then stained with haematoxylin and eosin to ensure the skin biopsy was embedded in the correct orientation. The structure and features within a control skin sample are illustrated in Figure 5-6. Features illustrated within this sample are the multi-layered epidermis including the outermost layer, known as the stratum corneum. Below the epidermis is the dermis, in which blood vessels, hair follicles and sebaceous glands can be identified (Figure 5-6).

It was decided to test the anti-human D6 antibody on skin sections using a 1:250 dilution. This concentration of antibody resulted in brown staining within the epidermis as well as within the connective tissue in the dermis (Figure 5-7). The isotype control stained skin section did not display any brown staining, which would suggest that the brown staining seen in the anti-human D6 antibody stained section is due to primary antibody binding (anti-human D6 antibody). However, in the D6 stained section, brown staining covered the whole tissue and as a result indicated that the staining was non-specific (Figure 5-7).



**Figure 5-6. Structure and features of human skin**

A skin biopsy was taken from a control patient, processed and sections were cut and stained with haematoxylin and eosin. Annotations illustrate epidermal and dermal compartments of skin as well as stratum corneum (SC), blood vessels (BV), hair follicles (HF) and sebaceous glands (SG). Magnification 100x.

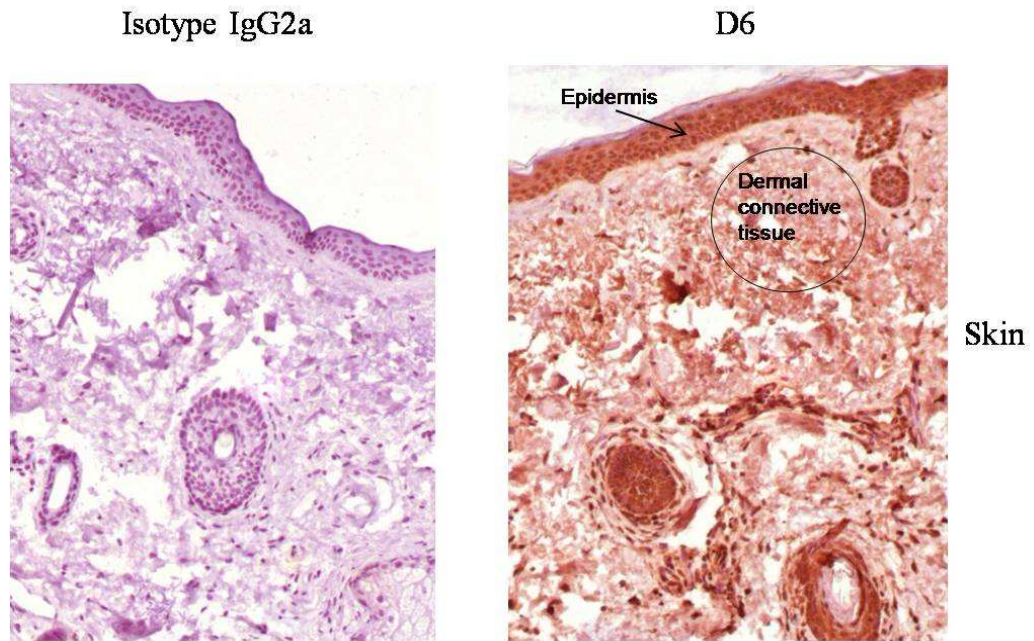


**Figure 5-7. D6 staining in skin section**

**Control skin sections were stained with either isotype IgG2a or anti-human D6 antibody (1:250 dilution). Magnification 100x.**

To optimise the anti-human D6 antibody for staining in human skin sections, decreasing concentrations of anti-human D6 antibody were tested using 1:300, 1:400 and 1:500 dilutions (Figure 5-8; 1:400 dilution not shown). Using 1:300 dilution of antibody, D6 was specifically expressed on syncytiotrophoblasts within placental sections as no brown staining appeared on syncytiotrophoblasts with the negative control, which was stained with isotype IgG2a antibody (Figure 5-8A). On the other hand, in the skin sections, brown staining was present in the epidermis and in hair follicles with no brown staining appearing in dermal connective tissues (Figure 5-8A). As no brown staining appeared in the negative control skin section, this suggested that the anti-human D6 antibody was working but possibly not specific to D6 and potentially cross-reacting to other proteins, for example in hair follicles. (Figure 5-8A). The 1:500 dilution of antibody also resulted in similar staining to the 1:300 dilution where brown staining occurring in the epidermis as well as hair follicles and no brown staining occurred in the negative control (Figure 5-8B). In addition, it was noted that in both 1:300 and 1:500 stained skin sections, the dermal connective tissue did not stain brown in comparison to the staining seen previously with a 1:250 dilution of antibody (Figure 5-7). This suggested that by increasing the dilution of the antibody, non-specific binding had been reduced slightly.

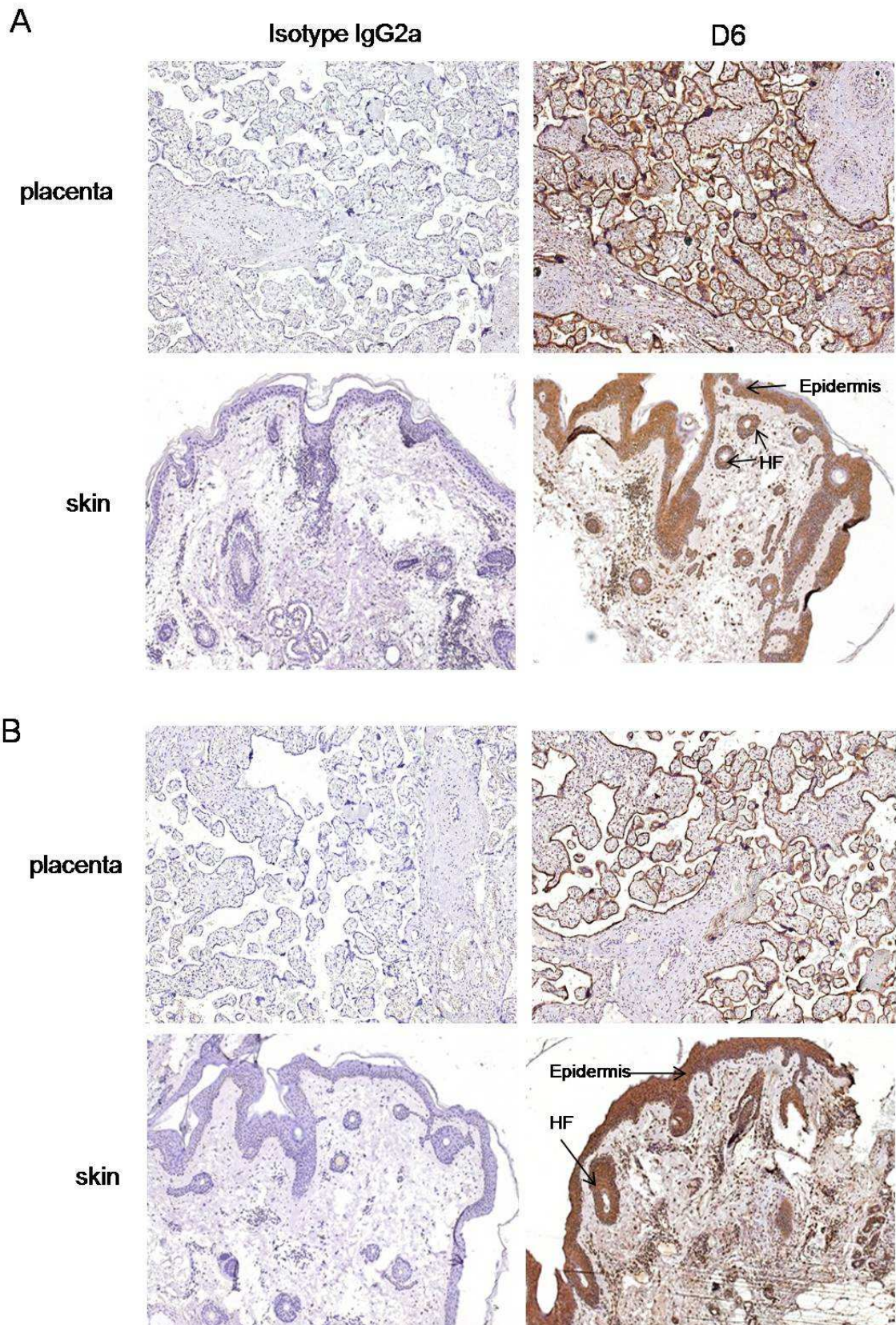


**Figure 5-8.** Different concentrations of primary antibody on human placenta and skin sections.

Placental and skin sections were stained with either isotype IgG2a antibody or anti-human D6 antibody. (A) Antibodies were used at 1:300 dilution (B) Antibodies were used at 1:500 dilution. HF indicates hair follicles. Magnification 50x.

To determine optimal conditions for D6 staining within skin sections and to reduce non-specific binding within the tissue, further dilutions, 1:750 and 1:1000 were tested. In the 1:750 dilution, D6 was seen to be expressed within the placenta indicated by brown staining using the anti-human D6 antibody (Figure 5-9A). Within the skin, brown staining was present within the epidermis (Figure 5-9A) however, it was noted that this was less intense than when the 1:500 dilution was used (Figure 5-8). This indicated that non-specific staining was reduced by using a lower concentration of anti-human D6 antibody. In the 1:1000 antibody dilution, brown staining still occurred in the epidermis and surrounding hair follicles in skin sections stained with the anti-human D6 antibody although no brown staining was seen in the negative control (Figure 5-9B). However, it was noted that several cells within the skin were stained brown and others did not (within black circle in Figure 5-9B). On closer examination, it was noted that there was non-specific staining in the epidermal tissue (indicated by the red arrow in Figure 5-10) yet not all the cells within the epidermis were stained brown (example within black circle in Figure 5-10). Within the dermis, there was a mixture of cells that had stained brown (examples in red circle in Figure 5-10), which could possibly be leukocytes and others cells did not. These data indicated that the D6 antibody may be specific for D6 expressing cells but there was still some staining within the epidermis, which was likely to be non-specific, and indicates cross-reactivity with other proteins within the epidermis.

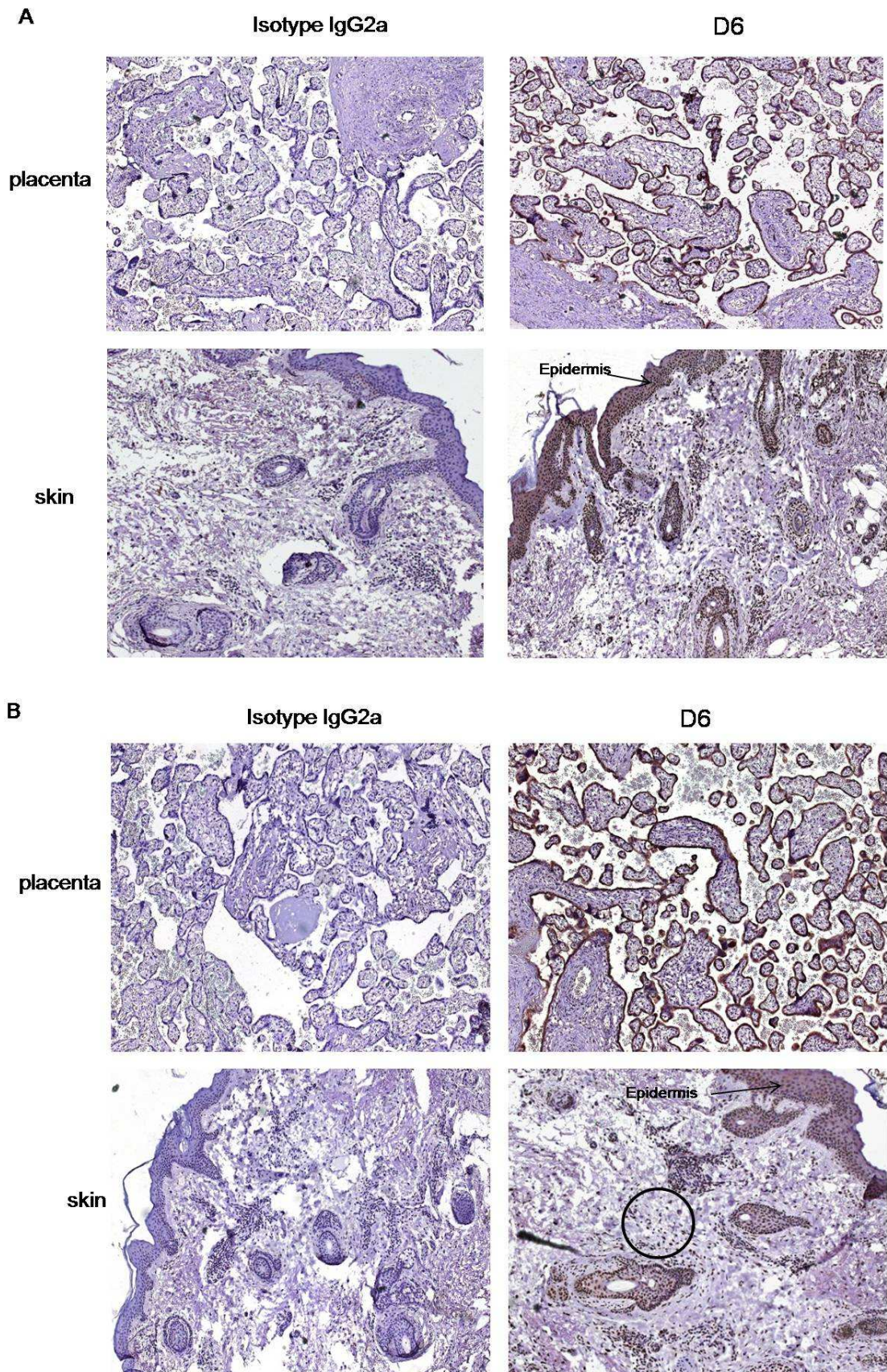


**Figure 5-9. Optimisation of primary antibody on human placenta and human skin sections using 1:750 and 1:1000 dilutions.**

Human placenta and skin sections were stained with either isotype IgG2a or anti-human D6 antibody (A) Sections were stained with primary antibody at 1:750 dilution (B) Primary antibody was used at 1:1000 dilution. Black circle contains some cells, which have stained brown which indicates that these cells express D6. Magnification 100x.

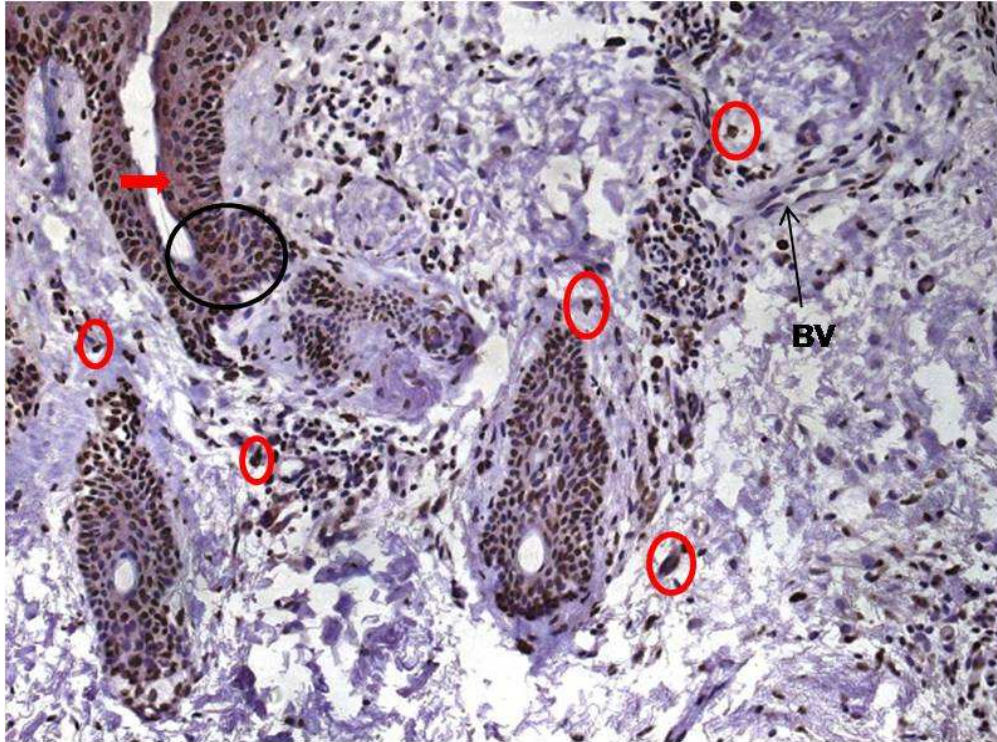


**Figure 5-10. D6 staining within human skin**

Human skin section was stained with anti-human D6 antibody (1:1000 dilution) and examined for positive brown staining. BV indicates a blood vessel. Red arrow denotes background staining in the epidermis. Red circles illustrate positive brown stained cells indicating D6 protein expression. Black circle highlights that some cells in the epidermis did not stain brown (negative for D6). Magnification x200.

In order to reduce non-specific staining within the epidermis, sections were tested with the extra steps of blocking endogenous biotin as well as reducing the time the tissues were incubated in DAB. There was less epidermal staining in both sets of skin sections, indicating that non-specific staining was reduced by the amount of time DAB was incubated with the samples and not by the use of avidin-biotin block in this case (Figure 5-11). Once again, there are positive stained cells within the epidermis and the dermis (Figure 5-11B). However, with non-specific staining still present in the epidermis, there is the possibility that positive brown stained cells are not D6 expressing cells and the antibody is cross-reactive with proteins on these cells. If these cells are positive for D6, they could be leukocytes as D6 has been reported to be expressed on B cells and dendritic cells as well as within atopic dermatitis (McKimmie et al., 2008, McKimmie and Graham, 2006). Further staining would be required to confirm the cell types. As for cells positively stained within the epidermis, this would suggest that D6, or the antibody is cross-reacting with proteins, expressed on keratinocytes, melanocytes and merkel cells or possibly by resident immune cells within the skin. Blood vessels did not stain positively for D6 and it was noted that using his clone of anti-human D6 antibody, positive brown staining was not seen on lymphatic vessels within control skin. With non-specific staining occurring in the skin, this clone of antibody may not be optimal for immunohistochemistry on skin.

Whilst trying to optimise the anti-human D6 antibody, the next step was to obtain, embed and cut psoriasis skin biopsies ready for immunohistochemistry staining. There were only five psoriasis patient samples available (lesional and non-lesional) however; several attempts to cut sections were unsuccessful. While trying to cut sections, the skin would ribbon, tear or the section would split down the middle, therefore not giving good sections to stain. To try to improve this, a new blade was used, embedded sections were left on ice longer but sections were still difficult to cut. Another possibility could be that the sections were not in the exact correct orientation during the embedding procedure.

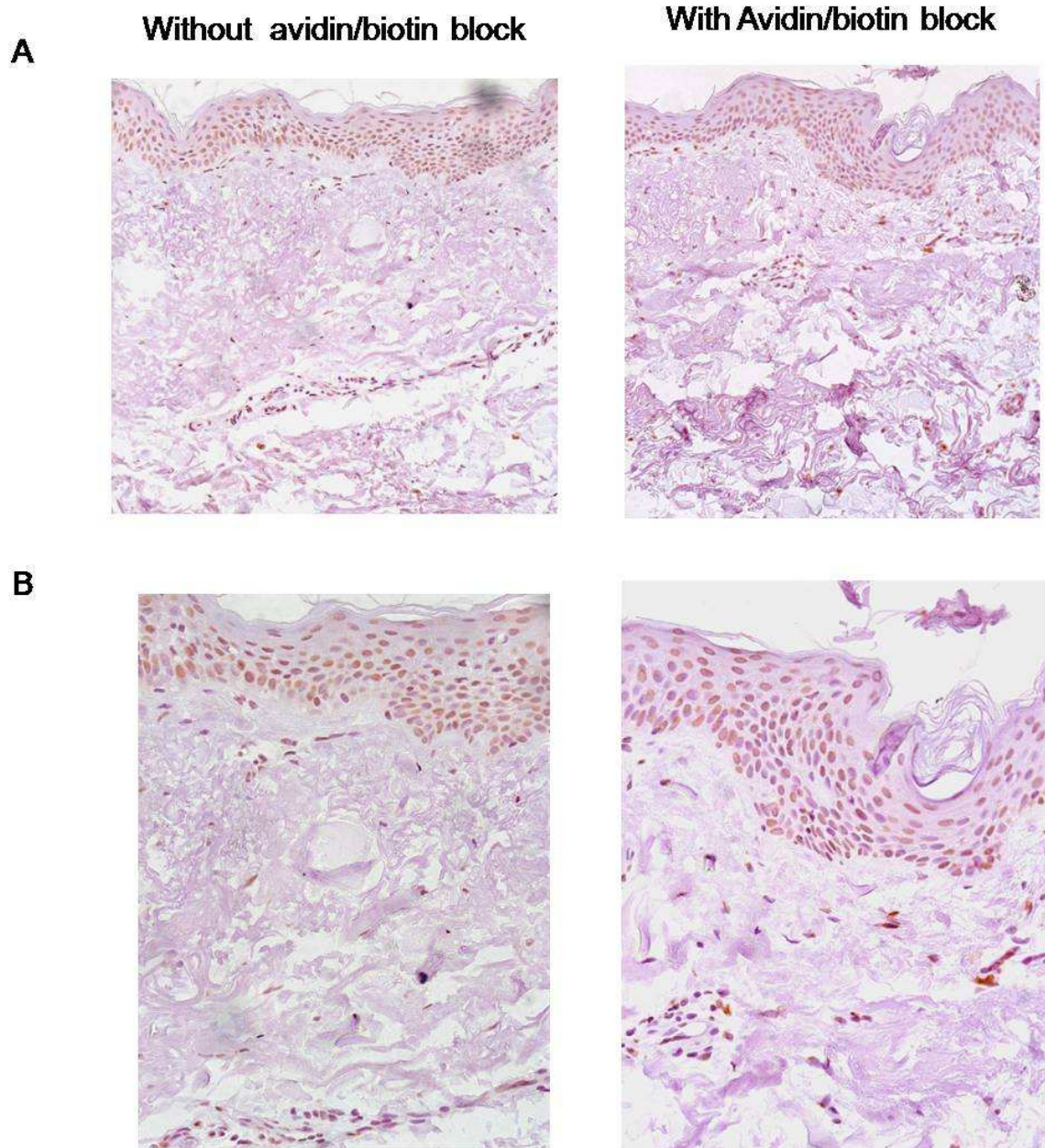


**Figure 5-11. Comparison using avidin/biotin block during D6 staining on human skin.**

**Skin sections were stained using 1:1000 dilution of anti-human D6 antibody. (A) Skin stained section without or without the use of avidin/biotin block. Magnification 200x (B) Skin sections with/without avidin biotin block, showing brown staining on some cells within the tissue. Same pictures as in (A) but magnification is 400x.**

## 5.5 D6 transcripts in peripheral blood

As described in section 5.3, D6 transcripts were elevated in psoriatic uninvolved skin compared to control skin. Therefore, it was decided to examine D6 transcript levels within the peripheral blood of psoriasis patients to determine if PBMCs had enhanced D6 expression compared to healthy controls. These cells may contribute to the enhanced expression of D6 within psoriatic uninvolved skin due to increased leukocyte infiltration. It was also decided to extend the analysis of D6 transcripts within peripheral blood to other inflammatory diseases, such as psoriatic arthritis (PsA) and rheumatoid arthritis (RA). Psoriatic arthritis is a chronic inflammatory disease that involves joint inflammation as well as the presence of psoriasis. Over time, cartilage within the joints is reduced and erosion of the bone occurs resulting in joint deformities leading to a reduced function and quality of life (Gladman et al., 2005). Rheumatoid arthritis is also chronic inflammatory disease that leads to swelling and destruction within the joints. The lining of the synovium becomes inflamed and hyperplastic due to infiltration of inflammatory cells (Sweeney and Firestein, 2004). Joint destruction occurs through cartilage damage and bone erosion leading to severe disability (Goldring, 2003). PsA and RA can be distinguished from each other by the psoriatic component and by the joints that are affected.

A small sample of peripheral blood was collected from control (n=12), psoriatic (n=12), psoriatic arthritis (n=15) and RA patients (n=15). Cells from peripheral blood were isolated and RNA was extracted from total PBMCs, which includes monocytes, T cells, B cells, myeloid dendritic cells and plasmacytoid dendritic cells, and analysed for D6 transcripts by QPCR. In the PBMCs from psoriasis patients, D6 transcripts were increased 2.3-fold compared to control PBMCs but the change was not significant (Figure 5-12). There was no significant difference in D6 transcripts in PBMCs within PsA patients compared to controls. However, there was a significant 2-fold decrease found in PBMCs from RA patients in comparison to controls (Figure 5-12). There was large variation in D6 transcripts within psoriasis patients and it is not known whether this variation correlates with disease severity at the time (Figure 5-12). In PsA patients, there are two distinct populations and it may be possible that these correlate with the presence of psoriatic lesions (Figure 5-12).

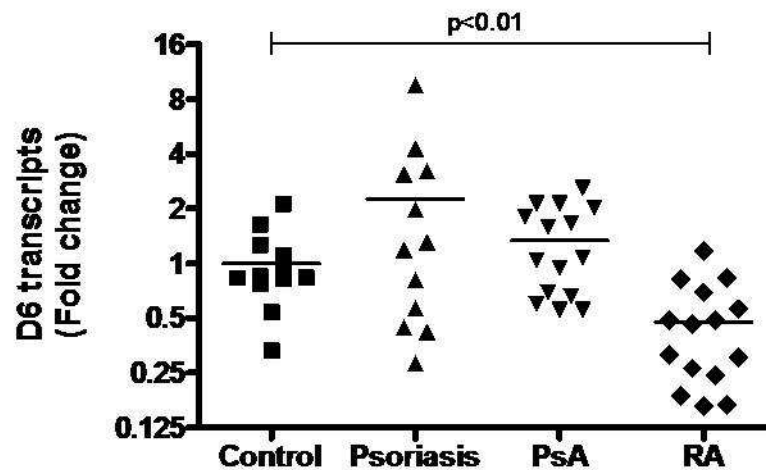


Figure 5-12. Levels of D6 transcripts in peripheral blood from human inflammatory diseases.

RNA was extracted from peripheral blood cells of control, psoriatic, psoriatic arthritis (PsA) or rheumatoid arthritis (RA) patients and examined for D6 transcripts. Levels were normalised using GAPDH as a housekeeping gene. D6 transcripts levels are expressed as fold change in comparison to controls. Control n=12, psoriasis n=12, psoriatic arthritis (PsA) n=15 and rheumatoid arthritis (RA) n=15.

## 5.6 D6 surface expression on peripheral blood cells

D6 transcript levels were found to be lower in peripheral blood of RA patients than in healthy controls. As a result, it was decided to examine PBMCs in more detail to determine which cell types were responsible for lower D6 expression in RA patients.

PBMCs were extracted from control or RA patient blood and examined for D6 expression on the cell surface by flow cytometry using an anti-human D6 antibody (McKimmie et al., 2008). To identify cell types, antibodies against lineage specific markers were used. CD3 was used to identify T cells, CD20 was used to identify B cells and monocytes were identified by CD14. Myeloid DCs were identified by CD1c expression and plasmacytoid DCs were identified by CD304 (BDCA4) expression.

PBMCs were profiled using forward and side scatter and the main population of cells were gated as show in Figure 5-13.

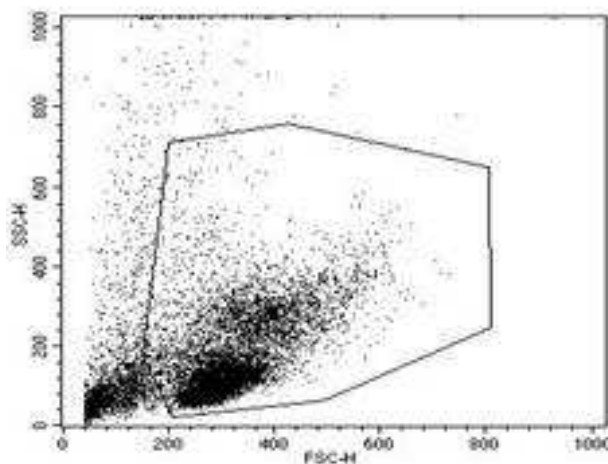


**Figure 5-13.** Profile of peripheral blood mononuclear cells from a healthy control patient.

Peripheral blood mononuclear cells were profiled by flow cytometry using forward and side scatter. The main population of cells were gated for further analysis.

Control PBMCs were stained with viaprobe to detect and exclude dead cells. Live cells do not stain positive for viaprobe. Live T lymphocytes were gated (R2) by selecting cells which were negative for viaprobe and stained positive for CD3 using an anti-human CD3 antibody, as shown in Figure 5-14A. The plots shown in Figure 5-14 are from one representative sample. A profile of CD3 positive T cells stained with isotype antibody or anti-human D6 antibody is shown in Figure 5-14B. T cells stained with isotype antibody had a mean fluorescent intensity (MFI) of 1.79 whereas D6 expressing CD3 positive cells had an MFI of 3.36. The corresponding histogram plot shows that T cells from a control patient weakly express D6 on their surface (Figure 5-14B). Live B cells were gated on CD20 positive cells (R2; Figure 5-14C) and were then analysed using either isotype antibody staining or anti-human D6 antibody. Isotype stained B cells had an MFI of 1.74 whereas B cells express different levels of surface D6 (fluorescent intensity spread is 3-3865) with an MFI of 49.76 (Figure 5-14D). Control B cells express surface D6 at various levels with some B cells expressing D6 at high levels.

Monocytes from controls were gated (R2) using an anti-human CD14 antibody (Figure 5-15A). Cells positively expressing CD14 were gated and analysed for expression of D6 (Figure 5-15A). In a representative sample, isotype stained monocytes had an MFI of 5.09 whereas D6 positive cells had an MFI of 53.83 (Figure 5-15B). It can be concluded that monocytes express surface D6 (Figure 5-11B).

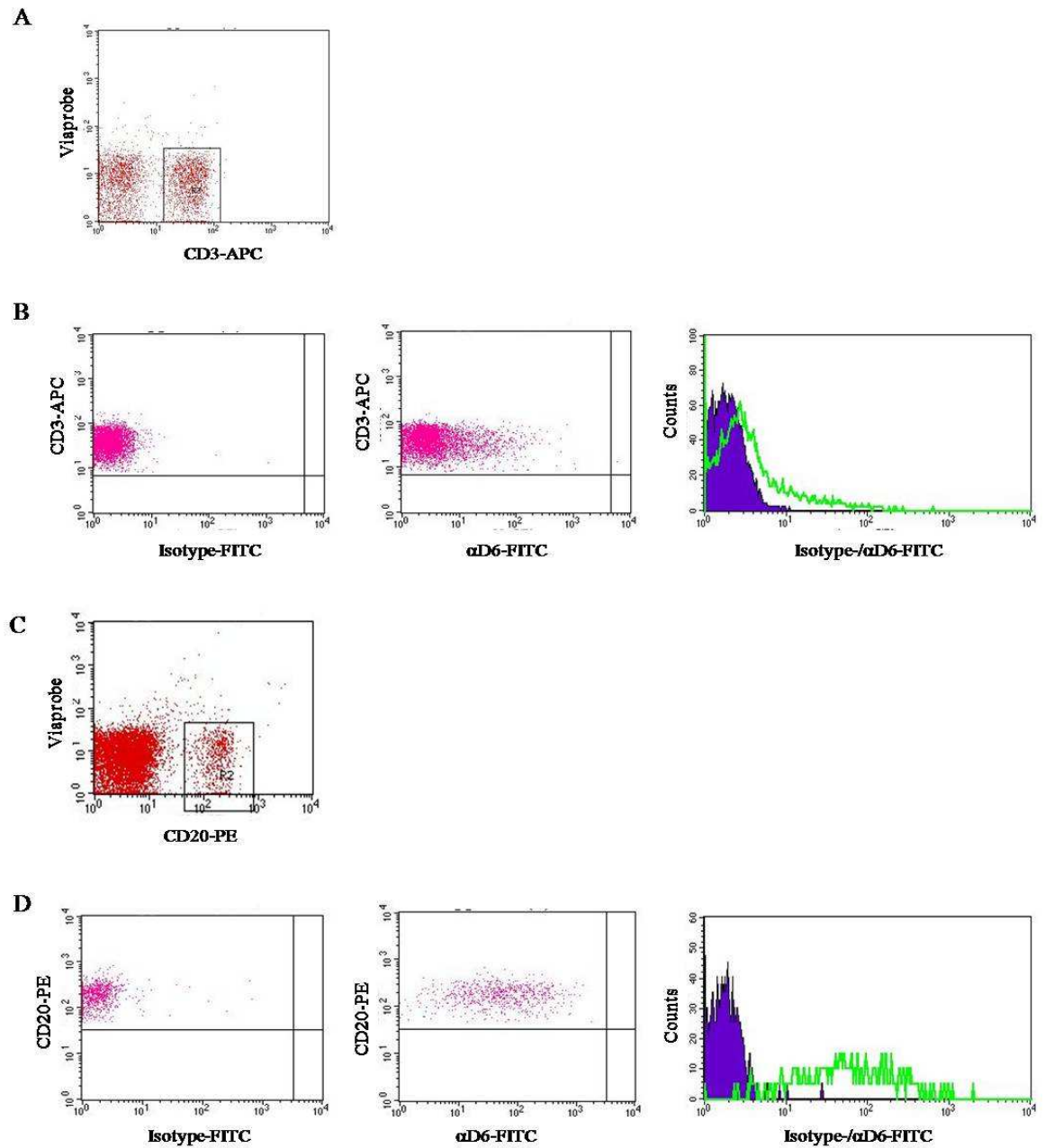


Figure 5-14. Analysis of D6 expression on control human T and B cells.

(A) Live positive CD3 T cells were gated using R2. (B) T cells gated through R2 were analysed using isotype or anti-human D6 antibody. A representative histogram showing T cells intensity for isotype (purple) and D6 (green). (C) Live B cells were gated using an anti-human CD20 antibody. (D) A representative plot of cells positive for CD20 and stained with either isotype control or anti-human D6 antibody. A representative overlay is shown plotting B cell fluorescent intensity for isotype (purple) and D6 (green).

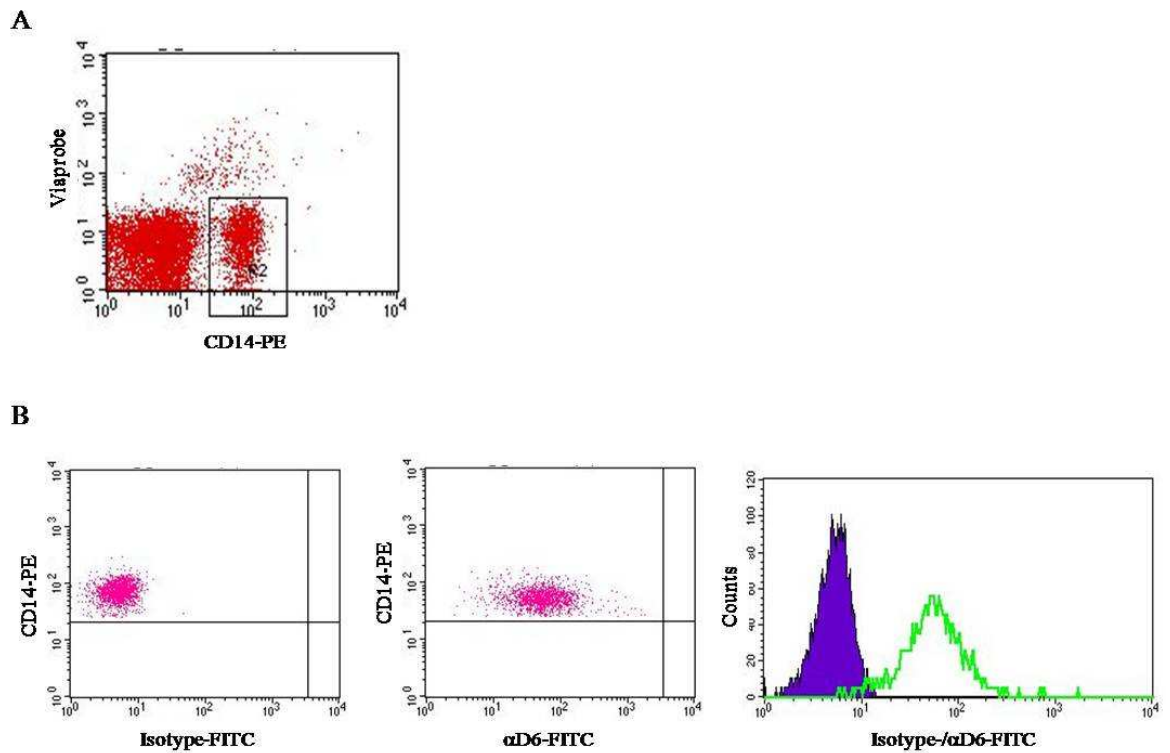


Figure 5-15. Analysis of D6 expression on control monocytes.

(A) Monocytes were gated using an anti-human CD14 antibody (R2) (B) Cells were gated through R2 and analysed for isotype and D6 expression. A representative histogram shows fluorescent intensity for isotype (purple) and D6 (green) positive monocytes.

There are two subtypes of dendritic cells in human PBMCs, myeloid and plasmacytoid dendritic cells, which are characterised by distinct lineage markers (Shortman and Liu, 2002). For mDCs, an antibody against CD1c was used and for pDCs, an antibody against CD304 (BDCA-4) was used. However, monocytes and B cells can also express these surface molecules and therefore identification of monocytes and B cells was required in order to exclude them from further analysis of dendritic cells. Cells were stained with a cocktail of antibodies in order to identify dendritic cells. Cells negative for CD14 and CD20 were gated through R2, therefore excluding monocytes and B cells respectively (Figure 5-16A). Cells gated in R2, which were positive for CD1c, were classed as mDCs (R3; Figure 5-16B). In a representative sample, mDCs, which stained positive for isotype control had an MFI of 3.32 whereas D6 positive cells gave an MFI of 44.21 (Figure 5-16B). Myeloid DCs express a range of D6 on their surface with some expressing very little D6 and some with high expression of D6, the fluorescent intensity ranged from 3 to 5474 (Figure 5-16B). Plasmacytoid DCs were also gated through R2, to exclude monocytes and B cells. Positively stained BDCA-4 (CD304) cells indicated that these cells were pDCs and were gated (R3) for further analysis (Figure 5-16C). Plasmacytoid DCs, in a representative sample, express very high levels of D6 (MFI is between 5 and 2916 with a mean of 268.3) as shown in Figure 5-16D.

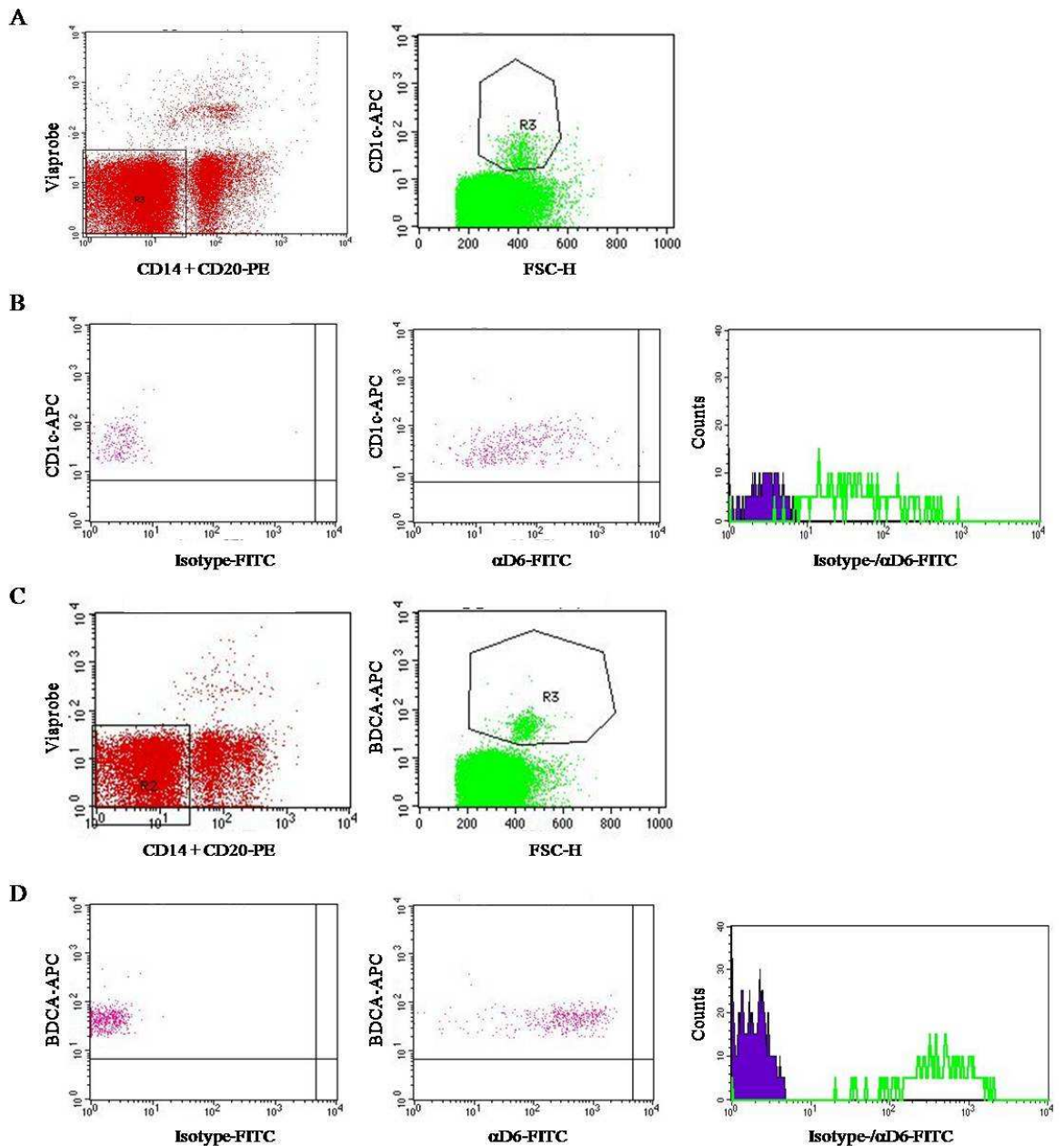
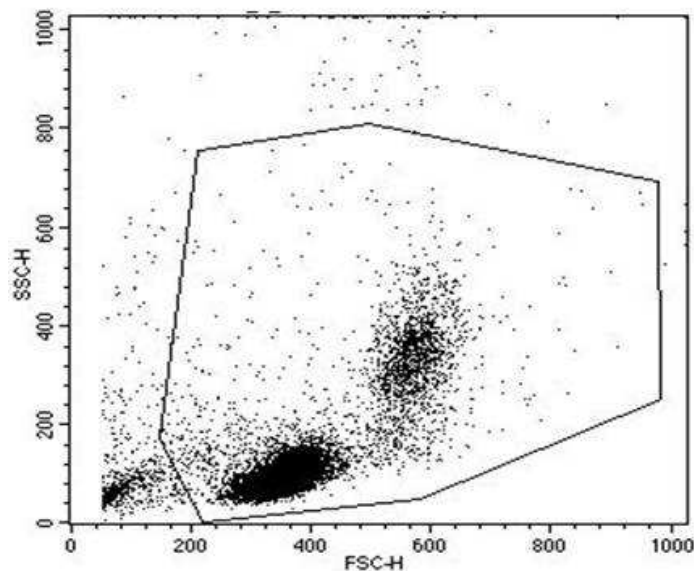


Figure 5-16. Analysis of D6 expression on control myeloid and plasmacytoid dendritic cells.

(A) Live cells were gated (R2) to exclude monocytes and B cells using anti-human CD14 and anti-human CD20 antibody and positive CD1c cells were gated (R3) as myeloid DCs. (B) Cells were gated through R3 and analysed for isotype and D6 expression. A representative histogram plot shows fluorescent intensity for isotype stained mDCs (purple) and D6 positive mDCs (green). (C) Live pDCs were gated to exclude monocytes and B cells (R2) and were gated using an anti-human BDCA-4 antibody (R3). (D) Representative plots of cells positive for CD20 and stained with either isotype control or anti-human D6 antibody. A representative histogram plot shows fluorescent intensity for isotype stained pDCs (purple) and D6 positive pDCs (green).

Peripheral blood was taken from RA patients and PBMCs were isolated. PBMCs were stained with antibodies specific for lineage markers to identify monocytes, T and B lymphocytes, myeloid and plasmacytoid dendritic cells as well as staining for surface D6 expression. PBMCs from RA patients were all gated using the same antibodies and parameters as the control peripheral mononuclear cells. A profile of PBMCs from one RA patient is shown in Figure 5-17, which is similar to control PBMCs although the profile will vary slightly from patient to patient.



**Figure 5-17. Cell profile of peripheral blood mononuclear cells from a rheumatoid arthritis patient using flow cytometry.**

**Peripheral blood mononuclear cells were profiled by flow cytometry using forward and side scatter. The main population of cells were gated for further analysis.**

Live T cells were identified using the anti-human CD3 antibody and were gated as shown in Figure 5-18A. T cells from one RA patient expressed low levels of D6, as the MFI was 3.65 and only shifted to 7.32 for D6 positive T cells (Figure 5-18B). B cells were gated using CD20 and an MFI of 3.52 was obtained with cells stained with isotype antibody whereas cells stained with anti-human D6 antibody resulted in an MFI of 190.16 with a spread of 12 to 1322. High levels of D6 was expressed on B cells from RA patients shown by a 2 log fold shift in the MFI of D6 positive cells compared to isotype stained cells (Figure 5-18D).

Monocytes from RA patient peripheral blood were gated using an anti-human CD14 antibody (Figure 5-19A). In a representative sample, isotype stained monocytes had an MFI of 8.55 and moved to 100.67 on D6 stained monocytes. The corresponding histogram shows that monocytes expressing D6 resulted in a log fold shift of the MFI compared to the isotype control. Therefore, D6 is expressed on monocytes within the peripheral blood of RA patients (Figure 5-19B).

Live mDCs from a RA patient were gated (Figure 5-20A) and isotype stained mDCs had an MFI of 5.22 whereas mDCs positively bound to D6 antibody yielded an MFI of 44.56 with a spread of 53-1241, resulting in a log-fold shift (Figure 5-20B). Although there were low numbers of mDCs, they express moderate levels of D6. Low numbers of pDCs were also seen yet pDCs express a broad and high range of D6 expression levels. In a representative sample, the MFI was 4.09 for isotype stained pDCs and positively D6 stained pDCs varied from 5-4598 with a mean of 359.34 resulting in a 2-log fold shift compared to the isotype control (Figure 5-20D).

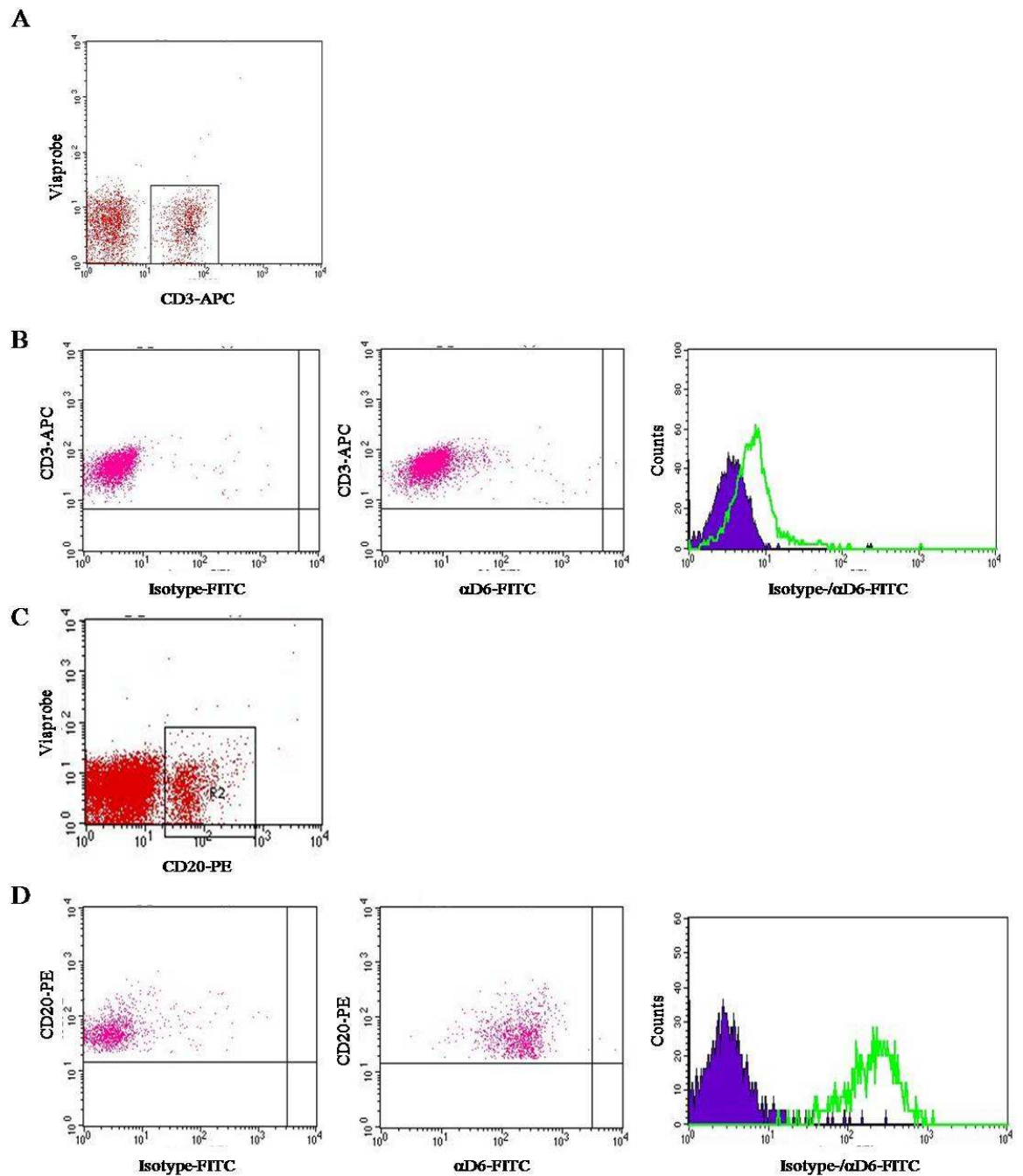


**Figure 5-18.** Analysis of D6 expression on T and B cells from a RA patient.

(A) Positive CD3 cells were gated and selected as T cells. (B) Cells were gated through R2 and analysed for isotype or D6 expression. A representative histogram plotting T cells intensity for isotype (purple) and D6 (green). (D) Live B cells were gated using an anti-human CD20 antibody. (E) Representative plots of cells positive for CD20 and stained with either isotype control or anti-human D6 antibody with a histogram plot showing T cell intensity for isotype (purple) and D6 (green).

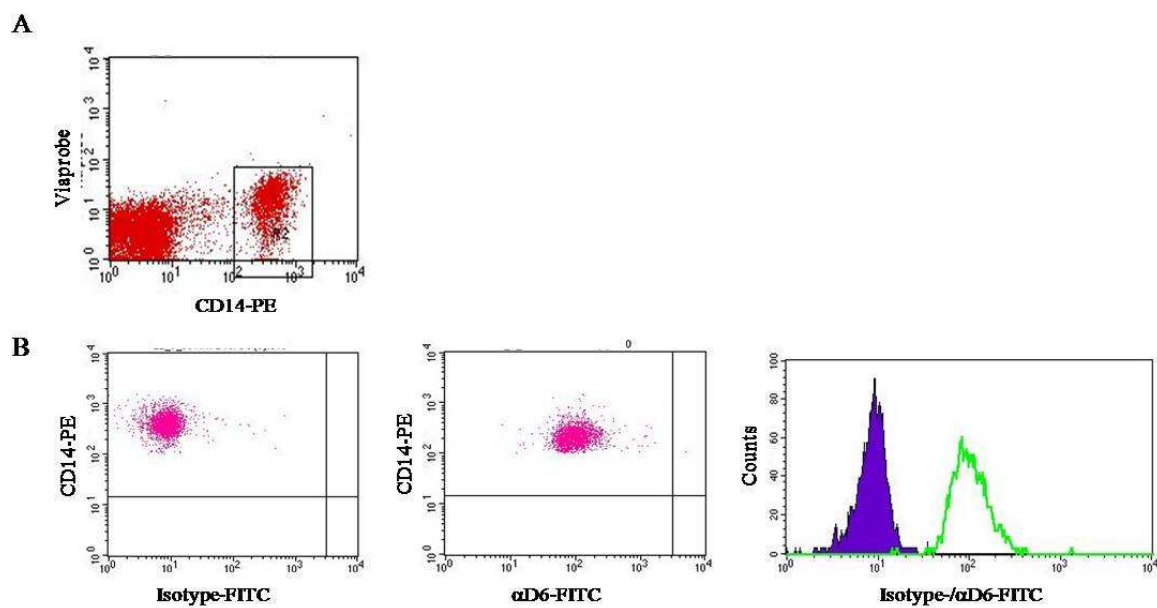
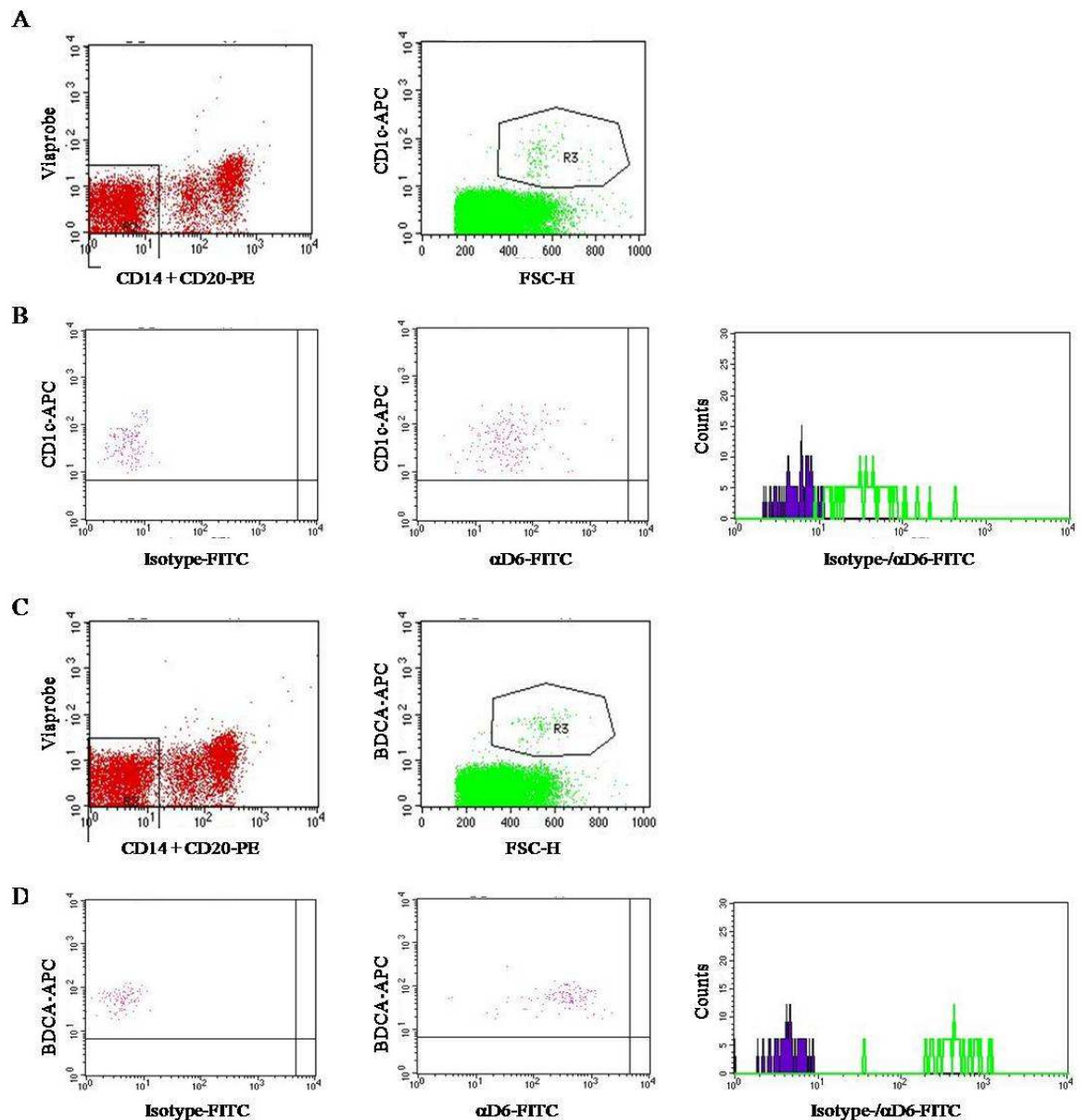


Figure 5-19. Analysis of D6 expression on monocytes from a RA patient.

Cells were gated through R1 and live cells were detected using viaprobe. (A) Monocytes were selected using an anti-human CD14 antibody and gated (R2) (B) Cells were gated through R2 and analysed for isotype control or D6 expression. A representative histogram shows fluorescent intensity for isotype (purple) and D6 (green) positive monocytes.



**Figure 5-20.** Analysis of D6 expression on myeloid and plasmacytoid dendritic cells from a RA patient.

Cells were gated through R1 and live cells were detected using viaprobe. (A) Live cells were gated using R2 to exclude monocytes and B cells and positive CD1c cells were gated and selected as myeloid DCs (R3). (B) Cells were gated through R3 and analysed for isotype and D6 expression. A representative overlay plotting fluorescent intensity for isotype positive (purple) and D6 positive (green) monocytes. (C) Live pDCs were gated to exclude monocytes and B cells (R2) and was gated using an anti-human BDCA-4 antibody (R3). (D) A representative overlay plot of cells positive for CD20 and stained with either isotype control or anti-human D6 antibody.

To compare D6 expression levels between healthy samples and RA patients, the corrected mean fluorescent intensity was calculated, by subtracting the MFI from the isotype control from MFI of D6, for each cell type. Overall, in control peripheral blood, pDCs and B cells expressed the highest levels of D6 on their surface, followed by mDCs and monocytes whereas T cells expressed very weak levels of D6 (Figure 5-21). This trend in levels of expression was similar to D6 expression found on leukocytes (McKimmie et al., 2008, McKimmie and Graham, 2006). In peripheral blood from RA patients, the trend of D6 expression on the same cell types was similar, in that B cells and pDCs expressed highest levels of surface D6 followed by mDCs and monocytes then T cells (Figure 5-21). However, D6 expression on B cells and mDCs was found to be significantly higher in RA patients than in healthy control patients (Figure 5-21). In addition, D6 expression was increased on T cells, monocytes and pDCs from RA patients compared to healthy control but were not significant (Figure 5-21). As a result, these data contradicted the D6 transcript levels data obtained earlier (Figure 5-12), where in peripheral blood, D6 transcript levels were lower in RA patients than in healthy controls.

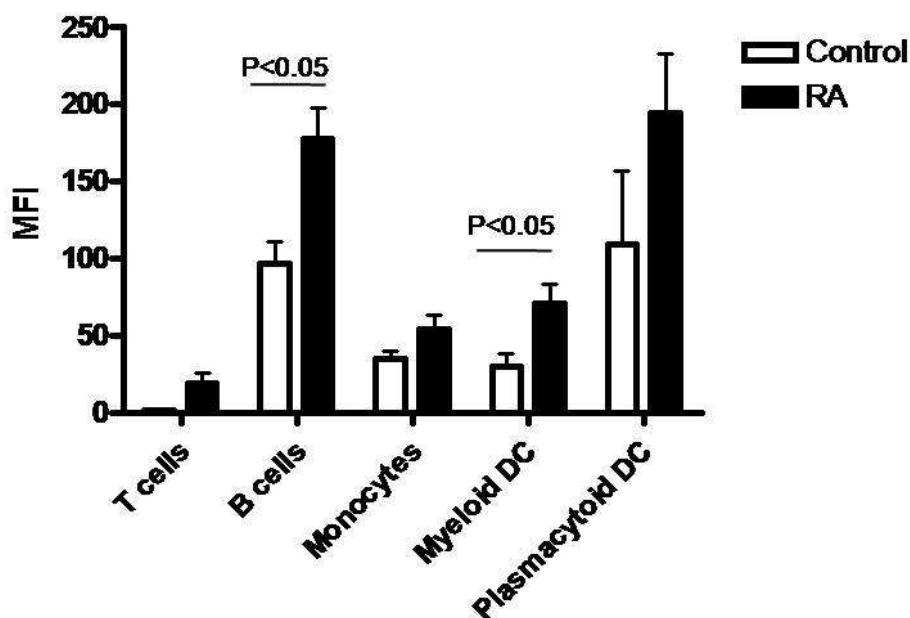


Figure 5-21. Analysis of D6 expression on peripheral blood cells in control and RA patients.

Peripheral blood cells were isolated from control (white) and RA patients (black) stained for specific lineage markers to identify T cells, B cells, monocytes, myeloid DCs and plasmacytoid DCs. D6 surface expression on these cells was detected by an anti-human D6 antibody and expression levels are represented as mean fluorescent intensity (MFI). Control n=6, RA n=9, column is mean  $\pm$  SEM.

Due to the apparent contradiction in these data, it was decided to reanalyse the QPCR data to try to find a possible explanation. Upon doing so, it was seen that the housekeeping gene, GAPDH, was significantly higher in peripheral blood of RA patients compared to healthy controls (Figure 5-22). Housekeeping genes are used to normalise sample cDNA levels to allow comparison of gene levels between samples. Having significantly higher levels of housekeeping gene within a sample group would skew the data because this would result in the transcript levels of D6 in the RA samples to be calculated lower than they actually are. This suggests that GAPDH is not the most suitable housekeeping gene to use in order to normalise the data, as an ideal housekeeping gene should be expressed at a constant level between control and test sample. There is evidence that GAPDH transcript levels can vary in nucleated blood cells between individuals (Bustin et al., 1999) as well as in whole blood from healthy and in pulmonary tuberculosis samples (Dheda et al., 2004). To correct for this, it would be more suitable to use a housekeeping gene that does not significantly change between peripheral blood of RA patients and control samples.

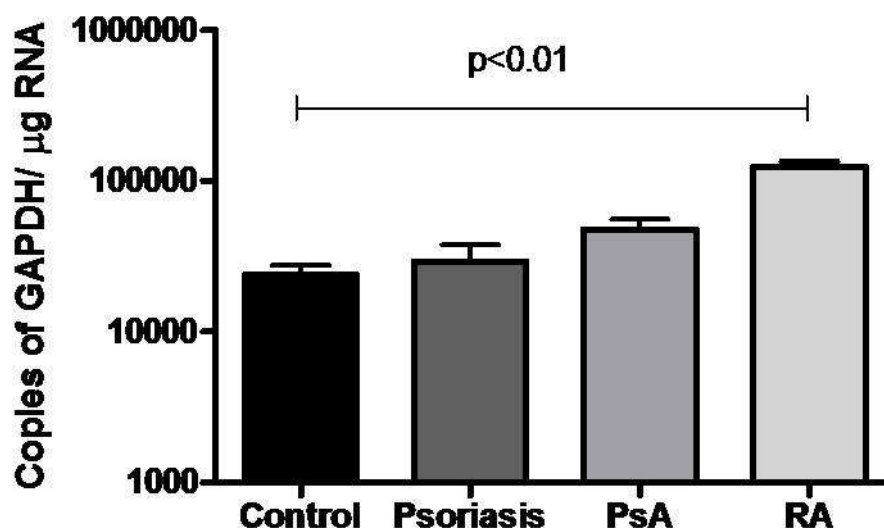


Figure 5-22 Copy numbers of GAPDH in control, psoriatic arthritis (PsA), rheumatoid arthritis (RA) and psoriasis patients.

RNA was extracted from peripheral blood cells converted to cDNA and diluted with nuclease free water. Levels of GAPDH transcripts were assessed by QPCR using SYBR Green. Control n=12, Psoriatic arthritis n=15, RA n=15 and psoriasis n=12. Columns are mean  $\pm$  SEM,

## 5.7 Summary of Chapter 5

In a cutaneous model of inflammation, absence of D6 results an exaggerated inflammatory response resulting in pathology similar to human psoriasis (Jamieson et al., 2005). This led to the hypothesis that D6 dysfunction may play a role in the pathogenesis of human psoriasis. To examine this possibility, the aim of the work within this chapter was to examine the expression of D6 within human psoriasis and other inflammatory diseases.

Analysis of skin biopsies from psoriatic (uninvolved and lesional samples) as well as control and atopic dermatitis samples revealed that D6 transcript expression was increased in psoriatic uninvolved skin. This suggests that D6 is dysfunctional within psoriatic patients in that D6 expression may be upregulated in uninvolved skin to limit skin inflammation. Anti-human D6 antibody was tested for use with psoriatic skin however obtaining good skin sections from these biopsies was difficult and results suggest that the antibody may not be ideal to use on skin by immunohistochemistry. Examination of D6 transcripts within peripheral blood revealed a non-significant 2.3 fold increase in D6 transcripts within psoriatic blood, no change in psoriatic arthritis blood and a 2 fold decrease in RA blood compared to control. However, it was discovered that GAPDH may not be a suitable housekeeping gene for peripheral blood from RA patients and that the 2-fold decrease in transcript levels was a false result. This was confirmed by the analysis of D6 expression on isolated cells from RA blood indicating that in fact B cells and mDCs expressed significantly higher levels of surface D6 in comparison to healthy control.

To conclude, the work within this chapter suggests that more studies are required to determine the correlation between D6 and inflammatory diseases especially regarding the mechanisms underlying the dysregulation of D6 in uninvolved skin of psoriasis patients.

**Chapter 6**

**General Discussion**

## 6 General Discussion

Inflammation is the body's response to internal or external insults such as tissue injury or infection (Medzhitov, 2008). Chemokines are key players in the inflammatory process by controlling the migration of leukocytes into tissues (Charo and Ransohoff, 2006). In particular, pro-inflammatory CC chemokines are involved, which signal through chemokine receptors present on various leukocytes (Murphy et al., 2000). A controlled inflammatory response results in the tissue returning to its normal physiological state and is beneficial to the body (Serhan et al., 2007). When inflammation becomes dysregulated, this can be detrimental as demonstrated by chronic inflammatory diseases. Although the initiation and maintenance of inflammatory processes is well understood, the mechanisms responsible for the resolution of inflammation are only just beginning to emerge.

D6 is an atypical chemokine receptor, which has the ability to bind inflammatory CC chemokines (Graham, 2009). D6 does not seem to signal (Graham, 2009) but studies suggest that D6 sequesters CC chemokines by constitutively moving to and from the cell surface in a ligand independent manner (Weber et al., 2004). Evidence has shown that D6 is a key mediator in the resolution of inflammation. D6 null mice display enhanced skin inflammation in response to TPA and complete Freund's adjuvant (Martinez de la Torre et al., 2005, Jamieson et al., 2005). Additionally, D6 null mice are susceptible to inflammation dependent tumour development (Nibbs et al., 2007). During skin inflammation, D6 has been shown to be involved in the clearance of CC chemokines at the site of inflammation (Jamieson et al., 2005). D6 null mice displayed enhanced recruitment of leukocytes to the lung after allergen exposure (Whitehead et al., 2007) and infection with *Mycobacterium tuberculosis* leads to enhanced local and systemic inflammation with increased CC chemokines and leukocyte infiltration (Di Liberto et al., 2008). In inflammation induced miscarriage models using LPS or anti-phospholipid antibodies, enhanced susceptibility to miscarriage occurs in D6 null mice and is associated with enhanced chemokines and leukocyte infiltration in the placenta (Martinez de la Torre et al., 2007). D6 has been implicated in the development of experimental colitis and is thought to regulate the production of IL-17A by  $\gamma\delta$  T cells in the later stages of the disease (Bordon et al., 2009).

Evidence indicated that D6 was involved in controlling cutaneous inflammation therefore, we hypothesised that increased expression of D6, using a transgenic approach, should be able to suppress cutaneous inflammation *in vivo*. To test this, transgenic mice were generated, in which the expression of D6 was targeted to epidermal keratinocytes. Validation studies confirmed ectopic expression of D6 in the epidermis and in keratinocytes from K14D6 mice, whilst D6 transcripts were absent from wild-type epidermis. In addition, D6 expressed from the transgene in K14D6 keratinocytes was functional, as demonstrated by the ability of K14D6 keratinocytes to bind CCL2 and progressively remove extracellular CCL3, both D6 ligands, in a D6 dependent manner. It is of note that only 45% of K14D6 keratinocytes were able to bind CCL2. These primary keratinocytes were isolated and cultured in keratinocytes growth media containing low concentrations of calcium and no fetal calf serum. As a result, culture of these keratinocytes should generate a homogenous population, which would proliferate but not differentiate due to the low concentration of calcium (Hennings et al., 1980). An explanation as to why only 45% keratinocytes were able to bind CCL2 is that the majority of D6 expression is inside the cell (Blackburn et al., 2004) and keratinocytes expressing low levels of surface D6 were not identified i.e. these cells were not able to bind high levels of CCL2. Retrospectively, it may have been of interest to confirm that D6 positive keratinocytes were keratin 14 expressing cells.

Having characterised the K14D6 transgenic mice, we examined whether ectopic expression of D6 within the skin was able to dampen down inflammation. We used a well-characterised model of skin inflammation previously used by colleagues, which involved application of TPA to murine dorsal skin once a day for three consecutive days (Jamieson et al., 2005). Work presented here shows that D6 null mice demonstrated an exaggerated cutaneous inflammatory response and wild-type mice had increased skin thickness four days after the last application of TPA compared to resting thickness. This was consistent with previous findings in a different strain of mice (Jamieson et al., 2005). K14D6 mice displayed no significant difference in skin thickness four days after the final application of TPA compared to resting skin thickness. In addition, the numbers of mast cells and epidermal T cells were reduced in inflamed K14D6 skin compared to inflamed wild-type skin. Within the skin, D6 is involved in regulating the levels of CC chemokines (Jamieson et al., 2005) and therefore the

most likely explanation is that by increasing D6 levels in K14D6 mice, lower levels of CC chemokines were present than in wild-type skin. As a result, this directly affected the recruitment of mast cells and T cells into the skin and subsequent inflammation.

In the epidermis, keratinocytes and Langerhans cells are rich sources of various chemokines, which can drain into the dermis. Following TPA stimulation, keratinocytes produce CCL3 and CCL5 (personal communication, Prof. G.Graham). Murine mast cells express CCR1, CCR2, CCR3 and CCR5 (Ma et al., 2002, Oliveira and Lukacs, 2001), which are all capable of supporting migration towards ligands which also bind to D6. Human mast cells also express a range of chemokine receptors. One of these is CCR3 (de Paulis et al., 2001) which is able to support migration towards CCL11 and CCL5 in the skin (Romagnani et al., 1999), both of which are D6 ligands. Activated T cells express various chemokine receptors (Bonecchi et al., 1998) including CCR4, which is implicated in the homing of T cells into inflamed skin (Reiss et al., 2001). In addition, activated T cells recruited into the skin during inflammation may release CXCL12 which influences the migration of mast cells (Brill et al., 2004), through the presence of CXCR4 on mast cells (Oliveira and Lukacs, 2001). Therefore, it is feasible that a reduction in mast cells and T cells recruited into the skin was due to a lower abundance of CC chemokines.

D6 may not just have an impact on the level of chemokines but also indirectly affect nearby leukocytes. In turn, this may affect the function and recruitment of leukocytes into the skin. Degranulation of mast cells can be mediated by chemokines, such as CCL3 binding to CCR1 (Miyazaki et al., 2005). One possibility is that D6 may affect degranulation of mast cells by scavenging CCL3 resulting in a reduction of the levels of histamine secreted from mast cells. Histamine mediates vasodilatation and is required for leukocyte infiltration into tissues.

The ability of K14D6 mice to dampen down cutaneous inflammation suggests that D6 has the potential to be therapeutic. By generating K14D6 transgenic mice, we have used a prophylactic approach. Therefore, the therapeutic ability of D6 remains to be examined. To assess this, one approach would be to induce and establish skin inflammation in the D6 null mice and assess whether D6 can

rescue the phenotype of the D6 null mice, i.e. dampen down the exaggerated skin inflammation. This could be tested using a 'gene gun', also known as particle mediated gene delivery (Yang et al., 2001). This method involves gold particles coated with plasmid DNA and directly delivered at high speed into the target tissue. In D6 null mice, skin inflammation would be initiated using the TPA induced inflammation model and then D6 would be expressed in the skin of the D6 null mice using the gene gun. The type of promoter used within the plasmid would determine the location of transgene expression. For example, using a CMV promoter, genes are expressed in the epidermis and dermis of the skin whereas when using a K14 promoter, genes are only expressed in the epidermis (Lin et al., 2001a). The gene gun technology has been used to deliver cytokines *in vivo* (Sun et al., 1995) and studies using IL-23 and IL-18 cDNA delivered by the gene gun have been shown to have anti-tumour effects in the skin (Wang et al., 2004b).

If D6 was indeed therapeutic, it may be useful in a variety of inflammatory diseases. In particular, pathologies involving CC chemokines could be targeted with D6. These include psoriasis, atopic dermatitis, rheumatoid arthritis, asthma, inflammatory bowel disease (as reviewed by D'Ambrosio et al., 2003). CC chemokines have also been implicated in atherosclerosis (Sheikine and Hansson, 2004) and transplantation (Colvin and Thomson, 2002)

In order to use D6 as a therapeutic agent against these diseases, development of additional methods to deliver D6 would be required. This could involve the use of viral delivery systems. Viral vectors are modified where their own viral genes are replaced with a gene of choice. The most common types of viruses used as vectors for gene therapy are retroviruses, adenoviruses and adeno-associated viruses, all with different properties and length of time in which the transgene is expressed. There is evidence that CC chemokines can be targeted using viral based gene therapy in a murine model of atherosclerosis. A chemokine binding protein derived from *Vaccinia* virus can block chemokine activity (Alcami et al., 1998) and gene therapy using an adenoviral mediated delivery system blocked CC chemokines (Bursill et al., 2006), inhibited recruitment of macrophages and reduced atherosclerotic plaque formation *in vivo* (Bursill et al., 2004). As adenoviral gene therapy results in short-term transgene expression, the viral chemokine binding protein has also been transferred using lentivirus

demonstrating that long-term inhibition of CC chemokines resulted in reduction of atherosclerotic plaques (Bursill et al., 2009). Alternative methods of gene delivery, which are non-viral, have also been developed. Non-viral methods include the use of naked plasmid DNA and synthetic vectors (Li and Huang, 2000). So far, although these non-viral methods are thought to be safer, the transfection efficiency of non-viral therapy is lower than viral delivery methods. Another approach altogether would be to use peptides, based on a short linear sequence from D6. Peptides have been derived based on the sequences of chemokine receptors. One example is the synthesis of a peptide using a short N-terminal fragment of CCR5 sequence (Chain et al., 2008). The peptide was used to generate antibodies which would be specific for CCR5 to reduce HIV infectivity (Chain et al., 2008). CCR3 is another receptor where peptides were synthesised based on the N-terminus of the receptor to characterise the binding properties between CCR3 and CCL11 (Ye et al., 2000). The development of the best delivery method for D6 may depend on the type of disease, where D6 is to be targeted and whether expression of the transgene is only required for short-term or longer.

*In vitro* studies suggest that D6 does not seem to have the ability to signal (Fra et al., 2003) however, D6 may signal via other mechanisms that do not elicit a calcium flux response. We have begun to examine this by isolating murine keratinocytes that express D6 ectopically at high levels and to determine the transcriptional consequences of ligand binding using microarray technology. Keratinocytes are capable of producing chemokines such as CCL5 and CCL2 upon stimulation with IFN- $\gamma$  or TNF- $\alpha$  (Li et al., 1996), which contribute to recruiting leukocytes into the skin during inflammation. Therefore, D6 may have had an impact on cellular transcription within these cells or scavenged the chemokines produced from it.

By analysing individual differential gene expression using rank products (Breitling et al., 2004b), one conclusion can be made from our microarray experiment. D6 was expressed at higher levels in K14D6 keratinocytes compared to wild-type. This was an expected result. By analysing groups of functional gene classes, our results from the microarray suggests that non-ligated D6 may have an impact on the transcription of some genes, in particular, chemokines. Although we do not provide firm evidence of this, it would be intriguing to examine whether D6's

ability to reduce the levels of CC chemokines, also regulates the transcription of these genes. It is of note that as a functional gene class, chemokines were downregulated in keratinocytes in the presence of non-ligated D6 (using iGA analysis) particularly CXCL4, CCL6 and CCL9. CXCL4 is involved in the migration of T lymphocytes mediated by CXCR3B, a splice variant of CXCR3 (Lasagni et al., 2003, Mueller et al., 2008). CCL6 and CCL9 are chemokines which to date have only been found in rodents, both which are able to bind to CCR1 (Lean et al., 2002, Ma et al., 2004). It is interesting to note that CCL6 and CCL9 both contain an extended N-terminal domain. Whilst there are no direct human homologues of CCL6 and CCL9, two chemokines CCL15 and CCL23 also contain extended N-termini and have only been found in humans (Berger et al., 1993, Youn et al., 1998). Studies have shown that all four can be truncated by proteases at their N-termini, which increases their signalling and chemotaxis ability through CCR1 (Berahovich et al., 2005). In addition, N-terminal truncated CCL15 and CCL23 are detected at high levels in synovial fluid from rheumatoid arthritis patients (Berahovich et al., 2005). One possibility may be that D6 inhibits the transcription of these genes, although the mechanisms are unclear, to prevent their release and limit the levels of potential potent chemoattractants during the inflammatory response. It may be that D6 it is unable to scavenge these chemokines once they are cleaved by proteases during inflammation. Evidence has shown that D6 is not able to scavenge a truncated form of CCL22 (Bonecchi et al., 2004) although it is of note that neither human nor murine D6 has been shown to bind CCL6, CCL9, CCL15 or CCL23. However, by inhibiting the transcription of genes for CCL6, CCL9 and CXCL4, D6 may indirectly affect the recruitment of cells into the tissue.

Other studies have examined the downstream consequences induced by CCL5 in human monocytes (Locati et al., 2002). CCL5 induced the upregulation of genes but did not suppress the transcription of any genes. CCL5 induced gene expression of several chemokines including CCL2, CCL3, CCL4 and CXCL8 as well as CCR1 and induced expression of molecules involved in matrix degradation, potentially amplifying leukocyte recruitment (Locati et al., 2002). Additionally, gene transcripts induced by CCL5 binding to CCR5 in human neuronal cells has also been examined. Upregulated genes induced by CCL5 included those involved in cell signalling and CCL5 in this context induced the downregulation of several

genes (Valerio et al., 2004). Therefore, depending on the cell type and the environment, chemokines can induce different transcriptional responses.

The microarray data generated in this study used primary cells that did not normally express D6. Human lymphatic endothelial cells express D6 (Nibbs et al., 2001, Vetrano et al., 2009) however D6 expression is lost when lymphatic endothelial cells have been cultured (Amatschek et al., 2007). It would be more suitable to use primary cells that express D6. In keeping with this consideration, leukocytes and murine B cells derived from the spleen have been found to express D6 (McKimmie et al., 2008) and in a separate study, expression of D6 on splenic B cells was located in marginal zone B cells (Kin et al., 2008). Although what role D6 has on B cells remains to be determined.

Studies performed in our lab illustrated that D6 was important in regulating the resolution of inflammation (Jamieson et al., 2005). Jamieson *et al.*, demonstrated that D6 null mice had enhanced levels of CC chemokines within the skin, which resulted in a psoriasis-like pathology. We decided to determine whether there was any association between D6 levels and human psoriasis. We obtained skin biopsies from control, psoriatic and atopic dermatitis patients. In some psoriatic patients, we obtained lesional and uninvolved skin from the same patient. Within this study, examination of D6 transcript levels revealed that there was no significant difference in D6 transcripts between atopic dermatitis, lesional psoriatic skin and control skin. Interestingly, D6 expression in psoriatic uninvolved skin was 8-fold higher than control and psoriatic lesional skin. Analysis of individual psoriatic patients, where we had matching uninvolved and lesional skin, revealed that 9 out of the 10 patients had increased expression of D6 mRNA in their uninvolved skin compared to their lesional skin. These data suggest that D6 expression is dysregulated in psoriatic uninvolved skin. These data were obtained from matched samples in psoriatic patients and therefore are internally controlled, further strengthening the evidence of the dysregulation of D6 expression in psoriatic uninvolved skin.

This led us to hypothesise that D6 is upregulated in uninvolved skin of psoriatic patients in order to suppress ongoing inflammation in the area. Gene expression profiles have revealed that there are differences between psoriatic lesional and uninvolved skin as well as psoriatic uninvolved and healthy skin (Itoh et al.,

2005, Zhou et al., 2003). Differences have also been shown in cytokines levels such as TNF- $\alpha$  and IL-1 $\beta$  (Uyemura et al., 1993) and expression levels of CXCL8 and CCL5 higher in uninvolved skin than normal skin have been shown as well as increased mRNA expression of IL-17 and IFN- $\gamma$  (Lowe et al., 2008). In addition, psoriatic lesional skin has increased transcript levels of IL-17A, IL-17F, IL-22 and IL-26, all Th17 derived cytokines, compared to normal skin (Wilson et al., 2007). Keratinocyte treatment with IL-22 and IL-17 resulted in upregulation of antimicrobial peptides such as  $\beta$ -defensins (Liang et al., 2006) suggesting a protective role for these cytokines in the skin. Indeed psoriatic lesions contain higher levels of antimicrobial peptides than normal skin (Harder and Schroder, 2005). However, in addition to anti-microbial properties,  $\beta$ -defensins can also bind CCR6 (Yang et al., 1999) and attract CCR6<sup>+</sup> T cells, such as Th17 cells into the skin. Additionally, Th17 cytokines can also stimulate CCL20 from keratinocytes (Harper et al., 2009) which can also bind CCR6, in turn this recruits more CCR6<sup>+</sup> Th17 cells into the skin and contributes to skin pathology. Subcutaneous injection of IL-23, a cytokine which enhances the proliferation of Th17 cells (Aggarwal et al., 2003), induced a psoriasis-like pathology *in vivo* (Chan et al., 2006) and IL-22 is a downstream mediator in this process (Zheng et al., 2007). IL-15 secretion can induce IL-17 (McInnes and Gracie, 2004) and has been implicated in psoriasis. Indeed, the use of anti-IL-15 antibodies *in vivo* resulted in resolution of psoriatic lesions (Villadsen et al., 2003). It is of note that the pathology displayed in D6 null mice after induction of inflammation by a chemical stimulant was dependent on IL-15 and IL-17 (personal communication Prof. G. Graham) therefore further confirming its similarity to human psoriasis. The presence of inflammatory cytokines and chemokines present within the uninvolved skin of psoriatic patients suggests the presence of ongoing low-level inflammation. As a result, D6 may be enhanced in uninvolved psoriatic skin to prevent a psoriatic lesion occurring. This then raises the question of how psoriatic lesions occur in these individuals, i.e. if D6 prevents psoriatic lesions in some areas, why does D6 not work in all areas. One possibility is that there is low-level ongoing inflammation in the psoriatic skin and lesions form when a reduction in the expression level of D6 occurs. D6 can be dynamically regulated, McKimmie *et al.*, have shown that LPS can downregulate D6 expression (McKimmie et al., 2008). Others have also shown that inflammatory mediators can upregulate D6 in a breast cancer cell line (Wu et al., 2008). This suggests the possibility that in the skin of psoriatic patients, an infection or trauma may

result in the downregulation of D6 levels and, in turn, a psoriatic lesion may erupt. A recent study revealed that D6 regulates the levels of IL-17 production by  $\gamma\delta$  T cells in the later stages of colitis (Bordon et al., 2009) therefore it may be possible that the lack of D6 in the skin may lead to the dysregulation of the IL-17 levels in the skin and contribute to the pathology of psoriasis.

Having examined the mRNA expression of D6 within psoriatic skin, we went on to examine the expression of the D6 protein within the skin. Previous studies revealed D6 protein to be expressed on lymphatic endothelial cells within the skin (Nibbs et al., 2001) and others have shown D6 expression on leukocytes within atopic dermatitis skin (McKimmie et al., 2008). In this study, the clone of antibody used is an alternative clone to that used previously to reveal D6 staining on lymphatic endothelial cells (Nibbs et al., 2001). The clone used in this study has been validated using HEK293 cells stably transfected with human D6 and detected by western blotting and flow cytometry (McCulloch et al., 2008). For use in immunohistochemistry, anti-human D6 staining was optimised using placental sections as a positive control and on control skin sections. Staining of control skin sections revealed positive D6 staining on leukocytes however, lymphatic endothelial vessels did not stain positive for D6. An explanation for this may be the use of different clones of antibody. One clone of antibody was specific for D6 expressed on lymphatic endothelial cells (Nibbs et al., 2001) whilst the other seems to be specific for D6 on leukocytes (McKimmie et al., 2008). This suggests that the different clones of the anti-human D6 antibodies have slightly altered specificities and bind different D6 epitopes on lymphatic endothelial cells and leukocytes. Different epitopes of D6 may occur because the N-terminus of D6 is glycosylated and also contains tyrosine residues which are sulphated (Blackburn et al., 2004). Therefore, the antibody used in this study may be specific for one epitope revealed on leukocytes for which the other antibody has lower affinity. Different antibody specificities using different clones of antibodies have also been demonstrated for another atypical chemokine receptor, DARC (Chaudhuri et al., 1997, Nielsen et al., 1997). It would be interesting to determine the location and number of leukocytes expressing D6 in psoriatic skin, including uninvolved and lesional skin biopsies, compared to control skin. To determine the specific leukocyte subset expressing D6, sections could be co-stained using antibodies specific for each subset of leukocytes. This would identify the leukocytes involved in the enhanced D6

expression in uninvolved psoriatic skin. The level of D6 protein expression by individual subsets of leukocytes could be determined by flow cytometry.

With enhanced D6 expression in uninvolved skin of psoriatic patients compared to controls, we decided to examine peripheral blood to determine if enhanced expression within the skin was a general phenomenon or only located within the skin in psoriatic patients. We also extended the study into other inflammatory diseases such as PsA and RA and examined D6 expression within these diseases. Peripheral blood mononuclear cells (PBMCs) from psoriasis patients displayed a non-significant 2.3-fold increase in D6 mRNA expression over normal PBMCs whereas PsA PBMCs showed no significant change in mRNA expression and RA PBMCs showed a significant 2-fold decrease. However, GAPDH levels in PBMCs from RA patients were increased compared to control peripheral blood mononuclear cells. Retrospectively, the housekeeping gene, GAPDH was not a suitable choice for a housekeeping gene for RA patients. In addition, there is evidence that GAPDH varies in nucleated blood cells between individuals (Bustin et al., 1999) and in peripheral blood cells from tuberculosis patients (Dheda et al., 2004). Subsequently, since completion of this work, a colleague has continued the research into psoriasis. The QPCR of peripheral blood from psoriasis patients has been repeated using TATA binding protein as the housekeeping gene and with increased sample size. In doing so, PBMCs from psoriatic patients displayed a 10-fold increase in D6 mRNA expression compared to controls, which correlates with the enhanced D6 expression observed in psoriatic uninvolved skin. Further work is required to determine whether enhanced expression of D6 in psoriatic peripheral blood is restricted to a distinct subset of leukocytes.

As mentioned above, before we had determined the problematic issue regarding GAPDH in this context, we had observed a 2-fold decrease in D6 transcripts within peripheral blood of RA patients. We resolved to examine surface D6 expression on specific leukocytes within peripheral blood to determine which cell types were expressing D6. Examination of D6 expression on specific subsets of leukocytes by flow cytometry revealed that expression of D6 was highest on B cells and dendritic cells. The trends in D6 expression on leukocyte subsets within control peripheral blood correlated with previous findings (McKimmie et al., 2008). Surface expression of D6 on B cells and mDCs from RA patients was

significantly increased on these cells compared to control B cells and mDCs. This data contradicted the QPCR data, which suggested that D6 transcripts in peripheral blood of RA patients were 2-fold lower than control peripheral blood. Retrospectively, it may have been useful to examine D6 transcript expression in each of the subpopulations of leukocytes from the same samples in which D6 protein expression was analysed.

All leukocytes analysed by flow cytometry revealed that D6 expression was increased on all cells in RA peripheral blood but this was only significantly different in B cells and mDCs compared to control. One reason for this enhanced D6 expression may be that RA can be considered a systemic inflammatory disease (with increased inflammatory mediators in the blood). Many chemokines and their receptors are implicated in the pathology of RA (Szekanecz et al., 2003). Within the blood, there are increased levels of inflammatory mediators and chemokines. Increased levels of CCR1 and CCR5 on RA peripheral blood monocytes and increased levels of CCL5 and CCL15 have also been reported in rheumatoid arthritis peripheral blood compared to controls (Haringman et al., 2006). An inflammatory environment surrounds PBMCs and it is possible that D6 is upregulated in the peripheral blood of RA patients to try to counteract the systemic inflammation. It would be interesting to correlate the expression of D6 on leukocytes from RA patients with the circulating levels of chemokines within their blood. This could be analysed by collecting peripheral blood from RA patients and using half to isolate PBMCs to examine surface D6 expression by flow cytometry and from the other half, plasma would be extracted to examine the levels of multiple chemokine at the same time. The chemokines and cytokines would be analysed using Luminex technology. In addition, as mentioned, a significant increase in D6 protein expression was observed in B cells and mDCs in RA patients compared to controls. Both these cells are involved in the adaptive response and play a role in antigen presentation. Therefore, D6 may be involved in the adaptive immune response. A recent study has revealed D6 expression on leukocytes within human rheumatoid synovium suggesting that D6 is involved in the pathogenesis of rheumatoid arthritis (McKimmie et al., 2008). The exact role of D6 in human or murine models of arthritis has not yet been determined.

Inflammation is an important mechanism within the body. However, there are many diseases driven by chronic inflammation, which are detrimental to our body. The work presented here shows that increased expression of D6 can suppress cutaneous inflammation *in vivo*; therefore, D6 has the potential to be of therapeutic value. Our microarray studies have indicated that non-ligated D6 may have a negative impact on the transcription of certain genes. Further work using a primary cell that naturally expresses D6 is required to determine the transcriptional response of cells to D6 after ligand binding. Additionally, this study shows evidence to suggest that D6 is dysregulated in inflammatory diseases suggesting D6 is involved in the pathogenesis of these inflammatory diseases.

## References

- ABBAS, A. K., MURPHY, K. M. & SHER, A. (1996) Functional diversity of helper T lymphocytes. *Nature*, 383, 787-93.
- ADAMS, G. B. & SCADDEN, D. T. (2006) The hematopoietic stem cell in its place. *Nat Immunol*, 7, 333-7.
- ADDISON, C. L., DANIEL, T. O., BURDICK, M. D., LIU, H., EHLERT, J. E., XUE, Y. Y., BUECHI, L., WALZ, A., RICHMOND, A. & STRIETER, R. M. (2000) The CXC chemokine receptor 2, CXCR2, is the putative receptor for ELR+ CXC chemokine-induced angiogenic activity. *J Immunol*, 165, 5269-77.
- ADRA, C. N., ZHU, S., KO, J. L., GUILLEMOT, J. C., CUERVO, A. M., KOBAYASHI, H., HORIUCHI, T., LELIAS, J. M., ROWLEY, J. D. & LIM, B. (1996) LAPT5: a novel lysosomal-associated multispansing membrane protein preferentially expressed in hematopoietic cells. *Genomics*, 35, 328-37.
- AFKARIAN, M., SEDY, J. R., YANG, J., JACOBSON, N. G., CEREB, N., YANG, S. Y., MURPHY, T. L. & MURPHY, K. M. (2002) T-bet is a STAT1-induced regulator of IL-12R expression in naive CD4+ T cells. *Nat Immunol*, 3, 549-57.
- AGGARWAL, S., GHILARDI, N., XIE, M. H., DE SAUVAGE, F. J. & GURNEY, A. L. (2003) Interleukin-23 promotes a distinct CD4 T cell activation state characterized by the production of interleukin-17. *J Biol Chem*, 278, 1910-4.
- AKINBI, H. T., EPAUD, R., BHATT, H. & WEAVER, T. E. (2000) Bacterial killing is enhanced by expression of lysozyme in the lungs of transgenic mice. *J Immunol*, 165, 5760-6.
- AKIRA, S., UEMATSU, S. & TAKEUCHI, O. (2006) Pathogen recognition and innate immunity. *Cell*, 124, 783-801.
- ALCAMI, A., SYMONS, J. A., COLLINS, P. D., WILLIAMS, T. J. & SMITH, G. L. (1998) Blockade of chemokine activity by a soluble chemokine binding protein from vaccinia virus. *J Immunol*, 160, 624-33.
- ALEXOPOULOU, L., HOLT, A. C., MEDZHITOV, R. & FLAVELL, R. A. (2001) Recognition of double-stranded RNA and activation of NF-kappaB by Toll-like receptor 3. *Nature*, 413, 732-8.
- ALIBERTI, J., HIENY, S., REIS E SOUSA, C., SERHAN, C. N. & SHER, A. (2002) Lipoxin-mediated inhibition of IL-12 production by DCs: a mechanism for regulation of microbial immunity. *Nat Immunol*, 3, 76-82.
- ALLEN, L. A. & ADEREM, A. (1996) Mechanisms of phagocytosis. *Curr Opin Immunol*, 8, 36-40.
- AMATSCHEK, S., KRIEHLER, E., BAUER, W., REININGER, B., MERANER, P., WOLPL, A., SCHWEIFER, N., HASLINGER, C., STINGL, G. & MAURER, D. (2007) Blood and lymphatic endothelial cell-specific differentiation programs are stringently controlled by the tissue environment. *Blood*, 109, 4777-85.
- ANDREJEVA, J., CHILDS, K. S., YOUNG, D. F., CARLOS, T. S., STOCK, N., GOODBOURN, S. & RANDALL, R. E. (2004) The V proteins of paramyxoviruses bind the IFN-inducible RNA helicase, mda-5, and inhibit

- its activation of the IFN-beta promoter. *Proc Natl Acad Sci U S A*, 101, 17264-9.
- ANGIOLILLO, A. L., SGADARI, C., TAUB, D. D., LIAO, F., FARBER, J. M., MAHESHWARI, S., KLEINMAN, H. K., REAMAN, G. H. & TOSATO, G. (1995) Human interferon-inducible protein 10 is a potent inhibitor of angiogenesis in vivo. *J Exp Med*, 182, 155-62.
- ARENBERG, D. A., KUNKEL, S. L., POLVERINI, P. J., MORRIS, S. B., BURDICK, M. D., GLASS, M. C., TAUB, D. T., IANNETTONI, M. D., WHYTE, R. I. & STRIETER, R. M. (1996) Interferon-gamma-inducible protein 10 (IP-10) is an angiostatic factor that inhibits human non-small cell lung cancer (NSCLC) tumorigenesis and spontaneous metastases. *J Exp Med*, 184, 981-92.
- AREND, W. P. (1991) Interleukin 1 receptor antagonist. A new member of the interleukin 1 family. *J Clin Invest*, 88, 1445-51.
- ARIEL, A., LI, P. L., WANG, W., TANG, W. X., FREDMAN, G., HONG, S., GOTLINGER, K. H. & SERHAN, C. N. (2005) The docosatriene protectin D1 is produced by TH2 skewing and promotes human T cell apoptosis via lipid raft clustering. *J Biol Chem*, 280, 43079-86.
- ARINOBU, Y., MIZUNO, S., CHONG, Y., SHIGEMATSU, H., IINO, T., IWASAKI, H., GRAF, T., MAYFIELD, R., CHAN, S., KASTNER, P. & AKASHI, K. (2007) Reciprocal activation of GATA-1 and PU.1 marks initial specification of hematopoietic stem cells into myeloerythroid and myelolymphoid lineages. *Cell Stem Cell*, 1, 416-27.
- ARITA, M., BIANCHINI, F., ALIBERTI, J., SHER, A., CHIANG, N., HONG, S., YANG, R., PETASIS, N. A. & SERHAN, C. N. (2005) Stereochemical assignment, antiinflammatory properties, and receptor for the omega-3 lipid mediator resolvin E1. *J Exp Med*, 201, 713-22.
- ASAHARA, T., MUROHARA, T., SULLIVAN, A., SILVER, M., VAN DER ZEE, R., LI, T., WITZENBICHLER, B., SCHATTEMAN, G. & ISNER, J. M. (1997) Isolation of putative progenitor endothelial cells for angiogenesis. *Science*, 275, 964-7.
- ASARNOW, D. M., KUZIEL, W. A., BONYHADI, M., TIGELAAR, R. E., TUCKER, P. W. & ALLISON, J. P. (1988) Limited diversity of gamma delta antigen receptor genes of Thy-1+ dendritic epidermal cells. *Cell*, 55, 837-47.
- AURRAND-LIONS, M., LAMAGNA, C., DANGERFIELD, J. P., WANG, S., HERRERA, P., NOURSHARGH, S. & IMHOF, B. A. (2005) Junctional adhesion molecule-C regulates the early influx of leukocytes into tissues during inflammation. *J Immunol*, 174, 6406-15.
- AUSTIN, L. M., OZAWA, M., KIKUCHI, T., WALTERS, I. B. & KRUEGER, J. G. (1999) The majority of epidermal T cells in Psoriasis vulgaris lesions can produce type 1 cytokines, interferon-gamma, interleukin-2, and tumor necrosis factor-alpha, defining TC1 (cytotoxic T lymphocyte) and TH1 effector populations: a type 1 differentiation bias is also measured in circulating blood T cells in psoriatic patients. *J Invest Dermatol*, 113, 752-9.
- AYABE, T., SATCHELL, D. P., WILSON, C. L., PARKS, W. C., SELSTED, M. E. & OUELLETTE, A. J. (2000) Secretion of microbicidal alpha-defensins by intestinal Paneth cells in response to bacteria. *Nat Immunol*, 1, 113-8.

- BABA, M., IMAI, T., NISHIMURA, M., KAKIZAKI, M., TAKAGI, S., HIESHIMA, K., NOMIYAMA, H. & YOSHIE, O. (1997) Identification of CCR6, the specific receptor for a novel lymphocyte-directed CC chemokine LARC. *J Biol Chem*, 272, 14893-8.
- BAEKKEVOLD, E. S., YAMANAKA, T., PALFRAMAN, R. T., CARLSEN, H. S., REINHOLT, F. P., VON ANDRIAN, U. H., BRANDTZAEG, P. & HARALDSEN, G. (2001) The CCR7 ligand elc (CCL19) is transcytosed in high endothelial venules and mediates T cell recruitment. *J Exp Med*, 193, 1105-12.
- BALABANIAN, K., LAGANE, B., INFANTINO, S., CHOW, K. Y., HARRIAGUE, J., MOEPPS, B., ARENZANA-SEISDEDOS, F., THELEN, M. & BACHELERIE, F. (2005) The chemokine SDF-1/CXCL12 binds to and signals through the orphan receptor RDC1 in T lymphocytes. *J Biol Chem*, 280, 35760-6.
- BALKWILL, F. (2003) Chemokine biology in cancer. *Semin Immunol*, 15, 49-55.
- BALKWILL, F. & MANTOVANI, A. (2001) Inflammation and cancer: back to Virchow? *Lancet*, 357, 539-45.
- BANCHEREAU, J. & STEINMAN, R. M. (1998) Dendritic cells and the control of immunity. *Nature*, 392, 245-52.
- BANDEIRA-MELO, C., BOZZA, P. T. & WELLER, P. F. (2002) The cellular biology of eosinophil eicosanoid formation and function. *J Allergy Clin Immunol*, 109, 393-400.
- BARLIC, J., KHANDAKER, M. H., MAHON, E., ANDREWS, J., DEVRIES, M. E., MITCHELL, G. B., RAHIMPOUR, R., TAN, C. M., FERGUSON, S. S. & KELVIN, D. J. (1999) beta-arrestins regulate interleukin-8-induced CXCR1 internalization. *J Biol Chem*, 274, 16287-94.
- BARNES, D. A., TSE, J., KAUFHOLD, M., OWEN, M., HESSELGESSER, J., STRIETER, R., HORUK, R. & PEREZ, H. D. (1998) Polyclonal antibody directed against human RANTES ameliorates disease in the Lewis rat adjuvant-induced arthritis model. *J Clin Invest*, 101, 2910-9.
- BARR, A. J., ALI, H., HARIBABU, B., SNYDERMAN, R. & SMRCKA, A. V. (2000) Identification of a region at the N-terminus of phospholipase C-beta 3 that interacts with G protein beta gamma subunits. *Biochemistry*, 39, 1800-6.
- BASSING, C. H., SWAT, W. & ALT, F. W. (2002) The mechanism and regulation of chromosomal V(D)J recombination. *Cell*, 109 Suppl, S45-55.
- BAUD, V. & KARIN, M. (2001) Signal transduction by tumor necrosis factor and its relatives. *Trends Cell Biol*, 11, 372-7.
- BAZAN, J. F., BACON, K. B., HARDIMAN, G., WANG, W., SOO, K., ROSSI, D., GREAVES, D. R., ZLOTNIK, A. & SCHALL, T. J. (1997) A new class of membrane-bound chemokine with a CX3C motif. *Nature*, 385, 640-4.
- BAZZONI, G. (2003) The JAM family of junctional adhesion molecules. *Curr Opin Cell Biol*, 15, 525-30.
- BAZZONI, G., MARTINEZ-ESTRADA, O. M., MUELLER, F., NELBOECK, P., SCHMID, G., BARTFAI, T., DEJANA, E. & BROCKHAUS, M. (2000) Homophilic interaction of junctional adhesion molecule. *J Biol Chem*, 275, 30970-6.
- BELLINGAN, G. J., CALDWELL, H., HOWIE, S. E., DRANSFIELD, I. & HASLETT, C. (1996) In vivo fate of the inflammatory macrophage during the resolution

of inflammation: inflammatory macrophages do not die locally, but emigrate to the draining lymph nodes. *J Immunol*, 157, 2577-85.

- BELTRANI, V. S. (1999) The clinical spectrum of atopic dermatitis. *J Allergy Clin Immunol*, 104, S87-98.
- BENNETT, C. L., CHRISTIE, J., RAMSDELL, F., BRUNKOW, M. E., FERGUSON, P. J., WHITESELL, L., KELLY, T. E., SAULSBURY, F. T., CHANCE, P. F. & OCHS, H. D. (2001) The immune dysregulation, polyendocrinopathy, enteropathy, X-linked syndrome (IPEX) is caused by mutations of FOXP3. *Nat Genet*, 27, 20-1.
- BERAHOVICH, R. D., MIAO, Z., WANG, Y., PREMACK, B., HOWARD, M. C. & SCHALL, T. J. (2005) Proteolytic activation of alternative CCR1 ligands in inflammation. *J Immunol*, 174, 7341-51.
- BERGER, E. A., DOMS, R. W., FENYO, E. M., KORBER, B. T., LITTMAN, D. R., MOORE, J. P., SATTENTAU, Q. J., SCHUITEMAKER, H., SODROSKI, J. & WEISS, R. A. (1998) A new classification for HIV-1. *Nature*, 391, 240.
- BERGER, M. S., KOZAK, C. A., GABRIEL, A. & PRYSTOWSKY, M. B. (1993) The gene for C10, a member of the beta-chemokine family, is located on mouse chromosome 11 and contains a novel second exon not found in other chemokines. *DNA Cell Biol*, 12, 839-47.
- BERRES, M. L., TRAUTWEIN, C., ZALDIVAR, M. M., SCHMITZ, P., PAUELS, K., LIRA, S. A., TACKE, F. & WASMUTH, H. E. (2009) The chemokine scavenging receptor D6 limits acute toxic liver injury in vivo. *Biol Chem*, 390, 1039-45.
- BIANCHI, M. E. (2007) DAMPs, PAMPs and alarmins: all we need to know about danger. *J Leukoc Biol*, 81, 1-5.
- BINGLE, L., BROWN, N. J. & LEWIS, C. E. (2002) The role of tumour-associated macrophages in tumour progression: implications for new anticancer therapies. *J Pathol*, 196, 254-65.
- BLACK, A. P., ARDERN-JONES, M. R., KASPROWICZ, V., BOWNESS, P., JONES, L., BAILEY, A. S. & OGG, G. S. (2007) Human keratinocyte induction of rapid effector function in antigen-specific memory CD4<sup>+</sup> and CD8<sup>+</sup> T cells. *Eur J Immunol*, 37, 1485-93.
- BLACK, R. A., RAUCH, C. T., KOZLOSKY, C. J., PESCHON, J. J., SLACK, J. L., WOLFSON, M. F., CASTNER, B. J., STOCKING, K. L., REDDY, P., SRINIVASAN, S., NELSON, N., BOIANI, N., SCHOOLEY, K. A., GERHART, M., DAVIS, R., FITZNER, J. N., JOHNSON, R. S., PAXTON, R. J., MARCH, C. J. & CERRETTI, D. P. (1997) A metalloproteinase disintegrin that releases tumour-necrosis factor-alpha from cells. *Nature*, 385, 729-33.
- BLACKBURN, P. E., SIMPSON, C. V., NIBBS, R. J., O'HARA, M., BOOTH, R., POULOS, J., ISAACS, N. W. & GRAHAM, G. J. (2004) Purification and biochemical characterization of the D6 chemokine receptor. *Biochem J*, 379, 263-72.
- BLANDER, J. M. & MEDZHITOV, R. (2006) Toll-dependent selection of microbial antigens for presentation by dendritic cells. *Nature*, 440, 808-12.
- BLANPAIN, C. & FUCHS, E. (2009) Epidermal homeostasis: a balancing act of stem cells in the skin. *Nat Rev Mol Cell Biol*, 10, 207-17.

- BLANPAIN, C., HORSLEY, V. & FUCHS, E. (2007) Epithelial stem cells: turning over new leaves. *Cell*, 128, 445-58.
- BLASCHKE, S., MIDDEL, P., DORNER, B. G., BLASCHKE, V., HUMMEL, K. M., KROCZEK, R. A., REICH, K., BENOEHR, P., KOZIOLEK, M. & MULLER, G. A. (2003) Expression of activation-induced, T cell-derived, and chemokine-related cytokine/lymphotactin and its functional role in rheumatoid arthritis. *Arthritis Rheum*, 48, 1858-72.
- BLUMBERG, H., DINH, H., TRUEBLOOD, E. S., PRETORIUS, J., KUGLER, D., WENG, N., KANALY, S. T., TOWNE, J. E., WILLIS, C. R., KUECHLE, M. K., SIMS, J. E. & PESCHON, J. J. (2007) Opposing activities of two novel members of the IL-1 ligand family regulate skin inflammation. *J Exp Med*, 204, 2603-14.
- BOE, A., BAIOCCHI, M., CARBONATTO, M., PAPOIAN, R. & SERLUPI-CRESCENZI, O. (1999) Interleukin 6 knock-out mice are resistant to antigen-induced experimental arthritis. *Cytokine*, 11, 1057-64.
- BOEHM, T. & BLEUL, C. C. (2007) The evolutionary history of lymphoid organs. *Nat Immunol*, 8, 131-5.
- BOISMENU, R. & HAVRAN, W. L. (1994) Modulation of epithelial cell growth by intraepithelial gamma delta T cells. *Science*, 266, 1253-5.
- BOISVERT, W. A., CURTISS, L. K. & TERKELTAUB, R. A. (2000) Interleukin-8 and its receptor CXCR2 in atherosclerosis. *Immunol Res*, 21, 129-37.
- BOL, D. K., KIGUCHI, K., GIMENEZ-CONTI, I., RUPP, T. & DIGIOVANNI, J. (1997) Overexpression of insulin-like growth factor-1 induces hyperplasia, dermal abnormalities, and spontaneous tumor formation in transgenic mice. *Oncogene*, 14, 1725-34.
- BOLDAJIPOUR, B., MAHABALESHWAR, H., KARDASH, E., REICHMAN-FRIED, M., BLASER, H., MININA, S., WILSON, D., XU, Q. & RAZ, E. (2008) Control of chemokine-guided cell migration by ligand sequestration. *Cell*, 132, 463-73.
- BONECCHI, R., BIANCHI, G., BORDIGNON, P. P., D'AMBROSIO, D., LANG, R., BORSATTI, A., SOZZANI, S., ALLAVENA, P., GRAY, P. A., MANTOVANI, A. & SINIGAGLIA, F. (1998) Differential expression of chemokine receptors and chemotactic responsiveness of type 1 T helper cells (Th1s) and Th2s. *J Exp Med*, 187, 129-34.
- BONECCHI, R., BORRONI, E. M., ANSELMO, A., DONI, A., SAVINO, B., MIROLO, M., FABBRI, M., JALA, V. R., HARIBABU, B., MANTOVANI, A. & LOCATI, M. (2008) Regulation of D6 chemokine scavenging activity by ligand- and Rab11-dependent surface up-regulation. *Blood*, 112, 493-503.
- BONECCHI, R., LOCATI, M., GALLIERA, E., VULCANO, M., SIRONI, M., FRA, A. M., GOBBI, M., VECCHI, A., SOZZANI, S., HARIBABU, B., VAN DAMME, J. & MANTOVANI, A. (2004) Differential recognition and scavenging of native and truncated macrophage-derived chemokine (macrophage-derived chemokine/CC chemokine ligand 22) by the D6 decoy receptor. *J Immunol*, 172, 4972-6.
- BONIFACE, K., GUIGNOUARD, E., PEDRETTI, N., GARCIA, M., DELWAIL, A., BERNARD, F. X., NAU, F., GUILLET, G., DAGREGORIO, G., YSSEL, H., LECRON, J. C. & MOREL, F. (2007) A role for T cell-derived interleukin 22 in psoriatic skin inflammation. *Clin Exp Immunol*, 150, 407-15.

- BONIZZI, G. & KARIN, M. (2004) The two NF-kappaB activation pathways and their role in innate and adaptive immunity. *Trends Immunol*, 25, 280-8.
- BONNET, D. (2002) Haematopoietic stem cells. *J Pathol*, 197, 430-40.
- BORDON, Y., HANSELL, C. A., SESTER, D. P., CLARKE, M., MOWAT, A. M. & NIBBS, R. J. (2009) The atypical chemokine receptor D6 contributes to the development of experimental colitis. *J Immunol*, 182, 5032-40.
- BORING, L., GOSLING, J., CLEARY, M. & CHARO, I. F. (1998) Decreased lesion formation in CCR2<sup>-/-</sup> mice reveals a role for chemokines in the initiation of atherosclerosis. *Nature*, 394, 894-7.
- BORISH, L. C. & STEINKE, J. W. (2003) 2. Cytokines and chemokines. *J Allergy Clin Immunol*, 111, S460-75.
- BORKOWSKI, T. A., LETTERIO, J. J., FARR, A. G. & UDEY, M. C. (1996) A role for endogenous transforming growth factor beta 1 in Langerhans cell biology: the skin of transforming growth factor beta 1 null mice is devoid of epidermal Langerhans cells. *J Exp Med*, 184, 2417-22.
- BORZI, R. M., MAZZETTI, I., CATTINI, L., UGUCCIONI, M., BAGGIOLINI, M. & FACCHINI, A. (2000) Human chondrocytes express functional chemokine receptors and release matrix-degrading enzymes in response to C-X-C and C-C chemokines. *Arthritis Rheum*, 43, 1734-41.
- BOS, J. D., DE RIE, M. A., TEUNISSEN, M. B. & PISKIN, G. (2005) Psoriasis: dysregulation of innate immunity. *Br J Dermatol*, 152, 1098-107.
- BOS, J. D. & KAPSENBERG, M. L. (1986) The skin immune system. *Immunology Today*, 7, 235-240.
- BOWCOCK, A. M. & KRUEGER, J. G. (2005) Getting under the skin: the immunogenetics of psoriasis. *Nat Rev Immunol*, 5, 699-711.
- BOYMAN, O., HEFTI, H. P., CONRAD, C., NICKOLOFF, B. J., SUTER, M. & NESTLE, F. O. (2004) Spontaneous development of psoriasis in a new animal model shows an essential role for resident T cells and tumor necrosis factor-alpha. *J Exp Med*, 199, 731-6.
- BOZIC, C. R., GERARD, N. P., VON UEXKULL-GULDENBAND, C., KOLAKOWSKI, L. F., JR., CONKLYN, M. J., BRESLOW, R., SHOWELL, H. J. & GERARD, C. (1994) The murine interleukin 8 type B receptor homologue and its ligands. Expression and biological characterization. *J Biol Chem*, 269, 29355-8.
- BREITLING, R., AMTMANN, A. & HERZYK, P. (2004a) Iterative Group Analysis (iGA): a simple tool to enhance sensitivity and facilitate interpretation of microarray experiments. *BMC Bioinformatics*, 5, 34.
- BREITLING, R., ARMENGAUD, P., AMTMANN, A. & HERZYK, P. (2004b) Rank products: a simple, yet powerful, new method to detect differentially regulated genes in replicated microarray experiments. *FEBS Lett*, 573, 83-92.
- BRESNIHAN, B., ALVARO-GRACIA, J. M., COBBY, M., DOHERTY, M., DOMLJAN, Z., EMERY, P., NUKI, G., PAVELKA, K., RAU, R., ROZMAN, B., WATT, I., WILLIAMS, B., AITCHISON, R., MCCABE, D. & MUSIKIC, P. (1998) Treatment of rheumatoid arthritis with recombinant human interleukin-1 receptor antagonist. *Arthritis Rheum*, 41, 2196-204.

- BRILL, A., BARAM, D., SELA, U., SALAMON, P., MEKORI, Y. A. & HERSHKOVIZ, R. (2004) Induction of mast cell interactions with blood vessel wall components by direct contact with intact T cells or T cell membranes in vitro. *Clin Exp Allergy*, 34, 1725-31.
- BRITSCHGI, M. R., LINK, A., LISSANDRIN, T. K. & LUTHER, S. A. (2008) Dynamic modulation of CCR7 expression and function on naive T lymphocytes in vivo. *J Immunol*, 181, 7681-8.
- BROXMEYER, H. E., ORSCHELL, C. M., CLAPP, D. W., HANGOC, G., COOPER, S., PLETT, P. A., LILES, W. C., LI, X., GRAHAM-EVANS, B., CAMPBELL, T. B., CALANDRA, G., BRIDGER, G., DALE, D. C. & SROUR, E. F. (2005) Rapid mobilization of murine and human hematopoietic stem and progenitor cells with AMD3100, a CXCR4 antagonist. *J Exp Med*, 201, 1307-18.
- BRUNKOW, M. E., JEFFERY, E. W., HJERRILD, K. A., PAEPER, B., CLARK, L. B., YASAYKO, S. A., WILKINSON, J. E., GALAS, D., ZIEGLER, S. F. & RAMSDELL, F. (2001) Disruption of a new forkhead/winged-helix protein, scurfin, results in the fatal lymphoproliferative disorder of the scurfy mouse. *Nat Genet*, 27, 68-73.
- BUCHAU, A. S. & GALLO, R. L. (2007) Innate immunity and antimicrobial defense systems in psoriasis. *Clin Dermatol*, 25, 616-24.
- BUCKLAND, K. F., O'CONNOR, E. C., COLEMAN, E. M., LIRA, S. A., LUKACS, N. W. & HOGABOAM, C. M. (2007) Remission of chronic fungal asthma in the absence of CCR8. *J Allergy Clin Immunol*, 119, 997-1004.
- BURNS, J. M., SUMMERS, B. C., WANG, Y., MELIKIAN, A., BERAHOVICH, R., MIAO, Z., PENFOLD, M. E., SUNSHINE, M. J., LITTMAN, D. R., KUO, C. J., WEI, K., MCMASTER, B. E., WRIGHT, K., HOWARD, M. C. & SCHALL, T. J. (2006) A novel chemokine receptor for SDF-1 and I-TAC involved in cell survival, cell adhesion, and tumor development. *J Exp Med*, 203, 2201-13.
- BURSILL, C. A., CASH, J. L., CHANNON, K. M. & GREAVES, D. R. (2006) Membrane-bound CC chemokine inhibitor 35K provides localized inhibition of CC chemokine activity in vitro and in vivo. *J Immunol*, 177, 5567-73.
- BURSILL, C. A., CHOUDHURY, R. P., ALI, Z., GREAVES, D. R. & CHANNON, K. M. (2004) Broad-spectrum CC-chemokine blockade by gene transfer inhibits macrophage recruitment and atherosclerotic plaque formation in apolipoprotein E-knockout mice. *Circulation*, 110, 2460-6.
- BURSILL, C. A., MCNEILL, E., WANG, L., HIBBITT, O. C., WADE-MARTINS, R., PATERSON, D. J., GREAVES, D. R. & CHANNON, K. M. (2009) Lentiviral gene transfer to reduce atherosclerosis progression by long-term CC-chemokine inhibition. *Gene Ther*, 16, 93-102.
- BUSTIN, S. A., GYSELMAN, V. G., WILLIAMS, N. S. & DORUDI, S. (1999) Detection of cytokeratins 19/20 and guanylyl cyclase C in peripheral blood of colorectal cancer patients. *Br J Cancer*, 79, 1813-20.
- BUTCHER, E. C. (1991) Leukocyte-endothelial cell recognition: three (or more) steps to specificity and diversity. *Cell*, 67, 1033-6.
- BUTLER, D. M., MALFAIT, A. M., MASON, L. J., WARDEN, P. J., KOLLIAS, G., MAINI, R. N., FELDMANN, M. & BRENNAN, F. M. (1997) DBA/1 mice expressing the human TNF-alpha transgene develop a severe, erosive arthritis: characterization of the cytokine cascade and cellular composition. *J Immunol*, 159, 2867-76.

- CAMPBELL, D. J. & BUTCHER, E. C. (2002) Rapid acquisition of tissue-specific homing phenotypes by CD4(+) T cells activated in cutaneous or mucosal lymphoid tissues. *J Exp Med*, 195, 135-41.
- CAMPBELL, J. J., HARALDSEN, G., PAN, J., ROTTMAN, J., QIN, S., PONATH, P., ANDREW, D. P., WARNKE, R., RUFFING, N., KASSAM, N., WU, L. & BUTCHER, E. C. (1999) The chemokine receptor CCR4 in vascular recognition by cutaneous but not intestinal memory T cells. *Nature*, 400, 776-80.
- CAMPBELL, J. J., HEDRICK, J., ZLOTNIK, A., SIANI, M. A., THOMPSON, D. A. & BUTCHER, E. C. (1998) Chemokines and the arrest of lymphocytes rolling under flow conditions. *Science*, 279, 381-4.
- CAPON, F., DI MEGLIO, P., SZAUB, J., PRESCOTT, N. J., DUNSTER, C., BAUMBER, L., TIMMS, K., GUTIN, A., ABKEVIC, V., BURDEN, A. D., LANCHBURY, J., BARKER, J. N., TREMBATH, R. C. & NESTLE, F. O. (2007) Sequence variants in the genes for the interleukin-23 receptor (IL23R) and its ligand (IL12B) confer protection against psoriasis. *Hum Genet*, 122, 201-6.
- CARGILL, M., SCHRODI, S. J., CHANG, M., GARCIA, V. E., BRANDON, R., CALLIS, K. P., MATSUNAMI, N., ARDLIE, K. G., CIVELLO, D., CATANESE, J. J., LEONG, D. U., PANKO, J. M., MCALLISTER, L. B., HANSEN, C. B., PAPPENFUSS, J., PRESCOTT, S. M., WHITE, T. J., LEPPERT, M. F., KRUEGER, G. G. & BEGOVICH, A. B. (2007) A large-scale genetic association study confirms IL12B and leads to the identification of IL23R as psoriasis-risk genes. *Am J Hum Genet*, 80, 273-90.
- CARMAN, C. V., SAGE, P. T., SCIUTO, T. E., DE LA FUENTE, M. A., GEHA, R. S., OCHS, H. D., DVORAK, H. F., DVORAK, A. M. & SPRINGER, T. A. (2007) Transcellular diapedesis is initiated by invasive podosomes. *Immunity*, 26, 784-97.
- CARMAN, C. V. & SPRINGER, T. A. (2003) Integrin avidity regulation: are changes in affinity and conformation underemphasized? *Curr Opin Cell Biol*, 15, 547-56.
- CARMELIET, P. (2005) Angiogenesis in life, disease and medicine. *Nature*, 438, 932-6.
- CARRENO, B. M. & COLLINS, M. (2002) The B7 family of ligands and its receptors: new pathways for costimulation and inhibition of immune responses. *Annu Rev Immunol*, 20, 29-53.
- CAUX, C., VANBERVLIET, B., MASSACRIER, C., AZUMA, M., OKUMURA, K., LANIER, L. L. & BANCHEREAU, J. (1994) B70/B7-2 is identical to CD86 and is the major functional ligand for CD28 expressed on human dendritic cells. *J Exp Med*, 180, 1841-7.
- CERADINI, D. J., KULKARNI, A. R., CALLAGHAN, M. J., TEPPER, O. M., BASTIDAS, N., KLEINMAN, M. E., CAPLA, J. M., GALIANO, R. D., LEVINE, J. P. & GURTNER, G. C. (2004) Progenitor cell trafficking is regulated by hypoxic gradients through HIF-1 induction of SDF-1. *Nat Med*, 10, 858-64.
- CHAIN, B. M., NOURSADEGHI, M., GARDENER, M., TSANG, J. & WRIGHT, E. (2008) HIV blocking antibodies following immunisation with chimaeric peptides coding a short N-terminal sequence of the CCR5 receptor. *Vaccine*, 26, 5752-9.

- CHAN, J. R., BLUMENSCHN, W., MURPHY, E., DIVEU, C., WIEKOWSKI, M., ABBONDANZO, S., LUCIAN, L., GEISSLER, R., BRODIE, S., KIMBALL, A. B., GORMAN, D. M., SMITH, K., DE WAAL MALEFYT, R., KASTELEIN, R. A., MCCLANAHAN, T. K. & BOWMAN, E. P. (2006) IL-23 stimulates epidermal hyperplasia via TNF and IL-20R2-dependent mechanisms with implications for psoriasis pathogenesis. *J Exp Med*, 203, 2577-87.
- CHAN, J. R., HYDUK, S. J. & CYBULSKY, M. I. (2001) Chemoattractants induce a rapid and transient upregulation of monocyte alpha4 integrin affinity for vascular cell adhesion molecule 1 which mediates arrest: an early step in the process of emigration. *J Exp Med*, 193, 1149-58.
- CHARO, I. F. & RANSOHOFF, R. M. (2006) The many roles of chemokines and chemokine receptors in inflammation. *N Engl J Med*, 354, 610-21.
- CHAUDHURI, A., NIELSEN, S., ELKJAER, M. L., ZBRZEZNA, V., FANG, F. & POGO, A. O. (1997) Detection of Duffy antigen in the plasma membranes and caveolae of vascular endothelial and epithelial cells of nonerythroid organs. *Blood*, 89, 701-12.
- CHAUDHURI, A., POLYAKOVA, J., ZBRZEZNA, V., WILLIAMS, K., GULATI, S. & POGO, A. O. (1993) Cloning of glycoprotein D cDNA, which encodes the major subunit of the Duffy blood group system and the receptor for the Plasmodium vivax malaria parasite. *Proc Natl Acad Sci U S A*, 90, 10793-7.
- CHEN, W., JIN, W., HARDEGEN, N., LEI, K. J., LI, L., MARINOS, N., MCGRADY, G. & WAHL, S. M. (2003) Conversion of peripheral CD4+CD25- naive T cells to CD4+CD25+ regulatory T cells by TGF-beta induction of transcription factor Foxp3. *J Exp Med*, 198, 1875-86.
- CHEN, X. & JENSEN, P. E. (2008) The role of B lymphocytes as antigen-presenting cells. *Arch Immunol Ther Exp (Warsz)*, 56, 77-83.
- CHENG, Z. J., ZHAO, J., SUN, Y., HU, W., WU, Y. L., CEN, B., WU, G. X. & PEI, G. (2000) beta-arrestin differentially regulates the chemokine receptor CXCR4-mediated signaling and receptor internalization, and this implicates multiple interaction sites between beta-arrestin and CXCR4. *J Biol Chem*, 275, 2479-85.
- CHENSUE, S. W., LUKACS, N. W., YANG, T. Y., SHANG, X., FRAIT, K. A., KUNKEL, S. L., KUNG, T., WIEKOWSKI, M. T., HEDRICK, J. A., COOK, D. N., ZINGONI, A., NARULA, S. K., ZLOTNIK, A., BARRAT, F. J., O'GARRA, A., NAPOLITANO, M. & LIRA, S. A. (2001) Aberrant in vivo T helper type 2 cell response and impaired eosinophil recruitment in CC chemokine receptor 8 knockout mice. *J Exp Med*, 193, 573-84.
- CHESNUTT, B. C., SMITH, D. F., RAFFLER, N. A., SMITH, M. L., WHITE, E. J. & LEY, K. (2006) Induction of LFA-1-dependent neutrophil rolling on ICAM-1 by engagement of E-selectin. *Microcirculation*, 13, 99-109.
- CHUNG, C. D., KUO, F., KUMER, J., MOTANI, A. S., LAWRENCE, C. E., HENDERSON, W. R., JR. & VENKATARAMAN, C. (2003) CCR8 is not essential for the development of inflammation in a mouse model of allergic airway disease. *J Immunol*, 170, 581-7.
- CHVATCHKO, Y., HOOGEWERF, A. J., MEYER, A., ALOUANI, S., JUILLARD, P., BUSER, R., CONQUET, F., PROUDFOOT, A. E., WELLS, T. N. & POWER, C. A. (2000) A key role for CC chemokine receptor 4 in lipopolysaccharide-induced endotoxic shock. *J Exp Med*, 191, 1755-64.

- CINAMON, G., SHINDER, V., SHAMRI, R. & ALON, R. (2004) Chemoattractant signals and beta 2 integrin occupancy at apical endothelial contacts combine with shear stress signals to promote transendothelial neutrophil migration. *J Immunol*, 173, 7282-91.
- CLARK, R. A., CHONG, B., MIRCHANDANI, N., BRINSTER, N. K., YAMANAKA, K., DOWGIERT, R. K. & KUPPER, T. S. (2006) The vast majority of CLA<sup>+</sup> T cells are resident in normal skin. *J Immunol*, 176, 4431-9.
- COCCHI, F., DEVICO, A. L., GARZINO-DEMO, A., ARYA, S. K., GALLO, R. C. & LUSSO, P. (1995) Identification of RANTES, MIP-1 alpha, and MIP-1 beta as the major HIV-suppressive factors produced by CD8<sup>+</sup> T cells. *Science*, 270, 1811-5.
- COLGAN, S. P., SERHAN, C. N., PARKOS, C. A., DELP-ARCHER, C. & MADARA, J. L. (1993) Lipoxin A4 modulates transmigration of human neutrophils across intestinal epithelial monolayers. *J Clin Invest*, 92, 75-82.
- COLOTTA, F., RE, F., MUZIO, M., BERTINI, R., POLENTARUTTI, N., SIRONI, M., GIRI, J. G., DOWER, S. K., SIMS, J. E. & MANTOVANI, A. (1993) Interleukin-1 type II receptor: a decoy target for IL-1 that is regulated by IL-4. *Science*, 261, 472-5.
- COLVIN, B. L. & THOMSON, A. W. (2002) Chemokines, their receptors, and transplant outcome. *Transplantation*, 74, 149-55.
- COMBADIÈRE, C., POTTEAUX, S., GAO, J. L., ESPOSITO, B., CASANOVA, S., LEE, E. J., DEBRE, P., TEDGUI, A., MURPHY, P. M. & MALLAT, Z. (2003) Decreased atherosclerotic lesion formation in CX3CR1/apolipoprotein E double knockout mice. *Circulation*, 107, 1009-16.
- COMERFORD, I., MILASTA, S., MORROW, V., MILLIGAN, G. & NIBBS, R. (2006) The chemokine receptor CX3CR1 mediates effective scavenging of CCL19 in vitro. *Eur J Immunol*, 36, 1904-16.
- CONSTANTIN, G., MAJEED, M., GIAGULLI, C., PICCIO, L., KIM, J. Y., BUTCHER, E. C. & LAUDANNA, C. (2000) Chemokines trigger immediate beta2 integrin affinity and mobility changes: differential regulation and roles in lymphocyte arrest under flow. *Immunity*, 13, 759-69.
- CONTENTO, R. L., MOLON, B., BOULARAN, C., POZZAN, T., MANES, S., MARULLO, S. & VIOLA, A. (2008) CXCR4-CCR5: a couple modulating T cell functions. *Proc Natl Acad Sci U S A*, 105, 10101-6.
- CONTI, P. & DIGIOACCHINO, M. (2001) MCP-1 and RANTES are mediators of acute and chronic inflammation. *Allergy Asthma Proc*, 22, 133-7.
- COOK, D. N., PROSSER, D. M., FORSTER, R., ZHANG, J., KUKLIN, N. A., ABBONDANZO, S. J., NIU, X. D., CHEN, S. C., MANFRA, D. J., WIEKOWSKI, M. T., SULLIVAN, L. M., SMITH, S. R., GREENBERG, H. B., NARULA, S. K., LIPP, M. & LIRA, S. A. (2000) CCR6 mediates dendritic cell localization, lymphocyte homeostasis, and immune responses in mucosal tissue. *Immunity*, 12, 495-503.
- COUSSENS, L. M. & WERB, Z. (2002) Inflammation and cancer. *Nature*, 420, 860-7.
- CULLINAN, E. B., KWEE, L., NUNES, P., SHUSTER, D. J., JU, G., MCINTYRE, K. W., CHIZZONITE, R. A. & LABOW, M. A. (1998) IL-1 receptor accessory

- protein is an essential component of the IL-1 receptor. *J Immunol*, 161, 5614-20.
- CUMANO, A. & GODIN, I. (2007) Ontogeny of the hematopoietic system. *Annu Rev Immunol*, 25, 745-85.
- CUNNINGHAM, S. A., RODRIGUEZ, J. M., ARRATE, M. P., TRAN, T. M. & BROCK, T. A. (2002) JAM2 interacts with alpha4beta1. Facilitation by JAM3. *J Biol Chem*, 277, 27589-92.
- CURNOCK, A. P., LOGAN, M. K. & WARD, S. G. (2002) Chemokine signalling: pivoting around multiple phosphoinositide 3-kinases. *Immunology*, 105, 125-36.
- D'AMBROSIO, D., PANINA-BORDIGNON, P. & SINIGAGLIA, F. (2003) Chemokine receptors in inflammation: an overview. *J Immunol Methods*, 273, 3-13.
- DALGLEISH, A. G., BEVERLEY, P. C., CLAPHAM, P. R., CRAWFORD, D. H., GREAVES, M. F. & WEISS, R. A. (1984) The CD4 (T4) antigen is an essential component of the receptor for the AIDS retrovirus. *Nature*, 312, 763-7.
- DAMBLY-CHAUDIERE, C., CUBEDO, N. & GHYSEN, A. (2007) Control of cell migration in the development of the posterior lateral line: antagonistic interactions between the chemokine receptors CXCR4 and CXCR7/RDC1. *BMC Dev Biol*, 7, 23.
- DARBONNE, W. C., RICE, G. C., MOHLER, M. A., APPLE, T., HEBERT, C. A., VALENTE, A. J. & BAKER, J. B. (1991) Red blood cells are a sink for interleukin 8, a leukocyte chemotaxin. *J Clin Invest*, 88, 1362-9.
- DARDALHON, V., AWASTHI, A., KWON, H., GALILEOS, G., GAO, W., SOBEL, R. A., MITSDOERFFER, M., STROM, T. B., ELYAMAN, W., HO, I. C., KHOURY, S., OUKKA, M. & KUCHROO, V. K. (2008) IL-4 inhibits TGF-beta-induced Foxp3+ T cells and, together with TGF-beta, generates IL-9+ IL-10+ Foxp3(-) effector T cells. *Nat Immunol*, 9, 1347-55.
- DAWICKI, W. & MARSHALL, J. S. (2007) New and emerging roles for mast cells in host defence. *Curr Opin Immunol*, 19, 31-8.
- DAWSON, T. C., LENTSCH, A. B., WANG, Z., COWHIG, J. E., ROT, A., MAEDA, N. & PEIPER, S. C. (2000) Exaggerated response to endotoxin in mice lacking the Duffy antigen/receptor for chemokines (DARC). *Blood*, 96, 1681-4.
- DE PAULIS, A., ANNUNZIATO, F., DI GIOIA, L., ROMAGNANI, S., CARFORA, M., BELTRAME, C., MARONE, G. & ROMAGNANI, P. (2001) Expression of the chemokine receptor CCR3 on human mast cells. *Int Arch Allergy Immunol*, 124, 146-50.
- DE RODA HUSMAN, A. M., KOOT, M., CORNELISSEN, M., KEET, I. P., BROUWER, M., BROERSEN, S. M., BAKKER, M., ROOS, M. T., PRINS, M., DE WOLF, F., COUTINHO, R. A., MIEDEMA, F., GOUDSMIT, J. & SCHUITEMAKER, H. (1997) Association between CCR5 genotype and the clinical course of HIV-1 infection. *Ann Intern Med*, 127, 882-90.
- DEL RIO, L., BENNOUNA, S., SALINAS, J. & DENKERS, E. Y. (2001) CXCR2 deficiency confers impaired neutrophil recruitment and increased susceptibility during *Toxoplasma gondii* infection. *J Immunol*, 167, 6503-9.
- DELEURAN, M., BUHL, L., ELLINGSEN, T., HARADA, A., LARSEN, C. G., MATSUSHIMA, K. & DELEURAN, B. (1996) Localization of monocyte

- chemotactic and activating factor (MCAF/MCP-1) in psoriasis. *J Dermatol Sci*, 13, 228-36.
- DENG, H., LIU, R., ELLMEIER, W., CHOE, S., UNUTMAZ, D., BURKHART, M., DI MARZIO, P., MARMON, S., SUTTON, R. E., HILL, C. M., DAVIS, C. B., PEIPER, S. C., SCHALL, T. J., LITTMAN, D. R. & LANDAU, N. R. (1996) Identification of a major co-receptor for primary isolates of HIV-1. *Nature*, 381, 661-6.
- DEVALARAJA, R. M., NANNEY, L. B., DU, J., QIAN, Q., YU, Y., DEVALARAJA, M. N. & RICHMOND, A. (2000) Delayed wound healing in CXCR2 knockout mice. *J Invest Dermatol*, 115, 234-44.
- DEVINE, S. M., FLOMENBERG, N., VESOLE, D. H., LIESVELD, J., WEISDORF, D., BADEL, K., CALANDRA, G. & DIPERSIO, J. F. (2004) Rapid mobilization of CD34+ cells following administration of the CXCR4 antagonist AMD3100 to patients with multiple myeloma and non-Hodgkin's lymphoma. *J Clin Oncol*, 22, 1095-102.
- DHEDA, K., HUGGETT, J. F., BUSTIN, S. A., JOHNSON, M. A., ROOK, G. & ZUMLA, A. (2004) Validation of housekeeping genes for normalizing RNA expression in real-time PCR. *Biotechniques*, 37, 112-4, 116, 118-9.
- DI LIBERTO, D., LOCATI, M., CACCAMO, N., VECCHI, A., MERAVIGLIA, S., SALERNO, A., SIRECI, G., NEBULONI, M., CACERES, N., CARDONA, P. J., DIELI, F. & MANTOVANI, A. (2008) Role of the chemokine decoy receptor D6 in balancing inflammation, immune activation, and antimicrobial resistance in Mycobacterium tuberculosis infection. *J Exp Med*.
- DIDICHENKO, S. A., TILTON, B., HEMMINGS, B. A., BALLMER-HOFER, K. & THELEN, M. (1996) Constitutive activation of protein kinase B and phosphorylation of p47phox by a membrane-targeted phosphoinositide 3-kinase. *Curr Biol*, 6, 1271-8.
- DINARELLO, C. A. (1996) Biologic basis for interleukin-1 in disease. *Blood*, 87, 2095-147.
- DING, Y., SHIMADA, Y., MAEDA, M., KAWABE, A., KAGANOI, J., KOMOTO, I., HASHIMOTO, Y., MIYAKE, M., HASHIDA, H. & IMAMURA, M. (2003) Association of CC chemokine receptor 7 with lymph node metastasis of esophageal squamous cell carcinoma. *Clin Cancer Res*, 9, 3406-12.
- DOITSIDOU, M., REICHMAN-FRIED, M., STEBLER, J., KOPRUNNER, M., DORRIES, J., MEYER, D., ESGUERRA, C. V., LEUNG, T. & RAZ, E. (2002) Guidance of primordial germ cell migration by the chemokine SDF-1. *Cell*, 111, 647-59.
- DOROSHENKO, T., CHALY, Y., SAVITSKIY, V., MASLAKOVA, O., PORTYANKO, A., GORUDKO, I. & VOITENOK, N. N. (2002) Phagocytosing neutrophils down-regulate the expression of chemokine receptors CXCR1 and CXCR2. *Blood*, 100, 2668-71.
- DORR, P., WESTBY, M., DOBBS, S., GRIFFIN, P., IRVINE, B., MACARTNEY, M., MORI, J., RICKETT, G., SMITH-BURCHNELL, C., NAPIER, C., WEBSTER, R., ARMOUR, D., PRICE, D., STAMMEN, B., WOOD, A. & PERROS, M. (2005) Maraviroc (UK-427,857), a potent, orally bioavailable, and selective small-molecule inhibitor of chemokine receptor CCR5 with broad-spectrum anti-human immunodeficiency virus type 1 activity. *Antimicrob Agents Chemother*, 49, 4721-32.

- DORSCHNER, R. A., PESTONJAMASP, V. K., TAMAKUWALA, S., OHTAKE, T., RUDISILL, J., NIZET, V., AGERBERTH, B., GUDMUNDSSON, G. H. & GALLO, R. L. (2001) Cutaneous injury induces the release of cathelicidin antimicrobial peptides active against group A Streptococcus. *J Invest Dermatol*, 117, 91-7.
- DRAGIC, T., LITWIN, V., ALLAWAY, G. P., MARTIN, S. R., HUANG, Y., NAGASHIMA, K. A., CAYANAN, C., MADDON, P. J., KOUP, R. A., MOORE, J. P. & PAXTON, W. A. (1996) HIV-1 entry into CD4+ cells is mediated by the chemokine receptor CC-CKR-5. *Nature*, 381, 667-73.
- DU, J., LUAN, J., LIU, H., DANIEL, T. O., PEIPER, S., CHEN, T. S., YU, Y., HORTON, L. W., NANNEY, L. B., STRIETER, R. M. & RICHMOND, A. (2002) Potential role for Duffy antigen chemokine-binding protein in angiogenesis and maintenance of homeostasis in response to stress. *J Leukoc Biol*, 71, 141-53.
- DUNCAN, G. S., ANDREW, D. P., TAKIMOTO, H., KAUFMAN, S. A., YOSHIDA, H., SPELLBERG, J., LUIS DE LA POMPA, J., ELIA, A., WAKEHAM, A., KARAN-TAMIR, B., MULLER, W. A., SENALDI, G., ZUKOWSKI, M. M. & MAK, T. W. (1999) Genetic evidence for functional redundancy of Platelet/Endothelial cell adhesion molecule-1 (PECAM-1): CD31-deficient mice reveal PECAM-1-dependent and PECAM-1-independent functions. *J Immunol*, 162, 3022-30.
- DUNNE, J. L., BALLANTYNE, C. M., BEAUDET, A. L. & LEY, K. (2002) Control of leukocyte rolling velocity in TNF-alpha-induced inflammation by LFA-1 and Mac-1. *Blood*, 99, 336-41.
- DUNNE, J. L., COLLINS, R. G., BEAUDET, A. L., BALLANTYNE, C. M. & LEY, K. (2003) Mac-1, but not LFA-1, uses intercellular adhesion molecule-1 to mediate slow leukocyte rolling in TNF-alpha-induced inflammation. *J Immunol*, 171, 6105-11.
- DUSTIN, M. L. (2002) The immunological synapse. *Arthritis Res*, 4 Suppl 3, S119-25.
- DVORAK, A. M. & FENG, D. (2001) The vesiculo-vacuolar organelle (VVO). A new endothelial cell permeability organelle. *J Histochem Cytochem*, 49, 419-32.
- ECKERT, R. L. & WELTER, J. F. (1996) Transcription factor regulation of epidermal keratinocyte gene expression. *Mol Biol Rep*, 23, 59-70.
- EL KHOURY, J., TOFT, M., HICKMAN, S. E., MEANS, T. K., TERADA, K., GEULA, C. & LUSTER, A. D. (2007) Ccr2 deficiency impairs microglial accumulation and accelerates progression of Alzheimer-like disease. *Nat Med*, 13, 432-8.
- ELIAS, P. M. (2007) The skin barrier as an innate immune element. *Semin Immunopathol*, 29, 3-14.
- ELSNER, J., PETERING, H., KLUTHE, C., KIMMIG, D., SMOLARSKI, R., PONATH, P. & KAPP, A. (1998) Eotaxin-2 activates chemotaxis-related events and release of reactive oxygen species via pertussis toxin-sensitive G proteins in human eosinophils. *Eur J Immunol*, 28, 2152-8.
- ENGELHARDT, B. & WOLBURG, H. (2004) Mini-review: Transendothelial migration of leukocytes: through the front door or around the side of the house? *Eur J Immunol*, 34, 2955-63.

- ETIENNE-MANNEVILLE, S., MANNEVILLE, J. B., ADAMSON, P., WILBOURN, B., GREENWOOD, J. & COURAUD, P. O. (2000) ICAM-1-coupled cytoskeletal rearrangements and transendothelial lymphocyte migration involve intracellular calcium signaling in brain endothelial cell lines. *J Immunol*, 165, 3375-83.
- FADOK, V. A., DE CATHELINÉAU, A., DALEKE, D. L., HENSON, P. M. & BRATTON, D. L. (2001) Loss of phospholipid asymmetry and surface exposure of phosphatidylserine is required for phagocytosis of apoptotic cells by macrophages and fibroblasts. *J Biol Chem*, 276, 1071-7.
- FAN, G. H., LAPIERRE, L. A., GOLDENRING, J. R. & RICHMOND, A. (2003) Differential regulation of CXCR2 trafficking by Rab GTPases. *Blood*, 101, 2115-24.
- FAN, X., PATERA, A. C., PONG-KENNEDY, A., DENO, G., GONSIORÉK, W., MANFRA, D. J., VASSILEVA, G., ZENG, M., JACKSON, C., SULLIVAN, L., SHARIF-RODRIGUEZ, W., OPDENAKKER, G., VAN DAMME, J., HEDRICK, J. A., LUNDELL, D., LIRA, S. A. & HIPKIN, R. W. (2007) Murine CXCR1 is a functional receptor for GCP-2/CXCL6 and interleukin-8/CXCL8. *J Biol Chem*, 282, 11658-66.
- FAURSCHOU, M. & BORREGAARD, N. (2003) Neutrophil granules and secretory vesicles in inflammation. *Microbes Infect*, 5, 1317-27.
- FELDMANN, M. (2002) Development of anti-TNF therapy for rheumatoid arthritis. *Nat Rev Immunol*, 2, 364-71.
- FELDMANN, M. & MAINI, R. N. (1999) The role of cytokines in the pathogenesis of rheumatoid arthritis. *Rheumatology (Oxford)*, 38 Suppl 2, 3-7.
- FELDMEYER, L., KELLER, M., NIKLAUS, G., HOHL, D., WERNER, S. & BEER, H. D. (2007) The inflammasome mediates UVB-induced activation and secretion of interleukin-1beta by keratinocytes. *Curr Biol*, 17, 1140-5.
- FENG, D., NAGY, J. A., PYNE, K., DVORAK, H. F. & DVORAK, A. M. (1998) Neutrophils emigrate from venules by a transendothelial cell pathway in response to FMLP. *J Exp Med*, 187, 903-15.
- FERGUSON, S. S. (2001) Evolving concepts in G protein-coupled receptor endocytosis: the role in receptor desensitization and signaling. *Pharmacol Rev*, 53, 1-24.
- FERRARI, D., PIZZIRANI, C., ADINOLFI, E., LEMOLI, R. M., CURTI, A., IDZKO, M., PANTHER, E. & DI VIRGILIO, F. (2006) The P2X7 receptor: a key player in IL-1 processing and release. *J Immunol*, 176, 3877-83.
- FORSTER, R., MATTIS, A. E., KREMMER, E., WOLF, E., BREM, G. & LIPP, M. (1996) A putative chemokine receptor, BLR1, directs B cell migration to defined lymphoid organs and specific anatomic compartments of the spleen. *Cell*, 87, 1037-47.
- FORSTER, R., SCHUBEL, A., BREITFELD, D., KREMMER, E., RENNER-MULLER, I., WOLF, E. & LIPP, M. (1999) CCR7 coordinates the primary immune response by establishing functional microenvironments in secondary lymphoid organs. *Cell*, 99, 23-33.
- FRA, A. M., LOCATI, M., OTERO, K., SIRONI, M., SIGNORELLI, P., MASSARDI, M. L., GOBBI, M., VECCHI, A., SOZZANI, S. & MANTOVANI, A. (2003) Cutting

- edge: scavenging of inflammatory CC chemokines by the promiscuous putatively silent chemokine receptor D6. *J Immunol*, 170, 2279-82.
- FRITZ, J. H., FERRERO, R. L., PHILPOTT, D. J. & GIRARDIN, S. E. (2006) Nod-like proteins in immunity, inflammation and disease. *Nat Immunol*, 7, 1250-7.
- FUHLBRIGGE, R. C., KIEFFER, J. D., ARMERDING, D. & KUPPER, T. S. (1997) Cutaneous lymphocyte antigen is a specialized form of PSGL-1 expressed on skin-homing T cells. *Nature*, 389, 978-81.
- FUJITA, T., MATSUSHITA, M. & ENDO, Y. (2004) The lectin-complement pathway-its role in innate immunity and evolution. *Immunol Rev*, 198, 185-202.
- FUJIYAMA, S., AMANO, K., UEHIRA, K., YOSHIDA, M., NISHIWAKI, Y., NOZAWA, Y., JIN, D., TAKAI, S., MIYAZAKI, M., EGASHIRA, K., IMADA, T., IWASAKA, T. & MATSUBARA, H. (2003) Bone marrow monocyte lineage cells adhere on injured endothelium in a monocyte chemoattractant protein-1-dependent manner and accelerate reendothelialization as endothelial progenitor cells. *Circ Res*, 93, 980-9.
- FUKUMA, N., AKIMITSU, N., HAMAMOTO, H., KUSUHARA, H., SUGIYAMA, Y. & SEKIMIZU, K. (2003) A role of the Duffy antigen for the maintenance of plasma chemokine concentrations. *Biochem Biophys Res Commun*, 303, 137-9.
- FUKUNAGA, A., KHASKHELY, N. M., SREEVIDYA, C. S., BYRNE, S. N. & ULLRICH, S. E. (2008) Dermal dendritic cells, and not Langerhans cells, play an essential role in inducing an immune response. *J Immunol*, 180, 3057-64.
- GABRIEL, S. E. (2008) Why do people with rheumatoid arthritis still die prematurely? *Ann Rheum Dis*, 67 Suppl 3, iii30-4.
- GALLI, S. J., GORDON, J. R. & WERSHIL, B. K. (1991) Cytokine production by mast cells and basophils. *Curr Opin Immunol*, 3, 865-72.
- GALLI, S. J., GRIMBALDESTON, M. & TSAI, M. (2008) Immunomodulatory mast cells: negative, as well as positive, regulators of immunity. *Nat Rev Immunol*, 8, 478-86.
- GALLIERA, E., JALA, V. R., TRENT, J. O., BONECCHI, R., SIGNORELLI, P., LEFKOWITZ, R. J., MANTOVANI, A., LOCATI, M. & HARIBABU, B. (2004) beta-Arrestin-dependent constitutive internalization of the human chemokine decoy receptor D6. *J Biol Chem*, 279, 25590-7.
- GALLO, R. C. & MONTAGNIER, L. (2003) The discovery of HIV as the cause of AIDS. *N Engl J Med*, 349, 2283-5.
- GALLUCCI, S. & MATZINGER, P. (2001) Danger signals: SOS to the immune system. *Curr Opin Immunol*, 13, 114-9.
- GAO, J. L., WYNN, T. A., CHANG, Y., LEE, E. J., BROXMEYER, H. E., COOPER, S., TIFFANY, H. L., WESTPHAL, H., KWON-CHUNG, J. & MURPHY, P. M. (1997) Impaired host defense, hematopoiesis, granulomatous inflammation and type 1-type 2 cytokine balance in mice lacking CC chemokine receptor 1. *J Exp Med*, 185, 1959-68.
- GAO, W., TOPHAM, P. S., KING, J. A., SMILEY, S. T., CSIZMADIA, V., LU, B., GERARD, C. J. & HANCOCK, W. W. (2000) Targeting of the chemokine receptor CCR1 suppresses development of acute and chronic cardiac allograft rejection. *J Clin Invest*, 105, 35-44.

- GARCIA-VICUNA, R., GOMEZ-GAVIRO, M. V., DOMINGUEZ-LUIS, M. J., PEC, M. K., GONZALEZ-ALVARO, I., ALVARO-GRACIA, J. M. & DIAZ-GONZALEZ, F. (2004) CC and CXC chemokine receptors mediate migration, proliferation, and matrix metalloproteinase production by fibroblast-like synoviocytes from rheumatoid arthritis patients. *Arthritis Rheum*, 50, 3866-77.
- GARDNER, L., PATTERSON, A. M., ASHTON, B. A., STONE, M. A. & MIDDLETON, J. (2004) The human Duffy antigen binds selected inflammatory but not homeostatic chemokines. *Biochem Biophys Res Commun*, 321, 306-12.
- GARDNER, L., WILSON, C., PATTERSON, A. M., BRESNIHAN, B., FITZGERALD, O., STONE, M. A., ASHTON, B. A. & MIDDLETON, J. (2006) Temporal expression pattern of Duffy antigen in rheumatoid arthritis: up-regulation in early disease. *Arthritis Rheum*, 54, 2022-6.
- GAZITT, Y. (2004) Homing and mobilization of hematopoietic stem cells and hematopoietic cancer cells are mirror image processes, utilizing similar signaling pathways and occurring concurrently: circulating cancer cells constitute an ideal target for concurrent treatment with chemotherapy and antineoplastic-specific antibodies. *Leukemia*, 18, 1-10.
- GEISSMANN, F., JUNG, S. & LITTMAN, D. R. (2003) Blood monocytes consist of two principal subsets with distinct migratory properties. *Immunity*, 19, 71-82.
- GENOVESE, M. C., MCKAY, J. D., NASONOV, E. L., MYSLER, E. F., DA SILVA, N. A., ALECOCK, E., WOODWORTH, T. & GOMEZ-REINO, J. J. (2008) Interleukin-6 receptor inhibition with tocilizumab reduces disease activity in rheumatoid arthritis with inadequate response to disease-modifying antirheumatic drugs: the tocilizumab in combination with traditional disease-modifying antirheumatic drug therapy study. *Arthritis Rheum*, 58, 2968-80.
- GERARD, C. & ROLLINS, B. J. (2001) Chemokines and disease. *Nat Immunol*, 2, 108-15.
- GERSZTEN, R. E., GARCIA-ZEPEDA, E. A., LIM, Y. C., YOSHIDA, M., DING, H. A., GIMBRONE, M. A., JR., LUSTER, A. D., LUSCINSKAS, F. W. & ROSENZWEIG, A. (1999) MCP-1 and IL-8 trigger firm adhesion of monocytes to vascular endothelium under flow conditions. *Nature*, 398, 718-23.
- GILLITZER, R., RITTER, U., SPANDAU, U., GOEBELER, M. & BROCKER, E. B. (1996) Differential expression of GRO- $\alpha$  and IL-8 mRNA in psoriasis: a model for neutrophil migration and accumulation in vivo. *J Invest Dermatol*, 107, 778-82.
- GILLITZER, R., WOLFF, K., TONG, D., MULLER, C., YOSHIMURA, T., HARTMANN, A. A., STINGL, G. & BERGER, R. (1993) MCP-1 mRNA expression in basal keratinocytes of psoriatic lesions. *J Invest Dermatol*, 101, 127-31.
- GINHOUX, F., TACKE, F., ANGELI, V., BOGUNOVIC, M., LOUBEAU, M., DAI, X. M., STANLEY, E. R., RANDOLPH, G. J. & MERAD, M. (2006) Langerhans cells arise from monocytes in vivo. *Nat Immunol*, 7, 265-73.
- GIRARDI, M. & HAYDAY, A. C. (2005) Immunosurveillance by gammadelta T cells: focus on the murine system. *Chem Immunol Allergy*, 86, 136-50.
- GIRARDI, M., LEWIS, J., GLUSAC, E., FILLER, R. B., GENG, L., HAYDAY, A. C. & TIGELAAR, R. E. (2002) Resident skin-specific gammadelta T cells provide

- local, nonredundant regulation of cutaneous inflammation. *J Exp Med*, 195, 855-67.
- GIRARDI, M., LEWIS, J. M., FILLER, R. B., HAYDAY, A. C. & TIGELAAR, R. E. (2006) Environmentally responsive and reversible regulation of epidermal barrier function by gammadelta T cells. *J Invest Dermatol*, 126, 808-14.
- GIRAUDO, E., INOUE, M. & HANAHAAN, D. (2004) An amino-bisphosphonate targets MMP-9-expressing macrophages and angiogenesis to impair cervical carcinogenesis. *J Clin Invest*, 114, 623-33.
- GLADMAN, D. D., ANTONI, C., MEASE, P., CLEGG, D. O. & NASH, P. (2005) Psoriatic arthritis: epidemiology, clinical features, course, and outcome. *Ann Rheum Dis*, 64 Suppl 2, ii14-7.
- GLASS, W. G., LIM, J. K., CHOLERA, R., PLETNEV, A. G., GAO, J. L. & MURPHY, P. M. (2005) Chemokine receptor CCR5 promotes leukocyte trafficking to the brain and survival in West Nile virus infection. *J Exp Med*, 202, 1087-98.
- GLASS, W. G., MCDERMOTT, D. H., LIM, J. K., LEKHONG, S., YU, S. F., FRANK, W. A., PAPE, J., CHESHER, R. C. & MURPHY, P. M. (2006) CCR5 deficiency increases risk of symptomatic West Nile virus infection. *J Exp Med*, 203, 35-40.
- GODSON, C., MITCHELL, S., HARVEY, K., PETASIS, N. A., HOGG, N. & BRADY, H. R. (2000) Cutting edge: lipoxins rapidly stimulate nonphlogistic phagocytosis of apoptotic neutrophils by monocyte-derived macrophages. *J Immunol*, 164, 1663-7.
- GOLDRING, S. R. (2003) Pathogenesis of bone and cartilage destruction in rheumatoid arthritis. *Rheumatology (Oxford)*, 42 Suppl 2, ii11-6.
- GONG, J. H., RATKAY, L. G., WATERFIELD, J. D. & CLARK-LEWIS, I. (1997) An antagonist of monocyte chemoattractant protein 1 (MCP-1) inhibits arthritis in the MRL-lpr mouse model. *J Exp Med*, 186, 131-7.
- GONZALEZ, E., KULKARNI, H., BOLIVAR, H., MANGANO, A., SANCHEZ, R., CATANO, G., NIBBS, R. J., FREEDMAN, B. I., QUINONES, M. P., BAMSHAD, M. J., MURTHY, K. K., ROVIN, B. H., BRADLEY, W., CLARK, R. A., ANDERSON, S. A., O'CONNELL R, J., AGAN, B. K., AHUJA, S. S., BOLOGNA, R., SEN, L., DOLAN, M. J. & AHUJA, S. K. (2005) The influence of CCL3L1 gene-containing segmental duplications on HIV-1/AIDS susceptibility. *Science*, 307, 1434-40.
- GORDON, S. (2002) Pattern recognition receptors: doubling up for the innate immune response. *Cell*, 111, 927-30.
- GORDON, S. (2003) Alternative activation of macrophages. *Nat Rev Immunol*, 3, 23-35.
- GOSLING, J., DAIRAGHI, D. J., WANG, Y., HANLEY, M., TALBOT, D., MIAO, Z. & SCHALL, T. J. (2000) Cutting edge: identification of a novel chemokine receptor that binds dendritic cell- and T cell-active chemokines including ELC, SLC, and TECK. *J Immunol*, 164, 2851-6.
- GOTSCH, U., JAGER, U., DOMINIS, M. & VESTWEBER, D. (1994) Expression of P-selectin on endothelial cells is upregulated by LPS and TNF-alpha in vivo. *Cell Adhes Commun*, 2, 7-14.

- GOYA, I., VILLARES, R., ZABALLOS, A., GUTIERREZ, J., KREMER, L., GONZALO, J. A., VARONA, R., CARRAMOLINO, L., SERRANO, A., PALLARES, P., CRIADO, L. M., KOLBECK, R., TORRES, M., COYLE, A. J., GUTIERREZ-RAMOS, J. C., MARTINEZ, A. C. & MARQUEZ, G. (2003) Absence of CCR8 does not impair the response to ovalbumin-induced allergic airway disease. *J Immunol*, 170, 2138-46.
- GRAHAM, G. J. (2009) D6 and the atypical chemokine receptor family: novel regulators of immune and inflammatory processes. *Eur J Immunol*, 39, 342-51.
- GRIMBALDESTON, M. A., NAKAE, S., KALESNIKOFF, J., TSAI, M. & GALLI, S. J. (2007) Mast cell-derived interleukin 10 limits skin pathology in contact dermatitis and chronic irradiation with ultraviolet B. *Nat Immunol*, 8, 1095-104.
- GROSSMAN, R. M., KRUEGER, J., YOURISH, D., GRANELLI-PIPERNO, A., MURPHY, D. P., MAY, L. T., KUPPER, T. S., SEHGAL, P. B. & GOTTLIEB, A. B. (1989) Interleukin 6 is expressed in high levels in psoriatic skin and stimulates proliferation of cultured human keratinocytes. *Proc Natl Acad Sci U S A*, 86, 6367-71.
- GROVES, R. W., MIZUTANI, H., KIEFFER, J. D. & KUPPER, T. S. (1995) Inflammatory skin disease in transgenic mice that express high levels of interleukin 1 alpha in basal epidermis. *Proc Natl Acad Sci U S A*, 92, 11874-8.
- GUDJONSSON, J. E., THORARINSSON, A. M., SIGURGEIRSSON, B., KRISTINSSON, K. G. & VALDIMARSSON, H. (2003) Streptococcal throat infections and exacerbation of chronic plaque psoriasis: a prospective study. *Br J Dermatol*, 149, 530-4.
- GUNN, M. D., KYUWA, S., TAM, C., KAKIUCHI, T., MATSUZAWA, A., WILLIAMS, L. T. & NAKANO, H. (1999) Mice lacking expression of secondary lymphoid organ chemokine have defects in lymphocyte homing and dendritic cell localization. *J Exp Med*, 189, 451-60.
- GUNN, M. D., TANGEMANN, K., TAM, C., CYSTER, J. G., ROSEN, S. D. & WILLIAMS, L. T. (1998) A chemokine expressed in lymphoid high endothelial venules promotes the adhesion and chemotaxis of naive T lymphocytes. *Proc Natl Acad Sci U S A*, 95, 258-63.
- GUPTA, G. P. & MASSAGUE, J. (2006) Cancer metastasis: building a framework. *Cell*, 127, 679-95.
- HADLEY, T. J., LU, Z. H., WASNIOWSKA, K., MARTIN, A. W., PEIPER, S. C., HESSELGESSER, J. & HORUK, R. (1994) Postcapillary venule endothelial cells in kidney express a multispecific chemokine receptor that is structurally and functionally identical to the erythroid isoform, which is the Duffy blood group antigen. *J Clin Invest*, 94, 985-91.
- HADLEY, T. J. & PEIPER, S. C. (1997) From malaria to chemokine receptor: the emerging physiologic role of the Duffy blood group antigen. *Blood*, 89, 3077-91.
- HAMRAH, P., YAMAGAMI, S., LIU, Y., ZHANG, Q., VORA, S. S., LU, B., GERARD, C. J. & DANA, M. R. (2007) Deletion of the chemokine receptor CCR1 prolongs corneal allograft survival. *Invest Ophthalmol Vis Sci*, 48, 1228-36.

- HANAHAH, D. & WEINBERG, R. A. (2000) The hallmarks of cancer. *Cell*, 100, 57-70.
- HANCOCK, W. W., LU, B., GAO, W., CSIZMADIA, V., FAIA, K., KING, J. A., SMILEY, S. T., LING, M., GERARD, N. P. & GERARD, C. (2000) Requirement of the chemokine receptor CXCR3 for acute allograft rejection. *J Exp Med*, 192, 1515-20.
- HARDER, J., BARTELS, J., CHRISTOPHERS, E. & SCHRODER, J. M. (1997) A peptide antibiotic from human skin. *Nature*, 387, 861.
- HARDER, J. & SCHRODER, J. M. (2005) Psoriatic scales: a promising source for the isolation of human skin-derived antimicrobial proteins. *J Leukoc Biol*, 77, 476-86.
- HARDTKE, S., OHL, L. & FORSTER, R. (2005) Balanced expression of CXCR5 and CCR7 on follicular T helper cells determines their transient positioning to lymph node follicles and is essential for efficient B-cell help. *Blood*, 106, 1924-31.
- HARINGMAN, J. J., SMEETS, T. J., REINDERS-BLANKERT, P. & TAK, P. P. (2006) Chemokine and chemokine receptor expression in paired peripheral blood mononuclear cells and synovial tissue of patients with rheumatoid arthritis, osteoarthritis, and reactive arthritis. *Ann Rheum Dis*, 65, 294-300.
- HARPER, E. G., GUO, C., RIZZO, H., LILLIS, J. V., KURTZ, S. E., SKORCHEVA, I., PURDY, D., FITCH, E., IORDANOV, M. & BLAUVELT, A. (2009) Th17 cytokines stimulate CCL20 expression in keratinocytes in vitro and in vivo: implications for psoriasis pathogenesis. *J Invest Dermatol*, 129, 2175-83.
- HARRAZ, M., JIAO, C., HANLON, H. D., HARTLEY, R. S. & SCHATTEMAN, G. C. (2001) CD34- blood-derived human endothelial cell progenitors. *Stem Cells*, 19, 304-12.
- HARRINGTON, L. E., HATTON, R. D., MANGAN, P. R., TURNER, H., MURPHY, T. L., MURPHY, K. M. & WEAVER, C. T. (2005) Interleukin 17-producing CD4+ effector T cells develop via a lineage distinct from the T helper type 1 and 2 lineages. *Nat Immunol*, 6, 1123-32.
- HARRIS, D. P., HAYNES, L., SAYLES, P. C., DUSO, D. K., EATON, S. M., LEPAK, N. M., JOHNSON, L. L., SWAIN, S. L. & LUND, F. E. (2000) Reciprocal regulation of polarized cytokine production by effector B and T cells. *Nat Immunol*, 1, 475-82.
- HASHIMOTO, C., HUDSON, K. L. & ANDERSON, K. V. (1988) The Toll gene of *Drosophila*, required for dorsal-ventral embryonic polarity, appears to encode a transmembrane protein. *Cell*, 52, 269-79.
- HAVRAN, W. L., CHIEN, Y. H. & ALLISON, J. P. (1991) Recognition of self antigens by skin-derived T cells with invariant gamma delta antigen receptors. *Science*, 252, 1430-2.
- HAYES, E. B. & GUBLER, D. J. (2006) West Nile virus: epidemiology and clinical features of an emerging epidemic in the United States. *Annu Rev Med*, 57, 181-94.
- HEESEN, M., BERMAN, M. A., CHAREST, A., HOUSMAN, D., GERARD, C. & DORF, M. E. (1998) Cloning and chromosomal mapping of an orphan chemokine receptor: mouse RDC1. *Immunogenetics*, 47, 364-70.

- HEIL, F., HEMMI, H., HOCHREIN, H., AMPENBERGER, F., KIRSCHNING, C., AKIRA, S., LIPFORD, G., WAGNER, H. & BAUER, S. (2004) Species-specific recognition of single-stranded RNA via toll-like receptor 7 and 8. *Science*, 303, 1526-9.
- HEINZEL, K., BENZ, C. & BLEUL, C. C. (2007) A silent chemokine receptor regulates steady-state leukocyte homing in vivo. *Proc Natl Acad Sci U S A*, 104, 8421-6.
- HEISSIG, B., HATTORI, K., DIAS, S., FRIEDRICH, M., FERRIS, B., HACKETT, N. R., CRYSTAL, R. G., BESMER, P., LYDEN, D., MOORE, M. A., WERB, Z. & RAFII, S. (2002) Recruitment of stem and progenitor cells from the bone marrow niche requires MMP-9 mediated release of kit-ligand. *Cell*, 109, 625-37.
- HEMMI, H., TAKEUCHI, O., KAWAI, T., KAISHO, T., SATO, S., SANJO, H., MATSUMOTO, M., HOSHINO, K., WAGNER, H., TAKEDA, K. & AKIRA, S. (2000) A Toll-like receptor recognizes bacterial DNA. *Nature*, 408, 740-5.
- HENNINGS, H., MICHAEL, D., CHENG, C., STEINERT, P., HOLBROOK, K. & YUSPA, S. H. (1980) Calcium regulation of growth and differentiation of mouse epidermal cells in culture. *Cell*, 19, 245-54.
- HIRANO, T., YASUKAWA, K., HARADA, H., TAGA, T., WATANABE, Y., MATSUDA, T., KASHIWAMURA, S., NAKAJIMA, K., KOYAMA, K., IWAMATSU, A. & ET AL. (1986) Complementary DNA for a novel human interleukin (BSF-2) that induces B lymphocytes to produce immunoglobulin. *Nature*, 324, 73-6.
- HIROTA, K., HASHIMOTO, M., YOSHITOMI, H., TANAKA, S., NOMURA, T., YAMAGUCHI, T., IWAKURA, Y., SAKAGUCHI, N. & SAKAGUCHI, S. (2007a) T cell self-reactivity forms a cytokine milieu for spontaneous development of IL-17+ Th cells that cause autoimmune arthritis. *J Exp Med*, 204, 41-7.
- HIROTA, K., YOSHITOMI, H., HASHIMOTO, M., MAEDA, S., TERADAI, S., SUGIMOTO, N., YAMAGUCHI, T., NOMURA, T., ITO, H., NAKAMURA, T., SAKAGUCHI, N. & SAKAGUCHI, S. (2007b) Preferential recruitment of CCR6-expressing Th17 cells to inflamed joints via CCL20 in rheumatoid arthritis and its animal model. *J Exp Med*, 204, 2803-12.
- HIXENBAUGH, E. A., GOECKELER, Z. M., PAPAIIYA, N. N., WYSOLMERSKI, R. B., SILVERSTEIN, S. C. & HUANG, A. J. (1997) Stimulated neutrophils induce myosin light chain phosphorylation and isometric tension in endothelial cells. *Am J Physiol*, 273, H981-8.
- HOGAN, S. P., ROSENBERG, H. F., MOQBEL, R., PHIPPS, S., FOSTER, P. S., LACY, P., KAY, A. B. & ROTHENBERG, M. E. (2008) Eosinophils: biological properties and role in health and disease. *Clin Exp Allergy*, 38, 709-50.
- HOLTMEIER, W., PFANDER, M., HENNEMANN, A., ZOLLNER, T. M., KAUFMANN, R. & CASPARY, W. F. (2001) The TCR-delta repertoire in normal human skin is restricted and distinct from the TCR-delta repertoire in the peripheral blood. *J Invest Dermatol*, 116, 275-80.
- HOMEY, B., ALENIUS, H., MULLER, A., SOTO, H., BOWMAN, E. P., YUAN, W., MCEVOY, L., LAUERMA, A. I., ASSMANN, T., BUNEMANN, E., LEHTO, M., WOLFF, H., YEN, D., MARXHAUSEN, H., TO, W., SEDGWICK, J., RUZICKA, T., LEHMANN, P. & ZLOTNIK, A. (2002) CCL27-CCR10 interactions regulate T cell-mediated skin inflammation. *Nat Med*, 8, 157-65.
- HOMEY, B., DIEU-NOSJEAN, M. C., WIESENBERN, A., MASSACRIER, C., PIN, J. J., OLDFHAM, E., CATRON, D., BUCHANAN, M. E., MULLER, A., DEWAAL

- MALEFYT, R., DENG, G., OROZCO, R., RUZICKA, T., LEHMANN, P., LEBECQUE, S., CAUX, C. & ZLOTNIK, A. (2000a) Up-regulation of macrophage inflammatory protein-3 alpha/CCL20 and CC chemokine receptor 6 in psoriasis. *J Immunol*, 164, 6621-32.
- HOMEY, B., WANG, W., SOTO, H., BUCHANAN, M. E., WIESENBERN, A., CATRON, D., MULLER, A., MCCLANAHAN, T. K., DIEU-NOSJEAN, M. C., OROZCO, R., RUZICKA, T., LEHMANN, P., OLDHAM, E. & ZLOTNIK, A. (2000b) Cutting edge: the orphan chemokine receptor G protein-coupled receptor-2 (GPR-2, CCR10) binds the skin-associated chemokine CCL27 (CTACK/ALP/ILC). *J Immunol*, 164, 3465-70.
- HORAI, R., SAIJO, S., TANIOKA, H., NAKAE, S., SUDO, K., OKAHARA, A., IKUSE, T., ASANO, M. & IWAKURA, Y. (2000) Development of chronic inflammatory arthropathy resembling rheumatoid arthritis in interleukin 1 receptor antagonist-deficient mice. *J Exp Med*, 191, 313-20.
- HORI, S., NOMURA, T. & SAKAGUCHI, S. (2003) Control of regulatory T cell development by the transcription factor Foxp3. *Science*, 299, 1057-61.
- HORUK, R., CHITNIS, C. E., DARBONNE, W. C., COLBY, T. J., RYBICKI, A., HADLEY, T. J. & MILLER, L. H. (1993) A receptor for the malarial parasite *Plasmodium vivax*: the erythrocyte chemokine receptor. *Science*, 261, 1182-4.
- HORUK, R., MARTIN, A., HESSELGESSER, J., HADLEY, T., LU, Z. H., WANG, Z. X. & PEIPER, S. C. (1996) The Duffy antigen receptor for chemokines: structural analysis and expression in the brain. *J Leukoc Biol*, 59, 29-38.
- HUANG, H., LI, F., CAIRNS, C. M., GORDON, J. R. & XIANG, J. (2001) Neutrophils and B cells express XCR1 receptor and chemotactically respond to lymphotactin. *Biochem Biophys Res Commun*, 281, 378-82.
- HUDAK, S., HAGEN, M., LIU, Y., CATRON, D., OLDHAM, E., MCEVOY, L. M. & BOWMAN, E. P. (2002) Immune surveillance and effector functions of CCR10(+) skin homing T cells. *J Immunol*, 169, 1189-96.
- HUMBLES, A. A., LU, B., FRIEND, D. S., OKINAGA, S., LORA, J., AL-GARAWI, A., MARTIN, T. R., GERARD, N. P. & GERARD, C. (2002) The murine CCR3 receptor regulates both the role of eosinophils and mast cells in allergen-induced airway inflammation and hyperresponsiveness. *Proc Natl Acad Sci U S A*, 99, 1479-84.
- HUYNH, M. L., FADOK, V. A. & HENSON, P. M. (2002) Phosphatidylserine-dependent ingestion of apoptotic cells promotes TGF-beta1 secretion and the resolution of inflammation. *J Clin Invest*, 109, 41-50.
- HWANG, S. T. (2004) Chemokine receptors in melanoma: CCR9 has a potential role in metastasis to the small bowel. *J Invest Dermatol*, 122, xiv-xv.
- HYDUK, S. J., CHAN, J. R., DUFFY, S. T., CHEN, M., PETERSON, M. D., WADDELL, T. K., DIGBY, G. C., SZASZI, K., KAPUS, A. & CYBULSKY, M. I. (2007) Phospholipase C, calcium, and calmodulin are critical for alpha4beta1 integrin affinity up-regulation and monocyte arrest triggered by chemoattractants. *Blood*, 109, 176-84.
- IMAI, T., BABA, M., NISHIMURA, M., KAKIZAKI, M., TAKAGI, S. & YOSHIE, O. (1997) The T cell-directed CC chemokine TARC is a highly specific biological ligand for CC chemokine receptor 4. *J Biol Chem*, 272, 15036-42.

- IMAI, T., CHANTRY, D., RAPORT, C. J., WOOD, C. L., NISHIMURA, M., GODISKA, R., YOSHIE, O. & GRAY, P. W. (1998) Macrophage-derived chemokine is a functional ligand for the CC chemokine receptor 4. *J Biol Chem*, 273, 1764-8.
- INFANTINO, S., MOEPPS, B. & THELEN, M. (2006) Expression and regulation of the orphan receptor RDC1 and its putative ligand in human dendritic and B cells. *J Immunol*, 176, 2197-207.
- INOHARA, N., OGURA, Y., CHEN, F. F., MUTO, A. & NUNEZ, G. (2001) Human Nod1 confers responsiveness to bacterial lipopolysaccharides. *J Biol Chem*, 276, 2551-4.
- IRIZARRY, R. A., HOBBS, B., COLLIN, F., BEAZER-BARCLAY, Y. D., ANTONELLIS, K. J., SCHERF, U. & SPEED, T. P. (2003) Exploration, normalization, and summaries of high density oligonucleotide array probe level data. *Biostatistics*, 4, 249-64.
- ISENSEE, J. & RUIZ NOPPINGER, P. (2007) Sexually dimorphic gene expression in mammalian somatic tissue. *Genet Med*, 4 Suppl B, S75-95.
- ITO, T., INABA, M., INABA, K., TOKI, J., SOGO, S., IGUCHI, T., ADACHI, Y., YAMAGUCHI, K., AMAKAWA, R., VALLADEAU, J., SAELAND, S., FUKUHARA, S. & IKEHARA, S. (1999) A CD1a<sup>+</sup>/CD11c<sup>+</sup> subset of human blood dendritic cells is a direct precursor of Langerhans cells. *J Immunol*, 163, 1409-19.
- ITOH, K., KAWASAKI, S., KAWAMOTO, S., SEISHIMA, M., CHIBA, H., MICHIBATA, H., WAKIMOTO, K., IMAI, Y., MINESAKI, Y., OTSUJI, M. & OKUBO, K. (2005) Identification of differentially expressed genes in psoriasis using expression profiling approaches. *Exp Dermatol*, 14, 667-74.
- IVANOV, II, MCKENZIE, B. S., ZHOU, L., TADOKORO, C. E., LEPELLEY, A., LAFAILLE, J. J., CUA, D. J. & LITTMAN, D. R. (2006) The orphan nuclear receptor ROR $\gamma$  directs the differentiation program of proinflammatory IL-17<sup>+</sup> T helper cells. *Cell*, 126, 1121-33.
- IWATA, M., HIRAKIYAMA, A., ESHIMA, Y., KAGECHIKA, H., KATO, C. & SONG, S. Y. (2004) Retinoic acid imprints gut-homing specificity on T cells. *Immunity*, 21, 527-38.
- JAMESON, J., UGARTE, K., CHEN, N., YACHI, P., FUCHS, E., BOISMENU, R. & HAVRAN, W. L. (2002) A role for skin gammadelta T cells in wound repair. *Science*, 296, 747-9.
- JAMESON, J. M., CAUVI, G., SHARP, L. L., WITHERDEN, D. A. & HAVRAN, W. L. (2005) Gammadelta T cell-induced hyaluronan production by epithelial cells regulates inflammation. *J Exp Med*, 201, 1269-79.
- JAMIESON, T., COOK, D. N., NIBBS, R. J., ROT, A., NIXON, C., MCLEAN, P., ALCAMI, A., LIRA, S. A., WIEKOWSKI, M. & GRAHAM, G. J. (2005) The chemokine receptor D6 limits the inflammatory response in vivo. *Nat Immunol*, 6, 403-11.
- JANEWAY, C. A., JR. & MEDZHITOV, R. (2002) Innate immune recognition. *Annu Rev Immunol*, 20, 197-216.
- JANG, M. H., SOUGAWA, N., TANAKA, T., HIRATA, T., HIROI, T., TOHYA, K., GUO, Z., UMEMOTO, E., EBISUNO, Y., YANG, B. G., SEOH, J. Y., LIPP, M., KIYONO, H. & MIYASAKA, M. (2006) CCR7 is critically important for

- migration of dendritic cells in intestinal lamina propria to mesenteric lymph nodes. *J Immunol*, 176, 803-10.
- JENKINS, M. K., KHORUTS, A., INGULLI, E., MUELLER, D. L., MCSORLEY, S. J., REINHARDT, R. L., ITANO, A. & PAPE, K. A. (2001) In vivo activation of antigen-specific CD4 T cells. *Annu Rev Immunol*, 19, 23-45.
- JOHNSON-LEGER, C. A., AURRAND-LIONS, M., BELTRAMINELLI, N., FASEL, N. & IMHOF, B. A. (2002) Junctional adhesion molecule-2 (JAM-2) promotes lymphocyte transendothelial migration. *Blood*, 100, 2479-86.
- JONES, D. A., ABBASSI, O., MCINTIRE, L. V., MCEVER, R. P. & SMITH, C. W. (1993) P-selectin mediates neutrophil rolling on histamine-stimulated endothelial cells. *Biophys J*, 65, 1560-9.
- KAMARI, Y., WERMAN-VENKERT, R., SHAISH, A., WERMAN, A., HARARI, A., GONEN, A., VORONOV, E., GROSSKOPF, I., SHARABI, Y., GROSSMAN, E., IWAKURA, Y., DINARELLO, C. A., APTE, R. N. & HARATS, D. (2007) Differential role and tissue specificity of interleukin-1alpha gene expression in atherogenesis and lipid metabolism. *Atherosclerosis*, 195, 31-8.
- KAPLAN, M. H., SCHINDLER, U., SMILEY, S. T. & GRUSBY, M. J. (1996) Stat6 is required for mediating responses to IL-4 and for development of Th2 cells. *Immunity*, 4, 313-9.
- KAPLANSKI, G., FARNARIER, C., KAPLANSKI, S., PORAT, R., SHAPIRO, L., BONGRAND, P. & DINARELLO, C. A. (1994) Interleukin-1 induces interleukin-8 secretion from endothelial cells by a juxtacrine mechanism. *Blood*, 84, 4242-8.
- KARSHOVSKA, E., ZERNECKE, A., SEVILMIS, G., MILLET, A., HRISTOV, M., COHEN, C. D., SCHMID, H., KROTZ, F., SOHN, H. Y., KLAUSS, V., WEBER, C. & SCHOBER, A. (2007) Expression of HIF-1alpha in injured arteries controls SDF-1alpha mediated neointima formation in apolipoprotein E deficient mice. *Arterioscler Thromb Vasc Biol*, 27, 2540-7.
- KARSUNKY, H., MERAD, M., COZZIO, A., WEISSMAN, I. L. & MANZ, M. G. (2003) Flt3 ligand regulates dendritic cell development from Flt3+ lymphoid and myeloid-committed progenitors to Flt3+ dendritic cells in vivo. *J Exp Med*, 198, 305-13.
- KEFFER, J., PROBERT, L., CAZLARIS, H., GEORGOPOULOS, S., KASLARIS, E., KIOUSSIS, D. & KOLLIAS, G. (1991) Transgenic mice expressing human tumour necrosis factor: a predictive genetic model of arthritis. *Embo J*, 10, 4025-31.
- KHOJA, H., WANG, G., NG, C. T., TUCKER, J., BROWN, T. & SHYAMALA, V. (2000) Cloning of CCRL1, an orphan seven transmembrane receptor related to chemokine receptors, expressed abundantly in the heart. *Gene*, 246, 229-38.
- KIMURA, A., NAKA, T. & KISHIMOTO, T. (2007) IL-6-dependent and -independent pathways in the development of interleukin 17-producing T helper cells. *Proc Natl Acad Sci U S A*, 104, 12099-104.
- KIN, N. W., CRAWFORD, D. M., LIU, J., BEHRENS, T. W. & KEARNEY, J. F. (2008) DNA microarray gene expression profile of marginal zone versus follicular B cells and idiotype positive marginal zone B cells before and after immunization with *Streptococcus pneumoniae*. *J Immunol*, 180, 6663-74.

- KISHIMOTO, T. (2005) Interleukin-6: from basic science to medicine--40 years in immunology. *Annu Rev Immunol*, 23, 1-21.
- KITA, H., WEILER, D. A., ABU-GHAZALEH, R., SANDERSON, C. J. & GLEICH, G. J. (1992) Release of granule proteins from eosinophils cultured with IL-5. *J Immunol*, 149, 629-35.
- KLARESKOG, L., STOLT, P., LUNDBERG, K., KALLBERG, H., BENGTSSON, C., GRUNEWALD, J., RONNELID, J., HARRIS, H. E., ULFGREN, A. K., RANTAPAA-DAHLQVIST, S., EKLUND, A., PADYUKOV, L. & ALFREDSSON, L. (2006) A new model for an etiology of rheumatoid arthritis: smoking may trigger HLA-DR (shared epitope)-restricted immune reactions to autoantigens modified by citrullination. *Arthritis Rheum*, 54, 38-46.
- KLEINERT, S., FEUCHTENBERGER, M., KNEITZ, C. & TONY, H. P. (2007) Psoriatic arthritis: clinical spectrum and diagnostic procedures. *Clin Dermatol*, 25, 519-23.
- KNAUT, H., WERZ, C., GEISLER, R. & NUSSLEIN-VOLHARD, C. (2003) A zebrafish homologue of the chemokine receptor Cxcr4 is a germ-cell guidance receptor. *Nature*, 421, 279-82.
- KOCH, A. E., KUNKEL, S. L., BURROWS, J. C., EVANOFF, H. L., HAINES, G. K., POPE, R. M. & STRIETER, R. M. (1991) Synovial tissue macrophage as a source of the chemotactic cytokine IL-8. *J Immunol*, 147, 2187-95.
- KOCH, A. E., KUNKEL, S. L., HARLOW, L. A., JOHNSON, B., EVANOFF, H. L., HAINES, G. K., BURDICK, M. D., POPE, R. M. & STRIETER, R. M. (1992) Enhanced production of monocyte chemoattractant protein-1 in rheumatoid arthritis. *J Clin Invest*, 90, 772-9.
- KOCK, A., SCHWARZ, T., KIRNBAUER, R., URBANSKI, A., PERRY, P., ANSEL, J. C. & LUGER, T. A. (1990) Human keratinocytes are a source for tumor necrosis factor alpha: evidence for synthesis and release upon stimulation with endotoxin or ultraviolet light. *J Exp Med*, 172, 1609-14.
- KOLLIAS, G., DOUNI, E., KASSIOTIS, G. & KONTOYIANNIS, D. (1999) On the role of tumor necrosis factor and receptors in models of multiorgan failure, rheumatoid arthritis, multiple sclerosis and inflammatory bowel disease. *Immunol Rev*, 169, 175-94.
- KOLLISCH, G., KALALI, B. N., VOELCKER, V., WALLICH, R., BEHRENDT, H., RING, J., BAUER, S., JAKOB, T., MEMPEL, M. & OLLERT, M. (2005) Various members of the Toll-like receptor family contribute to the innate immune response of human epidermal keratinocytes. *Immunology*, 114, 531-41.
- KOMATSU, T., MORIYA, N. & SHIOHARA, T. (1996) T cell receptor (TCR) repertoire and function of human epidermal T cells: restricted TCR V alpha-V beta genes are utilized by T cells residing in the lesional epidermis in fixed drug eruption. *Clin Exp Immunol*, 104, 343-50.
- KONDO, M., WEISSMAN, I. L. & AKASHI, K. (1997) Identification of clonogenic common lymphoid progenitors in mouse bone marrow. *Cell*, 91, 661-72.
- KRIEGLER, M., PEREZ, C., DEFAY, K., ALBERT, I. & LU, S. D. (1988) A novel form of TNF/cachectin is a cell surface cytotoxic transmembrane protein: ramifications for the complex physiology of TNF. *Cell*, 53, 45-53.

- KULKE, R., BORNSCHEUER, E., SCHLUTER, C., BARTELS, J., ROWERT, J., STICHERLING, M. & CHRISTOPHERS, E. (1998) The CXC receptor 2 is overexpressed in psoriatic epidermis. *J Invest Dermatol*, 110, 90-4.
- KUNKEL, E. J., KIM, C. H., LAZARUS, N. H., VIERRA, M. A., SOLER, D., BOWMAN, E. P. & BUTCHER, E. C. (2003) CCR10 expression is a common feature of circulating and mucosal epithelial tissue IgA Ab-secreting cells. *J Clin Invest*, 111, 1001-10.
- KUNKEL, E. J. & LEY, K. (1996) Distinct phenotype of E-selectin-deficient mice. E-selectin is required for slow leukocyte rolling in vivo. *Circ Res*, 79, 1196-204.
- KUPPER, T. S. & FUHLBRIGGE, R. C. (2004) Immune surveillance in the skin: mechanisms and clinical consequences. *Nat Rev Immunol*, 4, 211-22.
- KURIHARA, T., WARR, G., LOY, J. & BRAVO, R. (1997) Defects in macrophage recruitment and host defense in mice lacking the CCR2 chemokine receptor. *J Exp Med*, 186, 1757-62.
- LAPORTE, S. A., OAKLEY, R. H., ZHANG, J., HOLT, J. A., FERGUSON, S. S., CARON, M. G. & BARAK, L. S. (1999) The beta2-adrenergic receptor/betaarrestin complex recruits the clathrin adaptor AP-2 during endocytosis. *Proc Natl Acad Sci U S A*, 96, 3712-7.
- LASAGNI, L., FRANCALANCI, M., ANNUNZIATO, F., LAZZERI, E., GIANNINI, S., COSMI, L., SAGRINATI, C., MAZZINGHI, B., ORLANDO, C., MAGGI, E., MARRA, F., ROMAGNANI, S., SERIO, M. & ROMAGNANI, P. (2003) An alternatively spliced variant of CXCR3 mediates the inhibition of endothelial cell growth induced by IP-10, Mig, and I-TAC, and acts as functional receptor for platelet factor 4. *J Exp Med*, 197, 1537-49.
- LAUDANNA, C., KIM, J. Y., CONSTANTIN, G. & BUTCHER, E. (2002) Rapid leukocyte integrin activation by chemokines. *Immunol Rev*, 186, 37-46.
- LAWRENCE, M. B., KANSAS, G. S., KUNKEL, E. J. & LEY, K. (1997) Threshold levels of fluid shear promote leukocyte adhesion through selectins (CD62L,P,E). *J Cell Biol*, 136, 717-27.
- LAZZERI, E. & ROMAGNANI, P. (2005) CXCR3-binding chemokines: novel multifunctional therapeutic targets. *Curr Drug Targets Immune Endocr Metabol Disord*, 5, 109-18.
- LEAN, J. M., MURPHY, C., FULLER, K. & CHAMBERS, T. J. (2002) CCL9/MIP-1gamma and its receptor CCR1 are the major chemokine ligand/receptor species expressed by osteoclasts. *J Cell Biochem*, 87, 386-93.
- LEBRE, M. C., VAN DER AAR, A. M., VAN BAARSEN, L., VAN CAPEL, T. M., SCHUITEMAKER, J. H., KAPSENBERG, M. L. & DE JONG, E. C. (2007) Human keratinocytes express functional Toll-like receptor 3, 4, 5, and 9. *J Invest Dermatol*, 127, 331-41.
- LEE, D. M., FRIEND, D. S., GURISH, M. F., BENOIST, C., MATHIS, D. & BRENNER, M. B. (2002) Mast cells: a cellular link between autoantibodies and inflammatory arthritis. *Science*, 297, 1689-92.
- LEE, E., TREPICCHIO, W. L., OESTREICHER, J. L., PITTMAN, D., WANG, F., CHAMIAN, F., DHODAPKAR, M. & KRUEGER, J. G. (2004) Increased expression of interleukin 23 p19 and p40 in lesional skin of patients with psoriasis vulgaris. *J Exp Med*, 199, 125-30.

- LEE, J. S., FREVERT, C. W., THORNING, D. R., SEGERER, S., ALPERS, C. E., CARTRON, J. P., COLIN, Y., WONG, V. A., MARTIN, T. R. & GOODMAN, R. B. (2003a) Enhanced expression of Duffy antigen in the lungs during suppurative pneumonia. *J Histochem Cytochem*, 51, 159-66.
- LEE, J. S., FREVERT, C. W., WURFEL, M. M., PEIPER, S. C., WONG, V. A., BALLMAN, K. K., RUZINSKI, J. T., RHIM, J. S., MARTIN, T. R. & GOODMAN, R. B. (2003b) Duffy antigen facilitates movement of chemokine across the endothelium in vitro and promotes neutrophil transmigration in vitro and in vivo. *J Immunol*, 170, 5244-51.
- LEE, S. J., NAMKOONG, S., KIM, Y. M., KIM, C. K., LEE, H., HA, K. S., CHUNG, H. T., KWON, Y. G. & KIM, Y. M. (2006) Fractalkine stimulates angiogenesis by activating the Raf-1/MEK/ERK- and PI3K/Akt/eNOS-dependent signal pathways. *Am J Physiol Heart Circ Physiol*, 291, H2836-46.
- LEE, Y. K., TURNER, H., MAYNARD, C. L., OLIVER, J. R., CHEN, D., ELSON, C. O. & WEAVER, C. T. (2009) Late developmental plasticity in the T helper 17 lineage. *Immunity*, 30, 92-107.
- LEGLER, D. F., LOETSCHER, M., ROOS, R. S., CLARK-LEWIS, I., BAGGIOLINI, M. & MOSER, B. (1998) B cell-attracting chemokine 1, a human CXC chemokine expressed in lymphoid tissues, selectively attracts B lymphocytes via BLR1/CXCR5. *J Exp Med*, 187, 655-60.
- LENTSCH, A. B. (2002) The Duffy antigen/receptor for chemokines (DARC) and prostate cancer. A role as clear as black and white? *Faseb J*, 16, 1093-5.
- LETSCH, A., KEILHOLZ, U., SCHADENDORF, D., ASSFALG, G., ASEMISSEN, A. M., THIEL, E. & SCHEIBENBOGEN, C. (2004) Functional CCR9 expression is associated with small intestinal metastasis. *J Invest Dermatol*, 122, 685-90.
- LEUNG, D. Y. (1995) Atopic dermatitis: the skin as a window into the pathogenesis of chronic allergic diseases. *J Allergy Clin Immunol*, 96, 302-18; quiz 319.
- LEVOYE, A., BALABANIAN, K., BALEUX, F., BACHELERIE, F. & LAGANE, B. (2009) CXCR7 heterodimerizes with CXCR4 and regulates CXCL12-mediated G protein signaling. *Blood*, 113, 6085-93.
- LEVY, B. D., CLISH, C. B., SCHMIDT, B., GRONERT, K. & SERHAN, C. N. (2001) Lipid mediator class switching during acute inflammation: signals in resolution. *Nat Immunol*, 2, 612-9.
- LEVY, J. A., MACKEWICZ, C. E. & BARKER, E. (1996) Controlling HIV pathogenesis: the role of the noncytotoxic anti-HIV response of CD8+ T cells. *Immunol Today*, 17, 217-24.
- LEW, W., BOWCOCK, A. M. & KRUEGER, J. G. (2004) Psoriasis vulgaris: cutaneous lymphoid tissue supports T-cell activation and "Type 1" inflammatory gene expression. *Trends Immunol*, 25, 295-305.
- LEY, K., LAUDANNA, C., CYBULSKY, M. I. & NOURSHARGH, S. (2007) Getting to the site of inflammation: the leukocyte adhesion cascade updated. *Nat Rev Immunol*, 7, 678-89.
- LEY, K. & REUTERSHAN, J. (2006) Leucocyte-endothelial interactions in health and disease. *Handb Exp Pharmacol*, 97-133.

- LI, J., IRELAND, G. W., FARTHING, P. M. & THORNHILL, M. H. (1996) Epidermal and oral keratinocytes are induced to produce RANTES and IL-8 by cytokine stimulation. *J Invest Dermatol*, 106, 661-6.
- LI, S. & HUANG, L. (2000) Nonviral gene therapy: promises and challenges. *Gene Ther*, 7, 31-4.
- LI, Z., JIANG, H., XIE, W., ZHANG, Z., SMRCKA, A. V. & WU, D. (2000) Roles of PLC-beta2 and -beta3 and PI3Kgamma in chemoattractant-mediated signal transduction. *Science*, 287, 1046-9.
- LIANG, S. C., TAN, X. Y., LUXENBERG, D. P., KARIM, R., DUNUSSI-JOANNOPOULOS, K., COLLINS, M. & FOUSER, L. A. (2006) Interleukin (IL)-22 and IL-17 are coexpressed by Th17 cells and cooperatively enhance expression of antimicrobial peptides. *J Exp Med*, 203, 2271-9.
- LIAO, F., ALI, J., GREENE, T. & MULLER, W. A. (1997) Soluble domain 1 of platelet-endothelial cell adhesion molecule (PECAM) is sufficient to block transendothelial migration in vitro and in vivo. *J Exp Med*, 185, 1349-57.
- LIEHN, E. A., SCHOBER, A. & WEBER, C. (2004) Blockade of keratinocyte-derived chemokine inhibits endothelial recovery and enhances plaque formation after arterial injury in ApoE-deficient mice. *Arterioscler Thromb Vasc Biol*, 24, 1891-6.
- LILES, W. C., BROXMEYER, H. E., RODGER, E., WOOD, B., HUBEL, K., COOPER, S., HANGOC, G., BRIDGER, G. J., HENSON, G. W., CALANDRA, G. & DALE, D. C. (2003) Mobilization of hematopoietic progenitor cells in healthy volunteers by AMD3100, a CXCR4 antagonist. *Blood*, 102, 2728-30.
- LIN, E. Y. & POLLARD, J. W. (2007) Tumor-associated macrophages press the angiogenic switch in breast cancer. *Cancer Res*, 67, 5064-6.
- LIN, M. T., WANG, F., UITTO, J. & YOON, K. (2001a) Differential expression of tissue-specific promoters by gene gun. *Br J Dermatol*, 144, 34-9.
- LIN, W. J., NORRIS, D. A., ACHZIGER, M., KOTZIN, B. L. & TOMKINSON, B. (2001b) Oligoclonal expansion of intraepidermal T cells in psoriasis skin lesions. *J Invest Dermatol*, 117, 1546-53.
- LIU, J. P., BAKER, J., PERKINS, A. S., ROBERTSON, E. J. & EFSTRATIADIS, A. (1993) Mice carrying null mutations of the genes encoding insulin-like growth factor I (Igf-1) and type 1 IGF receptor (Igf1r). *Cell*, 75, 59-72.
- LIU, L., GRAHAM, G. J., DAMODARAN, A., HU, T., LIRA, S. A., SASSE, M., CANASTO-CHIBUQUE, C., COOK, D. N. & RANSOHOFF, R. M. (2006) Cutting edge: the silent chemokine receptor D6 is required for generating T cell responses that mediate experimental autoimmune encephalomyelitis. *J Immunol*, 177, 17-21.
- LIU, P., YU, Y. R., SPENCER, J. A., JOHNSON, A. E., VALLANAT, C. T., FONG, A. M., PATTERSON, C. & PATEL, D. D. (2008) CX3CR1 deficiency impairs dendritic cell accumulation in arterial intima and reduces atherosclerotic burden. *Arterioscler Thromb Vasc Biol*, 28, 243-50.
- LIU, R., PAXTON, W. A., CHOE, S., CERADINI, D., MARTIN, S. R., HORUK, R., MACDONALD, M. E., STUHLMANN, H., KOUP, R. A. & LANDAU, N. R. (1996) Homozygous defect in HIV-1 coreceptor accounts for resistance of some multiply-exposed individuals to HIV-1 infection. *Cell*, 86, 367-77.

- LIU, X. H., HADLEY, T. J., XU, L., PEIPER, S. C. & RAY, P. E. (1999) Up-regulation of Duffy antigen receptor expression in children with renal disease. *Kidney Int*, 55, 1491-500.
- LKRIEGOVA, E., TSYRULNYK, A., ARAKELYAN, A., MRAZEK, F., ORDELTOVA, M., PETZMANN, S., ZATLOUKAL, J., KOLEK, V., DU BOIS, R. M., POPPER, H. & PETREK, M. (2006) Expression of CCX CKR in pulmonary sarcoidosis. *Inflamm Res*, 55, 441-5.
- LOCATI, M., DEUSCHLE, U., MASSARDI, M. L., MARTINEZ, F. O., SIRONI, M., SOZZANI, S., BARTFAI, T. & MANTOVANI, A. (2002) Analysis of the gene expression profile activated by the CC chemokine ligand 5/RANTES and by lipopolysaccharide in human monocytes. *J Immunol*, 168, 3557-62.
- LOCKSLEY, R. M., KILLEEN, N. & LENARDO, M. J. (2001) The TNF and TNF receptor superfamilies: integrating mammalian biology. *Cell*, 104, 487-501.
- LOU, O., ALCAIDE, P., LUSCINSKAS, F. W. & MULLER, W. A. (2007) CD99 is a key mediator of the transendothelial migration of neutrophils. *J Immunol*, 178, 1136-43.
- LOWES, M. A., KIKUCHI, T., FUENTES-DUCULAN, J., CARDINALE, I., ZABA, L. C., HAIDER, A. S., BOWMAN, E. P. & KRUEGER, J. G. (2008) Psoriasis vulgaris lesions contain discrete populations of Th1 and Th17 T cells. *J Invest Dermatol*, 128, 1207-11.
- LU, Z. H., WANG, Z. X., HORUK, R., HESSELGESSER, J., LOU, Y. C., HADLEY, T. J. & PEIPER, S. C. (1995) The promiscuous chemokine binding profile of the Duffy antigen/receptor for chemokines is primarily localized to sequences in the amino-terminal domain. *J Biol Chem*, 270, 26239-45.
- LUAN, J., SHATTUCK-BRANDT, R., HAGHNEGHDAR, H., OWEN, J. D., STRIETER, R., BURDICK, M., NIRODI, C., BEAUCHAMP, D., JOHNSON, K. N. & RICHMOND, A. (1997) Mechanism and biological significance of constitutive expression of MGSA/GRO chemokines in malignant melanoma tumor progression. *J Leukoc Biol*, 62, 588-97.
- LUND, J. M., ALEXOPOULOU, L., SATO, A., KAROW, M., ADAMS, N. C., GALE, N. W., IWASAKI, A. & FLAVELL, R. A. (2004) Recognition of single-stranded RNA viruses by Toll-like receptor 7. *Proc Natl Acad Sci U S A*, 101, 5598-603.
- LUNDSTEDT, A. C., MCCARTHY, S., GUSTAFSSON, M. C., GODALY, G., JODAL, U., KARPMAN, D., LEIJONHUFVUD, I., LINDEN, C., MARTINELL, J., RAGNARSDOTTIR, B., SAMUELSSON, M., TRUEDSSON, L., ANDERSSON, B. & SVANBORG, C. (2007) A genetic basis of susceptibility to acute pyelonephritis. *PLoS One*, 2, e825.
- LUSSO, P. (2006) HIV and the chemokine system: 10 years later. *Embo J*, 25, 447-56.
- LUST, J. A., DONOVAN, K. A., KLINE, M. P., GREIPP, P. R., KYLE, R. A. & MAIHLE, N. J. (1992) Isolation of an mRNA encoding a soluble form of the human interleukin-6 receptor. *Cytokine*, 4, 96-100.
- MA, B., ZHU, Z., HOMER, R. J., GERARD, C., STRIETER, R. & ELIAS, J. A. (2004) The C10/CCL6 chemokine and CCR1 play critical roles in the pathogenesis of IL-13-induced inflammation and remodeling. *J Immunol*, 172, 1872-81.

- MA, Q., JONES, D. & SPRINGER, T. A. (1999) The chemokine receptor CXCR4 is required for the retention of B lineage and granulocytic precursors within the bone marrow microenvironment. *Immunity*, 10, 463-71.
- MA, W., BRYCE, P. J., HUMBLE, A. A., LAOUINI, D., YALCINDAG, A., ALENIUS, H., FRIEND, D. S., OETTGEN, H. C., GERARD, C. & GEHA, R. S. (2002) CCR3 is essential for skin eosinophilia and airway hyperresponsiveness in a murine model of allergic skin inflammation. *J Clin Invest*, 109, 621-8.
- MACKIEWICZ, A., SCHOOLTINK, H., HEINRICH, P. C. & ROSE-JOHN, S. (1992) Complex of soluble human IL-6-receptor/IL-6 up-regulates expression of acute-phase proteins. *J Immunol*, 149, 2021-7.
- MAINTZ, L. & NOVAK, N. (2007) Histamine and histamine intolerance. *Am J Clin Nutr*, 85, 1185-96.
- MAMDOUH, Z., CHEN, X., PIERINI, L. M., MAXFIELD, F. R. & MULLER, W. A. (2003) Targeted recycling of PECAM from endothelial surface-connected compartments during diapedesis. *Nature*, 421, 748-53.
- MANGAN, P. R., HARRINGTON, L. E., O'QUINN, D. B., HELMS, W. S., BULLARD, D. C., ELSON, C. O., HATTON, R. D., WAHL, S. M., SCHOEB, T. R. & WEAVER, C. T. (2006) Transforming growth factor-beta induces development of the T(H)17 lineage. *Nature*, 441, 231-4.
- MANTOVANI, A. (1999) The chemokine system: redundancy for robust outputs. *Immunol Today*, 20, 254-7.
- MANTOVANI, A., ALLAVENA, P. & SICA, A. (2004) Tumour-associated macrophages as a prototypic type II polarised phagocyte population: role in tumour progression. *Eur J Cancer*, 40, 1660-7.
- MARKS, S. C., JR. & LANE, P. W. (1976) Osteopetrosis, a new recessive skeletal mutation on chromosome 12 of the mouse. *J Hered*, 67, 11-18.
- MARSHALL, J. S. (2004) Mast-cell responses to pathogens. *Nat Rev Immunol*, 4, 787-99.
- MARTIN-FONTECHA, A., SEBASTIANI, S., HOPKEN, U. E., UGUCCIONI, M., LIPP, M., LANZAVECCHIA, A. & SALLUSTO, F. (2003) Regulation of dendritic cell migration to the draining lymph node: impact on T lymphocyte traffic and priming. *J Exp Med*, 198, 615-21.
- MARTIN-PADURA, I., LOSTAGLIO, S., SCHNEEMANN, M., WILLIAMS, L., ROMANO, M., FRUSCELLA, P., PANZERI, C., STOPPACCIARO, A., RUCO, L., VILLA, A., SIMMONS, D. & DEJANA, E. (1998) Junctional adhesion molecule, a novel member of the immunoglobulin superfamily that distributes at intercellular junctions and modulates monocyte transmigration. *J Cell Biol*, 142, 117-27.
- MARTINEZ DE LA TORRE, Y., BURACCHI, C., BORRONI, E. M., DUPOR, J., BONECCHI, R., NEBULONI, M., PASQUALINI, F., DONI, A., LAURI, E., AGOSTINIS, C., BULLA, R., COOK, D. N., HARIBABU, B., MERONI, P., RUKAVINA, D., VAGO, L., TEDESCO, F., VECCHI, A., LIRA, S. A., LOCATI, M. & MANTOVANI, A. (2007) Protection against inflammation- and autoantibody-caused fetal loss by the chemokine decoy receptor D6. *Proc Natl Acad Sci U S A*, 104, 2319-24.
- MARTINEZ DE LA TORRE, Y., LOCATI, M., BURACCHI, C., DUPOR, J., COOK, D. N., BONECCHI, R., NEBULONI, M., RUKAVINA, D., VAGO, L., VECCHI, A., LIRA,

- S. A. & MANTOVANI, A. (2005) Increased inflammation in mice deficient for the chemokine decoy receptor D6. *Eur J Immunol*, 35, 1342-6.
- MARTINON, F., PETRILLI, V., MAYOR, A., TARDIVEL, A. & TSCHOPP, J. (2006) Gout-associated uric acid crystals activate the NALP3 inflammasome. *Nature*, 440, 237-41.
- MARTINON, F. & TSCHOPP, J. (2007) Inflammatory caspases and inflammasomes: master switches of inflammation. *Cell Death Differ*, 14, 10-22.
- MATLOUBIAN, M., DAVID, A., ENGEL, S., RYAN, J. E. & CYSTER, J. G. (2000) A transmembrane CXC chemokine is a ligand for HIV-coreceptor Bonzo. *Nat Immunol*, 1, 298-304.
- MATSUI, T., AKAHOSHI, T., NAMAI, R., HASHIMOTO, A., KURIHARA, Y., RANA, M., NISHIMURA, A., ENDO, H., KITASATO, H., KAWAI, S., TAKAGISHI, K. & KONDO, H. (2001) Selective recruitment of CCR6-expressing cells by increased production of MIP-3 alpha in rheumatoid arthritis. *Clin Exp Immunol*, 125, 155-61.
- MATSUKAWA, A., KUDOH, S., SANO, G., MAEDA, T., ITO, T., LUKACS, N. W., HOGABOAM, C. M., KUNKEL, S. L. & LIRA, S. A. (2006) Absence of CC chemokine receptor 8 enhances innate immunity during septic peritonitis. *Faseb J*, 20, 302-4.
- MATTHEWS, V., SCHUSTER, B., SCHUTZE, S., BUSSMEYER, I., LUDWIG, A., HUNDHAUSEN, C., SADOWSKI, T., SAFTIG, P., HARTMANN, D., KALLEN, K. J. & ROSE-JOHN, S. (2003) Cellular cholesterol depletion triggers shedding of the human interleukin-6 receptor by ADAM10 and ADAM17 (TACE). *J Biol Chem*, 278, 38829-39.
- MCCULLOCH, C. V., MORROW, V., MILASTA, S., COMERFORD, I., MILLIGAN, G., GRAHAM, G. J., ISAACS, N. W. & NIBBS, R. J. (2008) Multiple roles for the C-terminal tail of the chemokine scavenger D6. *J Biol Chem*, 283, 7972-82.
- MCINNES, I. B. & GRACIE, J. A. (2004) Interleukin-15: a new cytokine target for the treatment of inflammatory diseases. *Curr Opin Pharmacol*, 4, 392-7.
- MCKENNA, H. J., STOCKING, K. L., MILLER, R. E., BRASEL, K., DE SMEDT, T., MARASKOVSKY, E., MALISZEWSKI, C. R., LYNCH, D. H., SMITH, J., PULENDRAN, B., ROUX, E. R., TEEPE, M., LYMAN, S. D. & PESCHON, J. J. (2000) Mice lacking flt3 ligand have deficient hematopoiesis affecting hematopoietic progenitor cells, dendritic cells, and natural killer cells. *Blood*, 95, 3489-97.
- MCKENZIE, R. C. & SABIN, E. (2003) Aberrant signalling and transcription factor activation as an explanation for the defective growth control and differentiation of keratinocytes in psoriasis: a hypothesis. *Exp Dermatol*, 12, 337-45.
- MCKIMMIE, C. S., FRASER, A. R., HANSELL, C., GUTIERREZ, L., PHILIPSEN, S., CONNELL, L., ROT, A., KUROWSKA-STOLARSKA, M., CARRENO, P., PRUENSTER, M., CHU, C. C., LOMBARDI, G., HALSEY, C., MCINNES, I. B., LIEW, F. Y., NIBBS, R. J. & GRAHAM, G. J. (2008) Hemopoietic cell expression of the chemokine decoy receptor D6 is dynamic and regulated by GATA1. *J Immunol*, 181, 3353-63.
- MCKIMMIE, C. S. & GRAHAM, G. J. (2006) Leucocyte expression of the chemokine scavenger D6. *Biochem Soc Trans*, 34, 1002-4.

- MCQUIBBAN, G. A., BUTLER, G. S., GONG, J. H., BENDALL, L., POWER, C., CLARK-LEWIS, I. & OVERALL, C. M. (2001) Matrix metalloproteinase activity inactivates the CXC chemokine stromal cell-derived factor-1. *J Biol Chem*, 276, 43503-8.
- MEDZHITOV, R. (2001) Toll-like receptors and innate immunity. *Nat Rev Immunol*, 1, 135-45.
- MEDZHITOV, R. (2007) Recognition of microorganisms and activation of the immune response. *Nature*, 449, 819-26.
- MEDZHITOV, R. (2008) Origin and physiological roles of inflammation. *Nature*, 454, 428-35.
- MEDZHITOV, R. & JANEWAY, C., JR. (2000) Innate immunity. *N Engl J Med*, 343, 338-44.
- MEDZHITOV, R., PRESTON-HURLBURT, P. & JANEWAY, C. A., JR. (1997) A human homologue of the *Drosophila* Toll protein signals activation of adaptive immunity. *Nature*, 388, 394-7.
- MENTEN, P., WUYTS, A. & VAN DAMME, J. (2002) Macrophage inflammatory protein-1. *Cytokine Growth Factor Rev*, 13, 455-81.
- METCALFE, D. D., BARAM, D. & MEKORI, Y. A. (1997) Mast cells. *Physiol Rev*, 77, 1033-79.
- METZ, M., PILIPONSKY, A. M., CHEN, C. C., LAMMEL, V., ABRINK, M., PEJLER, G., TSAI, M. & GALLI, S. J. (2006) Mast cells can enhance resistance to snake and honeybee venoms. *Science*, 313, 526-30.
- MIAO, Z., LUKER, K. E., SUMMERS, B. C., BERAHOVICH, R., BHOJANI, M. S., REHEMTULLA, A., KLEER, C. G., ESSNER, J. J., NASEVICIUS, A., LUKER, G. D., HOWARD, M. C. & SCHALL, T. J. (2007) CXCR7 (RDC1) promotes breast and lung tumor growth in vivo and is expressed on tumor-associated vasculature. *Proc Natl Acad Sci U S A*, 104, 15735-40.
- MIDDLETON, J., PATTERSON, A. M., GARDNER, L., SCHMUTZ, C. & ASHTON, B. A. (2002) Leukocyte extravasation: chemokine transport and presentation by the endothelium. *Blood*, 100, 3853-60.
- MILLAN, J., HEWLETT, L., GLYN, M., TOOMRE, D., CLARK, P. & RIDLEY, A. J. (2006) Lymphocyte transcellular migration occurs through recruitment of endothelial ICAM-1 to caveola- and F-actin-rich domains. *Nat Cell Biol*, 8, 113-23.
- MIN, B., PROUT, M., HU-LI, J., ZHU, J., JANKOVIC, D., MORGAN, E. S., URBAN, J. F., JR., DVORAK, A. M., FINKELMAN, F. D., LEGROS, G. & PAUL, W. E. (2004) Basophils produce IL-4 and accumulate in tissues after infection with a Th2-inducing parasite. *J Exp Med*, 200, 507-17.
- MITSUYAMA, K., TOMIYASU, N., SUZUKI, A., TAKAKI, K., TAKEDATSU, H., MASUDA, J., YAMASAKI, H., MATSUMOTO, S., TSURUTA, O., TOYONAGA, A. & SATA, M. (2006) A form of circulating interleukin-6 receptor component soluble gp130 as a potential interleukin-6 inhibitor in inflammatory bowel disease. *Clin Exp Immunol*, 143, 125-31.
- MIYAZAKI, D., NAKAMURA, T., TODA, M., CHEUNG-CHAU, K. W., RICHARDSON, R. M. & ONO, S. J. (2005) Macrophage inflammatory protein-1 $\alpha$  as a costimulatory signal for mast cell-mediated immediate hypersensitivity reactions. *J Clin Invest*, 115, 434-42.

- MOLON, B., GRI, G., BETTELLA, M., GOMEZ-MOUTON, C., LANZAVECCHIA, A., MARTINEZ, A. C., MANES, S. & VIOLA, A. (2005) T cell costimulation by chemokine receptors. *Nat Immunol*, 6, 465-71.
- MORALES, J., HOMEY, B., VICARI, A. P., HUDAK, S., OLDHAM, E., HEDRICK, J., OROZCO, R., COPELAND, N. G., JENKINS, N. A., MCEVOY, L. M. & ZLOTNIK, A. (1999) CTACK, a skin-associated chemokine that preferentially attracts skin-homing memory T cells. *Proc Natl Acad Sci U S A*, 96, 14470-5.
- MOROHASHI, H., MIYAWAKI, T., NOMURA, H., KUNO, K., MURAKAMI, S., MATSUSHIMA, K. & MUKAIDA, N. (1995) Expression of both types of human interleukin-8 receptors on mature neutrophils, monocytes, and natural killer cells. *J Leukoc Biol*, 57, 180-7.
- MORRISON, T. B., WEIS, J. J. & WITTEWER, C. T. (1998) Quantification of low-copy transcripts by continuous SYBR Green I monitoring during amplification. *Biotechniques*, 24, 954-8, 960, 962.
- MOSER, B., WOLF, M., WALZ, A. & LOETSCHER, P. (2004) Chemokines: multiple levels of leukocyte migration control. *Trends Immunol*, 25, 75-84.
- MOUSER, J. F. & HYAMS, J. S. (1999) Infliximab: a novel chimeric monoclonal antibody for the treatment of Crohn's disease. *Clin Ther*, 21, 932-42; discussion 931.
- MUELLER, A., MEISER, A., MCDONAGH, E. M., FOX, J. M., PETIT, S. J., XANTHOU, G., WILLIAMS, T. J. & PEASE, J. E. (2008) CXCL4-induced migration of activated T lymphocytes is mediated by the chemokine receptor CXCR3. *J Leukoc Biol*, 83, 875-82.
- MUELLER, W. & HERRMANN, B. (1979) Cyclosporin A for psoriasis. *N Engl J Med*, 301, 555.
- MUKAI, K., MATSUOKA, K., TAYA, C., SUZUKI, H., YOKOZEKI, H., NISHIOKA, K., HIROKAWA, K., ETORI, M., YAMASHITA, M., KUBOTA, T., MINEGISHI, Y., YONEKAWA, H. & KARASUYAMA, H. (2005) Basophils play a critical role in the development of IgE-mediated chronic allergic inflammation independently of T cells and mast cells. *Immunity*, 23, 191-202.
- MULLEN, A. C., HIGH, F. A., HUTCHINS, A. S., LEE, H. W., VILLARINO, A. V., LIVINGSTON, D. M., KUNG, A. L., CEREB, N., YAO, T. P., YANG, S. Y. & REINER, S. L. (2001) Role of T-bet in commitment of TH1 cells before IL-12-dependent selection. *Science*, 292, 1907-10.
- MULLER, A., HOMEY, B., SOTO, H., GE, N., CATRON, D., BUCHANAN, M. E., MCCLANAHAN, T., MURPHY, E., YUAN, W., WAGNER, S. N., BARRERA, J. L., MOHAR, A., VERASTEGUI, E. & ZLOTNIK, A. (2001) Involvement of chemokine receptors in breast cancer metastasis. *Nature*, 410, 50-6.
- MULLER, W. A. (2003) Leukocyte-endothelial-cell interactions in leukocyte transmigration and the inflammatory response. *Trends Immunol*, 24, 327-34.
- MULLER, W. A., WEIGL, S. A., DENG, X. & PHILLIPS, D. M. (1993) PECAM-1 is required for transendothelial migration of leukocytes. *J Exp Med*, 178, 449-60.
- MURAKAMI, T., CARDONES, A. R., FINKELSTEIN, S. E., RESTIFO, N. P., KLAUNBERG, B. A., NESTLE, F. O., CASTILLO, S. S., DENNIS, P. A. &

- HWANG, S. T. (2003) Immune evasion by murine melanoma mediated through CC chemokine receptor-10. *J Exp Med*, 198, 1337-47.
- MURPHY, K. M. & REINER, S. L. (2002) The lineage decisions of helper T cells. *Nat Rev Immunol*, 2, 933-44.
- MURPHY, M., KERR, P. & GRANT-KELS, J. M. (2007) The histopathologic spectrum of psoriasis. *Clin Dermatol*, 25, 524-8.
- MURPHY, P. M. (2002) International Union of Pharmacology. XXX. Update on chemokine receptor nomenclature. *Pharmacol Rev*, 54, 227-9.
- MURPHY, P. M., BAGGIOLINI, M., CHARO, I. F., HEBERT, C. A., HORUK, R., MATSUSHIMA, K., MILLER, L. H., OPPENHEIM, J. J. & POWER, C. A. (2000) International union of pharmacology. XXII. Nomenclature for chemokine receptors. *Pharmacol Rev*, 52, 145-76.
- NAGASAWA, T., HIROTA, S., TACHIBANA, K., TAKAKURA, N., NISHIKAWA, S., KITAMURA, Y., YOSHIDA, N., KIKUTANI, H. & KISHIMOTO, T. (1996) Defects of B-cell lymphopoiesis and bone-marrow myelopoiesis in mice lacking the CXC chemokine PBSF/SDF-1. *Nature*, 382, 635-8.
- NAGASAWA, T., TACHIBANA, K. & KAWABATA, K. (1999) A CXC chemokine SDF-1/PBSF: a ligand for a HIV coreceptor, CXCR4. *Adv Immunol*, 71, 211-28.
- NAIR, R. P., RUETHER, A., STUART, P. E., JENISCH, S., TEJASVI, T., HIREMAGALORE, R., SCHREIBER, S., KABELITZ, D., LIM, H. W., VOORHEES, J. J., CHRISTOPHERS, E., ELDER, J. T. & WEICHENTHAL, M. (2008) Polymorphisms of the IL12B and IL23R genes are associated with psoriasis. *J Invest Dermatol*, 128, 1653-61.
- NAITO, M., HAYASHI, S., YOSHIDA, H., NISHIKAWA, S., SHULTZ, L. D. & TAKAHASHI, K. (1991) Abnormal differentiation of tissue macrophage populations in 'osteopetrosis' (op) mice defective in the production of macrophage colony-stimulating factor. *Am J Pathol*, 139, 657-67.
- NAKAE, S., HO, L. H., YU, M., MONTEFORTE, R., IIKURA, M., SUTO, H. & GALLI, S. J. (2007) Mast cell-derived TNF contributes to airway hyperreactivity, inflammation, and TH2 cytokine production in an asthma model in mice. *J Allergy Clin Immunol*, 120, 48-55.
- NALDI, L. & GAMBINI, D. (2007) The clinical spectrum of psoriasis. *Clin Dermatol*, 25, 510-8.
- NEGUS, R. P., STAMP, G. W., HADLEY, J. & BALKWILL, F. R. (1997) Quantitative assessment of the leukocyte infiltrate in ovarian cancer and its relationship to the expression of C-C chemokines. *Am J Pathol*, 150, 1723-34.
- NEGUS, R. P., STAMP, G. W., RELF, M. G., BURKE, F., MALIK, S. T., BERNASCONI, S., ALLAVENA, P., SOZZANI, S., MANTOVANI, A. & BALKWILL, F. R. (1995) The detection and localization of monocyte chemoattractant protein-1 (MCP-1) in human ovarian cancer. *J Clin Invest*, 95, 2391-6.
- NEIL, S. J., AASA-CHAPMAN, M. M., CLAPHAM, P. R., NIBBS, R. J., MCKNIGHT, A. & WEISS, R. A. (2005) The promiscuous CC chemokine receptor D6 is a functional coreceptor for primary isolates of human immunodeficiency virus type 1 (HIV-1) and HIV-2 on astrocytes. *J Virol*, 79, 9618-24.

- NEOTE, K., MAK, J. Y., KOLAKOWSKI, L. F., JR. & SCHALL, T. J. (1994) Functional and biochemical analysis of the cloned Duffy antigen: identity with the red blood cell chemokine receptor. *Blood*, 84, 44-52.
- NEPTUNE, E. R., IIRI, T. & BOURNE, H. R. (1999) Galphai is not required for chemotaxis mediated by Gi-coupled receptors. *J Biol Chem*, 274, 2824-8.
- NESTLE, F. O., CONRAD, C., TUN-KYI, A., HOMEY, B., GOMBERT, M., BOYMAN, O., BURG, G., LIU, Y. J. & GILLIET, M. (2005) Plasmacytoid predendritic cells initiate psoriasis through interferon-alpha production. *J Exp Med*, 202, 135-43.
- NESTLE, F. O., FILGUEIRA, L., NICKOLOFF, B. J. & BURG, G. (1998) Human dermal dendritic cells process and present soluble protein antigens. *J Invest Dermatol*, 110, 762-6.
- NETELENBOS, T., ZUIJDERDIJN, S., VAN DEN BORN, J., KESSLER, F. L., ZWEEGMAN, S., HUIJGENS, P. C. & DRAGER, A. M. (2002) Proteoglycans guide SDF-1-induced migration of hematopoietic progenitor cells. *J Leukoc Biol*, 72, 353-62.
- NGUYEN, D. H. & TAUB, D. (2002) Cholesterol is essential for macrophage inflammatory protein 1 beta binding and conformational integrity of CC chemokine receptor 5. *Blood*, 99, 4298-306.
- NIBBS, R., GRAHAM, G. & ROT, A. (2003) Chemokines on the move: control by the chemokine "interceptors" Duffy blood group antigen and D6. *Semin Immunol*, 15, 287-94.
- NIBBS, R. J., GILCHRIST, D. S., KING, V., FERRA, A., FORROW, S., HUNTER, K. D. & GRAHAM, G. J. (2007) The atypical chemokine receptor D6 suppresses the development of chemically induced skin tumors. *J Clin Invest*, 117, 1884-92.
- NIBBS, R. J., KRIEHLER, E., PONATH, P. D., PARENT, D., QIN, S., CAMPBELL, J. D., HENDERSON, A., KERJASCHKI, D., MAURER, D., GRAHAM, G. J. & ROT, A. (2001) The beta-chemokine receptor D6 is expressed by lymphatic endothelium and a subset of vascular tumors. *Am J Pathol*, 158, 867-77.
- NIBBS, R. J., WYLIE, S. M., PRAGNELL, I. B. & GRAHAM, G. J. (1997a) Cloning and characterization of a novel murine beta chemokine receptor, D6. Comparison to three other related macrophage inflammatory protein-1alpha receptors, CCR-1, CCR-3, and CCR-5. *J Biol Chem*, 272, 12495-504.
- NIBBS, R. J., WYLIE, S. M., YANG, J., LANDAU, N. R. & GRAHAM, G. J. (1997b) Cloning and characterization of a novel promiscuous human beta-chemokine receptor D6. *J Biol Chem*, 272, 32078-83.
- NIBBS, R. J., YANG, J., LANDAU, N. R., MAO, J. H. & GRAHAM, G. J. (1999) LD78beta, a non-allelic variant of human MIP-1alpha (LD78alpha), has enhanced receptor interactions and potent HIV suppressive activity. *J Biol Chem*, 274, 17478-83.
- NICKOLOFF, B. J. (1991) The cytokine network in psoriasis. *Arch Dermatol*, 127, 871-84.
- NICOLAS, J. F., CHAMCHICK, N., THIVOLET, J., WIJDENES, J., MOREL, P. & REVILLARD, J. P. (1991) CD4 antibody treatment of severe psoriasis. *Lancet*, 338, 321.

- NIELSEN, S., CHAUDHURI, A. & POGO, A. O. (1997) Which are the nonerythroid cells that constitutively express the Duffy antigen? *Blood*, 90, 3231-3.
- NOTOHAMIPRODJO, M., SEGERER, S., HUSS, R., HILDEBRANDT, B., SOLER, D., DJAFARZADEH, R., BUCK, W., NELSON, P. J. & VON LUETTICHAU, I. (2005) CCR10 is expressed in cutaneous T-cell lymphoma. *Int J Cancer*, 115, 641-7.
- NOWELL, M. A., RICHARDS, P. J., HORIUCHI, S., YAMAMOTO, N., ROSE-JOHN, S., TOPLEY, N., WILLIAMS, A. S. & JONES, S. A. (2003) Soluble IL-6 receptor governs IL-6 activity in experimental arthritis: blockade of arthritis severity by soluble glycoprotein 130. *J Immunol*, 171, 3202-9.
- OHL, L., HENNING, G., KRAUTWALD, S., LIPP, M., HARDTKE, S., BERNHARDT, G., PABST, O. & FORSTER, R. (2003) Cooperating mechanisms of CXCR5 and CCR7 in development and organization of secondary lymphoid organs. *J Exp Med*, 197, 1199-204.
- OKA, Y., SARAIVA, L. R., KWAN, Y. Y. & KORSCHING, S. I. (2009) The fifth class of Galpha proteins. *Proc Natl Acad Sci U S A*, 106, 1484-9.
- OLIVEIRA, S. H. & LUKACS, N. W. (2001) Stem cell factor and igE-stimulated murine mast cells produce chemokines (CCL2, CCL17, CCL22) and express chemokine receptors. *Inflamm Res*, 50, 168-74.
- ONO, S. J., NAKAMURA, T., MIYAZAKI, D., OHBAYASHI, M., DAWSON, M. & TODA, M. (2003) Chemokines: roles in leukocyte development, trafficking, and effector function. *J Allergy Clin Immunol*, 111, 1185-99; quiz 1200.
- OPPMANN, B., LESLEY, R., BLOM, B., TIMANS, J. C., XU, Y., HUNTE, B., VEGA, F., YU, N., WANG, J., SINGH, K., ZONIN, F., VAISBERG, E., CHURAKOVA, T., LIU, M., GORMAN, D., WAGNER, J., ZURAWSKI, S., LIU, Y., ABRAMS, J. S., MOORE, K. W., RENNICK, D., DE WAAL-MALEFYT, R., HANNUM, C., BAZAN, J. F. & KASTELEIN, R. A. (2000) Novel p19 protein engages IL-12p40 to form a cytokine, IL-23, with biological activities similar as well as distinct from IL-12. *Immunity*, 13, 715-25.
- OSTERMANN, G., WEBER, K. S., ZERNECKE, A., SCHRODER, A. & WEBER, C. (2002) JAM-1 is a ligand of the beta(2) integrin LFA-1 involved in transendothelial migration of leukocytes. *Nat Immunol*, 3, 151-8.
- OUYANG, W., RANGANATH, S. H., WEINDEL, K., BHATTACHARYA, D., MURPHY, T. L., SHA, W. C. & MURPHY, K. M. (1998) Inhibition of Th1 development mediated by GATA-3 through an IL-4-independent mechanism. *Immunity*, 9, 745-55.
- OZAKI, H., ISHII, K., HORIUCHI, H., ARAI, H., KAWAMOTO, T., OKAWA, K., IWAMATSU, A. & KITA, T. (1999) Cutting edge: combined treatment of TNF-alpha and IFN-gamma causes redistribution of junctional adhesion molecule in human endothelial cells. *J Immunol*, 163, 553-7.
- PALCZEWSKI, K., KUMASAKA, T., HORI, T., BEHNKE, C. A., MOTOSHIMA, H., FOX, B. A., LE TRONG, I., TELLER, D. C., OKADA, T., STENKAMP, R. E., YAMAMOTO, M. & MIYANO, M. (2000) Crystal structure of rhodopsin: A G protein-coupled receptor. *Science*, 289, 739-45.
- PALUCKA, K. A., TAQUET, N., SANCHEZ-CHAPUIS, F. & GLUCKMAN, J. C. (1998) Dendritic cells as the terminal stage of monocyte differentiation. *J Immunol*, 160, 4587-95.

- PAPADAKIS, K. A., PREHN, J., MORENO, S. T., CHENG, L., KOUROUMALIS, E. A., DEEM, R., BREAVERMAN, T., PONATH, P. D., ANDREW, D. P., GREEN, P. H., HODGE, M. R., BINDER, S. W. & TARGAN, S. R. (2001) CCR9-positive lymphocytes and thymus-expressed chemokine distinguish small bowel from colonic Crohn's disease. *Gastroenterology*, 121, 246-54.
- PAPAYIANNI, A., SERHAN, C. N. & BRADY, H. R. (1996) Lipoxin A4 and B4 inhibit leukotriene-stimulated interactions of human neutrophils and endothelial cells. *J Immunol*, 156, 2264-72.
- PARHAM, C., CHIRICA, M., TIMANS, J., VAISBERG, E., TRAVIS, M., CHEUNG, J., PFLANZ, S., ZHANG, R., SINGH, K. P., VEGA, F., TO, W., WAGNER, J., O'FARRELL, A. M., MCCLANAHAN, T., ZURAWSKI, S., HANNUM, C., GORMAN, D., RENNICK, D. M., KASTELEIN, R. A., DE WAAL MALEFYT, R. & MOORE, K. W. (2002) A receptor for the heterodimeric cytokine IL-23 is composed of IL-12Rbeta1 and a novel cytokine receptor subunit, IL-23R. *J Immunol*, 168, 5699-708.
- PARK, H., LI, Z., YANG, X. O., CHANG, S. H., NURIEVA, R., WANG, Y. H., WANG, Y., HOOD, L., ZHU, Z., TIAN, Q. & DONG, C. (2005) A distinct lineage of CD4 T cells regulates tissue inflammation by producing interleukin 17. *Nat Immunol*, 6, 1133-41.
- PARKER, D. C. (1993) T cell-dependent B cell activation. *Annu Rev Immunol*, 11, 331-60.
- PASPARAKIS, M., COURTOIS, G., HAFNER, M., SCHMIDT-SUPPRIAN, M., NENCI, A., TOKSOY, A., KRAMPERT, M., GOEBELER, M., GILLITZER, R., ISRAEL, A., KRIEG, T., RAJEWSKY, K. & HAASE, I. (2002) TNF-mediated inflammatory skin disease in mice with epidermis-specific deletion of IKK2. *Nature*, 417, 861-6.
- PASSLICK, B., FLIEGER, D. & ZIEGLER-HEITBROCK, H. W. (1989) Identification and characterization of a novel monocyte subpopulation in human peripheral blood. *Blood*, 74, 2527-34.
- PATEL, D. D., ZACHARIAH, J. P. & WHICHARD, L. P. (2001) CXCR3 and CCR5 ligands in rheumatoid arthritis synovium. *Clin Immunol*, 98, 39-45.
- PATTERSON, A. M., SIDDALL, H., CHAMBERLAIN, G., GARDNER, L. & MIDDLETON, J. (2002) Expression of the duffy antigen/receptor for chemokines (DARC) by the inflamed synovial endothelium. *J Pathol*, 197, 108-16.
- PEASE, J. E. & WILLIAMS, T. J. (2006) The attraction of chemokines as a target for specific anti-inflammatory therapy. *Br J Pharmacol*, 147 Suppl 1, S212-21.
- PEICHEV, M., NAIYER, A. J., PEREIRA, D., ZHU, Z., LANE, W. J., WILLIAMS, M., OZ, M. C., HICKLIN, D. J., WITTE, L., MOORE, M. A. & RAFII, S. (2000) Expression of VEGFR-2 and AC133 by circulating human CD34(+) cells identifies a population of functional endothelial precursors. *Blood*, 95, 952-8.
- PEIPER, S. C., WANG, Z. X., NEOTE, K., MARTIN, A. W., SHOWELL, H. J., CONKLYN, M. J., OGBORNE, K., HADLEY, T. J., LU, Z. H., HESSELGESSER, J. & HORUK, R. (1995) The Duffy antigen/receptor for chemokines (DARC) is expressed in endothelial cells of Duffy negative individuals who lack the erythrocyte receptor. *J Exp Med*, 181, 1311-7.

- PELED, A., GRABOVSKY, V., HABLER, L., SANDBANK, J., ARENZANA-SEISDEDOS, F., PETIT, I., BEN-HUR, H., LAPIDOT, T. & ALON, R. (1999) The chemokine SDF-1 stimulates integrin-mediated arrest of CD34(+) cells on vascular endothelium under shear flow. *J Clin Invest*, 104, 1199-211.
- PENE, J., CHEVALIER, S., PREISSER, L., VENEREAU, E., GUILLEUX, M. H., GHANNAM, S., MOLES, J. P., DANGER, Y., RAVON, E., LESAUX, S., YSSEL, H. & GASCAN, H. (2008) Chronically inflamed human tissues are infiltrated by highly differentiated Th17 lymphocytes. *J Immunol*, 180, 7423-30.
- PERRIGOU, J. G., SAENZ, S. A., SIRACUSA, M. C., ALLENSPACH, E. J., TAYLOR, B. C., GIACOMIN, P. R., NAIR, M. G., DU, Y., ZAPH, C., VAN ROOIJEN, N., COMEAU, M. R., PEARCE, E. J., LAUFER, T. M. & ARTIS, D. (2009) MHC class II-dependent basophil-CD4+ T cell interactions promote T(H)2 cytokine-dependent immunity. *Nat Immunol*, 10, 697-705.
- PETERING, H., KLUTHE, C., DULKYS, Y., KIEHL, P., PONATH, P. D., KAPP, A. & ELSNER, J. (2001) Characterization of the CC chemokine receptor 3 on human keratinocytes. *J Invest Dermatol*, 116, 549-55.
- PETIT-FRERE, C., CLINGEN, P. H., GREWE, M., KRUTMANN, J., ROZA, L., ARLETT, C. F. & GREEN, M. H. (1998) Induction of interleukin-6 production by ultraviolet radiation in normal human epidermal keratinocytes and in a human keratinocyte cell line is mediated by DNA damage. *J Invest Dermatol*, 111, 354-9.
- PETIT, I., JIN, D. & RAFII, S. (2007) The SDF-1-CXCR4 signaling pathway: a molecular hub modulating neo-angiogenesis. *Trends Immunol*, 28, 299-307.
- PETRAI, I., ROMBOUITS, K., LASAGNI, L., ANNUNZIATO, F., COSMI, L., ROMANELLI, R. G., SAGRINATI, C., MAZZINGHI, B., PINZANI, M., ROMAGNANI, S., ROMAGNANI, P. & MARRA, F. (2008) Activation of p38(MAPK) mediates the angiostatic effect of the chemokine receptor CXCR3-B. *Int J Biochem Cell Biol*, 40, 1764-74.
- PHILLIPS, J. & EBERWINE, J. H. (1996) Antisense RNA Amplification: A Linear Amplification Method for Analyzing the mRNA Population from Single Living Cells. *Methods*, 10, 283-8.
- PHILLIPSON, M., HEIT, B., COLARUSSO, P., LIU, L., BALLANTYNE, C. M. & KUBES, P. (2006) Intraluminal crawling of neutrophils to emigration sites: a molecularly distinct process from adhesion in the recruitment cascade. *J Exp Med*, 203, 2569-75.
- PIGUET, P. F., GRAU, G. E., VESIN, C., LOETSCHER, H., GENTZ, R. & LESSLAUER, W. (1992) Evolution of collagen arthritis in mice is arrested by treatment with anti-tumour necrosis factor (TNF) antibody or a recombinant soluble TNF receptor. *Immunology*, 77, 510-4.
- PRINZ, J. C., VOLLMER, S., BOEHNCKE, W. H., MENSSEN, A., LAISNEY, I. & TROMMLER, P. (1999) Selection of conserved TCR VDJ rearrangements in chronic psoriatic plaques indicates a common antigen in psoriasis vulgaris. *Eur J Immunol*, 29, 3360-8.
- PROKSCH, E., BRANDNER, J. M. & JENSEN, J. M. (2008) The skin: an indispensable barrier. *Exp Dermatol*, 17, 1063-72.
- PRUENSTER, M., MUDDE, L., BOMBOSI, P., DIMITROVA, S., ZSAK, M., MIDDLETON, J., RICHMOND, A., GRAHAM, G. J., SEGERER, S., NIBBS, R. J. & ROT, A.

- (2009) The Duffy antigen receptor for chemokines transports chemokines and supports their promigratory activity. *Nat Immunol*, 10, 101-8.
- PTAK, W. & SZCZEPANIK, M. (1998) [Immunogerontology--aging of the immune system and its cause]. *Przegl Lek*, 55, 397-9.
- QUINONES, M. P., AHUJA, S. K., JIMENEZ, F., SCHAEFER, J., GARAVITO, E., RAO, A., CHENAUX, G., REDDICK, R. L., KUZIEL, W. A. & AHUJA, S. S. (2004) Experimental arthritis in CC chemokine receptor 2-null mice closely mimics severe human rheumatoid arthritis. *J Clin Invest*, 113, 856-66.
- QUIRICI, N., SOLIGO, D., CANEVA, L., SERVIDA, F., BOSSOLASCO, P. & DELILIERIS, G. L. (2001) Differentiation and expansion of endothelial cells from human bone marrow CD133(+) cells. *Br J Haematol*, 115, 186-94.
- RATAJCZAK, M. Z., MAJKA, M., KUCIA, M., DRUKALA, J., PIETRZKOWSKI, Z., PEIPER, S. & JANOWSKA-WIECZOREK, A. (2003) Expression of functional CXCR4 by muscle satellite cells and secretion of SDF-1 by muscle-derived fibroblasts is associated with the presence of both muscle progenitors in bone marrow and hematopoietic stem/progenitor cells in muscles. *Stem Cells*, 21, 363-71.
- RATAJCZAK, M. Z., ZUBA-SURMA, E., KUCIA, M., RECA, R., WOJAKOWSKI, W. & RATAJCZAK, J. (2006) The pleiotropic effects of the SDF-1-CXCR4 axis in organogenesis, regeneration and tumorigenesis. *Leukemia*, 20, 1915-24.
- RATZINGER, G., STOITZNER, P., EBNER, S., LUTZ, M. B., LAYTON, G. T., RAINER, C., SENIOR, R. M., SHIPLEY, J. M., FRITSCH, P., SCHULER, G. & ROMANI, N. (2002) Matrix metalloproteinases 9 and 2 are necessary for the migration of Langerhans cells and dermal dendritic cells from human and murine skin. *J Immunol*, 168, 4361-71.
- REBOLDI, A., COISNE, C., BAUMJOHANN, D., BENVENUTO, F., BOTTINELLI, D., LIRA, S., UCCELLI, A., LANZAVECCHIA, A., ENGELHARDT, B. & SALLUSTO, F. (2009) C-C chemokine receptor 6-regulated entry of TH-17 cells into the CNS through the choroid plexus is required for the initiation of EAE. *Nat Immunol*, 10, 514-23.
- REICHE, E. M., BONAMETTI, A. M., VOLTARELLI, J. C., MORIMOTO, H. K. & WATANABE, M. A. (2007) Genetic polymorphisms in the chemokine and chemokine receptors: impact on clinical course and therapy of the human immunodeficiency virus type 1 infection (HIV-1). *Curr Med Chem*, 14, 1325-34.
- REIF, K., EKLAND, E. H., OHL, L., NAKANO, H., LIPP, M., FORSTER, R. & CYSTER, J. G. (2002) Balanced responsiveness to chemoattractants from adjacent zones determines B-cell position. *Nature*, 416, 94-9.
- REISS, Y., PROUDFOOT, A. E., POWER, C. A., CAMPBELL, J. J. & BUTCHER, E. C. (2001) CC chemokine receptor (CCR)4 and the CCR10 ligand cutaneous T cell-attracting chemokine (CTACK) in lymphocyte trafficking to inflamed skin. *J Exp Med*, 194, 1541-7.
- REUTERSHAN, J., HARRY, B., CHANG, D., BAGBY, G. J. & LEY, K. (2009) DARC on RBC limits lung injury by balancing compartmental distribution of CXC chemokines. *Eur J Immunol*, 39, 1597-607.
- ROBAK, T., GLADALSKA, A., STEPIEN, H. & ROBAK, E. (1998) Serum levels of interleukin-6 type cytokines and soluble interleukin-6 receptor in patients with rheumatoid arthritis. *Mediators Inflamm*, 7, 347-53.

- ROBINSON, E., KEYSTONE, E. C., SCHALL, T. J., GILLET, N. & FISH, E. N. (1995) Chemokine expression in rheumatoid arthritis (RA): evidence of RANTES and macrophage inflammatory protein (MIP)-1 beta production by synovial T cells. *Clin Exp Immunol*, 101, 398-407.
- ROBINSON, S. C., SCOTT, K. A. & BALKWILL, F. R. (2002) Chemokine stimulation of monocyte matrix metalloproteinase-9 requires endogenous TNF-alpha. *Eur J Immunol*, 32, 404-12.
- ROMAGNANI, P., ANNUNZIATO, F., LASAGNI, L., LAZZERI, E., BELTRAME, C., FRANCALANCI, M., UGUCCIONI, M., GALLI, G., COSMI, L., MAURENZIG, L., BAGGIOLINI, M., MAGGI, E., ROMAGNANI, S. & SERIO, M. (2001) Cell cycle-dependent expression of CXC chemokine receptor 3 by endothelial cells mediates angiostatic activity. *J Clin Invest*, 107, 53-63.
- ROMAGNANI, P., DE PAULIS, A., BELTRAME, C., ANNUNZIATO, F., DENTE, V., MAGGI, E., ROMAGNANI, S. & MARONE, G. (1999) Tryptase-chymase double-positive human mast cells express the eotaxin receptor CCR3 and are attracted by CCR3-binding chemokines. *Am J Pathol*, 155, 1195-204.
- ROMANO, M., FAGGIONI, R., SIRONI, M., SACCO, S., ECHTENACHER, B., DI SANTO, E., SALMONA, M. & GHEZZI, P. (1997) Carrageenan-induced acute inflammation in the mouse air pouch synovial model. Role of tumour necrosis factor. *Mediators Inflamm*, 6, 32-8.
- ROOS, D., VAN BRUGGEN, R. & MEISCHL, C. (2003) Oxidative killing of microbes by neutrophils. *Microbes Infect*, 5, 1307-15.
- ROOS, R. S., LOETSCHER, M., LEGLER, D. F., CLARK-LEWIS, I., BAGGIOLINI, M. & MOSER, B. (1997) Identification of CCR8, the receptor for the human CC chemokine I-309. *J Biol Chem*, 272, 17251-4.
- ROSE-JOHN, S. & HEINRICH, P. C. (1994) Soluble receptors for cytokines and growth factors: generation and biological function. *Biochem J*, 300 ( Pt 2), 281-90.
- ROSENZWEIG, S. D. (2008) Inflammatory manifestations in chronic granulomatous disease (CGD). *J Clin Immunol*, 28 Suppl 1, S67-72.
- ROSU-MYLES, M., GALLACHER, L., MURDOCH, B., HESS, D. A., KEENEY, M., KELVIN, D., DALE, L., FERGUSON, S. S., WU, D., FELLOWS, F. & BHATIA, M. (2000) The human hematopoietic stem cell compartment is heterogeneous for CXCR4 expression. *Proc Natl Acad Sci U S A*, 97, 14626-31.
- ROT, A. & VON ANDRIAN, U. H. (2004) Chemokines in innate and adaptive host defense: basic chemokine grammar for immune cells. *Annu Rev Immunol*, 22, 891-928.
- ROTTMAN, J. B., SLAVIN, A. J., SILVA, R., WEINER, H. L., GERARD, C. G. & HANCOCK, W. W. (2000) Leukocyte recruitment during onset of experimental allergic encephalomyelitis is CCR1 dependent. *Eur J Immunol*, 30, 2372-7.
- ROTTMAN, J. B., SMITH, T. L., GANLEY, K. G., KIKUCHI, T. & KRUEGER, J. G. (2001) Potential role of the chemokine receptors CXCR3, CCR4, and the integrin alphaEbeta7 in the pathogenesis of psoriasis vulgaris. *Lab Invest*, 81, 335-47.

- ROZIS, G., BENLAHRECH, A., DURAISINGHAM, S., GOTCH, F. & PATTERSON, S. (2008) Human Langerhans' cells and dermal-type dendritic cells generated from CD34 stem cells express different toll-like receptors and secrete different cytokines in response to toll-like receptor ligands. *Immunology*, 124, 329-38.
- RUCKERT, R., ASADULLAH, K., SEIFERT, M., BUDAGIAN, V. M., ARNOLD, R., TROMBOTTO, C., PAUS, R. & BULFONE-PAUS, S. (2000) Inhibition of keratinocyte apoptosis by IL-15: a new parameter in the pathogenesis of psoriasis? *J Immunol*, 165, 2240-50.
- SADAGURSKI, M., YAKAR, S., WEINGARTEN, G., HOLZENBERGER, M., RHODES, C. J., BREITKREUTZ, D., LEROITH, D. & WERTHEIMER, E. (2006) Insulin-like growth factor 1 receptor signaling regulates skin development and inhibits skin keratinocyte differentiation. *Mol Cell Biol*, 26, 2675-87.
- SAKAGUCHI, S., ONO, M., SETOGUCHI, R., YAGI, H., HORI, S., FEHERVARI, Z., SHIMIZU, J., TAKAHASHI, T. & NOMURA, T. (2006) Foxp3<sup>+</sup> CD25<sup>+</sup> CD4<sup>+</sup> natural regulatory T cells in dominant self-tolerance and autoimmune disease. *Immunol Rev*, 212, 8-27.
- SALAS, A., SHIMAOKA, M., KOGAN, A. N., HARWOOD, C., VON ANDRIAN, U. H. & SPRINGER, T. A. (2004) Rolling adhesion through an extended conformation of integrin alphaLbeta2 and relation to alpha I and beta I-like domain interaction. *Immunity*, 20, 393-406.
- SALCEDO, R., YOUNG, H. A., PONCE, M. L., WARD, J. M., KLEINMAN, H. K., MURPHY, W. J. & OPPENHEIM, J. J. (2001) Eotaxin (CCL11) induces in vivo angiogenic responses by human CCR3<sup>+</sup> endothelial cells. *J Immunol*, 166, 7571-8.
- SALLUSTO, F. & LANZAVECCHIA, A. (1994) Efficient presentation of soluble antigen by cultured human dendritic cells is maintained by granulocyte/macrophage colony-stimulating factor plus interleukin 4 and downregulated by tumor necrosis factor alpha. *J Exp Med*, 179, 1109-18.
- SALLUSTO, F., LENIG, D., FORSTER, R., LIPP, M. & LANZAVECCHIA, A. (1999) Two subsets of memory T lymphocytes with distinct homing potentials and effector functions. *Nature*, 401, 708-12.
- SANKARAN, B., OSTERHOUT, J., WU, D. & SMRCKA, A. V. (1998) Identification of a structural element in phospholipase C beta2 that interacts with G protein betagamma subunits. *J Biol Chem*, 273, 7148-54.
- SANO, S., CHAN, K. S., CARBAJAL, S., CLIFFORD, J., PEAVEY, M., KIGUCHI, K., ITAMI, S., NICKOLOFF, B. J. & DIGIOVANNI, J. (2005) Stat3 links activated keratinocytes and immunocytes required for development of psoriasis in a novel transgenic mouse model. *Nat Med*, 11, 43-9.
- SANTOSO, S., SACHS, U. J., KROLL, H., LINDER, M., RUF, A., PREISSNER, K. T. & CHAVAKIS, T. (2002) The junctional adhesion molecule 3 (JAM-3) on human platelets is a counterreceptor for the leukocyte integrin Mac-1. *J Exp Med*, 196, 679-91.
- SASAI, M., SAEKI, Y., OHSHIMA, S., NISHIOKA, K., MIMA, T., TANAKA, T., KATADA, Y., YOSHIZAKI, K., SUEMURA, M. & KISHIMOTO, T. (1999) Delayed onset and reduced severity of collagen-induced arthritis in interleukin-6-deficient mice. *Arthritis Rheum*, 42, 1635-43.

- SCHAERLI, P., WILLIMANN, K., LANG, A. B., LIPP, M., LOETSCHER, P. & MOSER, B. (2000) CXC chemokine receptor 5 expression defines follicular homing T cells with B cell helper function. *J Exp Med*, 192, 1553-62.
- SHELLEKENS, G. A., DE JONG, B. A., VAN DEN HOOGEN, F. H., VAN DE PUTTE, L. B. & VAN VENROOIJ, W. J. (1998) Citrulline is an essential constituent of antigenic determinants recognized by rheumatoid arthritis-specific autoantibodies. *J Clin Invest*, 101, 273-81.
- SCHENKEL, A. R., MAMDOUH, Z., CHEN, X., LIEBMAN, R. M. & MULLER, W. A. (2002) CD99 plays a major role in the migration of monocytes through endothelial junctions. *Nat Immunol*, 3, 143-50.
- SCHENKEL, A. R., MAMDOUH, Z. & MULLER, W. A. (2004) Locomotion of monocytes on endothelium is a critical step during extravasation. *Nat Immunol*, 5, 393-400.
- SCHLAAK, J. F., BUSLAU, M., JOCHUM, W., HERMANN, E., GIRNDT, M., GALLATI, H., MEYER ZUM BUSCHENFELDE, K. H. & FLEISCHER, B. (1994) T cells involved in psoriasis vulgaris belong to the Th1 subset. *J Invest Dermatol*, 102, 145-9.
- SCHNEIDER, G. B., RELFSON, M. & NICOLAS, J. (1986) Pluripotent hemopoietic stem cells give rise to osteoclasts. *Am J Anat*, 177, 505-11.
- SCHOLS, D., STRUYF, S., VAN DAMME, J., ESTE, J. A., HENSON, G. & DE CLERCQ, E. (1997) Inhibition of T-tropic HIV strains by selective antagonization of the chemokine receptor CXCR4. *J Exp Med*, 186, 1383-8.
- SCHONEMEIER, B., KOLODZIEJ, A., SCHULZ, S., JACOBS, S., HOELLT, V. & STUMM, R. (2008) Regional and cellular localization of the CXCL12/SDF-1 chemokine receptor CXCR7 in the developing and adult rat brain. *J Comp Neurol*, 510, 207-20.
- SCHRODER, J. M. & CHRISTOPHERS, E. (1986) Identification of C5ades arg and an anionic neutrophil-activating peptide (ANAP) in psoriatic scales. *J Invest Dermatol*, 87, 53-8.
- SCHWAB, J. M., CHIANG, N., ARITA, M. & SERHAN, C. N. (2007) Resolvin E1 and protectin D1 activate inflammation-resolution programmes. *Nature*, 447, 869-74.
- SCHWAB, S. R. & CYSTER, J. G. (2007) Finding a way out: lymphocyte egress from lymphoid organs. *Nat Immunol*, 8, 1295-301.
- SCHWAEBLE, W. J. & REID, K. B. (1999) Does properdin crosslink the cellular and the humoral immune response? *Immunol Today*, 20, 17-21.
- SCHWANDNER, R., DZIARSKI, R., WESCHE, H., ROTHE, M. & KIRSCHNING, C. J. (1999) Peptidoglycan- and lipoteichoic acid-induced cell activation is mediated by toll-like receptor 2. *J Biol Chem*, 274, 17406-9.
- SCHWEICKART, V. L., EPP, A., RAPORT, C. J. & GRAY, P. W. (2000) CCR11 is a functional receptor for the monocyte chemoattractant protein family of chemokines. *J Biol Chem*, 275, 9550-6.
- SEGERER, S., REGELE, H., MAC, K. M., KAIN, R., CARTRON, J. P., COLIN, Y., KERJASCHKI, D. & SCHLONDORFF, D. (2000) The Duffy antigen receptor for chemokines is up-regulated during acute renal transplant rejection and crescentic glomerulonephritis. *Kidney Int*, 58, 1546-56.

- SERHAN, C. N., BRAIN, S. D., BUCKLEY, C. D., GILROY, D. W., HASLETT, C., O'NEILL, L. A., PERRETTI, M., ROSSI, A. G. & WALLACE, J. L. (2007) Resolution of inflammation: state of the art, definitions and terms. *Faseb J*, 21, 325-32.
- SERHAN, C. N., CLISH, C. B., BRANNON, J., COLGAN, S. P., CHIANG, N. & GRONERT, K. (2000) Novel functional sets of lipid-derived mediators with antiinflammatory actions generated from omega-3 fatty acids via cyclooxygenase 2-nonsteroidal antiinflammatory drugs and transcellular processing. *J Exp Med*, 192, 1197-204.
- SERHAN, C. N., HONG, S., GRONERT, K., COLGAN, S. P., DEVCHAND, P. R., MIRICK, G. & MOUSSIGNAC, R. L. (2002) Resolvins: a family of bioactive products of omega-3 fatty acid transformation circuits initiated by aspirin treatment that counter proinflammation signals. *J Exp Med*, 196, 1025-37.
- SHAMRI, R., GRABOVSKY, V., GAUGUET, J. M., FEIGELSON, S., MANEVICH, E., KOLANUS, W., ROBINSON, M. K., STAUNTON, D. E., VON ANDRIAN, U. H. & ALON, R. (2005) Lymphocyte arrest requires instantaneous induction of an extended LFA-1 conformation mediated by endothelium-bound chemokines. *Nat Immunol*, 6, 497-506.
- SHARMA, D. K., CHOUDHURY, A., SINGH, R. D., WHEATLEY, C. L., MARKS, D. L. & PAGANO, R. E. (2003) Glycosphingolipids internalized via caveolar-related endocytosis rapidly merge with the clathrin pathway in early endosomes and form microdomains for recycling. *J Biol Chem*, 278, 7564-72.
- SHARP, L. L., JAMESON, J. M., CAUVI, G. & HAVRAN, W. L. (2005) Dendritic epidermal T cells regulate skin homeostasis through local production of insulin-like growth factor 1. *Nat Immunol*, 6, 73-9.
- SHAW, S. K., MA, S., KIM, M. B., RAO, R. M., HARTMAN, C. U., FROIO, R. M., YANG, L., JONES, T., LIU, Y., NUSRAT, A., PARKOS, C. A. & LUSCINSKAS, F. W. (2004) Coordinated redistribution of leukocyte LFA-1 and endothelial cell ICAM-1 accompany neutrophil transmigration. *J Exp Med*, 200, 1571-80.
- SHEIKINE, Y. & HANSSON, G. K. (2004) Chemokines and atherosclerosis. *Ann Med*, 36, 98-118.
- SHEN, H., SCHUSTER, R., STRINGER, K. F., WALTZ, S. E. & LENTSCH, A. B. (2006) The Duffy antigen/receptor for chemokines (DARC) regulates prostate tumor growth. *Faseb J*, 20, 59-64.
- SHI, G., PARTIDA-SANCHEZ, S., MISRA, R. S., TIGHE, M., BORCHERS, M. T., LEE, J. J., SIMON, M. I. & LUND, F. E. (2007) Identification of an alternative G $\alpha$ -dependent chemokine receptor signal transduction pathway in dendritic cells and granulocytes. *J Exp Med*, 204, 2705-18.
- SHIRATO, K., KIMURA, T., MIZUTANI, T., KARIWA, H. & TAKASHIMA, I. (2004) Different chemokine expression in lethal and non-lethal murine West Nile virus infection. *J Med Virol*, 74, 507-13.
- SHORTMAN, K. & LIU, Y. J. (2002) Mouse and human dendritic cell subtypes. *Nat Rev Immunol*, 2, 151-61.
- SICA, A., SACCANI, A., BOTTAZZI, B., POLENTARUTTI, N., VECCHI, A., VAN DAMME, J. & MANTOVANI, A. (2000) Autocrine production of IL-10 mediates defective IL-12 production and NF-kappa B activation in tumor-associated macrophages. *J Immunol*, 164, 762-7.

- SIERRO, F., BIBEN, C., MARTINEZ-MUNOZ, L., MELLADO, M., RANSOHOFF, R. M., LI, M., WOHL, B., LEUNG, H., GROOM, J., BATTEN, M., HARVEY, R. P., MARTINEZ, A. C., MACKAY, C. R. & MACKAY, F. (2007) Disrupted cardiac development but normal hematopoiesis in mice deficient in the second CXCL12/SDF-1 receptor, CXCR7. *Proc Natl Acad Sci U S A*, 104, 14759-64.
- SIGMUNSDOTTIR, H. & BUTCHER, E. C. (2008) Environmental cues, dendritic cells and the programming of tissue-selective lymphocyte trafficking. *Nat Immunol*, 9, 981-7.
- SIGMUNSDOTTIR, H., PAN, J., DEBES, G. F., ALT, C., HABTEZION, A., SOLER, D. & BUTCHER, E. C. (2007) DCs metabolize sunlight-induced vitamin D3 to 'program' T cell attraction to the epidermal chemokine CCL27. *Nat Immunol*, 8, 285-93.
- SIGNORET, N., HEWLETT, L., WAVRE, S., PELCHEN-MATTHEWS, A., OPPERMAN, M. & MARSH, M. (2005) Agonist-induced endocytosis of CC chemokine receptor 5 is clathrin dependent. *Mol Biol Cell*, 16, 902-17.
- SIMS, J. E., GAYLE, M. A., SLACK, J. L., ALDERSON, M. R., BIRD, T. A., GIRI, J. G., COLOTTA, F., RE, F., MANTOVANI, A., SHANEBECK, K. & ET AL. (1993) Interleukin 1 signaling occurs exclusively via the type I receptor. *Proc Natl Acad Sci U S A*, 90, 6155-9.
- SIMS, J. E., NICKLIN, M. J., BAZAN, J. F., BARTON, J. L., BUSFIELD, S. J., FORD, J. E., KASTELEIN, R. A., KUMAR, S., LIN, H., MULERO, J. J., PAN, J., PAN, Y., SMITH, D. E. & YOUNG, P. R. (2001) A new nomenclature for IL-1-family genes. *Trends Immunol*, 22, 536-7.
- SINGH, S., SINGH, U. P., STILES, J. K., GRIZZLE, W. E. & LILLARD, J. W., JR. (2004) Expression and functional role of CCR9 in prostate cancer cell migration and invasion. *Clin Cancer Res*, 10, 8743-50.
- SMITH, C. H. & BARKER, J. N. (2006) Psoriasis and its management. *Bmj*, 333, 380-4.
- SOKOL, C. L., CHU, N. Q., YU, S., NISH, S. A., LAUFER, T. M. & MEDZHITOV, R. (2009) Basophils function as antigen-presenting cells for an allergen-induced T helper type 2 response. *Nat Immunol*, 10, 713-20.
- SONNICHSEN, B., DE RENZIS, S., NIELSEN, E., RIETDORF, J. & ZERIAL, M. (2000) Distinct membrane domains on endosomes in the recycling pathway visualized by multicolor imaging of Rab4, Rab5, and Rab11. *J Cell Biol*, 149, 901-14.
- SOZZANI, S., LUINI, W., BIANCHI, G., ALLAVENA, P., WELLS, T. N., NAPOLITANO, M., BERNARDINI, G., VECCHI, A., D'AMBROSIO, D., MAZZEO, D., SINIGAGLIA, F., SANTONI, A., MAGGI, E., ROMAGNANI, S. & MANTOVANI, A. (1998) The viral chemokine macrophage inflammatory protein-II is a selective Th2 chemoattractant. *Blood*, 92, 4036-9.
- SOZZANI, S., SALLUSTO, F., LUINI, W., ZHOU, D., PIEMONTE, L., ALLAVENA, P., VAN DAMME, J., VALITUTTI, S., LANZAVECCHIA, A. & MANTOVANI, A. (1995) Migration of dendritic cells in response to formyl peptides, C5a, and a distinct set of chemokines. *J Immunol*, 155, 3292-5.
- STANLEY, P. L., STEINER, S., HAVENS, M. & TRAMPOSCH, K. M. (1991) Mouse skin inflammation induced by multiple topical applications of 12-O-tetradecanoylphorbol-13-acetate. *Skin Pharmacol*, 4, 262-71.

- STEINMAN, L. (2007) A brief history of T(H)17, the first major revision in the T(H)1/T(H)2 hypothesis of T cell-mediated tissue damage. *Nat Med*, 13, 139-45.
- STEINMAN, R. M. & COHN, Z. A. (1973) Identification of a novel cell type in peripheral lymphoid organs of mice. I. Morphology, quantitation, tissue distribution. *J Exp Med*, 137, 1142-62.
- STEPHENS, L., SMRCKA, A., COOKE, F. T., JACKSON, T. R., STERNWEIS, P. C. & HAWKINS, P. T. (1994) A novel phosphoinositide 3 kinase activity in myeloid-derived cells is activated by G protein beta gamma subunits. *Cell*, 77, 83-93.
- STRATIS, A., PASPARAKIS, M., RUPEC, R. A., MARKUR, D., HARTMANN, K., SCHARFFETTER-KOCHANNEK, K., PETERS, T., VAN ROOIJEN, N., KRIEG, T. & HAASE, I. (2006) Pathogenic role for skin macrophages in a mouse model of keratinocyte-induced psoriasis-like skin inflammation. *J Clin Invest*, 116, 2094-104.
- STRIETER, R. M., BURDICK, M. D., GOMPERTS, B. N., BELPERIO, J. A. & KEANE, M. P. (2005) CXC chemokines in angiogenesis. *Cytokine Growth Factor Rev*, 16, 593-609.
- STRIETER, R. M., POLVERINI, P. J., KUNKEL, S. L., ARENBERG, D. A., BURDICK, M. D., KASPER, J., DZUIBA, J., VAN DAMME, J., WALZ, A., MARRIOTT, D. & ET AL. (1995) The functional role of the ELR motif in CXC chemokine-mediated angiogenesis. *J Biol Chem*, 270, 27348-57.
- STRUNK, D., EGGER, C., LEITNER, G., HANAU, D. & STINGL, G. (1997) A skin homing molecule defines the langerhans cell progenitor in human peripheral blood. *J Exp Med*, 185, 1131-6.
- STRUYF, S., PROOST, P. & VAN DAMME, J. (2003) Regulation of the immune response by the interaction of chemokines and proteases. *Adv Immunol*, 81, 1-44.
- SUGITA, K., KABASHIMA, K., ATARASHI, K., SHIMAUCHI, T., KOBAYASHI, M. & TOKURA, Y. (2007) Innate immunity mediated by epidermal keratinocytes promotes acquired immunity involving Langerhans cells and T cells in the skin. *Clin Exp Immunol*, 147, 176-83.
- SUGIYAMA, H., GYULAI, R., TOICHI, E., GARACZI, E., SHIMADA, S., STEVENS, S. R., MCCORMICK, T. S. & COOPER, K. D. (2005) Dysfunctional blood and target tissue CD4<sup>+</sup>CD25<sup>high</sup> regulatory T cells in psoriasis: mechanism underlying unrestrained pathogenic effector T cell proliferation. *J Immunol*, 174, 164-73.
- SUN, W. H., BURKHOLDER, J. K., SUN, J., CULP, J., TURNER, J., LU, X. G., PUGH, T. D., ERSHLER, W. B. & YANG, N. S. (1995) In vivo cytokine gene transfer by gene gun reduces tumor growth in mice. *Proc Natl Acad Sci U S A*, 92, 2889-93.
- SUTO, H., NAKAE, S., KAKURAI, M., SEDGWICK, J. D., TSAI, M. & GALLI, S. J. (2006) Mast cell-associated TNF promotes dendritic cell migration. *J Immunol*, 176, 4102-12.
- SWANSON, J. A. & HOPPE, A. D. (2004) The coordination of signaling during Fc receptor-mediated phagocytosis. *J Leukoc Biol*, 76, 1093-103.

- SWEENEY, S. E. & FIRESTEIN, G. S. (2004) Rheumatoid arthritis: regulation of synovial inflammation. *Int J Biochem Cell Biol*, 36, 372-8.
- SYMMONS, D., TURNER, G., WEBB, R., ASTEN, P., BARRETT, E., LUNT, M., SCOTT, D. & SILMAN, A. (2002) The prevalence of rheumatoid arthritis in the United Kingdom: new estimates for a new century. *Rheumatology (Oxford)*, 41, 793-800.
- SYRBE, U., SIVEKE, J. & HAMANN, A. (1999) Th1/Th2 subsets: distinct differences in homing and chemokine receptor expression? *Springer Semin Immunopathol*, 21, 263-85.
- SZABO, I., WETZEL, M. A. & ROGERS, T. J. (2001) Cell-density-regulated chemotactic responsiveness of keratinocytes in vitro. *J Invest Dermatol*, 117, 1083-90.
- SZANYA, V., ERMANN, J., TAYLOR, C., HOLNESS, C. & FATHMAN, C. G. (2002) The subpopulation of CD4+CD25+ splenocytes that delays adoptive transfer of diabetes expresses L-selectin and high levels of CCR7. *J Immunol*, 169, 2461-5.
- SZEKANECZ, Z., KIM, J. & KOCH, A. E. (2003) Chemokines and chemokine receptors in rheumatoid arthritis. *Semin Immunol*, 15, 15-21.
- TAGA, T., HIBI, M., HIRATA, Y., YAMASAKI, K., YASUKAWA, K., MATSUDA, T., HIRANO, T. & KISHIMOTO, T. (1989) Interleukin-6 triggers the association of its receptor with a possible signal transducer, gp130. *Cell*, 58, 573-81.
- TAKANAMI, I. (2003) Overexpression of CCR7 mRNA in nonsmall cell lung cancer: correlation with lymph node metastasis. *Int J Cancer*, 105, 186-9.
- TAKEUCHI, O., KAWAI, T., MUHLRADT, P. F., MORR, M., RADOLF, J. D., ZYCHLINSKY, A., TAKEDA, K. & AKIRA, S. (2001) Discrimination of bacterial lipoproteins by Toll-like receptor 6. *Int Immunol*, 13, 933-40.
- TAKEUCHI, O., SATO, S., HORIUCHI, T., HOSHINO, K., TAKEDA, K., DONG, Z., MODLIN, R. L. & AKIRA, S. (2002) Cutting edge: role of Toll-like receptor 1 in mediating immune response to microbial lipoproteins. *J Immunol*, 169, 10-4.
- TAKEUCHI, T., WATANABE, Y., TAKANO-SHIMIZU, T. & KONDO, S. (2006) Roles of jumonji and jumonji family genes in chromatin regulation and development. *Dev Dyn*, 235, 2449-59.
- TANG, P., HUNG, M. C. & KLOSTERGAARD, J. (1996) Human pro-tumor necrosis factor is a homotrimer. *Biochemistry*, 35, 8216-25.
- TAYLOR, P. R., TSONI, S. V., WILLMENT, J. A., DENNEHY, K. M., ROSAS, M., FINDON, H., HAYNES, K., STEELE, C., BOTTO, M., GORDON, S. & BROWN, G. D. (2007) Dectin-1 is required for beta-glucan recognition and control of fungal infection. *Nat Immunol*, 8, 31-8.
- TELFER, N. R., CHALMERS, R. J., WHALE, K. & COLMAN, G. (1992) The role of streptococcal infection in the initiation of guttate psoriasis. *Arch Dermatol*, 128, 39-42.
- TENNANT, S. M., HARTLAND, E. L., PHUMOONNA, T., LYRAS, D., ROOD, J. I., ROBINS-BROWNE, R. M. & VAN DRIEL, I. R. (2008) Influence of gastric acid on susceptibility to infection with ingested bacterial pathogens. *Infect Immun*, 76, 639-45.

- TERMEER, C., BENEDIX, F., SLEEMAN, J., FIEBER, C., VOITH, U., AHRENS, T., MIYAKE, K., FREUDENBERG, M., GALANOS, C. & SIMON, J. C. (2002) Oligosaccharides of Hyaluronan activate dendritic cells via toll-like receptor 4. *J Exp Med*, 195, 99-111.
- TEUNISSEN, M. B., KOOMEN, C. W., DE WAAL MALEFYT, R., WIERENGA, E. A. & BOS, J. D. (1998) Interleukin-17 and interferon-gamma synergize in the enhancement of proinflammatory cytokine production by human keratinocytes. *J Invest Dermatol*, 111, 645-9.
- THELEN, M. (2001) Dancing to the tune of chemokines. *Nat Immunol*, 2, 129-34.
- THIERFELDER, W. E., VAN DEURSEN, J. M., YAMAMOTO, K., TRIPP, R. A., SARAWAR, S. R., CARSON, R. T., SANGSTER, M. Y., VIGNALI, D. A., DOHERTY, P. C., GROSVELD, G. C. & IHLE, J. N. (1996) Requirement for Stat4 in interleukin-12-mediated responses of natural killer and T cells. *Nature*, 382, 171-4.
- THORNBERRY, N. A., BULL, H. G., CALAYCAY, J. R., CHAPMAN, K. T., HOWARD, A. D., KOSTURA, M. J., MILLER, D. K., MOLINEAUX, S. M., WEIDNER, J. R., AUNINS, J. & ET AL. (1992) A novel heterodimeric cysteine protease is required for interleukin-1 beta processing in monocytes. *Nature*, 356, 768-74.
- TONEGAWA, S. (1983) Somatic generation of antibody diversity. *Nature*, 302, 575-81.
- TOURNAMILLE, C., COLIN, Y., CARTRON, J. P. & LE VAN KIM, C. (1995) Disruption of a GATA motif in the Duffy gene promoter abolishes erythroid gene expression in Duffy-negative individuals. *Nat Genet*, 10, 224-8.
- TOURNAMILLE, C., LE VAN KIM, C., GANE, P., BLANCHARD, D., PROUDFOOT, A. E., CARTRON, J. P. & COLIN, Y. (1997) Close association of the first and fourth extracellular domains of the Duffy antigen/receptor for chemokines by a disulfide bond is required for ligand binding. *J Biol Chem*, 272, 16274-80.
- TOWNSON, J. R., BARCELLOS, L. F. & NIBBS, R. J. (2002) Gene copy number regulates the production of the human chemokine CCL3-L1. *Eur J Immunol*, 32, 3016-26.
- TOWNSON, J. R. & NIBBS, R. J. (2002) Characterization of mouse CCX-CKR, a receptor for the lymphocyte-attracting chemokines TECK/mCCL25, SLC/mCCL21 and MIP-3beta/mCCL19: comparison to human CCX-CKR. *Eur J Immunol*, 32, 1230-41.
- TURKSEN, K., KUPPER, T., DEGENSTEIN, L., WILLIAMS, I. & FUCHS, E. (1992) Interleukin 6: insights to its function in skin by overexpression in transgenic mice. *Proc Natl Acad Sci U S A*, 89, 5068-72.
- TZU, J. & KERDEL, F. (2008) From conventional to cutting edge: the new era of biologics in treatment of psoriasis. *Dermatol Ther*, 21, 131-41.
- UEHARA, S., GRINBERG, A., FARBER, J. M. & LOVE, P. E. (2002) A role for CCR9 in T lymphocyte development and migration. *J Immunol*, 168, 2811-9.
- ULLRICH, O., REINSCH, S., URBE, S., ZERIAL, M. & PARTON, R. G. (1996) Rab11 regulates recycling through the pericentriolar recycling endosome. *J Cell Biol*, 135, 913-24.

- ULLUM, H., COZZI LEPRI, A., VICTOR, J., ALADDIN, H., PHILLIPS, A. N., GERSTOFT, J., SKINHOJ, P. & PEDERSEN, B. K. (1998) Production of beta-chemokines in human immunodeficiency virus (HIV) infection: evidence that high levels of macrophage inflammatory protein-1beta are associated with a decreased risk of HIV disease progression. *J Infect Dis*, 177, 331-6.
- UYEMURA, K., YAMAMURA, M., FIVENSON, D. F., MODLIN, R. L. & NICKOLOFF, B. J. (1993) The cytokine network in lesional and lesion-free psoriatic skin is characterized by a T-helper type 1 cell-mediated response. *J Invest Dermatol*, 101, 701-5.
- VALERIO, A., FERRARIO, M., MARTINEZ, F. O., LOCATI, M., GHISI, V., BRESCIANI, L. G., MANTOVANI, A. & SPANO, P. (2004) Gene expression profile activated by the chemokine CCL5/RANTES in human neuronal cells. *J Neurosci Res*, 78, 371-82.
- VALLADEAU, J., RAVEL, O., DEZUTTER-DAMBUYANT, C., MOORE, K., KLEIJMEER, M., LIU, Y., DUVERT-FRANCES, V., VINCENT, C., SCHMITT, D., DAVOUST, J., CAUX, C., LEBECQUE, S. & SAELAND, S. (2000) Langerin, a novel C-type lectin specific to Langerhans cells, is an endocytic receptor that induces the formation of Birbeck granules. *Immunity*, 12, 71-81.
- VAN DER SLUIJS, P., HULL, M., WEBSTER, P., MALE, P., GOUD, B. & MELLMAN, I. (1992) The small GTP-binding protein rab4 controls an early sorting event on the endocytic pathway. *Cell*, 70, 729-40.
- VASSAR, R., ROSENBERG, M., ROSS, S., TYNER, A. & FUCHS, E. (1989) Tissue-specific and differentiation-specific expression of a human K14 keratin gene in transgenic mice. *Proc Natl Acad Sci U S A*, 86, 1563-7.
- VELDHOEN, M., UYTENHOVE, C., VAN SNICK, J., HELMBY, H., WESTENDORF, A., BUER, J., MARTIN, B., WILHELM, C. & STOCKINGER, B. (2008) Transforming growth factor-beta 'reprograms' the differentiation of T helper 2 cells and promotes an interleukin 9-producing subset. *Nat Immunol*, 9, 1341-6.
- VENKATESAN, S., ROSE, J. J., LODGE, R., MURPHY, P. M. & FOLEY, J. F. (2003) Distinct mechanisms of agonist-induced endocytosis for human chemokine receptors CCR5 and CXCR4. *Mol Biol Cell*, 14, 3305-24.
- VESTERGAARD, C., JUST, H., BAUMGARTNER NIELSEN, J., THESTRUP-PEDERSEN, K. & DELEURAN, M. (2004) Expression of CCR2 on monocytes and macrophages in chronically inflamed skin in atopic dermatitis and psoriasis. *Acta Derm Venereol*, 84, 353-8.
- VETRANO, S., BORRONI, E. M., SARUKHAN, A., SAVINO, B., BONECCHI, R., CORREALE, C., ARENA, V., FANTINI, M., RONCALLI, M., MALESCI, A., MANTOVANI, A., LOCATI, M. & DANESE, S. (2009) The lymphatic system controls intestinal inflammation and inflammation-associated colon cancer through the chemokine decoy receptor D6. *Gut*.
- VICARI, A. P., AIT-YAHIA, S., CHEMIN, K., MUELLER, A., ZLOTNIK, A. & CAUX, C. (2000) Antitumor effects of the mouse chemokine 6Ckine/SLC through angiostatic and immunological mechanisms. *J Immunol*, 165, 1992-2000.
- VIELHAUER, V., ALLAM, R., LINDENMEYER, M. T., COHEN, C. D., DRAGANOVICI, D., MANDELBAUM, J., ELTRICH, N., NELSON, P. J., ANDERS, H. J., PRUENSTER, M., ROT, A., SCHLONDORFF, D. & SEGERER, S. (2009)

Efficient renal recruitment of macrophages and T cells in mice lacking the duffy antigen/receptor for chemokines. *Am J Pathol*, 175, 119-31.

- VILCEK, J. & FELDMANN, M. (2004) Historical review: Cytokines as therapeutics and targets of therapeutics. *Trends Pharmacol Sci*, 25, 201-9.
- VILLADSEN, L. S., SCHUURMAN, J., BEURSKENS, F., DAM, T. N., DAGNAES-HANSEN, F., SKOV, L., RYGAARD, J., VOORHORST-OGINK, M. M., GERRITSEN, A. F., VAN DIJK, M. A., PARREN, P. W., BAADSGAARD, O. & VAN DE WINKEL, J. G. (2003) Resolution of psoriasis upon blockade of IL-15 biological activity in a xenograft mouse model. *J Clin Invest*, 112, 1571-80.
- VILLARES, R., CADENAS, V., LOZANO, M., ALMONACID, L., ZABALLOS, A., MARTINEZ, A. C. & VARONA, R. (2009) CCR6 regulates EAE pathogenesis by controlling regulatory CD4<sup>+</sup> T-cell recruitment to target tissues. *Eur J Immunol*, 39, 1671-81.
- VIVANCO, I. & SAWYERS, C. L. (2002) The phosphatidylinositol 3-Kinase AKT pathway in human cancer. *Nat Rev Cancer*, 2, 489-501.
- VOIGT, I., CAMACHO, S. A., DE BOER, B. A., LIPP, M., FORSTER, R. & BEREK, C. (2000) CXCR5-deficient mice develop functional germinal centers in the splenic T cell zone. *Eur J Immunol*, 30, 560-7.
- VOLIN, M. V., WOODS, J. M., AMIN, M. A., CONNORS, M. A., HARLOW, L. A. & KOCH, A. E. (2001) Fractalkine: a novel angiogenic chemokine in rheumatoid arthritis. *Am J Pathol*, 159, 1521-30.
- VOLLMER, S., MENSSSEN, A. & PRINZ, J. C. (2001) Dominant lesional T cell receptor rearrangements persist in relapsing psoriasis but are absent from nonlesional skin: evidence for a stable antigen-specific pathogenic T cell response in psoriasis vulgaris. *J Invest Dermatol*, 117, 1296-301.
- VON ANDRIAN, U. H. & MEMPEL, T. R. (2003) Homing and cellular traffic in lymph nodes. *Nat Rev Immunol*, 3, 867-78.
- VON HUNDELSHAUSEN, P., WEBER, K. S., HUO, Y., PROUDFOOT, A. E., NELSON, P. J., LEY, K. & WEBER, C. (2001) RANTES deposition by platelets triggers monocyte arrest on inflamed and atherosclerotic endothelium. *Circulation*, 103, 1772-7.
- WALPORT, M. J. (2001) Complement. First of two parts. *N Engl J Med*, 344, 1058-66.
- WANG, C., KANG, S. G., LEE, J., SUN, Z. & KIM, C. H. (2009) The roles of CCR6 in migration of Th17 cells and regulation of effector T-cell balance in the gut. *Mucosal Immunol*, 2, 173-83.
- WANG, C. R., LIU, M. F., HUANG, Y. H. & CHEN, H. C. (2004a) Up-regulation of XCR1 expression in rheumatoid joints. *Rheumatology (Oxford)*, 43, 569-73.
- WANG, H., PETERS, T., KESS, D., SINDRILARU, A., ORESHKOVA, T., VAN ROOIJEN, N., STRATIS, A., RENKL, A. C., SUNDERKOTTER, C., WLASCHEK, M., HAASE, I. & SCHARFFETTER-KOCHANNEK, K. (2006) Activated macrophages are essential in a murine model for T cell-mediated chronic psoriasiform skin inflammation. *J Clin Invest*, 116, 2105-14.

- WANG, J., KOBAYASHI, Y., SATO, A., KOBAYASHI, E. & MURAKAMI, T. (2004b) Synergistic anti-tumor effect by combinatorial gene-gun therapy using IL-23 and IL-18 cDNA. *J Dermatol Sci*, 36, 66-8.
- WANG, J., SHIOZAWA, Y., WANG, J., WANG, Y., JUNG, Y., PIENTA, K. J., MEHRA, R., LOBERG, R. & TAICHMAN, R. S. (2008) The role of CXCR7/RDC1 as a chemokine receptor for CXCL12/SDF-1 in prostate cancer. *J Biol Chem*, 283, 4283-94.
- WANG, W., SOTO, H., OLDHAM, E. R., BUCHANAN, M. E., HOMEY, B., CATRON, D., JENKINS, N., COPELAND, N. G., GILBERT, D. J., NGUYEN, N., ABRAMS, J., KERSHENOVICH, D., SMITH, K., MCCLANAHAN, T., VICARI, A. P. & ZLOTNIK, A. (2000) Identification of a novel chemokine (CCL28), which binds CCR10 (GPR2). *J Biol Chem*, 275, 22313-23.
- WANG, X., FEUERSTEIN, G. Z., GU, J. L., LYSKO, P. G. & YUE, T. L. (1995) Interleukin-1 beta induces expression of adhesion molecules in human vascular smooth muscle cells and enhances adhesion of leukocytes to smooth muscle cells. *Atherosclerosis*, 115, 89-98.
- WANG, X., ZINKEL, S., POLONSKY, K. & FUCHS, E. (1997) Transgenic studies with a keratin promoter-driven growth hormone transgene: prospects for gene therapy. *Proc Natl Acad Sci U S A*, 94, 219-26.
- WEBER, K. S., NELSON, P. J., GRONE, H. J. & WEBER, C. (1999) Expression of CCR2 by endothelial cells : implications for MCP-1 mediated wound injury repair and In vivo inflammatory activation of endothelium. *Arterioscler Thromb Vasc Biol*, 19, 2085-93.
- WEBER, M., BLAIR, E., SIMPSON, C. V., O'HARA, M., BLACKBURN, P. E., ROT, A., GRAHAM, G. J. & NIBBS, R. J. (2004) The chemokine receptor D6 constitutively traffics to and from the cell surface to internalize and degrade chemokines. *Mol Biol Cell*, 15, 2492-508.
- WEI, C. C., CHEN, W. Y., WANG, Y. C., CHEN, P. J., LEE, J. Y., WONG, T. W., CHEN, W. C., WU, J. C., CHEN, G. Y., CHANG, M. S. & LIN, Y. C. (2005) Detection of IL-20 and its receptors on psoriatic skin. *Clin Immunol*, 117, 65-72.
- WEI, L., DEBETS, R., HEGMANS, J. J., BENNER, R. & PRENS, E. P. (1999) IL-1 beta and IFN-gamma induce the regenerative epidermal phenotype of psoriasis in the transwell skin organ culture system. IFN-gamma up-regulates the expression of keratin 17 and keratinocyte transglutaminase via endogenous IL-1 production. *J Pathol*, 187, 358-64.
- WEINSTEIN, G. D., MCCULLOUGH, J. L. & ROSS, P. (1984) Cell proliferation in normal epidermis. *J Invest Dermatol*, 82, 623-8.
- WEISENSEEL, P., LAUMBACHER, B., BESGEN, P., LUDOLPH-HAUSER, D., HERZINGER, T., ROECKEN, M., WANK, R. & PRINZ, J. C. (2002) Streptococcal infection distinguishes different types of psoriasis. *J Med Genet*, 39, 767-8.
- WEISS, G., SHEMER, A. & TRAU, H. (2002) The Koebner phenomenon: review of the literature. *J Eur Acad Dermatol Venereol*, 16, 241-8.
- WHITEHEAD, G. S., WANG, T., DEGRAFF, L. M., CARD, J. W., LIRA, S. A., GRAHAM, G. J. & COOK, D. N. (2007) The chemokine receptor D6 has opposing effects on allergic inflammation and airway reactivity. *Am J Respir Crit Care Med*, 175, 243-9.

- WIEDERHOLT, T., VON WESTERNHAGEN, M., ZALDIVAR, M. M., BERRES, M. L., SCHMITZ, P., HELLERBRAND, C., MULLER, T., BERG, T., TRAUTWEIN, C. & WASMUTH, H. E. (2008) Genetic variations of the chemokine scavenger receptor D6 are associated with liver inflammation in chronic hepatitis C. *Hum Immunol*, 69, 861-6.
- WIEDOW, O., HARDER, J., BARTELS, J., STREIT, V. & CHRISTOPHERS, E. (1998) Antileukoprotease in human skin: an antibiotic peptide constitutively produced by keratinocytes. *Biochem Biophys Res Commun*, 248, 904-9.
- WILEY, H. E., GONZALEZ, E. B., MAKI, W., WU, M. T. & HWANG, S. T. (2001) Expression of CC chemokine receptor-7 and regional lymph node metastasis of B16 murine melanoma. *J Natl Cancer Inst*, 93, 1638-43.
- WILLIAMS, R. O., FELDMANN, M. & MAINI, R. N. (1992) Anti-tumor necrosis factor ameliorates joint disease in murine collagen-induced arthritis. *Proc Natl Acad Sci U S A*, 89, 9784-8.
- WILSON, N. J., BONIFACE, K., CHAN, J. R., MCKENZIE, B. S., BLUMENSCHN, W. M., MATTSON, J. D., BASHAM, B., SMITH, K., CHEN, T., MOREL, F., LECRON, J. C., KASTELEIN, R. A., CUA, D. J., MCCLANAHAN, T. K., BOWMAN, E. P. & DE WAAL MALEFYT, R. (2007) Development, cytokine profile and function of human interleukin 17-producing helper T cells. *Nat Immunol*, 8, 950-7.
- WOODLAND, D. L. & KOHLMEIER, J. E. (2009) Migration, maintenance and recall of memory T cells in peripheral tissues. *Nat Rev Immunol*, 9, 153-61.
- WU, F. Y., OU, Z. L., FENG, L. Y., LUO, J. M., WANG, L. P., SHEN, Z. Z. & SHAO, Z. M. (2008) Chemokine decoy receptor d6 plays a negative role in human breast cancer. *Mol Cancer Res*, 6, 1276-88.
- WU, L., GERARD, N. P., WYATT, R., CHOE, H., PAROLIN, C., RUFFING, N., BORSETTI, A., CARDOSO, A. A., DESJARDIN, E., NEWMAN, W., GERARD, C. & SODROSKI, J. (1996) CD4-induced interaction of primary HIV-1 gp120 glycoproteins with the chemokine receptor CCR-5. *Nature*, 384, 179-83.
- XU, J., GAO, X. P., RAMCHANDRAN, R., ZHAO, Y. Y., VOGEL, S. M. & MALIK, A. B. (2008) Nonmuscle myosin light-chain kinase mediates neutrophil transmigration in sepsis-induced lung inflammation by activating beta2 integrins. *Nat Immunol*, 9, 880-6.
- YAGO, T., WU, J., WEY, C. D., KLOPOCKI, A. G., ZHU, C. & MCEVER, R. P. (2004) Catch bonds govern adhesion through L-selectin at threshold shear. *J Cell Biol*, 166, 913-23.
- YANAGIHARA, S., KOMURA, E., NAGAFUNE, J., WATARAI, H. & YAMAGUCHI, Y. (1998) EBI1/CCR7 is a new member of dendritic cell chemokine receptor that is up-regulated upon maturation. *J Immunol*, 161, 3096-102.
- YANG, D., CHERTOV, O., BYKOVSKAIA, S. N., CHEN, Q., BUFFO, M. J., SHOGAN, J., ANDERSON, M., SCHRODER, J. M., WANG, J. M., HOWARD, O. M. & OPPENHEIM, J. J. (1999) Beta-defensins: linking innate and adaptive immunity through dendritic and T cell CCR6. *Science*, 286, 525-8.
- YANG, N. S., BURKHOLDER, J., MCCABE, D., NEUMANN, V. & FULLER, D. (2001) Particle-mediated gene delivery in vivo and in vitro. *Curr Protoc Hum Genet*, Chapter 12, Unit 12 6.

- YANG, X. O., PANOPOULOS, A. D., NURIEVA, R., CHANG, S. H., WANG, D., WATOWICH, S. S. & DONG, C. (2007) STAT3 regulates cytokine-mediated generation of inflammatory helper T cells. *J Biol Chem*, 282, 9358-63.
- YANG, Y. F., MUKAI, T., GAO, P., YAMAGUCHI, N., ONO, S., IWAKI, H., OBIKA, S., IMANISHI, T., TSUJIMURA, T., HAMAOKA, T. & FUJIWARA, H. (2002) A non-peptide CCR5 antagonist inhibits collagen-induced arthritis by modulating T cell migration without affecting anti-collagen T cell responses. *Eur J Immunol*, 32, 2124-32.
- YAO, D., ALEXANDER, C. L., QUINN, J. A., PORTER, M. J., WU, H. & GREENHALGH, D. A. (2006) PTEN loss promotes rasHa-mediated papillomatogenesis via dual up-regulation of AKT activity and cell cycle deregulation but malignant conversion proceeds via PTEN-associated pathways. *Cancer Res*, 66, 1302-12.
- YAROVINSKY, F., ZHANG, D., ANDERSEN, J. F., BANNENBERG, G. L., SERHAN, C. N., HAYDEN, M. S., HIENY, S., SUTTERWALA, F. S., FLAVELL, R. A., GHOSH, S. & SHER, A. (2005) TLR11 activation of dendritic cells by a protozoan profilin-like protein. *Science*, 308, 1626-9.
- YE, J., KOHLI, L. L. & STONE, M. J. (2000) Characterization of binding between the chemokine eotaxin and peptides derived from the chemokine receptor CCR3. *J Biol Chem*, 275, 27250-7.
- YIN, A. H., MIRAGLIA, S., ZANJANI, E. D., ALMEIDA-PORADA, G., OGAWA, M., LEARY, A. G., OLWEUS, J., KEARNEY, J. & BUCK, D. W. (1997) AC133, a novel marker for human hematopoietic stem and progenitor cells. *Blood*, 90, 5002-12.
- YONEYAMA, M., KIKUCHI, M., NATSUKAWA, T., SHINOBU, N., IMAIZUMI, T., MIYAGISHI, M., TAIRA, K., AKIRA, S. & FUJITA, T. (2004) The RNA helicase RIG-I has an essential function in double-stranded RNA-induced innate antiviral responses. *Nat Immunol*, 5, 730-7.
- YOSHIDA, H., HAYASHI, S., KUNISADA, T., OGAWA, M., NISHIKAWA, S., OKAMURA, H., SUDO, T., SHULTZ, L. D. & NISHIKAWA, S. (1990) The murine mutation osteopetrosis is in the coding region of the macrophage colony stimulating factor gene. *Nature*, 345, 442-4.
- YOUN, B. S., ZHANG, S. M., BROXMEYER, H. E., COOPER, S., ANTOL, K., FRASER, M., JR. & KWON, B. S. (1998) Characterization of CKbeta8 and CKbeta8-1: two alternatively spliced forms of human beta-chemokine, chemoattractants for neutrophils, monocytes, and lymphocytes, and potent agonists at CC chemokine receptor 1. *Blood*, 91, 3118-26.
- ZABALLOS, A., GUTIERREZ, J., VARONA, R., ARDAVIN, C. & MARQUEZ, G. (1999) Cutting edge: identification of the orphan chemokine receptor GPR-9-6 as CCR9, the receptor for the chemokine TECK. *J Immunol*, 162, 5671-5.
- ZARBOCK, A., SCHMOLKE, M., BOCKHORN, S. G., SCHARTE, M., BUSCHMANN, K., LEY, K. & SINGBARTL, K. (2007) The Duffy antigen receptor for chemokines in acute renal failure: A facilitator of renal chemokine presentation. *Crit Care Med*, 35, 2156-63.
- ZENZ, R., EFERL, R., KENNER, L., FLORIN, L., HUMMERICH, L., MEHIC, D., SCHEUCH, H., ANGEL, P., TSCHACHLER, E. & WAGNER, E. F. (2005) Psoriasis-like skin disease and arthritis caused by inducible epidermal deletion of Jun proteins. *Nature*, 437, 369-75.

- ZHANG, D., ZHANG, G., HAYDEN, M. S., GREENBLATT, M. B., BUSSEY, C., FLAVELL, R. A. & GHOSH, S. (2004) A toll-like receptor that prevents infection by uropathogenic bacteria. *Science*, 303, 1522-6.
- ZHENG, H., FLETCHER, D., KOZAK, W., JIANG, M., HOFMANN, K. J., CONN, C. A., SOSZYNSKI, D., GRABIEC, C., TRUMBAUER, M. E., SHAW, A. & ET AL. (1995) Resistance to fever induction and impaired acute-phase response in interleukin-1 beta-deficient mice. *Immunity*, 3, 9-19.
- ZHENG, Y., DANILENKO, D. M., VALDEZ, P., KASMAN, I., EASTHAM-ANDERSON, J., WU, J. & OUYANG, W. (2007) Interleukin-22, a T(H)17 cytokine, mediates IL-23-induced dermal inflammation and acanthosis. *Nature*, 445, 648-51.
- ZHOU, X., BAILEY-BUCKTROUT, S., JEKER, L. T. & BLUESTONE, J. A. (2009) Plasticity of CD4(+) FoxP3(+) T cells. *Curr Opin Immunol*, 21, 281-5.
- ZHOU, X., KRUEGER, J. G., KAO, M. C., LEE, E., DU, F., MENTER, A., WONG, W. H. & BOWCOCK, A. M. (2003) Novel mechanisms of T-cell and dendritic cell activation revealed by profiling of psoriasis on the 63,100-element oligonucleotide array. *Physiol Genomics*, 13, 69-78.
- ZHOU, Y., KURIHARA, T., RYSECK, R. P., YANG, Y., RYAN, C., LOY, J., WARR, G. & BRAVO, R. (1998) Impaired macrophage function and enhanced T cell-dependent immune response in mice lacking CCR5, the mouse homologue of the major HIV-1 coreceptor. *J Immunol*, 160, 4018-25.
- ZHU, J., GUO, L., WATSON, C. J., HU-LI, J. & PAUL, W. E. (2001) Stat6 is necessary and sufficient for IL-4's role in Th2 differentiation and cell expansion. *J Immunol*, 166, 7276-81.
- ZIEGLER-HEITBROCK, H. W. (2000) Definition of human blood monocytes. *J Leukoc Biol*, 67, 603-6.
- ZLOTNIK, A. & YOSHIE, O. (2000) Chemokines: a new classification system and their role in immunity. *Immunity*, 12, 121-7.
- ZOU, Y. R., KOTTMANN, A. H., KURODA, M., TANIUCHI, I. & LITTMAN, D. R. (1998) Function of the chemokine receptor CXCR4 in haematopoiesis and in cerebellar development. *Nature*, 393, 595-9.

# Appendix One

## Terminology used on the web pages automatically generated by FunAlyse, microarray data analysis software

<http://www.gla.ac.uk/functionalgenomics/rp/termin.html>

---

### Experiment report

#### Software

This refers to software that actually runs the whole analysis automatically. In particular it:

- • Generates a directory structure for a project and its experiments
- • Manages the security of the project
- • Performs *RMA* low-level analysis
- • Performs *RP* identification of differentially expressed genes for a number of between-group comparisons
- • Functionally annotates the list of *RP*-identified top genes
- • Performs *iGA* to find differentially expressed functional classes of genes (written by Rainer Breitling).
- • Presents the *RP* and *iGA* results in form of web pages and/or downloadable tab-delimited text files suitable for reading in Excel.

The software has been written and implemented by Pawel Herzyk in the Autumn 2003 – Spring 2004.

#### Project

Project refers to data that belongs to a particular researcher or a group of researchers. Each PI (principal investigator) can only have one project that can be divided into many experiments. Each project has associated:

- • **Name** - this is usually constructed from the PI's name e.g. john\_dav would be a name of a project owned by John Davis.
- • **Class** - this could be Microarray or Proteomics
- • **Type** - e.g. Affymetrix or Spotted depending on the type of microarrays used

#### Experiment

Each project can be divided into experiments. Each experiment contains data from a number of replicated (or not) samples corresponding to different conditions.

#### Array

This refers to an identifiable type of array e.g. U133 is the Affymetrix human array HG-U133.

#### Chip

Some Affymetrix arrays may consist of several subarrays. E.g. HG-U133 array is in fact represented by two arrays HG-U133A and HG-U133B. In this case we say that the array has two chips A and B. If the array has only one chip it is denoted as N (for none).

### Normalisation

This really is a shorthand for low-level analysis. In case of Affymetrix data this consists of

- • Background correction
- • Multichip normalisation on the probe level
- • Summary of the log-normalised probe level data into a probe-set level data

By default we use [Robust Multichip Average](#) (RMA) method implemented in module [Affy](#) in the [Bioconductor](#) microarray analysis software.

### Differential Expression

A method of identification of differentially expressed genes between two groups of replicated samples. We use the [RankProducts](#) method (RP) developed in University of Glasgow.

### Differentially expressed gene classes

A method for identification of functional gene classes that are differentially expressed in a given comparison. We use the [Iterative Group Analysis](#) method developed in the University of Glasgow.

### Baseline

For every comparison between two groups of replicated samples we select one of the groups as a reference (baseline). This is usually done upon suggestion from a researcher who owns the data.

### Treatment

This refers to the group of replicated samples that has not been selected as baseline. The software analyses the expression of a treatment group with respect to the baseline.

### Direction

This refers to the direction of the differential expression of the treatment with respect to the baseline:

- • *Positive* - means a list of genes with significantly higher expression in the treatment group than in the baseline group
- • *Negative* - means a list of genes with significantly lower expression in the treatment group than in the baseline group

### RPhtml

Results of RP in html format

### RPtext

Results of RP in tab-delimited text format

**iGAcla**

Results of iGA in **Classic** mode (html format). Look at paragraph **Mode** in section **iGA report** for more explanations.

**iGArep**

Results of iGA in **Representative** mode (html format). Look at paragraph **Mode** in section **iGA report** for more explanations.

**RP report****Comparison**

This refers to a comparison between two groups of replicated samples. E.g.:  
*Samples: A,B,C vs Samples: D,E,F* means that samples A,B,C correspond to the *treatment* group and D,E,F correspond to the *baseline* group.

**Probe-set ID**

The Affymetrix probe-set identifier

**RPscore**

This is a measure of differential expression calculated by the RP method. For every gene this is calculated as a geometric mean of fold-change ranks over the number of all possible between-chip comparisons contributing to a given between-group comparison.

**FDR**

This is a conservative estimate of False Discovery Rate. If you cut the differentially expressed gene-list at the particular position associated with a particular FDR then it shows the expected percentage of false positives.

**FCrma**

Before FunAlyse version 1.4.1 this is a mean fold-change over all possible between-chip comparisons contributing to a given between-group comparison. From FunAlyse version 1.4.1 onwards this is calculated as an antilog of a mean log-fold-change over all possible between-chip comparisons contributing to a given between-group comparison.

In both cases if you have two groups of three Affymetrix chips the FCrma is calculated over all nine comparisons.

**FCnom**

It has been demonstrated in the experiment where selected genes were spiked-in at known concentrations on the HG-U95A chip that the fold-changes calculated after RMA low-level analysis are significantly lower than the nominal fold-changes calculated from the spiked-in gene concentrations. The relation between these two fold-changes was calculated by a fitting procedure:

$$\log_2(\text{rma FC}) = 0.61 \times \log_2(\text{nominal FC})$$

Consequently, the FCnom corresponds to the mean nominal fold-change obtained from the rma fold-changes using the above equation over all possible between-chip comparisons contributing to a given between-group comparison. Please, treat it with caution as it is not known how universal the above equation is. Consult Figure 6 in the original paper [Cope et al. 2003](#) (PubMed [abstract](#)).

**Gene annotation database**

This is a database that contains functional annotation of your genes. Every gene in the reported list of differentially expressed genes has a hyperlink to it. Currently, we use the following databases:

- • Human, Mouse and Rat - [SOURCE](#) database
- • *Arabidopsis* - [MIPS](#) and [TAIR](#) databases
- • *Drosophila* - [FlyBase](#)
- • Yeast - [SGD](#) database

### **Gene symbol**

Common gene symbol used by biologists.

### **Gene ID**

Publicly used gene identifier.

### **Title**

Short functional annotation of a gene. This is very brief, you shouldn't rely on it too much.

### **iGA report**

#### **Mode**

The iGA module in the FunAnalyse software can work in two modes: **Classic** - all probe-sets on the chip are taking part in the iGA calculations. **Representative** - only one probe-set per gene is selected. This is to remove a bias towards a particular groups in case more than one probe-set represent a gene contributing to this group. A probe set producing the best **RPscore** in a given comparison (calculated separately for positive and negative expression) is selected as a *representative* for that gene. The non-redundant set of genes is defined differently for different organisms. For Human, Mouse and Rat they are defined using *Unigene IDs*, for Arabidopsis and Yeast they are defined on the base of *gene IDs* whilst for Drosophila it is based on *gene symbols*.

#### **Number of probe-sets on the chip**

A number of Affymetrix probe-sets on a given chip. In the **Classic** mode some probe-sets may refer to the same gene.

#### **Number of annotated probe-sets**

A number of probe-sets on a given chip that have functional annotation in the current Affymetrix annotation file that has been used for functional group construction.

#### **Number of groups**

A total number of functionally annotated gene-groups. They are pre-constructed independently of the microarray experiment. Usually we use GeneOntology (GO) annotations present in the Affymetrix annotation file but you may advise us to use other annotation sources.

#### **Number of singletons**

A number of functionally annotated gene-groups that contain a single gene. These are not particularly useful for iGA.

**Significance threshold**

A threshold for **P-value changed**. P-values lower than the threshold are considered statistically significant. (see also *P-value changed*)

**File Name**

A name of the input file that contains full list of genes sorted by RankProducts score **RPscore** that is our measure of gene differential expression.

**Annotations**

This is a name of the Affymetrix functional annotation file used for the functional group construction.

**Top changed groups**

A list of significantly differentially expressed gene-groups.

**Group Members**

Number of probe-sets that belong to a particular group.

**Changed Members**

Number of **group members** that have actually contributed to achieving a given **P-value changed** for this group.

**P-value changed**

This tells you what is a probability of a random event that 'that many' of **changed members** out of 'that many' **group members** has been found 'that high' on the RP list of 'that many' sorted genes. This is calculated from the hyper-geometric distribution. Consult [Figure 1 in the original paper](#)

**P-value**

Going down from the top of the RP list, for every encountered subset of a particular gene group we calculate the p-value that tells you how probable a random event is that such subset was found 'that high' on the RP list. This is calculated from the hyper-geometric distribution. In this context **P-value changed** is a smallest p-value over all the above subsets. Consult [Figure 1 in the original paper](#)

**Percent changed**

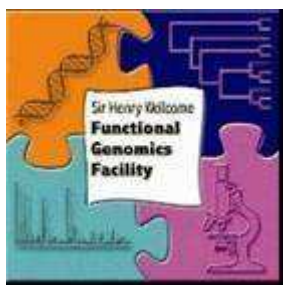
This is simply *changed members* over *group members* times 100.

**Rank**

This is rank of a particular gene in the list of differentially expressed genes. This list was created from the RP list by exclusion of genes that are not assigned to the functional gene-groups.

## Appendix Two

### The Rank Product (RP) differential expression analysis report



#### General Information

Experiment	VK1mouse4302
Normalisation	rma across replicates
Chip	one chip only
Comparison	Treatment samples: <b>K14D6 Control</b> vs Baseline samples: <b>WT Control</b>
RP comparison	not paired
Direction	Positive

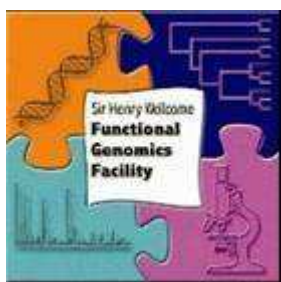
0	Probe-set ID	RPscore	FDR	FC_rma	FC_nom	"SOURCE"	"EntrezGene"	Gene Symbol	Title
1	1422111_at	1.00	0.00	49.59	603.20	BE631540	59289	Ccbp2	chemokine binding protein 2
2	1420512_at	206.84	15.50	2.66	4.96	NM_020265	56811	Dkk2	dickkopf homolog 2 (Xenopus laevis)
3	1450079_at	348.58	43.33	1.81	2.65	AK012873	27206	Nrk	Nik related kinase
4	1450871_a_at	359.51	34.50	1.48	1.90	X17502	12035	Bcat1	branched chain aminotransferase 1, cytosolic
5	1449484_at	389.02	32.20	1.56	2.08	AF031035	20856	Stc2	stanniocalcin 2
6	1418547_at	470.76	47.67	1.62	2.21	NM_009364	21789	Tfpi2	tissue factor pathway inhibitor 2
7	1437935_at	507.32	NA	1.57	2.09	BB821151	75033	4930486G11Rik	RIKEN cDNA 4930486G11 gene
8	1420991_at	511.93	NA	1.55	2.05	AK009959	107765	Ankrd1	ankyrin repeat domain 1 (cardiac muscle)
9	1448816_at	529.66	NA	1.75	2.51	NM_008968	19223	Ptgis	prostaglandin I2 (prostaglandin) synthase
10	1421038_a_at	531.04	NA	1.12	1.20	NM_008433	16534	Kcnn4	potassium intermediate/small conductance calcium-activated channel, subfamily N, member 4
11	1416405_at	607.93	NA	1.71	2.41	BC019502	12111	Bgn	biglycan
12	1448323_a_at	643.49	NA	1.71	2.40	BC019502	12111	Bgn	biglycan
13	1416200_at	667.15	NA	1.65	2.27	NM_133775	77125	9230117N10Rik	RIKEN cDNA 9230117N10 gene
14	1423607_at	680.73	NA	1.94	2.96	AK014312	17022	Lum	lumican
15	1427262_at	691.34	NA	1.87	2.78	L04961	213742	Xist	inactive X specific transcripts
16	1418815_at	723.08	NA	1.43	1.79	BC022107	12558	Cdh2	cadherin 2
17	1454672_at	798.97	NA	1.87	2.78	BE952212	---	---	---
18	1436448_a_at	821.49	NA	1.60	2.15	AA833146	19224	Ptgs1	prostaglandin-endoperoxide synthase 1
19	1455626_at	829.09	NA	1.07	1.12	AA987181	15405	Hoxa9	homeo box A9
20	1451016_at	832.05	NA	1.38	1.69	BB540964	15983	lfrd2	interferon-related

									developmental regulator 2
21	1416778_at	841.85	NA	1.68	2.34	BE197945	20324	Sdpr	serum deprivation response
22	1434278_at	855.72	NA	1.34	1.62	BG976607	17772	Mtm1	X-linked myotubular myopathy gene 1
23	1424186_at	887.84	NA	1.44	1.82	BG074158	67896	2610001E17Rik	RIKEN cDNA 2610001E17 gene
24	1439774_at	913.38	NA	1.62	2.20	BB051738	18933	Prrx1	paired related homeobox 1
25	1415834_at	946.19	NA	1.24	1.42	NM_026268	67603	Dusp6	dual specificity phosphatase 6
26	1416072_at	956.02	NA	1.45	1.85	NM_133654	12490	Cd34	CD34 antigen
27	1425458_a_at	966.35	NA	1.37	1.67	AF022072	14783	Grb10	growth factor receptor bound protein 10
28	1436319_at	980.06	NA	1.31	1.55	BB751459	240725	Sulf1	sulfatase 1
29	1434877_at	984.15	NA	1.53	2.01	AI152800	18164	Nptx1	neuronal pentraxin 1
30	1453252_at	994.13	NA	1.34	1.61	AK010138	71916	Dus4l	dihydrouridine synthase 4-like (S. cerevisiae)
31	1428960_at	1004.42	NA	1.35	1.63	AK017056	71233	4933434I06Rik	RIKEN cDNA 4933434I06 gene
32	1436936_s_at	1014.15	NA	1.74	2.49	BG806300	213742	Xist	inactive X specific transcripts
33	1425415_a_at	1016.60	NA	1.36	1.65	U75214	20510	Slc1a1	solute carrier family 1 (neuronal/epithelial high affinity glutamate transporter, system Xag), member 1
34	1427610_at	1020.80	NA	1.39	1.72	BC026631	109620	Dsp	desmoplakin
35	1449519_at	1023.57	NA	1.36	1.65	NM_007836	13197	Gadd45a	growth arrest and DNA-damage-inducible 45 alpha
36	1415998_at	1035.12	NA	1.38	1.69	NM_011694	22333	Vdac1	voltage-dependent anion channel 1
37	1437889_x_at	1046.43	NA	1.57	2.09	AI931862	12111	Bgn	biglycan
38	1427263_at	1065.74	NA	1.35	1.63	L04961	213742	Xist	inactive X specific transcripts
39	1428944_at	1089.81	NA	1.42	1.78	BB417360	231380	5730469D23Rik	RIKEN cDNA 5730469D23 gene
40	1448590_at	1187.50	NA	1.63	2.24	NM_009933	12833	Col6a1	procollagen, type VI, alpha 1
41	1436698_x_at	1189.66	NA	1.26	1.47	AV167328	407831	BC054438	cDNA sequence BC054438
42	1423606_at	1208.13	NA	1.57	2.09	BI110565	50706	Postn	periostin, osteoblast specific factor
43	1438989_s_at	1236.84	NA	1.31	1.56	BB386167	320860	B130021B11Rik	RIKEN cDNA B130021B11 gene
44	1455121_at	1248.43	NA	1.30	1.54	BB553784	212391	A630025C20Rik	RIKEN cDNA A630025C20 gene
45	1454904_at	1261.59	NA	1.29	1.52	BG976607	17772	Mtm1	X-linked myotubular myopathy gene 1
46	1421917_at	1262.81	NA	1.47	1.88	AW537708	18595	Pdgfra	platelet derived growth factor receptor, alpha polypeptide
47	1423271_at	1266.24	NA	1.31	1.57	AV239646	14619	Gjb2	gap junction membrane channel protein beta 2
48	1423110_at	1271.66	NA	1.67	2.32	BF227507	---	---	---
49	1450196_s_at	1289.33	NA	1.31	1.56	NM_030678	14936 14937	Gys1 /// Gys3	glycogen synthase 1, muscle /// glycogen synthase 3, brain
50	1431295_a_at	1318.68	NA	1.31	1.56	AK016910	71116	Stx18	syntaxin 18
51	1416121_at	1323.10	NA	1.72	2.43	M65143	16948	Lox	lysyl oxidase
52	1450757_at	1324.74	NA	1.38	1.69	NM_009866	12552	Cdh11	cadherin 11
53	1444368_at	1328.00	NA	1.30	1.54	BE956442	110834	Chrna3	Cholinergic receptor,

									nicotinic, alpha polypeptide 3 (Chrna3), mRNA
54	1420992_at	1331.31	NA	1.45	1.85	AK009959	107765	Ankrd1	ankyrin repeat domain 1 (cardiac muscle)
55	1450857_a_at	1334.16	NA	1.81	2.64	BF227507	12843	Col1a2	procollagen, type I, alpha 2
56	1452445_at	1339.62	NA	1.33	1.60	BC026874	338365	Slc41a2	solute carrier family 41, member 2
57	1453783_at	1344.55	NA	1.32	1.59	BE864772	70733	6330411E07Rik	RIKEN cDNA 6330411E07 gene
58	1449735_at	1372.35	NA	1.31	1.56	BG074689	---	---	---
59	1418601_at	1383.54	NA	0.96	0.94	NM_011921	26358	Aldh1a7	aldehyde dehydrogenase family 1, subfamily A7
60	1415802_at	1390.45	NA	1.29	1.51	NM_009196	20501	Slc16a1	solute carrier family 16 (monocarboxylic acid transporters), member 1
61	1442845_at	1412.33	NA	1.27	1.48	AV320517	320395	C130075A20Rik	RIKEN cDNA C130075A20 gene
62	1435945_a_at	1437.93	NA	0.95	0.92	BG865910	16534	Kcnn4	potassium intermediate/small conductance calcium-activated channel, subfamily N, member 4
63	1418736_at	1456.53	NA	1.32	1.58	BC003835	26879	B3galt3	UDP-Gal:betaGlcNAc beta 1,3-galactosyltransferase, polypeptide 3
64	1454174_a_at	1465.43	NA	1.29	1.51	AK021190	77644	C330007P06Rik	RIKEN cDNA C330007P06 gene
65	1456292_a_at	1479.27	NA	1.43	1.79	AV147875	22352	Vim	vimentin
66	1421817_at	1481.12	NA	1.20	1.35	AK019177	14782	Gsr	glutathione reductase 1
67	1422995_at	1485.51	NA	1.29	1.52	NM_138313	171543	Bmf	Bcl2 modifying factor
68	1419404_s_at	1487.00	NA	1.27	1.49	NM_009173	20437 20438	Siah1a /// Siah1b	seven in absentia 1A /// seven in absentia 1B
69	1435831_at	1515.03	NA	1.09	1.15	BB427704	22268	Upk1b	uroplakin 1B
70	1449475_at	1541.88	NA	1.31	1.55	NM_138652	192113	Atp12a	ATPase, H+/K+ transporting, nongastric, alpha polypeptide
71	1428796_at	1554.27	NA	1.29	1.53	AK017436	74503	5530401J07Rik	RIKEN cDNA 5530401J07 gene
72	1425092_at	1559.88	NA	1.16	1.28	AF183946	320873	Cdh10	cadherin 10
73	1452250_a_at	1581.58	NA	1.38	1.69	BI455189	12834	Col6a2	procollagen, type VI, alpha 2
74	1423744_x_at	1589.37	NA	1.31	1.56	BC006682	26905	Eif2s3x	eukaryotic translation initiation factor 2, subunit 3, structural gene X-linked
75	1449244_at	1621.01	NA	1.35	1.63	BC022107	12558	Cdh2	cadherin 2
76	1418157_at	1625.70	NA	1.32	1.58	NM_010151	13865	Nr2f1	nuclear receptor subfamily 2, group F, member 1
77	1430676_at	1636.38	NA	1.30	1.54	AK019854	12823	Col19a1	procollagen, type XIX, alpha 1
78	1450315_at	1638.11	NA	1.28	1.49	NM_030736	81011	V1rd14	vomeronal 1 receptor, D14
79	1451090_a_at	1643.54	NA	1.30	1.53	BC006682	26905	Eif2s3x	eukaryotic translation initiation factor 2, subunit 3, structural gene X-linked
80	1437672_at	1643.85	NA	1.27	1.48	AV286336	16369	Irs3	insulin receptor substrate 3

81	1418926_at	1648.07	NA	1.36	1.66	NM_011546	21417	Zfhx1a	zinc finger homeobox 1a
82	1427883_a_at	1666.33	NA	1.28	1.50	AW550625	12825	Col3a1	procollagen, type III, alpha 1
83	1440910_at	1680.56	NA	1.35	1.64	AW495307	Mm.381907	---	CDNA clone IMAGE:5252333
84	1450004_at	1685.90	NA	1.08	1.14	NM_021367	53603	Tslp	thymic stromal lymphopoietin
85	1426255_at	1696.96	NA	1.29	1.52	M20480	18039	Nefl	neurofilament, light polypeptide
86	1446584_at	1706.52	NA	1.29	1.52	BB485470	76299	Txndc4	Thioredoxin domain containing 4 (endoplasmic reticulum) (Txndc4), mRNA
87	1422567_at	1709.08	NA	1.29	1.51	NM_022018	63913	Niban	niban protein
88	1459085_at	1711.18	NA	1.27	1.49	BG066528	52305	D1Ert259e	DNA segment, Chr 1, ERATO Doi 259, expressed
89	1420650_at	1717.02	NA	1.27	1.48	NM_007496	11906	Atbf1	AT motif binding factor 1
90	1430342_at	1717.63	NA	1.28	1.51	BF011273	67589	4930518J20Rik	RIKEN cDNA 4930518J20 gene
91	1433491_at	1728.77	NA	1.27	1.49	BE951907	13822	Epb4.1l2	erythrocyte protein band 4.1-like 2
92	1437219_at	1729.38	NA	1.33	1.59	AW553541	16001	Igf1r	Insulin-like growth factor I receptor (Igf1r), mRNA
93	1416473_a_at	1735.26	NA	1.32	1.58	NM_020043	56741	Nope	neighbor of Punc E11
94	1449351_s_at	1736.95	NA	1.18	1.31	NM_019971	54635	Pdgfc	platelet-derived growth factor, C polypeptide
95	1450078_at	1760.15	NA	1.32	1.57	AK012873	27206	Nrk	Nik related kinase
96	1460039_at	1760.67	NA	1.30	1.53	BB035924	243653	Clec1a	C-type lectin domain family 1, member a
97	1437556_at	1761.93	NA	1.32	1.58	BF147593	80892	Zfhx4	zinc finger homeodomain 4
98	1458640_at	1768.52	NA	1.29	1.51	BB284122	Mm.37652	---	6 days neonate skin cDNA, RIKEN full-length enriched library, clone:A030007119 product:hypothetical protein, full insert sequence
99	1438148_at	1774.82	NA	1.10	1.17	BB829808	330122	Gm1960	gene model 1960, (NCBI)
100	1451332_at	1786.80	NA	1.22	1.39	BC021376	225207	Zfp521	zinc finger protein 521

## The Rank Product (RP) differential expression analysis report



General Information	
Experiment	VK1mouse4302
Normalisation	rma across replicates
Chip	one chip only
Comparison	Treatment samples: <b>WT + CCL3</b> vs Baseline samples: <b>WT Control</b>
RP comparison	not paired
Direction	Positive

0	Probe-set ID	RPscore	FDR	FC_r ma	FC_no m	"SOURCE"	"EntrezGene"	Gene Symbol	Title
1	1424754_at	145.79	14.00	2.46	4.38	<a href="#">BC024402</a>	<a href="#">109225</a>	Ms4a7	membrane-spanning 4-domains, subfamily A, member 7
2	1448995_at	171.94	9.50	2.10	3.39	<a href="#">NM_019932</a>	<a href="#">56744</a>	Cxcl4	chemokine (C-X-C motif) ligand 4
3	1448748_at	189.97	8.33	2.61	4.83	<a href="#">AF181829</a>	<a href="#">56193</a>	Plek	pleckstrin
4	1427883_a_at	224.73	10.25	3.72	8.61	<a href="#">AW550625</a>	<a href="#">12825</a>	Col3a1	procollagen, type III, alpha 1
5	1420512_at	228.64	8.20	3.50	7.79	<a href="#">NM_020265</a>	<a href="#">56811</a>	Dkk2	dickkopf homolog 2 (Xenopus laevis)
6	1418547_at	236.57	7.00	3.11	6.44	<a href="#">NM_009364</a>	<a href="#">21789</a>	Tfpi2	tissue factor pathway inhibitor 2
7	1423607_at	287.28	9.86	3.29	7.06	<a href="#">AK014312</a>	<a href="#">17022</a>	Lum	lumican
8	1450663_at	288.57	8.75	2.86	5.61	<a href="#">NM_011581</a>	<a href="#">21826</a>	Thbs2	thrombospondin 2
9	1438989_s_at	288.84	7.78	2.48	4.42	<a href="#">BB386167</a>	<a href="#">320860</a>	B130021B11Rik	RIKEN cDNA B130021B11 gene
10	1416136_at	296.29	7.20	2.71	5.12	<a href="#">NM_008610</a>	<a href="#">17390</a>	Mmp2	matrix metalloproteinase 2
11	1436970_a_at	303.38	7.55	3.20	6.74	<a href="#">AA499047</a>	<a href="#">18596</a>	Pdgfrb	platelet derived growth factor receptor, beta polypeptide
12	1448590_at	314.50	7.50	3.25	6.91	<a href="#">NM_009933</a>	<a href="#">12833</a>	Col6a1	procollagen, type VI, alpha 1
13	1448326_a_at	319.04	7.15	2.86	5.59	<a href="#">NM_013496</a>	<a href="#">12903</a>	Crabp1	cellular retinoic acid binding protein I
14	1452250_a_at	322.66	7.00	2.96	5.92	<a href="#">BI455189</a>	<a href="#">12834</a>	Col6a2	procollagen, type VI, alpha 2
15	1417381_at	329.93	7.00	2.13	3.47	<a href="#">NM_007572</a>	<a href="#">12259</a>	C1qa	complement component 1, q subcomponent, alpha polypeptide
16	1439364_a_at	335.60	6.88	2.65	4.95	<a href="#">BF147716</a>	<a href="#">17390</a>	Mmp2	matrix metalloproteinase 2
17	1422317_a_at	339.17	6.71	2.78	5.34	<a href="#">NM_010743</a>	<a href="#">17082</a>	Il1rl1	interleukin 1 receptor-like 1
18	1435943_at	373.12	8.39	2.55	4.63	<a href="#">AI647687</a>	<a href="#">13479</a>	Dpep1	dipeptidase 1 (renal)

19	1449154_at	394.70	9.68	2.21	3.68	<a href="#">NM_007729</a>	<a href="#">12814</a>	Col11a1	procollagen, type XI, alpha 1
20	1419598_at	397.90	9.35	2.16	3.53	<a href="#">NM_026835</a>	<a href="#">68774</a>	Ms4a6d	membrane-spanning 4-domains, subfamily A, member 6D
21	1436905_x_at	415.35	9.67	1.88	2.82	<a href="#">BB218107</a>	<a href="#">16792</a>	Laptm5	lysosomal-associated protein transmembrane 5
22	1423606_at	417.60	9.32	2.82	5.47	<a href="#">B1110565</a>	<a href="#">50706</a>	Postn	periostin, osteoblast specific factor
23	1418157_at	421.55	9.22	2.10	3.38	<a href="#">NM_010151</a>	<a href="#">13865</a>	Nr2f1	nuclear receptor subfamily 2, group F, member 1
24	1450757_at	437.53	10.04	2.56	4.67	<a href="#">NM_009866</a>	<a href="#">12552</a>	Cdh11	cadherin 11
25	1448929_at	439.43	9.72	1.97	3.03	<a href="#">NM_028784</a>	<a href="#">74145</a>	F13a1	coagulation factor XIII, A1 subunit
26	1419100_at	455.66	10.42	2.15	3.51	<a href="#">NM_009252</a>	<a href="#">20716</a>	Serpina3n	serine (or cysteine) peptidase inhibitor, clade A, member 3N
27	1416414_at	461.95	10.37	1.85	2.75	<a href="#">NM_133918</a>	<a href="#">100952</a>	Emilin1	elastin microfibril interfacier 1
28	1449368_at	469.99	10.50	2.97	5.97	<a href="#">NM_007833</a>	<a href="#">13179</a>	Dcn	decorin
29	1450857_a_at	470.68	10.17	3.18	6.68	<a href="#">BF227507</a>	<a href="#">12843</a>	Col1a2	procollagen, type I, alpha 2
30	1416121_at	472.91	9.97	3.12	6.45	<a href="#">M65143</a>	<a href="#">16948</a>	Lox	lysyl oxidase
31	1438672_at	475.20	9.87	1.96	3.02	<a href="#">B1134721</a>	<a href="#">170736</a>	Parvb	Parvin, beta (Parvb), mRNA
32	1421425_a_at	476.88	9.62	1.80	2.61	<a href="#">NM_030598</a>	<a href="#">53901</a>	Dscr111	Down syndrome critical region gene 1-like 1
33	1435477_s_at	482.60	9.64	2.03	3.19	<a href="#">BM224327</a>	<a href="#">14130</a>	Fcgr2b	Fc receptor, IgG, low affinity IIb
34	1416405_at	489.25	9.65	2.93	5.82	<a href="#">BC019502</a>	<a href="#">12111</a>	Bgn	biglycan
35	1418666_at	506.88	10.20	1.75	2.50	<a href="#">NM_008987</a>	<a href="#">19288</a>	Ptx3	pentraxin related gene
36	1423110_at	506.90	9.92	2.96	5.91	<a href="#">BF227507</a>	---	---	---
37	1424186_at	539.75	11.89	2.80	5.40	<a href="#">BG074158</a>	<a href="#">67896</a>	2610001E17Rik	RIKEN cDNA 2610001E17 gene
38	1437558_at	540.30	11.61	1.85	2.74	<a href="#">BM119919</a>	<a href="#">320860</a>	B130021B11Rik	RIKEN cDNA B130021B11 gene
39	1419728_at	546.18	11.62	1.93	2.95	<a href="#">NM_009141</a>	<a href="#">20311</a>	Cxcl5	chemokine (C-X-C motif) ligand 5
40	1418454_at	549.59	11.47	2.01	3.15	<a href="#">NM_015776</a>	<a href="#">50530</a>	Mfap5	microfibrillar associated protein 5
41	1448323_a_at	549.62	11.22	2.98	5.99	<a href="#">BC019502</a>	<a href="#">12111</a>	Bgn	biglycan
42	1420498_a_at	552.08	11.05	2.16	3.53	<a href="#">NM_023118</a>	<a href="#">13132</a>	Dab2	disabled homolog 2 (Drosophila)
43	1419473_a_at	566.01	11.88	1.99	3.10	<a href="#">NM_031161</a>	<a href="#">12424</a>	Cck	cholecystokinin
44	1423537_at	566.36	11.61	2.13	3.45	<a href="#">BB622036</a>	<a href="#">14432</a>	Gap43	growth associated protein 43
45	1421917_at	569.08	11.51	2.40	4.22	<a href="#">AW537708</a>	<a href="#">18595</a>	Pdgfra	platelet derived growth factor receptor, alpha polypeptide
46	1436698_x_at	575.44	11.67	1.92	2.91	<a href="#">AV167328</a>	<a href="#">407831</a>	BC054438	cDNA sequence BC054438
47	1416200_at	582.79	11.77	1.90	2.87	<a href="#">NM_133775</a>	<a href="#">77125</a>	9230117N10Rik	RIKEN cDNA 9230117N10 gene
48	1452905_at	585.62	11.65	2.60	4.79	<a href="#">AV015833</a>	<a href="#">17263330814</a>	Gtl2 /// Lphn1	GTL2, imprinted maternally expressed untranslated mRNA /// latrophilin 1
49	1419248_at	591.51	11.67	2.01	3.13	<a href="#">AF215668</a>	<a href="#">19735</a>	Rgs2	regulator of G-protein signaling 2
50	1420380_at	628.06	13.48	2.33	3.99	<a href="#">AF065933</a>	<a href="#">20296</a>	Ccl2	chemokine (C-C motif) ligand 2
51	1437889_x_at	657.21	15.35	2.68	5.04	<a href="#">A1931862</a>	<a href="#">12111</a>	Bgn	biglycan

52	1422571_at	657.44	15.06	2.69	5.06	<a href="#">NM_011581</a>	<a href="#">21826</a>	Thbs2	thrombospondin 2
53	1420804_s_at	659.19	14.89	1.80	2.63	<a href="#">NM_010819</a>	<a href="#">17474</a>	Clec4d	C-type lectin domain family 4, member d
54	1416221_at	661.34	14.85	2.60	4.80	<a href="#">BI452727</a>	<a href="#">14314</a>	Fstl1	folliculin-like 1
55	1448228_at	661.58	14.60	2.53	4.58	<a href="#">M65143</a>	<a href="#">16948</a>	Lox	lysyl oxidase
56	1448816_at	664.14	14.50	2.23	3.73	<a href="#">NM_008968</a>	<a href="#">19223</a>	Ptgis	prostaglandin I2 (prostacyclin) synthase
57	1426947_x_at	667.96	14.46	2.20	3.65	<a href="#">BI455189</a>	<a href="#">12834</a>	Col6a2	procollagen, type VI, alpha 2
58	1450430_at	672.42	14.72	1.74	2.47	<a href="#">NM_008625</a>	<a href="#">17533</a>	Mrc1	mannose receptor, C type 1
59	1452141_a_at	680.30	14.97	1.95	3.00	<a href="#">BC001991</a>	<a href="#">20363</a>	Sepp1	selenoprotein P, plasma, 1
60	1418599_at	682.21	14.87	1.77	2.55	<a href="#">NM_007729</a>	<a href="#">12814</a>	Col11a1	procollagen, type XI, alpha 1
61	1448162_at	694.27	15.39	1.91	2.90	<a href="#">BB250384</a>	<a href="#">22329</a>	Vcam1	vascular cell adhesion molecule 1
62	1448925_at	701.70	15.76	2.09	3.36	<a href="#">NM_007855</a>	<a href="#">13345</a>	Twist2	twist homolog 2 (Drosophila)
63	1437165_a_at	704.76	15.70	2.35	4.05	<a href="#">BB250811</a>	<a href="#">18542</a>	Pcolce	procollagen C-endopeptidase enhancer protein
64	1436448_a_at	706.91	15.59	2.24	3.77	<a href="#">AA833146</a>	<a href="#">19224</a>	Ptgs1	prostaglandin-endoperoxide synthase 1
65	1418601_at	711.64	15.65	3.17	6.64	<a href="#">NM_011921</a>	<a href="#">26358</a>	Aldh1a7	aldehyde dehydrogenase family 1, subfamily A7
66	1451978_at	721.02	16.06	2.24	3.75	<a href="#">AF357006</a>	<a href="#">16949</a>	Loxl1	lysyl oxidase-like 1
67	1439426_x_at	740.13	17.28	1.74	2.48	<a href="#">AV058500</a>	<a href="#">17110</a>	Lzp-s	P lysozyme structural
68	1447862_x_at	752.36	17.85	2.00	3.13	<a href="#">BB233297</a>	<a href="#">21826</a>	Thbs2	thrombospondin 2
69	1438405_at	763.85	18.36	2.41	4.22	<a href="#">BB791906</a>	<a href="#">14178</a>	Fgf7	fibroblast growth factor 7
70	1415983_at	766.61	18.29	1.57	2.10	<a href="#">NM_008879</a>	<a href="#">18826</a>	Lcp1	lymphocyte cytosolic protein 1
71	1450652_at	770.50	18.41	2.28	3.87	<a href="#">NM_007802</a>	<a href="#">13038</a>	Ctsk	cathepsin K
72	1436996_x_at	783.94	19.10	1.66	2.29	<a href="#">AV066625</a>	<a href="#">17110</a>	Lzp-s	P lysozyme structural
73	1450641_at	805.95	20.26	2.13	3.45	<a href="#">M24849</a>	<a href="#">22352</a>	Vim	vimentin
74	1425575_at	811.40	20.24	1.76	2.54	<a href="#">M68513</a>	<a href="#">13837</a>	Epha3	Eph receptor A3
75	1425528_at	821.92	20.69	2.20	3.63	<a href="#">L06502</a>	<a href="#">18933</a>	Prrx1	paired related homeobox 1
76	1418990_at	822.12	20.43	1.76	2.52	<a href="#">NM_025658</a>	<a href="#">66607</a>	Ms4a4d	membrane-spanning 4-domains, subfamily A, member 4D
77	1456292_a_at	853.38	22.35	2.11	3.39	<a href="#">AV147875</a>	<a href="#">22352</a>	Vim	vimentin
78	1449254_at	853.87	22.12	2.22	3.70	<a href="#">NM_009263</a>	<a href="#">20750</a>	Spp1	secreted phosphoprotein 1
79	1417266_at	868.30	22.85	1.87	2.80	<a href="#">BC002073</a>	<a href="#">20305</a>	Ccl6	chemokine (C-C motif) ligand 6
80	1418736_at	870.45	22.73	1.70	2.39	<a href="#">BC003835</a>	<a href="#">26879</a>	B3galt3	UDP-Gal:betaGlcNAc beta 1,3-galactosyltransferase, polypeptide 3
81	1425145_at	871.16	22.47	2.23	3.73	<a href="#">D13695</a>	<a href="#">17082</a>	Il1r1	interleukin 1 receptor-like 1
82	1425810_a_at	875.10	22.50	1.60	2.16	<a href="#">BF124540</a>	<a href="#">13007</a>	Csrp1	cysteine and glycine-rich protein 1
83	1448259_at	885.57	22.84	2.41	4.24	<a href="#">BI452727</a>	<a href="#">14314</a>	Fstl1	folliculin-like 1
84	1418945_at	889.73	22.88	1.95	2.99	<a href="#">NM_010809</a>	<a href="#">17392</a>	Mmp3	matrix metalloproteinase 3
85	1460227_at	894.34	22.94	1.95	2.98	<a href="#">BC008107</a>	<a href="#">21857</a>	Timp1	tissue inhibitor of metalloproteinase 1
86	1448591_at	897.68	22.99	1.61	2.17	<a href="#">NM_021281</a>	<a href="#">13040</a>	Ctss	cathepsin S
87	1418815_at	900.46	22.91	1.68	2.35	<a href="#">BC022107</a>	<a href="#">12558</a>	Cdh2	cadherin 2
88	1440397_at	908.51	23.31	1.74	2.47	<a href="#">BB464523</a>	---	---	---

89	1448620_at	920.24	23.66	1.76	2.53	<a href="#">NM_010188</a>	<a href="#">14131</a>	Fcgr3	Fc receptor, IgG, low affinity III
90	1449244_at	933.40	24.27	1.73	2.46	<a href="#">BC022107</a>	<a href="#">12558</a>	Cdh2	cadherin 2
91	1419599_s_at	937.95	24.34	1.58	2.12	<a href="#">NM_026835</a>	<a href="#">64382</a>	Ms4a11	membrane-spanning 4-domains, subfamily A, member 11
92	1439774_at	941.15	24.33	2.29	3.89	<a href="#">BB051738</a>	<a href="#">18933</a>	Prrx1	paired related homeobox 1
93	1460419_a_at	942.93	24.22	1.66	2.29	<a href="#">X59274</a>	<a href="#">18751</a>	Prkcb1	protein kinase C, beta 1
94	1427086_at	954.53	24.83	1.83	2.68	<a href="#">BM570006</a>	---	---	---
95	1416168_at	964.23	25.19	1.97	3.04	<a href="#">NM_011340</a>	<a href="#">20317</a>	Serpinf1	serine (or cysteine) peptidase inhibitor, clade F, member 1
96	1418492_at	967.73	25.18	2.19	3.62	<a href="#">NM_011825</a>	<a href="#">23893</a>	Grem2	gremlin 2 homolog, cysteine knot superfamily (Xenopus laevis)
97	1451867_x_at	982.96	26.14	2.00	3.13	<a href="#">AF177664</a>	<a href="#">11856</a>	Arhgap6	Rho GTPase activating protein 6
98	1427262_at	984.23	25.98	1.94	2.95	<a href="#">L04961</a>	<a href="#">213742</a>	Xist	inactive X specific transcripts
99	1448293_at	985.81	25.81	1.88	2.83	<a href="#">BB125261</a>	<a href="#">13591</a>	Ebf1	early B-cell factor 1
100	1447830_s_at	990.58	25.97	1.82	2.67	<a href="#">BB034265</a>	<a href="#">19735</a>	Rgs2	regulator of G-protein signaling 2
101	1417936_at	995.22	26.11	1.58	2.12	<a href="#">AF128196</a>	<a href="#">20308</a>	Ccl9	chemokine (C-C motif) ligand 9
102	1418511_at	1004.36	26.59	1.76	2.52	<a href="#">NM_019759</a>	<a href="#">56429</a>	Dpt	Dermatopontin
103	1434423_at	1014.89	27.27	1.70	2.38	<a href="#">BB138485</a>	---	---	---
104	1423311_s_at	1023.04	27.63	1.44	1.82	<a href="#">BQ177165</a>	<a href="#">21983</a>	Tpbp	trophoblast glycoprotein
105	1449408_at	1026.36	27.55	1.52	1.99	<a href="#">NM_023844</a>	<a href="#">67374</a>	Jam2	junction adhesion molecule 2
106	1438009_at	1038.87	28.45	1.42	1.79	<a href="#">W91024</a>	<a href="#">319171</a>	Hist1h2ao	histone 1, H2ao
107	1423477_at	1039.21	28.21	1.69	2.37	<a href="#">BB361162</a>	<a href="#">22771</a>	Zic1	zinc finger protein of the cerebellum 1
108	1437673_at	1039.26	27.95	1.60	2.15	<a href="#">AV164956</a>	<a href="#">Mm.257714</a>	---	Transcribed locus
109	1460208_at	1043.57	28.02	2.12	3.42	<a href="#">NM_007993</a>	<a href="#">14118</a>	Fbn1	fibrillin 1
110	1452296_at	1044.06	27.82	2.10	3.37	<a href="#">BM570006</a>	<a href="#">20564</a>	Slit3	slit homolog 3 (Drosophila)
111	1429022_at	1044.37	27.57	1.82	2.67	<a href="#">AK013587</a>	<a href="#">11517</a>	Adcyap1r1	adenylate cyclase activating polypeptide 1 receptor 1
112	1449984_at	1047.97	27.60	1.53	2.00	<a href="#">NM_009140</a>	<a href="#">20310</a>	Cxcl2	chemokine (C-X-C motif) ligand 2
113	1426640_s_at	1050.29	27.55	1.91	2.90	<a href="#">BB354684</a>	<a href="#">217410</a>	Trib2	tribbles homolog 2 (Drosophila)
114	1438118_x_at	1057.27	27.73	1.95	2.99	<a href="#">AV147875</a>	<a href="#">22352</a>	Vim	Vimentin
115	1426236_a_at	1071.93	28.56	1.67	2.32	<a href="#">AI391218</a>	<a href="#">14645</a>	Glul	glutamate-ammonia ligase (glutamine synthetase)
116	1440910_at	1084.85	29.08	1.65	2.27	<a href="#">AW495307</a>	<a href="#">Mm.381907</a>	---	CDNA clone IMAGE:5252333
117	1454830_at	1091.86	29.35	1.47	1.88	<a href="#">AV010392</a>	<a href="#">14119</a>	Fbn2	fibrillin 2
118	1423326_at	1092.49	29.13	1.97	3.03	<a href="#">BI151440</a>	<a href="#">12495</a>	Entpd1	ectonucleoside triphosphate diphosphohydrolase 1
119	1451332_at	1097.99	29.24	1.78	2.57	<a href="#">BC021376</a>	<a href="#">225207</a>	Zfp521	zinc finger protein 521
120	1416740_at	1100.12	29.12	2.04	3.22	<a href="#">AW744319</a>	<a href="#">12831</a>	Col5a1	procollagen, type V, alpha 1
121	1425357_a_at	1102.12	29.03	1.70	2.39	<a href="#">BC015293</a>	<a href="#">23892</a>	Grem1	gremlin 1
122	1437726_x_at	1102.12	28.80	1.57	2.10	<a href="#">BB111335</a>	<a href="#">12260</a>	C1qb	complement component 1, q subcomponent, beta polypeptide
123	1424542_at	1102.94	28.61	1.78	2.58	<a href="#">D00208</a>	<a href="#">20198</a>	S100a4	S100 calcium binding

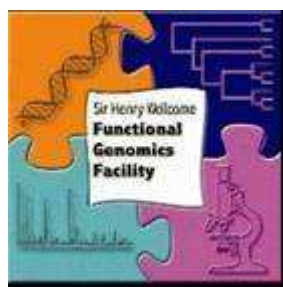
									protein A4
124	1448942_at	1113.88	29.19	1.89	2.85	<a href="#">NM_025331</a>	<a href="#">66066</a>	Gng11	guanine nucleotide binding protein (G protein), gamma 11
125	1420992_at	1116.76	29.22	1.82	2.67	<a href="#">AK009959</a>	<a href="#">107765</a>	Ankrd1	ankyrin repeat domain 1 (cardiac muscle)
126	1455494_at	1131.87	29.91	2.15	3.50	<a href="#">BI794771</a>	<a href="#">12842</a>	Col1a1	procollagen, type I, alpha 1
127	1419693_at	1144.97	30.70	1.89	2.83	<a href="#">NM_130449</a>	<a href="#">140792</a>	Colec12	collectin sub-family member 12
128	1457042_at	1147.07	30.63	1.73	2.45	<a href="#">BB328287</a>	<a href="#">58871</a>	AI256396	EST AI256396
129	1448606_at	1150.23	30.65	1.72	2.43	<a href="#">U70622</a>	<a href="#">14745</a>	Edg2	endothelial differentiation, lysophosphatidic acid G-protein-coupled receptor, 2
130	1423271_at	1150.59	30.44	1.65	2.28	<a href="#">AV239646</a>	<a href="#">14619</a>	Gjb2	gap junction membrane channel protein beta 2
131	1418892_at	1162.74	30.97	2.02	3.17	<a href="#">AF309564</a>	<a href="#">80837</a>	Rhoj	ras homolog gene family, member J
132	1455426_at	1172.64	31.50	1.97	3.04	<a href="#">AV226618</a>	<a href="#">13837</a>	Epha3	Eph receptor A3
133	1439380_x_at	1173.55	31.34	2.02	3.18	<a href="#">BB093563</a>	<a href="#">17263</a>	Gtl2	GTL2, imprinted maternally expressed untranslated mRNA
134	1429273_at	1174.13	31.18	1.87	2.80	<a href="#">AK014221</a>	<a href="#">73230</a>	Bmper	BMP-binding endothelial regulator
135	1448919_at	1178.48	31.22	1.85	2.74	<a href="#">NM_025422</a>	<a href="#">66205</a>	Cd302	CD302 antigen
136	1437360_at	1179.09	31.04	1.74	2.48	<a href="#">BB053591</a>	<a href="#">279653</a>	Pcdh19	protocadherin 19
137	1448201_at	1180.52	30.89	1.55	2.06	<a href="#">NM_009144</a>	<a href="#">20319</a>	Sfrp2	secreted frizzled-related sequence protein 2
138	1416778_at	1182.06	30.72	1.84	2.72	<a href="#">BE197945</a>	<a href="#">20324</a>	Sdpr	serum deprivation response
139	1435459_at	1185.11	30.68	1.87	2.79	<a href="#">BM936480</a>	<a href="#">55990</a>	Fmo2	flavin containing monooxygenase 2
140	1436791_at	1186.03	30.51	1.64	2.25	<a href="#">BB067079</a>	<a href="#">22418</a>	Wnt5a	wingless-related MMTV integration site 5A
141	1425951_a_at	1188.07	30.39	1.81	2.65	<a href="#">AF240358</a>	<a href="#">56620</a>	Clec4n	C-type lectin domain family 4, member n
142	1427919_at	1188.31	30.20	1.67	2.32	<a href="#">BC028307</a>	<a href="#">68792</a>	SrpX2	sushi-repeat-containing protein, X-linked 2
143	1442257_at	1192.88	30.28	1.56	2.08	<a href="#">BI134319</a>	<a href="#">Mm_204306</a>	---	12 days embryo female mullerian duct includes surrounding region cDNA, RIKEN full-length enriched library, clone:6820438B06 product:unclassifiable, full insert sequence
144	1420991_at	1194.70	30.18	1.44	1.81	<a href="#">AK009959</a>	<a href="#">107765</a>	Ankrd1	ankyrin repeat domain 1 (cardiac muscle)
145	1420394_s_at	1197.25	30.08	1.75	2.50	<a href="#">U05264</a>	<a href="#">14727</a> <a href="#">14728</a>	Gp49a /// Lilrb4	glycoprotein 49 A /// leukocyte immunoglobulin-like receptor, subfamily B, member 4
146	1456046_at	1198.63	30.01	1.62	2.20	<a href="#">AV319144</a>	<a href="#">17064</a>	C1qr1	complement component 1, q subcomponent, receptor 1
147	1452183_a_at	1204.70	30.21	1.75	2.50	<a href="#">Y13832</a>	<a href="#">17263</a>	Gtl2	GTL2, imprinted maternally expressed untranslated mRNA
148	1456014_s_at	1209.43	30.34	1.65	2.26	<a href="#">BB113173</a>	<a href="#">108101</a>	BC032204	cDNA sequence

									BC032204	
149	1452445_at	1213.81	30.38	1.76	2.53	<a href="#">BC026874</a>	<a href="#">338365</a>	Slc41a2	solute carrier family 41, member 2	
150	1422124_a_at	1214.38	30.20	1.50	1.94	<a href="#">NM_011210</a>	<a href="#">19264</a>	Ptprc	protein tyrosine phosphatase, receptor type, C	
151	1455688_at	1226.72	30.73	2.17	3.55	<a href="#">BB795075</a>	<a href="#">98434</a>	LOC98434	hypothetical LOC98434	
152	1450241_a_at	1231.15	30.84	1.78	2.56	<a href="#">NM_010161</a>	<a href="#">14017</a>	Evi2a	ecotropic viral integration site 2a	
153	1421045_at	1241.21	31.37	1.88	2.82	<a href="#">BB528408</a>	<a href="#">17534</a>	Mrc2	mannose receptor, C type 2	
154	1439327_at	1246.77	31.51	1.68	2.34	<a href="#">BB197647</a>	<a href="#">320924</a>	Ccbe1	collagen and calcium binding EGF domains 1	
155	1416072_at	1256.35	31.96	2.02	3.16	<a href="#">NM_133654</a>	<a href="#">12490</a>	Cd34	CD34 antigen	
156	1452366_at	1258.53	31.87	1.56	2.07	<a href="#">AV371987</a>	<a href="#">234356</a>	4732435N03Rik	RIKEN cDNA 4732435N03 gene	
157	1449473_s_at	1259.58	31.71	1.60	2.17	<a href="#">NM_011611</a>	<a href="#">21939</a>	Cd40	CD40 antigen	
158	1424131_at	1267.67	32.21	1.70	2.40	<a href="#">AF064749</a>	<a href="#">12835</a>	Col6a3	procollagen, type VI, alpha 3	
159	1423547_at	1267.81	32.02	1.63	2.23	<a href="#">AW208566</a>	<a href="#">17105</a>	Lyzs	Lysozyme	
160	1434877_at	1268.95	31.91	2.11	3.40	<a href="#">AI152800</a>	<a href="#">18164</a>	Nptx1	neuronal pentraxin 1	
161	1416468_at	1276.93	32.25	1.89	2.85	<a href="#">NM_013467</a>	<a href="#">11668</a>	Aldh1a1	aldehyde dehydrogenase family 1, subfamily A1	
162	1439181_at	1277.63	32.12	1.46	1.86	<a href="#">AV020760</a>	<a href="#">210104</a>	BC043301	cDNA sequence BC043301	
163	1428432_at	1283.31	32.37	1.55	2.06	<a href="#">BB813478</a>	<a href="#">71918</a>	2310047A01Rik	RIKEN cDNA 2310047A01 gene	
164	1433695_at	1284.05	32.23	1.62	2.21	<a href="#">BQ174762</a>	<a href="#">380686</a>	1500041B16Rik	RIKEN cDNA 1500041B16 gene	
165	1437056_x_at	1287.99	32.23	1.51	1.97	<a href="#">BB558800</a>	<a href="#">78892</a>	Crispld2	cysteine-rich secretory protein LCCL domain containing 2	
166	1436936_s_at	1289.80	32.15	1.75	2.49	<a href="#">BG806300</a>	<a href="#">213742</a>	Xist	inactive X specific transcripts	
167	1450826_a_at	1292.53	32.15	1.81	2.64	<a href="#">NM_011315</a>	<a href="#">20210</a>	Saa3	serum amyloid A 3	
168	1448194_a_at	1307.72	32.86	1.40	1.75	<a href="#">NM_023123</a>	<a href="#">14955</a>	H19	H19 fetal liver mRNA	
169	1437385_at	1309.05	32.76	1.85	2.74	<a href="#">AV264768</a>	<a href="#">320924</a>	Ccbe1	collagen and calcium binding EGF domains 1	
170	1450684_at	1318.88	33.22	1.70	2.38	<a href="#">NM_007960</a>	<a href="#">14009</a>	Etv1	ets variant gene 1	
171	1424382_at	1321.77	33.29	1.88	2.82	<a href="#">BC025602</a>	<a href="#">52377</a>	Rcn3	reticulocalbin 3, EF-hand calcium binding domain	
172	1451161_a_at	1330.77	33.72	1.42	1.78	<a href="#">U66888</a>	<a href="#">13733</a>	Emr1	EGF-like module containing, mucin-like, hormone receptor-like sequence 1	
173	1434298_at	1331.24	33.55	1.59	2.14	<a href="#">BQ174116</a>	<a href="#">24136</a>	Zfhx1b	zinc finger homeobox 1b	
174	1419442_at	1335.10	33.75	1.50	1.95	<a href="#">BC005429</a>	<a href="#">17181</a>	Matn2	matrilin 2	
175	1452339_at	1343.82	34.11	1.52	1.98	<a href="#">AL359935</a>	<a href="#">108153</a>	Adamts7	a disintegrin-like and metalloproteinase (reprolysin type) with thrombospondin type 1 motif, 7	
176	1448433_a_at	1347.37	34.24	1.75	2.50	<a href="#">NM_008788</a>	<a href="#">18542</a>	Pcolce	procollagen C-endopeptidase enhancer protein	
177	1420772_a_at	1362.23	35.11	1.40	1.74	<a href="#">NM_010286</a>	<a href="#">14605</a>	Tsc22d3	TSC22 domain family 3	
178	1456475_s_at	1367.93	35.22	1.58	2.13	<a href="#">BB216074</a>	<a href="#">19088</a>	Prkar2b	protein kinase, cAMP dependent regulatory, type II beta	

179	1417649_at	1371.14	35.28	1.87	2.79	<a href="#">NM_009876</a>	<a href="#">12577</a>	Cdkn1c	cyclin-dependent kinase inhibitor 1C (P57)
180	1428642_at	1376.30	35.43	1.57	2.09	<a href="#">AK018094</a>	<a href="#">76157</a>	Slc35d3	solute carrier family 35, member D3
181	1437903_at	1380.77	35.54	1.50	1.94	<a href="#">BB820958</a>	<a href="#">16948</a>	Lox	lysyl oxidase
182	1423327_at	1392.35	36.16	1.67	2.33	<a href="#">AK005645</a>	<a href="#">68172</a>	4930517K11Rik	RIKEN cDNA 4930517K11 gene
183	1449314_at	1406.49	36.84	1.71	2.41	<a href="#">NM_011766</a>	<a href="#">22762</a>	Zfpm2	zinc finger protein, multitype 2
184	1420249_s_at	1412.65	37.03	1.68	2.34	<a href="#">AV084904</a>	<a href="#">20305</a>	Ccl6	chemokine (C-C motif) ligand 6
185	1436659_at	1419.14	37.39	1.90	2.86	<a href="#">BB757120</a>	<a href="#">13175</a>	Dcamk1	Double cortin and calcium/calmodulin-dependent protein kinase-like 1, mRNA (cDNA clone IMAGE:5006471)
186	1427076_at	1420.25	37.26	1.65	2.27	<a href="#">L20315</a>	<a href="#">17476</a>	Mpeg1	macrophage expressed gene 1
187	1427300_at	1421.31	37.15	1.81	2.65	<a href="#">D49658</a>	<a href="#">16875</a>	Lhx8	LIM homeobox protein 8
188	1451289_at	1426.94	37.30	1.87	2.78	<a href="#">AW105916</a>	<a href="#">13175</a>	Dcamk1	double cortin and calcium/calmodulin-dependent protein kinase-like 1
189	1420688_a_at	1428.63	37.24	1.52	1.98	<a href="#">NM_011360</a>	<a href="#">20392</a>	Sgce	sarcoglycan, epsilon
190	1460292_a_at	1437.47	37.61	1.42	1.78	<a href="#">NM_053123</a>	<a href="#">93761</a>	Smarca1	SWI/SNF related, matrix associated, actin dependent regulator of chromatin, subfamily a, member 1
191	1452382_at	1439.22	37.55	1.83	2.68	<a href="#">BB542096</a>	---	---	---
192	1450079_at	1442.66	37.59	1.73	2.45	<a href="#">AK012873</a>	<a href="#">27206</a>	Nrk	Nik related kinase
193	1457753_at	1461.09	38.58	1.54	2.03	<a href="#">B1655907</a>	<a href="#">279572</a>	Tlr13	toll-like receptor 13
194	1421228_at	1472.68	39.19	1.67	2.33	<a href="#">AF128193</a>	<a href="#">20306</a>	Ccl7	chemokine (C-C motif) ligand 7
195	1424659_at	1507.79	41.70	1.77	2.56	<a href="#">BG963150</a>	<a href="#">20563</a>	Slit2	slit homolog 2 (Drosophila)
196	1433885_at	1507.90	41.49	1.72	2.44	<a href="#">BM240173</a>	<a href="#">544963</a>	Iqgap2	IQ motif containing GTPase activating protein 2
197	1417148_at	1546.39	44.16	1.51	1.96	<a href="#">NM_008809</a>	<a href="#">18596</a>	Pdgfrb	platelet derived growth factor receptor, beta polypeptide
198	1450852_s_at	1563.76	45.34	1.76	2.54	<a href="#">BQ173958</a>	<a href="#">14062</a>	F2r	coagulation factor II (thrombin) receptor
199	1451016_at	1573.54	45.88	1.31	1.55	<a href="#">BB540964</a>	<a href="#">15983</a>	Ildr2	interferon-related developmental regulator 2
200	1438530_at	1577.96	45.97	1.46	1.86	<a href="#">BB756069</a>	<a href="#">21788</a>	Tfpi	tissue factor pathway inhibitor
201	1450004_at	1598.64	47.40	1.21	1.36	<a href="#">NM_021367</a>	<a href="#">53603</a>	Tslp	thymic stromal lymphopoietin
202	1416805_at	1599.80	47.27	1.52	1.98	<a href="#">NM_133187</a>	<a href="#">68659</a>	1110032E23Rik	RIKEN cDNA 1110032E23 gene
203	1434325_x_at	1606.07	47.50	1.58	2.11	<a href="#">BB274009</a>	<a href="#">19085</a>	Prkar1b	protein kinase, cAMP dependent regulatory, type I beta
204	1422748_at	1619.25	48.26	1.74	2.48	<a href="#">NM_015753</a>	<a href="#">24136</a>	Zfhx1b	zinc finger homeobox 1b
205	1440969_at	1622.67	48.29	1.32	1.58	<a href="#">BE944957</a>	<a href="#">407797</a>	BC030308	cDNA sequence BC030308
206	1442082_at	1635.09	48.95	1.55	2.05	<a href="#">BB333624</a>	<a href="#">12267</a>	C3ar1	complement component 3a receptor 1

207	1424086_at	1638.55	48.96	1.52	1.99	<a href="#">BC025514</a>	<a href="#">102644</a>	D9Ucla1	DNA segment, Chr 9, University of California at Los Angeles 1
208	1431079_at	1641.74	48.98	1.59	2.13	<a href="#">BF148029</a>	<a href="#">69183</a>	C1qtnf2	C1q and tumor necrosis factor related protein 2
209	1432466_a_at	1647.20	49.19	1.48	1.89	<a href="#">AK019319</a>	<a href="#">11816</a>	Apoe	apolipoprotein E
210	1455393_at	1651.60	49.27	1.49	1.92	<a href="#">BB009037</a>	---	---	---
211	1427263_at	1653.60	49.18	1.39	1.73	<a href="#">L04961</a>	<a href="#">213742</a>	Xist	inactive X specific transcripts
212	1429514_at	1654.13	49.00	1.56	2.08	<a href="#">AW111876</a>	<a href="#">67916</a>	Ppap2b	phosphatidic acid phosphatase type 2B
213	1443673_x_at	1659.77	49.19	1.30	1.54	<a href="#">BB710847</a>	---	---	---
214	1432517_a_at	1664.55	49.35	1.41	1.76	<a href="#">AK006371</a>	<a href="#">18113</a>	Nnmt	nicotinamide N- methyltransferase
215	1456389_at	1669.64	49.54	1.47	1.88	<a href="#">BB244754</a>	<a href="#">24136</a>	Zfx1b	zinc finger homeobox 1b
216	1418826_at	1678.82	49.93	1.60	2.15	<a href="#">NM_027209</a>	<a href="#">69774</a>	Ms4a6b	membrane-spanning 4-domains, subfamily A, member 6B
217	1446085_at	1681.26	49.93	1.35	1.63	<a href="#">BB022048</a>	<a href="#">216233</a>	Socs2	Suppressor of cytokine signaling 2 (Socs2), mRNA

## The Rank Product (RP) differential expression analysis report



General Information	
Experiment	VK1mouse4302
Normalisation	rma across replicates
Chip	one chip only
Comparison	Treatment samples: <b>K14D6 + CCL3</b> vs Baseline samples: <b>TG Control</b>
RP comparison	not paired
Direction	Positive

0	Probe-set ID	RPscore	FDR	FC	rmaFC	FC_nom	"SOURCE"	"EntrezGene"	Gene Symbol	Title
1	1418601_at	97.20	3.00	3.31	7.11	NM_011921	26358	Aldh1a7	aldehyde dehydrogenase family 1, subfamily A7	
2	1436996_x_at	106.48	1.50	2.47	4.41	AV066625	17110	Lzp-s	P lysozyme structural	
3	1448591_at	110.66	1.33	2.33	4.01	NM_021281	13040	Ctss	cathepsin S	
4	1439426_x_at	132.50	1.50	2.33	4.01	AV058500	17110	Lzp-s	P lysozyme structural	
5	1423522_at	147.22	1.40	2.11	3.39	BB811478	18150	Npm3	nucleoplasmin 3	
6	1452141_a_at	162.85	1.50	2.31	3.96	BC001991	20363	Sepp1	selenoprotein P, plasma, 1	
7	1418666_at	199.63	2.71	2.18	3.58	NM_008987	19288	Ptx3	pentraxin related gene	
8	1416468_at	210.40	2.75	2.31	3.94	NM_013467	11668	Aldh1a1	aldehyde dehydrogenase family 1, subfamily A1	
9	1436905_x_at	234.40	3.67	1.89	2.85	BB218107	16792	Laptm5	lysosomal-associated protein transmembrane 5	
10	1448620_at	242.06	3.90	1.97	3.04	NM_010188	14131	Fcgr3	Fc receptor, IgG, low affinity III	
11	1427883_a_at	254.35	4.27	2.18	3.59	AW550625	12825	Col3a1	procollagen, type III, alpha 1	
12	1460197_a_at	279.37	5.17	2.22	3.71	NM_054098	117167	Steap4	STEAP family member 4	
13	1420504_at	296.41	6.38	1.61	2.18	AF320226	56774	Slc6a14	solute carrier family 6 (neurotransmitter transporter), member 14	
14	1424186_at	302.93	6.14	2.05	3.26	BG074158	67896	2610001E17Rik	RIKEN cDNA 2610001E17 gene	
15	1427747_a_at	305.98	5.87	1.79	2.61	X14607	16819	Lcn2	lipocalin 2	
16	1432466_a_at	313.90	5.94	1.92	2.92	AK019319	11816	ApoE	apolipoprotein E	
17	1417936_at	373.00	9.29	1.82	2.66	AF128196	20308	Ccl9	chemokine (C-C motif) ligand 9	
18	1423091_a_at	398.97	11.22	1.98	3.05	AK016567	14758	Gpm6b	glycoprotein m6b	
19	1452905_at	423.63	12.68	2.11	3.40	AV015833	17263 330814	Gtl2 /// Lphn1	GTL2, imprinted maternally expressed untranslated	

20	1449833_at	427.48	12.40	1.68	2.34	NM_011472	20760	Sprr2f	mRNA /// latrophilin 1 small proline-rich protein 2F
21	1417266_at	430.38	12.24	1.86	2.77	BC002073	20305	Ccl6	chemokine (C-C motif) ligand 6
22	1425087_at	435.11	12.23	1.60	2.16	BC021588	67693	2310003F16Rik	RIKEN cDNA 2310003F16 gene glycoprotein 49 A /// leukocyte
23	1420394_s_at	446.67	12.52	1.92	2.90	U05264	14727 14728	Gp49a /// Lilrb4	immunoglobulin- like receptor, subfamily B, member 4
24	1455494_at	463.36	13.08	1.86	2.77	BI794771	12842	Col1a1	procollagen, type I, alpha 1
25	1423547_at	464.59	12.56	1.85	2.73	AW208566	17105	Lyzs	lysozyme
26	1452250_a_at	482.72	13.31	1.90	2.85	BI455189	12834	Col6a2	procollagen, type VI, alpha 2
27	1435477_s_at	496.59	13.89	1.72	2.43	BM224327	14130	Fcgr2b	Fc receptor, IgG, low affinity IIb
28	1419100_at	508.00	14.46	1.85	2.75	NM_009252	20716	Serpina3n	serine (or cysteine) peptidase inhibitor, clade A, member 3N
29	1422939_at	508.61	13.97	1.53	2.01	NM_009126	383548	Serpina3b	serine (or cysteine) peptidase inhibitor, clade B (ovalbumin), member 3B
30	1448590_at	512.09	13.70	1.85	2.74	NM_009933	12833	Col6a1	procollagen, type VI, alpha 1
31	1420503_at	535.10	14.87	1.49	1.92	AF320226	56774	Slc6a14	solute carrier family 6 (neurotransmitter transporter), member 14
32	1435459_at	539.54	14.88	1.85	2.74	BM936480	55990	Fmo2	flavin containing monooxygenase 2
33	1422940_x_at	583.05	18.36	1.53	2.01	NM_009126	383548	Serpina3b	serine (or cysteine) peptidase inhibitor, clade B (ovalbumin), member 3B
34	1423271_at	591.98	18.88	1.45	1.83	AV239646	14619	Gjb2	gap junction membrane channel protein beta 2
35	1433530_at	613.80	20.00	1.51	1.96	BI694945	70164	2210411K19Rik	RIKEN cDNA 2210411K19 gene
36	1423537_at	615.70	19.67	1.87	2.79	BB622036	14432	Gap43	growth associated protein 43
37	1448326_a_at	627.16	20.08	1.75	2.51	NM_013496	12903	Crabp1	cellular retinoic acid binding protein I
38	1424754_at	644.48	21.11	1.55	2.05	BC024402	109225	Ms4a7	membrane- spanning 4- domains, subfamily A, member 7
39	1448259_at	653.72	21.44	1.76	2.52	BI452727	14314	Fstl1	follicle-stimulating inhibitor-like 1
40	1424843_a_at	663.67	21.62	1.48	1.89	BC004622	14455	Gas5	growth arrest specific 5
41	1438405_at	665.38	21.44	1.86	2.77	BB791906	14178	Fgf7	fibroblast growth factor 7
42	1449154_at	671.67	21.45	1.86	2.78	NM_007729	12814	Col11a1	procollagen, type XI, alpha 1
43	1436970_a_at	682.68	21.84	1.73	2.45	AA499047	18596	Pdgfrb	platelet derived

									growth factor receptor, beta polypeptide
44	1418599_at	696.26	22.52	1.81	2.65	NM_007729	12814	Col11a1	procollagen, type XI, alpha 1
45	1420804_s_at	720.74	24.69	1.57	2.09	NM_010819	17474	Clec4d	C-type lectin domain family 4, member d
46	1448756_at	729.95	25.20	1.40	1.74	NM_009114	20202	S100a9	S100 calcium binding protein A9 (calgranulin B)
47	1448748_at	730.24	24.68	1.55	2.05	AF181829	56193	Plek	pleckstrin
48	1417785_at	734.92	24.60	1.58	2.12	NM_134102	85031	Pla1a	phospholipase A1 member A
49	1416221_at	735.00	24.12	1.74	2.48	BI452727	14314	Fstl1	folliculin-like 1
50	1452296_at	738.70	24.00	1.72	2.43	BM570006	20564	Slit3	slit homolog 3 (Drosophila)
51	1448475_at	739.77	23.61	1.64	2.25	NM_133859	99543	Olfml3	olfactomedin-like 3
52	1424265_at	742.77	23.38	1.51	1.97	BC022734	74091	Npl	N-acetylneuraminic acid pyruvate lyase
53	1426947_x_at	743.55	22.98	1.75	2.51	BI455189	12834	Col6a2	procollagen, type VI, alpha 2
54	1440739_at	753.02	23.33	1.63	2.24	AW228853	22341	Vegfc	vascular endothelial growth factor C
55	1423110_at	757.87	23.31	1.76	2.53	BF227507	---	---	---
56	1418892_at	764.07	23.25	1.72	2.44	AF309564	80837	Rhoj	ras homolog gene family, member J
57	1448228_at	776.52	23.63	1.86	2.77	M65143	16948	Lox	lysyl oxidase
58	1419627_s_at	777.85	23.34	1.67	2.31	NM_020001	56620	Clec4n	C-type lectin domain family 4, member n
59	1419394_s_at	794.29	24.37	1.42	1.77	NM_013650	20201	S100a8	S100 calcium binding protein A8 (calgranulin A)
60	1435943_at	807.08	25.17	1.89	2.84	AI647687	13479	Dpep1	dipeptidase 1 (renal)
61	1448995_at	827.30	26.46	1.65	2.28	NM_019932	56744	Cxcl4	chemokine (C-X-C motif) ligand 4
62	1451718_at	827.63	26.06	1.45	1.84	BB768495	18823	Plp1	proteolipid protein (myelin) 1
63	1423259_at	834.40	26.32	1.56	2.07	BB121406	15904	Id4	inhibitor of DNA binding 4
64	1450857_a_at	834.80	25.92	1.71	2.41	BF227507	12843	Col1a2	procollagen, type I, alpha 2
65	1417649_at	835.68	25.65	1.86	2.76	NM_009876	12577	Cdkn1c	cyclin-dependent kinase inhibitor 1C (P57)
66	1449984_at	838.10	25.42	1.56	2.06	NM_009140	20310	Cxcl2	chemokine (C-X-C motif) ligand 2
67	1448293_at	858.04	26.76	1.58	2.12	BB125261	13591	Ebf1	early B-cell factor 1
68	1424382_at	861.21	26.69	1.67	2.31	BC025602	52377	Rcn3	reticulocalbin 3, EF-hand calcium binding domain
69	1457040_at	863.35	26.49	1.47	1.88	BE947711	246316	Lgi2	leucine-rich repeat LGI family, member 2
70	1419599_s_at	866.01	26.29	1.58	2.12	NM_026835	64382	Ms4a11	membrane-spanning 4-domains, subfamily A, member 11
71	1416121_at	870.48	26.28	1.71	2.42	M65143	16948	Lox	lysyl oxidase
72	1443790_x_at	902.84	28.36	1.37	1.68	AV208084	78108	4930414L22Rik	RIKEN cDNA 4930414L22 gene

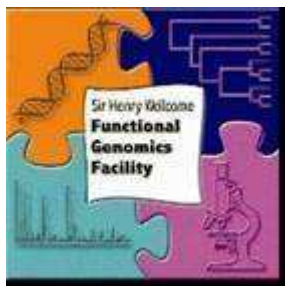
73	1448194_a_at	909.59	28.47	1.50	1.94	NM_023123	14955	H19	H19 fetal liver mRNA
74	1429273_at	914.94	28.57	1.70	2.39	AK014221	73230	Bmper	BMP-binding endothelial regulator
75	1419417_at	915.86	28.24	1.59	2.14	NM_009506	22341	Vegfc	vascular endothelial growth factor C
76	1437517_x_at	918.09	27.99	1.37	1.68	BB699605	20248	Serpib3a	serine (or cysteine) peptidase inhibitor, clade B (ovalbumin), member 3A
77	1449368_at	922.52	27.90	1.67	2.32	NM_007833	13179	Dcn	decorin
78	1450757_at	925.19	27.76	1.56	2.07	NM_009866	12552	Cdh11	cadherin 11
79	1439380_x_at	928.28	27.68	1.75	2.51	BB093563	17263	Gtl2	GTL2, imprinted maternally expressed untranslated mRNA
80	1457642_at	932.93	27.65	1.38	1.70	BB255999	70622	5730507N06Rik	RIKEN cDNA 5730507N06 gene
81	1420867_at	945.78	28.28	1.37	1.67	BB609648	56334	Tmed2	transmembrane emp24 domain trafficking protein 2
82	1437165_a_at	956.17	28.85	1.62	2.20	BB250811	18542	Pcolce	procollagen C-endopeptidase enhancer protein
83	1460250_at	971.86	30.01	1.57	2.10	BC021458	66042	Sostdc1	sclerostin domain containing 1
84	1448397_at	974.60	29.90	1.28	1.50	BC016507	14623	Gjb6	gap junction membrane channel protein beta 6
85	1420249_s_at	977.46	29.84	1.51	1.97	AV084904	20305	Ccl6	chemokine (C-C motif) ligand 6
86	1419463_at	978.22	29.53	1.55	2.04	AF108501	80797	Clca2	chloride channel calcium activated 2
87	1430655_at	988.47	29.91	1.47	1.88	BE685884	70800	4631405K08Rik	RIKEN cDNA 4631405K08 gene
88	1450652_at	993.62	30.05	1.63	2.24	NM_007802	13038	Ctsk	cathepsin K
89	1419483_at	1011.87	31.35	1.38	1.70	NM_009779	12267	C3ar1	complement component 3a receptor 1
90	1448323_a_at	1017.20	31.40	1.52	1.99	BC019502	12111	Bgn	biglycan
91	1443897_at	1022.26	31.38	1.44	1.82	BB200603	13198	Ddit3	DNA-damage inducible transcript 3
92	1432517_a_at	1022.64	31.12	1.51	1.97	AK006371	18113	Nnmt	nicotinamide N-methyltransferase
93	1438069_a_at	1027.87	31.16	1.38	1.70	BE446879	83486	Rbm5	RNA binding motif protein 5
94	1419598_at	1033.12	31.26	1.54	2.03	NM_026835	68774	Ms4a6d	membrane-spanning 4-domains, subfamily A, member 6D
95	1427086_at	1033.55	30.94	1.58	2.12	BM570006	---	---	---
96	1438403_s_at	1033.62	30.63	1.41	1.75	BF537798	80291	BC003324	CDNA sequence BC003324, mRNA (cDNA clone MGC:7036 IMAGE:3156139)
97	1450826_a_at	1039.65	30.82	1.61	2.18	NM_011315	20210	Saa3	serum amyloid A 3
98	1424903_at	1043.42	30.77	1.58	2.12	AF127244	20592	Jarid1d	jumonji, AT rich

										interactive domain 1D (Rbp2 like)
99	1423606_at	1051.64	31.16	1.71	2.42	BI110565	50706		Postn	periostin, osteoblast specific factor
100	1420499_at	1055.47	31.16	1.43	1.79	NM_008102	14528		Gch1	GTP cyclohydrolase 1
101	1439766_x_at	1058.94	31.08	1.52	1.99	BB089170	22341		Vegfc	vascular endothelial growth factor C
102	1433695_at	1062.92	31.13	1.51	1.97	BQ174762	380686		1500041B16Rik	RIKEN cDNA 1500041B16 gene
103	1420676_at	1070.91	31.50	1.38	1.71	NM_025984	67127		Sprr13	small proline rich-like 3
104	1455607_at	1087.25	32.29	1.55	2.05	BG072958	72780		Rspo3	R-spondin 3 homolog (Xenopus laevis)
105	1429297_at	1090.31	32.27	1.41	1.75	AK009018	71869		Serp1b12	serine (or cysteine) peptidase inhibitor, clade B (ovalbumin), member 12
106	1421228_at	1129.88	35.33	1.69	2.37	AF128193	20306		Ccl7	chemokine (C-C motif) ligand 7
107	1416779_at	1130.25	35.03	1.46	1.86	BE197945	20324		Sdpr	serum deprivation response
108	1435934_at	1144.23	35.91	1.43	1.80	AI643884	70316		Ndufab1	NADH dehydrogenase (ubiquinone) 1, alpha/beta subcomplex, 1
109	1434479_at	1161.59	37.06	1.49	1.93	AV246911	12831		Col5a1	Procollagen, type V, alpha 1 (Col5a1), mRNA
110	1416077_at	1162.52	36.79	1.54	2.03	NM_009627	11535		Adm	adrenomedullin
111	1422963_at	1167.55	36.90	1.31	1.56	NM_011475	20763		Sprr2i	small proline-rich protein 2I
112	1425357_a_at	1176.66	37.24	1.52	1.99	BC015293	23892		Grem1	gremlin 1
113	1460259_s_at	1182.29	37.41	1.52	1.99	AF108501	12722 80797		C1ca1 /// C1ca2	chloride channel calcium activated 1 /// chloride channel calcium activated 2
114	1435639_at	1183.14	37.14	1.43	1.80	BF580962	70045		2610528A11Rik	RIKEN cDNA 2610528A11 gene
115	1451939_a_at	1186.41	37.15	1.35	1.64	AB028050	51795		Srpx	sushi-repeat-containing protein
116	1436055_at	1204.38	38.34	1.52	1.99	AI506528	74488		Lrrc15	leucine rich repeat containing 15
117	1421492_at	1208.73	38.34	1.36	1.66	NM_019455	54486		Ptgds2	prostaglandin D2 synthase 2, hematopoietic
118	1448303_at	1210.06	38.14	1.41	1.76	NM_053110	93695		Gpnmb	glycoprotein (transmembrane) nmb
119	1422571_at	1215.82	38.34	1.69	2.35	NM_011581	21826		Thbs2	thrombospondin 2
120	1424542_at	1217.79	38.22	1.40	1.75	D00208	20198		S100a4	S100 calcium binding protein A4
121	1452138_a_at	1219.78	38.05	1.38	1.69	BB497528	70008		Ace2	angiotensin I converting enzyme (peptidyl-dipeptidase A) 2
122	1450618_a_at	1228.45	38.52	1.34	1.61	NM_011468	20755		Sprr2a	small proline-rich protein 2A
123	1416136_at	1242.21	39.27	1.71	2.41	NM_008610	17390		Mmp2	matrix metalloproteinase 2
124	1417256_at	1246.90	39.42	1.22	1.39	NM_008607	17386		Mmp13	matrix metalloproteinase

									13	
125	1417852_x_at	1252.74	39.53	1.40	1.74	AF047838	12722	Clca1	chloride channel calcium activated 1	
126	1419665_a_at	1253.73	39.26	1.38	1.69	NM_019738	56312	Nupr1	nuclear protein 1	
127	1435343_at	1255.50	39.16	1.53	2.00	BF715043	210293	Dock10	dedicator of cytokinesis 10	
128	1448061_at	1264.04	39.57	1.48	1.91	AA183642	---	---	---	
129	1416405_at	1265.70	39.38	1.45	1.85	BC019502	12111	Bgn	biglycan	
130	1418492_at	1266.15	39.11	1.52	1.99	NM_011825	23893	Grem2	gremlin 2 homolog, cysteine knot superfamily (Xenopus laevis)	
131	1448925_at	1268.43	38.96	1.54	2.02	NM_007855	13345	Twist2	twist homolog 2 (Drosophila)	
132	1449314_at	1270.69	38.87	1.46	1.86	NM_011766	22762	Zfpn2	zinc finger protein, multitype 2	
133	1443768_at	1273.77	38.83	1.41	1.75	BG101505	11848	Rhoa	Ras homolog gene family, member A (Rhoa), mRNA	
134	1417494_a_at	1273.90	38.54	1.55	2.06	BB332449	12870	Cp	ceruloplasmin	
135	1456379_x_at	1274.42	38.31	1.34	1.61	BB038556	227325	Dner	delta/notch-like EGF-related receptor	
136	1420380_at	1282.63	38.65	1.67	2.32	AF065933	20296	Ccl2	chemokine (C-C motif) ligand 2	
137	1417210_at	1294.04	39.26	1.55	2.05	NM_012011	26908	Eif2s3y	eukaryotic translation initiation factor 2, subunit 3, structural gene Y-linked	
138	1450430_at	1297.13	39.17	1.47	1.89	NM_008625	17533	Mrc1	mannose receptor, C type 1	
139	1422837_at	1299.90	39.14	1.24	1.43	NM_022886	64929	Scel	sciellin	
140	1419247_at	1311.81	39.72	1.45	1.84	AF215668	19735	Rgs2	regulator of G-protein signaling 2	
141	1416740_at	1314.96	39.72	1.47	1.88	AW744319	12831	Col5a1	procollagen, type V, alpha 1	
142	1422317_a_at	1327.48	40.41	1.74	2.48	NM_010743	17082	Il1rl1	interleukin 1 receptor-like 1	
143	1426302_at	1327.77	40.16	1.33	1.59	BC021368	214523	Tmprss4	transmembrane protease, serine 4	
144	1417009_at	1334.11	40.38	1.48	1.90	NM_023143	50909	C1r	complement component 1, r subcomponent	
145	1455426_at	1342.39	40.70	1.51	1.96	AV226618	13837	Epha3	Eph receptor A3	
146	1423634_at	1354.58	41.49	1.28	1.50	AI506986	57911	Gsdm1	gasdermin 1	
147	1444176_at	1375.02	42.96	1.32	1.58	AV204216	242341	Atp6v0d2	ATPase, H <sup>+</sup> transporting, V0 subunit D, isoform 2	
148	1420498_a_at	1377.68	42.91	1.53	2.00	NM_023118	13132	Dab2	disabled homolog 2 (Drosophila)	
149	1421194_at	1383.73	43.09	1.42	1.78	NM_010576	16401	Itga4	integrin alpha 4	
150	1455431_at	1391.19	43.42	1.35	1.63	AV371434	20537	Slc5a1	solute carrier family 5 (sodium/glucose cotransporter), member 1	
151	1434195_at	1405.67	44.29	1.45	1.83	BB042892	244954	Prss35	protease, serine, 35	
152	1428642_at	1410.00	44.40	1.41	1.75	AK018094	76157	Slc35d3	solute carrier family 35, member D3	
153	1416072_at	1415.04	44.40	1.46	1.85	NM_133654	12490	Cd34	CD34 antigen	
154	1450783_at	1415.15	44.11	1.30	1.54	NM_008331	15957	Ifit1	interferon-induced	

									protein with tetratricopeptide repeats 1
155	1455930_at	1424.05	44.67	1.30	1.54	BI651113	---	---	---
156	1455899_x_at	1427.58	44.75	1.31	1.56	BB241535	12702	Socs3	suppressor of cytokine signaling 3
157	1436530_at	1429.16	44.57	1.44	1.83	AA666504	Mm.24097	---	CDNA clone MGC:107680 IMAGE:6766535
158	1421045_at	1443.93	45.50	1.48	1.91	BB528408	17534	Mrc2	mannose receptor, C type 2
159	1439364_a_at	1450.22	45.77	1.62	2.20	BF147716	17390	Mmp2	matrix metalloproteinase 2
160	1449254_at	1464.84	46.70	1.36	1.66	NM_009263	20750	Spp1	secreted phosphoprotein 1
161	1437658_a_at	1475.87	47.36	1.33	1.60	AW552536	83673	Rnu22	RNA, U22 small nucleolar
162	1418266_at	1478.82	47.39	1.26	1.45	NM_009659	11686	Alox12b	arachidonate 12-lipoxygenase, 12R type
163	1444061_at	1482.07	47.46	1.29	1.51	BB150166	109314	A030004J04Rik	RIKEN cDNA A030004J04 gene
164	1417516_at	1492.32	48.02	1.31	1.56	NM_007837	13198	Ddit3	DNA-damage inducible transcript 3
165	1455573_at	1494.80	47.92	1.34	1.62	BE197934	16664	Krt1-14	keratin complex 1, acidic, gene 14
166	1448162_at	1495.67	47.71	1.46	1.86	BB250384	22329	Vcam1	vascular cell adhesion molecule 1
167	1416593_at	1501.01	47.82	1.40	1.74	AF276917	93692	Glrx1	glutaredoxin 1 (thioltransferase)
168	1454830_at	1502.75	47.65	1.41	1.76	AV010392	14119	Fbn2	fibrillin 2
169	1451332_at	1511.71	48.01	1.43	1.79	BC021376	225207	Zfp521	zinc finger protein 521
170	1416200_at	1524.31	48.78	1.20	1.36	NM_133775	77125	9230117N10Rik	RIKEN cDNA 9230117N10 gene
171	1429504_at	1538.85	49.65	1.36	1.65	BE134108	67225	Rnpc3	RNA-binding region (RNP1, RRM) containing 3

## The Rank Product (RP) differential expression analysis report



### General Information

Experiment	VK1mouse4302
Normalisation	rma across replicates
Chip	one chip only
Comparison	Treatment samples: <b>K14D6 + CCL3</b> vs Baseline samples: <b>WT + CCL3</b>
RP comparison	not paired
Direction	Positive

0	Probe-set ID	RPscore	FDR	FC_rma	FC_nom	"SOURCE"	"EntrezGene"	Gene Symbol	Title
1	1422111_at	1.28	0.00	35.02	340.86	BE631540	59289	Ccbp2	chemokine binding protein 2
2	1426438_at	186.44	12.00	3.97	9.59	AA210261	26900	Ddx3y	DEAD (Asp-Glu-Ala-Asp) box polypeptide 3, Y-linked
3	1417210_at	190.60	9.00	3.73	8.67	NM_012011	26908	Eif2s3y	eukaryotic translation initiation factor 2, subunit 3, structural gene Y-linked
4	1452077_at	280.18	21.25	2.31	3.95	AA210261	26900	Ddx3y	DEAD (Asp-Glu-Ala-Asp) box polypeptide 3, Y-linked
5	1420504_at	335.66	27.20	1.55	2.05	AF320226	56774	Slc6a14	solute carrier family 6 (neurotransmitter transporter), member 14
6	1426598_at	396.73	33.67	1.58	2.12	BB742957	22290 546404 546411	Uty /// LOC546404 /// LOC546411	ubiquitously transcribed tetratricopeptide repeat gene, Y chromosome /// similar to male-specific histocompatibility antigen H-YDb /// similar to male-specific histocompatibility antigen H-YDb
7	1424903_at	407.62	31.86	1.92	2.92	AF127244	20592	Jarid1d	jumonji, AT rich interactive domain 1D (Rbp2 like)
8	1417022_at	423.42	32.00	1.52	1.99	NM_007515	11989	Slc7a3	solute carrier family 7 (cationic amino acid transporter, y+ system), member 3
9	1426439_at	612.17	NA	1.80	2.62	AA210261	26900	Ddx3y	DEAD (Asp-Glu-Ala-Asp) box polypeptide 3, Y-linked
10	1423522_at	627.90	NA	1.50	1.95	BB811478	18150	Npm3	nucleoplasmin 3
11	1449484_at	698.90	NA	1.44	1.82	AF031035	20856	Stc2	stanniocalcin 2
12	1437935_at	710.40	NA	1.46	1.85	BB821151	75033	4930486G11 Rik	RIKEN cDNA 4930486G11 gene
13	1415862_at	729.26	NA	1.36	1.66	BB762957	22178	Tyrp1	tyrosinase-related protein 1

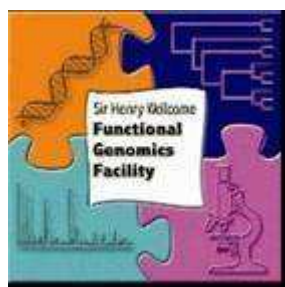
14	1420503_at	789.24	NA	1.38	1.69	AF320226	56774	Slc6a14	solute carrier family 6 (neurotransmitter transporter), member 14
15	1421003_at	826.18	NA	1.38	1.69	AA024025	56809	Gmeb1	glucocorticoid modulatory element binding protein 1
16	1455626_at	917.50	NA	1.14	1.24	AA987181	15405	Hoxa9	homeo box A9
17	1420901_a_at	948.05	NA	1.36	1.65	NM_010438	15275	Hk1	hexokinase 1
18	1418666_at	956.11	NA	1.22	1.38	NM_008987	19288	Ptx3	pentraxin related gene
19	1422523_at	973.05	NA	1.30	1.54	NM_021882	20431	Si	silver
20	1422481_at	977.84	NA	1.28	1.50	NM_008473	16678	Krt2-1	keratin complex 2, basic, gene 1
21	1437445_at	1076.16	NA	1.23	1.41	BB770967	17364	Trpm1	transient receptor potential cation channel, subfamily M, member 1
22	1452315_at	1120.02	NA	1.36	1.66	BB827235	16551	Kif11	kinesin family member 11
23	1417649_at	1128.63	NA	1.23	1.41	NM_009876	12577	Cdkn1c	cyclin-dependent kinase inhibitor 1C (P57)
24	1415861_at	1141.68	NA	1.24	1.43	BB762957	22178	Tyrp1	tyrosinase-related protein 1
25	1456095_at	1150.01	NA	1.19	1.33	BB769772	22173	Tyr	tyrosinase
26	1418028_at	1186.33	NA	1.26	1.46	NM_010024	13190	Dct	dopachrome tautomerase
27	1426065_a_at	1196.86	NA	1.36	1.65	BC012955	228775	Trib3	tribbles homolog 3 (Drosophila)
28	1421830_at	1228.50	NA	1.33	1.60	NM_009647	11639	Ak3l1	adenylate kinase 3 alpha-like 1
29	1456225_x_at	1241.53	NA	1.35	1.64	BB508622	228775	Trib3	tribbles homolog 3 (Drosophila)
30	1439409_x_at	1294.88	NA	1.23	1.40	BB006219	22178	Tyrp1	tyrosinase-related protein 1
31	1448397_at	1302.50	NA	1.25	1.44	BC016507	14623	Gjb6	gap junction membrane channel protein beta 6
32	1453252_at	1304.65	NA	1.33	1.59	AK010138	71916	Dus4l	dihydrouridine synthase 4-like (S. cerevisiae)
33	1452514_a_at	1305.71	NA	1.27	1.49	X65997	16590	Kit	kit oncogene
34	1421487_a_at	1318.38	NA	1.34	1.62	NM_010878	17973	Nck1	non-catalytic region of tyrosine kinase adaptor protein 1
35	1417717_a_at	1323.95	NA	1.24	1.41	NM_011661	22173	Tyr	tyrosinase
36	1425415_a_at	1375.67	NA	1.32	1.58	U75214	20510	Slc1a1	solute carrier family 1 (neuronal/epithelial high affinity glutamate transporter, system Xag), member 1
37	1448152_at	1414.85	NA	1.34	1.61	NM_010514	16002	Igf2	insulin-like growth factor 2
38	1450618_a_at	1420.44	NA	1.28	1.50	NM_011468	20755	Sprr2a	small proline-rich protein 2A
39	1426634_at	1471.30	NA	1.33	1.59	BB010989	230612	Slc5a9	solute carrier family 5 (sodium/glucose cotransporter), member 9
40	1419906_at	1473.87	NA	1.32	1.58	AV026552	15446	Hpgd	Hydroxyprostaglandin dehydrogenase 15 (NAD), mRNA (cDNA clone MGC:14001 IMAGE:4208980)
41	1442153_at	1480.86	NA	1.47	1.87	BB206087	Mm.385427	---	0 day neonate thymus cDNA, RIKEN full-length enriched library,

									clone:A430072F05 product:unclassifiable , full insert sequence
42	1437125_at	1503.50	NA	1.30	1.54	BB476448	12322	Camk2a	calcium/calmodulin- dependent protein kinase II alpha
									high mobility group box 1 /// RIKEN cDNA 4932431P20 gene /// high mobility group box 1-like /// similar to High mobility group protein 1 (HMG-1) (High mobility group protein B1) (Amphoterin) (Heparin-binding protein p30) /// similar to High mobility group protein 1 (HMG-1) (High mobility group protein B1) (Amphoterin) (Heparin-binding protein p30) /// similar to High mobility group protein 1 (HMG-1) (High mobility group protein B1) (Amphoterin) (Heparin-binding protein p30) /// similar to Ac2-008 /// similar to High mobility group protein 1 (HMG-1) (High mobility group protein B1) (Amphoterin) (Heparin-binding protein p30) /// similar to High mobility group protein 1 (HMG-1) (High mobility group protein B1) (Amphoterin) (Heparin-binding protein p30) /// similar to High mobility group protein 1 (HMG-1) (High mobility group protein B1) (Amphoterin) (Heparin-binding protein p30)
								Hmgb1 /// 4932431P20R ik /// Hmgb1l /// 114675 15289 213440 432959 433238 434174 544824 545506 545555 546331	
43	1448235_s_at	1517.76	NA	1.32	1.58	BF166000			
44	1448745_s_at	1519.00	NA	1.13	1.22	NM_008508	16939	Lor	loricrin
45	1446990_at	1553.36	NA	1.30	1.53	AW556192	18027	Nfia	nuclear factor I/A
46	1430635_at	1563.59	NA	1.21	1.37	BB774399	77836	Mlana	melan-A
47	1415998_at	1574.94	NA	1.32	1.57	NM_011694	22333	Vdac1	voltage-dependent anion channel 1
48	1429460_at	1583.55	NA	1.24	1.41	AK019508	78249	Gpr115	G protein-coupled receptor 115
49	1451718_at	1591.23	NA	1.13	1.23	BB768495	18823	Plp1	proteolipid protein (myelin) 1
50	1447625_at	1594.11	NA	1.26	1.47	BB286270	13559	E2f5	E2F transcription factor 5
51	1429565_s_at	1598.37	NA	1.02	1.03	AK004318	66203	Lce5a	late cornified envelope 5A
52	1449347_a_at	1603.63	NA	1.28	1.50	NM_021365	27083 434794	Xlr4b /// Xlr4a	X-linked lymphocyte- regulated 4B /// X- linked lymphocyte- regulated 4A
53	1429067_at	1612.21	NA	1.29	1.52	AK009171	69543	Capns2	calpain, small subunit 2
54	1449540_at	1628.21	NA	1.30	1.55	NM_023894	104384	Rhox9	reproductive homeobox on X chromosome, 9

55	1450976_at	1633.42	NA	1.28	1.50	AI987929	17988	Ndrp1	N-myc downstream regulated gene 1
56	1450079_at	1633.77	NA	1.09	1.15	AK012873	27206	Nrk	Nik related kinase
57	1448107_x_at	1655.08	NA	1.29	1.51	BC010754	16612	Klk6	kallikrein 6
58	1451613_at	1672.90	NA	1.10	1.17	AY027660	68723	Hnr	homerin
59	1419409_at	1700.51	NA	1.15	1.26	NM_026822	68720	Sprr15	small proline rich-like 5
60	1417516_at	1703.92	NA	1.30	1.53	NM_007837	13198	Ddit3	DNA-damage inducible transcript 3
61	1427663_a_at	1708.03	NA	1.30	1.55	BG921314	12750	Clk4	CDC like kinase 4
62	1448185_at	1724.45	NA	1.30	1.53	NM_022331	64209	Herpud1	homocysteine-inducible, endoplasmic reticulum stress-inducible, ubiquitin-like domain member 1
63	1452138_a_at	1747.88	NA	1.29	1.52	BB497528	70008	Ace2	angiotensin I converting enzyme (peptidyl-dipeptidase A) 2
64	1419905_s_at	1792.82	NA	1.07	1.11	AV026552	15446	Hpgd	hydroxyprostaglandin dehydrogenase 15 (NAD)
65	1420676_at	1794.82	NA	1.05	1.08	NM_025984	67127	Sprr13	small proline rich-like 3
66	1448612_at	1809.06	NA	1.31	1.55	NM_018754	55948	Sfn	stratifin
67	1416778_at	1837.15	NA	1.22	1.39	BE197945	20324	Sdpr	serum deprivation response
68	1416691_at	1841.81	NA	1.29	1.52	NM_019581	56055	Gtpbp2	GTP binding protein 2
69	1453218_at	1888.02	NA	1.01	1.01	AK003705	73719	1110014K05Rik	RIKEN cDNA 1110014K05 gene
70	1420867_at	1891.78	NA	1.28	1.50	BB609648	56334	Tmed2	transmembrane emp24 domain trafficking protein 2
71	1451064_a_at	1893.43	NA	1.28	1.49	BC004827	107272	Psat1	phosphoserine aminotransferase 1
72	1432032_a_at	1895.53	NA	1.29	1.52	AK015393	11876	Artn	artemin
73	1423271_at	1932.34	NA	1.15	1.26	AV239646	14619	Gjb2	gap junction membrane channel protein beta 2
74	1422989_a_at	1941.79	NA	1.28	1.50	NM_032418	13400	Dmpk	dystrophia myotonica-protein kinase
75	1450387_s_at	1943.45	NA	1.24	1.43	NM_009647	11639	Ak311	adenylate kinase 3 alpha-like 1
76	1420431_at	1953.13	NA	0.99	0.98	NM_009100	20129	Rptn	repetin
77	1420332_x_at	1953.24	NA	1.02	1.03	NM_027137	69611	Sprr17	small proline rich-like 7
78	1422639_at	1963.56	NA	1.13	1.23	NM_054084	116903	Calcb	calcitonin-related polypeptide, beta
79	1419591_at	1971.27	NA	1.21	1.36	NM_031378	83492	Mlze	melanoma-derived leucine zipper, extra-nuclear factor
80	1418283_at	1979.65	NA	1.29	1.51	NM_009903	12740	Cldn4	claudin 4
81	1448364_at	1979.87	NA	1.21	1.36	U95826	12452	Ccng2	cyclin G2
82	1416934_at	1988.26	NA	1.27	1.49	NM_019926	17772	Mtm1	X-linked myotubular myopathy gene 1
83	1457449_at	1991.14	NA	1.29	1.52	AW550676	241447	Lass6	Longevity assurance homolog 6 (S. cerevisiae), mRNA (cDNA clone MGC:67674 IMAGE:4224547)
84	1419254_at	1991.99	NA	1.29	1.51	BG076333	17768	Mthfd2	methylenetetrahydrofolate dehydrogenase (NAD+ dependent), methenyltetrahydrofol

									ate cyclohydrolase
85	1437703_at	1997.64	NA	1.26	1.47	BM229128	382156	LOC382156	similar to F-box- and WD40-repeat-containing protein
86	1444515_at	1999.14	NA	1.28	1.49	BM247709	338367	Myo1d	Myosin ID (Myo1d), mRNA
87	1429602_at	2011.21	NA	1.26	1.47	AK009888	69655	Cd164I2	D164 sialomucin-like 2
88	1437306_at	2022.54	NA	1.17	1.30	BG071013	232035	C130092O11 Rik	RIKEN cDNA C130092O11 gene
89	1457040_at	2026.45	NA	1.21	1.38	BE947711	246316	Lgi2	leucine-rich repeat LGI family, member 2
90	1436058_at	2041.03	NA	1.28	1.49	BB132493	58185	Rsad2	radical S-adenosyl methionine domain containing 2
91	1437809_x_at	2045.19	NA	1.26	1.46	AV296703	23872	Ets2	E26 avian leukemia oncogene 2, 3' domain
92	1430112_at	2045.22	NA	1.30	1.54	AK016965	269701 545804	Wdr66 /// LOC545804	WD repeat domain 66 /// similar to hypothetical protein MGC33630
93	1444000_at	2052.19	NA	1.28	1.49	BB448693	319786	B930059L03R ik	RIKEN cDNA B930059L03 gene
94	1424332_at	2054.71	NA	1.28	1.49	AF422144	224624	Rab40c	Rab40c, member RAS oncogene family
95	1436055_at	2071.43	NA	1.19	1.32	AI506528	74488	Lrrc15	leucine rich repeat containing 15
96	1418599_at	2077.45	NA	1.10	1.16	NM_007729	12814	Col11a1	procollagen, type XI, alpha 1
97	1422247_a_at	2095.05	NA	1.09	1.15	NM_009484	22290 546404	Uty /// LOC546404	ubiquitously transcribed tetratricopeptide repeat gene, Y chromosome /// similar to male-specific histocompatibility antigen H-YDb
98	1425880_x_at	2096.27	NA	1.26	1.46	AF290196	236537	Zfp352	zinc finger protein 352
99	1449033_at	2098.87	NA	1.12	1.20	AB013898	18383	Tnfrsf11b	tumor necrosis factor receptor superfamily, member 11b (osteoprotegerin)
100	1429297_at	2107.08	NA	1.17	1.29	AK009018	71869	Serpinb12	serine (or cysteine) peptidase inhibitor, clade B (ovalbumin), member 12

## The Rank Product (RP) differential expression analysis report



### General Information

Experiment	VK1mouse4302
Normalisation	rma across replicates
Chip	one chip only
Comparison	Treatment samples: <b>K14D6 Control</b> vs Baseline samples: <b>WT Control</b>
RP comparison	not paired
Direction	Negative

0	Probe-set ID	RPscore	FDR	FC_rma	FC_nom	"SOURCE"	"EntrezGene"	Gene Symbol	Title
1	1436996_x_at	80.91	0.00	-2.92	-5.79	AV066625	17110	Lzp-s	P lysozyme structural
2	1448591_at	99.49	0.50	-2.81	-5.44	NM_021281	13040	Ctss	cathepsin S
3	1439426_x_at	119.46	1.67	-2.73	-5.20	AV058500	17110	Lzp-s	P lysozyme structural
4	1419627_s_at	204.14	5.75	-2.04	-3.22	NM_020001	56620	Clec4n	C-type lectin domain family 4, member n
5	1436905_x_at	241.21	8.20	-2.02	-3.18	BB218107	16792	Laptm5	lysosomal-associated protein transmembrane 5
6	1420804_s_at	288.72	11.17	-1.84	-2.73	NM_010819	17474	Clec4d	C-type lectin domain family 4, member d
7	1453218_at	314.02	13.14	-1.94	-2.97	AK003705	73719	1110014K05Rik	RIKEN cDNA 1110014K05 gene
8	1448620_at	349.82	16.00	-1.84	-2.71	NM_010188	14131	Fcgr3	Fc receptor, IgG, low affinity III
9	1444061_at	391.54	19.33	-1.96	-3.01	BB150166	109314	A030004J04Rik	RIKEN cDNA A030004J04 gene
10	1423547_at	395.41	17.70	-1.88	-2.81	AW208566	17105	Lyzs	lysozyme
11	1419599_s_at	395.62	16.09	-1.74	-2.49	NM_026835	64382	Ms4a11	membrane-spanning 4-domains, subfamily A, member 11
12	1432466_a_at	412.07	17.00	-1.79	-2.60	AK019319	11816	Apoe	apolipoprotein E
13	1424903_at	436.82	18.77	-1.76	-2.53	AF127244	20592	Jarid1d	jumonji, AT rich interactive domain 1D (Rbp2 like)
14	1452141_a_at	458.61	20.36	-1.75	-2.50	BC001991	20363	Sepp1	selenoprotein P, plasma, 1
15	1456248_at	463.19	19.87	-1.87	-2.79	AV076385	69520	2310002A05Rik	RIKEN cDNA 2310002A05 gene
16	1420394_s_at	464.93	19.06	-1.73	-2.45	U05264	14727 14728	Gp49a /// Lilrb4	glycoprotein 49 A /// leukocyte immunoglobulin-like receptor, subfamily B,

									member 4
17	1419409_at	529.00	26.29	-1.75	-2.50	NM_026822	68720	Sprrl5	small proline rich-like 5
18	1429565_s_at	530.23	24.89	-1.86	-2.76	AK004318	66203	Lce5a	late cornified envelope 5A
19	1420332_x_at	533.51	23.89	-1.78	-2.57	NM_027137	69611	Sprrl7	small proline rich-like 7
20	1420550_at	577.80	28.95	-1.73	-2.46	AV014636	67828	1110055J05Rik	RIKEN cDNA 1110055J05 gene
21	1428980_at	601.17	30.43	-1.73	-2.46	AK003253	73731	1110001M24Rik	RIKEN cDNA 1110001M24 gene
22	1452077_at	626.85	32.00	-1.60	-2.15	AA210261	26900	Ddx3y	DEAD (Asp-Glu-Ala-Asp) box polypeptide 3, Y-linked
23	1448995_at	639.19	32.13	-1.32	-1.58	NM_019932	56744	Cxcl4	chemokine (C-X-C motif) ligand 4
24	1438069_a_at	646.43	31.58	-1.56	-2.07	BE446879	83486	Rbm5	RNA binding motif protein 5
25	1420350_at	648.49	30.68	-1.72	-2.44	NM_028625	73722	Sprrl2	small proline rich-like 2
26	1420676_at	662.44	31.35	-1.70	-2.38	NM_025984	67127	Sprrl3	small proline rich-like 3
27	1438558_x_at	665.94	30.52	-1.63	-2.22	AV009267	15220	Foxq1	Forkhead box Q1 (Foxq1), mRNA
28	1417808_at	667.50	29.68	-1.67	-2.31	NM_025621	66533	2310050C09Rik	RIKEN cDNA 2310050C09 gene
29	1423505_at	674.00	29.52	-1.49	-1.93	BB114067	21345	Tagln	transgelin
30	1417936_at	686.95	30.53	-1.61	-2.19	AF128196	20308	Ccl9	chemokine (C-C motif) ligand 9
31	1449265_at	718.21	34.00	-1.54	-2.03	BC008152	12362	Casp1	caspase 1
32	1420431_at	719.47	33.00	-1.59	-2.14	NM_009100	20129	Rptn	repetin
33	1423522_at	723.58	32.58	-1.57	-2.09	BB811478	18150	Npm3	nucleoplasmin 3
34	1417275_at	731.55	32.50	-1.31	-1.55	NM_010762	17153	Mal	myelin and lymphocyte protein, T-cell differentiation protein
35	1432828_at	737.75	32.57	-1.52	-1.98	BF607489	---	---	---
36	1426438_at	764.20	35.17	-1.54	-2.04	AA210261	26900	Ddx3y	DEAD (Asp-Glu-Ala-Asp) box polypeptide 3, Y-linked
37	1420741_x_at	791.06	37.41	-1.65	-2.28	NM_029667	76585	2310069N01Rik	RIKEN cDNA 2310069N01 gene
38	1427735_a_at	805.16	38.18	-1.53	-2.00	M12233	11459	Acta1	actin, alpha 1, skeletal muscle
39	1431554_a_at	806.43	37.38	-1.60	-2.15	AK003395	71790	Anxa9	annexin A9
40	1422963_at	808.90	36.98	-1.61	-2.19	NM_011475	20763	Sprr2i	small proline-rich protein 2I
41	1425951_a_at	814.54	36.80	-1.51	-1.97	AF240358	56620	Clec4n	C-type lectin domain family 4, member n
42	1457777_at	817.53	36.43	-1.58	-2.11	AV240142	57911	Gsdm1	gasdermin 1
43	1449833_at	833.07	37.70	-1.59	-2.14	NM_011472	20760	Sprr2f	small proline-rich protein 2F
44	1435477_s_at	834.99	37.02	-1.58	-2.11	BM224327	14130	Fcgr2b	Fc receptor, IgG, low affinity IIb
45	1423634_at	852.30	38.13	-1.58	-2.12	AI506986	57911	Gsdm1	gasdermin 1
46	1449071_at	854.10	37.59	-1.50	-1.95	NM_022879	17898	Myl7	myosin, light polypeptide 7, regulatory
47	1456001_at	854.64	36.83	-1.60	-2.17	AV071932	Mm.387664	---	CDNA clone MGC:118457

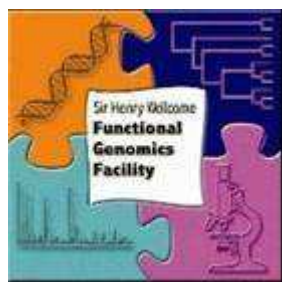
IMAGE:30288561

48	1426598_at	863.01	37.17	-1.48	-1.90	BB742957	22290 546404 546411	Uty /// LOC546404 /// LOC546411	ubiquitously transcribed tetratricopeptide repeat gene, Y chromosome /// similar to male-specific histocompatibility antigen H-YDb /// similar to male-specific histocompatibility antigen H-YDb
49	1423542_at	869.86	37.16	-1.56	-2.08	BB283507	23993	Klk7	kallikrein 7 (chymotryptic, stratum corneum)
50	1417210_at	874.20	36.80	-1.48	-1.91	NM_012011	26908	Eif2s3y	eukaryotic translation initiation factor 2, subunit 3, structural gene Y-linked
51	1453092_at	875.77	36.14	-1.66	-2.29	AK009010	74175	2300002G24Rik	RIKEN cDNA 2300002G24 gene
52	1418188_a_at	879.22	36.19	-1.50	-1.95	AF146523	72289	Malat1	metastasis associated lung adenocarcinoma transcript 1 (non-coding RNA)
53	1416468_at	881.14	35.64	-1.40	-1.75	NM_013467	11668	Aldh1a1	aldehyde dehydrogenase family 1, subfamily A1
54	1440966_at	882.57	35.20	-1.43	-1.79	BB248730	57438	March7	membrane-associated ring finger (C3HC4) 7
55	1448291_at	890.87	35.47	-1.40	-1.74	NM_013599	17395	Mmp9	matrix metalloproteinase 9
56	1427910_at	890.93	34.84	-1.61	-2.18	AK003744	73720	Cst6	cystatin E/M
57	1418601_at	896.13	34.77	-1.04	-1.06	NM_011921	26358	Aldh1a7	aldehyde dehydrogenase family 1, subfamily A7
58	1420677_x_at	931.87	38.52	-1.57	-2.10	NM_025984	67127	Sprr13	small proline rich-like 3
59	1460569_x_at	933.90	38.10	-1.47	-1.87	AW611462	12739	Cldn3	claudin 3
60	1438403_s_at	944.91	38.80	-1.46	-1.86	BF537798	80291	BC003324	CDNA sequence BC003324, mRNA (cDNA clone MGC:7036 IMAGE:3156139)
61	1455900_x_at	948.87	38.64	-1.59	-2.14	BB041811	21817	Tgm2	transglutaminase 2, C polypeptide
62	1437277_x_at	957.49	38.84	-1.49	-1.92	BB550124	21817	Tgm2	transglutaminase 2, C polypeptide
63	1449902_at	961.33	38.57	-1.50	-1.95	AV014636	66195	1110058A15Rik	RIKEN cDNA 1110058A15 gene
64	1417266_at	967.76	38.66	-1.72	-2.43	BC002073	20305	Ccl6	chemokine (C-C motif) ligand 6
65	1435934_at	984.76	39.83	-1.43	-1.80	AI643884	70316	Ndufab1	NADH dehydrogenase (ubiquinone) 1, alpha/beta subcomplex, 1
66	1450430_at	1019.27	43.24	-1.50	-1.95	NM_008625	17533	Mrc1	mannose receptor, C type 1
67	1432558_a_at	1032.55	44.00	-1.22	-1.39	AK019046	17153	Mal	myelin and lymphocyte protein, T-cell

68	1457254_x_at	1041.76	44.28	-1.63	-2.22	BB302103	432460	LOC432460	differentiation protein similar to RIKEN cDNA 6330442E10 gene
69	1456211_at	1061.10	45.87	-1.48	-1.90	BB003937	---	---	---
70	1447807_s_at	1066.37	45.89	-1.44	-1.82	AV336001	211945	Plekhh1	pleckstrin homology domain containing, family H (with MyTH4 domain) member 1
71	1419549_at	1071.67	45.93	-1.35	-1.63	NM_007482	11846	Arg1	arginase 1, liver
72	1420377_at	1074.00	45.62	-1.27	-1.48	BG071333	20450	St8sia2	ST8 alpha-N-acetylneuraminide alpha-2,8-sialyltransferase 2
73	1417061_at	1090.52	46.88	-1.46	-1.86	AF226613	53945	Slc40a1	solute carrier family 40 (iron-regulated transporter), member 1
74	1427268_at	1091.98	46.50	-1.55	-2.04	J03458	433621 545581	LOC433621 /// LOC545581	similar to Acidic ribosomal phosphoprotein P0 /// similar to Acidic ribosomal phosphoprotein P0
75	1435906_x_at	1103.69	47.03	-1.46	-1.85	BE197524	14469	Gbp2	guanylate nucleotide binding protein 2
76	1454849_x_at	1104.74	46.59	-1.38	-1.69	BB433678	12759	Clu	clusterin
77	1452378_at	1116.67	47.32	-1.47	-1.88	AW012617	72289	Malat1	metastasis associated lung adenocarcinoma transcript 1 (non-coding RNA)
78	1451601_a_at	1121.06	47.27	-1.54	-2.02	BC025823	216892	BC011467	cDNA sequence BC011467
79	1426439_at	1135.14	48.33	-1.50	-1.95	AA210261	26900	Ddx3y	DEAD (Asp-Glu-Ala-Asp) box polypeptide 3, Y-linked
80	1451613_at	1142.37	48.46	-1.48	-1.89	AY027660	68723	Hnr	hornerin
81	1448982_at	1158.63	49.88	-1.50	-1.94	NM_011177	19144	Prss18	protease, serine, 18
82	1448169_at	1202.81	NA	-1.31	-1.56	NM_010664	16668	Krt1-18	keratin complex 1, acidic, gene 18
83	1449959_x_at	1203.90	NA	-1.50	-1.95	NM_026335	67718	Sprl9	small proline rich-like 9
84	1435462_at	1214.16	NA	-1.46	-1.86	BQ176176	433022	LOC433022	hypothetical LOC433022
85	1437458_x_at	1221.73	NA	-1.37	-1.67	AV075715	12759	Clu	clusterin
86	1419605_at	1240.04	NA	-1.44	-1.81	NM_010796	17312	Mgl1	macrophage galactose N-acetyl-galactosamine specific lectin 1
87	1450633_at	1243.32	NA	-1.48	-1.91	NM_020036	80796	Calm4	calmodulin 4
88	1427963_s_at	1246.05	NA	-1.47	-1.88	BE979765	103142	Rdh9	retinol dehydrogenase 9
89	1429540_at	1247.88	NA	-1.49	-1.92	AK008979	72383	Cnfn	cornifelin
90	1422837_at	1249.20	NA	-1.43	-1.80	NM_022886	64929	Scel	sciellin
91	1429060_at	1255.39	NA	-1.42	-1.77	AK020483	72289	Malat1	metastasis associated lung adenocarcinoma transcript 1 (non-

coding RNA)									
92	1429230_at	1256.39	NA	-1.46	-1.87	AK003996	68668	1110030O19Rik	RIKEN cDNA 1110030O19 gene
93	1421398_at	1264.34	NA	-1.37	-1.67	NM_053166	94089	Trim7	tripartite motif protein 7
94	1450792_at	1273.33	NA	-1.38	-1.69	NM_011662	22177	Tyrobp	TYRO protein tyrosine kinase binding protein
95	1418283_at	1274.46	NA	-1.34	-1.62	NM_009903	12740	Cldn4	claudin 4
96	1418626_a_at	1277.22	NA	-1.34	-1.61	NM_013492	12759	Clu	clusterin
97	1436917_s_at	1289.32	NA	-1.34	-1.62	BB491018	67839	Gpsm1	G-protein signalling modulator 1 (AGS3-like, C. elegans)
98	1417917_at	1307.06	NA	-1.38	-1.69	NM_009922	12797	Cnn1	calponin 1
99	1436329_at	1314.80	NA	-1.42	-1.79	AV346607	13655	Egr3	early growth response 3
100	1429537_at	1315.93	NA	-1.34	-1.61	BG277020	66625	5730406M06Rik	RIKEN cDNA 5730406M06 gene

## The Rank Product (RP) differential expression analysis report



General Information	
Experiment	VK1mouse4302
Normalisation	rma across replicates
Chip	one chip only
Comparison	Treatment samples: <b>WT + CCL3</b> vs Baseline samples: <b>WT Control</b>
RP comparison	not paired
Direction	Negative

0	Probe-set ID	RPscore	FDR	FC_rma	FC_nom	"SOURCE"	"EntrezGene"	Gene Symbol	Title
1	1426438_at	228.87	45.00	-4.27	-10.81	AA210261	26900	Ddx3y	DEAD (Asp-Glu-Ala-Asp) box polypeptide 3, Y-linked
2	1453218_at	263.41	32.50	-1.59	-2.15	AK003705	73719	1110014K05Rik	RIKEN cDNA 1110014K05 gene
3	1451613_at	265.52	22.00	-1.70	-2.39	AY027660	68723	Hnrn	Hornerin
4	1452077_at	302.93	23.50	-2.63	-4.88	AA210261	26900	Ddx3y	DEAD (Asp-Glu-Ala-Asp) box polypeptide 3, Y-linked
5	1417210_at	319.33	21.20	-3.57	-8.06	NM_012011	26908	Eif2s3y	eukaryotic translation initiation factor 2, subunit 3, structural gene Y-linked
6	1419409_at	332.57	19.83	-1.63	-2.22	NM_026822	68720	Sprr15	small proline rich-like 5
7	1429565_s_at	387.48	28.00	-1.55	-2.05	AK004318	66203	Lce5a	late cornified envelope 5A
8	1420431_at	415.16	30.12	-1.58	-2.11	NM_009100	20129	Rptn	Repetin
9	1424903_at	443.01	32.11	-2.14	-3.49	AF127244	20592	Jarid1d	jumonji, AT rich interactive domain 1D (Rbp2 like)
10	1420332_x_at	453.86	30.90	-1.49	-1.92	NM_027137	69611	Sprr17	small proline rich-like 7
11	1452292_at	494.01	36.36	-1.51	-1.97	AV271093	---	---	---
12	1426598_at	506.99	35.75	-1.84	-2.72	BB742957	22290 546404 546411	Uty /// LOC546404 /// LOC546411	ubiquitously transcribed tetratricopeptide repeat gene, Y chromosome /// similar to male-specific histocompatibility antigen H-YDb /// similar to male-specific histocompatibility antigen H-YDb
13	1427268_at	508.76	33.62	-1.53	-2.00	J03458	433621 545581	LOC433621 /// LOC545581	similar to Acidic ribosomal phosphoprotein P0 /// similar to Acidic ribosomal phosphoprotein P0
14	1426439_at	544.39	36.79	-1.98	-3.07	AA210261	26900	Ddx3y	DEAD (Asp-Glu-Ala-

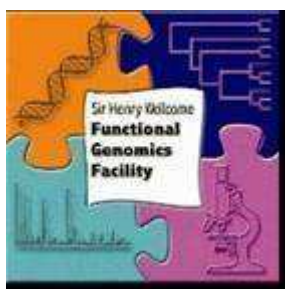
									Asp) box polypeptide 3, Y-linked
15	1428980_at	574.12	38.80	-1.47	-1.87	AK003253	73731	1110001M24Rik	RIKEN cDNA 1110001M24 gene
16	1448745_s_at	646.92	NA	-1.45	-1.84	NM_008508	16939	Lor	Loricrin
17	1420350_at	652.06	NA	-1.42	-1.78	NM_028625	73722	Sprrl2	small proline rich-like 2
18	1417275_at	698.11	NA	-1.44	-1.82	NM_010762	17153	Mal	myelin and lymphocyte protein, T-cell differentiation protein
19	1419906_at	708.68	NA	-1.46	-1.86	AV026552	15446	Hpgd	Hydroxyprostaglandin dehydrogenase 15 (NAD), mRNA (cDNA clone MGC:14001 IMAGE:4208980)
20	1429996_at	786.08	NA	-1.42	-1.77	BB207765	70760	6330417A16Rik	RIKEN cDNA 6330417A16 gene
21	1459635_at	854.52	NA	-1.41	-1.76	BG144294	13383	Dlgh1	Discs, large homolog 1 (Drosophila) (Dlgh1), mRNA
22	1417808_at	911.39	NA	-1.45	-1.84	NM_025621	66533	2310050C09Rik	RIKEN cDNA 2310050C09 gene
23	1420677_x_at	949.26	NA	-1.38	-1.69	NM_025984	67127	Sprrl3	small proline rich-like 3
24	1444472_at	961.17	NA	-1.39	-1.72	BB154631	235344	Sik2	SNF1-like kinase 2 (Snf1k2), mRNA
25	1442153_at	962.32	NA	-1.57	-2.10	BB206087	Mm.385427	---	0 day neonate thymus cDNA, RIKEN full-length enriched library, clone:A430072F05 product:unclassifiable, full insert sequence
26	1420550_at	1016.33	NA	-1.34	-1.61	AV014636	67828	1110055J05Rik	RIKEN cDNA 1110055J05 gene
27	1420183_at	1037.45	NA	-1.37	-1.67	AI036317	16939	Lor	Loricrin (Lor), mRNA
28	1432558_a_at	1074.86	NA	-1.36	-1.65	AK019046	17153	Mal	myelin and lymphocyte protein, T-cell differentiation protein
29	1452315_at	1119.09	NA	-1.31	-1.56	BB827235	16551	Kif11	kinesin family member 11
30	1429772_at	1124.63	NA	-1.35	-1.64	BB085537	18845	Plxna2	plexin A2
31	1453405_at	1164.96	NA	-1.38	-1.70	AK019180	78390	2610311B01Rik	RIKEN cDNA 2610311B01 gene
32	1457065_at	1166.06	NA	-1.49	-1.93	BB530943	22268	Upk1b	uroplakin 1B
33	1423952_a_at	1173.29	NA	-1.45	-1.84	BC010337	110310	Krt2-7	keratin complex 2, basic, gene 7
34	1441100_at	1188.84	NA	-1.37	-1.68	BB496952	103537	Mbtd1	mbt domain containing 1
35	1420377_at	1217.31	NA	-1.22	-1.39	BG071333	20450	St8sia2	ST8 alpha-N-acetylneuraminide alpha-2,8-sialyltransferase 2
36	1419905_s_at	1217.46	NA	-1.31	-1.55	AV026552	15446	Hpgd	hydroxyprostaglandin dehydrogenase 15 (NAD)
37	1437782_at	1225.80	NA	-1.36	-1.67	BE651445	66797	Ctnap2	contactin associated protein-like 2
38	1423320_at	1241.37	NA	-1.41	-1.76	AI507229	66705	Dnase1l2	deoxyribonuclease 1-like 2
39	1419549_at	1252.27	NA	-1.44	-1.82	NM_007482	11846	Arg1	arginase 1, liver
40	1420676_at	1258.55	NA	-1.28	-1.51	NM_025984	67127	Sprrl3	small proline rich-like 3
41	1449451_at	1259.55	NA	-1.34	-1.62	NM_025867	66957	Serpnb11	serine (or cysteine) peptidase inhibitor, clade B (ovalbumin), member 11
42	1421316_at	1264.83	NA	-1.38	-1.69	NM_025413	66195	1110058A15Rik	RIKEN cDNA 1110058A15 gene

43	1420741_x_at	1275.58	NA	-1.30	-1.53	NM_029667	76585	2310069N01Rik	RIKEN cDNA 2310069N01 gene
44	1418855_at	1285.55	NA	-1.37	-1.68	NM_028628	73730	1110008K04Rik	RIKEN cDNA 1110008K04 gene
45	1449902_at	1286.42	NA	-1.32	-1.57	AV014636	66195	1110058A15Rik	RIKEN cDNA 1110058A15 gene
46	1424927_at	1315.09	NA	-1.35	-1.63	BC025083	73690	Glipr1	GLI pathogenesis-related 1 (glioma)
47	1440789_at	1329.47	NA	-1.35	-1.64	BB243938	18007	Neo1	Neogenin
48	1440966_at	1338.11	NA	-1.37	-1.67	BB248730	57438	March7	membrane-associated ring finger (C3HC4) 7
49	1456248_at	1352.60	NA	-1.29	-1.52	AV076385	69520	2310002A05Rik	RIKEN cDNA 2310002A05 gene
50	1448393_at	1356.41	NA	-1.42	-1.78	BC008104	53624	Cldn7	claudin 7
51	1416613_at	1364.07	NA	-1.10	-1.17	BI251808	13078	Cyp1b1	cytochrome P450, family 1, subfamily b, polypeptide 1
52	1430440_at	1368.33	NA	-1.34	-1.61	AK015363	74660	4930442J19Rik	RIKEN cDNA 4930442J19 gene
53	1455464_x_at	1377.32	NA	-1.41	-1.76	BB427704	---	---	---
54	1422760_at	1398.06	NA	-1.28	-1.49	NM_0111061	18602	Padi4	peptidyl arginine deiminase, type IV
55	1420413_at	1405.23	NA	-1.34	-1.62	NM_0111990	26570	Slc7a11	solute carrier family 7 (cationic amino acid transporter, y+ system), member 11
56	1447625_at	1406.24	NA	-1.30	-1.54	BB286270	13559	E2f5	E2F transcription factor 5
57	1456001_at	1416.63	NA	-1.34	-1.61	AV071932	Mm.387664	---	CDNA clone MGC:118457 IMAGE:30288561
58	1460569_x_at	1420.12	NA	-1.37	-1.68	AW611462	12739	Cldn3	claudin 3
59	1444192_at	1434.52	NA	-1.32	-1.58	BB460651	---	---	---
60	1450633_at	1435.50	NA	-1.34	-1.62	NM_020036	80796	Calm4	calmodulin 4
61	1418283_at	1436.80	NA	-1.31	-1.57	NM_009903	12740	Cldn4	claudin 4
62	1439845_at	1440.73	NA	-1.33	-1.60	BQ174438	Mm.348429	---	Transcribed locus
63	1419529_at	1441.16	NA	-1.20	-1.34	NM_031252	83430	Il23a	interleukin 23, alpha subunit p19
64	1457077_at	1456.56	NA	-1.34	-1.61	BB306048	245683	---	PREDICTED: similar to hypothetical protein FLJ34960 [Mus musculus], mRNA sequence
65	1453252_at	1459.43	NA	-1.27	-1.48	AK010138	71916	Dus4l	dihydrouridine synthase 4-like (S. cerevisiae)
66	1438558_x_at	1519.98	NA	-1.31	-1.55	AV009267	15220	Foxq1	Forkhead box Q1 (Foxq1), mRNA
67	1454299_at	1522.69	NA	-1.31	-1.55	AV250295	74587	4833422B07Rik	RIKEN cDNA 4833422B07 gene
68	1454632_at	1530.52	NA	-1.32	-1.58	AV328515	268567	6330442E10Rik	RIKEN cDNA 6330442E10 gene
69	1449071_at	1534.40	NA	-1.37	-1.68	NM_022879	17898	Myl7	myosin, light polypeptide 7, regulatory
70	1445916_at	1537.46	NA	-1.34	-1.62	BG070994	11964	Atp6v1a1	ATPase, H+ transporting, V1 subunit A1, mRNA (cDNA clone MGC:6531 IMAGE:2651677)
71	1418496_at	1549.18	NA	-1.36	-1.65	NM_008259	15375	Foxa1	forkhead box A1
72	1451601_a_a_t	1553.22	NA	-1.30	-1.53	BC025823	216892	BC011467	cDNA sequence BC011467
73	1416368_at	1580.84	NA	-1.23	-1.40	NM_010357	14860	Gsta4	glutathione S-transferase, alpha 4
74	1459415_at	1594.42	NA	-1.31	-1.56	BB204258	---	---	---

75	1458871_at	1611.25	NA	-1.34	-1.62	BB148290	243084	Tmprss11e	transmembrane protease, serine 11e
76	1427593_at	1632.56	NA	-1.31	-1.55	BB620112	93679	Trim8	tripartite motif protein 8
77	1418423_s_at	1637.78	NA	-1.30	-1.53	AF425083	20709 20710 544923 93806	Serpib9f /// Serpib9e /// Serpib9g /// LOC54492 3	serine (or cysteine) peptidase inhibitor, clade B, member 9f /// serine (or cysteine) peptidase inhibitor, clade B, member 9e /// serine (or cysteine) peptidase inhibitor, clade B, member 9g /// similar to OTTMUSP0000000064 1
78	1442750_at	1639.79	NA	-1.30	-1.54	BG067768	97884	D230016N 13Rik	UDP-GalNAc:betaGlcNAc beta 1,3-galactosaminyltransferase, polypeptide 2, mRNA (cDNA clone MGC:103263 IMAGE:30735904)
79	1425671_at	1644.06	NA	-1.31	-1.56	AF093257	26556	Homer1	homer homolog 1 (Drosophila)
80	1444562_at	1655.13	NA	-1.32	-1.58	BE690666	100763	Ube3c	Ubiquitin protein ligase E3C, mRNA (cDNA clone IMAGE:5353408)
81	1419619_at	1661.35	NA	-1.32	-1.57	NM_028770	74127	1200016G 03Rik	RIKEN cDNA 1200016G03 gene
82	1444349_at	1661.40	NA	-1.24	-1.42	BG071091	---	---	---
83	1422639_at	1680.58	NA	-1.32	-1.57	NM_054084	116903	Calcbl	calcitonin-related polypeptide, beta
84	1420647_a_a t	1681.19	NA	-1.25	-1.44	NM_031170	16691 434261	Krt2-8 /// LOC43426 1	keratin complex 2, basic, gene 8 /// similar to cytokeratin EndoA - mouse
85	1422247_a_a t	1685.22	NA	-1.28	-1.50	NM_009484	22290 546404	Uty /// LOC54640 4	ubiquitously transcribed tetratricopeptide repeat gene, Y chromosome /// similar to male-specific histocompatibility antigen H-YDb
86	1447807_s_at	1688.22	NA	-1.34	-1.62	AV336001	211945	Plekhh1	pleckstrin homology domain containing, family H (with MyTH4 domain) member 1
87	1446570_at	1692.91	NA	-1.31	-1.56	BB469236	---	---	---
88	1448169_at	1698.16	NA	-1.23	-1.40	NM_010664	16668	Krt1-18	keratin complex 1, acidic, gene 18
89	1415861_at	1699.74	NA	-1.22	-1.39	BB762957	22178	Tyrp1	tyrosinase-related protein 1
90	1445477_at	1711.48	NA	-1.31	-1.55	BE952410	Mm.26390	---	Retrotransposon ETn insertion in p53 mRNA
91	1435831_at	1713.42	NA	-1.42	-1.79	BB427704	22268	Upk1b	uroplakin 1B
92	1435321_at	1719.91	NA	-1.34	-1.61	BM117827	77569	3732412D 22Rik	RIKEN cDNA 3732412D22 gene
93	1444202_at	1743.05	NA	-1.30	-1.54	BI965268	546051	LOC54605 1	similar to hypothetical protein LOC80139
94	1455679_at	1748.59	NA	-1.29	-1.51	BE457727	109019	5830411E1 0Rik	RIKEN cDNA 5830411E10 gene
95	1438216_at	1751.69	NA	-1.27	-1.48	BG143502	68750	1110037N 09Rik	PREDICTED: hypothetical protein LOC68750 [Mus musculus], mRNA sequence
96	1435154_at	1760.27	NA	-1.24	-1.43	AV099404	245128	LOC24512 8	similar to solute carrier family 7 (cationic amino acid transporter, y+ system), member 3
97	1426941_at	1764.77	NA	-1.26	-1.47	BC020027	---	---	---

98	1420371_at	1787.33	NA	-1.29	-1.52	BI646094	20650	Sntb2	syntrophin, basic 2
99	1443915_at	1788.56	NA	-1.30	-1.55	BE957160	74600	Mrpl47	mitochondrial ribosomal protein L47
100	1436686_at	1789.49	NA	-1.31	-1.55	AA165749	68036	Zfp706	zinc finger protein 706

## The Rank Product (RP) differential expression analysis report



### General Information

Experiment	VK1mouse4302
Normalisation	rma across replicates
Chip	one chip only
Comparison	Treatment samples: <b>K14D6 + CCL3</b> vs Baseline samples: <b>K14D6 Control</b>
RP comparison	not paired
Direction	Negative

0	Probe-set ID	RPscore	FDR	FC_rma	FC_nom	"SOURCE"	"EntrezGene"	Gene Symbol	Title
1	1452292_at	123.91	2.00	-1.85	-2.74	AV271093	---	---	---
2	1436319_at	264.52	29.00	-1.62	-2.21	BB751459	240725	Sulf1	sulfatase 1
3	1435831_at	294.66	26.67	-1.60	-2.17	BB427704	22268	Upk1b	uroplakin 1B
4	1434172_at	360.64	34.00	-1.44	-1.81	BQ177934	---	---	---
5	1450377_at	538.35	NA	-1.55	-2.04	AI385532	21825	Thbs1	thrombospondin 1
6	1446481_at	543.55	NA	-1.49	-1.93	BB534411	11787	Apbb2	Amyloid beta (A4) precursor protein-binding, family B, member 2, mRNA (cDNA clone MGC:100042 IMAGE:30550087)
7	1435989_x_at	576.03	NA	-1.52	-1.99	AW322280	434261	LOC434261	similar to cytokeratin EndoA - mouse
8	1457479_at	603.21	NA	-1.44	-1.81	AW536823	22596	Xrcc5	X-ray repair complementing defective repair in Chinese hamster cells 5, mRNA (cDNA clone IMAGE:2647262)
9	1427262_at	649.58	NA	-1.42	-1.77	L04961	213742	Xist	inactive X specific transcripts
10	1456661_at	657.15	NA	-1.50	-1.94	BM293452	16468	Jarid2	Jumonji, AT rich interactive domain 2, mRNA (cDNA clone IMAGE:3589616)
11	1427610_at	674.96	NA	-1.47	-1.88	BC026631	109620	Dsp	desmoplakin
12	1417275_at	680.37	NA	-1.46	-1.85	NM_010762	17153	Mal	myelin and lymphocyte protein, T-cell differentiation protein
13	1424598_at	683.47	NA	-1.44	-1.81	BC021452	13209	Ddx6	DEAD (Asp-Glu-Ala-Asp) box polypeptide 6
14	1455464_x_at	694.70	NA	-1.47	-1.88	BB427704	---	---	---
15	1445641_at	703.61	NA	-1.47	-1.88	BB727879	---	---	---
16	1427263_at	741.08	NA	-1.32	-1.58	L04961	213742	Xist	inactive X specific transcripts

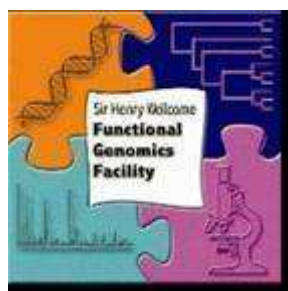
17	1440722_at	771.22	NA	-1.39	-1.72	BB284387	52013	D19Erttd386e	DNA segment, Chr 19, ERATO Doi 386, expressed (D19Erttd386e), mRNA
18	1420377_at	813.18	NA	-1.24	-1.41	BG071333	20450	St8sia2	ST8 alpha-N-acetyl-neuraminidase alpha-2,8-sialyltransferase 2
19	1433902_at	819.15	NA	-1.36	-1.66	BB469300	243574	Kbtbd8	kelch repeat and BTB (POZ) domain containing 8
20	1460302_at	852.47	NA	-1.42	-1.77	AI385532	21825	Thbs1	thrombospondin 1
21	1420647_a_at	861.38	NA	-1.45	-1.83	NM_031170	16691 434261	Krt2-8 /// LOC434261	keratin complex 2, basic, gene 8 /// similar to cytokeratin EndoA - mouse
22	1438200_at	874.34	NA	-1.42	-1.78	BB065799	240725	Sulf1	sulfatase 1
23	1443393_at	878.47	NA	-1.44	-1.81	BB201890	75788	Smurf1	SMAD specific E3 ubiquitin protein ligase 1, mRNA (cDNA clone MGC:28022 IMAGE:3660965)
24	1440014_at	917.67	NA	-1.41	-1.76	AW553510	107975	Pacs1	Phosphofurin acidic cluster sorting protein 1 (Pacs1), mRNA
25	1425092_at	920.21	NA	-1.27	-1.49	AF183946	320873	Cdh10	cadherin 10
26	1454904_at	923.49	NA	-1.34	-1.61	BG976607	17772	Mtm1	X-linked myotubular myopathy gene 1
27	1423691_x_at	923.68	NA	-1.44	-1.82	M21836	16691	Krt2-8	keratin complex 2, basic, gene 8
28	1437219_at	951.33	NA	-1.42	-1.77	AW553541	16001	Igf1r	Insulin-like growth factor I receptor (Igf1r), mRNA
29	1439760_x_at	963.24	NA	-1.37	-1.68	BB219662	22268	Upk1b	uropod 1B
30	1442961_at	969.72	NA	-1.37	-1.67	BG071782	---	---	---
31	1456712_at	981.56	NA	-1.34	-1.62	AV231984	209707	A830039H10Rik	RIKEN cDNA A830039H10 gene
32	1436039_at	1012.68	NA	-1.32	-1.58	BM245957	Mm.85165	---	Transcribed locus, moderately similar to XP_488601.1 PREDICTED: hypothetical protein XP_488601 [Mus musculus]
33	1454544_at	1035.15	NA	-1.38	-1.70	AK020650	78850	9530078B04Rik	RIKEN cDNA 9530078B04 gene
34	1421811_at	1059.53	NA	-1.37	-1.68	AI385532	21825	Thbs1	thrombospondin 1
35	1447408_at	1082.37	NA	-1.42	-1.79	BM201377	71175	4933421G18Rik	Nipped-B homolog (Drosophila) (Nipbl), transcript variant B, mRNA
36	1445642_at	1088.29	NA	-1.36	-1.65	AV156411	213409	Lemd1	LEM domain containing 1
37	1439843_at	1107.13	NA	-1.34	-1.62	AI840829	12326	Camk4	calcium/calmodulin-dependent protein kinase IV
38	1457429_s_at	1114.50	NA	-1.33	-1.59	BB549174	226866	Gm106	gene model 106, (NCBI)
39	1442535_at	1123.07	NA	-1.38	-1.70	BB533591	Mm.216110	---	Adult male hypothalamus cDNA, RIKEN full-length enriched library, clone:A230075A13 product:unclassified, full insert

									sequence
40	1438148_at	1133.18	NA	-1.18	-1.30	BB829808	330122	Gm1960	gene model 1960, (NCBI)
41	1455134_at	1137.25	NA	-1.34	-1.62	AF031164	242474	D730040F13Rik	RIKEN cDNA D730040F13 gene (D730040F13Rik), mRNA
42	1436982_at	1143.42	NA	-1.35	-1.63	BB788270	213988	Tnrc6b	trinucleotide repeat containing 6b
43	1427072_at	1147.74	NA	-1.38	-1.69	BM119481	236920	Stard8	START domain containing 8
44	1427056_at	1173.34	NA	-1.35	-1.64	AV228731	235130	Adamts15	a disintegrin-like and metallopeptidase (reprolysin type) with thrombospondin type 1 motif, 15
45	1441629_at	1191.73	NA	-1.31	-1.55	BB451601	---	---	---
46	1416368_at	1195.00	NA	-1.31	-1.56	NM_010357	14860	Gsta4	glutathione S-transferase, alpha 4
47	1445786_at	1208.94	NA	-1.34	-1.61	BB539247	109880	Braf	Braf transforming gene
48	1454672_at	1232.33	NA	-1.36	-1.65	BE952212	---	---	---
49	1427537_at	1236.24	NA	-1.37	-1.67	BC026387	223650	Eppk1	epiplakin 1
50	1450988_at	1265.15	NA	-1.30	-1.54	BB751088	14160	Lgr5	leucine rich repeat containing G protein coupled receptor 5
51	1441501_at	1268.76	NA	-1.32	-1.58	AV382262	66870	Serbp1	Serpine1 mRNA binding protein 1
52	1459443_at	1273.18	NA	-1.31	-1.56	BM248133	16535	Kcnq1	KCNQ1b mRNA for Q1-type potassium channel spliced variant
53	1455059_at	1297.80	NA	-1.31	-1.55	BB104941	109278	9430093I07Rik	RIKEN cDNA 9430093I07 gene
54	1421038_a_at	1306.61	NA	-1.38	-1.70	NM_008433	16534	Kcnn4	potassium intermediate/small conductance calcium-activated channel, subfamily N, member 4
55	1427982_s_at	1313.46	NA	-1.34	-1.61	BF582734	---	---	---
56	1446196_at	1314.47	NA	-1.29	-1.52	BB105328	15364	Hmga2	high mobility group AT-hook 2
57	1437534_at	1318.78	NA	-1.34	-1.63	AU019880	106529	Gpsn2	ES cells cDNA, RIKEN full-length enriched library, clone:2410016D23 product:SC2 homolog [Rattus sp], full insert sequence
58	1435945_a_at	1339.40	NA	-1.36	-1.67	BG865910	16534	Kcnn4	potassium intermediate/small conductance calcium-activated channel, subfamily N, member 4
59	1458068_at	1355.02	NA	-1.33	-1.60	BB374785	74370	4932417H02Rik	Raptor mRNA for p150 target of rapamycin (TOR)-scaffold protein containing WD-repeats
60	1446616_at	1357.47	NA	-1.30	-1.55	AW551961	---	---	---
61	1430425_at	1368.44	NA	-1.34	-1.61	AW493494	237979	Sdk2	sidekick homolog 2 (chicken)
62	1431528_at	1375.82	NA	-1.34	-1.61	BE225800	76042	5830427D02Rik	RIKEN cDNA

									5830427D02 gene
63	1440343_at	1385.12	NA	-1.31	-1.55	BQ174267	73086	Rps6ka5	ribosomal protein S6 kinase, polypeptide 5
64	1418480_at	1432.73	NA	-1.29	-1.52	NM_023785	57349	Cxcl7	chemokine (C-X-C motif) ligand 7
65	1424112_at	1435.45	NA	-1.33	-1.60	BG092290	16004	Igf2r	insulin-like growth factor 2 receptor
66	1439129_at	1466.83	NA	-1.31	-1.55	AW495734	68813	1110060D06Rik	RIKEN cDNA 1110060D06 gene
67	1447294_at	1470.87	NA	-1.34	-1.61	BB730861	103583	Fbxw11	F-box and WD-40 domain protein 11
68	1439545_at	1478.26	NA	-1.31	-1.55	BM240227	18181	Nrf1	Nuclear respiratory factor 1, mRNA (cDNA clone MGC:5646 IMAGE:3496661)
69	1457262_at	1479.82	NA	-1.34	-1.62	BB024162	233789	2610207I05Rik	RIKEN cDNA 2610207I05 gene
70	1441652_at	1489.70	NA	-1.27	-1.48	BB185152	12168	Bmpr2	bone morphogenic protein receptor, type II (serine/threonine kinase)
71	1453125_at	1492.31	NA	-1.25	-1.44	BM508495	20666	Sox11	SRY-box containing gene 11
72	1432358_at	1495.44	NA	-1.30	-1.54	AK003577	73732	1110008I14Rik	RIKEN cDNA 1110008I14 gene
73	1458663_at	1502.50	NA	-1.35	-1.64	AI552833	16795	Large	Like-glycosyltransferase (Large), mRNA
74	1448169_at	1520.27	NA	-1.38	-1.69	NM_010664	16668	Krt1-18	keratin complex 1, acidic, gene 18
75	1455965_at	1521.30	NA	-1.21	-1.37	BG064671	---	---	---
76	1418547_at	1532.31	NA	-0.89	-0.82	NM_009364	21789	Tfpi2	tissue factor pathway inhibitor 2
77	1439571_at	1535.73	NA	-1.30	-1.53	BB820889	319683	E230008J23Rik	RIKEN cDNA E230008J23 gene
78	1438575_a_at	1538.08	NA	-1.32	-1.58	BG143413	Mm.254833	---	Transcribed locus
79	1455377_at	1542.74	NA	-1.28	-1.49	BB795572	70892	4921517B04Rik	RIKEN cDNA 4921517B04 gene
80	1424927_at	1546.63	NA	-1.27	-1.49	BC025083	73690	Glipr1	GLI pathogenesis-related 1 (glioma)
81	1444218_at	1549.04	NA	-1.29	-1.52	AI117684	76539	D19ErtD737e	DNA segment, Chr 19, ERATO Doi 737, expressed
82	1428719_at	1549.16	NA	-1.28	-1.50	AK008551	207685 547243 70018	2010309G21Rik /// LOC207685 /// LOC547243	RIKEN cDNA 2010309G21 gene /// hypothetical protein LOC207685 /// similar to Ig lambda-2 chain
83	1423071_x_at	1585.19	NA	-1.28	-1.50	AW549928	270335 434328 544983 545175 545584 546326	LOC270335 /// LOC434328 /// LOC544983 /// LOC545175 /// LOC545584 /// LOC546326	hypothetical gene supported by BC019681; BC027236 /// hypothetical LOC434328 /// similar to RIKEN cDNA 2610524H06 gene /// similar to LOC381508 protein /// similar to LOC381508 protein /// similar to LOC381508 protein
84	1450923_at	1592.44	NA	-1.30	-1.53	BF144658	21808	Tgfb2	transforming growth factor, beta 2

85	1436790_a_at	1598.23	NA	-1.27	-1.48	BG072739	20666	Sox11	SRY-box containing gene 11
86	1433201_at	1599.52	NA	-1.26	-1.45	AK010214	70290	2310079F09Rik	RIKEN cDNA 2310079F09 gene
87	1416612_at	1605.67	NA	-1.21	-1.37	BI251808	13078	Cyp1b1	cytochrome P450, family 1, subfamily b, polypeptide 1
88	1422324_a_at	1615.75	NA	-1.17	-1.29	NM_008970	19227	Pthlh	parathyroid hormone-like peptide
89	1445943_at	1617.75	NA	-1.28	-1.49	BG071766	---	---	---
90	1460571_at	1618.37	NA	-1.27	-1.48	BM208197	192119	Dicer1	Double-strand-specific ribonuclease MDCR
91	1428944_at	1625.90	NA	-1.23	-1.41	BB417360	231380	5730469D23Rik	RIKEN cDNA 5730469D23 gene
92	1416613_at	1628.60	NA	-1.17	-1.29	BI251808	13078	Cyp1b1	cytochrome P450, family 1, subfamily b, polypeptide 1
93	1459646_at	1631.73	NA	-1.16	-1.27	BM899994	328779	Hs3st6	heparan sulfate (glucosamine) 3-O-sulfotransferase 6
94	1457065_at	1646.08	NA	-1.30	-1.53	BB530943	22268	Upk1b	uropod protein 1B
95	1435154_at	1648.01	NA	-1.26	-1.46	AV099404	245128	LOC245128	similar to solute carrier family 7 (cationic amino acid transporter, y+ system), member 3
96	1458657_at	1648.43	NA	-1.29	-1.52	AA822260	69538	Antxr1	Tumor endothelial marker 8 precursor (Tem8)
97	1437554_at	1666.56	NA	-1.30	-1.54	BM232239	18810	Plec1	plectin 1
98	1441688_at	1671.69	NA	-1.29	-1.52	AV343428	319654	6430537I21Rik	RIKEN cDNA 6430537I21 gene
99	1447143_at	1683.35	NA	-1.35	-1.64	BM115076	---	---	---
100	1458021_at	1684.30	NA	-1.29	-1.51	BB550531	69024	Snx15	Sorting nexin 15, mRNA (cDNA clone MGC:27611 IMAGE:4503873)

## The Rank Product (RP) differential expression analysis report



### General Information

Experiment	VK1mouse4302
Normalisation	rma across replicates
Chip	one chip only
Comparison	Treatment samples: <b>K14D6 + CCL3</b> vs Baseline samples: <b>WT + CCL3</b>
RP comparison	not paired
Direction	Negative

0	Probe-set ID	RPscore	FDR	FC_rma	FC_nom	"SOURCE"	"EntrezGene"	Gene Symbol	Title
1	1436905_x_at	145.03	10.00	-2.01	-3.15	BB218107	16792	Laptn5	lysosomal-associated protein transmembrane 5
2	1436996_x_at	154.19	5.50	-1.96	-3.01	AV066625	17110	Lzp-s	P lysozyme structural
3	1439426_x_at	163.17	3.67	-2.04	-3.21	AV058500	17110	Lzp-s	P lysozyme structural
4	1420804_s_at	186.83	4.50	-2.12	-3.43	NM_010819	17474	Clec4d	C-type lectin domain family 4, member d
5	1448591_at	204.23	4.60	-1.93	-2.95	NM_021281	13040	Ctss	cathepsin S
6	1448748_at	236.28	6.33	-1.96	-3.01	AF181829	56193	Plek	pleckstrin
7	1424754_at	377.58	22.14	-1.93	-2.93	BC024402	109225	Ms4a7	membrane-spanning 4-domains, subfamily A, member 7
8	1448995_at	378.78	19.62	-1.69	-2.36	NM_019932	56744	Cxcl4	chemokine (C-X-C motif) ligand 4
9	1418547_at	381.87	17.89	-1.70	-2.39	NM_009364	21789	Tfpi2	tissue factor pathway inhibitor 2
10	1448929_at	407.64	20.70	-1.82	-2.68	NM_028784	74145	F13a1	coagulation factor XIII, A1 subunit
11	1419599_s_at	418.00	20.82	-1.74	-2.49	NM_026835	64382	Ms4a11	membrane-spanning 4-domains, subfamily A, member 11
12	1450430_at	418.30	19.08	-1.77	-2.55	NM_008625	17533	Mrc1	mannose receptor, C type 1
13	1417266_at	421.12	17.92	-1.73	-2.46	BC002073	20305	Ccl6	chemokine (C-C motif) ligand 6
14	1438989_s_at	421.60	16.86	-1.56	-2.08	BB386167	320860	B130021B11Rik	RIKEN cDNA B130021B11 gene
15	1425951_a_at	427.86	16.67	-2.06	-3.28	AF240358	56620	Clec4n	C-type lectin domain family 4, member n
16	1435477_s_at	462.57	19.31	-1.86	-2.77	BM224327	14130	Fcgr2b	Fc receptor, IgG, low affinity IIb
17	1419598_at	502.33	23.24	-1.83	-2.69	NM_026835	68774	Ms4a6d	membrane-spanning 4-domains, subfamily A, member 6D
18	1423547_at	562.57	31.33	-1.66	-2.30	AW208566	17105	Lyzs	lysozyme
19	1417381_at	565.86	30.11	-1.82	-2.68	NM_007572	12259	C1qa	complement component 1, q

20	1419627_s_at	572.64	29.65	-1.78	-2.57	NM_020001	56620	Clec4n	subcomponent, alpha polypeptide C-type lectin domain family 4, member n
21	1449254_at	640.21	37.48	-1.75	-2.50	NM_009263	20750	Spp1	secreted phosphoprotein 1
22	1449368_at	646.39	36.95	-1.39	-1.71	NM_007833	13179	Dcn	decorin
23	1442082_at	694.46	43.87	-1.75	-2.51	BB333624	12267	C3ar1	complement component 3a receptor 1
24	1419473_a_at	698.40	42.71	-1.63	-2.23	NM_031161	12424	Cck	cholecystokinin
25	1448620_at	730.34	46.00	-1.64	-2.25	NM_010188	14131	Fcgr3	Fc receptor, IgG, low affinity III
26	1419728_at	740.66	45.88	-1.53	-2.02	NM_009141	20311	Cxcl5	chemokine (C-X-C motif) ligand 5
27	1427262_at	754.73	46.93	-1.47	-1.88	L04961	213742	Xist	inactive X specific transcripts
28	1417936_at	783.45	NA	-1.41	-1.75	AF128196	20308	Ccl9	chemokine (C-C motif) ligand 9
29	1434172_at	791.18	NA	-1.58	-2.12	BQ177934	---	---	---
30	1437558_at	793.08	NA	-1.45	-1.84	BM119919	320860	B130021B11Rik	RIKEN cDNA B130021B11 gene
31	1420394_s_at	840.89	NA	-1.58	-2.11	U05264	14727 14728	Gp49a /// Lilrb4	glycoprotein 49 A /// leukocyte immunoglobulin- like receptor, subfamily B, member 4
32	1444176_at	840.89	NA	-1.71	-2.41	AV204216	242341	Atp6v0d2	ATPase, H+ transporting, V0 subunit D, isoform 2
33	1443673_x_at	888.70	NA	-1.38	-1.70	BB710847	---	---	---
34	1456858_at	912.26	NA	-1.42	-1.77	BB075339	229357	Gpr149	G protein-coupled receptor 149
35	1440969_at	918.41	NA	-1.40	-1.74	BE944957	407797	BC030308	cDNA sequence BC030308
36	1438672_at	929.31	NA	-1.42	-1.77	BI134721	170736	Parvb	Parvin, beta (Parvb), mRNA
37	1436568_at	929.37	NA	-1.62	-2.20	AU016127	67374	Jam2	junction adhesion molecule 2
38	1427263_at	952.72	NA	-1.37	-1.67	L04961	213742	Xist	inactive X specific transcripts
39	1452141_a_at	985.76	NA	-1.48	-1.90	BC001991	20363	Sepp1	selenoprotein P, plasma, 1
40	1415983_at	985.90	NA	-1.49	-1.92	NM_008879	18826	Lcp1	lymphocyte cytosolic protein 1
41	1443775_x_at	995.49	NA	-1.39	-1.71	AV165539	380993	Zfp406	zinc finger protein 406
42	1434877_at	1003.29	NA	-1.31	-1.56	AI152800	18164	Nptx1	neuronal pentraxin 1
43	1418511_at	1011.43	NA	-1.49	-1.92	NM_019759	56429	Dpt	dermatopontin
44	1441688_at	1032.11	NA	-1.37	-1.68	AV343428	319654	6430537121Rik	RIKEN cDNA 6430537121 gene
45	1420249_s_at	1057.30	NA	-1.60	-2.16	AV084904	20305	Ccl6	chemokine (C-C motif) ligand 6
46	1427268_at	1059.33	NA	-1.15	-1.26	J03458	433621 545581	LOC433621 /// LOC545581	similar to Acidic ribosomal phosphoprotein P0 /// similar to Acidic ribosomal phosphoprotein P0
47	1425575_at	1062.51	NA	-1.50	-1.95	M68513	13837	Epha3	Eph receptor A3
48	1448169_at	1089.52	NA	-1.47	-1.88	NM_010664	16668	Krt1-18	keratin complex 1, acidic, gene 18
49	1451289_at	1091.74	NA	-1.44	-1.82	AW105916	13175	Dcamk1	double cortin and calcium/calmodulin-

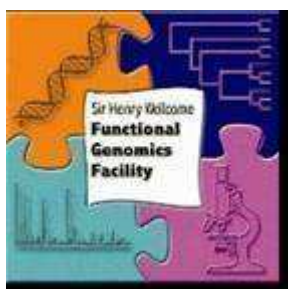
										dependent protein kinase-like 1
50	1423477_at	1107.54	NA	-1.45	-1.85	BB361162	22771		Zic1	zinc finger protein of the cerebellum 1
51	1422340_a_at	1114.62	NA	-1.45	-1.83	NM_009610	11468		Actg2	actin, gamma 2, smooth muscle, enteric
52	1416811_s_at	1118.89	NA	-1.33	-1.59	NM_007796	13024 13025		Ctla2a /// Ctla2b	cytotoxic T lymphocyte-associated protein 2 alpha /// cytotoxic T lymphocyte-associated protein 2 beta
53	1422135_at	1132.40	NA	-1.36	-1.65	NM_011980	26465		Zfp146	zinc finger protein 146
54	1419872_at	1139.33	NA	-1.50	-1.94	AI323359	12978		Csf1r	colony stimulating factor 1 receptor
55	1442257_at	1142.86	NA	-1.38	-1.70	BI134319	Mm.204306		---	12 days embryo female mullerian duct includes surrounding region cDNA, RIKEN full-length enriched library, clone:6820438B06 product:unclassified, full insert sequence
56	1418826_at	1150.73	NA	-1.56	-2.07	NM_027209	69774		Ms4a6b	membrane-spanning 4-domains, subfamily A, member 6B
57	1448471_a_at	1190.30	NA	-1.33	-1.59	NM_007796	13024		Ctla2a	cytotoxic T lymphocyte-associated protein 2 alpha
58	1450652_at	1201.01	NA	-1.36	-1.66	NM_007802	13038		Ctsk	cathepsin K
59	1422124_a_at	1203.52	NA	-1.40	-1.74	NM_011210	19264		Ptpnc	protein tyrosine phosphatase, receptor type, C
60	1418157_at	1236.99	NA	-1.31	-1.56	NM_010151	13865		Nr2f1	nuclear receptor subfamily 2, group F, member 1
61	1435943_at	1256.04	NA	-1.22	-1.38	AI647687	13479		Dpep1	dipeptidase 1 (renal)
62	1427115_at	1268.28	NA	-1.32	-1.58	M74753	17883		Myh3	myosin, heavy polypeptide 3, skeletal muscle, embryonic
63	1419609_at	1270.76	NA	-1.43	-1.79	AV231648	12768		Ccr1	chemokine (C-C motif) receptor 1
64	1427076_at	1270.97	NA	-1.59	-2.14	L20315	17476		Mpeg1	macrophage expressed gene 1
65	1423505_at	1271.94	NA	-1.37	-1.67	BB114067	21345		Tagln	transgelin
66	1416613_at	1274.71	NA	-1.18	-1.31	BI251808	13078		Cyp1b1	cytochrome P450, family 1, subfamily b, polypeptide 1
67	1440145_at	1317.38	NA	-1.38	-1.70	BB831986	15101		H60	PREDICTED: histocompatibility 60 [Mus musculus], mRNA sequence
68	1423691_x_at	1322.52	NA	-1.43	-1.79	M21836	16691		Krt2-8	keratin complex 2, basic, gene 8
69	1440295_at	1329.05	NA	-1.36	-1.65	BB130189	68832		1110057K04Rik	RIKEN cDNA 1110057K04 gene
70	1434129_s_at	1340.14	NA	-1.50	-1.95	BG917242	218454		Lhfp12	lipoma HMGIC fusion partner-like 2
71	1456046_at	1342.16	NA	-1.53	-2.00	AV319144	17064		C1qr1	complement component 1, q subcomponent, receptor 1

72	1429693_at	1354.44	NA	-1.44	-1.82	AK017619	13132	Dab2	disabled homolog 2 (Drosophila)
73	1439364_a_at	1380.07	NA	-1.18	-1.32	BF147716	17390	Mmp2	matrix metalloproteinase 2
74	1435989_x_at	1384.32	NA	-1.42	-1.77	AW322280	434261	LOC434261	similar to cyokeratin EndoA - mouse
75	1416136_at	1387.90	NA	-1.20	-1.34	NM_008610	17390	Mmp2	matrix metalloproteinase 2
76	1454656_at	1389.76	NA	-1.38	-1.69	AV271736	219140	Spata13	spermatogenesis associated 13
77	1433525_at	1395.56	NA	-1.44	-1.82	AW558570	13617	Ednra	endothelin receptor type A
78	1451161_a_at	1448.52	NA	-1.41	-1.75	U66888	13733	Emr1	EGF-like module containing, mucin-like, hormone receptor-like sequence 1
79	1456014_s_at	1456.21	NA	-1.53	-2.02	BB113173	108101	BC032204	cDNA sequence BC032204
80	1458299_s_at	1458.03	NA	-1.40	-1.75	BB820441	18037	Nfkbie	nuclear factor of kappa light polypeptide gene enhancer in B-cells inhibitor, epsilon
81	1420498_a_at	1458.52	NA	-1.35	-1.63	NM_023118	13132	Dab2	disabled homolog 2 (Drosophila)
82	1436970_a_at	1465.52	NA	-1.39	-1.72	AA499047	18596	Pdgfrb	platelet derived growth factor receptor, beta polypeptide
83	1426236_a_at	1466.34	NA	-1.40	-1.74	AI391218	14645	Glul	glutamate-ammonia ligase (glutamine synthetase)
84	1452382_at	1471.67	NA	-1.34	-1.62	BB542096	---	---	---
85	1456475_s_at	1475.79	NA	-1.41	-1.76	BB216074	19088	Prkar2b	protein kinase, cAMP dependent regulatory, type II beta
86	1424443_at	1476.00	NA	-1.43	-1.79	AV378394	107769 29877	Hdgfrp3 /// Tm6sf1	hepatoma-derived growth factor, related protein 3 /// transmembrane 6 superfamily member 1
87	1444061_at	1484.12	NA	-1.18	-1.32	BB150166	109314	A030004J04Rik	RIKEN cDNA A030004J04 gene
88	1435343_at	1488.16	NA	-1.41	-1.77	BF715043	210293	Dock10	dedicator of cytokinesis 10
89	1420431_at	1495.23	NA	-1.01	-1.02	NM_009100	20129	Rptn	repetin
90	1429210_at	1498.92	NA	-1.44	-1.83	BE290548	237759	Col23a1	procollagen, type XXIII, alpha 1
91	1437726_x_at	1518.53	NA	-1.39	-1.71	BB111335	12260	C1qb	complement component 1, q subcomponent, beta polypeptide
92	1427883_a_at	1520.30	NA	-1.33	-1.60	AW550625	12825	Col3a1	procollagen, type III, alpha 1
93	1432466_a_at	1521.93	NA	-1.37	-1.69	AK019319	11816	ApoE	apolipoprotein E
94	1451867_x_at	1535.31	NA	-1.57	-2.09	AF177664	11856	Arhgap6	Rho GTPase activating protein 6
95	1438975_x_at	1543.90	NA	-1.32	-1.59	AV361868	224454	Zdhc14	zinc finger, DHHC domain containing 14
96	1419090_x_at	1558.48	NA	-1.31	-1.55	NM_010644	16618	Klk26	kallikrein 26
97	1449038_at	1558.98	NA	-1.31	-1.56	NM_008288	15483	Hsd11b1	hydroxysteroid 11-beta dehydrogenase 1
98	1448061_at	1560.02	NA	-1.43	-1.80	AA183642	---	---	---

99	1427484_at	1561.14	NA	-1.31	-1.55	BB650819	319670	Eml5	echinoderm microtubule associated protein like 5
100	1455660_at	1567.23	NA	-1.61	-2.19	BB769628	12983	Csf2rb1	colony stimulating factor 2 receptor, beta 1, low-affinity (granulocyte- macrophage)

## Appendix Three

### Iterative Group Analysis (iGA) report on the differentially expressed functional gene classes



#### General Information

Mode	Representative
Number of genes on chip	23155
Number of annotated genes	15986
Number of groups	8092
Number of singletons	2867
Significance threshold	1.2e-04
File name	K14D6 Control v WT Control positive

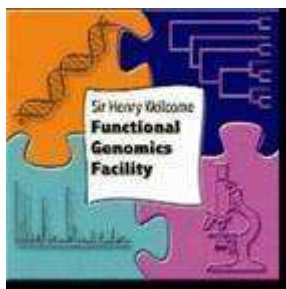
Top Changed Groups	Group Members	Changed Members	P-Value Changed	Percent Changed
<b>5581 - collagen</b>	34	5	1.9e-07	14.71
<b>7169 - transmembrane receptor protein tyrosine kinase signaling pathway</b>	76	6	4.3e-06	7.89
<b>30020 - extracellular matrix structural constituent conferring tensile strength</b>	29	4	4.5e-06	13.79
<b>IPR008160 - Collagen triple helix repeat</b>	65	5	5.1e-06	7.69
<b>IPR000233 - Cadherin cytoplasmic region</b>	12	3	7.8e-06	25.00
<b>6817 - phosphate transport</b>	84	5	1.8e-05	5.95
<b>1516 - prostaglandin biosynthesis</b>	9	2	2.9e-05	22.22
<b>5201 - extracellular matrix structural constituent</b>	47	4	3.2e-05	8.51
<b>5229 - intracellular calcium activated chloride channel activity</b>	3	3	1.0e-04	100.00

#### Changed group breakdown:

Group	P-value	Probe-set ID	Rank	Gene ID	Gene Symbol	Title
<b>5581 - collagen</b>	6.6e-02	1448590_at	32	NM_009933	Col6a1	procollagen, type VI, alpha 1
	3.8e-03	1450857_a_at	43	BF227507	Col1a2	procollagen, type I, alpha 2
	2.1e-04	1452250_a_at	55	BI455189	Col6a2	procollagen, type VI, alpha 2
	6.7e-06	1430676_at	58	AK019854	Col19a1	procollagen, type XIX, alpha 1
<a href="#">show the whole group</a>	1.9e-07	1427883_a_at	62	AW550625	Col3a1	procollagen, type III, alpha 1
<b>7169 - transmembrane receptor protein tyrosine kinase signaling pathway</b>	1.6e-01	1421917_at	36	AW537708	Pdgfra	platelet derived growth factor receptor, alpha polypeptide
	1.5e-02	1416121_at	40	M65143	Lox	lysyl oxidase
	1.1e-03	1450857_a_at	43	BF227507	Col1a2	procollagen, type I, alpha 2
	3.2e-04	1437219_at	69	AW553541	Igf1r	Insulin-like growth factor I receptor (Igf1r), mRNA

	3.0e-05	1436970_a_at	76	AA499047	Pdgfrb	platelet derived growth factor receptor, beta polypeptide
<a href="#">show the whole group</a>	4.3e-06	1419248_at	90	AF215668	Rgs2	regulator of G-protein signaling 2
<b>30020 - extracellular matrix structural constituent conferring tensile strength</b>	5.7e-02	1448590_at	32	NM_009933	Col6a1	procollagen, type VI, alpha 1
	2.7e-03	1450857_a_at	43	BF227507	Col1a2	procollagen, type I, alpha 2
	1.3e-04	1452250_a_at	55	BI455189	Col6a2	procollagen, type VI, alpha 2
<a href="#">show the whole group</a>	4.5e-06	1427883_a_at	62	AW550625	Col3a1	procollagen, type III, alpha 1
<b>IPR008160 - Collagen triple helix repeat</b>	1.2e-01	1448590_at	32	NM_009933	Col6a1	procollagen, type VI, alpha 1
	1.3e-02	1450857_a_at	43	BF227507	Col1a2	procollagen, type I, alpha 2
	1.4e-03	1452250_a_at	55	BI455189	Col6a2	procollagen, type VI, alpha 2
	9.0e-05	1430676_at	58	AK019854	Col19a1	procollagen, type XIX, alpha 1
<a href="#">show the whole group</a>	5.1e-06	1427883_a_at	62	AW550625	Col3a1	procollagen, type III, alpha 1
<b>IPR000233 - Cadherin cytoplasmic region</b>	1.0e-02	1418815_at	14	BC022107	Cdh2	cadherin 2
	4.2e-04	1450757_at	41	NM_009866	Cdh11	cadherin 11
<a href="#">show the whole group</a>	7.8e-06	1425092_at	54	AF183946	Cdh10	cadherin 10
<b>6817 - phosphate transport</b>	1.6e-01	1448590_at	32	NM_009933	Col6a1	procollagen, type VI, alpha 1
	2.1e-02	1450857_a_at	43	BF227507	Col1a2	procollagen, type I, alpha 2
	3.0e-03	1452250_a_at	55	BI455189	Col6a2	procollagen, type VI, alpha 2
	2.4e-04	1430676_at	58	AK019854	Col19a1	procollagen, type XIX, alpha 1
<a href="#">show the whole group</a>	1.8e-05	1427883_a_at	62	AW550625	Col3a1	procollagen, type III, alpha 1
<b>1516 - prostaglandin biosynthesis</b>	4.5e-03	1448816_at	8	NM_008968	Ptgis	prostaglandin I2 (prostacyclin) synthase
<a href="#">show the whole group</a>	2.9e-05	1436448_a_at	15	AA833146	Ptgs1	prostaglandin-endoperoxide synthase 1
<b>5201 - extracellular matrix structural constituent</b>	9.0e-02	1448590_at	32	NM_009933	Col6a1	procollagen, type VI, alpha 1
	7.1e-03	1450857_a_at	43	BF227507	Col1a2	procollagen, type I, alpha 2
	5.6e-04	1452250_a_at	55	BI455189	Col6a2	procollagen, type VI, alpha 2
<a href="#">show the whole group</a>	3.2e-05	1427883_a_at	62	AW550625	Col3a1	procollagen, type III, alpha 1
<b>5229 - intracellular calcium activated chloride channel activity</b>	2.7e-02	1460259_s_at	144	AF108501	Clca1 /// Clca2	chloride channel calcium activated 1 /// chloride channel calcium activated 2
	4.0e-04	1419463_at	164	AF108501	Clca2	chloride channel calcium activated 2
	1.0e-04	1417853_at	343	AF047838	Clca1	chloride channel calcium activated 1

**Iterative Group Analysis (iGA) report on the differentially expressed functional gene classes**



### General Information

Mode	Representative
Number of genes on chip	23155
Number of annotated genes	16003
Number of groups	8107
Number of singletons	2867
Significance threshold	1.2e-04
File name	WT +CCL3 V WT Control Positive

Top Changed Groups	Group Members	Changed Members	P-Value Changed	Percent Changed
<b>IPR008160 - Collagen triple helix repeat</b>	71	8	7.6e-11	11.27
<b>6817 - phosphate transport</b>	84	7	1.3e-10	8.33
<b>5201 - extracellular matrix structural constituent</b>	48	8	4.3e-10	16.67
<b>30020 - extracellular matrix structural constituent conferring tensile strength</b>	29	5	1.1e-09	17.24
<b>5581 - collagen</b>	35	5	2.9e-09	14.29
<b>IPR000885 - Fibrillar collagen, C-terminal</b>	11	5	3.2e-09	45.45
<b>IPR001811 - Small chemokine, interleukin-8 like</b>	31	6	1.8e-08	19.35
<b>8009 - chemokine activity</b>	38	6	6.4e-08	15.79
<b>7169 - transmembrane receptor protein tyrosine kinase signaling pathway</b>	76	6	4.7e-07	7.89
<b>IPR007237 - CD20/IgE Fc receptor beta subunit</b>	15	4	5.5e-07	26.67
<b>IPR000372 - Cysteine-rich flanking region, N-terminal</b>	39	5	2.2e-06	12.82
<b>1527 - microfibril</b>	6	3	3.8e-06	50.00
<b>30023 - extracellular matrix constituent conferring elasticity</b>	2	2	4.9e-06	100.00
<b>6935 - chemotaxis</b>	87	6	9.4e-06	6.90
<b>8201 - heparin binding</b>	57	5	2.3e-05	8.77
<b>Inflammatory_Response_Pathway - GenMAPP</b>	40	3	4.1e-05	7.50
<b>Eicosanoid_Synthesis - GenMAPP</b>	21	3	4.6e-05	14.29
<b>IPR001007 - von Willebrand factor, type C</b>	22	2	5.0e-05	9.09
<b>IPR001695 - Lysyl oxidase</b>	4	2	7.2e-05	50.00
<b>5229 - intracellular calcium activated chloride channel activity</b>	3	3	9.8e-05	100.00
<b>50766 - positive regulation of phagocytosis</b>	21	3	1.1e-04	14.29
<b>5588 - collagen type V</b>	3	3	1.2e-04	100.00

### Changed group breakdown:

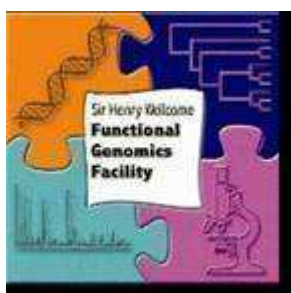
Group	P-value	Probe-set ID	Rank	Gene ID	Gene Symbol	Title
<b>IPR008160 - Collagen triple helix repeat</b>	1.8e-02	1427883_a_at	4	AW550625	Col3a1	procollagen, type III, alpha 1
	1.0e-03	1448590_at	11	NM_009933	Col6a1	procollagen, type VI, alpha 1
	2.3e-05	1452250_a_at	13	BI455189	Col6a2	procollagen, type VI, alpha 2
	3.4e-07	1417381_at	14	NM_007572	C1qa	complement component 1, q subcomponent, alpha polypeptide
	8.9e-09	1449154_at	17	NM_007729	Col11a1	procollagen, type XI,

	1.1e-09	1416414_at	25	NM_133918	Emilin1	alpha 1 elastin microfibril interfacer 1
	1.0e-10	1450857_a_at	27	BF227507	Col1a2	procollagen, type I, alpha 2
<a href="#">show the whole group</a>	7.6e-11	1423110_at	34	BF227507	---	---
<b>6817 - phosphate transport</b>	2.1e-02	1427883_a_at	4	AW550625	Col3a1	procollagen, type III, alpha 1
	1.5e-03	1448590_at	11	NM_009933	Col6a1	procollagen, type VI, alpha 1
	3.8e-05	1452250_a_at	13	BI455189	Col6a2	procollagen, type VI, alpha 2
	6.8e-07	1417381_at	14	NM_007572	C1qa	complement component 1, q subcomponent, alpha polypeptide
	2.1e-08	1449154_at	17	NM_007729	Col11a1	procollagen, type XI, alpha 1
	2.9e-09	1416414_at	25	NM_133918	Emilin1	elastin microfibril interfacer 1
<a href="#">show the whole group</a>	1.3e-10	1450857_a_at	27	BF227507	Col1a2	procollagen, type I, alpha 2
<b>5201 - extracellular matrix structural constituent</b>	1.2e-02	1427883_a_at	4	AW550625	Col3a1	procollagen, type III, alpha 1
	4.8e-04	1448590_at	11	NM_009933	Col6a1	procollagen, type VI, alpha 1
	7.1e-06	1452250_a_at	13	BI455189	Col6a2	procollagen, type VI, alpha 2
	1.6e-07	1449154_at	17	NM_007729	Col11a1	procollagen, type XI, alpha 1
	1.5e-08	1450857_a_at	27	BF227507	Col1a2	procollagen, type I, alpha 2
	2.2e-07	1460208_at	87	NM_007993	Fbn1	fibrillin 1
	1.1e-08	1454830_at	93	AV010392	Fbn2	fibrillin 2
<a href="#">show the whole group</a>	4.3e-10	1416740_at	96	AW744319	Col5a1	procollagen, type V, alpha 1
<b>30020 - extracellular matrix structural constituent conferring tensile strength</b>	7.2e-03	1427883_a_at	4	AW550625	Col3a1	procollagen, type III, alpha 1
	1.7e-04	1448590_at	11	NM_009933	Col6a1	procollagen, type VI, alpha 1
	1.5e-06	1452250_a_at	13	BI455189	Col6a2	procollagen, type VI, alpha 2
	2.0e-08	1449154_at	17	NM_007729	Col11a1	procollagen, type XI, alpha 1
<a href="#">show the whole group</a>	1.1e-09	1450857_a_at	27	BF227507	Col1a2	procollagen, type I, alpha 2
<b>5581 - collagen</b>	8.7e-03	1427883_a_at	4	AW550625	Col3a1	procollagen, type III, alpha 1
	2.5e-04	1448590_at	11	NM_009933	Col6a1	procollagen, type VI, alpha 1
	2.7e-06	1452250_a_at	13	BI455189	Col6a2	procollagen, type VI, alpha 2
	4.5e-08	1449154_at	17	NM_007729	Col11a1	procollagen, type XI, alpha 1
<a href="#">show the whole group</a>	2.9e-09	1450857_a_at	27	BF227507	Col1a2	procollagen, type I, alpha 2
<b>IPR000885 - Fibrillar collagen, C-terminal</b>	2.7e-03	1427883_a_at	4	AW550625	Col3a1	procollagen, type III, alpha 1
	5.8e-05	1449154_at	17	NM_007729	Col11a1	procollagen, type XI, alpha 1
	7.0e-07	1450857_a_at	27	BF227507	Col1a2	procollagen, type I, alpha 2
	5.6e-09	1423110_at	34	BF227507	---	---
<a href="#">show the whole group</a>	3.2e-09	1416740_at	96	AW744319	Col5a1	procollagen, type V, alpha 1
<b>IPR001811 - Small chemokine,</b>	3.9e-03	1448995_at	2	NM_019932	Cxcl4	chemokine (C-X-C

<b>interleukin-8 like</b>						motif) ligand 4
	2.1e-03	<a href="#">1419728_at</a>	35	<a href="#">NM_009141</a>	Cxcl5	chemokine (C-X-C motif) ligand 5
	8.8e-05	<a href="#">1420380_at</a>	45	<a href="#">AF065933</a>	Ccl2	chemokine (C-C motif) ligand 2
	7.6e-06	<a href="#">1417266_at</a>	66	<a href="#">BC002073</a>	Ccl6	chemokine (C-C motif) ligand 6
	4.5e-07	<a href="#">1417936_at</a>	81	<a href="#">AF128196</a>	Ccl9	chemokine (C-C motif) ligand 9
<a href="#">show the whole group</a>	1.8e-08	<a href="#">1449984_at</a>	90	<a href="#">NM_009140</a>	Cxcl2	chemokine (C-X-C motif) ligand 2
<b>8009 - chemokine activity</b>	4.7e-03	<a href="#">1448995_at</a>	2	<a href="#">NM_019932</a>	Cxcl4	chemokine (C-X-C motif) ligand 4
	3.1e-03	<a href="#">1419728_at</a>	35	<a href="#">NM_009141</a>	Cxcl5	chemokine (C-X-C motif) ligand 5
	1.6e-04	<a href="#">1420380_at</a>	45	<a href="#">AF065933</a>	Ccl2	chemokine (C-C motif) ligand 2
	1.8e-05	<a href="#">1417266_at</a>	66	<a href="#">BC002073</a>	Ccl6	chemokine (C-C motif) ligand 6
	1.3e-06	<a href="#">1417936_at</a>	81	<a href="#">AF128196</a>	Ccl9	chemokine (C-C motif) ligand 9
<a href="#">show the whole group</a>	6.4e-08	<a href="#">1449984_at</a>	90	<a href="#">NM_009140</a>	Cxcl2	chemokine (C-X-C motif) ligand 2
<b>7169 - transmembrane receptor protein tyrosine kinase signaling pathway</b>	4.7e-02	<a href="#">1436970_a_at</a>	10	<a href="#">AA499047</a>	Pdgfrb	platelet derived growth factor receptor, beta polypeptide
	7.2e-03	<a href="#">1450857_a_at</a>	27	<a href="#">BF227507</a>	Col1a2	procollagen, type I, alpha 2
	3.1e-04	<a href="#">1416121_at</a>	28	<a href="#">M65143</a>	Lox	lysyl oxidase
	3.8e-05	<a href="#">1421917_at</a>	40	<a href="#">AW537708</a>	Pdgfra	platelet derived growth factor receptor, alpha polypeptide
	2.0e-06	<a href="#">1419248_at</a>	44	<a href="#">AF215668</a>	Rgs2	regulator of G-protein signaling 2
<a href="#">show the whole group</a>	4.7e-07	<a href="#">1425575_at</a>	62	<a href="#">M68513</a>	Epha3	Eph receptor A3
<b>IPR007237 - CD20/IgE Fc receptor beta subunit</b>	9.4e-04	<a href="#">1424754_at</a>	1	<a href="#">BC024402</a>	Ms4a7	membrane-spanning 4-domains, subfamily A, member 7
	1.2e-04	<a href="#">1419598_at</a>	18	<a href="#">NM_026835</a>	Ms4a6d	membrane-spanning 4-domains, subfamily A, member 6D
	2.7e-05	<a href="#">1418990_at</a>	64	<a href="#">NM_025658</a>	Ms4a4d	membrane-spanning 4-domains, subfamily A, member 4D
<a href="#">show the whole group</a>	5.5e-07	<a href="#">1419599_s_at</a>	74	<a href="#">NM_026835</a>	Ms4a11	membrane-spanning 4-domains, subfamily A, member 11
<b>IPR000372 - Cysteine-rich flanking region, N-terminal</b>	1.7e-02	<a href="#">1423607_at</a>	7	<a href="#">AK014312</a>	Lum	lumican
	1.8e-03	<a href="#">1449368_at</a>	26	<a href="#">NM_007833</a>	Dcn	decorin
	6.3e-05	<a href="#">1416405_at</a>	32	<a href="#">BC019502</a>	Bgn	biglycan
	4.8e-05	<a href="#">1423311_s_at</a>	83	<a href="#">BQ177165</a>	Tpbp	trophoblast glycoprotein
<a href="#">show the whole group</a>	2.2e-06	<a href="#">1452296_at</a>	88	<a href="#">BM570006</a>	Slit3	slit homolog 3 (Drosophila)
<b>1527 - microfibril</b>	1.3e-02	<a href="#">1418454_at</a>	36	<a href="#">NM_015776</a>	Mfap5	microfibrillar associated protein 5
	4.3e-04	<a href="#">1460208_at</a>	87	<a href="#">NM_007993</a>	Fbn1	fibrillin 1
<a href="#">show the whole group</a>	3.8e-06	<a href="#">1454830_at</a>	93	<a href="#">AV010392</a>	Fbn2	fibrillin 2
<b>30023 - extracellular matrix constituent conferring elasticity</b>	3.1e-03	<a href="#">1416414_at</a>	25	<a href="#">NM_133918</a>	Emilin1	elastin microfibril interfacier 1
	4.9e-06	<a href="#">1418454_at</a>	36	<a href="#">NM_015776</a>	Mfap5	microfibrillar associated protein 5
<b>6935 - chemotaxis</b>	1.1e-02	<a href="#">1448995_at</a>	2	<a href="#">NM_019932</a>	Cxcl4	chemokine (C-X-C motif) ligand 4

	1.5e-02	1419728_at	35	NM_009141	Cxcl5	chemokine (C-X-C motif) ligand 5
	1.9e-03	1420380_at	45	AF065933	Ccl2	chemokine (C-C motif) ligand 2
	4.5e-04	1417266_at	66	BC002073	Ccl6	chemokine (C-C motif) ligand 6
	7.8e-05	1417936_at	81	AF128196	Ccl9	chemokine (C-C motif) ligand 9
<a href="#">show the whole group</a>	9.4e-06	1449984_at	90	NM_009140	Cxcl2	chemokine (C-X-C motif) ligand 2
<b>8201 - heparin binding</b>	7.1e-03	1448995_at	2	NM_019932	Cxcl4	chemokine (C-X-C motif) ligand 4
	3.4e-04	1450663_at	8	NM_011581	Thbs2	thrombospondin 2
	4.7e-05	1423606_at	20	BI110565	Postn	periostin, osteoblast specific factor
<a href="#">show the whole group</a>	2.3e-05	1416221_at	47	BI452727	Fstl1	follicle-stimulating-like 1
	2.3e-05	1416740_at	96	AW744319	Col5a1	procollagen, type V, alpha 1
<b>Inflammatory_Response_Pathway - GenMAPP</b>	1.0e-02	1427883_a_at	4	AW550625	Col3a1	procollagen, type III, alpha 1
	2.2e-04	1416136_at	9	NM_008610	Mmp2	matrix metalloproteinase 2
<a href="#">show the whole group</a>	4.1e-05	1450857_a_at	27	BF227507	Col1a2	procollagen, type I, alpha 2
<b>Eicosanoid_Synthesis - GenMAPP</b>	2.1e-02	1435943_at	16	AI647687	Dpep1	dipeptidase 1 (renal)
	1.8e-03	1448816_at	48	NM_008968	Ptgis	prostaglandin I2 (prostacyclin) synthase
<a href="#">show the whole group</a>	4.6e-05	1436448_a_at	54	AA833146	Ptgs1	prostaglandin-endoperoxide synthase 1
<b>IPR001007 - von Willebrand factor, type C</b>	5.5e-03	1427883_a_at	4	AW550625	Col3a1	procollagen, type III, alpha 1
<a href="#">show the whole group</a>	5.0e-05	1450663_at	8	NM_011581	Thbs2	thrombospondin 2
<b>IPR001695 - Lysyl oxidase</b>	7.0e-03	1416121_at	28	M65143	Lox	lysyl oxidase
<a href="#">show the whole group</a>	7.2e-05	1451978_at	56	AF357006	Loxl1	lysyl oxidase-like 1
<b>5229 - intracellular calcium activated chloride channel activity</b>	3.2e-02	1419463_at	172	AF108501	Clca2	chloride channel calcium activated 2
	7.0e-04	1417852_x_at	230	AF047838	Clca1	chloride channel calcium activated 1
	9.8e-05	1460259_s_at	262	AF108501	Clca1 /// Clca2	chloride channel calcium activated 1 /// chloride channel calcium activated 2
<b>50766 - positive regulation of phagocytosis</b>	4.0e-02	1435477_s_at	31	BM224327	Fcgr2b	Fc receptor, IgG, low affinity IIb
	8.5e-04	1418666_at	33	NM_008987	Ptx3	pentraxin related gene
<a href="#">show the whole group</a>	1.1e-04	1448620_at	73	NM_010188	Fcgr3	Fc receptor, IgG, low affinity III
<b>5588 - collagen type V</b>	1.8e-02	1416740_at	96	AW744319	Col5a1	procollagen, type V, alpha 1
	6.3e-04	1422437_at	215	AV229424	Col5a2	procollagen, type V, alpha 2
	1.2e-04	1419703_at	492	NM_016919	Col5a3	procollagen, type V, alpha 3

## Iterative Group Analysis (iGA) report on the differentially expressed functional gene classes



### General Information

Mode	Representative
Number of genes on chip	23155
Number of annotated genes	15988
Number of groups	8102
Number of singletons	2879
Significance threshold	1.2e-04
File name	K14D6 + CCL3 v K14D6 control positive

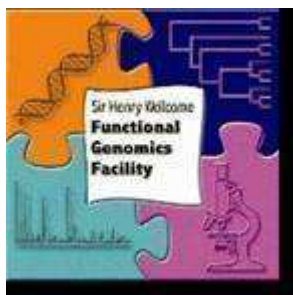
Top Changed Groups	Group Members	Changed Members	P-Value Changed	Percent Changed
<b>30020 - extracellular matrix structural constituent conferring tensile strength</b>	29	7	1.9e-10	24.14
<b>5581 - collagen</b>	35	7	6.9e-10	20.00
<b>8201 - heparin binding</b>	57	8	1.7e-09	14.04
<b>5201 - extracellular matrix structural constituent</b>	48	7	6.8e-09	14.58
<b>IPR000885 - Fibrillar collagen, C-terminal</b>	10	4	2.4e-08	40.00
<b>IPR008160 - Collagen triple helix repeat</b>	72	6	1.5e-07	8.33
<b>6817 - phosphate transport</b>	85	7	3.9e-07	8.24
<b>6935 - chemotaxis</b>	87	7	3.9e-07	8.05
<b>IPR001811 - Small chemokine, interleukin-8 like</b>	31	5	5.7e-07	16.13
<b>8009 - chemokine activity</b>	38	5	1.6e-06	13.16
<b>50766 - positive regulation of phagocytosis</b>	21	3	3.9e-06	14.29
<b>19864 - IgG binding</b>	5	2	2.2e-05	40.00
<b>IPR001614 - Myelin proteolipid protein PLP</b>	3	2	3.1e-05	66.67
<b>IPR007237 - CD20/IgE Fc receptor beta subunit</b>	14	3	3.8e-05	21.43
<b>IPR001916 - Glycoside hydrolase, family 22</b>	8	2	5.0e-05	25.00
<b>IPR002086 - Aldehyde dehydrogenase</b>	26	2	5.3e-05	7.69
<b>45576 - mast cell activation</b>	9	2	7.7e-05	22.22
<b>3796 - lysozyme activity</b>	10	2	8.1e-05	20.00
<b>IPR001751 - Calcium-binding protein, S-100/ICaBP type</b>	15	3	9.3e-05	20.00
<b>5229 - intracellular calcium activated chloride channel activity</b>	3	3	9.4e-05	100.00
<b>IPR002227 - Tyrosinase</b>	3	3	9.8e-05	100.00
<b>IPR002035 - von Willebrand factor, type A</b>	44	4	1.1e-04	9.09

Changed group breakdown:						
Group	P-value	Probe-set ID	Rank	Gene ID	Gene Symbol	Title
<b>30020 - extracellular matrix structural constituent conferring tensile strength</b>	1.8e-02	1427883_a_at	10	AW550625	Col3a1	procollagen, type III, alpha 1
	6.5e-04	1455494_at	21	BI794771	Col1a1	procollagen, type I, alpha 1
	9.3e-06	1452250_a_at	23	BI455189	Col6a2	procollagen, type VI, alpha 2
	1.5e-07	1448590_at	27	NM_009933	Col6a1	procollagen, type VI, alpha 1
	4.3e-09	1449154_at	35	NM_007729	Col11a1	procollagen, type XI, alpha 1
	5.2e-10	1450857_a_at	54	BF227507	Col1a2	procollagen, type I, alpha 2
	<a href="#">show the whole group</a>	1.9e-10	1434479_at	87	AV246911	Col5a1
<b>5581 - collagen</b>	2.2e-02	1427883_a_at	10	AW550625	Col3a1	procollagen, type III, alpha 1
	9.5e-04	1455494_at	21	BI794771	Col1a1	procollagen, type I, alpha 1
	1.7e-05	1452250_a_at	23	BI455189	Col6a2	procollagen, type VI, alpha 2
	3.3e-07	1448590_at	27	NM_009933	Col6a1	procollagen, type VI, alpha 1
	1.2e-08	1449154_at	35	NM_007729	Col11a1	procollagen, type XI, alpha 1
	1.7e-09	1450857_a_at	54	BF227507	Col1a2	procollagen, type I, alpha 2
	<a href="#">show the whole group</a>	6.9e-10	1434479_at	87	AV246911	Col5a1
<b>8201 - heparin binding</b>	4.9e-02	1432466_a_at	14	AK019319	Apoe	apolipoprotein E
	6.1e-03	1448259_at	33	BI452727	Fstl1	follostatin-like 1
	7.9e-04	1448995_at	51	NM_019932	Cxcl4	chemokine (C-X-C motif) ligand 4
	2.0e-04	1423606_at	81	BI110565	Postn	periostin, osteoblast specific factor
	1.3e-05	1421228_at	85	AF128193	Ccl7	chemokine (C-C motif) ligand 7
	6.3e-07	1434479_at	87	AV246911	Col5a1	Procollagen, type V, alpha 1 (Col5a1), mRNA
	4.3e-08	1448303_at	95	NM_053110	GpnmB	glycoprotein (transmembrane) nmb
<a href="#">show the whole group</a>	1.7e-09	1422571_at	96	NM_011581	Thbs2	thrombospondin 2

<b>5201 - extracellular matrix structural constituent</b>	3.0e-02	1427883_a_at	10	AW550625	Col3a1	procollagen, type III, alpha 1
	1.8e-03	1455494_at	21	BI794771	Col1a1	procollagen, type I, alpha 1
	4.3e-05	1452250_a_at	23	BI455189	Col6a2	procollagen, type VI, alpha 2
	1.2e-06	1448590_at	27	NM_009933	Col6a1	procollagen, type VI, alpha 1
	6.0e-08	1449154_at	35	NM_007729	Col11a1	procollagen, type XI, alpha 1
	1.2e-08	1450857_a_at	54	BF227507	Col1a2	procollagen, type I, alpha 2
<a href="#">show the whole group</a>	6.8e-09	1434479_at	87	AV246911	Col5a1	Procollagen, type V, alpha 1 (Col5a1), mRNA
<b>IPR000885 - Fibrillar collagen, C-terminal</b>	6.2e-03	1427883_a_at	10	AW550625	Col3a1	procollagen, type III, alpha 1
	2.1e-04	1449154_at	35	NM_007729	Col11a1	procollagen, type XI, alpha 1
	2.5e-06	1423110_at	45	BF227507	---	---
	<a href="#">show the whole group</a>	2.4e-08	1450857_a_at	54	BF227507	Col1a2
<b>IPR008160 - Collagen triple helix repeat</b>	4.4e-02	1427883_a_at	10	AW550625	Col3a1	procollagen, type III, alpha 1
	4.8e-03	1452250_a_at	23	BI455189	Col6a2	procollagen, type VI, alpha 2
	2.4e-04	1448590_at	27	NM_009933	Col6a1	procollagen, type VI, alpha 1
	1.8e-05	1449154_at	35	NM_007729	Col11a1	procollagen, type XI, alpha 1
	1.7e-06	1423110_at	45	BF227507	---	---
	<a href="#">show the whole group</a>	1.5e-07	1450857_a_at	54	BF227507	Col1a2
<b>6817 - phosphate transport</b>	5.2e-02	1427883_a_at	10	AW550625	Col3a1	procollagen, type III, alpha 1
	5.5e-03	1455494_at	21	BI794771	Col1a1	procollagen, type I, alpha 1
	2.4e-04	1452250_a_at	23	BI455189	Col6a2	procollagen, type VI, alpha 2
	1.2e-05	1448590_at	27	NM_009933	Col6a1	procollagen, type VI, alpha 1
	1.1e-06	1449154_at	35	NM_007729	Col11a1	procollagen, type XI, alpha 1
	4.0e-07	1450857_a_at	54	BF227507	Col1a2	procollagen, type I, alpha 2
	<a href="#">show the whole group</a>	3.9e-07	1434479_at	87	AV246911	Col5a1
<b>6935 - chemotaxis</b>	7.9e-02	1417936_at	15	AF128196	Ccl9	chemokine (C-C motif) ligand 9
	4.7e-03	1417266_at	19	BC002073	Ccl6	chemokine (C-C motif) ligand 6
	2.4e-03	1419394_s_at	49	NM_013650	S100a8	S100 calcium binding protein A8 (calgranulin A)
	1.7e-04	1448995_at	51	NM_019932	Cxcl4	chemokine (C-X-C motif) ligand 4
	1.3e-05	1449984_at	56	NM_009140	Cxcl2	chemokine (C-X-C motif) ligand 2
	2.6e-06	1419483_at	72	NM_009779	C3ar1	complement component 3a receptor 1
	<a href="#">show the whole group</a>	3.9e-07	1421228_at	85	AF128193	Ccl7
<b>IPR001811 - Small chemokine, interleukin-8 like</b>	2.9e-02	1417936_at	15	AF128196	Ccl9	chemokine (C-C motif) ligand 9
	6.1e-04	1417266_at	19	BC002073	Ccl6	chemokine (C-C motif) ligand 6
	1.3e-04	1448995_at	51	NM_019932	Cxcl4	chemokine (C-X-C motif) ligand 4
	4.0e-06	1449984_at	56	NM_009140	Cxcl2	chemokine (C-X-C motif) ligand 2
	<a href="#">show the whole group</a>	5.7e-07	1421228_at	85	AF128193	Ccl7
<b>8009 - chemokine activity</b>	3.5e-02	1417936_at	15	AF128196	Ccl9	chemokine (C-C motif) ligand 9
	9.2e-04	1417266_at	19	BC002073	Ccl6	chemokine (C-C motif) ligand 6
	2.4e-04	1448995_at	51	NM_019932	Cxcl4	chemokine (C-X-C motif) ligand 4
	9.1e-06	1449984_at	56	NM_009140	Cxcl2	chemokine (C-X-C motif) ligand 2
	<a href="#">show the whole group</a>	1.6e-06	1421228_at	85	AF128193	Ccl7

<b>50766 - positive regulation of phagocytosis</b>	7.9e-03	1418666_at	6	NM_008987	Ptx3	pentraxin related gene
	5.9e-05	1448620_at	9	NM_010188	Fcgr3	Fc receptor, IgG, low affinity III
<a href="#">show the whole group</a>	3.9e-06	1435477_s_at	24	BM224327	Fcgr2b	Fc receptor, IgG, low affinity IIb
<b>19864 - IgG binding</b>	2.8e-03	1448620_at	9	NM_010188	Fcgr3	Fc receptor, IgG, low affinity III
<a href="#">show the whole group</a>	2.2e-05	1435477_s_at	24	BM224327	Fcgr2b	Fc receptor, IgG, low affinity IIb
<b>IPR001614 - Myelin proteolipid protein PLP</b>	3.0e-03	1423091_a_at	16	AK016567	Gpm6b	glycoprotein m6b
<a href="#">show the whole group</a>	3.1e-05	1451718_at	52	BB768495	Plp1	proteolipid protein (myelin) 1
<b>IPR007237 - CD20/IgE Fc receptor beta subunit</b>	2.8e-02	1424754_at	32	BC024402	Ms4a7	membrane-spanning 4-domains, subfamily A, member 7
	1.2e-03	1419599_s_at	60	NM_026835	Ms4a11	membrane-spanning 4-domains, subfamily A, member 11
<a href="#">show the whole group</a>	3.8e-05	1419598_at	77	NM_026835	Ms4a6d	membrane-spanning 4-domains, subfamily A, member 6D
<b>IPR001916 - Glycoside hydrolase, family 22</b>	1.0e-03	1436996_x_at	2	AV066625	Lzp-s	P lysozyme structural
<a href="#">show the whole group</a>	5.0e-05	1423547_at	22	AW208566	Lyzs	lysozyme
<b>IPR002086 - Aldehyde dehydrogenase</b>	1.6e-03	1418601_at	1	NM_011921	Aldh1a7	aldehyde dehydrogenase family 1, subfamily A7
<a href="#">show the whole group</a>	5.3e-05	1416468_at	7	NM_013467	Aldh1a1	aldehyde dehydrogenase family 1, subfamily A1
<b>45576 - mast cell activation</b>	5.1e-03	1448620_at	9	NM_010188	Fcgr3	Fc receptor, IgG, low affinity III
<a href="#">show the whole group</a>	7.7e-05	1435477_s_at	24	BM224327	Fcgr2b	Fc receptor, IgG, low affinity IIb
<b>3796 - lysozyme activity</b>	1.3e-03	1436996_x_at	2	AV066625	Lzp-s	P lysozyme structural
<a href="#">show the whole group</a>	8.1e-05	1423547_at	22	AW208566	Lyzs	lysozyme
<b>IPR001751 - Calcium-binding protein, S-100/CaBP type</b>	3.5e-02	1448756_at	38	NM_009114	S100a9	S100 calcium binding protein A9 (calgranulin B)
	9.4e-04	1419394_s_at	49	NM_013650	S100a8	S100 calcium binding protein A8 (calgranulin A)
<a href="#">show the whole group</a>	9.3e-05	1424542_at	97	D00208	S100a4	S100 calcium binding protein A4
<b>5229 - intracellular calcium activated chloride channel activity</b>	1.3e-02	1419463_at	70	AF108501	Clca2	chloride channel calcium activated 2
	9.6e-05	1460259_s_at	91	AF108501	Clca1 /// Clca2	chloride channel calcium activated 1 /// chloride channel calcium activated 2
	9.4e-05	1417852_x_at	102	AF047838	Clca1	chloride channel calcium activated 1
<b>IPR002227 - Tyrosinase</b>	2.8e-02	1415862_at	150	BB762957	Tyrp1	tyrosinase-related protein 1
	6.2e-04	1417717_a_at	214	NM_011661	Tyr	tyrosinase
	9.8e-05	1418028_at	257	NM_010024	Dct	dopachrome tautomerase
<b>IPR002035 - von Willebrand factor, type A</b>	6.1e-02	1452250_a_at	23	BI455189	Col6a2	procollagen, type VI, alpha 2
	2.5e-03	1448590_at	27	NM_009933	Col6a1	procollagen, type VI, alpha 1
	9.4e-04	1419463_at	70	AF108501	Clca2	chloride channel calcium activated 2
<a href="#">show the whole group</a>	1.1e-04	1460259_s_at	91	AF108501	Clca1 /// Clca2	chloride channel calcium activated 1 /// chloride channel calcium activated 2

**Iterative Group Analysis (iGA) report on the differentially expressed functional gene classes**



### General Information

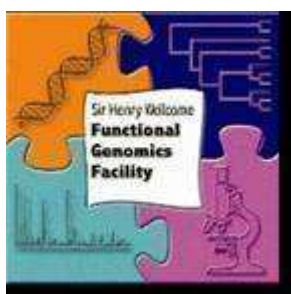
Mode	Representative
Number of genes on chip	23155
Number of annotated genes	15966
Number of groups	8086
Number of singletons	2867
Significance threshold	1.2e-04
File name	K14D6 + CCL3 v WT + CCL3 Positive

Top Changed Groups	Group Members	Changed Members	P-Value Changed	Percent Changed
<b>6583 - melanin biosynthesis from tyrosine</b>	6	4	3.4e-11	66.67
<b>1533 - cornified envelope</b>	14	5	1.2e-08	35.71
<b>IPR003347 - Transcription factor jumonji, jmjC</b>	21	3	3.9e-08	14.29
<b>42470 - melanosome</b>	7	3	6.8e-08	42.86
<b>IPR002227 - Tyrosinase</b>	2	2	1.6e-06	100.00
<b>15171 - amino acid transporter activity</b>	18	2	2.5e-05	11.11
<b>31424 - keratinization</b>	23	3	4.3e-05	13.04

Changed group breakdown:						
Group	P-value	Probe-set ID	Rank	Gene ID	Gene Symbol	Title
<b>6583 - melanin biosynthesis from tyrosine</b>	3.8e-03	1415862_at	10	BB762957	Tyrp1	tyrosinase-related protein 1
	1.2e-05	1422523_at	15	NM_021882	Si	silver
	3.4e-08	1456095_at	20	BB769772	Tyr	tyrosinase
	3.4e-11	1418028_at	21	NM_010024	Dct	dopachrome tautomerase
<a href="#">show the whole group</a>						
<b>1533 - cornified envelope</b>	2.6e-02	1450618_a_at	30	NM_011468	Sprr2a	small proline-rich protein 2A
	4.2e-04	1448745_s_at	35	NM_008508	Lor	loricrin
	9.1e-06	1451613_at	48	AY027660	Hrnr	hornerin
	1.8e-07	1420431_at	60	NM_009100	Rptn	repetin
	1.2e-08	1422837_at	94	NM_022886	Scel	sciellin
<a href="#">show the whole group</a>						
<b>IPR003347 - Transcription factor jumonji, jmjC</b>	2.6e-03	1426438_at	2	AA210261	Ddx3y	DEAD (Asp-Glu-Ala-Asp) box polypeptide 3, Y-linked
	1.6e-05	1426598_at	5	BB742957	Uty /// LOC546404 /// LOC546411	ubiquitously transcribed tetratricopeptide repeat gene, Y chromosome /// similar to male-specific histocompatibility antigen H-YDb /// similar to male-specific histocompatibility antigen H-YDb
	3.9e-08	1424903_at	6	AF127244	Jarid1d	jumonji, AT rich interactive domain 1D (Rbp2 like)
<a href="#">show the whole group</a>						
<b>42470 - melanosome</b>	4.4e-03	1415862_at	10	BB762957	Tyrp1	tyrosinase-related protein 1
	3.1e-05	1456095_at	20	BB769772	Tyr	tyrosinase
	6.8e-08	1418028_at	21	NM_010024	Dct	dopachrome tautomerase
<a href="#">show the whole group</a>						

<b>IPR002227 - Tyrosinase</b>	1.3e-03	<a href="#">1415862_at</a>	10	<a href="#">BB762957</a>	Tyrp1	tyrosinase-related protein 1
	1.6e-06	<a href="#">1418028_at</a>	21	<a href="#">NM_010024</a>	Dct	dopachrome tautomerase
<b>15171 - amino acid transporter activity</b>	4.5e-03	<a href="#">1420504_at</a>	4	<a href="#">AF320226</a>	Slc6a14	solute carrier family 6 (neurotransmitter transporter), member 14
	<a href="#">show the whole group</a>	2.5e-05	<a href="#">1417022_at</a>	7	<a href="#">NM_007515</a>	Slc7a3
<b>31424 - keratinization</b>	4.2e-02	<a href="#">1450618_a_at</a>	30	<a href="#">NM_011468</a>	Sprr2a	small proline-rich protein 2A
	1.1e-03	<a href="#">1448745_s_at</a>	35	<a href="#">NM_008508</a>	Lor	loricrin
<a href="#">show the whole group</a>	4.3e-05	<a href="#">1451613_at</a>	48	<a href="#">AY027660</a>	Hrnr	hornerin

## Iterative Group Analysis (iGA) report on the differentially expressed functional gene classes



### General Information

Mode	Representative
Number of genes on chip	23155
Number of annotated genes	15976

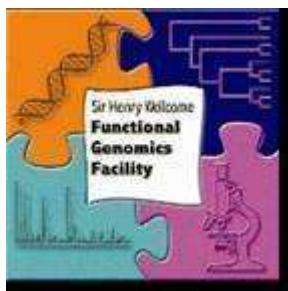
Number of groups	8057
Number of singletons	2885
Significance threshold	1.2e-04
File name	K14D6 Control v WT Control Negative

Top Changed Groups	Group Members	Changed Members	P-Value Changed	Percent Changed
<b>1533 - cornified envelope</b>	14	7	9.3e-13	50.00
<b>31424 - keratinization</b>	23	4	4.1e-06	17.39
<b>IPR001916 - Glycoside hydrolase, family 22</b>	8	2	4.6e-06	25.00
<b>3796 - lysozyme activity</b>	10	2	7.4e-06	20.00
<b>16998 - cell wall catabolism</b>	16	2	2.0e-05	12.50
<b>IPR001811 - Small chemokine, interleukin-8 like</b>	31	4	2.2e-05	12.90
<b>19835 - cytolysis</b>	20	2	3.1e-05	10.00
<b>19864 - IgG binding</b>	5	2	4.1e-05	40.00
<b>8009 - chemokine activity</b>	38	4	5.0e-05	10.53
<b>6935 - chemotaxis</b>	87	5	1.1e-04	5.75
<b>IPR002227 - Tyrosinase</b>				

Changed group breakdown:							
Group	P-value	Probe-set ID	Rank	Gene ID	Gene Symbol	Title	
<b>1533 - cornified envelope</b>	2.1e-02	1420431_at	24	NM_009100	Rptn	repetin	
	6.0e-04	1427910_at	42	AK003744	Cst6	cystatin E/M	
	1.4e-05	1427268_at	55	J03458	LOC433621 /// LOC545581	similar to Acidic ribosomal phosphoprotein P0 /// similar to Acidic ribosomal phosphoprotein P0	
	1.6e-07	1451613_at	59	AY027660	Hnr	hornerin	
	2.0e-09	1429540_at	66	AK008979	Cnfn	cornifelin	
	9.5e-12	1422837_at	67	NM_022886	Scel	sciellin	
<a href="#">show the whole group</a>	9.3e-13	1448745_s_at	77	NM_008508	Lor	loricrin	
<b>31424 - keratinization</b>	4.2e-02	1422963_at	30	NM_011475	Sprr2i	small proline-rich protein 2I	
	9.6e-04	1449833_at	32	NM_011472	Sprr2f	small proline-rich protein 2F	
	8.0e-05	1451613_at	59	AY027660	Hnr	hornerin	
	<a href="#">show the whole group</a>	4.1e-06	1448745_s_at	77	NM_008508	Lor	loricrin
<b>IPR001916 - Glycoside hydrolase, family 22</b>	5.0e-04	1436996_x_at	1	AV066625	Lzp-s	P lysozyme structural	
	<a href="#">show the whole group</a>	4.6e-06	1423547_at	7	AW208566	Lyzs	lysozyme
<b>3796 - lysozyme activity</b>	6.3e-04	1436996_x_at	1	AV066625	Lzp-s	P lysozyme structural	
	<a href="#">show the whole group</a>	7.4e-06	1423547_at	7	AW208566	Lyzs	lysozyme
<b>16998 - cell wall catabolism</b>	1.0e-03	1436996_x_at	1	AV066625	Lzp-s	P lysozyme structural	
	<a href="#">show the whole group</a>	2.0e-05	1423547_at	7	AW208566	Lyzs	lysozyme
<b>IPR001811 - Small chemokine, interleukin-8 like</b>	3.2e-02	1448995_at	17	NM_019932	Cxcl4	chemokine (C-X-C motif) ligand 4	
	8.2e-04	1417936_at	22	AF128196	Ccl9	chemokine (C-C motif) ligand 9	
	1.1e-04	1417266_at	48	BC002073	Ccl6	chemokine (C-C motif) ligand 6	
	<a href="#">show the whole group</a>	2.2e-05	1449984_at	86	NM_009140	Cxcl2	chemokine (C-X-C motif) ligand 2
	<b>19835 - cytolysis</b>	1.3e-03	1436996_x_at	1	AV066625	Lzp-s	P lysozyme structural
<a href="#">show the whole group</a>	3.1e-05	1423547_at	7	AW208566	Lyzs	lysozyme	
<b>19864 - IgG binding</b>	1.9e-03	1448620_at	6	NM_010188	Fcgr3	Fc receptor, IgG, low affinity III	
	<a href="#">show the whole group</a>	4.1e-05	1435477_s_at	33	BM224327	Fcgr2b	Fc receptor, IgG, low affinity IIb

<b>8009 - chemokine activity</b>	4.0e-02	1448995_at	17	NM_019932	Cxcl4	chemokine (C-X-C motif) ligand 4
	1.2e-03	1417936_at	22	AF128196	Ccl9	chemokine (C-C motif) ligand 9
	2.0e-04	1417266_at	48	BC002073	Ccl6	chemokine (C-C motif) ligand 6
<a href="#">show the whole group</a>	5.0e-05	1449984_at	86	NM_009140	Cxcl2	chemokine (C-X-C motif) ligand 2
<b>6935 - chemotaxis</b>	8.9e-02	1448995_at	17	NM_019932	Cxcl4	chemokine (C-X-C motif) ligand 4
	6.3e-03	1417936_at	22	AF128196	Ccl9	chemokine (C-C motif) ligand 9
	2.3e-03	1417266_at	48	BC002073	Ccl6	chemokine (C-C motif) ligand 6
	8.6e-04	1419483_at	78	NM_009779	C3ar1	complement component 3a receptor 1
<a href="#">show the whole group</a>	1.1e-04	1449984_at	86	NM_009140	Cxcl2	chemokine (C-X-C motif) ligand 2
<b>IPR002227 - Tyrosinase</b>	4.3e-02	1418028_at	233	NM_010024	Dct	dopachrome tautomerase
	2.7e-03	1415861_at	474	BB762957	Tyrp1	tyrosinase-related protein 1
	1.2e-04	1417717_a_at	477	NM_011661	Tyr	tyrosinase

**Iterative Group Analysis (iGA) report on the differentially expressed functional gene classes**



### General Information

Mode	Representative
Number of genes on chip	23155
Number of annotated genes	15960
Number of groups	8038
Number of singletons	2867
Significance threshold	1.2e-04
File name	WT + CCL3 V WT Control Negative

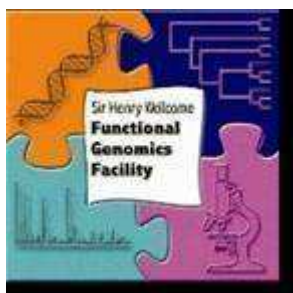
Top Changed Groups	Group Members	Changed Members	P-Value Changed	Percent Changed
<b>1533 - cornified envelope</b>	14	4	8.0e-11	28.57
<b>42470 - melanosome</b>	7	4	4.6e-08	57.14
<b>IPR003347 - Transcription factor jumonji, jmjC</b>	18	3	6.7e-08	16.67
<b>5882 - intermediate filament</b>	93	8	9.3e-08	8.60
<b>IPR001664 - Intermediate filament protein</b>	57	6	4.5e-07	10.53
<b>6583 - melanin biosynthesis from tyrosine</b>	6	3	4.4e-06	50.00
<b>IPR001751 - Calcium-binding protein, S-100/ICaBP type</b>	14	2	7.1e-06	14.29
<b>IPR002227 - Tyrosinase</b>	2	2	2.5e-05	100.00
<b>16338 - calcium-independent cell-cell adhesion</b>	22	3	2.5e-05	13.64
<b>42383 - sarcolemma</b>	14	3	4.6e-05	21.43
<b>42802 - identical protein binding</b>	81	4	6.0e-05	4.94
<b>IPR004031 - PMP-22/EMP/MP20 and claudin family</b>	30	3	6.5e-05	10.00
<b>31424 - keratinization</b>	23	2	8.9e-05	8.70
<b>5200 - structural constituent of cytoskeleton</b>	91	5	1.0e-04	5.49

Changed group breakdown:						
Group	P-value	Probe-set ID	Rank	Gene ID	Gene Symbol	Title
<b>1533 - cornified envelope</b>	1.8e-03	1451613_at	2	AY027660	Hnr	hornerin
	7.1e-06	1420431_at	5	NM_009100	Rptn	repetin
	4.5e-08	1427268_at	9	J03458	LOC433621 /// LOC545581	similar to Acidic ribosomal phosphoprotein P0 /// similar to Acidic ribosomal phosphoprotein P0
	8.0e-11	1448745_s_at	10	NM_008508	Lor	loricrin
<a href="#">show the whole group</a>						
<b>42470 - melanosome</b>	2.7e-02	1415861_at	63	BB762957	Tyrp1	tyrosinase-related protein 1
	5.1e-04	1418028_at	80	NM_010024	Dct	dopachrome tautomerase
	5.0e-06	1449896_at	85	NM_053015	Mlph	melanophilin
	4.6e-08	1456095_at	98	BB769772	Tyr	tyrosinase
<a href="#">show the whole group</a>						
<b>IPR003347 - Transcription factor jumonji, jmjC</b>	1.1e-03	1426438_at	1	AA210261	Ddx3y	DEAD (Asp-Glu-Ala-Asp) box polypeptide 3, Y-linked
	1.8e-05	1424903_at	6	AF127244	Jarid1d	jumonji, AT rich interactive domain 1D (Rbp2 like)
	6.7e-08	1426598_at	8	BB742957	Uty /// LOC546404 ///	ubiquitously transcribed tetratricopeptide repeat gene,
<a href="#">show the whole group</a>						

					LOC546411	Y chromosome /// similar to male-specific histocompatibility antigen H-YDb /// similar to male-specific histocompatibility antigen H-YDb
<b>5882 - intermediate filament</b>	2.3e-02	<a href="#">1429565_s_at</a>	4	<a href="#">AK004318</a>	Lce5a	late cornified envelope 5A
	6.6e-03	<a href="#">1423952_a_at</a>	21	<a href="#">BC010337</a>	Krt2-7	keratin complex 2, basic, gene 7
	4.5e-03	<a href="#">1419619_at</a>	57	<a href="#">NM_028770</a>	1200016G03Rik	RIKEN cDNA 1200016G03 gene
	3.8e-04	<a href="#">1420647_a_at</a>	59	<a href="#">NM_031170</a>	Krt2-8 /// LOC434261	keratin complex 2, basic, gene 8 /// similar to cytokeratin EndoA - mouse
	3.0e-05	<a href="#">1448169_at</a>	62	<a href="#">NM_010664</a>	Krt1-18	keratin complex 1, acidic, gene 18
	6.1e-06	<a href="#">1435989_x_at</a>	78	<a href="#">AW322280</a>	LOC434261	similar to cytokeratin EndoA - mouse
	4.8e-07	<a href="#">1423691_x_at</a>	82	<a href="#">M21836</a>	Krt2-8	keratin complex 2, basic, gene 8
	<a href="#">show the whole group</a>	9.3e-08	<a href="#">1438849_at</a>	97	<a href="#">BB144669</a>	2310030B04Rik
<b>IPR001664 - Intermediate filament protein</b>	7.2e-02	<a href="#">1423952_a_at</a>	21	<a href="#">BC010337</a>	Krt2-7	keratin complex 2, basic, gene 7
	1.8e-02	<a href="#">1419619_at</a>	57	<a href="#">NM_028770</a>	1200016G03Rik	RIKEN cDNA 1200016G03 gene
	1.2e-03	<a href="#">1420647_a_at</a>	59	<a href="#">NM_031170</a>	Krt2-8 /// LOC434261	keratin complex 2, basic, gene 8 /// similar to cytokeratin EndoA - mouse
	7.0e-05	<a href="#">1448169_at</a>	62	<a href="#">NM_010664</a>	Krt1-18	keratin complex 1, acidic, gene 18
	8.4e-06	<a href="#">1435989_x_at</a>	78	<a href="#">AW322280</a>	LOC434261	similar to cytokeratin EndoA - mouse
	<a href="#">show the whole group</a>	4.5e-07	<a href="#">1423691_x_at</a>	82	<a href="#">M21836</a>	Krt2-8
<b>6583 - melanin biosynthesis from tyrosine</b>	2.3e-02	<a href="#">1415861_at</a>	63	<a href="#">BB762957</a>	Tyrp1	tyrosinase-related protein 1
	3.7e-04	<a href="#">1418028_at</a>	80	<a href="#">NM_010024</a>	Dct	dopachrome tautomerase
	<a href="#">show the whole group</a>	4.4e-06	<a href="#">1456095_at</a>	98	<a href="#">BB769772</a>	Tyr
<b>IPR001751 - Calcium-binding protein, S-100/ICaBP type</b>	1.8e-03	<a href="#">1451613_at</a>	2	<a href="#">AY027660</a>	Hnr	hornerin
	<a href="#">show the whole group</a>	7.1e-06	<a href="#">1420431_at</a>	5	<a href="#">NM_009100</a>	Rptn
<b>IPR002227 - Tyrosinase</b>	7.9e-03	<a href="#">1415861_at</a>	63	<a href="#">BB762957</a>	Tyrp1	tyrosinase-related protein 1
	2.5e-05	<a href="#">1418028_at</a>	80	<a href="#">NM_010024</a>	Dct	dopachrome tautomerase
<b>16338 - calcium-independent cell-cell adhesion</b>	4.7e-02	<a href="#">1448393_at</a>	35	<a href="#">BC008104</a>	Cldn7	claudin 7
	1.4e-03	<a href="#">1460569_x_at</a>	40	<a href="#">AW611462</a>	Cldn3	claudin 3
	<a href="#">show the whole group</a>	2.5e-05	<a href="#">1418283_at</a>	42	<a href="#">NM_009903</a>	Cldn4
<b>42383 - sarcolemma</b>	5.1e-02	<a href="#">1420647_a_at</a>	59	<a href="#">NM_031170</a>	Krt2-8 /// LOC434261	keratin complex 2, basic, gene 8 /// similar to cytokeratin EndoA - mouse
	2.1e-03	<a href="#">1435989_x_at</a>	78	<a href="#">AW322280</a>	LOC434261	similar to cytokeratin EndoA - mouse
	<a href="#">show the whole group</a>	4.6e-05	<a href="#">1423691_x_at</a>	82	<a href="#">M21836</a>	Krt2-8
<b>42802 - identical protein binding</b>	5.4e-02	<a href="#">1420350_at</a>	11	<a href="#">NM_028625</a>	Sprl2	small proline rich-like 2
	1.4e-02	<a href="#">1448393_at</a>	35	<a href="#">BC008104</a>	Cldn7	claudin 7
	1.1e-03	<a href="#">1460569_x_at</a>	40	<a href="#">AW611462</a>	Cldn3	claudin 3

<a href="#">show the whole group</a>	6.0e-05	1418283_at	42	NM_009903	Cldn4	claudin 4
<b>IPR004031 - PMP-22/EMP/MP20 and claudin family</b>	6.4e-02	1448393_at	35	BC008104	Cldn7	claudin 7
	2.5e-03	1460569_x_at	40	AW611462	Cldn3	claudin 3
<a href="#">show the whole group</a>	6.5e-05	1418283_at	42	NM_009903	Cldn4	claudin 4
<b>31424 - keratinization</b>	2.9e-03	1451613_at	2	AY027660	Hrnr	hornerin
<a href="#">show the whole group</a>	8.9e-05	1448745_s_at	10	NM_008508	Lor	loricrin
<b>5200 - structural constituent of cytoskeleton</b>	5.6e-02	1448745_s_at	10	NM_008508	Lor	loricrin
	6.3e-03	1423952_a_at	21	BC010337	Krt2-7	keratin complex 2, basic, gene 7
	4.6e-03	1420647_a_at	59	NM_031170	Krt2-8 /// LOC434261	keratin complex 2, basic, gene 8 /// similar to cytokeratin EndoA - mouse
	4.3e-04	1448169_at	62	NM_010664	Krt1-18	keratin complex 1, acidic, gene 18
<a href="#">show the whole group</a>	1.0e-04	1423691_x_at	82	M21836	Krt2-8	keratin complex 2, basic, gene 8

## Iterative Group Analysis (iGA) report on the differentially expressed functional gene classes



### General Information

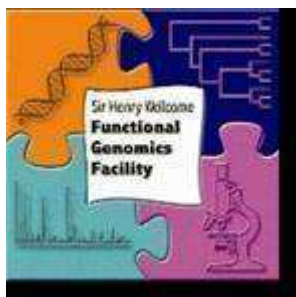
Mode	Representative
Number of genes on chip	23155
Number of annotated genes	15969
Number of groups	8045
Number of singletons	2869
Significance threshold	1.2e-04
File name	K14D6 +CCL3 vs K14D6 Control negative

Top Changed Groups	Group Members	Changed Members	P-Value Changed	Percent Changed
IPR001101 - Plectin repeat	8	4	3.8e-08	50.00
42383 - sarcolemma	14	3	6.1e-07	21.43
30018 - Z disc	27	3	4.8e-06	11.11
9613 - response to pest, pathogen or parasite	31	3	7.4e-06	9.68
IPR001664 - Intermediate filament protein	59	4	3.7e-05	6.78
46716 - muscle maintenance	4	2	5.7e-05	50.00
IPR002017 - Spectrin repeat	19	3	1.1e-04	15.79

Changed group breakdown:						
Group	P-value	Probe-set ID	Rank	Gene ID	Gene Symbol	Title
IPR001101 - Plectin repeat	5.0e-03	1427610_at	10	BC026631	Dsp	desmoplakin
	1.1e-04	1427537_at	32	BC026387	Eppk1	epiplakin 1
	3.4e-06	1437554_at	64	BM232239	Plec1	plectin 1
<a href="#">show the whole group</a>	3.8e-08	1428847_a_at	79	BM248206	Macf1	microtubule-actin crosslinking factor 1
42383 - sarcolemma	5.2e-03	1435989_x_at	6	AW322280	LOC434261	similar to cytokeratin EndoA - mouse
	7.4e-05	1420647_a_at	15	NM_031170	Krt2-8 /// LOC434261	keratin complex 2, basic, gene 8 /// similar to cytokeratin EndoA - mouse
<a href="#">show the whole group</a>	6.1e-07	1423691_x_at	20	M21836	Krt2-8	keratin complex 2, basic, gene 8
30018 - Z disc	1.0e-02	1435989_x_at	6	AW322280	LOC434261	similar to cytokeratin EndoA - mouse
	2.9e-04	1420647_a_at	15	NM_031170	Krt2-8 ///	keratin complex 2, basic, gene 8

					LOC434261	8 /// similar to cytokeratin EndoA - mouse
<a href="#">show the whole group</a>	4.8e-06	<a href="#">1423691_x_at</a>	20	<a href="#">M21836</a>	Krt2-8	keratin complex 2, basic, gene 8
<b>9613 - response to pest, pathogen or parasite</b>	1.2e-02	<a href="#">1435989_x_at</a>	6	<a href="#">AW322280</a>	LOC434261	similar to cytokeratin EndoA - mouse
	3.8e-04	<a href="#">1420647_a_at</a>	15	<a href="#">NM_031170</a>	Krt2-8 /// LOC434261	keratin complex 2, basic, gene 8 /// similar to cytokeratin EndoA - mouse
<a href="#">show the whole group</a>	7.4e-06	<a href="#">1423691_x_at</a>	20	<a href="#">M21836</a>	Krt2-8	keratin complex 2, basic, gene 8
<b>IPR001664 - Intermediate filament protein</b>	2.2e-02	<a href="#">1435989_x_at</a>	6	<a href="#">AW322280</a>	LOC434261	similar to cytokeratin EndoA - mouse
	1.4e-03	<a href="#">1420647_a_at</a>	15	<a href="#">NM_031170</a>	Krt2-8 /// LOC434261	keratin complex 2, basic, gene 8 /// similar to cytokeratin EndoA - mouse
	5.2e-05	<a href="#">1423691_x_at</a>	20	<a href="#">M21836</a>	Krt2-8	keratin complex 2, basic, gene 8
<a href="#">show the whole group</a>	3.7e-05	<a href="#">1448169_at</a>	51	<a href="#">NM_010664</a>	Krt1-18	keratin complex 1, acidic, gene 18
<b>46716 - muscle maintenance</b>	4.8e-03	<a href="#">1454904_at</a>	19	<a href="#">BG976607</a>	Mtm1	X-linked myotubular myopathy gene 1
<a href="#">show the whole group</a>	5.7e-05	<a href="#">1458663_at</a>	50	<a href="#">AI552833</a>	Large	Like-glycosyltransferase (Large), mRNA
<b>IPR002017 - Spectrin repeat</b>	1.2e-02	<a href="#">1427610_at</a>	10	<a href="#">BC026631</a>	Dsp	desmoplakin
	2.6e-03	<a href="#">1437554_at</a>	64	<a href="#">BM232239</a>	Plec1	plectin 1
<a href="#">show the whole group</a>	1.1e-04	<a href="#">1428847_a_at</a>	79	<a href="#">BM248206</a>	Macf1	microtubule-actin crosslinking factor 1

**Iterative Group Analysis (iGA) report on the differentially expressed functional gene classes**



### General Information

Mode	Representative
Number of genes on chip	23155
Number of annotated genes	15985
Number of groups	8056
Number of singletons	2858
Significance threshold	1.2e-04
File name	K14D6 + CCL3 v WT + CCL3 negative

Top Changed Groups	Group Members	Changed Members	P-Value Changed	Percent Changed
<b>IPR007237 - CD20/IgE Fc receptor beta subunit</b>	15	4	8.0e-08	26.67
<b>IPR001811 - Small chemokine, interleukin-8 like</b>	31	4	1.4e-07	12.90
<b>6935 - chemotaxis</b>	87	5	2.1e-07	5.75
<b>8009 - chemokine activity</b>	38	4	3.3e-07	10.53
<b>30595 - immune cell chemotaxis</b>	5	3	3.4e-07	60.00
<b>19864 - IgG binding</b>	5	2	1.8e-05	40.00
<b>IPR001916 - Glycoside hydrolase, family 22</b>	8	2	2.6e-05	25.00
<b>3796 - lysozyme activity</b>	10	2	4.2e-05	20.00
<b>42383 - sarcolemma</b>	14	3	5.4e-05	21.43
<b>IPR001304 - C-type lectin</b>	99	3	6.3e-05	3.03
<b>45576 - mast cell activation</b>	9	2	6.5e-05	22.22
<b>16998 - cell wall catabolism</b>	16	2	1.1e-04	12.50

Changed group breakdown:						
Group	P-value	Probe-set ID	Rank	Gene ID	Gene Symbol	Title
<b>IPR007237 - CD20/IgE Fc receptor beta subunit</b>	5.6e-03	1424754_at	6	BC024402	Ms4a7	membrane-spanning 4-domains, subfamily A, member 7
	3.7e-05	1419599_s_at	10	NM_026835	Ms4a11	membrane-spanning 4-domains, subfamily A, member 11
	3.0e-07	1419598_at	15	NM_026835	Ms4a6d	membrane-spanning 4-domains, subfamily A, member 6D
	<a href="#">show the whole group</a>	8.0e-08	1418826_at	46	NM_027209	Ms4a6b
<b>IPR001811 - Small chemokine, interleukin-8 like</b>	1.3e-02	1448995_at	7	NM_019932	Cxcl4	chemokine (C-X-C motif) ligand 4
	2.4e-04	1417266_at	12	BC002073	Ccl6	chemokine (C-C motif) ligand 6
	1.1e-05	1419728_at	23	NM_009141	Cxcl5	chemokine (C-X-C motif) ligand 5
	<a href="#">show the whole group</a>	1.4e-07	1417936_at	25	AF128196	Ccl9
<b>6935 - chemotaxis</b>	3.7e-02	1448995_at	7	NM_019932	Cxcl4	chemokine (C-X-C motif) ligand 4
	1.9e-03	1417266_at	12	BC002073	Ccl6	chemokine (C-C motif) ligand 6

	1.7e-04	1442082_at	20	BB333624	C3ar1	complement component 3a receptor 1
	6.7e-06	1419728_at	23	NM_009141	Cxcl5	chemokine (C-X-C motif) ligand 5
<a href="#">show the whole group</a>	2.1e-07	1417936_at	25	AF128196	Ccl9	chemokine (C-C motif) ligand 9
<b>8009 - chemokine activity</b>	1.7e-02	1448995_at	7	NM_019932	Cxcl4	chemokine (C-X-C motif) ligand 4
	3.6e-04	1417266_at	12	BC002073	Ccl6	chemokine (C-C motif) ligand 6
	2.1e-05	1419728_at	23	NM_009141	Cxcl5	chemokine (C-X-C motif) ligand 5
<a href="#">show the whole group</a>	3.3e-07	1417936_at	25	AF128196	Ccl9	chemokine (C-C motif) ligand 9
<b>30595 - immune cell chemotaxis</b>	2.2e-03	1448995_at	7	NM_019932	Cxcl4	chemokine (C-X-C motif) ligand 4
	1.2e-05	1449254_at	18	NM_009263	Spp1	secreted phosphoprotein 1
<a href="#">show the whole group</a>	3.4e-07	1419609_at	53	AV231648	Ccr1	chemokine (C-C motif) receptor 1
<b>19864 - IgG binding</b>	4.4e-03	1435477_s_at	14	BM224327	Fcgr2b	Fc receptor, IgG, low affinity IIb
<a href="#">show the whole group</a>	1.8e-05	1448620_at	22	NM_010188	Fcgr3	Fc receptor, IgG, low affinity III
<b>IPR001916 - Glycoside hydrolase, family 22</b>	1.0e-03	1436996_x_at	2	AV066625	Lzp-s	P lysozyme structural
<a href="#">show the whole group</a>	2.6e-05	1423547_at	16	AW208566	Lyzs	lysozyme
<b>3796 - lysozyme activity</b>	1.3e-03	1436996_x_at	2	AV066625	Lzp-s	P lysozyme structural
<a href="#">show the whole group</a>	4.2e-05	1423547_at	16	AW208566	Lyzs	lysozyme
<b>42383 - sarcolemma</b>	5.0e-02	1423691_x_at	58	M21836	Krt2-8	keratin complex 2, basic, gene 8
	1.4e-03	1435989_x_at	64	AW322280	LOC434261	similar to cytokeratin EndoA - mouse
<a href="#">show the whole group</a>	5.4e-05	1420647_a_at	87	NM_031170	Krt2-8 /// LOC434261	keratin complex 2, basic, gene 8 /// similar to cytokeratin EndoA - mouse
<b>IPR001304 - C-type lectin</b>	1.8e-02	1420804_s_at	3	NM_010819	Clec4d	C-type lectin domain family 4, member d
	2.0e-03	1450430_at	11	NM_008625	Mrc1	mannose receptor, C type 1
<a href="#">show the whole group</a>	6.3e-05	1425951_a_at	13	AF240358	Clec4n	C-type lectin domain family 4, member n
<b>45576 - mast cell activation</b>	7.9e-03	1435477_s_at	14	BM224327	Fcgr2b	Fc receptor, IgG, low affinity IIb
<a href="#">show the whole group</a>	6.5e-05	1448620_at	22	NM_010188	Fcgr3	Fc receptor, IgG, low affinity III
<b>16998 - cell wall catabolism</b>	2.0e-03	1436996_x_at	2	AV066625	Lzp-s	P lysozyme structural
<a href="#">show the whole group</a>	1.1e-04	1423547_at	16	AW208566	Lyzs	lysozyme